ANTIMICROBIALS AND ANTICANCERS OF BACTERIAL ORIGINS

EDITED BY: Tomasz M. Karpiński, Ana R. Freitas and Bingyun Li
PUBLISHED IN: Frontiers in Microbiology

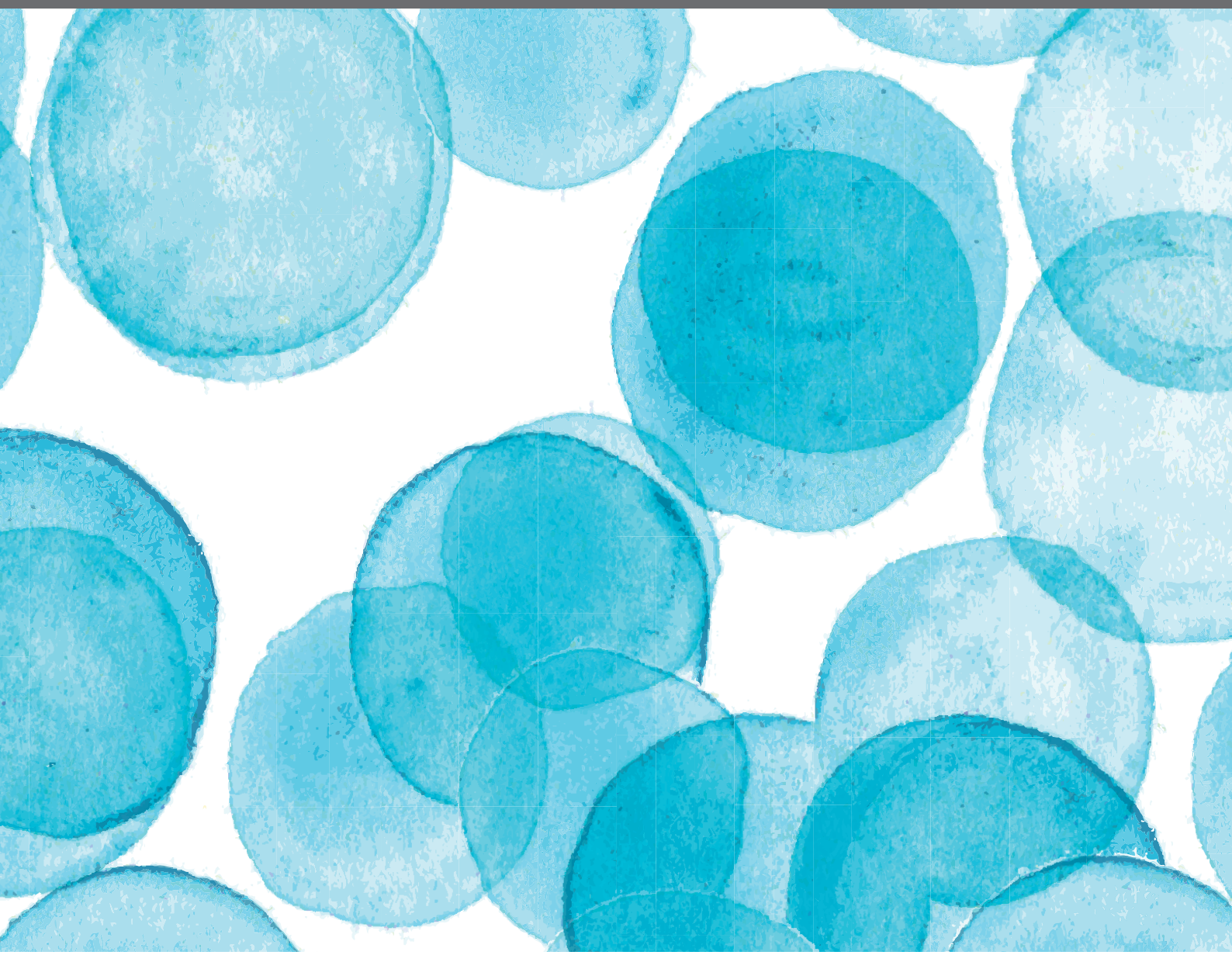

frontiers Research Topics

frontiers

ISSN 1664-8714
ISBN 978-2-88963-806-2
DOI 10.3389/978-2-88963-806-2

About Frontiers

Frontiers is more than just an open-access publisher of scholarly articles: it is a pioneering approach to the world of academia, radically improving the way scholarly research is managed. The grand vision of Frontiers is a world where all people have an equal opportunity to seek, share and generate knowledge. Frontiers provides immediate and permanent online open access to all its publications, but this alone is not enough to realize our grand goals.

Frontiers Journal Series

The Frontiers Journal Series is a multi-tier and interdisciplinary set of open-access, online journals, promising a paradigm shift from the current review, selection and dissemination processes in academic publishing. All Frontiers journals are driven by researchers for researchers; therefore, they constitute a service to the scholarly community. At the same time, the Frontiers Journal Series operates on a revolutionary invention, the tiered publishing system, initially addressing specific communities of scholars, and gradually climbing up to broader public understanding, thus serving the interests of the lay society, too.

Dedication to Quality

Each Frontiers article is a landmark of the highest quality, thanks to genuinely collaborative interactions between authors and review editors, who include some of the world's best academicians. Research must be certified by peers before entering a stream of knowledge that may eventually reach the public - and shape society; therefore, Frontiers only applies the most rigorous and unbiased reviews.
Frontiers revolutionizes research publishing by freely delivering the most outstanding research, evaluated with no bias from both the academic and social point of view. By applying the most advanced information technologies, Frontiers is catapulting scholarly publishing into a new generation.

What are Frontiers Research Topics?

Frontiers Research Topics are very popular trademarks of the Frontiers Journals Series: they are collections of at least ten articles, all centered on a particular subject. With their unique mix of varied contributions from Original Research to Review Articles, Frontiers Research Topics unify the most influential researchers, the latest key findings and historical advances in a hot research area! Find out more on how to host your own Frontiers Research Topic or contribute to one as an author by contacting the Frontiers Editorial Office: researchtopics@frontiersin.org

ANTIMICROBIALS AND ANTICANCERS OF BACTERIAL ORIGINS

Topic Editors:
Tomasz M. Karpiński, Poznan University of Medical Sciences, Poland
Ana R. Freitas, University of Porto, Portugal
Bingyun Li, West Virginia University, United States

Citation: Karpiński, T. M., Freitas, A. R., Li, B., eds. (2020). Antimicrobials and Anticancers of Bacterial Origins. Lausanne: Frontiers Media SA.
doi: 10.3389/978-2-88963-806-2

Table of Contents

frontiers in Microbiology

EDITORIAL
published: 30 April 2020
doi: 10.3389/fmicb.2020.00842

Editorial: Antimicrobials and Anticancers of Bacterial Origins

Ana R. Freitas[1]*, *Tomasz M. Karpiński*[2] *and Bingyun Li*[3]

[1] UCIBIO/REQUIMTE, Departamento de Ciências Biológicas, Laboratório de Microbiologia, Faculdade de Farmácia, Universidade Do Porto, Porto, Portugal, [2] Chair and Department of Medical Microbiology, Poznań University of Medical Sciences, Poznań, Poland, [3] Department of Orthopaedics, School of Medicine, West Virginia University, Morgantown, WV, United States

Keywords: non-ribosomal peptide, bacterial toxin, anticancer activity, antimicrobial activity, antibiotic, bacteriocin, bacterial enzyme

Editorial on the Research Topic

Antimicrobials and Anticancers of Bacterial Origins

OPEN ACCESS

Edited by:
Fabian Cieplik, University Medical Center Regensburg, Germany

Reviewed by:
Rodolfo García-Contreras, National Autonomous University of Mexico, Mexico
César de la Fuente, University of Pennsylvania, United States

***Correspondence:**
Ana R. Freitas
anarpf@gmail.com; afreitas@ff.up.pt

Specialty section:
This article was submitted to Antimicrobials, Resistance and Chemotherapy, a section of the journal Frontiers in Microbiology

Received: *18 March 2020*
Accepted: *08 April 2020*
Published: *30 April 2020*

Citation:
Freitas AR, Karpiński TM and Li B (2020) Editorial: Antimicrobials and Anticancers of Bacterial Origins. Front. Microbiol. 11:842. doi: 10.3389/fmicb.2020.00842

Infectious diseases kill more than 17 million people a year according to the World Health Organization (WHO; https://www.who.int/whr/1996/media_centre/press_release). Among them, healthcare-associated infections caused by antimicrobial resistant (AMR) bacteria are increasingly hard to treat, threatening our progress in healthcare and life expectancy, and have a tremendous social and economic impact worldwide (https://www.who.int/news-room/fact-sheets/detail/antibiotic-resistance). In Europe alone, AMR causes 33,000 deaths and costs 1.5 billion per year in healthcare and productivity losses (EU Commission, 2017; Cassini et al., 2019). More than 2.8 million AMR infections occur in the United States each year, and more than 35,000 people die as a result (CDC, 2019). Patients with AMR infections may need to be hospitalized for more than 13 days, adding over 8 million hospital days annually (Ventola, 2015). Current strategies to counteract this worrying scenario include the investment on R&D to develop new antibiotics.

Cancer is another leading cause of morbidity and mortality worldwide; cancer was responsible for 8.8 million deaths in 2015. Similar to AMR infections, the resistance to classic cancer chemotherapeutic agents and/or novel targeted drugs has been recognized for decades and is a significant obstacle to the success of chemotherapy in cancer treatments.

It is clear that the greatest challenges in treating infections and cancers is the resistance to the treatments and the lack of new antimicrobial or anticancer drugs. Microorganisms themselves have been the richest source of antibiotics/anticancer drugs with currently unknown or unculturable bacteria being one of the greatest sources of novel bioactive molecules. Both antimicrobial and anticancer drugs can be obtained from bacteria of natural environments or the gut microbiota, and some drugs like actinomycin D and bleomycin may have dual antimicrobial and anticancer properties (Karpinski and Adamczak, 2018). The papers published in this Research Topic (seven Research Articles and three Reviews) have reinforced the diversity of bioactive molecules with antimicrobial and anticancer properties that can be found in natural bacteria, as illustrated further bellow.

Rodrigues et al. reviewed bacterial proteins and peptides called bacteriocins including colicin, pyocin, nisin, microcin, laterosporulin, pediocin, plantaricin, duramycin, etc. These unique proteins and peptides can be synthesized by Gram-positive (e.g., *Lactococcus lactis*, *Lactobacillus plantarum*) or Gram-negative (e.g., *Escherichia coli*, *Pseudomonas aeruginosa*) bacteria and were shown to present *in vitro* and/or *in vivo* antimicrobial and anticancer properties.

Baquero et al. comprehensively reviewed the main chemical substances arising from the action of the gut microbiota that might inhibit bacterial replication or reduce microbial viability. The role of microcins, which are small peptides produced by Gram-negative organisms (mostly *Enterobacteriaceae*) and are able to inhibit other bacteria, has been highlighted as effectors of intermicrobial interactions. The microcin's history and classification, mechanisms of action, and mechanisms involved in microcin's immunity (in microcin producers) and resistance (non-producers) were elegantly reviewed.

Shafiee et al. reviewed the targeted application of diphtheria toxin, one of the most frequently studied immunotoxins, in treating cancers. Strategies using cancer specific/targeted ligands and gene therapies were discussed.

In the study of Marcolefas et al. a variety of materials were collected from the high Arctic habitats, which are characterized by high salt and prolonged subzero temperatures, and analyzed for antimicrobial properties. Two Arctic microbial isolates presented antimicrobial activity either against foodborne pathogens at refrigeration temperatures or against clinically relevant pathogens (e.g., *Staphylococcus aureus, Enterococcus faecium, Acinetobacter baumannii*). This suggested that Arctic microbial diversity might be a promising source for antibiotics with unique low-temperature antimicrobial properties.

Qin et al. described a novel class I bacteriocin (Subtilin L-Q11) purified from a *Bacillus subtilis* strain L-Q11 of an orchard soil in Beijing, China. This novel bacteriocin showed optimal physicochemical features including high thermostability, pH-tolerance, resistance to chemical reagents, and sensitivity to various human proteases, and inhibition of growth of Gram-positive human pathogens (*Staphylococcus aureus* and *Enterococcus faecalis*) and food spoilage bacteria (e.g., *Bacillus cereus*). The most consistent activity of inhibition was observed against *Staphylococcus aureus*. Subtilin L-Q11 could be a potential antimicrobial drug for food preservation.

Zhao et al. reported a *Pseudomonas* sp. genome of a 11K1 strain isolated from rhizosphere in China by performing *in silico* and genetic analyses of putative secondary metabolite biosynthetic clusters. It was previously known that this strain exhibited strong inhibitory activity against plant pathogenic fungi and bacteria. Two putative novel cyclic lipopeptide biosynthetic clusters (brasmycin and braspeptin) were now identified to contribute to such antifungal activities by affecting biofilm formation and colony morphology.

The study by Cebrián et al. focused on the identification, design, and production of new lantibiotics, a class of polycyclic peptide antibiotics, with enhanced activity against *Clostridium difficile*. They used a strategy of genome mining, heterologous expression, design of new hybrid lantibiotics, and cloning and expressing the designed peptides in *Lactococcus lactis*. One peptide was found to present a high heterologous production level and high specificity/activity against clostridial species, making it a potential alternative to traditional antibiotics for treating *Clostridium difficile* infections.

Pérez Navarro et al. assessed the action of fluopsin C (a metalloantibiotic produced by *Pseudomonas* spp.) against multidrug-resistant and clinically-relevant bacterial species (*Staphylococcus aureus, Enterococcus faecium, Klebsiella pneumoniae*) through *in vitro* and *in vivo* experiments. Although further studies are needed to clarify the pharmokinetic and toxicity properties, fluopsin C and its derivatives have potential to serve as alternatives in treating multidrug-resistant infections caused by Gram-positive and Gram-negative bacterial species.

Can antimicrobial drugs be used for anticancer purposes or vice versa? Several antimicrobial drugs (e.g., antimicrobial peptides) were tested for their potential anticancer properties in the study of Varas et al.. For instance, the antimicrobial peptide microcin E492 produced by Gram-negative *Klebsiella pneumoniae* was found to present *in vitro* and *in vivo* anticancer properties against colorectal cancer cells. Models based on zebrafish were developed and may be efficient in screening pre-clinical anticancer drugs. Meanwhile, commonly used anticancer drugs (e.g., mitomycin C, etoposide, camptothecin, doxorubicin, 5-fluorouracil, cisplatin) were also repurposed for antimicrobial applications according to Domalaon et al. Mitomycin C, augmented with tobramycin-ciprofloxacin hybrids, was found to display antimicrobial activities against multidrug-resistant Gram-negative bacteria including *Pseudomonas aeruginosa*, *Acinetobacter baumannii*, *Escherichia coli*, *Klebsiella pneumoniae*, and *Enterobacter cloacae*. Therefore, there are drugs that can be used for both antimicrobial and anticancer purposes, and repurposing FDA approved drugs could be time- and cost-effective in discovering new antimicrobial or anticancer drugs.

Taken together, these studies illustrate the versatility of bioactive molecules from natural products and highlight the importance of using cutting-edge methodologies to boost the discovery of new antimicrobial and anticancer compounds.

AUTHOR CONTRIBUTIONS

All authors listed have made a substantial, direct and intellectual contribution to the work, and approved it for publication.

FUNDING

BL acknowledges the financial support from the Office of the Assistant Secretary of Defense for Health Affairs through the Medical Research Program, Discovery Awards under Award Nos. W81XWH1710603 and W81XWH1810203.

ACKNOWLEDGMENTS

The Editors are grateful to all authors that participated in this Research Topic and to all (external or editorial board member) reviewers, who have contributed significantly to its success. AF acknowledges the Junior Research Position (CEECIND/02268/2017) granted by FCT/MCTES.

REFERENCES

Cassini, A., Högberg, L. D., Plachouras, D., Plachouras, A., Hoxha, A., Simonsen, G. S., et al. (2019). Attributable deaths and disability-adjusted life-years caused by infections with antibiotic-resistant bacteria in the EU and the European Economic Area in 2015: a Population-level Modelling Analysis. *Lancet Infect Dis.* 19, 56–66. doi: 10.1016/s1473-3099(18)30605-4

CDC (2019). *Antibiotic Resistance Threats in the United States, 2019*. Atlanta, GA: U.S. Department of Health and Human Services, CDC. Available online at: https://www.cdc.gov/drugresistance/pdf/threats-report/2019-ar-threats-report-508.pdf

EU Commission (2017). *A European One Health Action Plan against Antimicrobial Resistance (AMR)*. Available online at: https://ec.europa.eu/health/amr/sites/health/files/antimicrobial_resistance/docs/amr_2017_action-plan.pdf

Karpinski, T. M., and Adamczak, A. (2018). Anticancer activity of bacterial proteins and peptides. *Pharmaceutics*. 10:E54. doi: 10.3390/pharmaceutics10020054

Ventola, C. L. (2015). The antibiotic resistance crisis: part 1: causes and threats. *P T* 40, 277–283.

Conflict of Interest: The authors declare that the research was conducted in the absence of any commercial or financial relationships that could be construed as a potential conflict of interest.

frontiers in Microbiology

ORIGINAL RESEARCH
published: 19 March 2020
doi: 10.3389/fmicb.2020.00405

Exploiting Zebrafish Xenografts for Testing the *in vivo* Antitumorigenic Activity of Microcin E492 Against Human Colorectal Cancer Cells

Macarena A. Varas[1], Carlos Muñoz-Montecinos[2], Violeta Kallens[2], Valeska Simon[3], Miguel L. Allende[2], Andrés E. Marcoleta[1] and Rosalba Lagos[1]**

[1] *Laboratorio de Biología Estructural y Molecular BEM, Departamento de Biología, Facultad de Ciencias, Universidad de Chile, Santiago, Chile,* [2] *Departamento de Biología, Facultad de Ciencias, FONDAP Center for Genome Regulation, Universidad de Chile, Santiago, Chile,* [3] *Laboratorio de Inmunología, Departamento de Biología, Facultad de Ciencias, Universidad de Chile, Santiago, Chile*

OPEN ACCESS

Edited by:
Tomasz M. Karpiński, Poznan University of Medical Sciences, Poland

Reviewed by:
Koshy Philip, University of Malaya, Malaysia
Piyush Baindara, University of Arkansas for Medical Sciences, United States
Jianhua Wang, Feed Research Institute (CAAS), China

***Correspondence:**
Andrés E. Marcoleta
amarcoleta@uchile.cl
Rosalba Lagos
rolagos@uchile.cl

Specialty section:
This article was submitted to Antimicrobials, Resistance and Chemotherapy, a section of the journal Frontiers in Microbiology

Received: *21 August 2019*
Accepted: *26 February 2020*
Published: *19 March 2020*

Citation:
Varas MA, Muñoz-Montecinos C, Kallens V, Simon V, Allende ML, Marcoleta AE and Lagos R (2020) Exploiting Zebrafish Xenografts for Testing the in vivo Antitumorigenic Activity of Microcin E492 Against Human Colorectal Cancer Cells. Front. Microbiol. 11:405. doi: 10.3389/fmicb.2020.00405

One of the approaches to address cancer treatment is to develop new drugs not only to obtain compounds with less side effects, but also to have a broader set of alternatives to tackle the resistant forms of this pathology. In this regard, growing evidence supports the use of bacteria-derived peptides such as bacteriocins, which have emerged as promising anti-cancer molecules. In addition to test the activity of these molecules on cancer cells in culture, their *in vivo* antitumorigenic properties must be validated in animal models. Although the standard approach for such assays employs experiments in nude mice, at the initial stages of testing, the use of high-throughput animal models would permit rapid proof-of-concept experiments, screening a high number of compounds, and thus increasing the possibilities of finding new anti-cancer molecules. A validated and promising alternative animal model are zebrafish larvae harboring xenografts of human cancer cells. Here, we addressed the anti-cancer properties of the antibacterial peptide microcin E492 (MccE492), a bacteriocin produced by *Klebsiella pneumoniae*, showing that this peptide has a marked cytotoxic effect on human colorectal cancer cells *in vitro*. Furthermore, we developed a zebrafish xenograft model using these cells to test the antitumor effect of MccE492 *in vivo*, demonstrating that intratumor injection of this peptide significantly reduced the tumor cell mass. Our results provide, for the first time, evidence of the *in vivo* antitumoral properties of a bacteriocin tested in an animal model. This evidence strongly supports the potential of this bacteriocin for the development of novel anti-cancer therapies.

Keywords: microcin E492, antitumorigenic peptide, zebrafish xenograft, bacteriocin, colorectal cancer, human cell lines, cytotoxicity, *Klebsiella pneumoniae*

INTRODUCTION

Cancer is one of the leading causes of death in the world and, for this reason, research focused on the search of new agents that inhibit the proliferation of tumors is highly relevant. A promising area of research involves the study of therapeutic peptides and proteins produced by bacteria, including bacteriocins. Bacteriocins, besides their characteristic antibacterial properties, have a

potential role as anticancer agents. The use of bacteria or their products against cancer has already been tested at different levels. For instance, a treatment with mixed extracts from *Streptococcus pyogenes* and *Serratia marscensces* (currently known as Coley toxins) on unresectable tumors was successfully administrated more than 100 years ago (Karpiński and Adamczak, 2018; reviewed in Baindara et al., 2018; Ashu et al., 2019). Similarly, the study of different bacteriocins and their antineoplasic properties has a long history and has included colicins, pyocins, pediocins, and microcins (reviewed in Lagos, 2007; Cornut et al., 2008). Over the past few years there has been a renewed interest in exploring anticancer properties of other bacteriocins, and among them are laterosporulin10 (Baindara et al., 2017), nisin ZP (Kamarajan et al., 2015), nisin (Joo et al., 2012), plantaricin P1053 (De Giani et al., 2019), and others (reviewed in Kaur and Kaur, 2015; Baindara et al., 2018; Karpiński and Adamczak, 2018; Ashu et al., 2019). Microcins are a class of bacteriocins with a molecular mass of <10 kDa produced by Gram-negative bacteria, principally *Enterobactericeae*. A previous study on microcin E492 (MccE492) reported on its capacity to inhibit the proliferation of cancer cells *in vitro* (Hetz et al., 2002; Lagos et al., 2009). MccE492 is a pore-forming bacteriocin displaying toxic activity on several strains of the family *Enterobacteriaceae* (de Lorenzo and Pugsley, 1985; Lagos et al., 1993, 2001). This bacteriocin was isolated from *Klebsiella pneumoniae* RYC492 (de Lorenzo, 1984), and the genetic determinants necessary for its production were cloned and expressed in *Escherichia coli* (Wilkens et al., 1997). The steps for MccE92 synthesis, post-translational modification, processing, export and uptake from target cells are shown in **Figure 1A** (Thomas et al., 2004; Strahsburger et al., 2005; Lagos et al., 2009; Marcoleta et al., 2013a). The gene cluster encoding for active MccE492 is located in the genomic island GI-E492 (Marcoleta et al., 2013b, 2016), which was found to be highly prevalent among liver abscess-associated strains of *K. pneumoniae* (Marcoleta et al., 2016, 2018; Lam et al., 2018). A striking characteristic of MccE492 is that it forms amyloid fibers both *in vivo* and *in vitro* (**Figure 1A**; Bieler et al., 2005; Arranz et al., 2012; Marcoleta et al., 2013a; Aguilera et al., 2016). Regarding its cytotoxic activity, MccE492 was toxic to different malignant cell lines (HeLa, Jurkat, and RJ2.25), and did not have effect on KG-1 and a primary culture from human tonsils (Hetz et al., 2002). This study, however, did not include malignant cell lines derived from intestinal cancer, which could be a relevant target since MccE492 is produced by *K. pneumoniae*, known to colonize the intestine. To explore its potential use as an antitumor, the toxic activity of this bacteriocin should be tested *in vivo* in an animal model. The gold standard for such assays are nude mice; however, these studies are lengthy and costly for exploratory and proof-of-concept approaches. To overcome these drawbacks, the use of zebrafish as an alternative model for pre-clinical anti-cancer drug tests has gained importance (Wertman et al., 2016; Wyatt et al., 2017; Hill et al., 2018; Letrado et al., 2018; Hason and Bartůněk, 2019). This animal model has multiple advantages, among them, the possibility of concurrently examining a large number of individuals (allowing more statistically robust analyses), the duration of the experiments is brief, and a high number of experiments can be conducted at an affordable cost. Furthermore, the use of zebrafish larvae has allowed the development of human xenograft tumors showing histological features and gene expression patterns similar to those of the original human tumor. Another advantage is the optical transparency of the larvae, which allows real time tracking of individual cancer cells and tumor growth evaluation by non-invasive imaging, without the need to fix and sacrifice the animals (reviewed in White et al., 2013). Currently, zebrafish is being used for xenotransplantation of human cancers to evaluate the drug response of tumors from patient-derived biopsy specimens (reviewed in Veinotte et al., 2014). Fior et al. (2017), testing different colorectal cancers, demonstrated the usefulness of this model to predict the response of a specific cancer to a given therapy using patient-derived xenografts in zebrafish. These findings support the use of this model to test bacteriocins as anticancer compounds in colorectal tumors. Preliminary but not conclusive results from our laboratory (Lagos et al., 2009) suggested the possible antitumoral activity of McccE492 tested on tumors derived from colorectal cancer cells developed in nude mice. To demonstrate if indeed MccE492 has antitumor capacity *in vivo*, we decided to exploit the zebrafish model. Here, we tested the effect of MccE492 on two human colorectal cancer cell lines *in vitro*, and used one of them to develop a zebrafish xenograft model to assess the effect of direct MccE492 intratumoral injection on tumor growth.

MATERIALS AND METHODS

Microcin E492 Purification

Escherichia coli BL21 DE3 cells were transformed with the pMccE492 plasmid carrying a 13-kbp segment of the microcin E492 production cluster, originally cloned from *Klebsiella pneumoniae* RYC492 (Aguilera et al., 2016). An overnight culture of these cells grown in LB broth (10 g/L tryptone, 10 g/L NaCl and 5 g/L yeast extract) were typically used to inoculate (1:1000) 2 L of M9 medium supplemented with citrate and glucose (2 g/L each) and ampicillin (100 μg/mL). Cells were grown at 37°C with shaking (180 rpm) during 12–14 h, and then the supernatant was collected by centrifugation at 6,500 × g during 30 min at 4°C. Then, the supernatant was filtered through a 0.22 μm polyethersulfone membrane (Steritop, Millipore). The cell-free medium was incubated at 4°C during 2 h with 10 g of Bondapak C18 resin (Waters) previously activated overnight in 100% acetonitrile (ACN). The resin was filtered by negative pressure through a Buchner funnel, washed with 200 mL of 40% methanol, then with 200 mL of 25% ACN, and finally eluted with a 30–100% ACN stepwise gradient in fractions of 50 mL each. MccE492-enriched fractions were dialyzed twice for 2 h against 40 volumes of nanopure water and then lyophilized and stored at −20°C. For mock purification control, BL21 (DE3) cells were transformed with pJ053 plasmid, a pMccE492 derivative lacking the genes *mceA* (encoding the MccE492 precursor) and *mceB* (encoding MccE492 immunity protein). The downstream purification procedure was the same than for MccE492 purification.

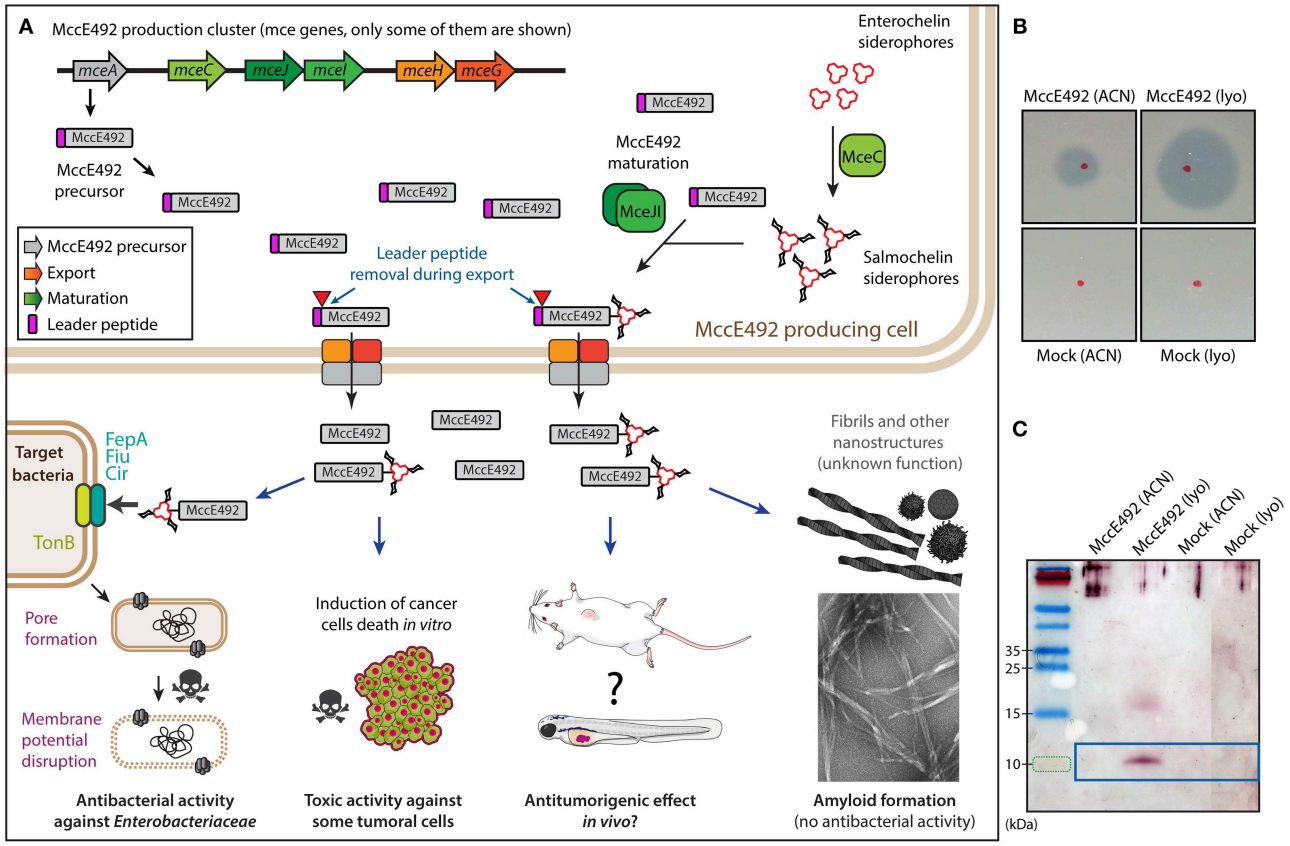

FIGURE 1 | (A) Main features of microcin E492 peptide and its production by bacterial cells, through the expression of the *mce* genes from the MccE492 gene cluster. The *mceA* gene encodes the microcin precursor that includes a leader peptide that is removed during the export by ABC exporters encoded by *mceHG*. During maturation, salmochelin (a glycosylated enterochelin derivative synthetized by MceC) is attached to MccE492 C-terminus by MceIJ. Mature MccE492 is recognized and internalized by catechol siderophore receptors of the target bacterial cell, and once in the periplasm it inserts into the cytoplasmic membrane in a TonB-dependent process forming pores that lead to a toxic effect through the disruption of the membrane potential of the cell. Additionally, under certain conditions, MccE492 aggregates into amyloid fibers and rod-shaped nanostructures, leading to the loss of its antibacterial activity. MccE492 also has toxic activity *in vitro* against some tumor cell lines, although its *in vivo* antitumoral effect has not been validated in animal models. For simplicity, several genes from the MccE492 gene cluster are not included, among them the immunity gene *mceB* that is encoded in an operon with the structural gene *mceA*. **(B)** Antibacterial activity assay of a representative MccE492 preparation (either the ACN fraction or after lyophilization) assessed through the detection of growth inhibition halos over sensitive bacterial lawns. The red dots correspond to the zone of the lawn where the drops of MccE492 or the mock preparation were placed. **(C)** SDS-PAGE and immunoblot of a representative MccE492 preparation (either the ACN fraction or after lyophilization), revealed with a monoclonal anti-MccE492 antibody. The last lane of the immunoblot image (showing mock purification) was spliced together with the first 3 lanes, to avoid showing blank (non-loaded) lanes.

MccE492 Activity Assay on Plates

Antibacterial activity determination in plates was performed mixing an aliquot of 0.3 mL of ~1 × 10^7 cells/mL of the *E. coli* indicator strain BL21 (DE3) with 3 mL of LB soft agar (0.7% w/v agar), and overlaying onto LB agar plates. Then, 3 μL drops of MccE492 preparations were spotted onto the top agar and incubated overnight at 37°C. Antibacterial activity was detected by the formation of growth inhibition halos.

SDS-PAGE and Immunoblotting

Sodium dodecyl sulfate-polyacrylamide gel electrophoresis (SDS-PAGE) was performed as described by Schägger and von Jagow (1987). Nitrocellulose membranes (Millipore) were used for immunoblot transfer (1 h, 350 mA, using chilled 25 mM Tris-HCl, 190 mM glycine, 20% methanol, as the transfer buffer). MccE492 was detected with a mouse monoclonal antibody raised against a synthetic MccE492 peptide (antiserum dilution, 1:1,000; Genscript) and with a goat anti-mouse alkaline phosphatase-conjugated secondary antibody (dilution 1:2,500). The alkaline phosphatase colorimetric reaction was performed as described by Marcoleta et al. (2013a). Briefly, the membrane was washed with FAL buffer (100 mM Tris-HCl [pH 9.5], 100 mM NaCl, 5 mM $MgCl_2$) and incubated in 10 ml of a mixture of BCIP (5-bromo-4-chloro-3′-indolylphosphate p-toluidine salt) and NBT (nitroblue tetrazolium chloride; 0.3 and 0.15 mg/mL in FAL buffer, respectively), until an optimal signal was observed.

Cancer Cell Lines and Culture Conditions

The human colorectal adenocarcinoma cell lines with epithelial morphology HT29 and SW620 were directly acquired from the

European Collection of Authenticated Cell Cultures (Catalog No. 91072201 and 87051203, respectively). Cells lines were maintained in 75 cm^2 flasks (T75) at 37°C and 5% CO_2 in Iscove's Modified Dulbecco's medium (IMDM) or RPMI 1640 medium supplemented with 10% fetal calf serum (FCS).

Viability Assays

SW620 and HT29 cells were seeded at 2.5×10^5 cells/well in 24-well plates before MccE492 or control treatments (phosphate-buffered saline (PBS) or mock). MccE492 was added to each well using a final concentration of 0, 30, or 60 μg/mL, and the mixture was incubated for 24 h. After incubation, cells of each well were trypsinized, suspended in PBS, and divided into two cytometry tubes. The viability was measured by staining the cells with 30 nM of Sytox Green dead cell stain (Invitrogen, Catalog No. S34860) and incubated for 20 min at room temperature protected from light. After incubation, 50 μL of Liquid Counting Beads (BD, Catalog No. 335925) were added to quantify the number of cells. Viability assays were analyzed by flow cytometry using a FACScan (Becton Dickinson) with BD FACSDiva™ Software.

Zebrafish Husbandry and Maintenance

Zebrafish (*Danio rerio*) embryos of the Tab5 strain were obtained by natural spawning according to Kimmel et al. (1995). Fertilized eggs were raised in Petri dishes at 28°C containing E3 medium (5 mM NaCl, 0.17 mM KCl, 0.33 mM $CaCl_2$, 0.3 mM $MgSO_4$, and 0.1 % methylene blue) on a 14 h:10 h light/dark cycle until transplantation. After introduction of human cells, embryos were grown at 34°C and in darkness, to avoid bleaching of stained human cells. All procedures were conducted following the recommendations described previously for the use of zebrafish in biomedical research (Cartner et al., 2020) and complied with the guidelines of the Animal Use Ethics Committee of the University of Chile and the Bioethics Advisory Committee of Fondecyt-Conicyt (funding agency).

Zebrafish Xenograft Development

Prior to transplantation into zebrafish larvae, human cancer cells SW620 were stained with Vybrant™ DiD Cell-Labeling Solution (ThermoFisher) according to the manufacturer's instructions, in order to visualize and track them inside larvae. Stained cells were suspended in PBS at a final concentration of 50 cells/nL and loaded into borosilicate glass capillary needles. ∼500 cells were injected into the perivitelline space (PVS) of 48 h post fertilization (hpf) embryos anesthetized with tricaine (0.02%, Sigma-Aldrich) and mounted in low-melting point agarose (1%). After injection, xenograft-harboring larvae were maintained at 34°C until the end of the experiment. To assure the homogeneity of the xenografts subjected to the different treatments, at 24 h post injection (hpi), successfully injected xenografts were selected choosing larvae displaying a tumor of similar size. After selection of the cohort, the tumors were photographed using an Olympus MVX10 stereomicroscope with a total magnification of 16,3X. Afterwards, larvae were individualized and maintained in 48-well plates until the end of the experiment.

Intratumoral Microcin E492 Administration in Zebrafish Xenografts

Twenty four hours after transplantation of tumor cells, xenograft-harboring zebrafish larvae were anesthetized and mounted into an agarose layer. Then, larvae were injected with ∼5 nl of 1 mg/ml mcce492 (equivalent to 5 ng), or the same volume of the mock purification or PBS. Then, larvae were dismounted, washed carefully to remove agarose remnants and tricaine, and then kept in E3 at 34°C. An average of 50 xenografts were injected per condition. this procedure was repeated 48 h after cell transplantation.

Evaluation of Tumor Size in Zebrafish Xenografts

At 5 dpf, individualized larvae were anesthetized with tricaine [0.02% (w/v)] and mounted in a layer of low melting point agarose (1%), allowing the tumors to be photographed using an Olympus MVX10 stereomicroscope with a total magnification of 16.3X, as described previously (Varas et al., 2019). The tumor area was quantified in 3-dpf and 5-dpf larvae using Image J software. The relative tumor size (5 dpf/3 dpf) was calculated and plotted using GraphPad software.

Statistical Analyses

Cell viability experiments conducted by flow cytometry were performed in biological duplicates. From the total event acquired, only singlets were counted, and the average percent population (P1, P2, and P3) was determined for each condition. Statistical significance of differences in cell populations size was assessed using a two-way ANOVA test with a Dunnet's post-test. Differences were considered significant with a $P < 0.05$.

For zebrafish xenograft experiments, the statistical significance of differences in tumor cell mass was determined using a two-way ANOVA test with a Dunnet's post-test. Differences were considered significant with a $P < 0.05$. The total number of individuals considered for each condition of this experiment was 50.

RESULTS AND DISCUSSION

MccE492 Shows Toxicity Against HT29 and SW620 Human Colorectal Cancer Cells *in vitro*

First, we aimed to select suitable cancer cell lines to conduct the study and set up the zebrafish xenograft model. After reviewing the literature, the cell lines HT29 and SW620 were selected considering the following relevant features: (1) they are of human origin; (2) they are from colorectal cancer and thus originate from the intestine, the place in which this bacteriocin is likely to be produced by enteric bacteria; and (3) they have been successfully used in xenograft transplantation experiments with zebrafish, as reported previously (Fior et al., 2017). Both cell lines were obtained directly from the European Collection of Authenticated Cell Cultures to perform the experiments described below. As a negative control we selected Human Embryonic Kidney 293

(HEK-293) cells, mainly because they have a non-tumoral origin (Graham et al., 1977; Brodaczewska et al., 2016) and because we found that these cells were unable to proliferate and form foci of growth after transplantation in zebrafish larvae (**Supplementary Figure 1A**).

We purified the MccE492 peptide from culture supernatants of *E. coli* cells transformed with the pMccE492 plasmid, which carries the gene cluster allowing the production and export of mature MccE492 (further details can be found in the Methods section). After the purification process, MccE492 was eluted in acetonitrile-water mixtures, which were then lyophilized to remove the solvent and to concentrate the peptide. Additionally, a control "mock" purification was prepared following the same steps than used for MccE492, but starting with cultures of *E. coli* cells transformed with a pMccE492 derivative lacking the *mceB* and *mceA* genes (encoding the MccE492 precursor and immunity protein, respectively), but carrying functional copies of the rest of the MccE492 cluster genes. By using this control, we aimed to eliminate any possible contribution of possible contaminant proteins present in the MccE492 preparation to the antitumorigenic effect to be studied. We evaluated the presence of MccE492 in the purified fractions (before and after lyophilization) monitoring the antibacterial activity against sensitive *E. coli* lawns, observed as the formation of growth inhibition halos (**Figure 1B**). MccE492 antibacterial activity was detected in 40% ACN fractions obtained from *E. coli* cells transformed with pMccE492, as well as in lyophilized preparations obtained from these fractions (suspended in PBS). Conversely, no antibacterial activity on MccE492 sensitive cells was observed with the purification obtained from the control strain. Also, we corroborated the presence of the MccE492 peptide by means of SDS-PAGE and immunoblotting using a monoclonal antibody prepared against this microcin. Although undetectable in the ACN fractions, a defined band corresponding to 10 kDa, and a more diffuse band between 15 and 20 kDa were observed in the lyophilized MccE492 preparation, but not in the mock control (**Figure 1C**). Although MccE492 has a molecular mass of ∼8 kDa, it typically migrates anomalously in SDS-PAGE gels as a size corresponding to 10 kDa and also shows species with higher molecular mass that would correspond to SDS-resistant oligomers (Marcoleta et al., 2013a; Aguilera et al., 2016).

Next, we evaluated the toxic activity of microcin E492 against the selected human colorectal cancer cell lines. To this end, 2.5×10^5 cells of each line were seeded per well in 24-well plates. After 24 h, they were treated with 0 (PBS control), 30, or 60 μg/mL of MccE492, or with the mock purification for a period of 24 h. After incubation, cell viability was measured by flow cytometry using the Sytox Green Dead Cell Stain (Invitrogen) and Liquid Counting Beads (BD) for an accurate determination of the number of cells. For HT29 cells (**Figure 2A**), in absence of treatment (PBS) or upon mock treatment, the viable cell population (defined as P1) was around 71%. Two additional populations were observed, corresponding to dead cells (P3), accounting for 22–22.5% of the total population, and cells with compromised viability (P2), probably including mainly apoptotic cells, corresponding to 6.3–6.8%. MccE492 caused a marked dose-dependent decrease in cancer cell viability, which dropped to 66.4 and 50% upon treatment with 30 or 60 μg/mL microcin suspensions, respectively. Moreover, this effect was accompanied by a significant increase mainly in the P2 population ($p < 0.001$, Two-way ANOVA with Dunnet's multiple comparison test), especially after treatment with the higher MccE492 dose, where compromised cells increased to 26.5% of the total population. This indicates that MccE492 has a strong cytotoxic effect on HT29 cells *in vitro*, likely inducing an apoptotic response. As expected, MccE492 did not present a cytotoxic effect on an *in vitro* culture of HEK-293 cells (**Supplementary Figure 1B**).

A less marked effect was observed with the SW620 line (**Figure 2B**). Viability of untreated cells and cells subjected to mock treatment was around 83% (P1), showing a less marked reduction to 76 and 69% upon treatment with 30 or 60 μg/mL MccE492, respectively. As observed for HT29, this decrease was concomitant with an increase mainly in P2 cells ($p < 0.05$), and to a lesser extent, with the increment of dead cells (P3). Although SW620 cells presented a higher resistance to the MccE492 effect when compared to HT29 cells, both of them showed significant sensitivity to the toxic effect of this bacteriocin, supporting the observations made previously using other cancer cell lines like HeLa, Jurkat, and RJ2.25 (Hetz et al., 2002). The apoptotic effect of MccE492 has only been characterized previously in HeLa cells, and this phenomenon was associated with the release of calcium from intracellular stores, probably triggered after MccE492 pore-formation either in the mitochondria or in the cell membrane (Hetz et al., 2002).

It has been reported that the SW480 cell line, which is related to SW620, is sensitive to nisin, another bacteriocin (Ahmadi et al., 2017). The exposure to 1–4 mg/mL of nisin had a cytotoxic effect over SW480 colon cancer cells. The SW480 line was derived from the same patient as SW620 (used in this study), but the former proceeds from the primary tumor while SW620 was isolated 6 months later from a lymph node metastasis (Hewitt et al., 2000). Additional evidence indicated that nisin induced apoptosis in head and neck squamous cell carcinoma, as evidenced by an increase of intracellular calcium concentration, cell cycle arrest, and increased CHAC1 activation, a cation transporter and pro-apoptotic component of the unfolded protein response (Joo et al., 2012). Of note, another study reported that roughly 100 μM (∼300 μg/mL) nisin had a strong cytotoxic effect over Caco-2 and HT29 colorectal cancer cell lines (Maher and McClean, 2006). This is a significantly lower dose, as compared to the IC50 reported for SW480 (Ahmadi et al., 2017). In agreement with these results, we also observed decreased susceptibility of SW620 cells to the bacteriocin-mediated cytotoxic effect, compared to HT29 cells. Additionally, the bacteriocin enterocin-B produced by *Enterococcus faecium* exhibited cytotoxic activity against HeLa, HT29, and other cancer cell lines, causing hallmark apoptotic morphological changes such as membrane blebbing, smaller nuclei, apoptotic body formation and nuclear fragmentation (Ankaiah et al., 2018).

Another antimicrobial peptide targeting the membrane showing anti-cancer activity is KL15, designed *in silico* based on the sequences of bacteriocins m2163 and m2386 from *Lactobacillus casei* ATCC 334 (Chen et al., 2015).

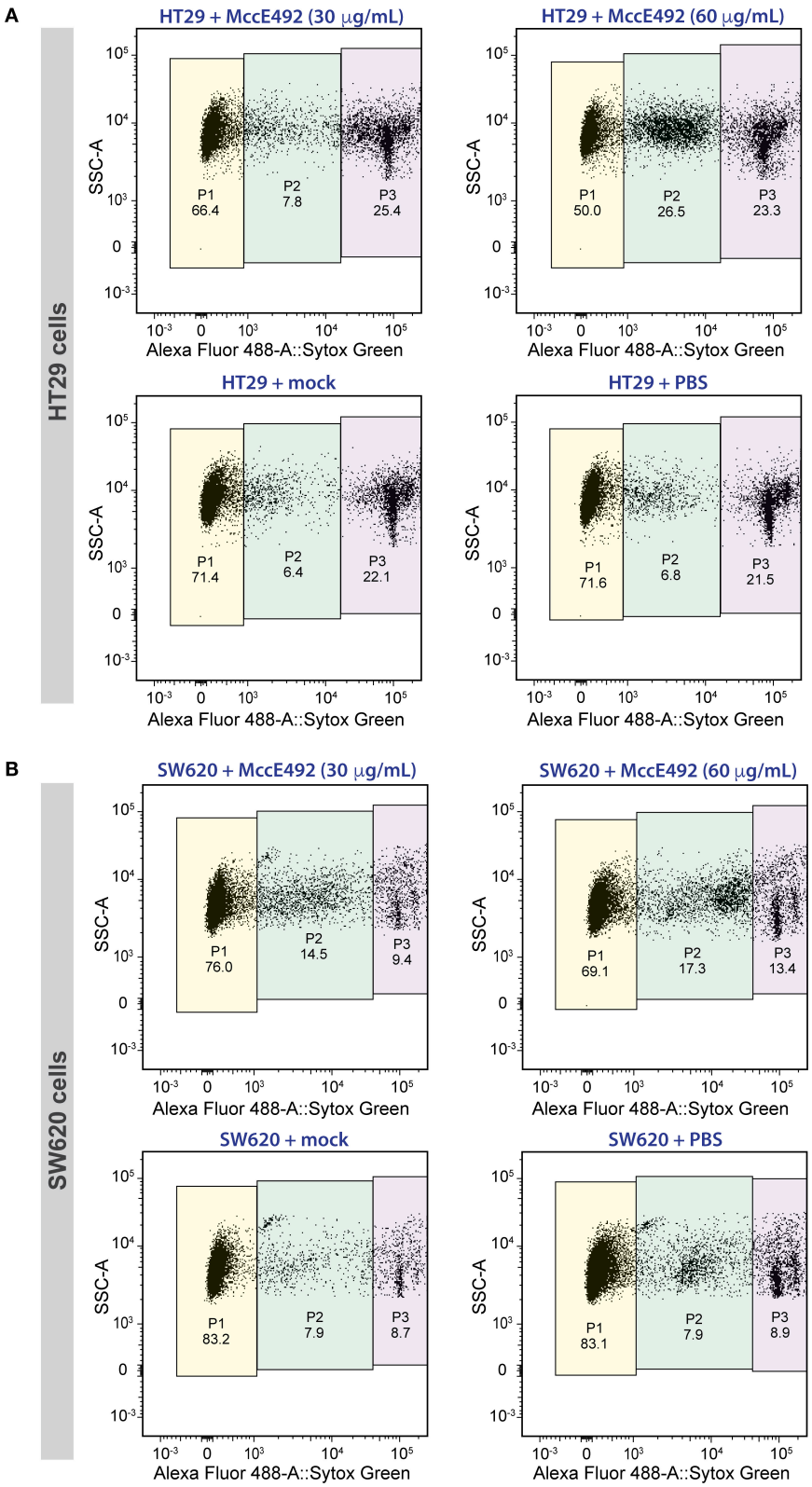

FIGURE 2 | Microcin E492 induces cytotoxicity over human colorectal cancer cell lines *in vitro*. HT29 **(A)** and SW620 **(B)** cells were incubated during 24 h with MccE492, a mock purification, or PBS, and the cell viability was determined through flow cytometry using the Sytox Green Dead Cell stain (Invitrogen) and liquid counting beads. Colored areas denote the three populations distinguished (P1-P3), and the numbers under each population label indicate the percentage from the total population. Each plot shows a total of 10,000 cells.

KL15 displayed an anti-proliferative effect on SW480 cells inducing morphological changes and increasing membrane permeability. Also in this case, a limited pro-apoptotic effect was observed in these cells, further evidencing the reduced sensitivity of the SW480 and SW620 cell lines to pro-apoptotic bacteriocins. In this regard, Chen et al. (2015) proposed that KL15-mediated cytotoxicity over SW480 cells could be exerted through the activation of a non-apoptotic cell death pathway or by regulated necrosis (Berghe et al., 2014) involving hyperactivation of poly(ADP-ribose) polymerase (PARP-1), mitochondrial permeability changes, and formation of necrosomes and inflammasomes. An additional example of bacteriocins with cytotoxic activity over human cancer cells *in vitro* is a pediocin produced by *Pediococcus acidilactici* K2a2-3, which caused a ∼55% growth inhibition of HT29 human colon adenocarcinoma cells (Villarante et al., 2011). Also, the 6.2-kDa Enterococcal anti-proliferative peptide (Entap) showed antiproliferative activity against cell lines of human gastric adenocarcinoma (AGS) and colorectal adenocarcinoma (HT29) (reviewed in Karpiński and Adamczak, 2018).

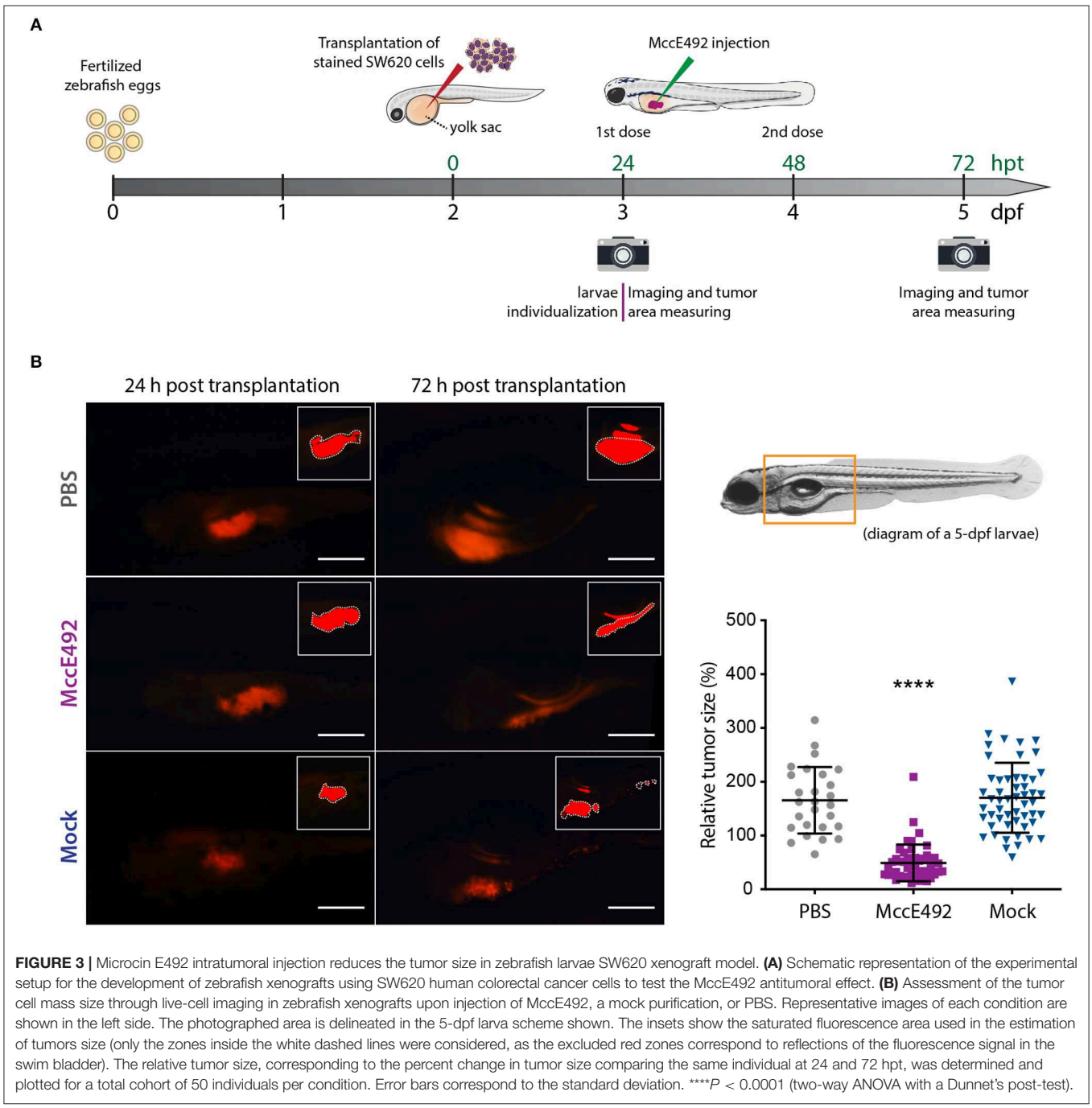

FIGURE 3 | Microcin E492 intratumoral injection reduces the tumor size in zebrafish larvae SW620 xenograft model. **(A)** Schematic representation of the experimental setup for the development of zebrafish xenografts using SW620 human colorectal cancer cells to test the MccE492 antitumoral effect. **(B)** Assessment of the tumor cell mass size through live-cell imaging in zebrafish xenografts upon injection of MccE492, a mock purification, or PBS. Representative images of each condition are shown in the left side. The photographed area is delineated in the 5-dpf larva scheme shown. The insets show the saturated fluorescence area used in the estimation of tumors size (only the zones inside the white dashed lines were considered, as the excluded red zones correspond to reflections of the fluorescence signal in the swim bladder). The relative tumor size, corresponding to the percent change in tumor size comparing the same individual at 24 and 72 hpt, was determined and plotted for a total cohort of 50 individuals per condition. Error bars correspond to the standard deviation. ****$P < 0.0001$ (two-way ANOVA with a Dunnet's post-test).

Intratumoral Injection of MccE492 Reduces Tumor Growth in Zebrafish Xenografts of SW620 Human Colorectal Cancer Cells

Upon corroborating the cytoxicity of MccE49 over the tested cancer colorectal cells *in vitro*, we attempted to use them to develop a xenograft model using zebrafish larvae. Initially, both the HT29 and SW620 cell lines were explored for this purpose. However, in our hands, the transplantation of HT29 cells was less successful, as we could not achieve the xenografts efficiently in a large number of individuals. Thus, we decided to focus our efforts in developing SW620 xenografts, establishing the experimental set up schematized in **Figure 3A**. Prior to the transplantation, SW620 cells were fluorescently labeled using the Vybrant™ DiD Cell-Labeling Solution (ThermoFisher), in order to track cancer cells and tumor development inside larvae by live-cell imaging. ∼500 cells were transplanted into individualized 2-dpf zebrafish larvae through injection into the perivitelline space, maintaining xenograft-bearing larvae at 34°C throughout the whole experiment. Twenty four hours post transplantation (hpt), the developing xenograft tumor was photographed to estimate its size using a fluorescence stereomicroscope, as described in the Methods section. Immediately after, either MccE492 (5 nL of 1 mg/mL solution in PBS) or an equivalent volume of the mock purification or PBS (used as MccE492 vehicle) were injected into the xenograft, and a second dose was applied at 48 hpt. Finally, at 72 hpt a second photograph of the xenograft was obtained and the relative tumor size was estimated (the tumor size measured at 72 hpt divided by the tumor size of the same individual at 24 hpt). This temporal frame was selected mainly because after 72 hpt, transplanted cells significantly dilute the fluorescent label due to proliferation, and zebrafish larvae progressively become less transparent, hampering an accurate evaluation of the tumor size.

As shown in **Figure 3B**, the analysis of a total cohort of 50 individuals from at least three biological replicates of the entire assay, indicated that MccE492 treatment -but not the mock treatment- significantly reduced the tumor size ($P < 0.0001$), compared to the group that received the PBS injection. Pictures of representative larvae from each condition are shown, in which the insets correspond to the saturated fluorescence area considered to accurately estimate the tumor size, as described previously (Zhao et al., 2011; Fior et al., 2017; Avci et al., 2018). The zone of the larvae shown in the pictures corresponds to that marked in the 5-dpf larva diagram. Our results indicate that MccE492 has a strong antitumoral activity on human colorectal SW620 cancer cells *in vivo*, supporting its potential use as an anti-cancer agent. Moreover, upon measuring the survival after 8 dpf of 50 xenografts per condition injected with either MccE492 or PBS, no significant changes were observed (98 and 92%, respectively), supporting that MccE492 has not a deleterious effect on larvae at longer times.

Previous works, by several research groups, point out the high potential of zebrafish larvae to carry out drug screening and for disease modeling (reviewed in Lu et al., 2017). As used here, larvae can be kept singly in multi-well plates allowing us to track the temporal evolution of transplanted human cancer cells in each individual through live-cell imaging. This set up allows simultaneous multiple non-invasive evaluations. Also, the reduced volume of the wells containing the larvae during the assays results advantageous when the drug availability is limited or in large-scale assays involving several conditions and numerous cohorts, where the total amount and number of compounds to be tested multiplies. In particular, the zebrafish xenograft approach has been especially exploited to study the behavior of human colon cancer cell lines and in colorectal tumor cells derived from patients (reviewed in Lobert et al., 2016). In a previous study, labeled human colorectal cancer cells of the lines SW620 and SW480 were injected into the yolk sac or perivitelline space of 2-dpf zebrafish embryos. The cancer cells then proliferated, migrated, and formed compact masses near the intestinal lumen surface (Haldi et al., 2006). Moreover, it was shown that the relative metastatic capacity of colorectal cancer cell lines *in vitro* and in *in vivo* mouse models is recapitulated in zebrafish. Likewise, SW620 cells reported as highly invasive on *in vitro* transwell migration assays were found to disseminate widely in zebrafish larvae a few days after transplantation (Teng et al., 2013). Conversely, HT29 cells that are not invasive *in vitro*, behave as non-metastatic inside larvae. Our results also indicate that the SW620 line is highly invasive, forming secondary tumors in a high number of individuals. The correlation between the known metastatic potential of cancer cells and their *in vivo* behavior upon transplantation into zebrafish allows (1) the evaluation of the metastatic potential of primary patient-derived tumors, and (2) the testing of compounds that will potentially reduce the invasiveness of these cells.

As a highly promising contribution in the field of personalized diagnostics and medicine, zebrafish xenograft models can be used for the evaluation of customized anti-cancer drug schemes. In this context, primary patient-derived biopsy specimens, often difficult to grow *in vitro*, can be used to isolate cancer cells and to establish xenografts in zebrafish, which after a few days are ready for testing the response of the cells to different anti-cancer agents. This is critical considering that currently patients go through multiple rounds of trial-and-error approaches to find the best treatment, with the consequence of adverse effects without therapeutic improvement, as well as the loss of valuable time before starting an effective treatment. In this sense, a recent study reported that colorectal cancer xenografts developed in zebrafish, starting from resected tumor samples from patients, constitute an advantageous *in vivo* model for testing differential therapy responses (Fior et al., 2017). The authors directly compared xenografts developed in zebrafish and in mouse, observing a good correlation between the relative sensitivities to anti-cancer agents in the two models. Also, several cell lines were tested in parallel including the closely related SW480 and SW620. Remarkably, they observed distinct proliferation dynamics, metastatic potential, and response to therapy between the isogenic tumors formed by these lines, revealing differential responses between primary and metastatic tumors to the tested drugs.

In summary, our data support MccE492 as a new antitumorigenic compound produced by bacteria. This polypeptide presents multiple advantages: it is small and

very stable, resistant to proteases and to harsh conditions including boiling (de Lorenzo, 1984; Lagos et al., 1993), being stability one of the main requirements for a compound with potential pharmacological use. The fact that it is produced by bacteria also provides the possibility for direct delivery through a therapeutic infection with a probiotic. Finally, using the zebrafish model with many different types of xenografted cancers broadens the possibilities of finding successful targets for MccE492 antitumoral activity.

DATA AVAILABILITY STATEMENT

All datasets generated for this study are included in the article/**Supplementary Material**.

ETHICS STATEMENT

The animal study was reviewed and approved by Comité de Etica, Facultad de Ciencias, Universidad de Chile.

AUTHOR CONTRIBUTIONS

MV, AM, MA, and RL conceived this study. MV and VS designed and performed the flow cytometry experiments and analyzed the data. MV, CM-M, VK, and AM performed the experiments with zebrafish larvae. AM, MV, and RL wrote the manuscript. All authors contributed with valuable discussions and edition, approving the final version of manuscript.

FUNDING

This work was funded by FONDECYT 3170449 grant to MV and FONDECYT 1140430 to RL. MA was funded by FONDAP 15090007.

ACKNOWLEDGMENTS

We are very grateful to Dr. María Rosa Bono and Leonardo Vargas from Facultad de Ciencias, Universidad de Chile, for their help and advice during FACS assays (FONDEQUIP EQM140016) and for the maintenance of the malignant cell lines. We also thank Marcelo Veloso for his support in MccE492 purifications.

SUPPLEMENTARY MATERIAL

The Supplementary Material for this article can be found online at: https://www.frontiersin.org/articles/10.3389/fmicb.2020.00405/full#supplementary-material

REFERENCES

Aguilera, P., Marcoleta, A., Lobos-Ruiz, P., Arranz, R., Valpuesta, J. M., Monasterio, O., et al. (2016). Identification of key amino acid residues modulating intracellular and *in vitro* microcin E492 amyloid formation. *Front. Microbiol.* 7:35. doi: 10.3389/fmicb.2016.00035

Ahmadi, S., Ghollasi, M., and Hosseini, H. M. (2017). The apoptotic impact of nisin as a potent bacteriocin on the colon cancer cells. *Microb. Pathog.* 111, 193–197. doi: 10.1016/j.micpath.2017.08.037

Ankaiah, D., Palanichamy, E., Antonyraj, C. B., Ayyanna, R., Perumal, V., Ahamed, S. I. B., et al. (2018). Cloning, overexpression, purification of bacteriocin enterocin-B and structural analysis, interaction determination of enterocin-A, B against pathogenic bacteria and human cancer cells. *Int. J. Biol. Macromol.* 116, 502–512. doi: 10.1016/j.ijbiomac.2018.05.002

Arranz, R., Mercado, G., Martín-Benito, J., Giraldo, R., Monasterio, O., Lagos, R., et al. (2012). Structural characterization of microcin E492 amyloid formation: identification of the precursors. *J. Struct. Biol.* 178, 54–60. doi: 10.1016/j.jsb.2012.02.015

Ashu, E. E., Xu, J., and Yuan, Z.-C. (2019). Bacteria in cancer therapeutics: a framework for effective therapeutic bacterial screening and identification. *J. Cancer* 10, 1781–1793. doi: 10.7150/jca.31699

Avci, M. E., Keskus, A. G., Targen, S., Isilak, M. E., Ozturk, M., Atalay, R. C., et al. (2018). Development of a novel zebrafish xenograft model in ache mutants using liver cancer cell lines. *Sci. Rep.* 8:1570. doi: 10.1038/s41598-018-19817-w

Baindara, P., Gautam, A., Raghava, G. P., and Korpole, S. (2017). Anticancer properties of a defensin like class IId bacteriocin laterosporulin 10. *Sci. Rep.* 7:46541. doi: 10.1038/srep46541

Baindara, P., Korpole, S., and Grover, V. (2018). Bacteriocins: perspective for the development of novel anticancer drugs. *Appl. Microbiol. Biotechnol.* 102, 10393–10408. doi: 10.1007/s00253-018-9420-8

Berghe, T. V., Linkermann, A., Jouan-Lanhouet, S., Walczak, H., and Vandenabeele, P. (2014). Regulated necrosis: the expanding network of non-apoptotic cell death pathways. *Nat. Rev. Mol. Cell Biol.* 15, 135–147. doi: 10.1038/nrm3737

Bieler, S., Estrada, L., Lagos, R., Baeza, M., Castilla, J., and Soto, C. (2005). Amyloid formation modulates the biological activity of a bacterial protein. *J. Biol. Chem.* 280, 26880–26885. doi: 10.1074/jbc.M502031200

Brodaczewska, K. K., Szczylik, C., Fiedorowicz, M., Porta, C., and Czarnecka, A. M. (2016). Choosing the right cell line for renal cell cancer research. *Mol. Cancer* 15:83. doi: 10.1186/s12943-016-0565-8

Cartner, S., Durboraw, E., and Watts, A. (2020). "Regulations, policies and guidelines pertaining to the use of zebrafish in biomedical research," in *The Zebrafish in Biomedical Research*, eds S. C. Cartner, J. S. Eisen, S. C. Farmer, K. J. Guillemin, M. L. Kent, and G. E. Sanders (London: Academic Press), 451–459.

Chen, Y. C., Tsai, T. L., Ye, X. H., and Lin, T. H. (2015). Anti-proliferative effect on a colon adenocarcinoma cell line exerted by a membrane disrupting antimicrobial peptide KL15. *Cancer Biol. Ther.* 16, 1172–1183. doi: 10.1080/15384047.2015.1056407

Cornut, G., Fortin, C., and Soulières, D. (2008). Antineoplastic properties of bacteriocins: revisiting potential active agents. *Am. J. Clin. Oncol.* 31, 399–404. doi: 10.1097/COC.0b013e31815e456d

De Giani, A., Bovio, F., Forcella, M., Fusi, P., Sello, G., and Di Gennaro, P. (2019). Identification of a bacteriocin-like compound from *Lactobacillus plantarum* with antimicrobial activity and effects on normal and cancerogenic human intestinal cells. *AMB Expr.* 9:88. doi: 10.1186/s13568-019-0813-6

de Lorenzo, V. (1984). Isolation and characterization of microcin E492 from *Klebsiella pneumoniae*. *Arch. Microbiol.* 139, 72–75. doi: 10.1007/BF00692715

de Lorenzo, V., and Pugsley, A. P. (1985). Microcin E492, a low molecular weight peptide antibiotic which causes depolarization of *Escherichia coli* cytoplasmic membrane. *Antimicrob. Agents Chemother.* 27, 666–669. doi: 10.1128/AAC.27.4.666

Fior, R., Póvoa, V., Mendes, R. V., Carvalho, T., Gomes, A., Figueiredo, N., et al. (2017). Single-cell functional and chemosensitive profiling of combinatorial colorectal therapy in zebrafish xenografts. *Proc. Natl. Acad. Sci. U.S.A.* 114, E8234–E8243. doi: 10.1073/pnas.1618389114

Graham, F. L., Smiley, J., Russell, W. C., and Nairn, R. (1977). Characteristics of a human cell line transformed by DNA from human adenovirus Type 5. *J. Gen. Virol.* 36, 59–74. doi: 10.1099/0022-1317-36-1-59

Haldi, M., Ton, C., Seng, W. L., and McGrath, P. (2006). Human melanoma cells transplanted into zebrafish proliferate, migrate, produce melanin, form masses and stimulate angiogenesis in zebrafish. *Angiogenesis* 9, 139–151. doi: 10.1007/s10456-006-9040-2

Hason, M., and Bartůněk, P. (2019). Zebrafish models of cancer—new insights on modeling human cancer in a non-mammalian vertebrate. *Genes* 10:935. doi: 10.3390/genes10110935

Hetz, C., Bono, M. R., Barros, F., and Lagos, R. (2002). Microcin E492, a channel forming bacteriocin from *Klebsiella pneumoniae*, induces apoptosis in some human cell lines. *Proc. Natl. Acad. Sci. U.S.A.* 99, 2696–2701. doi: 10.1073/pnas.052709699

Hewitt, R. E., McMarlin, A., Kleiner, D., Wersto, R., Martin, P., Tsokos, M., et al. (2000). Validation of a model of colon cancer progression. *J. Pathol.* 192, 446–454. doi: 10.1002/1096-9896(2000)9999:9999<::AID-PATH775>3.0.CO;2-K

Hill, D., Chen, L., Snaar-Jagalska, E., and Chaudhry, B. (2018). Embryonic zebrafish xenograft assay of human cancer metastasis. *F100Res.*7:1682. doi: 10.12688/f1000research.16659.1

Joo, N. E., Ritchie, K., Kamarajan, P., Miao, D., and Kapila, Y. L. (2012). Nisin, an apoptogenic bacteriocin and food preservative, attenuates HNSCC tumorigenesis via CHAC1. *Cancer Med.* 1, 295–305. doi: 10.1002/cam4.35

Kamarajan, P., Hayami, T., Matte, B., Liu, Y., Danciu, T., Ramamoorthy, A., et al. (2015). Nisin ZP, a bacteriocin and food preservative, inhibits head and neck cancer tumorigenesis and prolongs survival. *PLoS ONE* 10:7.e0131008. doi: 10.1371/journal.pone.0131008

Karpiński, T., and Adamczak, A. (2018). Anticancer activity of bacterial proteins and peptides. *Pharmaceutics* 10:E54. doi: 10.3390/pharmaceutics10020054

Kaur, S., and Kaur, S. (2015). Bacteriocins as potential anticancer agents. *Front. Pharmacol.* 6:272. doi: 10.3389/fphar.2015.00272

Kimmel, C. B., Ballard, W. W., Kimmel, S. R., Ullmann, B., and Schilling, T. F. (1995). Stages of embryonic development of the zebrafish. *Dev. Dynam.* 203, 253–310. doi: 10.1002/aja.1002030302

Lagos, R. (2007). "Cytotoxic activity of bacteriocins against eukaryotic cells," *in Research and Applications in Bacteriocins,* eds M. A. Riley and O. Gillor (Norfolk: Horizon Bioscience), 81–93.

Lagos, R., Baeza, M., Corsini, G., Hetz, C., Strahsburger, E., Castillo, J. A., et al. (2001). Structure, organization and characterization of the gene cluster involved in the production of microcin E492, a channel-forming bacteriocin. *Mol. Microbiol.* 42, 229–243. doi: 10.1046/j.1365-2958.2001.02630.x

Lagos, R., Tello, M., Mercado, G., García, V., and Monasterio, O. (2009). Antibacterial and antitumorigenic properties of microcin E492, a pore-forming bacteriocin. *Curr. Pharm. Biotechnol.* 10, 74–85. doi: 10.2174/138920109787048643

Lagos, R., Wilkens, M., Vergara, C., Cecchi, X., and Monasterio, O. (1993). Microcin E492 forms ion channels in phospholipid bilayer membranes. *FEBS Lett.* 321, 145–148. doi: 10.1016/0014-5793(93)80096-D

Lam, M. M., Wyres, K. L., Duchêne, S., Wick, R. R., Judd, L. M., Gan, Y. H., et al. (2018). Population genomics of hypervirulent *Klebsiella pneumoniae* clonal-group 23 reveals early emergence and rapid global dissemination. *Nat. Commun.* 9:2703. doi: 10.1038/s41467-018-05114-7

Letrado, P., de Miguel, I., Lamberto, I., Díez-Martínez, R., and Oyarzabal, J. (2018). Zebrafish: speeding up the cancer drug discovery process. *Cancer Res.* 78, 6048–6058. doi: 10.1158/0008-5472.CAN-18-1029

Lobert, V. H., Mouradov, D., and Heath, J. K. (2016). "Focusing the spotlight on the zebrafish intestine to illuminate mechanisms of colorectal cancer," in *Cancer and Zebrafish* (Cham: Springer), 411–437.

Lu, J. W., Ho, Y. J., Ciou, S. C., and Gong, Z. (2017). Innovative disease model: zebrafish as an *in vivo* platform for intestinal disorder and tumors. *Biomedicines* 5:E58. doi: 10.3390/biomedicines5040058

Maher, S., and McClean, S. Investigation of the cytotoxicity of eukaryotic and prokaryotic antimicrobial peptides in intestinal epithelial cells *in vitro*. (2006). *Biochem. Pharmacol.* 71,1289–1298. doi: 10.1016/j.bcp.2006.01.012

Marcoleta, A., Gutiérrez-Cortez, S., Maturana, D., Monasterio, O., and Lagos, R. (2013b). Whole-genome sequence of the microcin E492-producing strain *Klebsiella pneumoniae* RYC492. *Genome Announc.* 1, e00178–e00113. doi: 10.1128/genomeA.00178-13

Marcoleta, A., Marín, M., Mercado, G., Valpuesta, J. M., Monasterio, O., and Lagos, R. (2013a). Microcin E492 amyloid formation is retarded by posttranslational modification. *J. Bacteriol.* 195, 3995–4004. doi: 10.1128/JB.00564-13

Marcoleta, A. E., Berríos-Pastén, C., Nuñez, G., Monasterio, O., and Lagos, R. (2016). *Klebsiella pneumoniae* asparagine tDNAs are integration hotspots for different genomic islands encoding microcin E492 production determinants and other putative virulence factors present in hypervirulent strains. *Front. Microbiol.* 7:849. doi: 10.3389/fmicb.2016.00849

Marcoleta, A. E., Varas, M. A., Ortiz-Severín, J., Vásquez, L., Berríos-Pastén, C., Sabag, A., et al. (2018). Evaluating different virulence traits of *Klebsiella pneumoniae* using the social amoeba *Dictyostelium discoideum* and zebrafish larvae as host models. *Front. Cell. Infect. Microbiol.* 8:30. doi: 10.3389/fcimb.2018.00030

Schägger, H., and von Jagow, G. (1987). Tricine-sodium dodecyl sulfate-polyacrylamide gel electrophoresis for the separation of proteins in the range from 1 to 100 kDa. *Anal. Biochem.* 166, 368–379. doi: 10.1016/0003-2697(87)90587-2

Strahsburger, E., Baeza, M., Monasterio, O., and Lagos, R. (2005). Cooperative uptake of microcin E492 by receptors FepA, fiu and cir, and inhibition by the siderophore enterochelin and its dimeric and trimeric hydrolysis products. *Antimicrob. Agents Chemother.* 49, 3083–3086 doi: 10.1128/AAC.49.7.3083-3086.2005

Teng, Y., Xie, X., Walker, S., White, D. T., Mumm, J. S., and Cowell, J. K. (2013). Evaluating human cancer cell metastasis in zebrafish. *BMC Cancer* 13:453. doi: 10.1186/1471-2407-13-453

Thomas, X., Destoumieux-Garzón, D., Peduzzi, J., Alfonso, C., Blond, A., Birlirakis, N., et al. (2004). Siderophore peptide, a new type of post-translationally modified antibacterial peptide with potent activity. *J. Biol. Chem.* 279, 28233–28242. doi: 10.1074/jbc.M400228200

Varas, M. A., Ortíz-Severín, J., Marcoleta, A. E., Santiviago, C. A., Allende, M. L., and Chávez, F. P. (2019). "Static immersion and injection methods for live cell imaging of foodborne pathogen infections in zebrafish larvae," in *Foodborne Bacterial Pathogens*, ed A. Bridier (New York, NY: Humana Press), 183–190. Available online at: https://link.springer.com/book/10.1007/978-1-4939-9000-9#editorsandaffiliations

Veinotte, C. J., Dellaire, G., and Berman, J. N. (2014). Hooking the big one: the potential of zebrafish xenotransplantation to reform cancer drug screening in the genomic era. *Dis. Model. Mech.* 7, 745–754. doi: 10.1242/dmm.015784

Villarante, K. I., Elegado, F. B., Iwatani, S., Zendo, T., Sonomoto, K., and de Guzman, E. E. (2011). Purification, characterization and *in vitro* cytotoxicity of the bacteriocin from *Pediococcus acidilactici* K2a2-3 against human colon adenocarcinoma (HT29) and human cervical carcinoma (HeLa) cells. *World J. Microbiol. Biotechnol.* 27, 975–980. doi: 10.1007/s11274-010-0541-1

Wertman, J., Veinotte, C. J., Dellaire, G., and Berman, J. N. (2016). "The zebrafish xenograft platform: evolution of a novel cancer model and preclinical screening tool," in *Cancer and Zebrafish*, ed D. Langenau (Cham: Springer), 289–314. Available online at: https://link.springer.com/book/10.1007/978-3-319-30654-4#editorsandaffiliations

White, R., Rose, K., and Zon, L. (2013). Zebrafish cancer: the state of the art and the path forward. *Nat. Rev. Cancer* 13, 624–636. doi: 10.1038/nrc3589

Wilkens, M., Villanueva, J. E., Cofré, J., Chnaiderman, J., and Lagos, R. (1997). Cloning and expression in *Escherichia coli* of genetic determinants for production of and immunity to microcin E492 from *Klebsiella pneumoniae*. *J. Bacteriol.* 179, 4789–4794. doi: 10.1128/JB.179.15.4789-4794.1997

Wyatt, R. A., Trieu, N. P. V., and Crawford, B. D. (2017). Zebrafish Xenograft: an evolutionary experiment in tumour biology. *Genes* 8:220. doi: 10.3390/genes8090220

Zhao, C., Wang, X., Zhao, Y., Li, Z., Lin, S., Wei, Y., et al. (2011). A novel xenograft model in zebrafish for high-resolution investigating dynamics of neovascularization in tumors. *PLoS ONE.* 6:e21768. doi: 10.1371/journal.pone.0021768

Conflict of Interest: The authors declare that the research was conducted in the absence of any commercial or financial relationships that could be construed as a potential conflict of interest.

frontiers in Microbiology

REVIEW
published: 09 October 2019
doi: 10.3389/fmicb.2019.02261

Microcins in *Enterobacteriaceae*: Peptide Antimicrobials in the Eco-Active Intestinal Chemosphere

Fernando Baquero[1], Val F. Lanza[2], Maria-Rosario Baquero[3], Rosa del Campo[1] and Daniel A. Bravo-Vázquez[3]*

[1] Department of Microbiology, Ramón y Cajal University Hospital, Ramón y Cajal Institute for Health Research (IRYCIS), Madrid, Spain, [2] Bioinformatics Unit, Ramón y Cajal University Hospital, Ramón y Cajal Institute for Health Research (IRYCIS), Madrid, Spain, [3] Department of Microbiology, Alfonso X El Sabio University, Villanueva de la Cañada, Spain

OPEN ACCESS

Edited by:
Tomasz M. Karpiński, Poznań University of Medical Sciences, Poland

Reviewed by:
Konstantin Severinov, Rutgers, The State University of New Jersey, United States
David Šmajs, Masaryk University, Czechia
Sylvie Françoise Rebuffat, Muséum National d'Histoire Naturelle, France

***Correspondence:**
Fernando Baquero
baquero@bitmailer.net

Specialty section:
This article was submitted to Antimicrobials, Resistance and Chemotherapy, a section of the journal Frontiers in Microbiology

Received: *22 May 2019*
Accepted: *17 September 2019*
Published: *09 October 2019*

Citation:
Baquero F, Lanza VF, Baquero M-R, del Campo R and Bravo-Vázquez DA (2019) Microcins in Enterobacteriaceae: Peptide Antimicrobials in the Eco-Active Intestinal Chemosphere. Front. Microbiol. 10:2261. doi: 10.3389/fmicb.2019.02261

Microcins are low-molecular-weight, ribosomally produced, highly stable, bacterial-inhibitory molecules involved in competitive, and amensalistic interactions between *Enterobacteriaceae* in the intestine. These interactions take place in a highly complex chemical landscape, the intestinal eco-active chemosphere, composed of chemical substances that positively or negatively influence bacterial growth, including those originated from nutrient uptake, and those produced by the action of the human or animal host and the intestinal microbiome. The contribution of bacteria results from their effect on the host generated molecules, on food and digested food, and organic substances from microbial origin, including from bacterial degradation. Here, we comprehensively review the main chemical substances present in the human intestinal chemosphere, particularly of those having inhibitory effects on microorganisms. With this background, and focusing on *Enterobacteriaceae*, the most relevant human pathogens from the intestinal microbiota, the microcin's history and classification, mechanisms of action, and mechanisms involved in microcin's immunity (in microcin producers) and resistance (non-producers) are reviewed. Products from the chemosphere likely modulate the ecological effects of microcin activity. Several cross-resistance mechanisms are shared by microcins, colicins, bacteriophages, and some conventional antibiotics, which are expected to produce cross-effects. Double-microcin-producing strains (such as microcins MccM and MccH47) have been successfully used for decades in the control of pathogenic gut organisms. Microcins are associated with successful gut colonization, facilitating translocation and invasion, leading to bacteremia, and urinary tract infections. In fact, *Escherichia coli* strains from the more invasive phylogroups (e.g., B2) are frequently microcinogenic. A publicly accessible APD3 database http://aps.unmc.edu/AP/ shows particular genes encoding microcins in 34.1% of *E. coli* strains (mostly MccV, MccM, MccH47, and MccI47), and much less in *Shigella* and *Salmonella* (<2%). Some 4.65% of *Klebsiella pneumoniae* are microcinogenic (mostly with MccE492), and even less in *Enterobacter* or *Citrobacter*

(mostly MccS). The high frequency and variety of microcins in some *Enterobacteriaceae* indicate key ecological functions, a notion supported by their dominance in the intestinal microbiota of biosynthetic gene clusters involved in the synthesis of post-translationally modified peptide microcins.

Keywords: microcins, chemosphere, colicins, bacteriocins, molecular ecology, *Enterobacteriaceae*, competition

INTRODUCTION

The intestinal tract of mammals is a highly complex environment. It is an open environment partly influenced by factors external to the host, including food, swallowed environmental microorganisms (including those from the intestines of the same or other mammals), and abiotic environmental features. Consequently, the external microbial environment is "represented" in the intestine and can be considered an "invironment," a shared space where the interior and the exterior of the organism merge (Baquero, 2012). The biotic part of the intestinal environment is essentially endowed by the functions of the host in the upper intestine, but the environment of the distal ileum and colonic space is dominated by highly diverse gut microbiota composed of trillions of microbes (Lozupone et al., 2012) with associations between themselves and the host in complex interactive networks. These networks have been refined during a long coevolutionary trajectory (Ley et al., 2008a,b), starting probably in vertebrates (525 million years ago), and refined later in mammals (200 million years ago); thus, our current intestinal microbiota can almost be considered another human organ (Baquero and Nombela, 2012). The intestinal chemosphere, the ensemble of chemical molecules in the lumen and on the surfaces of the gut, is particularly relevant to understanding the regulatory ecology of the microbiome. In this review, an important group of peptide-derived effectors of bacterial origin, the microcins, are examined in detail. However, it is critical to understand that the ecological effects of these molecules are necessarily modulated by a complex constellation of other chemicals, the chemosphere, influencing the composition, physiology, and the resilience of the microbiota.

Until recently, a conservative, reductive view of understanding the biological phenomena has favored the concept that a single (or few) molecular or biological entity is sufficient to explain the variation in frequency of particular bacterial populations in the individual host. Given this single-entity approach has been shown to be untrue, it should be presented with a more integrative perspective (Baquero, 2015).

In this review, we summarize basic knowledge to help the reader understand the role of a group of ribosomally synthesized, low-molecular-weight peptidic molecules with antimicrobial effects, the microcins, which influence bacterial interactions. Our aim is to suggest that the ecological activity of microcins should be understood within a much larger frame of ecological influences exerted by many other chemical compounds in the intestine, the intestinal eco-active chemosphere. We use the term "eco-active" to clarify that we restricted our interest to chemicals that play a role as factors of the local microbial ecology; i.e., bacterial growth-promoting molecules, growth-inhibiting (or killer) substances, and chemicals influencing bacterial genetic variation, genetic regulation, bacterial interactions, and colonization efficiency.

THE INTESTINAL CHEMOSPHERE: MOLECULAR ECOLOGY

The term "molecular ecology" had been proposed by one of the discoverers of microcins, the biochemist Carlos Asensio, as early as 1975 (Asensio, 1976). He posited it was "necessary to change the focus of the biochemist's outlook on nature; a change of mood and style," focusing more on a new attitude in search of ecological perspectives at a molecular level. This visionary approach was based on his early experiences, shared with one of the authors of this review (FB), concerning the first description of microcins, and low-molecular-weight antimicrobial agents produced by gut enterobacteria.

The Intestinal Chemosphere and the Molecular Ecology of the Gut

The concept of a chemosphere at the core of the earliest studies on intestinal microorganisms, such as the work of Powers and Levine (1937), is also implicit in much later studies (Russell et al., 2013; Lee and Hase, 2014; Donia and Fischbach, 2015; Milshteyn et al., 2018). The microbiota works in a molecular chemosphere to which the microbiota itself contributes. In this review, we focus only on the fraction of the chemosphere comprised of natural chemical compounds present in the intestinal lumen (particularly in the large intestine), and not those that are part of or are tightly bound to the bacterial or host surfaces. The chemosphere is frequently subject to natural fluctuations, which are both the cause and the consequence of changes in the microbial community. Until very recently, the chemical environment of the gut has remained poorly defined, and therefore the "Molecular Ecology" of the environment where the microbiota was functioning had been poorly accessible. In recent years, the development of metabolomic approaches (mostly using proton nuclear magnetic resonance and mass spectrometry) has contributed to this field, attempting to define a human "fecal metabolome," comprised of small molecules from digested food, mainly metabolites (and residues from metabolites) of human origin, and more importantly from the effects of microbiota acting on human, food, or microbial organic substances, or resulting from bacterial degradation (Matsumoto et al., 2012; Xu et al., 2015; Milshteyn et al., 2018). Multiomics approaches in combination with metabolic modeling will soon contribute to a more complete view of chemical flows in the intestinal microbiota (Sieow et al., 2019).

The number of detectable metabolites in the gut is vast. All these chemical substances might, by themselves or in combination, serve as molecular mediators of microbe-microbe, and microbe-host interactions (Lustri et al., 2017). An advancing field of research, following earlier studies on microbiota and intestinal nutrients (Hooper et al., 2002) is focusing on the "metabobiome," that is, the network structure linking the composition of the intestinal microbiota and the intestinal metabolome (Xu et al., 2015). The gut microbiota has a considerable effect on the profile of mammalian blood metabolites (Wikoff et al., 2009). Given there is a core microbiota established in many (or most) human individuals (Turnbaugh et al., 2009), there should also be an accessory microbiota only present in distinct groups of individuals (Saric et al., 2007). Correspondingly, there should be a core and an accessory microbiota-derived metabolome (Xu et al., 2015). Part of the "species barriers" in transmission of bacteria among heterogeneous hosts (such as humans and food animals) could be due to discordances in the metabolic chemosphere of the intestine required for bacterial colonization in each type of host (Baquero, 2018; Nagpal et al., 2018). Bioinformatic approaches that are focused on the detection of secondary metabolites from the microbiota could be critical to casting light on this issue (Weber and Kim, 2016; Ozdemir et al., 2018). The variety of microbial metabolites in the gut is currently being explored by bioinformatic methods, such as ClusterFinder, to detect the biosynthetic gene clusters encoded in the genomes of the human microbiome (Donia and Fischbach, 2015). Gene clusters involved in the production of known oligosaccharide and ribosomally synthesized, post-translationally modified peptides (including microcins) were frequently identified, and this number could be further increased, given many biosynthetic clusters remain uncharacterized.

In any case, the abundance and complexity of the known microbiota-generated metabolites are overwhelming. Only the sub-metabolome of amine- and phenol-containing metabolites in fecal samples might comprise over 5000 different molecules (Xu et al., 2015). Compounds derived from dietary polyphenols, including chlorogenic acids, tannins, and flavonoids play an important role in the ecology of the intestinal microbiota (Popa et al., 2015). Carbohydrates, lipids, and proteins acquired from food or excreted by the host into the gut and eventually degraded or modified by the microbiota are also part of the chemosphere.

Mucins are particularly important as substrates for bacterial activity (Tailford et al., 2015; Corfield, 2018). In the neonatal period, human milk contains hundreds of glycans, including mucins, glycosaminoglycans, glycoproteins, and particularly human milk oligosaccharides, influencing the composition of the microbiota, mainly by modulating bacterial binding to intestinal surfaces, as in the case of *Escherichia coli* (Newburg and Morelli, 2014). Lipids in the milk, mostly free fatty acids, also have a role in microbiota construction. In infants, and also in adults, a number of bacterial gut populations have the ability to forage on glycans provided by the mucus layer covering the surface of the gastrointestinal tract, and are eventually released in the lumen by cell detachment. As a consequence, α- and β- linked N-acetyl-galactosamine, galactose, and N-acetyl-glucosamine can be incorporated into the chemosphere. Mucin glycans probably play a key role in selecting microbial communities along and across the gastrointestinal tract (Kashyap et al., 2013a,b; Tailford et al., 2015).

Dietary fiber- or host-derived (such as epithelial mucus) glycans produce many metabolites and can degrade into short-chain fatty acids such as acetate, butyrate, and propionate. This degradation requires a consortium of microorganisms linked by a trophic chain (Turroni et al., 2008). Other short-chain fatty acids, such as isobutyric, valeric, 2-/3-methylbutyric, caproic, and isocaproic are derived from amino acid metabolism. Phosphatidylethanolamine, derived from membrane lipids from animal hosts and bacteria, is degraded to glycerol and ethanolamine. Ethanolamine is a significant nutrient for gut microorganisms (Garsin, 2010; Kaval et al., 2018), as are probably phosphoinositides, sphingolipids, cholesterol, and eicosanoids (Bäckhed and Crawford, 2010). Bacterial action on dietary phospholipids (phosphoglycerides) such as choline, carnitine, or lecithin (phosphatidyl choline) gives rise to trimethylamine-N-oxide, acting as an osmolyte, assuring bacterial cell wall replication under stress and counteracting the effect of urea (Mukherjee et al., 2005; Lee and Hase, 2014).

Amino acids are actively produced by intestinal bacteria as electron acceptors in a highly anaerobic environment, frequently used together with reductive amino acid metabolites, such as phenylpropionic acid, and phenylacetic acid (Donia and Fischbach, 2015). Indole, a tryptophan metabolite, serves as a signaling molecule in bacterial interactions. It is from aliphatic amino acids, such as arginine, proline, and ornithine, that δ-aminovaleric acid is produced; threonine or methionine are the source of α-aminobutyric acid.

Proteins are present in vast amounts in the intestinal chemosphere. A gene catalog database of the human gut microbiome indicates the presence of nearly 10 million proteins; however, most of them are clearly intracellular proteins that are only available after bacterial lysis (Zhang et al., 2016). Proteins from the microbiota and the host are the target of metaproteomics (Xiong et al., 2015). From the approximately 6000 proteins that have been detected in the gut by metaproteomics, some two-thirds of them are of microbial origin (Verberkmoes et al., 2009; Erickson et al., 2012). More recent studies have identified more than 100,000 unique peptides associated with the microbiota (Cheng et al., 2017). The diversity of proteins is enhanced by post-translational modifications (by hydroxylation, methylation, citrullination, acetylation, phosphorylation, methyl-thiolation, S-nitrosylation, and nitration); in *E. coli* more than 5000 post-translational modification events been identified (Olsen and Mann, 2013). As in the metabolome, there is apparently a "core proteome" consisting of core functional categories (Verberkmoes et al., 2009). The intestinal proteome differs in the various intestinal regions, where variation in the local microbiota influences protein abundance and diversity (Lichtman et al., 2016).

In fact, there should be, at least in the colonic space, a wealth of molecules released by lysed bacteria (cell debris), including not only intracytoplasmic small molecules, nucleic acids, and proteins (many likely of ribosomal origin), but more

importantly bacterial membranes releasing lipopolysaccharides (glycolipids), lipoproteins, phospholipids, and peptidoglycan fragments, resulting from lysis of bacterial cell envelopes. It has been estimated that approximately one-third of bacteria in the gut are dead organisms (Ben-Amor et al., 2005). However, the contribution of "bacterial waste" to the intestinal chemosphere remains scarcely investigated.

The microbiota influences the intestinal chemosphere by altering the production and/or consumption of simple chemical molecules such as water, oxygen, hydrogen, nitrogen, carbon monoxide, carbon dioxide, hydrogen peroxide, nitrogen oxide, sulfates, ammonium, methane, and ethylene, and metals serving as nutrients or cofactors. In particular, microbiota and oxygen balance in the gut are deeply linked (Vacca, 2017). Given most of the microbiota is composed of strict anaerobic organisms, when oxygen availability increases, as occurs during antibiotic therapy, these populations are reduced, favoring facultative-aerobic organisms, such as *Enterobacteriaceae* (Rivera-Chávez et al., 2017). Finally, among the metals, iron is widely considered as a nutrient for microbiota. In fact, it is one of the main chemicals involved in biological competition, including competition among bacterial populations and also with the host (Kortman et al., 2014). Changes in gut iron availability alters the microbiota, frequently favoring rapid-growing bacteria, such as some intestinal pathogens (Jaeggi et al., 2015).

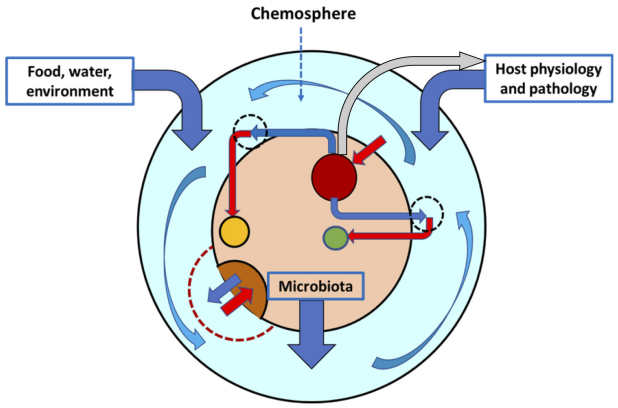

FIGURE 1 | The intestinal chemosphere. The chemosphere (light blue layer) is the ensemble of chemical molecules of dietary and environmental origin, released (dark blue vertical arrows) by the physiological or pathological functions of the host or by the complex bacterial communities colonizing the intestine. The chemosphere surrounds the gut microbiota (inner beige circle), composed of a variety of bacterial populations (dark red, brown, and yellow circles). These populations contribute to the chemosphere with chemicals (dark blue angled arrows) that result, probably in combination with other local chemicals, in the growth or inhibition of the same or other populations (red arrows). The chemosphere might have local differentiations with sets of chemicals (hatched circles), but an important part of it is flowing (curved blue arrows). Some components of the microbiota can regulate the secretion of chemicals by the host (gray arrow).

The Intestinal Chemosphere as a Field of Microbial Interactions

Reciprocal interactions are probably the most frequent processes in microbial gut ecology and are deeply influenced by the intestinal chemosphere. The microbiota determines an important part of the chemosphere, and the chemosphere constitutes the common chemical environment of the microbiota (**Figure 1**). A long and common evolutionary history of microbial organisms within their chemospheres has refined and stabilized intermicrobial interactions so they produce reciprocal effects on the interacting partners. In fact, the microbiota not only provides chemicals to the chemosphere, but some of these compounds, such as tryptamine, can activate the epithelial protein-coupled receptor to increase colonic secretion, probably for the benefit of some populations (Bhattarai et al., 2018). The microbe-driven modification of the intestinal chemosphere in the intestine could be a major factor influencing pathogen restriction, a topic thus far insufficiently investigated (Rangan and Hang, 2017).

Competition dominates species and clonal interactions in the bacterial world (Foster and Bell, 2012; Stubbendieck and Straight, 2016), and most probably the diversity and stability of the intestinal microbiota depends on competitive interactions (Coyte et al., 2015). Given the local coexistence of populations competing in the intestinal chemosphere for the same energy sources, nutrients, and attachment surfaces, the multiplication of the fittest reduces the reproductive possibilities of the competitor (exploitative competition) (Hibbing et al., 2010). However, this antagonistic interaction rarely produces the extinction of the competitor. Environmental fluctuation/variation might favor this competitor in other (sometimes immediate) circumstances. Also, because punctual competition could be for the mutual benefit of "being together" (coexistence mutualism) in the presence of certain substrates or conditions, so that the maintenance of both earlier contenders is assured faced with a third competitor negatively influencing both. This concept has been presented as a case similar to the game "rock-paper-scissors" (Czárán et al., 2002). In addition, and as was mentioned earlier, collective-cooperative trophic actions involving various bacterial populations are required to degrade particular compounds of the chemosphere, such as glycans from dietary fiber or epithelial mucus.

Later in this review we analyze in some detail the fact that the intestinal microbial ecology includes a wealth of interactions in which the growth of some bacterial populations is inhibited by others, either more efficient in the competition for limited vital resources, or excreting toxic substances which are released in the chemosphere, which is termed interference competition (Hibbing et al., 2010). At first sight, these types of effects can be considered an indirect, coincidental, or unintentional allelopathy. However, it is difficult to decide whether the spectrum of allelochemicals (such as metabolites) released by particular groups or ensembles of groups in the microbiota has evolved to maintain a healthy species diversity based on negative interactions (Abrudan et al., 2012).

Directed allelopathy or amensalism, in which one bacterial population inhibits the growth of or kills another one in a non-reciprocal manner, likely resulting in a benefit for the offender, is much more specific in shaping microbial ecology than interference competition based in fight for nutrients.

Amensalism might facilitate long-term genome evolution, given the DNA released from killed cells can be incorporated into the aggressor's genome (García-Bayona and Comstock, 2018). The involved allelochemicals are considered "antibacterial compounds," frequently "secondary metabolites" produced in the late stages of growth or during a stationary phase. It is of note that antimicrobials produced by bacteria cannot necessarily be considered (in our anthropocentric view) as weapons against "others," but more as signaling agents (Linares et al., 2006; Chikindas et al., 2018), probably acting along gradients. In fact, the maintenance of species diversity requires a non-extinction outcome, even in amensalistic interactions. In this respect, it should be debated whether allelopathic substances have evolved as an attack or defense strategy. Experimental results have suggested that antibiotic production does not improve the ability of producers to invade a population of sensitive cells (Wiener, 1996). On the contrary, established colicin-producing populations in structured habitats, which allow the achievement of a critical (high) population density, can overcome potential susceptible competitors (Chao and Levin, 1981; Durrett and Levin, 1997). This view is supported by the frequent production of allelopathic substances in populations with slow growth or during a stationary phase, such as when they reach high density in structured habitats. Whether allelopathy is triggered by different types of stress is an interesting possibility to consider; certainly, competition occurs more frequently under limiting conditions. However, the production of allelotoxic compounds might require investing energy in costly biosynthetic processes, whereas an alternative immunity/resistance-based "defensive strategy" could be evolutionarily preferred (García-Gutiérrez et al., 2019). This view suggests that the protection of population borders is critical, probably preventing niche invasions that can provoke local extinctions. Finally, the antibacterial activity of some allelopathic agents is highly dependent on the surrounding chemosphere; for instance, on the available carbon sources, trypsin, or carbon dioxide (García-Bayona and Comstock, 2018).

Microbial Growth Inhibitors in the Chemosphere

The ecological effects of intestinal chemical substances influence many dimensions. One aspect is their inhibitory effects on bacterial growth. In fact, intestinal microbiota can be considered a potential source of novel antimicrobials (Mousa et al., 2017). In the context of this review, we focus on metabolites and compounds arising from the action of intestinal bacteria that might inhibit bacterial replication or reduce microbial viability. As noted above, when defining the intestinal chemosphere, we are considering the chemical growth inhibitors that are available in the lumen, not those that are dependent on bacterial surfaces, such as those mediating contact inhibition (Willett et al., 2015; Chen et al., 2018).

Dietary Polyphenols and Carbohydrate Metabolites as Bacterial Growth Inhibitors

A number of phytochemicals, particularly polyphenols, are frequently bacterial growth inhibitors. In particular, flavonoids have direct antibacterial activity, eventually potentiating the effect of other antimicrobials (Cushnie and Lamb, 2011). It has been proposed that dietary flavonoids such as quercetin might even protect against some pathogens (Popa et al., 2015). Chlorogenic acids are extremely frequent in nature (approximately 400 have been reported), and among them, acyl-quinic acids are the most studied (Clifford et al., 2017). Chlorogenic acids have antimicrobial effects, and given these promote the increase in permeability of the outer and plasma bacterial membranes, they might also increase the effects of potentially active substances inhibiting microorganisms excluded by these barriers (Lou et al., 2011). Dietary fiber and polyphenols are metabolized to short-chain fatty acids and phenolic acids by the colonic microbiota (Russell and Duthie, 2011).

Short chain fatty acids resulting from the effect of microbiota on carbohydrates and polyphenols, mostly derived from the diet, are fermented by the gut microbiota and are in turn important effectors of microbial growth restriction. This inhibition occurs both by lowering pH, and by a pH-independent antibacterial effect. *Firmicutes* species mainly produce butyrate, whereas *Bacteroidetes* primarily produce acetate and propionate (den Besten et al., 2013; Ridaura et al., 2013). In newborns, the early (human milk-promoted) overgrowth of acetate-producing *Bifidobacterium* prevents a dangerous massive colonization with opportunistic, mostly Gram-negative, pathogens (Underwood et al., 2015). This modulation of the microbiota by acetate has inspired probiotic strategies using *Bifidobacterium* to correct metabolic disorders (Fukuda et al., 2011; Aoki et al., 2017).

Organic salts such as lactate and citrate have a growth-inhibitory activity on some species of microbiota (Zhitnitsky et al., 2017). Part of this activity is simply due to the pH effect. In fact, pH has a significant role in determining the species composition of human colonic microbiota; mildly acidic pH restricts Gram-negative bacteria, including *Enterobacteriaceae* and *Bacteroidetes*, particularly in the presence of short-chain fatty acids (such as acetate), favoring the growth of low-pH-tolerant microorganisms (Duncan et al., 2009). However, citrate has antibacterial activity independent of the pH effect on organisms of the colonic microbiota, such as *Fusobacterium* (Nagaoka et al., 2010).

Bile Acid and Lipid Bacterial Growth Inhibitors

The gut microbiota deconjugates and subsequently metabolizes the primary bile acids, cholic and chenodeoxycholic acid (cholesterol derivatives), into secondary bile acids, including terpenoids (Donia and Fischbach, 2015); bile salt hydrolases are key enzymes in the process (Jones et al., 2008). Both conjugated and unconjugated bile salts have direct antimicrobial activity (Sannasiddappa et al., 2017) and indirect actions on microbiota by modulating innate immunity. Inhibition occurs particularly in the proximal intestine; thus, if bile excretion is prevented, it results in bacterial overgrowth in the gut (Hofmann and Eckmann, 2006). The direct effects of bile salts in several Gram-negative bacteria probably result from action on membranes, which is in part compensated by the induction of efflux pumps (Thanassi et al., 1997; Rosenberg et al., 2003). Inhibition of Gram-negatives results in an increase in the proportion of Gram-positive bacteria (Friedman et al., 2018).

Lipids such as fatty alcohols, free fatty acids, and monoglycerides of fatty acids have antibacterial effects both on Gram-positive and Gram-negative bacteria, most probably due to damage to the bacterial envelopes (Thormar and Hilmarsson, 2007; Bergsson et al., 2011). Part of the antibacterial activity of milk is due to lipids, mostly medium-chain saturated, and long-chain unsaturated fatty acids and their monoglycerides released by lipases in the gastrointestinal tract (Isaacs, 2001).

Protein- and Amino Acid-Derived Bacterial Growth Inhibitors

Polyaminated molecules, biogenic amines, and polyamines are small polycation molecules derived from aromatic or cationic amino acids by decarboxylation, a process that can be mediated by intestinal microorganisms. *Bacteroides* (most importantly *B. thetaiotaomicron*) and *Fusobacterium* are important producers; however, polyamines are also produced by a "consortia" of other bacteria exchanging metabolites and forming collective chemical pathways (Matsumoto and Benno, 2007; Sakanaka et al., 2016; Nakamura et al., 2018). Polyamines include spermidine, homospermidine, norspermidine, putrescine, cadaverine, and 1,3-diaminopropane. The rate of production and degradation of biogenic amines and polyamines has consequences in microbial ecology (Pugin et al., 2017; Tofalo et al., 2019). Polyamines such as putrescine, spermine, and spermidine are known to be antibacterials, effective against Gram-positive bacteria (Bachracht and Weinstein, 1970). However, these compounds can also alter bacterial membrane permeability in Gram-negatives and in fact can serve as potential scaffolds for new antibacterial agents (Blanchet et al., 2016). In addition, polyamines can act as regulators of bacteriocin production, thus indirectly influencing competitive bacterial interactions (Yi-Hsuan and Chen-Chung, 2006).

Secretory N-acyl homoserine lactones mediating bacterial *quorum-sensing* in bacterial populations might also have antibacterial activity (Pomini and Marsaioli, 2008; John et al., 2016; Saroj et al., 2017). Indole-based intercellular communication molecules might also have antibacterial effects, eventually enhancing the effect of antibiotics (Biswas et al., 2015). Recently, it has been shown that *quorum-sensing* molecules involved in interspecies cell-to-cell communication, such as the signal autoinducer-2 from *E. coli*, influences the species composition of gut microbiota (Bivar, 2018).

Intestinal unconjugated bilirubin, resulting from the catabolism of hemes (from senescent erythrocytes), has a weak antimicrobial activity against *E. coli* and *Klebsiella pneumoniae* (Terzi et al., 2016). Biliverdin might influence inflammatory mediators (Overhaus et al., 2006). Finally, non-ribosomal peptides of bacterial origin are rarely found to be associated with mammals' microbiota (Donia and Fischbach, 2015).

Host Defense Antimicrobial Peptides and Proteins

Host defense antimicrobial molecules produced by epithelial cells of the intestine can be secreted into the intestinal lumen of mammals, such as antimicrobial peptides (α-defensins, β-defensins, and cathelicidins), protective carbohydrate-bonding proteins (C-type lectins), and RNAses (Gallo and Hooper, 2012; Meade and O'Farrelly, 2019). Secretion of these molecules is frequently controlled by bacterial-originated signals and might influence the composition of the microbial community (Salzman et al., 2010). However, they remain mostly attached to the inner and outer mucus layers of epithelium, embedded in the mucin glycoprotein layer (Meyer-Hoffert et al., 2008; Dupont et al., 2014). Given detached fragments of this mucin layer can serve as a source of bacterial nutrients, a possible effect of these antimicrobial peptides in the gut lumen, and not only on the epithelial surfaces, cannot be excluded. Finally, immunoglobulins, particularly secretory IgA, are produced by plasma cells and transported into the lumen through the intestinal epithelial cells but remain surface-attached to block epithelial receptors (Mantis et al., 2011). These large antimicrobial proteins also have effects on the microbiota composition, particularly on *Proteobacteria* (Mirpuri et al., 2014).

Bacteriocins

In 1925, André Gratia, a Belgian microbiologist, was the first to detect antagonisms between *Enterobacteriaceae* strains (Gratia, 1925), and this early work was followed by that of Pierre Fredericq (Fredericq and Levine, 1947), who identified colicins, the first bacteriocins. Bacteriocins, ribosomally synthesized proteins, are specific effectors of bacterial inhibition or death, and they are particularly active on phylogenetic relatives of the producer (Cotter et al., 2005, 2013). Bacteriocins are considered important modulators of intestinal microbiota (Lenski and Riley, 2002; Kirkup and Riley, 2004; Corr et al., 2007; Angelakis et al., 2013; Million et al., 2013). The classification of bacteriocins, a heterogeneous group of substances of various bacterial origins, is a highly debatable and even confusing issue (Chikindas et al., 2018), even though the various classification proposals do not differ in the essential (Klaenhammer, 1993; Van Belkum and Stiles, 2000; Kemperman et al., 2003; Heng and Tagg, 2006; Arnison et al., 2013; Balciunas et al., 2013; Alvarez-Sieiro et al., 2016; Dicks et al., 2018). Two clearly recognizable broad groups, are the long thermolabile peptides, including colicins, and a heterogeneous ensemble of small thermostable peptides, including the microcins. Lantibiotics (lanthionine and methyllanthionine containing peptides) are also thermostable. Note that thermostability is often correlated with resistance to proteolysis (Daniel et al., 1982), an important trait for stability in the intestinal environment. A systematic search of previously described bacteriocin molecules (n = 1360, 1000 of them from Gram-positives) has been performed on 317 genomes of the gut microbiota (Drissi et al., 2015). *Firmicutes* and *Bacteroidetes*, the most predominant phyla in the human microbiota, produce the largest number of bacteriocins. However, based on the chemical structure, the authors suggest that bacteriocins produced by *Proteobacteria,* which are rich in cationic charges and α-helices, might have higher antibacterial activity (Drissi et al., 2015).

THE MICROCINS

Historical Background of the Discovery of Microcins

Microcins were originally defined as eco-active, low-molecular-weight excreted molecules (less than 10 kDa), such as amino acids and short ribosomally synthesized peptides produced by Gram-negative organisms, and presenting resistance to proteases, extreme pH, and high temperatures. Microcins were discovered in 1974 in the process of identify effectors of enterobacterial sequential displacements in the microbiota of newborns (Baquero and Asensio, 1976). Even though the number of species cumulatively increases with time in newborns, the absolute number of bacterial cells is extremely high from the early days. The microcin's historical screening was performed in conditions resembling the high-density colonization of the colonic space, using minimal media to mimic possible nutritional deficiency, and was designed to detect only low-molecular-weight molecules, microcins (meaning small bacteriocins), which are able to pass and exert activity through cellophane membranes, excluding molecules over 10,000 Da. This screening excluded conventional bacteriocins, large proteins that could be degraded by intestinal proteases. Low-molecular-weight growth-inhibitory substances were consistently detected in *Enterobacteriaceae* from the human newborn intestine (15% of the tested strains). The first comprehensive review on microcins was in 1984 (Baquero and Moreno, 1984). At this time, these growth-inhibitory substances were identified as small peptides and occasionally as amino acids or amino acid-derived compounds. Other secondary metabolites or chemical substances of bacterial origin with low molecular weight and high antimicrobial activity are apparently very rare or are produced in small amounts. The possibility that microcins could be considered as potential drugs was considered from this early period, and in fact the microcins remain as promising, but not yet developed, antibacterial agents (Gillor et al., 2004; Zucca et al., 2011; Collin and Maxwell, 2019). Although the designation "microcins" currently refers mainly to ribosomally synthesized peptides, for the purposes of this review we would like to recapitulate the original "functional" meaning as small eco-active molecules mediating bacterial interactions in the gut. However, we should acknowledge that amino acids and amino acid derivatives with antimicrobial activity do not correspond in a strict sense to microcins as they are understood today, and they should in fact be considered as "historical microcins."

Historical Amino Acid or Amino Acid-Derived Microcins; Secreted Amino Acids as Inhibitors

In early studies focusing on low-molecular-weight inhibitors excreted by *Enterobacteriaceae*, several excreted amino acids and amino acid-derived compounds were included among microcins. This was the case for L-valine, which inhibits growth of *E. coli* strain K-12 due to repression of the aceto-hydroxybutyrate-forming system, leading to an inhibitory shortage of isoleucine. Also, methionine derivatives, such as microcin 15 m, inhibit the first enzyme of the methionine biosynthetic pathway, homoserine-O-trans-succinylase (Baquero et al., 1984). Early research on microcins (Baquero and Asensio, 1976) had indicated that among *Enterobacteriaceae* from the neonatal human intestine, 3% hyperexcreted L-valine, and 7% putative methionine derivatives (such as microcin 93 m), the inhibitory activity being reversed by adding methionine (10 mg/ml) (Aguilar et al., 1982). In other studies, *E. coli* excretion of D-alanine has been detected; in general, the bacterial excretion of D-amino acids might have bacterial growth-inhibitory activity. Either glycine or D-amino acids inhibit the growth of *E. coli* (Hishinuma et al., 1969), altering lipoprotein binding in the outer membrane (Tsuruoka et al., 1984), and triggering biofilm disassembly (Kolodkin-Gal et al., 2010). D-amino acids also induce in eukaryotic (intestinal?) cells the toxic formation of superoxides, and trigger apoptosis (Bardaweel et al., 2013). In particular, D-arginine is probably involved in microbial interactions and contributes to microecological diversity (Álvarez et al., 2018). Despite the possible importance of these findings, research on the physiology and ecological consequences of bacterial secretion of amino acids and amino acid derivatives in complex ecosystems remains very limited (Krämer, 1994), and only in recent years has it been systematically investigated (Aliashkevich et al., 2018).

Microcins as Small Peptides

In more recent times, the term "microcins" has been applied essentially to small peptides secreted by microorganisms (mostly *Enterobacteriaceae*) that are able to inhibit other bacteria. Microcins are non-SOS-inducible, ribosomally synthesized peptides, in some cases only active after post-translational modification. In 1949, the Belgian microbiologist Pierre Fredericq named the antagonistic substance previously described by Gratia in 1925 as "colicin V." The possibility that this low-molecular-weight molecule could be considered a microcin was acknowledged by Fredericq in a personal face-to-face *ad hoc* meeting in Liège with one of the authors of this review (FB). Low molecular weight was in fact instrumental to differentiating them from colicins in the microcin kick-off consensus conference at the Alhambra, Granada, Spain, in 1983, which was attended by top international experts in the field including Volkmar Braun, Roberto Kolter, Jordan Konisky, Claude Lazdunsky, Bauke Oudega, Anthony Pugsley, and Maxime Schwartz. Thirty years later, in 2013, a consensus on universal nomenclature of ribosomally synthesised and post-translationally modified peptides (RiPPs) was presented (Arnison et al., 2013). Most of these active RiPPs are initially synthesized as a long precursor peptide, typically ∼20–110 residues in length, encoded by a structural gene. The "core peptide" is the region that is transformed in the bioactive molecule. Microcins were recognized as a separate family among these natural products (Arnison et al., 2013).

The Functions of Microcins

Microcins had been discovered as molecules influencing interbacterial interactions in complex microbial ecosystems, regulating microbial communities; this basic ecological function is at the core of this review. In addition to this basic

function (Chung and Raffatellu, 2019), other interactions are also influenced by microcin-producing organisms, involving not only the microbial community but also the human or animal hosting the microbiota.

Microcins might have functions involving interactions with eukaryotic host cells. An important aspect is if microcins can cross the intestinal-blood barrier to produce systemic effects on the host (Dicks et al., 2018). Some microcins, such as MccJ25, have interactions with integrins, eukaryotic transmembrane receptors involved in cells' extracellular matrix adhesion and potentially regulating the cell cycle (Hegemann et al., 2014). In fact, the lasso peptide MccJ25 can act as a pro-apoptotic eukaryotic antimicrobial peptide, thus being potentially active in anticancer therapy (Soudy et al., 2017), as are other bacteriocins and microcins (Cornut et al., 2008). Strains producing microcins MccH and MccM, as the Nissle strain, tends to target neoplastic cells (Stritzker et al., 2007), and MccE492 has antitumorigenic properties (Lagos et al., 2009). It has been proposed that the decrease in potentially antineoplastic bacteriocins and microcins in healthy individuals might contribute to the initiation of non-advanced colorectal neoplasia; however, when neoplasia is advanced, a higher frequency of microcinogenic strains occurs (Kohoutova et al., 2014). Microcins are part of complex gene clusters, such as the colibactin gene cluster located in the genetic island KPHPI208 of *K. pneumoniae*, likely inducing some degree of host DNA damage (e.g., regulatory functions and genotoxicity) (Lai et al., 2014). Similarly, *E. coli* Nissle, 1917 harbors a gene cluster, the "pks island" allow production of colibactin, causing potential genotoxicity (Olier et al., 2012). In addition, some microcins, such as those producing accumulation of oxazole compounds derived from MccB17 and other thiazole/oxazole-modified microcin-producing bacterial strains, might significantly influence host immune responses, leading to intestinal inflammatory effects (eventually providing food for the microbe). In general, they have an immunoregulatory effect mediated by the glycoprotein CD1d-restricted pathways, thus influencing antigen-presentation functions (Iyer et al., 2018).

Finally, microcins and microcin-related molecules might also have regulatory functions inside the bacterial cell. MccC triggers the stringent response and persistence in both sensitive and producing cells (Piskunova et al., 2017). Microcins might have functions related to bacterial maintenance of mobile genetic elements, such as plasmids; thus, acting as a post-segregational killing mechanism; that is, bacteria losing a plasmid are penalized with cell death (Fedorec et al., 2019).

The Microcin Classification

Approximately 15 peptidic microcin molecules have been identified, but the chemical structure is only known for 8 of them. Peptidic microcins are currently grouped into 2 classes (Rebuffat, 2012). Class I peptidic microcins, such as microcins MccB17, MccC, MccD93, and MccJ25 are small (less than 5 kDa) plasmid-encoded peptides requiring extensive backbone post-translational modifications. The term "post-translational thiazole/oxazole-modified microcins" (TOMMs) has also been suggested for MccB17 related bacteriocins (Melby et al., 2014). Class II peptidic microcins (Duquesne et al., 2007b; Vassiliadis et al., 2011; Santos et al., 2017) are larger (5–10 kDa), and can be subdivided into class IIa, including the plasmid-mediated microcins MccL, MccV, and MccS, not requiring post-translational modifications and having, respectively 2, 1, or no disulfide bond(s); and class IIb, such as the chromosomally encoded microcins MccE492, MccM, and MccH47, and carrying (MccM, MccH47, and MccI47) or not a C-terminal post-translational modification, involving a catechol-siderophore moiety (Patzer et al., 2003; Vassiliadis et al., 2010).

Microcins' Mechanisms of Action

Microcins are antibiotic peptides, blocking vital functions in the target cell. They act by forming pores in the bacterial membrane (MccV, MccE492, and MccL), inhibiting aspartyl-tRNA synthetase, essential in protein synthesis (MccC), inhibiting the DNA gyrase GyrB, resulting in double DNA breaks (MccB17). Some others block the secondary RNA polymerase channel, impairing transcription and acting on cytochromes to inhibit cellular respiration (MccJ25), impairing the cellular proton channel (MccH47 and probably MccM and MccI), or the ATP synthase (MccH47). Some modes of action have been studied in detail and others remain to be confirmed. Colicins, much larger polypeptides, mainly act by pore formation, nuclease activity (DNase, 16S rRNase, and tRNase activities), and blocking peptidoglycan synthesis (colicin M).

Antimicrobial production should be balanced with appropriate mechanisms of self-protection by the producing organisms (immunity). Among others, these mechanisms involve acetyltransferases (MccC), production of immunity proteins (Class IIb microcins), efflux pumps (MccB17, MccJ25, and ppGpp-regulated), or inhibition of DNA gyrase supercoiling activity (MccB17), which are detailed later.

Once the peptides or their derivatives with antibacterial activity are released from the producer cell, action on other bacterial cells requires uptake mechanisms. Uptake depends frequently on outer membrane receptors, mainly OmpF and OmpC, but also on receptors involved in iron uptake (FhuA, FepA, Cir, and Fiu). Several microcins use the "Trojan horse" strategy of mimicking essential nutrients (such as essential amino acids or iron-siderophores) to be incorporated into the cell. Frequently, failure in nutrient uptake mechanisms results in microcin resistance in non-producer organisms. Next, in a simplified manner, we will review the main modes of action of these antibiotic peptides.

Class I microcins

The Microcin B17 (MccB17) structural gene, *mcbA*, encodes a 69-amino acid inactive precursor that undergoes at least 2 steps of post-translational modification, leading to the formation of oxazole and thiazole rings, and resulting in the toxic MccB17 molecule. These steps are performed by the McbBCD enzyme complex in subsequent reactions of cyclization, dehydration, and dehydrogenation involving the dipeptides Gly-Ser (oxazole) and Gly-Cys (thiazole), present in the MccB17 unmodified precursor (Li et al., 1996). Modification of the tripeptides Gly-Ser-Cys and Gly-Cys-Ser leads to the formation of oxazole-thiazole and thiazole-oxazole, respectively.

The discovery of the process of MccB17 peptide maturation has been instrumental for overall progress of the field of biological synthesis of oxazoles-thiazoles and, more importantly, of post-translational modification (Yorgey et al., 1994). The recent elucidation of the microcin B synthase octameric protein complex has been instrumental to understand the process of conversion of a ribosomally synthesized peptide in a DNA gyrase inhibitor, culminating 30 years of research (Ghilarov et al., 2019). Interestingly, compounds very similar to microcin B can target molecular machines other than gyrase. A full set of MccB17 homologous proteins was identified in the genome of *K. pneumoniae*; one of them, klebsazolicin from *K. pneumoniae* subsp. *ozenae* is targeting the 70S ribosome, obstructing the peptide exit tunnel, and overmapping with group B streptogramins (Metelev et al., 2017b).

Mature MccB17 is exported outside the cell by a specific ABC transporter (McbE–McbF). TldD/TldE is a protease that removes the leader peptide from the MccB17 precursor, allowing MccB17 export by the McbE–McbF transport system (Allali et al., 2002; Tsibulskaya et al., 2017). The leader peptide does not intervene in microcin activity. The lethal cellular target of MccB17 is the GyrB subunit of DNA gyrase (Vizan et al., 1991). Inhibition of GyrB results in an impairment of DNA replication in sensitive cells, producing an SOS response (Herrero et al., 1986). Alterations in DNA packaging by MccB17 might increase the bacterial mutation rate, as in the case of novobiocin, also targeting GyrB (Chang et al., 2003). Most of the studies of MccB17 have been performed with *E. coli* strains; however, there are reports of MccB17-like activities in environmental *Pseudomonas*, such as *P. syringae* and *P. antarctica* (Metelev et al., 2013; Lee et al., 2017), encoded with an almost identical genetic structures to that of MccB17.

Microcin J25 (MccJ25) is a 21-amino acid antimicrobial peptide with a lasso structure. The study of lasso peptides has generated increasing interest due to their high stability and possible bioengineering applications in the design of enzyme inhibitors or to antagonize receptors (Rosengren and Craik, 2009). Lasso peptides are a class of ribosomally synthesized peptides, with a unique three-dimensional structure produced by a lasso peptide synthetase, and the formation of a macrolactam ring (Rebuffat et al., 2004; Ducasse et al., 2012; Yan et al., 2012; Sumida et al., 2019). Microcin J25 is active against *Salmonella* species and *E. coli* (Lopez et al., 2007). To enter into target cells, MccJ25 uses the outer membrane protein FhuA, the receptor for ferrichrome (a hydroxamate siderophore) involved in iron uptake (Salomón and Farías, 1993). Klebsidin, an MccJ25-like lasso peptide from *Klebsiella*, likely has a species-specific short host range, given it is only internalized in *E. coli* when expressing the FhuA homolog from *Klebsiella pneumoniae* (Metelev et al., 2017a). Once MccJ25 reaches the periplasmic space, it interacts with the inner membrane protein SbmA to enter the cytoplasm (Salomón and Farías, 1995). MccJ25 inhibits at least 2 intracellular targets, the secondary channel of RNA polymerase (Adelman et al., 2004; Braffman et al., 2019), resulting in transcription impairment, and the cytochromes bd-I and bo3, leading to inhibition of cellular respiration (Galván et al., 2018).

Microcin C (MccC). In this review we use the designation MccC, but in the literature the acronym McC has been used, to avoid confusion with the *mccC* gene, encoding an microcin C transport protein. Microcin C is the smallest microcin known to date. In fact, it is the smallest peptide of ribosomal origin, encoded by the smallest *E. coli* gene, of only 21 bp (González-Pastor et al., 1994). It is built by only seven amino acids forming an N-formylated heptapeptide with covalently attached C-terminal adenosine monophosphate and a propylamine group attached to the phosphate (Guijarro et al., 1995). This phosphorus atom determines the chirality of the microcin, and might condition its antibacterial activity (Severinov et al., 2007). The length of the peptide is evolutionarily conserved, given larger peptides strongly reduce MccC production and activity (Zukher et al., 2019). In *Yersinia*, the peptide-cytidine antibiotic is activated inside the cell by the TldD/E protease, suggesting that proteolytic processing might optimize activity and reduce toxicity (Tsibulskaya et al., 2017). MccC enters the target cells by the porin OmpF in the outer membrane and is then guided through the inner membrane by YejABEF, an ABC transporter (Novikova et al., 2007). In fact, microcin uses the Trojan horse strategy to penetrate the cell, through N-acylphosphoramidate, deceiving target cells. Once inside, it becomes toxic after being processed (Metlitskaya et al., 2006). First, the microcin will undergo excision of the formyl group at the N-terminus; then, in a second step, the peptide domain will be removed, with the active molecule mimicking the aspartyl adenylate, acting as a strong inhibitor of aspartyl-tRNA synthetase and inhibiting protein synthesis at the translation step (Metlitskaya et al., 2009).

Class IIa microcins

Microcin V (MccV), previously named colicin V, is an 88-amino acid peptide encoded by the *cvaC* gene. It contains a disulphide bond in the C-terminal sequence that is formed during post-translational modification. MccV is secreted by *E. coli* through a specific exporter composed of the proteins CvaA, CvaB, and TolC; MccV is only bactericidal after it is exported (Zhang et al., 1995) and is active against related bacteria belonging to the genera *Escherichia*, *Klebsiella*, *Salmonella*, and *Shigella* (Håvarstein et al., 1994). MccV is recognized only by Cir, an outer membrane receptor for catecholate siderophores, and its uptake is dependent on the TonB complex, providing the necessary proton motive force (Chehade and Braun, 1988). Moreover, MccV activity also depends on the cytoplasmic membrane protein SdaC, also involved in serine uptake (Gérard et al., 2005). The activity of MccV is related to membrane channel formation and disruption of membrane potential (Yang and Konisky, 1984).

Microcin L (MccL) is a peptide produced by the strain *E. coli* LR05 that exhibits strong antibacterial activity against related *Enterobacteriaceae*, including the *Salmonella enterica* serovars Typhimurium and Enteritidis (Sablé et al., 2003). MccL uptake requires the outer membrane receptor Cir, similar to MccV. Moreover, like MccV activity, MccL activity depends on the inner membrane protein TonB that

transduces the proton motive force to transport iron siderophore complexes across the outer membrane. The MccL target is probably the bacterial membrane. In a preliminary study, it had been observed that high levels of MccL disrupt the inner membrane potential of *E. coli* cells; however, no permeabilization of the membrane had been detected (Morin et al., 2011).

Microcin N (MccN) is active against *E. coli* and *S.* Typhimurium but not against *Listeria monocytogenes* or *Campylobacter jejuni* (Wooley et al., 1999). To date, its uptake and mechanism of action are unknown. MccN displays sequence similarities with the class IIb MccE492 (Lagos et al., 1999), but lacks the C-terminal region necessary for recognition by catecholate siderophore receptors. Thus, focusing on the sequence identities, it has been suggested that MccN could have a target similar to MccE492, and both probably need ManY/ManZ inner membrane proteins (Bieler et al., 2006).

Microcin S (MccS), like microcins MccM and MccH47, was discovered by investigating the reason for the successful effect of a probiotic extensively used in functional gastrointestinal disorders. In this case, it was produced by *E. coli* G3/10, a component of the probiotic drug Symbioflor 2. MccS is encoded in the megaplasmid pSYM1 and has a genetic organization similar to other class IIa microcins, and it is the largest of all known microcins (11.67 kDa). MccS is lethal to the virulent enterohemorrhagic and enteropathogenic *E. coli*, but the mechanism of action has not been elucidated with certainty (Zschüttig et al., 2012, 2015).

Microcin PDI (MccPDI). The term "PDI" is an acronym for "proximity-dependent inhibition," given a close physical proximity between producer and susceptible strains is required. An MccPDI precursor protein (McpM) interacts with a conserved motif of the outer membrane porin OmpF on susceptible cells, ultimately resulting in lethal membrane damage (Eberhart et al., 2012; Lu et al., 2019). Other proximity-dependent (or contact-dependent) inhibition phenomena acting on stationary-phase bacteria have been described, sometimes secondary to the overproduction of bacterial glycogen; however, the mechanism of inhibition remains elusive (Lemonnier et al., 2007; Navarro Llorens et al., 2010).

Class IIb microcins

Microcin E492 (MccE492) was isolated for the first time from *K. pneumoniae* (de Lorenzo, 1984), and is active against closely related bacteria. The chromosomal genes needed for active microcin production were cloned in *E. coli* for heterologous expression and characterization (Wilkens et al., 1997). The presence of a serine-rich region located at the C-terminus was surprising. The precursor of microcin undergoes a post-translational modification before being secreted. In the glycosylation process, the C-terminal serine is bound through an O-glycosidic link to a linear trimer of N-2,3-(dihydroxybenzoyl)-L-serine (DHBS) (Thomas et al., 2004). DHBS is a catechol siderophore, similar to other siderophores such as enterobactin and salmochelin. These molecules bind to iron and import it into cells via high-affinity receptors so that the producer strains become more competitive when placed in an iron-poor environment. In addition, the siderophore-microcin complex binds ferric iron selectively through the catecholate receptor, and could work as a siderophore (Thomas et al., 2004). MccE492 recognizes FepA, Fiu, and/or Cir as receptors in the outer membrane. The main receptor is FepA (Strahsburger et al., 2005). It should be remembered that MccV is only recognized by the Cir catechol-siderophore receptor. Once more, the complex formed by the inner membrane proteins, TonB-ExbB-ExbD, uses the proton motive power from the cytoplasmic membrane to convey energy to the outer membrane, allowing microcin intake (Thomas et al., 2004). Although the serine-rich region at the C-terminus is important for recognition by catecholate-siderophore receptors, it is not required for the microcin activity (Bieler et al., 2006). Once in the periplasmic space, MccE492 interacts with the inner membrane proteins ManY/ManZ of the mannose permease and induces channel or pore formation, and TonB-dependent inner membrane depolarization, followed by cell death (Bieler et al., 2006). However, it is unknown whether microcin has other targets in the cytoplasm (Destoumieux-Garzón et al., 2006).

Microcin H47 (MccH47), microcin M (MccM), and probably microcin I (MccI47) belong, just as MccE472, to the catechol siderophore microcin group (Vassiliadis et al., 2010). Antimicrobial activities are restricted to some species of *Enterobacteriaceae*. These peptides have a serine-rich domain at the C-terminus that is necessary for recognition by the outer membrane receptors but not required for activity (Bieler et al., 2006). Catecholate receptors (FhuA, Cir, and Fiu) in *E. coli* and (IroN, Cir, and FepA) in *Salmonella*, are essential for recognizing the siderophore microcin (Patzer et al., 2003) and lead microcins to the periplasmic space. Mutations in catecholate receptors have been associated with microcin resistance (Vassiliadis et al., 2010). The antibiotic activity of MccE492 requires the integrity of mannose permease (ManX/ManY/ManZ), but this is not the case for MccH47 or MccM (Vassiliadis et al., 2011; Peduzzi and Vandervennet, unpublished data). Interestingly, post-translational modifications increase the antibacterial activity for all class IIb microcins by mimicking the natural siderophores.

The proton channel is the minimal structure necessary for ATP synthase and is sufficient for MccH47 antibiotic action (Rodríguez and Lavina, 2003). The target of MccH47 is the F0F1 ATP synthase, and particularly its F0 membrane element, which serves as a proton channel. To date, the mechanisms of action of MccM and MccI are not known, although it is suspected that they act in the same way as MccH47, impairing the cellular proton channel. MccV acts similarly, and in fact, it has been suggested that MccH47 is probably related to MccV (Azpiroz et al., 2001; Azpiroz and Laviña, 2007).

Microcin N (MccN) is also known as microcin 24 (O'Brien and Mahanty, 1994). The uptake of MccN is dependent on the presence of SemA and/or TonB. Both are genes that code for membrane proteins within *E. coli* and are involved in microcin resistance and sensitivity. The mechanism of action has not been elucidated, but MccN appears to have DNAse activity (O'Brien, 1996).

Mechanisms of Immunity and Mechanisms of Resistance to Microcins

Immunity to microcins should be clearly distinguished from microcin resistance. Immunity explains the absence of "self-killing" in producing strains (this has been previously described); however, resistance means acquired insusceptibility to external microcins. Resistance might complement immunity in producer strains; for instance, an excreted microcin might not be internalized again because of a "resistance" mutation in a porin. Most mechanisms of resistance to microcins involve mutations. The possibility of acquisition of microcin-inactivating enzymes by horizontal gene transfer has not yet been investigated but cannot be ruled out. Whether self-immunity mechanisms can be converted into acquired-resistance mechanisms is a possibility, as occurs with antibiotics (Benveniste and Davies, 1973). Certainly, mutational resistance might evolve in microcin-susceptible bacteria during amensalistic-competitive interactions. A number of resistance mutations might have significant biological costs for the bacterial cell (e.g., reducing permeability) or specific uptake mechanisms (e.g., siderophores).

Specific immunity proteins and/or non-specific resistance proteins are required for the viability of the microcin producer bacteria (Kolter and Moreno, 1992). Most importantly, immunity proteins expel microcins using ATP-binding cassette transporters (Beis and Rebuffat, 2019). Immunity genes are typically encoded in the same operon, close to the genes involved in microcin production, such as structural genes, post-translational modification genes, and secretion genes (Baquero and Moreno, 1984). The elucidation of the microcin immunity protein structure will cast some light on the mechanisms of immunity, just as with bacteriocin immunity systems in lactic acid bacteria (Klaenhammer, 1993; Bastos et al., 2015).

The evolution of microcin production in combination with specific self-protection immunity mechanisms remains uncertain, but it is an attractive field of basic evolutionary research. In the following section, immunity and resistance to microcins are considered according to the 2 major microcin groups (class I and II) (Gaillard-Gendron et al., 2000; Pons et al., 2002).

Immunity and resistance to class I microcins

Immunity to several microcins in this group, including MccB17, MccC, MccJ25, and MccD93, involves the presence of efflux pumps. Concerning specific immunity to microcin B17, the expression of 3 genes, present in the microcin gene cluster, is required. These genes, *mcbE*, *mcbF*, and *mcbG* encode the 3 proteins McbE, McbF, and McbG, respectively. McbE and McbF constitute the microcin export system; their activity is needed for resistance to MccB17. McbG is a pentapeptide protein that protects cells that synthesize MccB17 from its own action, blocking the inhibition of DNA gyrase (Garrido et al., 1988). It is only when these 3 genes are expressed that cells are fully immune to their own toxic peptide. If one of the 3 genes is repressed, partial immunity phenotypes are shown. Whether the McbG mechanism of immunity contributes to the protection of fluoroquinolones in bacteria producing MccB17 is an interesting possibility. The widespread target-protection Qnr proteins involved in plasmid-mediated resistance to fluoroquinolones belong to the pentapeptide repeat family and share sequence homology with McbG (Tran and Jacoby, 2002; Rodríguez-Martínez et al., 2011). The first studies indicated that a plasmid carrying the entire MccB17 operon or a vector that expresses only the *mcbG* gene produces a 2–8× decrease in sensitivity to quinolones (Lomovskaya et al., 1996). However, the expression of Qnr does not produce resistance to MccB17 (Jacoby et al., 2015).

In *Escherichia coli*, resistance to external MccB17 occurs by mutations in OmpF, the outer membrane porin F, in the inner membrane SbmA transporter protein, and in the target of antimicrobial action, GyrB (tryptophan at position 751 is replaced by arginine). This mutational change in topoisomerase does not influence the susceptibility to coumarins or quinolones (del Castillo et al., 2001; Mathavan and Beis, 2012).

Regarding Microcin C, self-immunity of producing strains requires an efflux pump, and also number of enzymes able to detoxify MccC. This is the case of the MccE acetyltransferase, which is also protective against a number of toxic aminoacyl-nucleotides (Agarwal et al., 2011). MccE is homologous to the chromosomally encoded acetyltransferase, RimL, acting on L12 ribosome proteins, which also provide MccC and albomycin (a hydroxamate-type siderophore antibiotic) resistance (Novikova et al., 2010; Kazakov et al., 2014). In addition, a serine carboxypeptidase MccF protects against MccC (Agarwal et al., 2012). The carboxypeptidase MccF is similar to *E. coli* LdcA, acting on cell murotetrapeptides (Tikhonov et al., 2010).

Resistance to external MccC in non-producers occurs by mutations in YejABEF, an ABC transporter, preventing the uptake of the compound (Novikova et al., 2007). Orthologs of some of these MccC detoxifying enzymes might occur in non-MccC-producing bacteria, which could be protected (resistance) from the action of this microcin (Nocek et al., 2012). As probably strains producing MccC have a strong effect on intestinal competitors, the possibility of a flow of MccC detoxifying enzymes by horizontal gene transfer cannot be excluded.

Immunity to microcin J25 involves the protein McjD, ensuring highly specific export of MccJ25 and self-immunity to the peptide (Clarke and Campopiano, 2007; Gu et al., 2015; Husada et al., 2018; Romano et al., 2018) and possibly YojI (Vincent and Morero, 2009). They are efflux pumps that require TolC to extract the microcin from the producing bacteria (Delgado et al., 1999). Resistance to MccJ25 in *E. coli*-sensitive strains involves alterations in the outer membrane receptor FhuA (a siderophore receptor, explaining cross-resistance with albomycin, and a sideromycin) and the inner membrane proteins TonB, ExbB, ExbD, and SbmA. Given microcin J25 inhibits *E. coli* RNA polymerase, mutations in RpoB and RpoC are associated with resistance (Yuzenkova et al., 2002).

Immunity and resistance to class II microcins

Self-immunity for class II microcins involves membrane-associated small peptides, ranging from 51 to 144 amino acids, which protects the producing strain from its own antibacterial

product in a highly specific way. Thus far, the 3-dimensional structure of these peptides has not been elucidated.

The protein involved in immunity to microcin V, MccV (formerly colicin V), has a molecular weight of approximately 6.5 kDa (Frick et al., 1981). The genetic determinant of MccV immunity protein, *cvi,* is located in a 700-base-pair fragment downstream from the region involved in its production (Gilson et al., 1987). The expression of the *cvi* gene was assessed under conditions of iron excess or depletion and immunoblots have shown that production of the immunity protein Cvi is iron dependent. The *cvi* promoter was located approximately 50 bp upstream from the *cvi* structural gene and was associated with a previously identified Fur binding site. The *cvi* promoter is also consistently inducible by iron depletion, and like other genes, encodes a transporter accessory protein, *cvaA* (Boyer and Tai, 1998). Resistance to MccV in non-producing cells has been analyzed in *E. coli* by transposon mutagenesis. Mutants in the *sdaC* (also called *dcrA*) gene, which is involved in serine uptake and is required for C1 phage adsorption, eliminate the bactericidal activity of this microcin (Gérard et al., 2005). Mutations in OmpF porin also result in MccV resistance (Jeanteur et al., 1994).

Immunity to MccL in producing organisms involves the *mclL* immunity gene, which was identified upstream of the *mclC* structural gene, and encodes a 51-amino acid protein with 2 potential transmembrane domains (Sablé et al., 2003; Pons et al., 2004). Resistance to MccL results from deficient uptake mediated by the outer membrane receptor Cir (colicin I receptor). Moreover, MccL bactericidal activity has been shown to depend on the TonB protein that transduces the proton motive force of the cytoplasmic membrane to transport iron-siderophore complexes across the outer membrane (Morin et al., 2011).

Immunity to microcins MccE492, MccH47, MccM, and MccI47 in the producer strains is provided by the inner membrane proteins, MceB, MchB, McmI, and MchS3, highly conserved in class IIb microcins, containing a putative transmembrane region (Duquesne et al., 2007a). The gene *mceB*, which encodes a protein of 95 amino acids, has been found in the strain *K. pneumoniae* RYC492. The gene *mchB* has been found in the microcin producer strains *E. coli* H47, *E. coli* CA46, *E. coli* CA58, and *E. coli* Nissle, 1917, and in all cases confers self-immunity to MccH47. The gene *mcmI*, has been found in the strains *E. coli* CA46, *E. coli* CA58, and *E. coli* Nissle, 1917, and confers self-immunity to microcin M. The strain *E. coli* H47 contains a truncated *mcmI* gene version that is not functional. The gene *mch*S3 has been found in the strains *E. coli* H47, *E. coli* CA46, and *E. coli* CA58, although the structural gene of MccI47, *mchS2*, is only present in the strains *E. coli* H47 and *E. coli* CA46 (Laviña et al., 1990; Patzer et al., 2003; Poey et al., 2006; Vassiliadis et al., 2010).

Microcin E492 immunity is negatively regulated by MceF (Tello Reyes, 2006). The gene *mceF* shows many similarities to the gene *mcmM*, which encodes a protein of 228 amino acids and 7 transmembrane domains and is present in the strains *E. coli* CA46, *E. coli* CA58, and *E. coli* Nissle, 1917. No evidence has been found that *mcmM* is necessary for immunity to MccM or MccH47 (Bravo-Vázquez, Doctoral Thesis). A sequence encoding for a 156-amino acid protein with 3 transmembrane domains, McmT, presumptively associated with MccH47 and MccM immunity, was cloned from *E. coli* Nissle, 1917, the producer strain. The plasmid containing the *mcmT* gene provided resistance in the recipient strain to MccH47 and MccM, and partial resistance to MccE492 and MccV (Bravo-Vázquez, Doctoral Thesis). A homologous MccT protein was found in *E. coli* O157:H7, the same region also containing the gene *mchA*, encoding a glycosyl transferase, essential in the biosynthetic pathway of MccE492, MccH47, MccM, and MccI47 (Bravo-Vázquez, Doctoral Thesis).

Mutations in three *E. coli* K12 genes, *tonB*, *exbB*, and *semA*, reduce sensitivity to MccE492 in non-producing strains; *tonB* and *exbB* genes had previously been shown to be involved in the uptake of siderophore (Pugsley et al., 1986).

Immunity to MccS depends on the gene *mcsI* encoding a 216-amino acid protein of the CAAX amino terminal protease protein family (Zschüttig et al., 2012).

Immunity to MccPDI involves a protein (McpI) that forms a multimeric cytoplasmic complex with itself; however, the detailed mechanisms remain unknown (Lu et al., 2019). Non-producer resistant *E. coli* strains display a mutation in a critical amino acid residue involved in the interaction of MccPDI with the outer membrane porin F (OmpF). Resistance mutations are present not only in this protein (or in OmpR), but also in AtpA, AtpF (ATP synthase), DsbA, and DsbB (probably involved in microcin-OmpF binding) (Zhao et al., 2015; Lu et al., 2019).

The gene *mtfI* encodes for MccN (Mcc24) immunity (O'Brien and Mahanty, 1994), and as in the previous 2 cases, it is also a protein with several transmembrane domains. MccN is closely related to MccE492, but lacking post-translational modifications (Corsini et al., 2010). The self-immunity phenotype is achieved in MccN producers by reducing the expression of the Mar operon regulator, MarR (multiple-antibiotic-resistance), which results in a phenotype resistance to other antimicrobial compounds (Carlson et al., 2001).

Microcins in *Enterobacteriaceae*

Inside *Enterobacteriaceae*, the production of microcins appears to be preferentially associated with some lineages. The first studies on microcins, using phenotypic methods, had estimated that 15% of *E. coli* strains isolated from newborns were microcin producers (Asensio et al., 1976). In fact, among the *Enterobacteriaceae* genomes of the publicly accessible National Centre for Biotechnology Information database, 34.1% of those corresponding to *E. coli* contain specific microcin gene sequences as defined in the APD3 (see text footnote 1) antimicrobial peptide database (Wang et al., 2016). Most of the various microcins are represented in *E. coli*, and are dominated by MccV (8.58%), MccM (7.43%), MccH47 (7.18%), and MccI47 (4.26%), with all other microcins at a frequency below 2%. Among the *Shigella sonnei* (closely related to *E. coli*) genomes examined, only 1.59% contained microcin genes; however, as in *E. coli*, a large variety of microcin genes were found, dominated by MccV (0.55%) and MccPDI (0.24%). *Shigella flexneri* is infrequently microcinogenic (0.54% of the strains). *S. enterica* has a low number of microcin

producers (1.59%), and predominantly MccV (1.3%). *K. pneumoniae* harbors microcin genes in 4.65% of the strains, mostly MccE492 (4.19%), which was first discovered in this species. This microcin surprisingly was absent in *E. coli*; however, it was also scarcely represented (0.19%) in *Enterobacter cloacae*, a species with a low proportion of microcin producers (0.38%). Although *Citrobacter freundii* has 3.29% of microcinogenic strains, MccS was exclusively found, as in other *Citrobacter* species. However, MccS is the microcin more extensively distributed among Enterobacterial species. MccV was not found in either *Enterobacter* or *Citrobacter*. Another bioinformatic analysis has revealed that microcin C-like adenylated peptides are widespread and are encoded by both Gram-negative (including *Yersinia*) and Gram-positive bacteria, and even by cyanobacteria (Bantysh et al., 2014).

It is tempting to suggest that the high proportion of microcinogenic strains in *E. coli* and the diversity of microcins in this species, compared with other *Enterobacteriaceae*, correspond to a highly competitive lifestyle inside multiple intestinal subniches (microniches) in which even weak microcins can play a substantial ecological role (Majeed et al., 2013). Bacteria with fewer and more specific niches (including intracellularity), such as *Shigella* or *Salmonella*, are much less microcinogenic. In addition, *Klebsiella*, *Citrobacter*, and *Enterobacter*, which have a much broader environmental lifestyle (Sánchez-Valenzuela et al., 2017), have distinctive microcins that are rarely found in *E. coli*, even though the number of available genomic sequences is larger than that of other organisms. Strains of the environmental species *Serratia marcescens* might contain analogs to MccN (Gerc et al., 2014).

Inside *E. coli* species, other authors have applied bioinformatic methods for microcin gene searching. The phylogenetic classification of *E. coli* reflects macro-evolutionary events, bacterial sub-speciation-like processes that take place over long periods of time and space (Wirth et al., 2006; Turrientes et al., 2014). Respectively for the A, B1, B2, and D main *E. coli* phylogenetic lineages, MccV was found in 37, 29, 29, and 23% of the strains; MccM in 10, 12, 34, and 21%; MccB17 in 8, 10, 11, and 19%; MccC7 in 2, 2, 1, and 2%; and MccJ25 and MccL were only found in the B2 (1 and 1%, respectively) and D (2 and 1%, respectively) phylogroups. Thus, MccB17 was most common in phylogroup D, and MccV in phylogroup A (Micenková et al., 2016b).

The association between *E. coli* bacteremia and microcin production appears particularly solid in cases associated with urinary tract infections (Micenková et al., 2017). In the case of phylogroup B2, in which many high-risk clones are located, such as the globally widespread, highly invasive, and antibiotic-resistant clone O25B-ST131, the proportion of microcin producers duplicates the colicin-producing strains (Micenková et al., 2016a,b).

As stated earlier, microcins are not exclusive from *Enterobacteriaceae*. A genome-mining search in anaerobic bacteria has demonstrated that these quantitatively dominant populations of the gut microbiota also produce a significant proportion (approximately 25% in a heterogeneous sample of only 211 genomes) of RiPPs, frequently in conjunction with polyketides or non-ribosomal peptides (Letzel et al., 2014).

Ensembles of Microcins and Colicins

Ensembles of inhibitory entities of microbial origin might exert stronger or broader spectrum inhibitory effects on competing organisms. On the other hand, these ensembles constitute a natural "combination strategy," thus reducing the possibility of selection of single-entity mutants (a mutant resistant to one of the antibacterial compounds will probably be killed by the other one/s). Mutual killing assures biodiversity (Abrudan et al., 2012; Coyte et al., 2015). Finally, asymmetric ensembles could assure the permanence of natural species and clone diversity according to the previously mentioned rock-paper-scissors model (Czárán et al., 2002; Lenski and Riley, 2002; Kirkup and Riley, 2004; Reichenbach et al., 2007), and that might also occur at higher hierarchical levels, as for coexistence of small bacterial communities (**Figure 2**).

The formation of ensembles is certainly facilitated by horizontal gene transfer. Soon after the microcin discovery, the relevance of plasmids in microcin gene transfer was highlighted (Baquero et al., 1978). In fact, most microcins are plasmid-mediated; those of chromosomal location tend to be associated with genomic islands. For instance, the genes involved in the production and immunity of MccM and MccH47 in *E. coli* Nissle, 1917 are located in genomic island I, originated from horizontal genetic transfer (Grozdanov et al., 2004; Bravo-Vázquez, 2009). Microcins can be either chromosomally or plasmid encoded, whereas colicins have been found only on plasmids.

Interestingly, *E. coli* microcinogenic strains frequently express more than 1 microcin (even 4 in the same strain) (Sablé et al., 2003). Such coexistence might foster microcin evolution, including recombinatorial processes facilitated by the modular structure of some of these peptides. This has been suggested for MccV and MccH47, which might recombine genetic sequences corresponding to uptake and toxic modular domains (Azpiroz and Laviña, 2007). The frequent association of the microcins MccH47 and MccM in the same strain can also be favored by common systems of secretion and immunity.

Colicin-colicin, colicin-microcin, and microcin-microcin combinations were found to coincide in particular *E. coli* strains much more often than would be expected by chance. This combination occurs particularly in strains belonging to the phylogroup B2 and with associations between MccH47 and MccM; colicin Ia and MccV; colicins B and M; colicins E1 and M; and colicins E1 and Ia (Gordon and O'Brien, 2006). In colicinogenic enterohaemorrhagic strains, more than one-half of the strains produce multiple colicins, mostly B, E2/E7, and M (Schamberger and Díez-González, 2004). In general, as much as 40% of the *E. coli* strains in the intestine also show coexpression of colicins and microcins (Micenková et al., 2016a). For instance, the microcins MccH47 and MccM are produced by strains that are also producing colicin H (*E. coli* CA56) or colicin G (*E. coli* K58) (Patzer et al., 2003). Coexistence of genetic determinants of microcins and colicins in the same cell provides the opportunity for a recombinatorial exchange of fragments or eventually, the loss of one of these

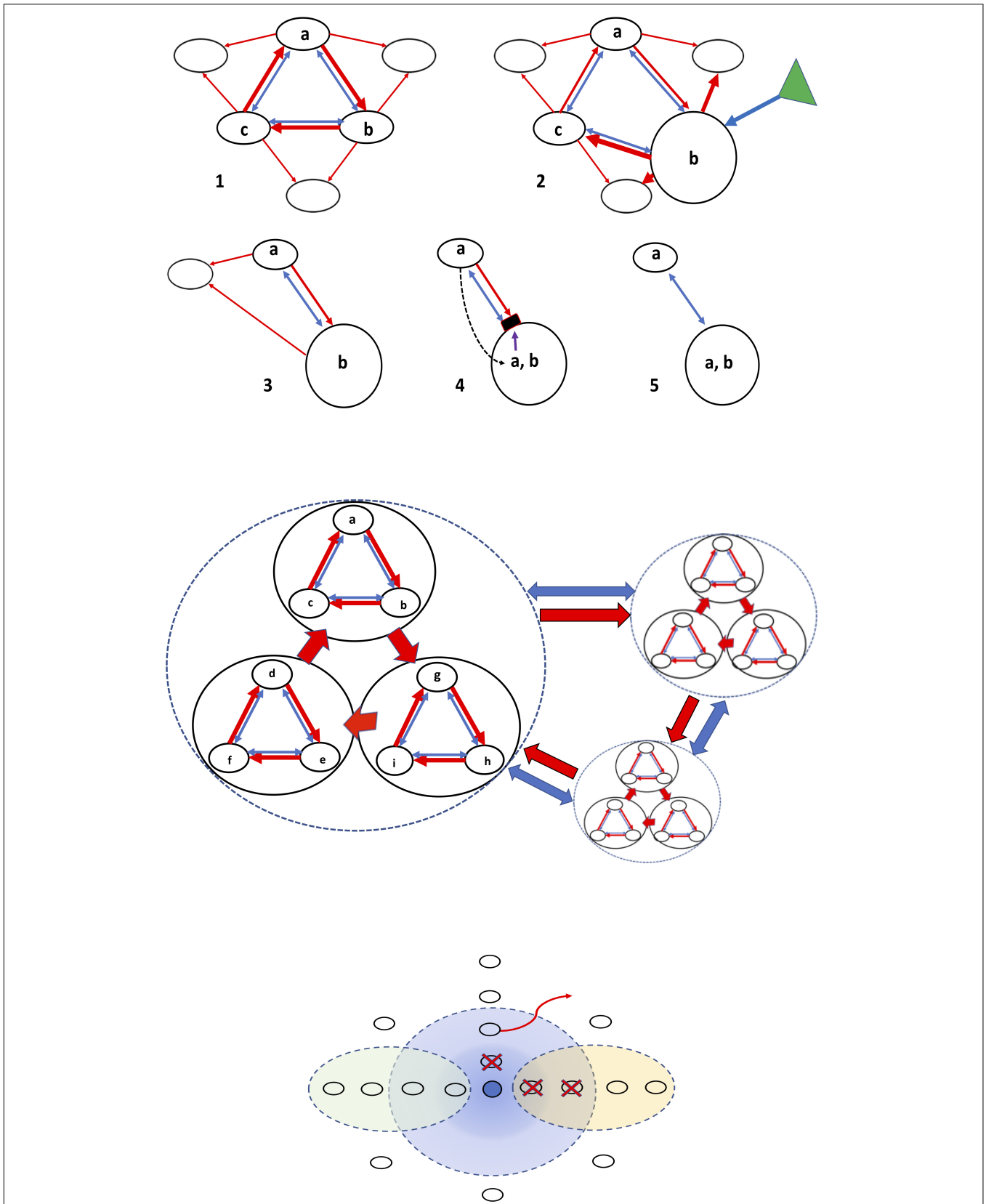

FIGURE 2 | Continued

FIGURE 2 | Structure of bacterial interactions and the influence of chemosphere. The structure and evolution of the microbiome is based in antagonistic and cooperative interactions in a complex chemical environment, the chemosphere. **Top panel**, antagonistic (red arrows) and cooperative (blue arrows) interactions among three bacterial populations producing different inhibitors (a–c). (1) The rock-paper-scissors dynamics, assuring coexistence of all three populations, which is enhanced by the cooperative blue bonds. This ensemble of populations cooperates in the inhibition of other competing bacteria (empty circles). (2) Under the influence of chemosphere (green triangle) one of the populations (b) increases in size, producing the collapse of the former equilibrium (3). In (4), because of the maintained coexistence with (a) and the high population size of (b), resistance to (a) might evolve in (b), or genes encoding (a) can be acquired by (b) via horizontal gene transfer, and a new, simpler coexistence might occur (5). **Middle panel**, the rock-paper-scissors dynamics at a higher hierarchical scale; ensembles of bacterial populations act as single entities able to compete and cooperate with other microbial ensembles. **Lower panel**, in the center, the dark blue circle represents a bacterial population excreting a "blue" microcin. The concentration of this bacteriocin is high near the producer, but diffusion gives rise to progressively lower concentrations (light blue). White circles, bacteria competing with the blue one, which (vertical line) are killed (red X) at high bacteriocin concentrations, or, at lower ones, prevented to be established (red curved arrow) in this area. In the left oval green circle, diffusion of a local chemosphere component antagonizing the production or effect of microcin, now unable to kill the competitors. In the yellow oval circle at the right, diffusion of a chemosphere component enhancing the effect of the bacteriocin, now able to kill even at very low concentrations.

functions. The frequent colicins B and M are usually encoded adjacently on the same plasmid in *E. coli*; in some strains, this plasmid contains a remnant of the MccV operon next to a truncated colicin B activity gene, indicating recombination events between colicin BM and MccV plasmids (Christenson and Gordon, 2009). Moreover, the expression of a colicin (microcin?) from one producer can induce colicin production in a second producer and *vice versa* (Majeed et al., 2011). Secreted amino acid-based inhibitors, such as homoserine-transacetylase inhibitors (historical microcins Mcc93 and Mcc15) or peptidic microcins also coexist in the same strain (Aguilar et al., 1983).

In a previous section we detailed the mechanisms of resistance to microcins in non-microcin producers. Several mechanisms of microcin resistance, such as *E. coli* OmpF mutants, provide cross-resistance to other microcins, colicins, and even bacteriophages and antibiotics. In fact, there is a complex landscape in which resistance to each one of these entities might select for resistance to others. Another example is the mutants in FhuA, the *E. coli* outer membrane receptor for ferrichrome-iron (Destoumieux-Garzón et al., 2005). This protein also acts as the receptor for the phages T1, T5, UC-1, and f80 for colicin M (one of the smallest colicins, 29.4 kDa), and for the antibiotics albomycin, some rifamycins, and the microcin J25. Of course, mutations in common import mechanisms will produce resistance to all inhibitors using these systems; this resistance occurs with colicins and microcins using the active import Ton system (TonB, ExbB, and ExbD proteins), at the expense of energy provided by the proton motive force of the cytoplasmic membrane (Braun et al., 2002). Finally, although not addressed in this review, membrane-permeabilizing antimicrobial peptides present in the gut might sensitize bacterial cells to the effect of some microcins (Pomares et al., 2010).

The Ecological Significance of Microcins

The discovery of microcins was driven by the search for molecular mediators of bacterial displacements in the neonatal gut, and this ecological view was expressed very early in their study (de Lorenzo and Aguilar, 1984). The production of antimicrobial small antibiotic peptides by bacteria appears to be a widespread strategy in maintaining diversity in the intestinal microbiota. For example, bioinformatic detection of biosynthetic gene clusters in microbiota has revealed the numerical dominance of those involved in synthesis of the main microcin-related molecules, RiPPs (Arnison et al., 2013; Donia et al., 2014).

Microcins are eco-active molecules that are active in *Enterobacteriaceae* as mediators of inter- and intraspecies competition. An unintended natural experiment lasting for a century (1917–2019) has provided evidence for this assertion. An oral preparation of the strain *E. coli* Nissle, 1917 (Jacobi and Malfertheiner, 2011) has been used for over 100 years as a useful probiotic preparation for therapy of bacterial intestinal diseases, starting during the First World War (Nissle, 1916, 1918; Henker et al., 2007; Sonnenborn and Schulze, 2009). *E. coli* Nissle, 2017 has been also detected in swine herds, with similar protective effects against pathogens (Kleta et al., 2006). In the first years of the 21st century, it was discovered that *E. coli* Nissle 1917 produce 2 microcins, MccM and MccH47 (Patzer et al., 2003). A mutant *E. coli* Nissle 1917 strain unable to secrete these microcins was unable to outcompete other *E. coli* and *S. enterica* in the inflamed intestine, whereas the wild strain produced this ecological effect (Sassone-Corsi et al., 2016). Evidence for the ecological effects of other microcins are available, such as for MccV (Boubezari et al., 2018), the most abundant among the *E. coli* microcins (see above).

These results confirmed much earlier preliminary work on the effects of microcins on microbial gut interactions (Baquero and Asensio, 1979; Jorge, 1984). It would be expected that microcinogenic *E. coli* strains could reach higher population densities in the gut, facilitating translocation (and consequently bacteremia), and urinary tract infections. This association has already been reported (Azpiroz et al., 2009; Budič et al., 2011).

As previously stated, concerning microcin ecological functions in interbacterial interactions, microcins constitute defensive rather than attack molecules (Rebuffat, 2012). Most microcins are produced and excreted during a stationary phase, and are regulated by, for example, *rpoS* (RNA polymerase sigma factor), *ompR* (DNA-binding transcriptional dual regulator), and *spoT* (bifunctional (p)ppGpp synthase/hydrolase) (Moreno et al., 2002). These populations are, compared with invaders, of a higher population size, facilitating a sufficient local concentration of the inhibitor (Wiener, 1996). High cell density or local inflammation also increases competition for critical nutrients, such as iron, in such a way that favors the uptake of siderophore-microcins (Sassone-Corsi et al., 2016). In general, there is

always a link between nutritional stress and competitive behavior in biology.

MICROCINS IN THE INTESTINAL CHEMOSPHERE

In this review, the role of microcins as effectors of intermicrobial interactions has been highlighted. At the same time, we wanted to relativize the view of "single molecules" as the main characters of bacterial displacements, and in general, of microbial ecology. As previously stated, the microecological effects (microbe-microbe and microbe-environment) of individual cell metabolism might be critical in shaping the interactive dynamics and evolution of microbial ecosystems (Klitgord and Segrè, 2011). According to the postulate of "Molecular Ecology" (Asensio, 1976), any particular molecule inhibiting bacterial growth is necessarily surrounded by many others, which might have effects on the growth or inhibition of bacterial populations and/or in the production or stability of this molecule. The secretion of amino acids and amino acid derivatives with inhibitory activity might modify the uptake, export, and biosynthesis of bacterial peptides (Payne, 1977). Amino acid-based inhibitors (historically included as microcins) share with some peptidic microcins the "Trojan horse" strategy of mimicking essential nutrients (such as essential amino acids or iron-siderophores to penetrate inside the target cell).

The Eco-Active Chemosphere

We have used the term "eco-active" to designate the part of the chemosphere constituted by chemicals able to play a role as factors of intestinal microbial ecology; i.e., growth-promoting molecules, growth-inhibiting (or killer) substances, and chemicals influencing bacterial genetic variation, genetic regulation, bacterial interactions, and colonization efficiency (**Table 1**). We are far from understanding in detail how this ensemble of chemical factors determines the microecological structure of the intestinal microbiota. A major limitation is the lack of knowledge about the spatial structure and organization of microenvironments (Baquero, 2015). It can be predicted that ensembles of bioactive molecules occur in microcompartments of the gut, which are dominated by particular microbial ensembles (Earle et al., 2015). How this constellation of molecules interacts and influences bacterial populations is an inconceivably complex issue. The possibility of intermolecular interactions between these molecules and with the microbiota depends on the "physics" and spatial dynamics of the system (intestinal ecophysics). For instance, the non-directional peristaltic movements of the colonic content assure complex mixing of bacterial populations (Ley et al., 2006) and of molecules from the chemosphere. However, bacterial populations in the gut probably interact at the microscopic scale inside clumps or aggregates, and these ensembles have their own chemospheres (Sonnenburg et al., 2005). In fact, specific chemospheres should be part of the "common niches" constructed by microbial

TABLE 1 | Compounds in the intestinal chemosphere with antimicrobial effects, and their basic mechanisms of action.

Polyphenols	
• Quercetin	
• Chlorogenic acids	Bacterial membrane permeabilization
Short-chain fatty acids	
• Acetate	Lowering pH
• Propionate	pH-independent effects
• Butyrate	
Organic salts	
• Lactate	Lowering pH
• Citrate	pH-independent effects
Bile acids, lipids	
• Secondary bile acids and terpenoids	Disruption of cell membranes
• Short and medium-chain saturated fatty acids	Indirect effect: modulation of local innate immunity
• Long-chain unsaturated fatty acids	
• Fatty alcohols and fatty acid monoglycerides	
Polyaminated molecules	
• Spermidine, homospermidine, and norspermidine	Disruption of cell membranes
• Putrescine, cadaverine, and 1,3-diaminopropane	Regulation of bacteriocin production
Intercellular signaling molecules	
• Homoserine lactones	Bacterial membrane permeabilization
• Indole-based signaling molecules	Quorum-sensing signaling
Haem catabolism	
• Unconjugated bilirubin	Unknown, antioxidant effects?
• Biliverdin	
Host defense secreted antimicrobials	
• α-defensins, β-defensins, and cathelicidins	Antimicrobial peptides and disruption of cell membranes
• C-type lectins RNAses	Protective carbohydrate-bonding proteins Cytokine induction and endosomal pathways suppressing bacteria
Immunoglobulins	
• Secretory IgA	Capture bacterial cells (immune exclusion), facilitating immunological, and physical removal of bacteria
Bacteriocins	
• Colicins (class I–III)	Membrane pore formation and nuclease activity
• Historical amino acid-based microcins	Interference with amino acid metabolism
• Class I peptidic microcins (post-translational thiazole/oxazole-modified microcins)	Membrane pore formation, impairing cellular proton channel, protein synthesis inhibition, inhibition of DNA gyrase,inhibition of cellular respiration, plasmid post-segregational killing, and bacterial persistence phenotype
• Class IIa peptidic microcins	
• Class IIb peptidic microcins	

consortia. However, all local chemospheres are open and fluctuating systems and are therefore influenced by the larger chemosphere in which they are embedded. Fluctuations in the chemosphere as a result of dietary changes and the host's physiological, pathological, or therapeutic circumstances likely influence the complex microbiota. Combined cocausal effects are eventually able to influence the production, release, or the activity of growth-promoting and inhibitory substances. Not being part of the natural chemosphere, chemotherapeutic substances directly stressing the microbiota (such as antimicrobial agents), affecting the functionality of the intestine (such as drugs influencing peristalsis, cholagogues, or antacids) or influencing host immunity (such as corticoids, immunodepressive agents) could alter (stress) intestinal microecology and favor the bacterial expression of eco-active substances (Taymaz-Nikerel et al., 2013; Baquero, 2015; Gillis et al., 2018).

Microcin Activity in Their Natural Chemosphere

Most of the studies published on the antimicrobial activity of microcins have been based on *in vitro* studies, in highly simplified environments. The intestinal chemosphere, variable in time and space, might determine particular configurations of interacting bacterial populations, and therefore the local effects of microcins are difficult to anticipate. *In vitro* models of the intestinal environment have been explored to predict the effect of microcins under gut conditions. For instance, MccJ25 was relatively stable under gastric conditions, but not in the duodenum conditions, being degraded by elastase I, and less efficiently α-chymotrypsin (Naimi et al., 2018). It has been shown that microcin inhibition does not occur in a rich nutrient system containing mucins or nucleic acids, as these molecules may bind peptides and suppress their antimicrobial activity (Ran et al., 2017). In the above section "The Intestinal Chemosphere and the Molecular Ecology of the Gut," the basic compounds serving as bacterial nutrients in the chemosphere were considered. Changes in their absolute or relative concentrations should modify the growth rate and cell number of bacterial populations, and consequently their susceptibility to growth inhibitors or their ability to act as inhibitors of other populations (**Figure 2**). In **Table 1** we summarize the main compounds in the intestinal chemosphere possessing antimicrobial activity. Certainly, the final effect of a microcin on a bacterial population depends on compounds facilitating bacterial growth, such as those acting as nutrients (reviewed in section "The Intestinal Chemosphere: Molecular Ecology"). Of particular importance are those nutrients that are critical but present at very low concentrations, which constitute important competition attractors, such as iron. In fact, siderophores frequently act in the internalization of microcins. Most importantly, microcins probably interact with many other bacterial inhibitors in the gut, either in a competitive or cooperative manner; however, this remains an almost unexplored field of research. The list of chemicals with inhibitory activity in **Table 1** allows us to distinguish 2 main types of inhibitors. Many of them correspond to chemicals altering or disrupting bacterial membranes, likely increasing permeability to external compounds. A few (mostly microcins and colicins) have more specific modes of action, targeting cellular processes, such as protein synthesis or DNA replication, but also altering membrane integrity. We can easily conceive of a possible synergy between compounds altering cellular structures (membranes) and those inhibiting specific cellular processes, generally with higher intrinsic activity. This distinction has previously been considered by other authors, suggesting that bacteria from the gut seem to produce many bacteriocins with low activity and small number of highly effective bacteriocins (Drissi et al., 2015). Overall, the activity of microcins might be modulated by the chemosphere composition, which constitutes the main message of this review. Interventions to specifically modify the human and animal chemosphere will likely have important consequences in the epidemiology of normal and pathogenic microbiota, and in controlling antibiotic resistance (Baquero et al., 2013; Kashyap et al., 2013b). New developments in the study of the complex chemical microecology of the gut, the field of Asensio's "Molecular Ecology" (Asensio, 1976), are certainly needed to obtain more realistic conclusions about the role of microcins in the interactive processes influencing the structure of microbiota.

AUTHOR CONTRIBUTIONS

FB and DB-V wrote the manuscript. All authors listed have made a substantial, direct and intellectual contribution to the work, and approved it for publication.

FUNDING

FB was supported by a grant from the Madrid Regional Government and the Structural Funds of the European Union (InGEMICS-C; S2017/BMD-3691), the CIBER (CIBER in Epidemiology and Public Health, CIBERESP; CB06/02/0053), PI15/00818, integrated in the Spanish 2013–2016 R+D+i State Plans, and cofounded by the Instituto de Salud Carlos III and the European Regional Development Fund (ERDF, "A way to achieve Europe"). RC is the recipient of the Vertex grant IIS-2017-106179.

ACKNOWLEDGMENTS

This review is dedicated to Felipe Moreno, the key pioneer in microcin genetics; also to two of the initial but essential workers on biochemistry and early taxonomy of microcins (based on cross-activity and resistance), respectively, José-Claudio Pérez-Díaz and Flora Sánchez. Most importantly, we honor the memory of the biochemist and microbe-lover Carlos Asensio (1925–1982), who co-discovered microcins and coined the concept of "Molecular Ecology." The detailed work of three outstanding referees significantly increased the quality of this review.

REFERENCES

Abrudan, M. I., Brown, S., Rozen, D. E. (2012). Killing as means of promoting biodiversity. *Biochem. Soc. Trans.* 40, 1512–1516. doi: 10.1042/BST20120196

Adelman, K., Yuzenkova, J., La Porta, A., Zenkin, N., Lee, J., Lis, J. T., et al. (2004). Molecular mechanism of transcription inhibition by peptide antibiotic microcin J25. *Mol. Cell* 14, 753–762. doi: 10.1016/j.molcel.2004.05.017

Agarwal, V., Metlitskaya, A., Severinov, K., and Nair, S. K. (2011). Structural basis for microcin C7 inactivation by the MccE acetyltransferase. *J. Biol. Chem.* 286, 21295–21303. doi: 10.1074/jbc.M111.226282

Agarwal, V., Tikhonov, A., Metlitskaya, A., Severinov, K., and Nair, S. K. (2012). Structure and function of a serine carboxypeptidase adapted for degradation of the protein synthesis antibiotic microcin C7. *Proc. Natl. Acad. Sci. U.S.A.* 109, 4425–4430. doi: 10.1073/pnas.1114224109

Aguilar, A., Baquero, F., Martínez, J. L., and Asensio, C. (1983). Microcin 15n: a second antibiotic from *Escherichia coli* LP15. *J. Antibiot.* 36, 325–327. doi: 10.7164/antibiotics.36.325

Aguilar, A., Pérez-Díaz, J. C., Baquero, F., and Asensio, C. (1982). Microcin 15m from *Escherichia coli*: mechanism of antibiotic action. *Antimicrob. Agents Chemother.* 121, 381–386. doi: 10.1128/aac.21.3.381

Aliashkevich, A., Alvarez, L., and Cava, F. (2018). New insights into the mechanisms and biological roles of D-amino acids in complex eco-systems. *Front. Microbiol.* 9:683. doi: 10.3389/fmicb.2018.00683

Allali, N., Afif, H., Couturier, M., and Van Melderen, L. (2002). The highly conserved TldD and TldE proteins of *Escherichia coli* are involved in microcin B17 processing and in CcdA degradation. *J. Bacteriol.* 184, 3224–3231. doi: 10.1128/jb.184.12.3224-3231.2002

Álvarez, L., Aliashkevich, A., de Pedro, M. A., and Cava, F. (2018). Bacterial secretion of D-arginine controls environmental microbial biodiversity. *ISME J.* 12, 438–450. doi: 10.1038/ismej.2017.176

Alvarez-Sieiro, P., Montalbán-López, M., Mu, D., and Kuipers, O. (2016). Bacteriocins of lactic acid bacteria: extending the family. *Appl. Microbiol. Biotechnol.* 7, 2939–2951. doi: 10.1007/s00253-016-7343-9

Angelakis, E., Merhej, V., and Raoult, D. (2013). Related actions of probiotics and antibiotics on gut microbiota and weight modification. *Lancet Infect. Dis.* 13, 889–899. doi: 10.1016/S1473-3099(13)70179-8

Aoki, R., Kamikado, K., Suda, W., Takii, H., and Mikami, Y., Suganuma, N. et al. (2017). A proliferative probiotic *Bifidobacterium* strain in the gut ameliorates progression of metabolic disorders via microbiota modulation and acetate elevation. *Sci. Rep.* 7:43522. doi: 10.1038/srep43522

Arnison, P. G., Bibb, M. J., Bierbaum, G., Bowers, A. A., Bugni, T. S., and Bulaj, G. et al. (2013). Ribosomally synthesized and post-translationally modified peptide natural products: overview and recommendations for a universal nomenclature. *Nat. Prod. Rep.* 30, 108–160. doi: 10.1039/c2np20085f

Asensio, C. (1976). Molecular ecology. in *Reflections in Biochemistry* eds A. Kornberg, BL. Horecker, L. Cornudella, J. Oro (Pergamon Press, Oxford), 235–240.

Asensio, C., Pérez-Díaz, J. C., Martínez, M. C., and Baquero, F. (1976). A new family of low molecular weight antibiotics from enterobacteria. *Biochem. Biophys. Res. Comm.* 69,7–14. doi: 10.1016/s0006-291x(76)80264-1

Azpiroz, M. F., and Laviña, M. (2007). Modular structure of microcin H47 and colicin V. *Antimicrob. Agents Chemother.* 51, 2412–2419. doi: 10.1128/aac.01606-06

Azpiroz, M. F., Poey, M. E., and Laviña, M. (2009). Microcins and urovirulence in *Escherichia coli*. *Microb. Pathog.* 47, 274–280. doi: 10.1016/j.micpath.2009.09.003

Azpiroz, M. F., Rodrìguez, E., and Laviña, M. (2001). The structure, function, and origin of the microcin H47 ATP-binding cassette exporter indicate its relatedness to that of colicin V. A*ntimicrob. Agents Chemother*. 45, 969–972. doi: 10.1128/aac.45.3.969-972.2001

Bachracht, U., and Weinstein, A. J. (1970). Effect of aliphatic polyamines on growth and macromolecular syntheses in bacteria. *J. Gen. Microbiol.* 60, 159–165. doi: 10.1099/00221287-60-2-159

Bäckhed, F., and Crawford, P. A. (2010). Coordinated regulation of the metabolome and lipidome at the host-microbial interface. *Biochim. Biophys. Acta* 1801, 240–245. doi: 10.1016/j.bbalip.2009.09.009

Balciunas, E. M., Martinez, F. A. C., Todorov, S. D., de Melo Franco, B. D. G., Converti, A., and de Souza Oliveira, R. P. (2013). Novel biotechnological applications of bacteriocins: a review. *Food Control* 32, 134–142. doi: 10.1016/j.foodcont.2012.11.025

Bantysh, O., Serebryakova, M., Makarova, K. S., Dubiley, S., Datsenko, K. A., and Severinov, K. (2014). Enzymatic synthesis of bioinformatically predicted microcin C-like compounds encoded by diverse bacteria. *mBio* 5:e01059-14. doi: 10.1128/mBio.01059-14

Baquero, F. (2012). Metagenomic epidemiology: a public health need for the control of antimicrobial resistance. *Clin. Microbiol. Infect.* 18, 67–73. doi: 10.1111/j.1469-0691.2012.03860.x

Baquero, F. (2015). Causes and interventions: need of a multiparametric analysis of microbial ecobiology. Characterizing microenvironments. *Environ. Microbiol. Rep.* 7, 13–14. doi: 10.1111/1758-2229.12242

Baquero, F. (2018). Causality in biological transmission: forces and energies. *Microbiol. Spectrum* 6:MTB-0018-2016.

Baquero, F., and Asensio, C. (1979). Microcins as ecological effectors in human intestinal flora: preliminary findings. in *New Criteria for Antimicrobial Therapy: Maintenance of Digestive Tract Colonization Resistance*, eds D. van der Waaij, J. Verhoef (Excerpta Medica, Amsterdam). 90–94.

Baquero, F., Bouanchaud, D., Martinez-Perez, M. C., and Fernandez, C. (1978). Microcin plasmids: a group of extrachromosomal elements coding for low-molecular-weight antibiotics in *Escherichia coli*. *J. Bacteriol.* 135, 342–347.

Baquero, F., and Moreno, F. (1984). The microcins. *FEMS Microbiol. Lett.* 23, 117–124.

Baquero, F., Moreno, F., and Kolter, R. (1984). Bacterial microcins: a new family of antibiotics. *APUA Newslett.* 2, 1–7.

Baquero, F., and Nombela, C. (2012). The microbiome as a human organ. *Clin. Microbiol. Infect.* 18, 2–4. doi: 10.1111/j.1469-0691.2012.03916.x

Baquero, F., Tedim, A. S. P., and Coque, T. M. (2013). Antibiotic resistance shaping multi-level population biology of bacteria. *Front. Microbiol.* 4:15. doi: 10.3389/fmicb.2013.00015

Baquero, F., and Asensio, C. (1976). Microcinas. in *Aspectos Actuales de las Relaciones Huésped-Parásito e Intermicrobianas*, eds Portolés A, Baquero, F. eds (Basic Monographies of the Spanish Society of Microbiology: Madrid). 2, 169–196.

Bardaweel, S. K., Abu-Dahab, R., and Almomani, N. F. (2013). An *in vitro* based investigation into the cytotoxic effects of D-amino acids. *Acta Pharm.* 63, 467–478. doi: 10.2478/acph-2013-0032

Bastos, M., Coelho, M., and Santos, O. (2015). Resistance to bacteriocins producedby Gram-positive bacteria. *Microbiology* 161, 683–700. doi: 10.1099/mic.0.082289-0

Beis, K., and Rebuffat, S. (2019). Multifaceted ABC transporters associated to microcin and bacteriocin export. *Res. Microbiol.* S0923-2508(19)30081-6. doi: 10.1016/j.resmic.2019.07.002

Ben-Amor, K., Heilig, H., Smidt, H., Vaughan, E. E., Abee, T., and de Vos, W. M. (2005). Genetic diversity of viable, injured, and dead fecal bacteria assessed by fluorescence-activated cell sorting and 16S rRNA gene analysis. *Appl. Environ. Microbiol.* 71, 4679–4689 doi: 10.1128/aem.71.8.4679-4689.2005

Benveniste, R., and Davies, J. (1973). Aminoglycoside antibiotic-inactivating enzymes in actinomycetes similar to those present in clinical isolates of antibiotic-resistant bacteria. *Proc. Natl. Acad. Sci. U.S.A.* 70, 2276–2280. doi: 10.1073/pnas.70.8.2276

Bergsson, G., Hilmarsson, H., and Thormar, H. (2011). Antibacterial, antiviral and antifungal activities of lipids. in *Lipids and Essential Oils as Antimicrobial Agents*. ed H. Thormar (John Wiley and Sons, Ltd.: Chichester).

Bhattarai, Y., Williams, B. B., Battaglioli, E. J., Whitaker, W. R., Till, L., Grover, M., et al. (2018). Gut microbiota-produced tryptamine activates an epithelial G-protein-coupled receptor to increase colonic secretion. *Cell Host Microb.* 23, 775–785. doi: 10.1016/j.chom.2018.05.004

Bieler, S., Silva, F., Soto, C., and Belin, D. (2006). Bactericidal activity of both secreted and non-secreted microcin E492 requires the mannose permease. *J. Bacteriol.* 188, 7049–7061. doi: 10.1128/jb.00688-06

Biswas, N. N., Kutty, S. K., Barraud, N., Iskander, G. M., Griffith, R., and Rice, S. A. et al. (2015). Indole-based novel small molecules for the modulation of bacterial signaling pathways. *Org. Biomol. Chem.* 13, 925–933. doi: 10.1039/c4ob02096k

Bivar, X. K. (2018). Bacterial interspecies quorum sensing in the mammalian gut microbiota. *C. R. Biol.* 341 297–299. doi: 10.1016/j.crvi.2018.03.006

Blanchet, M., Borselli, D., and Brunel, J. M. (2016). Polyamine derivatives: a revival of an old neglected scaffold to fight resistant Gram-negative bacteria? *Future Med. Chem. Future Sci.* 8, 963–973. doi: 10.4155/fmc-2016-0011

Boubezari, M. T., Idoui, T., Hammami, R., Fernandez, B., Gomaa, A., and Fliss, I. (2018). Bacteriocinogenic properties of *Escherichia coli* P2C isolated from pig gastrointestinal tract: purification and characterization of microcin V. *Arch. Microbiol.* 200 771–782. doi: 10.1007/s00203-018-1482-6

Boyer, E. A., and Tai, P. C. (1998). Characterization of the *cvaA* and *cvi* promoters of the colicin V export system: iron-dependent transcription of *cvaA* is modulated by downstream sequences. *J. Bacteriol.* 180, 1662–1672.

Braffman, N. R., Piscotta, F. J., Hauver, J., Campbell, E. A., Link, A. J., and Darst, S. A. (2019). Structural mechanism of transcription inhibition by lasso peptides microcin J25 and capistruin. *Proc. Natl Acad. Sci. U.S.A.* 116, 1273–1278. doi: 10.1073/pnas.1817352116

Braun, V., Patzer, S. I., and Hantke, K. (2002). Ton-dependent colicins and microcins: modular design and evolution. *Biochimie* 84, 365–380. doi: 10.1016/s0300-9084(02)01427-x

Bravo-Vázquez, D. A. (2009). *Caracterización genética y funcional del sistema microcina MccH47/MccM en el probiótico Escherichia coli Nissle 1917*. Repository Doctoral Theses, Universidad Autónoma de Madrid: Madrid.

Budiè, M., Rijavec, M., Petkovšek, Ž., and Žgur-Bertok, D. (2011). *Escherichia coli* bacteriocins: antimicrobial efficacy and prevalence among isolates from patients with bacteraemia. *PLoS One* 6:e28769. doi: 10.1371/journal.pone.0028769

Carlson, S. A., Frana, T. S., and Griffith, R. W. (2001). Antibiotic resistance in *Salmonella enterica* serovar Typhimurium exposed to microcin-producing *Escherichia coli*. *Appl. Environ. Microbiol.* 67, 3763–3766. doi: 10.1128/aem.67.8.3763-3766.2001

Chang, H., Drouillard, N., Fayed, S., Minhas, A., and Song, R. (2003). Investigating the effects of DNA packaging on natural mutation frequency. *J. Exp. Microbiol. Immunol.* 3, 78–86.

Chao, L., and Levin, B. R. (1981). Structured habitats and the evolution of anticompetitor toxins in bacteria. *Proc. Nat. Acad. Sci. U.S.A.* 78, 6324–6328. doi: 10.1073/pnas.78.10.6324

Chehade, H., and Braun, V. (1988). Iron-regulated synthesis and uptake of colicin V. *FEMS Microbiol. Lett.* 52, 177-182.

Chen, H., Fang, Q., Tu, Q., Liu, C., Yin, J., and Yin, Y. et al. (2018). Identification of a contact-dependent growth inhibition system in the probiotic *Escherichia coli* Nissle 1917. *FEMS Microbiol. Lett.* 365:fny102. doi: 10.1093/femsle/fny102

Cheng, K., Ning, Z., Zhang, X., Li, L., Liao, B., Mayne, J., et al. (2017). MetaLab: an automated pipeline for metaproteomic data analysis. *Microbiome* 5:157. doi: 10.1186/s40168-017-0375-2

Chikindas, M. L., Weeks, R., Drider, D., Chistyakov, V. A., and Dicks, L. M. (2018). Functions and emerging applications of bacteriocins. *Curr. Opin. Biotechnol.* 49, 23–28. doi: 10.1016/j.copbio.2017.07.011

Christenson, J. K., and Gordon, D. M. (2009). Evolution of colicin BM plasmids: the loss of the colicin B activity gene. *Microbiology* 155, 1645–1655. doi: 10.1099/mic.0.026666-0

Chung, LK, and Raffatellu, M. (2019). G.I. pros: antimicrobial defense in the gastrointestinal tract. *Semin. Cell Dev. Biol.* 88, 129–137. doi: 10.1016/j.semcdb.2018.02.001

Clarke, D. J., and Campopiano, D. J. (2007). Maturation of McjA precursor peptide into active microcin MccJ25. *Org. Biomol. Chem.* 5, 2564–2566.

Clifford, M. N., Jaganath, I. B., Ludwig, I. A., and Crozier, A. (2017). Chlorogenic acids and the acyl-quinic acids: discovery, biosynthesis, bioavailability and bioactivity. *Nat. Prod. Rep.* 34, 1391–1421. doi: 10.1039/c7np00030h

Collin, F., and Maxwell, A. (2019). The microbial toxin microcin B17: prospects for the development of new antibacterial agents. *J. Mol. Biol.* 431, 3400–3426. doi: 10.1016/j.jmb.2019.05.050

Corfield, A. P. (2018). The interaction of the gut microbiota with the mucus barrier in health and disease in human. *Microorganisms* 6:E78. doi: 10.3390/microorganisms6030078

Cornut, G., Fortin, C., and Soulières, D. (2008). Antineoplastic properties of bacteriocins: revisiting potential active agents. *Am. J. Clin. Oncol.* 31:399–404. doi: 10.1097/COC.0b013e31815e456d

Corr, S. C., Li, Y., Riedel, C. U., O'Toole, P. W., Hill, C., and Gahan, C. G. (2007). Bacteriocin production as a mechanism for the antiinfective activity *of Lactobacillus salivarius* UCC118. *Proc. Natl. Acad. Sci. U.S.A.* 104, 7617–7621. doi: 10.1073/pnas.0700440104

Corsini, G., Karahanian, E., Tello, M., Fernandez, K., Rivero, D., and Saavedra, J. M., et al. (2010). Purification and characterization of the antimicrobial peptide microcin N. *FEMS Microbiol. Lett.* 312, 119–125. doi: 10.1111/j.1574-6968.2010.02106.x

Cotter, P. D., Hill, C., and Ross, R. P. (2005). Food microbiology: bacteriocins: developing innate immunity for food. *Nat. Rev. Microbiol.* 3, 777–788. doi: 10.1038/nrmicro1273

Cotter, P. D., Ross, R. P., and Hill, C. (2013). Bacteriocins – a viable alternative to antibiotics? *Nat. Rev. Microbiol.* 11, 95–105. doi: 10.1038/nrmicro2937

Coyte, K. Z., Schluter, J., and Foster, K. R. (2015). The ecology of the microbiome: networks, competition, and stability. *Science* 350, 663–666. doi: 10.1126/science.aad2602

Cushnie, T. P., and Lamb, A. J. (2011). Recent advances in understanding the antibacterial properties of flavonoids. *Int. J. Antimicrob. Aging* 38, 99–107. doi: 10.1016/j.ijantimicag.2011.02.014

Czárán, T. L., Hoekstra, R. F., and Pagie, L. (2002). Chemical warfare between microbes promotes biodiversity. *Proc. Natl. Acad. Sci. U.S.A.* 99, 786–790. doi: 10.1073/pnas.012399899

Daniel, R. M., Cowan, D. A., Morgan, H. W., and Curran, M. P. (1982). A correlation between protein thermostability and resistance to proteolysis. *Biochem. J.* 207, 641–644. doi: 10.1042/bj2070641

de Lorenzo, V. (1984). Isolation and characterization of microcin E492 from *Klebsiella pneumoniae*. *Arch. Microbiol.* 139, 72–75. doi: 10.1007/bf00692715

de Lorenzo, V., and Aguilar, A. (1984). Antibiotics from gram-negative bacteria: do they play a role in microbial ecology? *Trends Biochem. Sci.* 9, 266–269. doi: 10.1016/0968-0004(84)90161-0

del Castillo, F. J., del Castillo, I., and Moreno, F. (2001). Construction and characterization of mutations at codon 751 of the *Escherichia coli* gyrB gene that confer resistance to the antimicrobial peptide microcin B17 and alter the activity of DNA gyrase. *J. Bacteriol.* 183, 2137–2140. doi: 10.1128/jb.183.6.2137-2140.2001

Delgado, M. A., Solbiati, J. O., Chiuchiolo, M. J., Farías, R. N., and Salomón, R. A. (1999). *Escherichia coli* outer membrane protein TolC is involved in production of the peptide antibiotic microcin J25. *J. Bacteriol.* 181, 1968–1970.

den Besten, G., van Eunen, K., Groen, A. K., Venema, K., Reijngoud, D. J., and Bakker, B. M. (2013). The role of short-chain fatty acids in the interplay between diet, gut microbiota, and host energy metabolism. *J. Lipid Res.* 54, 2325–2340. doi: 10.1194/jlr.R036012

Destoumieux-Garzón, D., Duquesne, S., Peduzzi, J., Goulard, C., Desmadril, M., Letellier, L., et al. (2005). The iron-siderophore transporter FhuA is the receptor for the antimicrobial peptide microcin J25: role of the microcin Val11–Pro16 β-hairpin region in the recognition mechanism. *Biochem. J.* 389, 869–876. doi: 10.1042/bj20042107

Destoumieux-Garzón, D., Peduzzi, J., Thomas, X., Djediat, C., and Rebuffat, S. (2006). Parasitism of iron-siderophore receptors of *Escherichia coli* by the siderophore-peptide microcin E492m and its unmodified counterpart. *Biometals* 19, 181–191. doi: 10.1007/s10534-005-4452-9

Dicks, L. M., Dreyer, L., Smith, C., and Van Staden, A. D. (2018). A review: the fate of bacteriocins in the human gastro-intestinal tract: do they cross the gut–blood barrier? *Front. Microbiol.* 9:2297. doi: 10.3389/fmicb.2018.02297

Donia, M. S., Cimermancic, P., Schulze, C. J., Wieland Brown, L. C., and Martin, J. Mitreva, M. et al. (2014). A systematic analysis of biosynthetic gene clusters in the human microbiome reveals a common family of antibiotics. *Cell* 158, 1402–1414. doi: 10.1016/j.cell.2014.08.032

Donia, M. S., and Fischbach, M. A. (2015). Small molecules from the human microbiota. *Science* 349:1254766. doi: 10.1126/science.1254766

Drissi, F., Buffet, S., Raoult, D., and Merhej, V. (2015). Common occurrence of antibacterial agents in human intestinal microbiota. *Front. Microbiol.* 6:441. doi: 10.3389/fmicb.2015.00441

Ducasse, R., Yan, K. P., Goulard, C., Blond, A., Li, Y., Lescop, E., et al. (2012). Sequence determinants governing the topology and biological activity of a lasso peptide, microcin J25. *ChemBioChem* 13, 371–380. doi: 10.1002/cbic.201100702

Duncan, S. H., Louis, P., Thomson, J. M., and Flint, H. J. (2009). The role of pH in determining the species composition of the human colonic microbiota. *Environ. Microbiol.* 11, 2112–2122. doi: 10.1111/j.1462-2920.2009.01931.x

Dupont, A., Heinbockel, L., Brandenburg, K., and Hornef, M. W. (2014). Antimicrobial peptides and the enteric mucus layer act in concert to protect the intestinal mucosa. *Gut Microb.* 5, 761–765. doi: 10.4161/19490976.2014.972238

Duquesne, S., Destoumieux-Garzón, D., Peduzzi, J., and Rebuffat, S. (2007a). Microcins, gene-encoded antibacterial peptides from enterobacteria. *Nat. Prod. Rep.* 24, 708–734.

Duquesne, S., Petit, V., Peduzzi, J., and Rebuffat, S. (2007b). Structural and functional diversity of microcins, gene-encoded antibacterial peptides from enterobacteria. *J. Mol. Microbiol. Biotech.* 13, 200–209. doi: 10.1159/000104748

Durrett, R., and Levin, S. (1997). Allelopathy in spatially distributed populations. *J. Theor. Biol.* 185, 165–171. doi: 10.1006/jtbi.1996.0292

Earle, K. A., Billings, G., Sigal, M., Lichtman, J. S., Hansson, G. C., Elias, J. E., et al. (2015). Quantitative imaging of gut microbiota spatial organization. *Cell Host Microb.* 18, 478–488. doi: 10.1016/j.chom.2015.09.002

Eberhart, L. J., Deringer, J. R., Brayton, K. A., Sawant, A. A., Besser, T. E., and Call, DR. (2012). Characterization of a novel microcin that kills enterohemorrhagic *Escherichia coli* O157:H7 and O26. *Appl. Environ. Microbiol.* 78, 6592–6599. doi: 10.1128/AEM.01067-12

Erickson, A. R., Cantarel, B. L., Lamendella, R., Darzi, Y., Mongodin, E. F., and Pan, C. et al. (2012). Integrated metagenomics/metaproteomics reveals human host-microbiota signatures of Crohn's disease. *PLoS One* 7:e49138. doi: 10.1371/journal.pone.0049138

Fedorec, A. J. H., Ozdemir, T., Doshi, A., Ho, Y. K., Rosa, L., Rutter, J., et al. (2019). Two new plasmid post-segregational killing mechanisms for the implementation of synthetic gene networks in *Escherichia coli*. *iScience* 14, 323–334. doi: 10.1016/j.isci.2019.03.019

Foster, K. R., and Bell, T. (2012). Competition, not cooperation, dominates interactions among culturable microbial species. *Curr. Biol.* 22, 1845–1850. doi: 10.1016/j.cub.2012.08.005

Fredericq, P., and Levine, M. (1947). Antibiotic interrelationships among the enteric group of bacteria. *J. Bacteriol.* 54:785.

Frick, K. K., Quackenbush, R. L., and Konisky, J. (1981). Cloning of immunity and structural genes for colicin V. *J. Bacteriol.* 148, 498–507.

Friedman, E. S., Li, Y., Shen, T. D., Jiang, J., Chau, L., Adorini, L., et al. (2018). FXR-dependent modulation of the human small intestinal microbiome by the bile acid derivative obeticholic acid. *Gastroenterology* 155, 1741–1752. doi: 10.1053/j.gastro.2018.08.022

Fukuda, S., Toh, H., Hase, K., Oshima, K., Nakanishi, Y., and Yoshimura, K. et al. (2011). *Bifidobacteria* can protect from enteropathogenic infection through production of acetate. *Nature* 469, 543–547. doi: 10.1038/nature09646

Gaillard-Gendron, S., Vignon, D., Cottenceau, G., Graber, M., Zorn, N., van Dorsselaer, A., et al. (2000). Isolation, purification and partial amino acid sequence of a highly hydrophobic new microcin named microcin L produced by *Escherichia coli*. *FEMS Microbiol. Lett.* 193, 95–98. doi: 10.1016/s0378-1097(00)00467-5

Gallo, R. L., and Hooper, L. V. (2012). Epithelial antimicrobial defence of the skin and intestine. *Nat. Rev. Immunol.* 12, 503–516. doi: 10.1038/nri3228

Galván, A. E., Chalon, M. C., Schurig-Briccio, L. A., Salomón, R. A., Minahk, C. J., Gennis, R. B., et al. (2018). Cytochromes bd-I and bo3 are essential for the bactericidal effect of microcin J25 on *Escherichia coli* cells. *Biochim. Biophys. Acta Bioenerget.* 1859, 110–118. doi: 10.1016/j.bbabio.2017.10.006

García-Bayona, L., and Comstock, L. E. (2018). Bacterial antagonism in host-associated microbial communities. *Science* 361:eaat2456. doi: 10.1126/science.aat2456

García-Gutiérrez, E., Mayer, M. J., Cotter, P. D., and Narbad, A. (2019). Gut microbiota as a source of novel antimicrobials. *Gut Microbes* 10, 1–21. doi: 10.1080/19490976.2018.1455790

Garrido, M. C., Herrero, M., Kolter, R., and Moreno, F. (1988). The export of the DNA replication inhibitor microcin B17 provides immunity for the host cell. *EMBO J.* 7, 1853–1862. doi: 10.1002/j.1460-2075.1988.tb03018.x

Garsin, D. A. (2010). Ethanolamine utilization in bacterial pathogens: roles and regulation. *Nat. Rev. Microbiol.* 8, 290–295. doi: 10.1038/nrmicro2334

Gérard, F., Pradel, N., and Wu, L. F. (2005). Bactericidal activity of colicin V is mediated by an inner membrane protein, SdaC, of *Escherichia coli*. *J. Bacteriol.* 187, 1945–1950. doi: 10.1128/jb.187.6.1945-1950.2005

Gerc, A. J., Stanley-Wall, N. R., and Coulthurst, S. J. (2014). Role of the phosphopantetheinyl-transferase enzyme, PswP, in the biosynthesis of antimicrobial secondary metabolites by *Serratia marcescens* Db10. *Microbiology* 160, 1609–1617. doi: 10.1099/mic.0.078576-0

Ghilarov, D., Stevenson, C. E., Travin, D. Y., Piskunova, J., Serebryakova, M., Maxwell, A., et al. (2019). Architecture of microcin B17 synthetase: an octameric protein complex converting a ribosomally synthesized peptide into a DNA Gyrase poison. *Mol. Cell.* 73, 749–762. doi: 10.1016/j.molcel.2018.11.032

Gillis, C. C., Hughes, E. R., Spiga, L., Winter, M. G., Zhu, W., Furtado de Carvalho, T., et al. (2018). Dysbiosis-associated change in host metabolism generates lactate to support *salmonella* growth. *Cell Host Microbe* 23, 54–64. doi: 10.1016/j.chom.2017.11.006

Gillor, O., Kirkup, B. C., and Riley, M. A. (2004). Colicins and microcins: the next generation antimicrobials. *Adv. Appl. Microbiol.* 54, 129–146. doi: 10.1016/s0065-2164(04)54005-4

Gilson, L., Mahanty, H. K., and Kolter, R. (1987). Four plasmid genes are required for colicin V synthesis, export, and immunity. *J. Bacteriol.* 169, 2466–2470. doi: 10.1128/jb.169.6.2466-2470.1987

González-Pastor, J. E., San Millán, J. L., and Moreno, F. (1994). The smallest known gene. *Nature* 369:281. doi: 10.1038/369281a0

Gordon, D. M., and O'Brien, C. L. (2006). Bacteriocin diversity and the frequency of multiple bacteriocin production in *Escherichia coli*. *Microbiology* 152, 3239–3244. doi: 10.1099/mic.0.28690-0

Gratia, A. (1925). Sur un remarquable exemple d'antagonisme entre deux souches de colibacille. *Compt. Rend. Soc. Biol.* 93, 1040–1043.

Grozdanov, L., Raasch, C., Schulze, J., Sonnenborn, U., Gottschalk, G., Hacker, J., et al. (2004). Analysis of the genome structure of the nonpathogenic probiotic *Escherichia coli* strain Nissle 1917. *J. Bacteriol.* 186, 5432–5441. doi: 10.1128/jb.186.16.5432-5441.2004

Gu, R. X., Corradi, V., Singh, G., Choudhury, H. G., Beis, K., and Tieleman, D. P. (2015). Conformational changes of the antibacterial peptide ATP binding cassette transporter McjD revealed by molecular dynamics simulations. *Biochemistry* 54, 5989–5998. doi: 10.1021/acs.biochem.5b00753

Guijarro, J. I., González-Pastor, J. E., Baleux, F., San Millán, J. L., Castilla, M. A., Rico, M., et al. (1995). Chemical structure and translation inhibition studies of the antibiotic microcin C7. *J. Biol. Chem.* 270, 23520–23532. doi: 10.1074/jbc.270.40.23520

Håvarstein, L. S., Holo, H., and Nes, I. F. (1994). The leader peptide of colicin V shares consensus sequences with leader peptides that are common among peptide bacteriocins produced by gram-positive bacteria. *Microbiology* 140, 2383–2389. doi: 10.1099/13500872-140-9-2383

Hegemann, J. D., De Simone, M., Zimmermann, M., Knappe, T. A., Xie, X., Di Leva, F. S., et al. (2014). Rational improvement of the affinity and selectivity of integrin binding of grafted lasso peptides. *J. Med. Chem.* 57, 5829–5834. doi: 10.1021/jm5004478

Heng, N. C., and Tagg, J. R. (2006). What's in a name? Class distinction for bacteriocins. *Nat. Rev. Microbiol.* 4:160. doi: 10.1038/nrmicro1273-c1

Henker, J., Laass, M. W., Blokhin, B. M., Maydannik, V. G., Bolbot, Y. K., Elze, M., et al. (2007). The probiotic *Escherichia coli* strain Nissle 1917 (EcN) stops acute diarrhoea in infants and toddlers. *Eur. J. Pediatr.* 166, 311–318. doi: 10.1007/s00431-007-0419-x

Herrero, M., Kolter, R., and Moreno, F. (1986). Effects of microcin B17 on microcin B17-immune cells. *J. Gen. Microbiol.* 132, 403–410. doi: 10.1099/00221287-132-2-403

Hibbing, M. E., Fuqua, C., Parsek, M. R., and Peterson, S. B. (2010). Bacterial competition: surviving and thriving in the microbial jungle. *Nat. Rev. Microbiol.* 8, 15–25. doi: 10.1038/nrmicro2259

Hishinuma, F., Izaki, K., and Takahashi, H. (1969). Effects of glycine and D-amino acids on growth of various microorganisms. *Agric. Biol. Chem.* 33, 1577–1586. doi: 10.1080/00021369.1969.10859511

Hofmann, A. F., and Eckmann, L. (2006). How bile acids confer gut mucosal protection against bacteria. *Proc. Natl. Acad. Sci. U.S.A.* 103, 4333–4334. doi: 10.1073/pnas.0600780103

Hooper, L. V., Midtvedt, T., and Gordon, J. I. (2002). How host-microbial interactions shape the nutrient environment of the mammalian intestine. *Ann. Rev. Nutr.* 22, 283–307. doi: 10.1146/annurev.nutr.22.011602.092259

Husada, F., Bountra, K., Tassis, K., de Boer, M., Romano, M., Rebuffat, S., et al. (2018). Conformational dynamics of the ABC transporter McjD seen by singlemolecule FRET. *EMBO J.* 37:e100056. doi: 10.15252/embj.2018100056

Isaacs, C. E. (2001). The antimicrobial function of milk lipids. *Adv. Nutr. Res.* 10, 271–285. doi: 10.1007/978-1-4615-0661-4_13

Iyer, S. S., Gensollen, T., Gandhi, A., Oh, S. F., Neves, J. F., Collin, F., et al. (2018). Dietary and microbial oxazoles induce intestinal inflammation by modulating aryl hydrocarbon receptor responses. *Cell* 173, 1123–1134. doi: 10.1016/j.cell.2018.04.037

Jacobi, C. A., and Malfertheiner, P. (2011). *Escherichia coli* Nissle 1917 (Mutaflor®): new insights into an old probiotic bacterium. *Digest. Dis.* 29, 600–607. doi: 10.1159/000333307

Jacoby, G. A., Corcoran, M. A., and Hooper, D. C. (2015). Protective effect of Qnr on agents other than quinolones that target DNA gyrase. *Antimicrob. Agents Chemother.* 59, 6689–6695. doi: 10.1128/AAC.01292-15

Jaeggi, T., Kortman, G. A., Moretti, D., Chassard, C., Holding, P., Dostal, A., et al. (2015). Iron fortification adversely affects the gut microbiome, increases pathogen abundance and induces intestinal inflammation in Kenyan infants. *Gut* 64, 731–742. doi: 10.1136/gutjnl-2014-307720

Jeanteur, D., Schirmer, T., Fourel, D., Simonet, V., Rummel, G., Widmer, C., et al. (1994). Structural and functional alterations of a colicin-resistant mutant of OmpF porin from *Escherichia coli*. *Proc. Natl. Acad. Sci. U.S.A.* 91, 10675–10679. doi: 10.1073/pnas.91.22.10675

John, J., Saranathan, R., Adigopula, L. N., Thamodharan, V., Singh, S. P., Lakshmi, T. P., et al. (2016). The quorum sensing molecule N-acyl homoserine lactone produced by *Acinetobacter baumannii* displays antibacterial and anticancer properties. *Biofouling* 32, 1029–1047. doi: 10.1080/08927014.2016.1221946

Jones, B. V., Begley, M., Hill, C., Gahan, C. G., and Marchesi, J. R. (2008). Functional and comparative metagenomic analysis of bile salt hydrolase activity in the human gut microbiome. *Proc. Natl. Acad. Sci. U.S.A.* 105, 13580–13585. doi: 10.1073/pnas.0804437105

Jorge, A. F. (1984). *Interacciones Microbianas Amensalistas de la Flora Intestinal*. Doctoral dissertation, Universidad Complutense de Madrid: Madrid.

Kashyap, P. C., Marcobal, A., Ursell, L. K., Larauche, M., Duboc, H., Earle, K. A., et al. (2013a). Complex interactions among diet, gastrointestinal transit, and gut microbiota in humanized mice. *Gastroenterology* 144, 967–977. doi: 10.1053/j.gastro.2013.01.047

Kashyap, P. C., Marcobal, A., Ursell, L. K., Smits, S. A., Sonnenburg, E. D., Costello, E. K., et al. (2013b). Genetically dictated change in host mucus carbohydrate landscape exerts a diet-dependent effect on the gut microbiota. *Proc. Natl. Acad. Sci. U.S.A.* 110, 17059–17064. doi: 10.1073/pnas.1306070110

Kaval, K. G., Singh, K. V., Cruz, M. R., DebRoy, S., Winkler, W. C., Murray, B. E., et al. (2018). Loss of ethanolamine utilization in *Enterococcus faecalis* increases gastrointestinal tract colonization. *mBio* 9:e00790-18. doi: 10.1128/mBio.00790-18

Kazakov, T., Kuznedelov, K., Semenova, E., Mukhamedyarov, D., Datsenko, K. A., Metlitskaya, A., et al. (2014). The RimL transacetylase provides resistance to translation inhibitor microcin C. *J. Bacteriol.* 196, 3377–3385. doi: 10.1128/JB.01584-14

Kemperman, R., Kuipers, A., Karsens, H., Nauta, A., Kuipers, O., and Kok, J. (2003). Identification and characterization of two novel clostridial bacteriocins, circularin A and closticin 574. *Appl. Environ. Microbiol.* 69, 1589–1597. doi: 10.1128/aem.69.3.1589-1597.2003

Kirkup, B. C., and Riley, M. A. (2004). Antibiotic-mediated antagonism leads to a bacterial game of rock–paper–scissors *in vivo*. *Nature* 428, 412–414. doi: 10.1038/nature02429

Klaenhammer, T. R. (1993). Genetics of bacteriocins produced by lactic acid bacteria. *FEMS Microbiol. Rev.* 12, 39–86.

Kleta, S., Steinrück, H., Breves, G., Duncker, S., Laturnus, C., Wieler, L. H., et al. (2006). Detection and distribution of probiotic *Escherichia coli* Nissle 1917 clones in swine herds in Germany. *J. Appl. Microbiol.* 101, 1357–1366. doi: 10.1111/j.1365-2672.2006.03019.x

Klitgord, . N., and Segrè, D. (2011). Ecosystems biology of microbial metabolism. *Curr. Opin. Biotechnol.* 22, 541–546

Kohoutova, D., Smajs, D., Moravkova, P., Cyrany, J., Moravkova, M., Forstlova, M., et al. (2014). *Escherichia coli* strains of phylogenetic group B2 and D and bacteriocin production are associated with advanced colorectal neoplasia. *BMC Infect. Dis.* 14:733. doi: 10.1186/s12879-014-0733-7

Kolodkin-Gal, I., Romero, D., Cao, S., Clardy, J., Kolter, R., and Losick, R. (2010). D-amino acids trigger biofilm disassembly. *Science* 328, 627–629. doi: 10.1126/science.1188628

Kolter, R., and Moreno, F. (1992). Genetics of ribosomally synthesized peptide antibiotics. *Ann. Rev. Microbiol.* 46, 141–163.

Kortman, G. A., Raffatellu, M., Swinkels, D. W., and Tjalsma, H. (2014). Nutritional iron turned inside out: intestinal stress from a gut microbial perspective. *FEMS Microbiol. Rev.* 38, 1202–1234. doi: 10.1111/1574-6976.12086

Krämer, R. (1994). Secretion of amino acids by bacteria: physiology and mechanism. *FEMS Microbiol. Rev.* 13, 75–93. doi: 10.1016/0168-6445(94)90102-3

Lagos, R., Tello, M., Mercado, G., García, V., and Monasterio, O. (2009). Antibacterial and antitumorigenic properties of microcin E492, a pore-forming bacteriocin. *Curr. Pharm. Biotechnol.* 10, 74–85. doi: 10.2174/138920109787048643

Lagos, R., Villanueva, J. E., and Monasterio, O. (1999). Identification and properties of the genes encoding microcin E492 and its immunity protein. *J. Bacteriol.* 18, 212–217.

Lai, Y. C., Lin, A. C., Chiang, M. K., Dai, Y. H., Hsu, C. C., Lu, M. C., et al. (2014). Genotoxic *Klebsiella pneumoniae* in Taiwan. *PLoS One* 9:e96292. doi: 10.1371/journal.pone.0096292

Laviña, M., Gaggero, C., and Moreno, F. (1990). Microcin H47, a chromosome-encoded microcin antibiotic of *Escherichia coli*. *J. Bacteriol.* 172, 6585–6588. doi: 10.1128/jb.172.11.6585-6588.1990

Lee, J., Cho, Y. J., Yang, J. Y., Jung, Y. J., Hong, S. G., and Kim, O. S. (2017). Complete genome sequence of *Pseudomonas antarctica* PAMC 27494, a bacteriocin-producing psychrophile isolated from Antarctica. *J. Biotechnol.* 259, 15–18. doi: 10.1016/j.jbiotec.2017.08.013

Lee, W. J., and Hase, K. (2014). Gut microbiota-generated metabolites in animal health and disease. *Nat. Chem. Biol.* 10, 416–424. doi: 10.1038/nchembio.1535

Lemonnier, M., Levin, B. R., Romeo, T., Garner, K., Baquero, M. R., Mercante, J., et al. (2007). The evolution of contact-dependent inhibition in non-growing populations of *Escherichia coli*. *Proc. R. Soc. B Biol. Sci.* 275, 3–10. doi: 10.1098/rspb.2007.1234

Lenski, R. E., and Riley, M. A. (2002). Chemical warfare from an ecological perspective. *Proc. Natl. Acad. Sci. U.S.A.* 99, 556–558. doi: 10.1073/pnas.022641999

Letzel, A. C., Pidot, S. J., and Hertweck, C. (2014). Genome mining for ribosomally synthesized and post-translationally modified peptides (RiPPs) in anaerobic bacteria. *BMC Genomics* 15:983. doi: 10.1186/1471-2164-15-983

Ley, R. E., Hamady, M., Lozupone, C., Turnbaugh, P. J., Ramey, R. R., Bircher, J. S., et al. (2008a). Evolution of mammals and their gut microbes. *Science* 320, 1647–1651.

Ley, R. E., Lozupone, C. A., Hamady, M., Knight, R., and Gordon, J. I. (2008b). Worlds within worlds: evolution of the vertebrate gut microbiota. *Nat. Rev. Microbiol.* 6, 776–788. doi: 10.1038/nrmicro1978

Ley, R. E., Peterson, D. A., and Gordon, J. I. (2006). Ecological and evolutionary forces shaping microbial diversity in the human intestine. *Cell* 124, 837–848. doi: 10.1016/j.cell.2006.02.017

Li, Y. M., Milne, J. C., Madison, L. L., Kolter, R., and Walsh, C. T. (1996). From peptide precursors to oxazole and thiazole-containing peptide antibiotics: microcin B17 synthase. *Science* 274, 1188–1193. doi: 10.1126/science.274.5290.1188

Lichtman, J. S., Alsentzer, E., Jaffe, M., Sprockett, S., Masutani, E., Ikwa, E., et al. (2016). The effect of microbial colonization on the host proteome varies by gastrointestinal location. *ISME J.* 10, 1170–1181. doi: 10.1038/ismej.2015.187

Linares, J. F., Gustafsson, I., Baquero, F., and Martinez, J. L. (2006). Antibiotics as intermicrobial signaling agents instead of weapons. *Proc. Natl. Acad. Sci. U.S.A.* 103, 19484–19489. doi: 10.1073/pnas.0608949103

Lomovskaya, O., Kawai, F., and Matin, A. (1996). Differential regulation of the mcb and emr operons of *Escherichia coli*: role of mcb in multidrug resistance. *Antimicrob. Agents Chemother.* 40, 1050–1052. doi: 10.1128/aac.40.4.1050

Lopez, F. E., Vincent, P. A., Zenoff, A. M., Salomón, R. A., and Farías, R. N. (2007). Efficacy of microcin J25 in biomatrices and in a mouse model of *Salmonella* infection. *J. Antimicrob. Chemother.* 59, 676–680. doi: 10.1093/jac/dkm009

Lou, Z., Wang, H., Zhu, S., Ma, C., and Wang, Z. (2011). Antibacterial activity and mechanism of action of chlorogenic acid. *J. Food Sci.* 76, 398–403. doi: 10.1111/j.1750-3841.2011.02213.x

Lozupone, C. A., Stombaugh, J. I., Gordon, J. I., Jansson, J. K., and Knight, R. (2012). Diversity, stability and resilience of the human gut microbiota. *Nature* 489, 220–230. doi: 10.1038/nature11550

Lu, S. Y., Graça, T., Avillan, J. J., Zhao, Z., and Call, D. R. (2019). Microcin PDI inhibits antibiotic-resistant strains of *Escherichia coli* and *Shigella* through a mechanism of membrane disruption and protection by homotrimer self-immunity. *Appl. Environ. Microbiol.* 85:e00371-19. doi: 10.1128/AEM.00371-19

Lustri, B. C., Sperandio, V., and Moreira, C. G. (2017). Bacterial chat: intestinal metabolites and signals in host-microbiota-pathogen interactions. *Infect. Immun.* 85:e00476-17. doi: 10.1128/IAI.00476-17

Majeed, H., Gillor, O., Kerr, B., and Riley, M. A. (2011). Competitive interactions in *Escherichia coli* populations: the role of bacteriocins. *ISME J.* 5, 71–81. doi: 10.1038/ismej.2010.90

Majeed, H., Lampert, A., Ghazaryan, L., and Gillor, O. (2013). The weak shall inherit: bacteriocin-mediated interactions in bacterial populations. *PLoS One* 8:e63837. doi: 10.1371/journal.pone.0063837

Mantis, N. J., Rol, N., and Corthésy, B. (2011). Secretory IgA's complex roles in immunity and mucosal homeostasis in the gut. *Mucosal Immunol.* 4, 603–611. doi: 10.1038/mi.2011.41

Mathavan, I., and Beis, K. (2012). The role of bacterial membrane proteins in the internalization of microcin MccJ25 and MccB17. *Biochem. Soc. Trans.* 40, 1539–1543. doi: 10.1042/BST20120176

Matsumoto, M., and Benno, Y. (2007). The relationship between microbiota and polyamine concentration in the human intestine: a pilot study. *Microbiol. Immunol.* 51, 25–35. doi: 10.1111/j.1348-0421.2007.tb03887.x

Matsumoto, M., Kibe, R., Ooga, T., Aiba, Y., Kurihara, S., Sawaki, E., et al. (2012). Impact of intestinal microbiota on intestinal luminal metabolome. *Sci. Rep.* 2:233. doi: 10.1038/srep00233

Meade, K. G., and O'Farrelly, C. (2019). β-Defensins: farming the microbiome for homeostasis and health. *Front. Immunol.* 9:3072. doi: 10.3389/fimmu.2018.03072

Melby, J. O., Li, X., and Mitchell, D. A. (2014). Orchestration of enzymatic processing by thiazole/oxazole-modified microcin dehydrogenases. *Biochemistry* 53, 413–422. doi: 10.1021/bi401529y

Metelev, M., Arseniev, A., Bushin, L. B., Kuznedelov, K., Artamonova, T. O., Kondratenko, R., et al. (2017a). Acinetodin and Klebsidin, RNA polymerase targeting lasso peptides produced by human isolates of *Acinetobacter gyllenbergii* and *Klebsiella pneumoniae*. *ACS Chem. Biol.* 12, 814–824. doi: 10.1021/acschembio.6b01154

Metelev, M., Osterman, I. A., Ghilarov, D., Khabibullina, N. F., Yakimov, A., Shabalin, K., et al. (2017b). Klebsazolicin inhibits 70S ribosome by obstructing the peptide exit tunnel. *Nat. Chem. Biol.* 13, 1129–1136. doi: 10.1038/nchembio.2462

Metelev, M., Serebryakova, M., Ghilarov, D., Zhao, Y., and Severinov, K. (2013). Structure of microcin B-like compounds produced by *Pseudomonas syringae* and species specificity of their antibacterial action. *J. Bacteriol.* 195, 4129–4137. doi: 10.1128/JB.00665-13

Metlitskaya, A., Kazakov, T., Kommer, A., Pavlova, O., Praetorius-Ibba, M., Ibba, M., et al. (2006). Aspartyl-tRNA synthetase is the target of peptide nucleotide antibiotic microcin C. *J. Biol. Chem.* 281, 18033–18042. doi: 10.1074/jbc.m513174200

Metlitskaya, A., Kazakov, T., Vondenhoff, G. H., Novikova, M., Shashkov, A., Zatsepin, T., et al. (2009). Maturation of the translation inhibitor microcin C. *J. Bacteriol.* 191, 2380–2387. doi: 10.1128/JB.00999-08

Meyer-Hoffert, U., Hornef, M. W., Henriques-Normark, B., Axelsson, L. G., Midtvedt, T., Pütsep, K., et al. (2008). Secreted enteric antimicrobial activity localises to the mucus surface layer. *Gut* 57, 764–771. doi: 10.1136/gut.2007.141481

Micenková, L., Beòová, A., Frankovièová, L., Bosák, J., Vrba, M., Ševèíková, A., et al. (2017). Human *Escherichia coli* isolates from hemocultures: septicemia linked to urogenital tract infections is caused by isolates harboring more virulence genes than bacteraemia linked to other conditions. *Int. J. Med. Microbiol.* 307, 182–189. doi: 10.1016/j.ijmm.2017.02.003

Micenková, L., Bosák, J., Štaudová, B., Kohoutová, D., Čejková, D., Woznicová, V., et al. (2016a). Microcin determinants are associated with B2 phylogroup of human fecal *Escherichia coli* isolates. *Microbiologyopen* 5, 490–498. doi: 10.1002/mbo3.345

Micenková, L., Bosák, J., Vrba, M., Ševèíková, A., and Šmajs, D. (2016b). Human extraintestinal pathogenic *Escherichia coli* strains differ in prevalence of virulence factors, phylogroups, and bacteriocin determinants. *BMC Microbiol.* 16:218. doi: 10.1186/s12866-016-0835-z

Million, M., Lagier, J. C., Yahav, D., and Paul, M. (2013). Gut bacterial microbiota and obesity. *Clin. Microbiol. Infect.* 19, 305–313. doi: 10.1111/1469-0691.12172

Milshteyn, A., Colosimo, D. A., and Brady, S. F. (2018). Accessing bioactive natural products from the human microbiome. *Cell Host Microbe* 23, 725–736. doi: 10.1016/j.chom.2018.05.013

Mirpuri, J., Raetz, M., Sturge, C. R., Wilhelm, C. L., Benson, A., Savani, R. C., et al. (2014). *Proteobacteria*-specific IgA regulates maturation of the intestinal microbiota. *Gut Microbes* 5, 28–39. doi: 10.4161/gmic.26489

Moreno, F., Gónzalez-Pastor, J. E., Baquero, M. R., and Bravo, D. (2002). The regulation of microcin B, C and J operons. *Biochimie* 84, 521–529. doi: 10.1016/s0300-9084(02)01452-9

Morin, N., Lanneluc, I., Connil, N., Cottenceau, M., Pons, A. M., and Sablé, S. (2011). Mechanism of bactericidal activity of microcin L in *Escherichia coli* and *Salmonella enterica*. *Antimicrob. Agents Chemother.* 55, 997–1007. doi: 10.1128/AAC.01217-10

Mousa, W. K., Athar, B., Merwin, N. J., and Magarvey, N. A. (2017). Antibiotics and specialized metabolites from the human microbiota. *Nat. Prod. Rep.* 34, 1302–1331. doi: 10.1039/c7np00021a

Mukherjee, A., Santra, M. K., Beuria, T. K., and Panda, D. (2005). A natural osmolyte trimethylamine N-oxide promotes assembly and bundling of the bacterial cell division protein, FtsZ and counteracts the denaturing effects of urea. *FEBS J.* 272, 2760–2772. doi: 10.1111/j.1742-4658.2005.04696.x

Nagaoka, S., Murata, S., Kimura, K., Mori, T., and Hojo, K. (2010). Antimicrobial activity of sodium citrate against *Streptococcus pneumoniae* and several oral bacteria. *Lett. Appl. Microbiol.* 51, 546–551. doi: 10.1111/j.1472-765X.2010.02932.x

Nagpal, R., Wang, S., Solberg Woods, L. C., Seshie, O., Chung, S. T., Shively, C. A., et al. (2018). Comparative microbiome signatures and short-chain fatty acids in mouse, rat, non-human primate, and human feces. *Front. Microbiol.* 9:2897. doi: 10.3389/fmicb.2018.02897

Naimi, S., Zirah, S., Hammami, R., Fernandez, B., Rebuffat, S., and Fliss, I. (2018). Fate and biological activity of the antimicrobial lasso peptide microcin J25 under gastrointestinal tract conditions. *Front. Microbiol.* 9:1764. doi: 10.3389/fmicb.2018.01764

Nakamura, A., Ooga, T., and Matsumoto, M. (2018). Intestinal luminal putrescine is produced by collective biosynthetic pathways of the commensal microbiome. *Gut Microbes* 5, 1–13. doi: 10.1080/19490976.2018.1494466

Navarro Llorens, J. M., Tormo, A., and Martinez-Garcia, E. (2010). Stationary phase in gram-negative bacteria. *FEMS Microbiol. Rev.* 34, 476–495. doi: 10.1111/j.1574-6976.2010.00213.x

Newburg, D. S., and Morelli, L. (2014). Human milk and infant intestinal mucosal glycans guide succession of the neonatal intestinal microbiota. *Pediat. Res.* 77, 115–120. doi: 10.1038/pr.2014.178

Nissle, A. (1916). Uber die grundlagen einer neuen ursächlichen bekämpfung der pathologischen darmflora. *Deut. Med. Wochenschr.* 42, 1181–1184. doi: 10.1055/s-0028-1135392

Nissle, A. (1918). Die antagonistische behandlung chronischer darmstörungen mit colibakterien. *Med. Klin.* 2, 29–33.

Nocek, B., Tikhonov, A., Babnigg, G., Gu, M., Zhou, M., Makarova, K. S., et al. (2012). Structural and functional characterization of microcin C resistance peptidase MccF from *Bacillus anthracis*. *J. Mol. Biol.* 420, 366–383. doi: 10.1016/j.jmb.2012.04.011

Novikova, M., Kazakov, T., Vondenhoff, G. H., Semenova, E., Rozenski, J., Metlytskaya, A., et al. (2010). MccE provides resistance to protein synthesis inhibitor microcin C by acetylating the processed form of the antibiotic. *J. Biol. Chem.* 285, 12662–12669. doi: 10.1074/jbc.M109.080192

Novikova, M., Metlitskaya, A., Datsenko, K., Kazakov, T., Kazakov, A., Wanner, B., et al. (2007). The *Escherichia coli* Yej transporter is required for the uptake of translation inhibitor microcin C. *J. Bacteriol.* 189, 8361–8365. doi: 10.1128/jb.01028-07

O'Brien, G. J. (1996). *Molecular Analysis of Microcin 24: Genetics, Secretion and Mode of Action of a Novel Microcin*. Doctoral dissertation, University of Canterbury: Christchurch.

Olier, M., Marcq, I., Salvador-Cartier, C., Secher, T., Dobrindt, U., Boury, M., et al. (2012). Genotoxicity of *Escherichia coli* Nissle 1917 strain cannot be dissociated from its probiotic activity. *Gut Microbes* 3, 501–509. doi: 10.4161/gmic.21737

Olsen, J. V., and Mann, M. (2013). Status of large-scale analysis of post-translational modifications by mass spectrometry. *Mol. Cell. Proteom.* 12, 3444–3452. doi: 10.1074/mcp.o113.034181

Overhaus, M., Moore, A. B., Barbato, J., Behrendt, F. F., Doering, J. G., and Bauer, A. J. (2006). Biliverdin protects against polymicrobial sepsis by modulating inflammatory mediators. *Am. J. Physiol. Gastrointest. Liver Physiol.* 290, G695–G703.

Ozdemir, T., Fedorec, A. J., Danino, T., and Barnes, C. P. (2018). Synthetic biology and engineered live biotherapeutics: toward increasing system complexity. *Cell Syst.* 7, 5–16. doi: 10.1016/j.cels.2018.06.008

O'Brien, G. J., and Mahanty, H. K. (1994). Colicin 24, a new plasmid-borne colicin from a uropathogenic strain of *Escherichia coli*. *Plasmid* 31, 288–296. doi: 10.1006/plas.1994.1030

Patzer, S., Baquero, M. R., Bravo, D., Moreno, F., and Hantke, K. (2003). The colicin G, H and X determinants encode microcins M and H47, which might utilize the catecholate siderophore receptors FepA, Cir, Fiu and IroN. *Microbiology* 149, 2557–2570. doi: 10.1099/mic.0.26396-0

Payne, J. W. (1977). Transport and hydrolysis of peptides by microorganisms. *Ciba Found. Symp.* 50, 305–334. doi: 10.1002/9780470720318.ch17

Piskunova, J., Maisonneuve, E., Germain, E., Gerdes, K., and Severinov, K. (2017). Peptide-nucleotide antibiotic Microcin C is a potent inducer of stringent response and persistence in both sensitive and producing cells. *Mol. Microbiol.* 104, 463–471. doi: 10.1111/mmi.13640

Poey, M. E., Azpiroz, M. F., and Laviña, M. (2006). Comparative analysis of chromosome-encoded microcins. *Antimicrob. Agents Chemother.* 50, 1411–1418. doi: 10.1128/aac.50.4.1411-1418.2006

Pomares, M. F., Delgado, M. A., Corbalán, N. S., Farías, R. N., and Vincent, P. A. (2010). Sensitization of microcin J25-resistant strains by a membrane-permeabilizing peptide. *Appl. Environ. Microbiol.* 76, 6837–6842. doi: 10.1128/AEM.00307-10

Pomini, A. M., and Marsaioli, A. J. (2008). Absolute configuration and antimicrobial activity of acylhomoserine lactones. *J. Nat. Prod.* 71, 1032–1036. doi: 10.1021/np800127b

Pons, A. M., Delalande, F., Duarte, M., Benoit, S., Lanneluc, I., Sablé, S., et al. (2004). Genetic analysis and complete primary structure of microcin L. *Antimicrob. Agents Chemother.* 48, 505–513. doi: 10.1128/aac.48.2.505-513.2004

Pons, A. M., Lanneluc, I., Cottenceau, G., and Sablé, S. (2002). New developments in non-post translationally modified microcins. *Biochimie* 84, 531–537. doi: 10.1016/s0300-9084(02)01416-5

Popa, D. E., Dragoi, C. M., Arsene, A. L., Dumitrescu, I. B., Nicolae, A. C., Velescu, B. S., et al. (2015). The relationship between phenolic compounds from diet and microbiota. *Food Funct.* 6, 2424–2439. doi: 10.1039/c5fo00322a

Powers, M. J., and Levine, M. (1937). Effect of metabolites on growth, and differentiation in the colon-group. *Proc. Soc. Exp. Biol. Med.* 36, 274–276. doi: 10.3181/00379727-36-9197p

Pugin, P., Barcik, W., Westermann, P., Heider, A., Wawrzyniak, M., Hellings, P., et al. (2017). A wide diversity of bacteria from the human gut produces and degrades biogenic amines. *Microb. Ecol. Health Dis.* 28:1353881. doi: 10.1080/16512235.2017.1353881

Pugsley, A. P., Moreno, F., and De Lorenzo, V. (1986). Microcin E492 insensitive mutants of *Escherichia coli* K12. *Microbiology* 132, 3253–3259. doi: 10.1099/00221287-132-12-3253

Ran, R., Zeng, H., Zhao, D., Liu, R., and Xu, X. (2017). The novel property of heptapeptide of microcin C7 in affecting the cell growth of *Escherichia coli*. *Molecules* 22:E432. doi: 10.3390/molecules22030432

Rangan, K. J., and Hang, H. C. (2017). Biochemical mechanisms of pathogen restriction by intestinal bacteria. *Trends Biochem. Sci.* 42, 887–898. doi: 10.1016/j.tibs.2017.08.005

Rebuffat, S. (2012). Microcins in action: amazing defence strategies of *Enterobacteria*. *Biochem. Soc. Trans.* 40, 1456–1462. doi: 10.1042/BST20120183

Rebuffat, S., Blond, A., Destoumieux-Garzón, D., Goulard, C., and Peduzzi, J. (2004). Microcin J25, from the macrocyclic to the lasso structure: implications for biosynthetic, evolutionary and biotechnological perspectives. *Curr. Prot. Pept. Sci.* 5, 383–391. doi: 10.2174/1389203043379611

Reichenbach, T., Mobilia, M., and Frey, E. (2007). Mobility promotes and jeopardizes biodiversity in rock-paper-scissors games. *Nature* 448, 1046–1049. doi: 10.1038/nature06095

Ridaura, V. K., Faith, J. J., Rey, F. E., Cheng, J., Duncan, A. E., Kau, A. L., et al. (2013). Gut microbiota from twins discordant for obesity modulate metabolism in mice. *Science* 341:1241214. doi: 10.1126/science.1241214

Rivera-Chávez, F., Lopez, C. A., and Bäumler, A. J. (2017). Oxygen as a driver of gut dysbiosis. *Free Radic. Biol. Med.* 105, 93–101. doi: 10.1016/j.freeradbiomed.2016.09.022

Rodríguez, E., and Lavina, M. (2003). The proton channel is the minimal structure of ATP synthase necessary and sufficient for microcin H47 antibiotic action. *Antimicrob. Agents Chemother.* 47, 181–187. doi: 10.1128/aac.47.1.181-187.2003

Rodríguez-Martínez, J. M., Cano, M. E., Velasco, C., Martínez-Martínez, L., and Pascual, A. (2011). Plasmid-mediated quinolone resistance: an update. *J. Infect. Chemother.* 17, 149–182. doi: 10.1007/s10156-010-0120-2

Romano, M., Fusco, G., Choudhury, H. G., Mehmood, S., Robinson, C. V., Zirah, S., et al. (2018). Structural basis for natural product selection and export by bacterial ABC transporters. *ACS Chem. Biol.* 13, 1598–1609. doi: 10.1021/acschembio.8b00226

Rosenberg, E. Y., Bertenthal, D., Nilles, M. L., Bertrand, K. P., and Nikaido, H. (2003). Bile salts and fatty acids induce the expression of *Escherichia coli* AcrAB multidrug efflux pump through their interaction with Rob regulatory protein. *Mol. Microbiol.* 48, 1609–1619. doi: 10.1046/j.1365-2958.2003.03531.x

Rosengren, K. J., and Craik, D. J. (2009). How bugs make lassos. *Chem. Biol.* 16, 1211–1212. doi: 10.1016/j.chembiol.2009.12.004

Russell, W., and Duthie, G. (2011). Plant secondary metabolites and gut health: the case for phenolic acids. *Proc. Nutr. Soc.* 70, 389–396. doi: 10.1017/S0029665111000152

Russell, W., Hoyles, L., Flint, H. J., and Dumas, M. E. (2013). Colonic bacterial metabolites and host health. *Curr. Opin. Microbiol.* 16, 246–254. doi: 10.1016/j.mib.2013.07.002

Sablé, S., Duarte, M., Bravo, D., Lanneluc, I., Pons, A. M., Cottenceau, G., et al. (2003). Wild-type *Escherichia coli* producing microcins B17, D93, J25, and L; cloning of genes for microcin L production and immunity. *Can. J. Microbiol.* 49, 357–361. doi: 10.1139/w03-047

Sakanaka, M., Sugiyama, Y., Kitakata, A., Katayama, T., and Kurihara, S. (2016). Carboxyspermidine decarboxylase of the prominent intestinal microbiota species *Bacteroides thetaiotaomicron* is required for spermidine biosynthesis and contributes to normal growth. *Amino Acids* 48, 2443–2451. doi: 10.1007/s00726-016-2233-0

Salomón, R. A., and Farías, R. N. (1993). The FhuA protein is involved in microcin 25 uptake. *J. Bacteriol.* 175, 7741–7742. doi: 10.1128/jb.175.23.7741-7742.1993

Salomón, R. A., and Farías, R. N. (1995). The peptide antibiotic microcin 25 is imported through the TonB pathway and the SbmA protein. *J. Bacteriol.* 177, 3323–3325. doi: 10.1128/jb.177.11.3323-3325.1995

Salzman, N. H., Hung, K., Haribhai, D., Chu, H., Karlsson-Sjöberg, J., Amir, E., et al. (2010). Enteric defensins are essential regulators of intestinal microbial ecology. *Nat. Immunol.* 11, 76–83. doi: 10.1038/ni.1825

Sánchez-Valenzuela, A., Morales, E., Rodríguez, M., López-Espinosa, M. J., Coque, M. T., Sunyer, J., et al. (2017). Copper-resistance in *Enterobacteriaceae* and other *Proteobacteria* from children's intestine. *J. Environ. Health. Sci.* 3, 1–13.

Sannasiddappa, T. H., Lund, P. A., and Clarke, S. R. (2017). In vitro antibacterial activity of unconjugated and conjugated bile salts on *Staphylococcus aureus*. *Front. Microbiol.* 8:1581. doi: 10.3389/fmicb.2017.01581

Santos, V. L., Nardi Drummond, R. M., and Dias-Souza, M. V. (2017). "Bacteriocins as antimicrobial and antibiofilm agents," in *Current Developments in Biotechnology and Bioengineering: Human and Animal Health Applications*, eds V. T. Soccol, A. Pandey, and R. R. Resende (Amsterdam: Elsevier B.V), 403–436. doi: 10.1016/b978-0-444-63660-7.00016-4

Saric, J., Wang, Y., Li, J., Coen, M., Utzinger, J., Marchesi, J. R., et al. (2007). Species variation in the fecal metabolome gives insight into differential gastrointestinal function. *J. Proteom. Res.* 7, 352–360. doi: 10.1021/pr070340k

Saroj, S. D., Holmer, L., Berengueras, J. M., and Jonsson, A. B. (2017). Inhibitory role of acyl homoserine lactones in hemolytic activity and viability of *Streptococcus pyogenes* M6 S165. *Sci. Rep.* 7:44902. doi: 10.1038/srep44902

Sassone-Corsi, M., Nuccio, S. P., Liu, H., Hernandez, D., Vu, C. T., Takahashi, A. A., et al. (2016). Microcins mediate competition among *Enterobacteriaceae* in the inflamed gut. *Nature* 540, 280–283. doi: 10.1038/nature20557

Schamberger, G. P., and Díez-González, F. (2004). Characterization of colicinogenic *Escherichia coli* strains inhibitory to enterohemorrhagic *Escherichia coli*. *J. Food Protect.* 67, 486–492. doi: 10.4315/0362-028x-67.3.486

Severinov, K., Semenova, E., Kazakov, A., Kazakov, T., and Gelfand, M. S. (2007). Low-molecular-weight post-translationally modified microcins. *Mol. Microbiol.* 65, 1380–1394. doi: 10.1111/j.1365-2958.2007.05874.x

Sieow, B. F. L., Numinen, T. J., Ling, H., and Chang, M. W. (2019). Meta-omics and metabolic modelling assisted deciphering of human microbiota metabolism. *Biotechnol. J.* 14:e1800445.

Sonnenborn, U., and Schulze, J. (2009). The non-pathogenic *Escherichia coli* strain Nissle 1917–features of a versatile probiotic. *Microb. Ecol. Health Dis.* 21, 122–158.

Sonnenburg, J. L., Xu, J., Leip, D. D., Chen, C. H., Westover, B. P., Weatherford, J., et al. (2005). Glycan foraging in vivo by an intestine-adapted bacterial symbiont. *Science* 307, 1955–1959. doi: 10.1126/science.1109051

Soudy, R., Etayash, H., Bahadorani, K., Lavasanifar, A., and Kaur, K. (2017). Breast cancer targeting peptide binds keratin 1: a new molecular marker for targeted drug delivery to breast cancer. *Mol. Pharm.* 14, 593–604. doi: 10.1021/acs.molpharmaceut.6b00652

Strahsburger, E., Baeza, M., Monasterio, O., and Lagos, R. (2005). Cooperative uptake of microcin E492 by receptors FepA, Fiu, and Cir and inhibition by the siderophore enterochelin and its dimeric and trimeric hydrolysis products. *J. Bacteriol.* 49, 3083–3086. doi: 10.1128/aac.49.7.3083-3086.2005

Stritzker, J., Weibel, S., Hill, P. J., Oelschlaeger, T. A., Goebel, W., and Szalay, A. A. (2007). Tumor-specific colonization, tissue distribution, and gene induction by probiotic *Escherichia coli* Nissle 1917 in live mice. *Int. J. Med. Microbiol.* 297, 151–162. doi: 10.1016/j.ijmm.2007.01.008

Stubbendieck, R. M., and Straight, P. D. (2016). Multifaceted interfaces of bacterial competition. *J. Bacteriol.* 198, 2145–2155. doi: 10.1128/JB.00275-16

Sumida, T., Dubiley, S., Wilcox, B., Severinov, K., and Tagami, S. (2019). Structural basis of leader peptide recognition in lasso peptide biosynthesis pathway. *ACS Chem. Biol.* 14, 1619–1627. doi: 10.1021/acschembio.9b00348

Tailford, L. E., Crost, E. H., Kavanaugh, D., and Juge, N. (2015). Mucin glycan foraging in the human gut microbiome. *Front. Gen.* 6:81. doi: 10.3389/fgene.2015.00081

Taymaz-Nikerel, H., De Mey, M., Baart, G., Maertens, J., Heijnen, J. J., and van Gulik, W. (2013). Changes in substrate availability in *Escherichia coli* lead to rapid metabolite, flux and growth rate responses. *Metab. Engin.* 16, 115–129. doi: 10.1016/j.ymben.2013.01.004

Tello Reyes, M. C. (2006). *La Especificidad, Exportación y Procesamiento de la Microcina E492 y Colicina V Dependen del Dominio ABC de sus Transportadores*. Doctoral Thesis, Chile University: Santiago.

Terzi, H. A., Kardes, H., Atasoy, A. R., Aykan, S. B., Karakece, E., Ustundag, G. H., et al. (2016). The antibacterial effects of bilirubin on gram-negative bacterial agents of sepsis. *Biomed. Res.* 27, 207–209.

Thanassi, D. G., Cheng, L. W., and Nikaido, H. (1997). Active efflux of bile salts by *Escherichia coli*. *J. Bacteriol.* 179, 2512–2518. doi: 10.1128/jb.179.8.2512-2518.1997

Thomas, X., Destoumieux-Garzón, D., Peduzzi, J., Afonso, C., Blond, A., Birlirakis, N., et al. (2004). Siderophore peptide, a new type of post-translationally modified antibacterial peptide with potent activity. *J. Biol. Chem.* 279, 28233–28242. doi: 10.1074/jbc.m400228200

Thormar, H., and Hilmarsson, H. (2007). The role of microbicidal lipids in host defense against pathogens and their potential as therapeutic agents. *Chem. Phys. Lipids* 150, 1–11. doi: 10.1016/j.chemphyslip.2007.06.220

Tikhonov, A., Kazakov, T., Semenova, E., Serebryakova, M., Vondenhoff, G., Van Aerschot, A., et al. (2010). The mechanism of microcin C resistance provided by the MccF peptidase. *J. Biol. Chem.* 285, 37944–37952. doi: 10.1074/jbc.M110.179135

Tofalo, R., Cocchi, S., and Suzzi, G. (2019). Polyamines and gut microbiota. *Front. Nutr.* 6:16. doi: 10.3389/fnut.2019.00016

Tran, J. H., and Jacoby, G. A. (2002). Mechanism of plasmid-mediated quinolone resistance. *Proc. Natl. Acad. Sci. U.S.A.* 99, 5638–5642. doi: 10.1073/pnas.082092899

Tsibulskaya, D., Mokina, O., Kulikovsky, A., Piskunova, J., Severinov, K., Serebryakova, M., et al. (2017). The product of *Yersinia pseudotuberculosis* mcc operon is a peptide-cytidine antibiotic activated inside producing cells by the TldD/E protease. *J. Am. Chem. Soc.* 139, 16178–16187. doi: 10.1021/jacs.7b07118

Tsuruoka, T., Tamura, A., Miyata, A., Takei, T., Iwamatsu, K., Inouye, S., et al. (1984). Penicillin-insensitive incorporation of D-amino acids into cell wall peptidoglycan influences the amount of bound lipoprotein in *Escherichia coli*. *J. Bacteriol.* 160, 889–894.

Turnbaugh, P. J., Hamady, M., Yatsunenko, T., Cantarel, B. L., Duncan, A., Ley, R. E., et al. (2009). A core gut microbiome in obese and lean twins. *Nature* 457, 480–484. doi: 10.1038/nature07540

Turrientes, M. C., González-Alba, J. M., del Campo, R., Baquero, M. R., Cantón, R., Baquero, F., et al. (2014). Recombination blurs phylogenetic groups routine assignment in *Escherichia coli*: setting the record straight. *PLoS One* 9:e105395. doi: 10.1371/journal.pone.0105395

Turroni, F., Ribbera, A., Foroni, E., van Sinderen, D., and Ventura, M. (2008). Human gut microbiota and *Bifidobacteria*: from composition to functionality. *Antonie Van Leeuwenhoek* 94, 35–50. doi: 10.1007/s10482-008-9232-4

Underwood, M. A., German, J. B., Lebrilla, C. B., and Mills, D. A. (2015). *Bifidobacterium longum* subspecies *infantis*: champion colonizer of the infant gut. *Pediat. Res.* 77, 229–235. doi: 10.1038/pr.2014.156

Vacca, I. (2017). The microbiota maintains oxygen balance in the gut. *Nat. Rev. Microbiol.* 15, 574–575. doi: 10.1038/nrmicro.2017.112

Van Belkum, M. J., and Stiles, M. E. (2000). Nonlantibiotic antibacterial peptides from lactic acid bacteria. *Nat. Prod. Rep.* 17, 323–335. doi: 10.1039/a801347k

Vassiliadis, G., Destoumieux-Garzón, D., Lombard, C., Rebuffat, S., and Peduzzi, J. (2010). Isolation and characterization of two members of the siderophore-microcin family, microcins M and H47. *Antimicrob. Agents Chemother.* 54, 288–297. doi: 10.1128/AAC.00744-09

Vassiliadis, G., Destoumieux-Garzón, D., and Peduzzi, J. (2011). "Class II microcins," in *Prokaryotic Antimicrobial Peptides*, eds D. Drider and S. Rebuffat (New York, NY: Springer), 309–332. doi: 10.1007/978-1-4419-7692-5_16

Verberkmoes, N. C., Russell, A. L., Shah, M., Godzik, A., Rosenquist, M., Halfvarson, J., et al. (2009). Shotgun metaproteomics of the human distal gut microbiota. *ISME J.* 3, 179–189. doi: 10.1038/ismej.2008.108

Vincent, P. A., and Morero, R. D. (2009). The structure and biological aspects of peptide antibiotic microcin J25. *Curr. Med. Chem.* 16, 538–539.

Vizan, J. L., Hernández-Chico, C., del Castillo, I., and Moreno, F. (1991). The peptide antibiotic microcin B17 induces double-strand cleavage of DNA mediated by *E. coli DNA gyrase*. *EMBO J.* 10, 467–476. doi: 10.1002/j.1460-2075.1991.tb07969.x

Wang, G., Li, X., and Wang, Z. (2016). APD3: the antimicrobial peptide database as a tool for research and education. *Nucleic Acids Res.* 44, D1087–D1093. doi: 10.1093/nar/gkv1278

Weber, T., and Kim, H. U. (2016). The secondary metabolite bioinformatics portal: computational tools to facilitate synthetic biology of secondary metabolite production. *Synth. Syst. Biotechnol.* 1, 69–79. doi: 10.1016/j.synbio.2015.12.002

Wiener, P. (1996). Experimental studies on the ecological role of antibiotic production in bacteria. *Evol. Ecol.* 10, 405–421. doi: 10.1007/bf01237726

Wikoff, W. R., Anfora, A. T., Liu, J., Schultz, P. G., Lesley, S. A., Peters, E. C., et al. (2009). Metabolomics analysis reveals large effects of gut microflora on mammalian blood metabolites. *Proc. Natl. Acad. Sci. U.S.A.* 10, 3698–3703. doi: 10.1073/pnas.0812874106

Wilkens, M., Villanueva, J., Cofré, J., Chnaiderman, J., and Lagos, R. (1997). Cloning and expression in *Escherichia coli* of genetic determinants for production of and immunity to microcin E492 from *Klebsiella pneumoniae*. *J. Bacteriol.* 179, 4789–4794. doi: 10.1128/jb.179.15.4789-4794.1997

Willett, J. L., Gucinski, G. C., Fatherree, J. P., Low, D. A., and Hayes, C. S. (2015). Contact-dependent growth inhibition toxins exploit multiple independent cell-entry pathways. *Proc. Natl. Acad. Sci. U.S.A.* 112, 11341–11346. doi: 10.1073/pnas.1512124112

Wirth, T., Falush, D., Lan, R., Colles, F., Mensa, P., Wieler, L. H., et al. (2006). Sex and virulence in *Escherichia coli*: an evolutionary perspective. *Mol. Microbiol.* 60, 1136–1151. doi: 10.1111/j.1365-2958.2006.05172.x

Wooley, R. E., Gibbs, P. S., and Shotts, E. B. (1999). Inhibition of *Salmonella* Typhimurium in the chicken intestinal tract by a transformed avirulent avian *Escherichia coli*. *Avian. Dis.* 43, 245–250.

Xiong, W., Abraham, P. E., Li, Z., Pan, C., and Hettich, R. L. (2015). Microbial metaproteomics for characterizing the range of metabolic functions and activities of human gut microbiota. *Proteomics* 15, 3424–3438. doi: 10.1002/pmic.201400571

Xu, W., Chen, D., Wang, N., Zhang, T., Zhou, R., Huan, T., et al. (2015). Development of high-performance chemical isotope labeling LC-MS for profiling the human fecal metabolome. *Anal. Chem.* 87, 829–836. doi: 10.1021/ac503619q

Yan, K. P., Li, Y., Zirah, S., Goulard, C., Knappe, T. A., Marahiel, M. A., et al. (2012). Dissecting the maturation steps of the lasso peptide microcin J25 in vitro. *ChemBioChem* 13, 1046–1052. doi: 10.1002/cbic.201200016

Yang, C. C., and Konisky, J. (1984). Colicin V-treated *Escherichia coli* does not generate membrane potential. *J. Bacteriol.* 158, 757–759.

Yi-Hsuan, P., and Chen-Chung, L. (2006). The critical roles of polyamines regulating ColE7 production and restricting ColE7 uptake of the colicin-producing *Escherichia coli*. *J. Biol. Chem.* 281, 13083–13091. doi: 10.1074/jbc.m511365200

Yorgey, P., Lee, J., Kördel, J., Vivas, E., Warner, P., Jebaratnam, D., et al. (1994). Posttranslational modifications in microcin B17 define an additional class of DNA gyrase inhibitor. *Proc. Natl. Acad. Sci. U.S.A.* 91, 4519–4523. doi: 10.1073/pnas.91.10.4519

Yuzenkova, J., Delgado, M., Nechaev, S., Savalia, D., Epshtein, V., Artsimovitch, I., et al. (2002). Mutations of bacterial RNA polymerase leading to resistance to microcin J25. *J. Biol. Chem.* 277, 50867–50875. doi: 10.1074/jbc.m209425200

Zhang, L. J., Fath, M. J., Mahanty, H. K., Tai, P. C., and Kolter, R. (1995). Genetic analysis of the colicin V secretion pathway. *Genetics* 141, 25–32.

Zhang, X., Ning, Z. B., Mayne, J., Moore, J. I., Li, J., Butcher, J., et al. (2016). MetaPro-IQ: a universal metaproteomic approach to studying human and mouse gut microbiota. *Microbiome* 4:31. doi: 10.1186/s40168-016-0176-z

Zhao, Z., Eberhart, L. J., Orfe, L. H., Lu, S. Y., Besser, T. E., and Call, D. R. (2015). Genome-wide screening identifies six genes that are associated with susceptibility to *Escherichia coli* microcin PDI. *Appl. Environ. Microbiol.* 81, 6953–6963. doi: 10.1128/AEM.01704-15

Zhitnitsky, D., Rose, J., and Lewinson, O. (2017). The highly synergistic, broad spectrum, antibacterial activity of organic acids and transition metals. *Sci. Rep.* 7:44554. doi: 10.1038/srep44554

Zschüttig, A., Auerbach, C., Meltke, S., Eichhorn, C., Brandt, M., Blom, J., et al. (2015). Complete sequence of probiotic symbioflor 2 *Escherichia coli* strain G3/10 and draft sequences of symbioflor 2 *E. coli* strains G1/2, G4/9, G5, G6/7, and G8. *Genome Announc.* 3:e01330-14. doi: 10.1128/genomeA.01330-14

Zschüttig, A., Zimmermann, K., Blom, J., Goesmann, A., Pöhlmann, C., and Gunzer, F. (2012). Identification and characterization of microcin S, a new antibacterial peptide produced by probiotic *Escherichia coli* G3/10. *PLoS One* 7:e33351. doi: 10.1371/journal.pone.0033351

Zucca, M., Scutera, M. S., and Savoia, D. (2011). New antimicrobial frontiers. *Med. Chem.* 11, 888–900. doi: 10.2174/138955711796575498

Zukher, I., Pavlov, M., Tsibulskaya, D., Kulikovsky, A., Zyubko, T., Bikmetov, D., et al. (2019). Reiterative synthesis by the ribosome and recognition of the N-terminal formyl group by biosynthetic machinery contribute to evolutionary conservation of the length of antibiotic microcin C peptide precursor. *mBio* 10:e00768-19. doi: 10.1128/mBio.00768-19

Conflict of Interest: The authors declare that the research was conducted in the absence of any commercial or financial relationships that could be construed as a potential conflict of interest.

frontiers in Microbiology

ORIGINAL RESEARCH
published: 24 September 2019
doi: 10.3389/fmicb.2019.02154

Design and Expression of Specific Hybrid Lantibiotics Active Against Pathogenic *Clostridium* spp.

*Rubén Cebrián, Alicia Macia-Valero, Afif P. Jati and Oscar P. Kuipers**

Department of Molecular Genetics, Groningen Biomolecular Sciences and Biotechnology Institute, Faculty of Science and Engineering, University of Groningen, Groningen, Netherlands

Clostridium difficile has been reported as the most common cause of nosocomial diarrhea (antibiotic-associated diarrhea), resulting in significant morbidity and mortality in hospitalized patients. The resistance of the clostridial spores to antibiotics and their side effects on the gut microbiota are two factors related to the emergence of infection and its relapses. Lantibiotics provide an innovative alternative for cell growth inhibition due to their dual mechanism of action (membrane pore-forming and cell wall synthesis inhibition) and low resistance rate. Based on the fact that bacteriocins are usually active against bacteria closely related to the producer strains, a new dual approach combining genome mining and synthetic biology was performed, by designing new lantibiotics with high activity and specificity toward *Clostridium*. We first attempted the heterologous expression of putative lantibiotics identified following *Clostridium* genome mining. Subsequently, we designed new hybrid lantibiotics combining the start or end of the putative clostridial peptides and the start or end parts of nisin. The designed peptides were cloned and expressed using the nisin biosynthetic machinery in *Lactococcus lactis*. From the 20 initial peptides, only 1 fulfilled the requirements established in this work to be considered as a good candidate: high heterologous production level and high specificity/activity against clostridial species. The high specificity and activity observed for the peptide AMV10 makes it an interesting candidate as an alternative to traditional antibiotics in the treatment of *C. difficile* infections, avoiding side effects and protecting the normal gut microbiota.

Keywords: genome mining, *Clostridium difficile*, antimicrobial susceptibility, lantibiotic design, nisin

OPEN ACCESS

Edited by:
Tomasz M. Karpiński, Poznań University of Medical Sciences, Poland

Reviewed by:
Sander H. J. Smits, Heinrich-Heine-Universität Düsseldorf (HHU), Germany
Melinda J. Mayer, Quadram Institute, United Kingdom

****Correspondence:***
Oscar P. Kuipers
o.p.kuipers@rug.nl

Specialty section:
This article was submitted to Antimicrobials, Resistance and Chemotherapy, a section of the journal Frontiers in Microbiology

Received: *14 May 2019*
Accepted: *02 September 2019*
Published: *24 September 2019*

Citation:
Cebrián R, Macia-Valero A, Jati AP and Kuipers OP (2019) Design and Expression of Specific Hybrid Lantibiotics Active Against Pathogenic Clostridium spp. Front. Microbiol. 10:2154. doi: 10.3389/fmicb.2019.02154

INTRODUCTION

The genus *Clostridium* comprises about 150 metabolically diverse species of Gram-positive, endospore-forming anaerobic bacteria that are ubiquitous in virtually all anoxic habitats where organic compounds are present, including soils, aquatic sediments, and the intestinal tracts of animals and humans (Udaondo et al., 2017). Although almost all *Clostridium* spp. are commensal strains, some species of clostridia (e.g., *C. perfringens*, *C. botulinum*, *C. tetani*, or *C. difficile*) are known to be opportunistic, toxin-producing pathogens in both animals and humans (Cassir et al., 2016; Kiu and Hall, 2018; Czepiel et al., 2019). Between the pathogenic clostridia, *C. difficile* is gaining increased attention from the research community because of its ability to escape the

biocidal action of antibiotics and because of the growing number of infections especially in hospitals, where *C. difficile* is one of the most common acquired infections (Czepiel et al., 2019). In fact, *C. difficile* has been recognized as the most frequent pathogen in nosocomial diseases in Europe, causing diarrhea or pseudomembranous colitis. It has always been related to the elderly until the start of the new millennium, when numerous studies have described several outbreaks in Europe (Bauer et al., 2011), with more than 150,000 cases per year of *C. difficile* infection and a 20-fold increase of mortality. Those events have been attributed to the emergence of new and more virulent strains (Mastrantonio and Rupnik, 2018). The guidelines for treatment against *C. difficile* infections include non-antimicrobial therapies such as fecal microbiota transplantation (FMT). There has been evidence of the effectiveness of FMT (Ramai et al., 2019). In fact, in most cases, this is sufficient for full resolution of the disease (∼25% of patients) (Collins and Auchtung, 2017). Although FMT is recommended for *C. difficile* treatment, some adverse effects as nausea, abdominal pain, and FMT−related diarrhea have been observed in about 20% of the cases, and more severe adverse effects happen in about the 3% of the cases (Wang et al., 2016; Cheng et al., 2019). In terms of antimicrobial treatments, some antibiotics such as vancomycin and metronidazole are used. Nevertheless, these antibiotics do not affect spores, and for this reason, the treatments have to be administered for a prolonged time. Antibiotics also lead to the disruption of the gut microbiota because of their low specificity, allowing the pathogen to proliferate and colonize the human gut after the treatment (Mathias et al., 2019). Moreover, the misuse of antibiotics has a central role in the emergence of novel and more virulent strains, characterized by higher antibiotic resistance and toxin production (Yakob et al., 2015; Candel-Pérez et al., 2019; Fatima and Aziz, 2019). Several different strains have been reported to show a decrease in susceptibility or to be resistant to more than one antibiotic (Peng et al., 2017). Factors and mechanisms responsible for resistance include chromosomal genes, mobile genetic elements, biofilm formation and modification of antibiotic targets or metabolic pathways, among others. As a result, the development of novel specific antimicrobial compounds against *Clostridium* spp. turn out to be a necessity and a very relevant line of investigation.

Recent studies showed the potential of lantibiotics as an alternative to conventional antibiotics (van Heel et al., 2011; Hudson and Mitchell, 2018; Lewies et al., 2018). The term lantibiotic refers to lanthionine containing peptides with antimicrobial activity. They are ribosomally synthesized peptides produced mainly by Gram-positive bacteria and characterized by the presence of the atypical amino acid as dehydrobutyrine and dehydroalanine (formed after dehydration of threonine and serine residues respectively). These amino acids can react with the SH group of a cysteine forming a thioether-linked amino acid called lanthionine or a methyl-lanthionine ring, increasing the stability of the peptides (de Vos et al., 1995; van Kraaij et al., 1999; Alvarez-Sieiro et al., 2016; Repka et al., 2017). Lantibiotics are also characterized by their low resistance level of their targets. This is because most of them have multiple modes of actions: pore-forming on the cell walls causing ATP leakage or the sequestration of cell wall precursor lipid II, that inhibits the cell wall synthesis and the replication (Sahl et al., 1995; Breukink and de Kruijff, 2006; Hasper et al., 2006).

The combination of genome mining and synthetic biology approaches can be used for the identification of novel lantibiotics and then employ the modularity and the orthogonality of engineering into the design of novel powerful antimicrobial peptides (van Heel et al., 2016; Montalbán-López et al., 2017; Schmitt et al., 2019). *In silico* analysis of putative lantibiotic genes using bioinformatic tools as BAGEL4 or Anti-Smash (Weber et al., 2015; van Heel et al., 2018) provides an accurate prediction of putative novel lantibiotics. BAGEL4 software can analyze DNA sequences by two different approaches. First, an indirect approach which is the context of bacteriocin- or RiPP gene-based mining and then a direct approach, which is structural gene-based mining directly via Glimmer software for finding genes in microbes (van Heel et al., 2018, 4). These approaches improve the success rate by reducing the false positive probability and minimize manual evaluation of results. Also, anti-SMASH is an application that predicts putative bacteriocin genes as well as their biochemical properties, and further details including gene cluster description, annotation, and genomic loci for the biosynthetic pathway (Weber et al., 2015). Combination of BAGEL4 and anti-SMASH for genome mining gives accurate information for identification of unknown lantibiotic genes in various organisms. Afterward, the new DNA sequence encoding the putative lanthipeptide gene can be fused to the nisin leader sequence and expressed heterologously in *Lactococcus lactis* (Montalbán-López et al., 2017). Alternatively, the design of hybrid lantibiotics by a combination of known ones, with enhanced antimicrobial activity has also been described as a potent tool for the identification of new drugs (Schmitt et al., 2019).

With some exceptions, bacteriocin/lantibiotics are usually active against strains closely related to the producer one (Yang et al., 2014; Todorov et al., 2019). The use of new peptides with high specific activity against *Clostridium* spp. and with low or no activity against other bacteria would provide a good strategy in the treatment of *C. difficile* infections, minimizing or limiting one of the most unwanted side effects of traditional antibiotics after prolonged treatments, i.e., gut microbiota modification. This alteration is related to the recurrence of the infection and also to other pathologies such as diarrhea (Nelson, 2007; Song et al., 2008).

This study is focused on the identification, design, and production of new lantibiotics with enhanced activity against *C. difficile*. These new peptides must fulfill three requirements: high heterologous production using the nisin biosynthetic machinery, and high specificity and activity toward *C. difficile*.

MATERIALS AND METHODS

Microorganisms, Plasmids, and Growth Conditions

The strains used in this work and the plasmid designs are listed in **Table 1**. *Escherichia coli* strains were grown in LB medium at 37°C and shaking. *Lactococcus* and *Lactobacillus*

TABLE 1 | Strains and plasmids used in this work.

Strain	Characteristic/purpose	References
Escherichia coli TOP-10	*mcrA*, Δ(*mrr-hsdRMS-mcrBC*), *Phi80lacZ*(*del*)*M15*, Δ*lacX74*, *deoR*, *recA1*, *araD139*, Δ(*ara-leu*)*7697*, *galU*, *galK*, *rpsL*(*SmR*), *endA1*, *nupG*	Thermo Fisher Scientific
pUC57-$Clos_x$	Amp^R, synthetic gene design	This work
pUC57-AMV_x	Amp^R, synthetic gene design	This work
Lactococcus lactis NZ9000	*pep*N:*nisRK*	de Ruyter et al., 1996
pIL253 pNZe-NisP8H	Ery^R, Cm^R, NisP producer strain	Montalbán-López et al., 2018
pTLR-BTC	Ery^R, *pepN:nisRK*, *nisBTC* genes cloned from pIL3-BTC into pTLR plasmid	Lab collection
pTLR-BTC pNZ8048	Ery^R, Cm^R, *pepN:nisRK*, *nis*BTC	This work
pIL3-BTC pNZ8048-NisA	Ery^R, Cm^R, NisA producer strain	van Heel et al., 2013
pTLR-BTC pNZ8048-Clos2	Ery^R, Cm^R, synthetic gene *clos2* cloned fused to nisin leader under P_{nis} promoter in pNZ8048-NisA	This work
pTLR-BTC pNZ8048-Clos4	Ery^R, Cm^R, synthetic gene *clos4* cloned fused to nisin leader under P_{nis} promoter in pNZ8048-NisA	This work
pTLR-BTC pNZ8048-Clos5	Ery^R, Cm^R, synthetic gene *clos5* cloned fused to nisin leader under P_{nis} promoter in pNZ8048-NisA	This work
pTLR-BTC pNZ8048-Clos12	Ery^R, Cm^R, synthetic gene *clos12* cloned fused to nisin leader under P_{nis} promoter in pNZ8048-NisA	This work
pTLR-BTC pNZ8048-Clos14	Ery^R, Cm^R, synthetic gene *clos14* cloned fused to nisin leader under P_{nis} promoter in pNZ8048-NisA	This work
pTLR-BTC pNZ8048-Clos15	Ery^R, Cm^R, synthetic gene *clos15* cloned fused to nisin leader under P_{nis} promoter in pNZ8048-NisA	This work
pTLR-BTC pNZ8048-Clos16	Ery^R, Cm^R, synthetic gene *clos16* cloned fused to nisin leader under P_{nis} promoter in pNZ8048-NisA	This work
pTLR-BTC pNZ8048-Clos17	Ery^R, Cm^R, synthetic gene *clos17* cloned fused to nisin leader under P_{nis} promoter in pNZ8048-NisA	This work
pTLR-BTC pNZ8048-Clos22	Ery^R, Cm^R, synthetic gene *clos22* cloned fused to nisin leader under P_{nis} promoter in pNZ8048-NisA	This work
pTLR-BTC pNZ8048-Clos24	Ery^R, Cm^R, synthetic gene *clos24* cloned fused to nisin leader under P_{nis} promoter in pNZ8048-NisA	This work
pTLR-BTC pNZ8048-AMV1	Ery^R, Cm^R, synthetic gene *AMV1* cloned fused to nisin leader under P_{nis} promoter in pNZ8048-NisA	This work
pTLR-BTC pNZ8048-AMV2	Ery^R, Cm^R, synthetic gene *AMV2* cloned fused to nisin leader under P_{nis} promoter in pNZ8048-NisA	This work
pTLR-BTC pNZ8048-AMV3	Ery^R, Cm^R, synthetic gene *AMV3* cloned fused to nisin leader under P_{nis} promoter in pNZ8048-NisA	This work
pTLR-BTC pNZ8048-AMV4	Ery^R, Cm^R, synthetic gene *AMV4* cloned fused to nisin leader under P_{nis} promoter in pNZ8048-NisA	This work
pTLR-BTC pNZ8048-AMV5	Ery^R, Cm^R, synthetic gene *AMV5* cloned fused to nisin leader under P_{nis} promoter in pNZ8048-NisA	This work
pTLR-BTC pNZ8048-AMV6	Ery^R, Cm^R, synthetic gene *AMV6* cloned fused to nisin leader under P_{nis} promoter in pNZ8048-NisA	This work
pTLR-BTC pNZ8048-AMV7	Ery^R, Cm^R, synthetic gene *AMV7* cloned fused to nisin leader under P_{nis} promoter in pNZ8048-NisA	This work
pTLR-BTC pNZ8048-AMV8	Ery^R, Cm^R, synthetic gene *AMV8* cloned fused to nisin leader under P_{nis} promoter in pNZ8048-NisA	This work
pTLR-BTC pNZ8048-AMV9	Ery^R, Cm^R, synthetic gene *AMV9* cloned fused to nisin leader under P_{nis} promoter in pNZ8048-NisA	This work
pTLR-BTC pNZ8048-AMV10	Ery^R, Cm^R, synthetic gene *AMV10* cloned fused to nisin leader under P_{nis} promoter in pNZ8048-NisA	This work
Clostridium beijerinckii NIZO B504	Indicator strain	Lab collection
C. botulinum CECT551	Indicator strain	CECT
C. difficile CECT531	Indicator strain	CECT
C. ihumii AP5	Indicator strain	Merhej et al., 2015
C. sporogenes C22/10	Indicator strain	Aktypis et al., 1998
C. tyrobutyricum NIZO B574	Indicator strain	Lab collection
Bacillus cereus ATCC10987	Indicator strain	ATCC
Enterococcus faecalis LMG8222	Indicator strain	LMG
E. faecium LMG16003	Indicator strain	LMG
Listeria monocytogenes LMG10470	Indicator strain	LMG
Lactobacillus plantarum WCFS1	Indicator strain	Kleerebezem et al., 2003
Lactococcus lactis MG1363	Indicator strain	Wegmann et al., 2007
Staphylococcus aureus LMG8224	Indicator strain	LMG
Streptococcus salivarius HSISS3	Indicator strain	Van den Bogert et al., 2013

ATCC, American Type Culture Collection; CECT, Spanish Type Culture Collection; LMG, Belgian Co-ordinated Collections of Microorganism.

strains were grown in M17 + 0.5% of glucose (GM17) at 30°C without shaking. *Bacillus*, *Enterococcus*, *Listeria*, *Staphylococcus*, and *Streptococcus* strains were grown as described above but at 37°C. *Clostridium* strains were grown in Reinforced Clostridium Medium (RCM) at 37°C in anaerobiosis in a Coy Anaerobic Chamber. For solid media, agar at 1.2% was added. For Amp^R resistant plasmids selection in *E. coli*, 100 μg/mL of ampicillin were added, while 5 or 10 μg/mL of chloramphenicol/erythromycin were added for *L. lactis* selection.

Genome Mining of Various *Clostridium* Strains and Synthetic Gene Design

Identification of novel putative lantibiotic genes was performed using BAGEL4 (van Heel et al., 2018) and antiSMASH (Weber et al., 2015). 563 genomes from *Clostridium* spp. strains and 43 of the recently separated *Paeniclostridium sordelii* genus (Sasi Jyothsna et al., 2016) deposited on the NCBI database were mined. Novelty, completeness of the gene cluster and the presence of lantibiotics-related protein domains, as the NisC interaction domain FxLx in the putative leader (van der Meer et al., 1994; Abts et al., 2013; Plat et al., 2013), were considered in the selection of the putative lantibiotic genes. Twenty synthetic genes (GeneScript) were designed by optimizing the codon usage to *L. lactis* using the Jcat program (Grote et al., 2005). The first 10, with the selected-putative-lantibiotic genes identified after genome mining (pUC-$Clos_x$) and the second 10 by the combination of the first or last rings of the putative lantibiotics with the first or last rings of nisin (pUC57-AMV_x). To simplify the cloning, the genes were designed with 5′ and 3′ tags: TCGAGTTCAAAAAAAGATTCAGGTGCTAGC-gene-TAACTTTGAACCAAAATTAGAAAACCC in the case of the $Clos_x$ genes and AMV_x hybrids with the last part of nisin, and ATTACAAGTATAAGCTTATGTACACCCGGGTGT-gene-TAACTTTGAACCAAAATTAGAAAACCC in the case of AMV_x hybrids with the first part of nisin. The plasmids with the designed genes were transformed into chemo-competent cells of *E. coli* TOP-10 (Green and Rogers, 2013) and then cloned into *L. lactis*.

Molecular Cloning

The designed plasmids pUC57-$Clos_x$ were isolated, and each gene was amplified with specific primers designed for USER ligation (Geu-Flores et al., 2007), Clos-USER-fw and Pep-USER-rv, and cloned into pNZ8048-NisA (van Heel et al., 2013) fused to nisin leader (instead nisin) and under P*nis* control. The backbone of pNZ8048-NisA was amplified using the primers Leader-USER-rv and pNZ-USER-fw. The same amounts of fragment and backbone were mixed and ligated using USER (NEB) enzyme according to the suppliers. After that, the ligation was dialyzed against ultra-pure water and transformed into electrocompetent cells of *L. lactis* NZ9000 pTLR-BTC (Holo and Nes, 1995), where the nisin processing enzymes (*nis*BC) and the transporter (*nis*T) were present. In the case of the other synthetic genes (pUC57-AMV_x), the same procedure was performed with some differences regarding the primers used. For the hybrid peptides with the first part of nisin fused to the last part of the putative lantibiotics, the genes were amplified using Pep-USER-fw and Pep-USER-rv primers, while the primers Rab-USER-rv and pNZ-USER-fw were used for the backbone. For those hybrid peptides in which the last rings of nisin were fused to the first rings of the putative lantibiotics, Clos-USER-fw and Pep-USER-rv were used for the amplification of the genes, while pNZery-USER-fw and Leader-USER-rv were used for the backbone. The primer sequences and the PCR conditions are listed in **Table 2**. Finally, the different plasmids pNZ-$Clos_x$ or pNZ-AMV_x were isolated, and the correct sequences of the peptides were confirmed by sequencing (Macrogen Europe, Amsterdam, Netherlands).

Peptide Expression, Purification, Quantification, and Characterization

Initially, TCA precipitation (Sambrook et al., 1990) was performed in order to identify the peptides with better expression. Briefly, 50 mL of minimal expression medium (MEM) (Rink et al., 2005) was inoculated at 2% from an overnight culture of the producer strains grown in GM17 with the corresponding antibiotics. The cells were incubated at 30°C until the $OD_{600\,nm}$ reached 0.4–0.6, and at this point, nisin at 10 ng/mL was added to induce the expression. The culture was left in the same conditions overnight. The cells were removed and TCA at 10% (final concentration) was added to the supernatants, that were placed on ice for 2 h. Finally, the peptides were collected by centrifuging at 10,000 rpm for 1 h at 4°C, washed with cold acetone and resuspended in 0.5 mL of 0.05% acetic acid. The peptides were analyzed by Matrix-Assisted Laser Desorption/Ionization with a Time-Of-Flight detector (MALDI-ToF) and those peptides detected were selected for a large-scale purification using 1 L of MEM medium.

After the induction and incubation, the peptides were purified as described by Cebrián et al. (2012). Briefly, the culture pH was raised to 6 and mixed with Sephadex CM-25 (Sigma–Aldrich) (previously swollen overnight in distilled water at 4°C) at 1:10

TABLE 2 | Primers and PCR conditions used in this work.

Name	Sequence	PCR conditions
Pep-USER-fw	AGTATAAGCT*U*ATGTACA CCCGGGTGT	1× 95°C 3 min, 30× (95°C 30 s, 55°C 30 s, 68°C 30 s), 1× 68°C 3 min
Pep-USER-rv	ACCGCATGCT*U*CTCGAGGGTTT TCTAATTTTGGTTCAAAG	
Clos-USER-fw	ATCTTGTTTCAG*U*TTCAAAAAAA GATTCAGGTGCTAGCCCACGT	
pNZ-USER-fw	AAGCATGCGG*U*CTTTGAACCA AAATTAGAAAACCAAGGCTTG	1× 95°C 3 min, 30× (95°C 30 s, 55°C 30 s, 68°C 5 min), 1× 68°C 6 min
Leader-USER-rv	ACTGAAACAAGA*U*CAAGATT AAAATCTTTTGTTGAC	
Rab-USER-rv	AAGCTTATAC*U*TGTAATGCGT GGTGATGCACCTGAATC	
pNZ-Cm-fw	CATGCAGGATTGTTTATGAA CTCTATTCAGGAATTGTCAG	1× 95°C 3 min, 30× (95°C 30 s, 55°C 30 s, 68°C 1 min), 1× 68°C 3 min
pNZ-*Sph*I-rv	TCGCCGCATGCTATCAA TCAAAGCAACACGTGC	

In italic and underlined the uracil nucleotide required for USER ligation.

(vol:vol). The mixture was shaken for 1 h, and then the CM-25 was decanted and placed into a chromatographic column. The CM-25 was washed with 1 L of distilled water, and the peptides were eluted with 800 mL NaCl 2 M distributed in 50 mL fractions. The active fractions were applied on reverse-phase C18 chromatography for a second purification step. Isopropanol:acetonitrile (2:1) 0.1% trifluoroacetic acid (TFA) was used as organic phase (solvent B) while 0.1% of TFA in distillated water was used as aqueous phase (solvent A). The peptides were eluted from the C18 column with 10 mL of different percentages of solvent B (10, 20, 30, 40, 50, 60, and 80%). Finally, the fractions were lyophilized, and the peptides resuspended in 1 mL of solvent A.

To obtain highly pure peptides, the previous active fractions were purified by reverse-phase C4 HPLC. For the purification, the Jupiter 5 μ C4 300A column (Phenomenex) was equilibrated in 5% of solvent B, and then a linear gradient 5–60% of solvent B was applied to elute the peptides. The *L. lactis* NZ9000 pIL253 pNZe-NisP8H strain was used as a sensitive strain in the different purification steps.

Active fractions were lyophilized, resuspended in solvent A, and quantified using a Quantus^{TM} fluorometer (Promega) and the Qubit^{TM} Protein Assay Kit (Thermo Scientific) according to the suppliers. Briefly, the samples were diluted 100-fold in 1× NanoOrange reagent working solution (1× NanoOrange protein quantitation diluent + 500-fold diluted NanoOrange protein quantification reagent), and the samples were incubated in the dark for 10 min at 93°C and then at room temperature for 20 min. After that, the fluorescence of the samples was measured in the Quantus^{TM} fluorometer (Promega). Nisin at known concertation was used as a reference.

For the nisin leader cleavage, NisP was purified from the supernatant of 1 L of *L. lactis* NZ9000 pIL253 pNZe-NisP8H [a soluble NisP producer strain (Montalbán-López et al., 2018)] in MEM medium after a nisin induction (10 ng/mL) using a Histrap^{TM} excel column (GE Healthcare) according to the suppliers. NisP was eluted with 20 mL of elution buffer (50 mM of NaH_2PO_4, 0.5 M NaCl, 200 mM imidazole, 20% of glycerol, pH 8) aliquoted and stored at −80°C. The ratio prenisin:NisP was optimized in 1:0.005 (prenisin 10% TCA precipitated supernatant:purified NisP) after 1 h at 37°C. The leader cleavage efficiency of the peptides was analyzed. For this, the purified peptides were mixed with NisP in the previous conditions, and the leader cleavage monitored each 1 h during 3 h using MALDI-ToF.

Finally, the dehydration level of the peptides was determined after the cleavage by MALDI-ToF according to the methodology described by van Heel et al. (2013). The average expected masses were calculated using the ProtParm program (Wilkins et al., 1999) and the percentage of each dehydration peak was calculated approximately as an average of the intensity of each peak after several MALDI-ToF analyses. The best peptides were analyzed for the ring formation using *N*-ethylmaleimide (NEM) reaction according to Yang and van der Donk (2015) methodology.

Antimicrobial Test

Minimal inhibitory concentration (MIC) measurements using a 96-well plate microdilution method and spot overlay assays were performed as systems for antimicrobial testing. Clinical and Laboratory Standards Institute (CLSI) indications were followed as far as possible. Mueller Hinton Agar (Difco, Thermo scientific) was used in the spot overlay screening test for the indicator strains (Hockett and Baltrus, 2017). In this case, NisP and the peptides were mixed as above and spotted (5 μl) on the indicator strains. For the MIC test, NisP was added into the liquid medium (RCM) in a relation 1:0.005 and then, serial dilutions of the peptides (from 32 to 0.003 μg/mL) were performed by triplicate. Finally, the indicator strains were added at 10^5 CFU/mL. All assays with *Clostridium* were performed in a Coy Anaerobic Chamber.

RESULTS

Lantibiotics Genome Mining of *Clostridium* spp.

In general, *Clostridium* spp. are organisms relatively difficult to grow, and require complex media as well as anaerobiosis. The identification of antimicrobial peptides in this genus is usually hard, and their production at high levels is challenging. In order to identify new lantibiotics specific and active against pathogenic *Clostridium* strains as *C. difficile*, two bioinformatics programs were used. Firstly, high-throughput screening of genomic data was accomplished using AntiSMASH (Weber et al., 2015) and then small putative lantibiotic ORFs were identified using BAGEL4 (van Heel et al., 2018). 563 genomes belonging to 110 *Clostridium* species, as well as 43 strains of *P. sordelii* that had been entirely sequenced and stored in Genebank NCBI, were mined.

All genomes were uploaded on the AntiSMASH program for the first selection of possible lantibiotic sequences identification. From the 606 initial genomes, only 17 were identified harboring putative lantibiotics sequences. They were downloaded and analyzed with BAGEL4. Finally, 54 putative lantibiotic genes were detected (**Supplementary Table S1**). Among all putative lantibiotic detected, 10 genes were selected for heterologous expression in *L. lactis* NZ9000 pTLR-BTC.

Putative Lantibiotics Selection, Expression, and Characterization From *Clostridium* spp.

Lantibiotics Selection

Based on novelty, the presence of all modification enzymes in the cluster (**Figure 1**) and the presence of some lantibiotic-related domains, 10 putative lantibiotic genes (**Table 3**) were selected, synthesized, and cloned, fused to the nisin leader under the P_{nis} promoter in pNZ-8048. The designed plasmids were transformed into *L. lactis* NZ9000 cells pTLR-BTC, which provides the rest of the genes necessary for their biosynthesis. Leader sequences were assigned manually considering the known leader cutting site for other lantibiotics (presence of P in the cleavage area, GG motifs, similar cutting site to known lantibiotics), the distance from the FxLx box (Abts et al., 2013), or the position of the first C (**Table 3**). In order to ensure the novelty of the selected peptides, a BLASTp analysis was performed for each one.

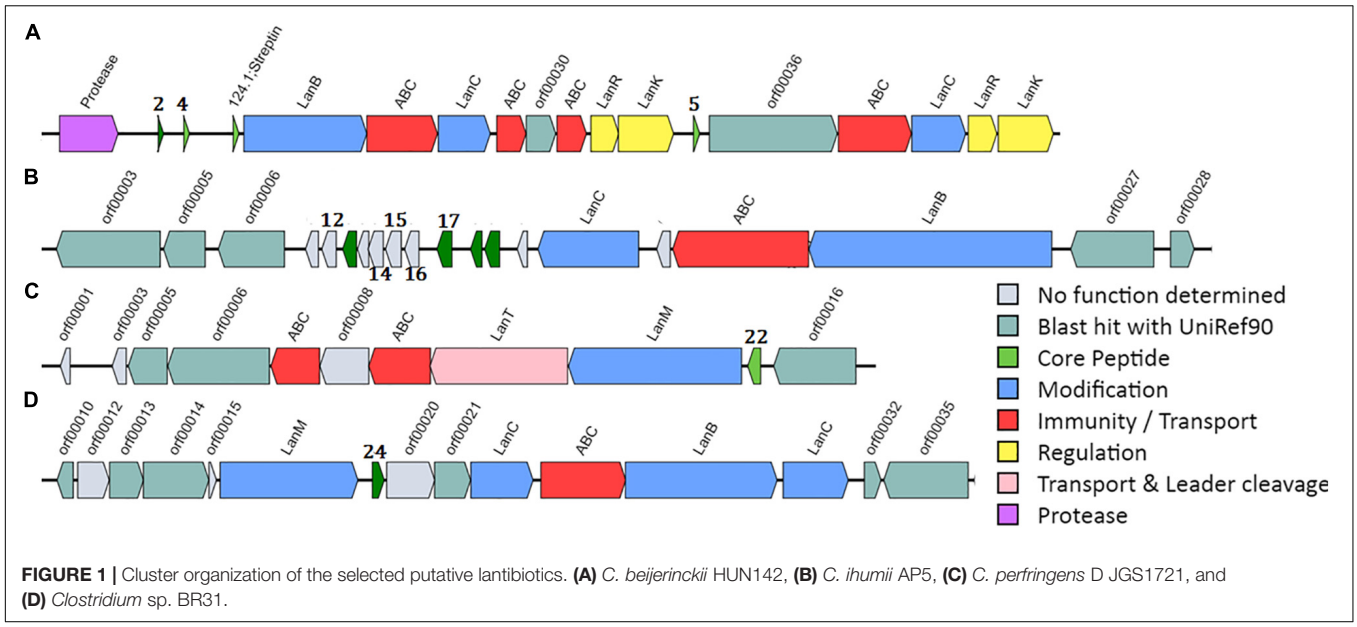

FIGURE 1 | Cluster organization of the selected putative lantibiotics. **(A)** *C. beijerinckii* HUN142, **(B)** *C. ihumii* AP5, **(C)** *C. perfringens* D JGS1721, and **(D)** *Clostridium* sp. BR31.

TABLE 3 | Putative lantibiotic sequences selected for *L. lactis* heterologous expression.

Name	Strain	Putative leader	Putative core peptide	S + T
Clos2	*C. beijerinckii* HUN142	VGKLDD**FDLD**VKVKINSKKGIKPS	YLSLTPKCTSLCPTNVFVCISKRCK	6
Clos4		MGKLDD**FDLD**VKVKATPKGGVKPS	ITSRILCTSSCYTQFIQCHDRV	6
Clos5		MGKLDN**FDLD**VKIKKDEKRGVKPS	VTSYSACTPGCATSLFRTCLTRSCKGC	9
Clos12	*C. ihumii* AP5	MPNYKE**FDLD**IRNEKNNLKSMNSKKRSD**GG**	TCYYSCGCKTNEGNSCGKVCFTDTIVCGTDFDGR	7
Clos14		MPNYKD**FDLD**IQNIKMNKINDKRRYPI	SDKRDDMSMCVCKKTDVCKTHETDSCNNGLCFESGKCTWV	8
Clos15		MPNYKD**FDLD**IQNSKLGVDSSRKVLPP	TFSYEYDKLSECRCRPKTQTCATHCSCATYCNGSCNQHTDCAL	10
Clos16		MPNYKE**FDLD**IRNSKNGINMYGPSAVIVP	ATDGGGKKTVCGRTCNGSACNPNSCQTRCIKPAD	6
Clos17		MPNYKD**FDLD**IQNNKSSVNSIKTTTMPP	TFSYEYDQYSECVCKPKTRNSCVTYCNGSCNQHTDCTL	9
Clos22	*C. perfringens* D JGS1721	MMKQLDKKSKTGIYVQVASDKELELLV**GG**	AGAGFIKTLTKDCPEVVSQVCGSFFGWVSACKNC	5
Clos24	*Clostridium* sp. BR31	MDD**FDLD**LRKIAENGNSANALSASDMITSEIISK	VTETITRTFKGQCVSVETPTTGMTSACCKKGGTDVEPQCVP	11

In bold, domain related to the peptide processing. S and T positions are indicated in green while C positions are in red.

In the case of the putative lantibiotics from *C. beijerinckii* HUN142 (Clos2, Clos4, and Clos5 in this study), the complete set of biosynthetic genes including putative modification enzymes, ABC transporters, regulation, immunity, and protease protein was identified in the cluster, which shows similarity to the class I lantibiotic biosynthetic genes cluster (**Figure 1A**). Interestingly, this cluster appears to be duplicated. One part could be related to Clos2 and Clos4 production and the other one with Clos5 production. Based on BLASTp homology (NCBI) analysis, these peptides belong to the gallidermin/nisin family, but low level of homology and/or similarity was observed except for Clos5. In this case, the putative lipid II binding domain region (CTPGCA) is the same as for gallidermin or nisin. Another putative antimicrobial peptide corresponding to streptin but with two modifications (G2N and M6A) was also identified in this cluster.

Clostridium ihumii AP5 is a new species of *Clostridium* isolated from a French Caucasian female with anorexia nervosa (Merhej et al., 2015). Surprisingly, 11 putative lantibiotic genes were identified after the mining in this strain and only one *lan*BTC putative system (**Figure 1B**). In their sequences, they are quite diverse, limiting the similarities to the first 15 aa of the leader peptide (**Supplementary Table S1**). After a BLASTp analysis of these peptides, no homologies were found, and no other lantibiotic has been described with similar characteristics. For this reason, 5 of them (Clos12, Clos14, Clos15, Clos16, and Clos17) were selected for their heterologous expression.

One single component lantibiotic from Class II lanthipeptides was found in *C. perfringens* D JGS1721 coded (**Figure 1C**) as Clos22 and identified as type A(II) lantibiotic which is known to have two domains, a linear N-terminal region and a globular C-terminal region. These types of lantibiotics show a slightly different mode of action than the type A(I) lantibiotics since they only can inhibit cell wall synthesis by the interaction with the lipid II (no pore-forming activity). After a BLASTp analysis, a 52% of identity with the predicted lantibiotic columbicin A was observed.

Taken from the newest study about *Clostridium* sp. BR31, this species was previously known as novel species in the genus of *Clostridium* as was still listed in *Clostridium* genome databases when this study started, but recently it had a new order in

taxonomy and was declared as a new genus in *Clostridium* cluster XIVa, in the family Lachnospiraceae. This species now is designated as *Merdimonas faecis gen. nov.*, sp. nov (Seo et al., 2017). An a-typical cluster structure was observed for this strain, with two *lan*C genes separated by *lan*T and *lan*B, as well as the presence of the *lan*M gene upstream of the structural gen (**Figure 1D**). The unusual distribution of the cysteines in the peptide makes it difficult to place it inside the lantibiotics groups. No homologies were found with other lantibiotics after the BLASTp analysis.

Lantibiotics Expression and Characterization

As a first approximation, 10% TCA precipitation was performed, and the samples were analyzed by MALDI-ToF. Unfortunately, from the 10 peptides, only Clos2, Clos4, and Clos5 were observed. So, these strains were selected for a larger purification using 1 L of MEM medium, CM-25, C18, and RP-HPLC (**Figure 2A**).

The production levels obtained for the peptides in comparison with nisin were not high, being the lowest for Clos4. Many peaks were also observed indicating different levels of dehydration (hetero-dehydration) (**Figure 2A**). The peptides were analyzed by MALDI-ToF, and a strong hetero-dehydration, as well as degradation of the peptides, was observed, specifically in the case of Clos4 and Clos5. According to the observed masses, N-terminal degradation of the peptide leader (MSTKDFNLDLV and/or MSTKDFNLDLVSV degradation) could be related to this (**Figure 3**).

Finally, in order to establish the dehydration levels for each peptide and because of the high ratio of N-terminal degradation, the peptides were digested with NisP. Firstly, the efficiency of the cleavage was analyzed monitoring the leader release during 3 h. In the case of these peptides, almost all the peptides were cleaved after this time. However, the efficiency was much lower than for nisin during the first and second hour (**Supplementary Figure S1**). The percentage of each dehydration level was approximately calculated considering the intensity of each peak after MALDI-ToF (**Figure 4** and **Table 4**) (the results were similar for different MALDI-ToF analyzed samples). In general, low dehydration levels were observed. In the case of Clos2, 11.4% of the observed peptide was non dehydrated, while 29.9% were with -3 H_2O and only the 2.4% of the peptide was fully dehydrated (-6 H_2O) (**Table 4**). In the case of Clos4, it was the best dehydrated, no full dehydrated peptides (-6 H_2O) were observed, and 21, 35, and 26.5% of dehydration was observed for -5, -4, and -3 H_2O, respectively (**Table 3**). A 5.8% of the peptide was no dehydrated. Finally, for Clos5, the 6.1% of the peptide was fully dehydrated (-9 H_2O), but the higher dehydration range was -6 H_2O (22.7%) (**Table 4**).

Antimicrobial Activity Test

One milliliter fractions of the HPLC was collected between minutes 15 and 25. These fractions were lyophilized and stored. Because the state of dehydration is essential for the activity, and the activity of the peptides against different bacteria could be related to the state of dehydration, the four fractions corresponding to the main peaks of each lantibiotic were resuspended in 1 mL of solvent A and were assayed against Gram-positive bacteria using spot overlay test (5 μL drops). In **Figure 3**, the antimicrobial activity is represented. NisP was previously added into the plates for the leader cleavage. No activity was observed for the peptides Clos2, Clos4, and Clos5 against the tested bacteria, except for *B. cereus* ATCC10987 for which a small halo was observed for the fraction 4 of each peptide. Finally, the same test was performed against three strains

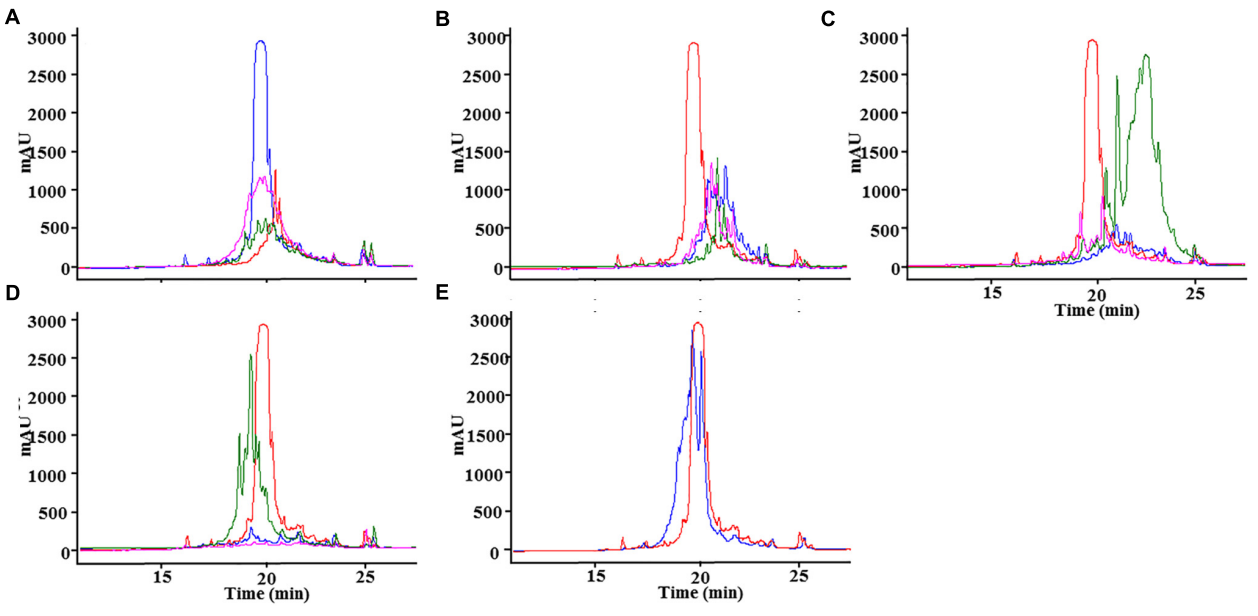

FIGURE 2 | RP-HPLC chromatogram for: **(A)** nisin (blue), Clos2 (red), Clos4 (green), and Clos5 (pink) peptides. **(B)** Nisin (red), AMV1 (green), AMV2 (pink), AMV3 (blue). **(C)** Nisin (red), AMV4 (blue), AMV5 (green), AMV6 (pink). **(D)** Nisin (red), AMV7 (green), AMV8 (blue), AMV9 (pink). **(E)** Nisin (red), AMV10 (blue).

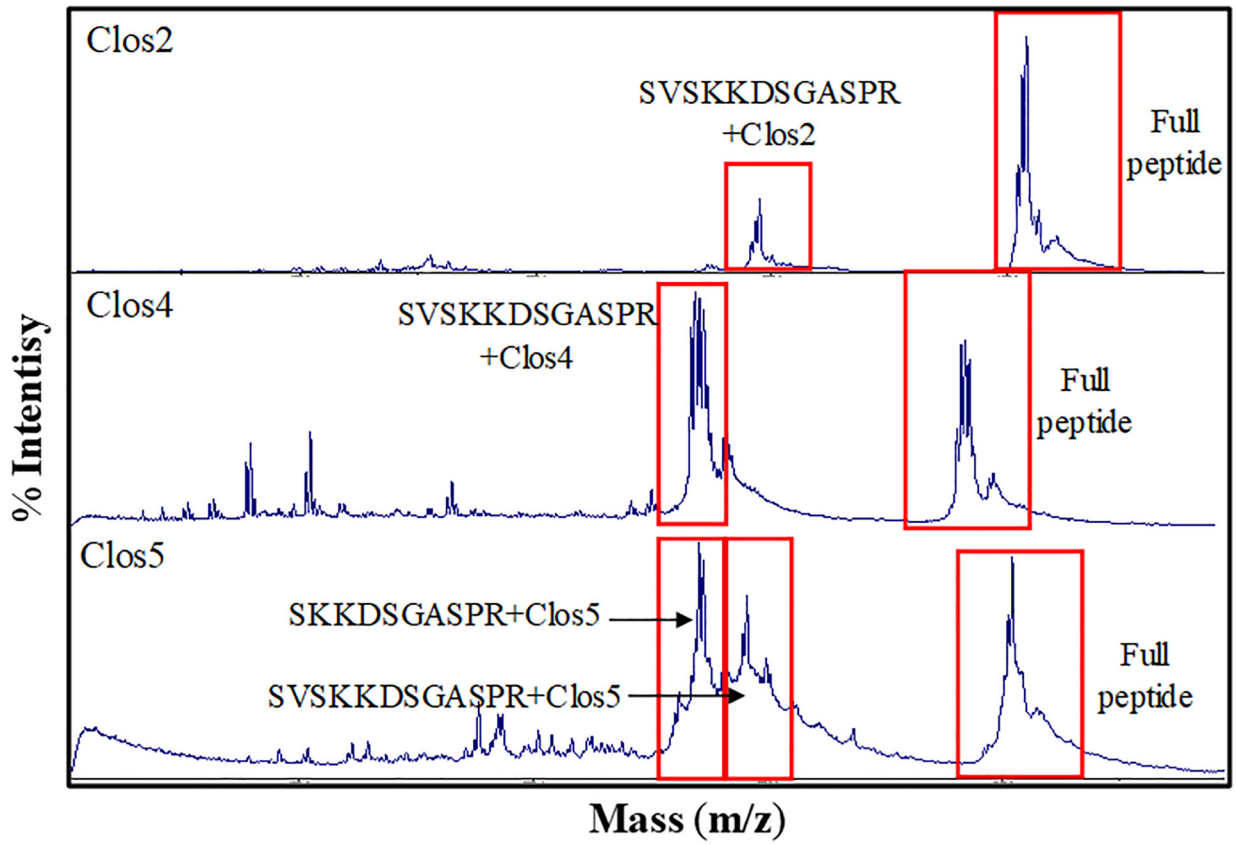

FIGURE 3 | MALDI-ToF chromatogram for $Clos_x$ peptides indicating different degradation levels.

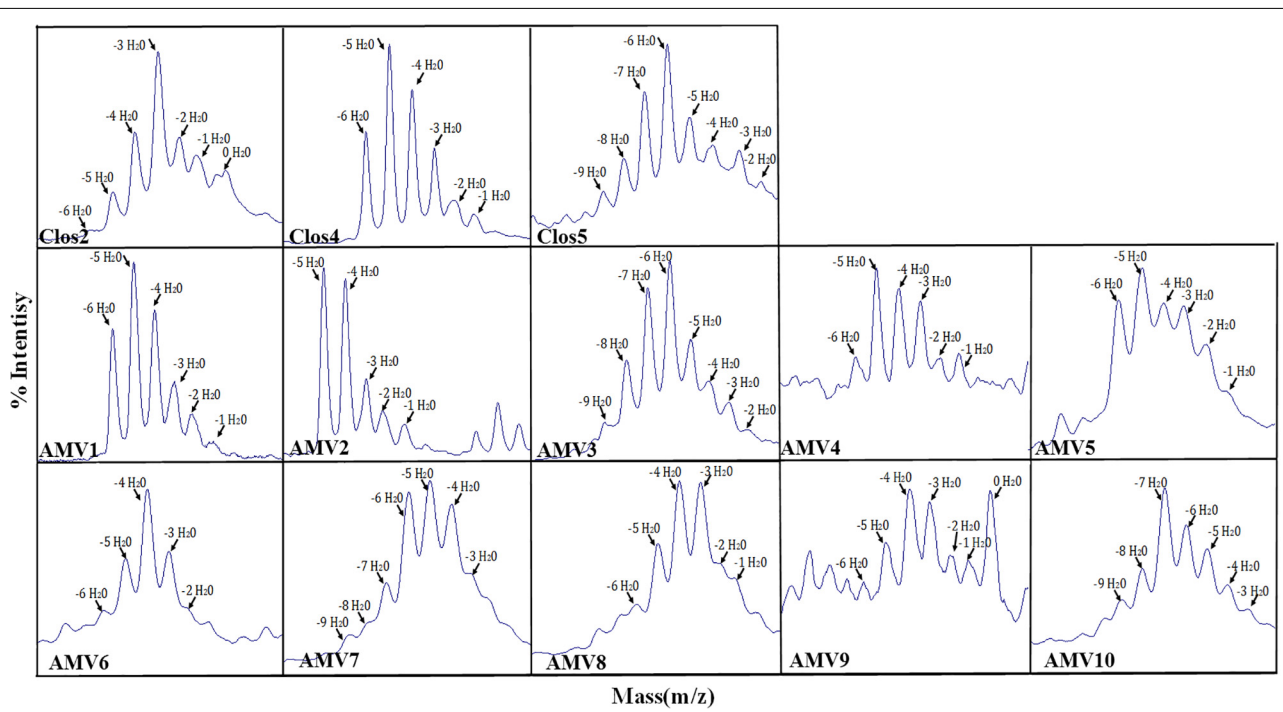

FIGURE 4 | MALDI-Tof of the designed peptides after the leader cleavage, indicating the dehydration level.

TABLE 4 | Molecular weight for the different AMV peptides and abundance.

Dehy	Clos2		Clos4		Clos5		AMV1		AMV2		AMV3		AMV4	
	MW	%	MW	%	MW	%	MW	%	MW	%	MW	%	MW	%
0	2805.4	11.4	2575.0	5.8	2817.3	–	2571.1	–	2485.9	–	2823.4	–	3021.5	–
1	2787.4	14.1	2557.0	8.3	2799.3	–	2553.1	2.67	2467.9	6.3	2805.4	–	3003.5	17.3
2	2769.4	16.7	2539.0	17.1	2781.3	7.3	2535.1	6.41	2449.9	9.0	2787.4	4.5	2985.5	17.0
3	2751.4	29.9	2521.0	26.6	2763.3	10.8	2517.1	11.63	2431.9	15.0	2769.4	8.1	2967.5	25.1
4	2733.4	17.4	2503.0	35.3	2745.3	11.3	2499.1	21.38	2413.9	33.7	2751.4	11.0	2949.5	27.9
5	2715.4	8.1	2485.0	20.9	2727.3	14.6	2481.1	30.87	2395.9	36.0	2733.4	17.0	2931.5	30.1
6	2697.4	2.4	2467.0	–	2709.3	22.7	2463.1	27.03			2715.4	27.9	2913.5	17.0
7					2691.3	17.4					2697.4	24.8	2895.5	–
8					2673.3	9.8					2679.4	14.0		
9					2655.3	6.1					2661.4	5.3		

Dehy	AMV5		AMV6		AMV7		AMV8		AMV9		AMV10	
	MW	%	MW	%	MW	%	MW	%	MW	%	MW	%
0	3186.8	–	3406.9	–	3732.5	–	3713.5	–	3808.5	18.8	3587.3	–
1	3168.8	4.2	3388.9	–	3714.5	–	3695.5	8.1	3790.5	11.5	3569.3	–
2	3150.8	11.2	3370.9	10.1	3696.5	–	3677.5	12.0	3772.5	11.9	3551.3	–
3	3132.8	19.5	3352.9	20.5	3678.5	11.8	3659.5	23.5	3754.5	17.1	3533.3	8.6
4	3114.8	19.9	3334.9	30.4	3660.5	20.1	3641.5	23.6	3736.5	18.6	3515.3	11.4
5	3096.8	24.5	3316.9	19.1	3642.5	22.8	3623.5	16.2	3718.5	12.8	3497.3	15.9
6	3078.8	20.6	3298.9	11.0	3624.5	21.8	3605.5	9.0	3700.5	9.2	3479.3	18.7
7	3060.8	–	3280.9	9.0	3606.5	11.1	3587.5	7.7	3682.5	–	3461.3	22.8
8					3588.5	6.9					3443.3	13.2
9					3570.5	5.4					3425.3	9.4
10											3407.3	–

In the case of AMV6, the masses are corresponding to the peptide AMV6 without the C-terminal part ESGKCTWV.

of *Clostridium* (**Figure 5**), but unfortunately, no antimicrobial activity was observed.

Chimeric Peptide Design, Expression, and Characterization

Since the specificity toward *Clostridium* could be related to the lipid II binding domain or with the other rings, and because of the relatively high activity of nisin against *Clostridium*, we decided to design new lantibiotics by a synthetic biology approach combining different parts of the putative lantibiotics and nisin.

Peptide Design

Ten different peptides were designed (**Table 5** and **Figure 6**). Five peptides were designed based on the peptides Clos2, Clos4, and Clos5 and the other five based on the other lantibiotics identified after the mining. Originality and new lantibiotic structure design were also considered. Depending on the nisin part used in the fusion, three kinds of peptides were designed. The first group contains those peptides for which the first two rings of nisin were fused to the last part of the putative lantibiotics. AMV1 was designed in this line by the fusion of nisin AB rings and the putative last two rings of Clos2, AMV2 with the putative last ring of Clos4 and AMV3 with the putative last three rings of Clos5. The idea, in this case, was to design the new peptides with the structure close to the wild putative lantibiotic peptide (**Figure 6**).

Another group of chimeric peptides consisted of those for which the first three rings of nisin and the last part of the putative lantibiotics were combined. AMV4 was designed by the fusion of the nisin ABC rings and the last putative ring of Clos12, obtaining a peptide with four putative rings and a long C terminal tail. AMV5, obtained by the fusion with the last putative two rings of Clos22, obtaining a peptide with five putative rings (as nisin) and with a putative end ring (as described for many other lantibiotics). AMV6 was obtained by the fusion with the last three putative rings of Clos14, obtaining a long lantibiotic with six putative rings and a tail (**Table 5** and **Figure 6**).

Finally, another group was containing peptides with the first part of *Clostridium* peptide and the last part from nisin. AMV7 and AMV10, with the first two rings of Clos2 and Clos4, respectively, and the last three rings of nisin, obtaining peptides with five putative rings closely to nisin. The peptides AMV8 and AMV9 were designed with the first putative two rings of Clos14 and Clos22, respectively, and the last two rings of nisin (with the hinge region included) (**Table 5** and **Figure 6**).

AMV_x Cloning, Expression, and Characterization

As before, each peptide was independently cloned fused to the nisin leader and under control of the P_{nis} promoter in pNZ8048 and transformed into *L. lactis* NZ9000 pTLR-BTC strains. TCA precipitation and MALDI-ToF analysis were also performed,

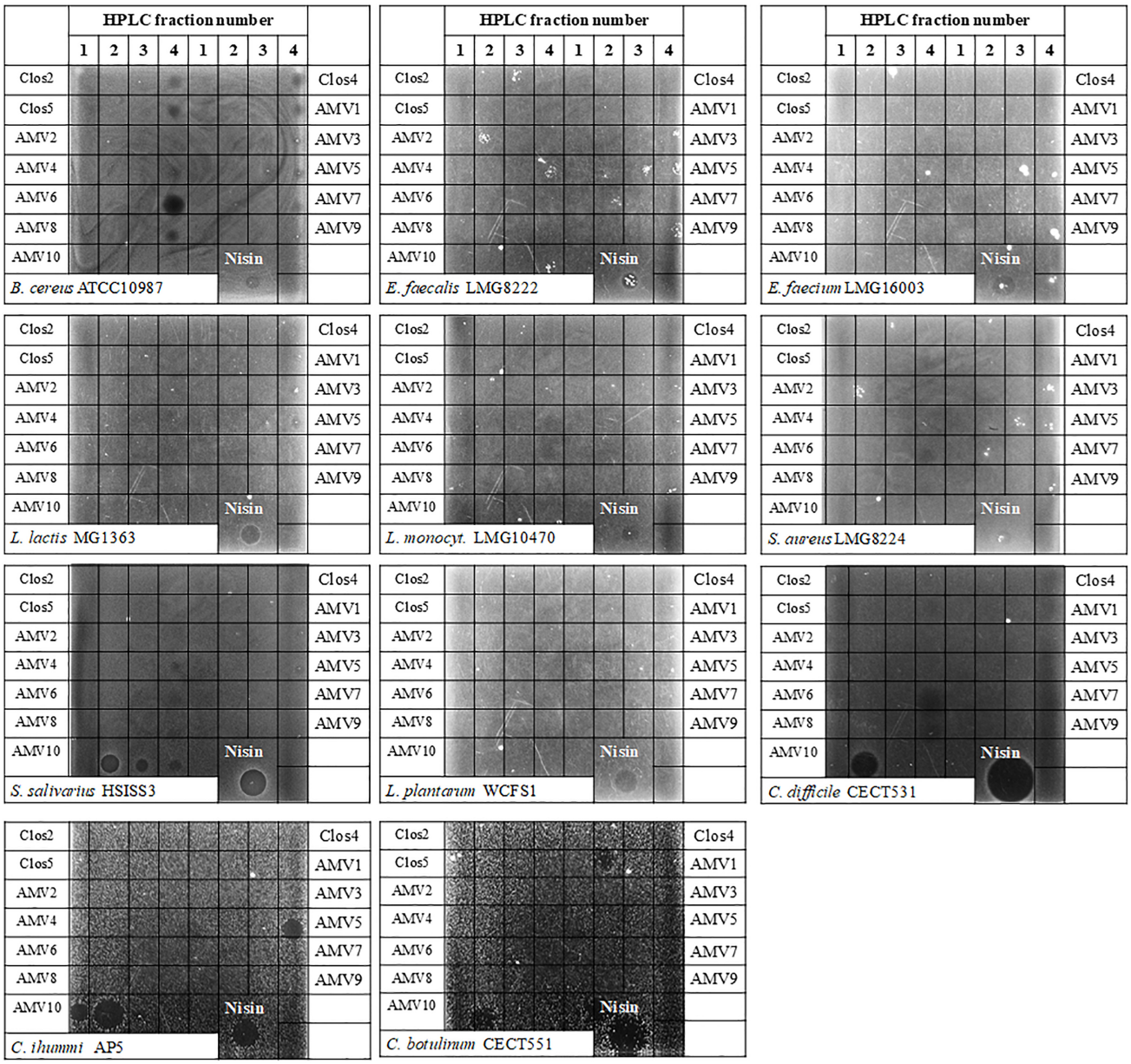

FIGURE 5 | Spot-overlay test of HPLC purified fractions against Gram-positive indicator strains.

finding the peptides in the supernatant in all the cases, so 1 L purification was performed using the methodology described for $Clos_x$ peptides.

The best peptide production levels were obtained for AMV5, AMV7, and AMV10, and moderate levels of production were obtained for AMV1, AMV2, and AMV3 (**Figures 2B–E**). In the case of AMV4, AMV6, AMV8, and AMV9, the production levels were very low (especially for AMV9) (**Figure 2**). As before, many peaks were observed for each peptide, suggesting different dehydration levels. As before, after MALDI-ToF analysis different degradation levels for the peptides were observed, but interestingly the N-terminal leader degradation was stronger in the case of the peptides for which the first part of nisin was used (**Figure 7**). This fact was especially observed in the case of the peptides AMV1, AMV2, AMV3, AMV4, AMV5, and AMV6, and to a lesser extent for the peptides AMV7, AMV8, AMV9, and AMV10 (**Figure 7**). In some cases, the N-terminal degradation also affected the designed peptides as in AMV5, where peaks without the first I or without the first ring (ITSILC) were observed. Interestingly, this fragment was not fully dehydrated, suggesting that the ring protects from degradation. Another example is the peptide AMV9. In this case, the complete nisin leader was observed as well as the core peptide without the first four aa (AGAG). This piece could have been released

TABLE 5 | Sequence of the nisin hybrid designed peptides.

Peptides	Sequence	S + T
Nisin	ITSISLCTPGCKTGALMGCNMKTATCHCSIHVSK	9
AMV1	ITSISLCTPGCPTNVFVCISKRCK	7
AMV2	ITSISLCTPGCYTQFIQCHDRV	5
AMV3	ITSISLCTPGCATSLFRTCLTRSCKGC	9
AMV4	ITSISLCTPGCKTGALMGCTIVCGTDFDGR	7
AMV5	ITSISLCTPGCKTGALMGCSFFGWVSACKNC	7
AMV6	ITSISLCTPGCKTGALMGCKTHETDSCNNGLCFESGKCTWV	10
AMV7	YLSLTPKCTSLCKTGALMGCNMKTATCHCSIHVSK	9
AMV8	ISDKRDDMSMCVCKKTDVCNMKTATCHCSIHVSK	7
AMV9	AGAGFIKTLTKDCPEVVSQVCNMKTATCHCSIHVSK	7
AMV10	ITSRILCTSSCKTGALMGCNMKTATCHCSIHVSK	10

In shading the nisin part of the peptides. S and T positions are indicated in green while C positions are in red.

spontaneously or by a specific protease, where this sequence could be targeted. In the case of the peptides, AMV2, AMV4, and AMV6, also a putative C-terminal degradation was detected, although the peptide with higher degradation rate was AMV4. HDRV C-Ter degradation was observed for AMV2, ESGKCTWV C-Ter degradation for AMV6, and until IVCGTDFDGR in the case of AMV4.

As before, and in order to establish the dehydration level for each peptide, they were digested with NisP. The leader cleavage efficiency was also checked for these peptides, and in general, after 3 h of incubation the leader was released entirely in all the peptides with the exception of AMV5 where the leader cleavage efficiency was a bit lower (**Supplementary Figure S2**). The percentage of dehydration was approximately calculated considering the intensity of each peak in the MADI-ToF (**Figure 4** and **Table 4**). Only the peptides AMV1, AMV2, AMV3, AMV6, AMV7, and AMV8 were fully dehydrated, but in general, all were dehydrated to a greater or lesser extent (**Table 4**).

AMV_x Antimicrobial Activity and Ring Formation

As in the case of the $Clos_x$ firstly, the four HPLC fractions corresponding to the main peaks were assayed against different Gram-positive bacteria and *Clostridium*. In general, the peptides were not active against the Gram-positive bacteria assayed (**Figure 5**) with the exception of *B. cereus*. In this case, fraction 4 of the truncated peptide AMV6 displayed an evident antimicrobial activity, while others as AMV1 or 8 displayed a weak activity. Interestingly, the fractions 2, 3, and 4 of peptide AMV10 showed antimicrobial activity against *Streptococcus salivarius* but not against the rest of the tested bacteria (**Figure 5**).

In the case of *Clostridium* (**Figure 5**), two of the designed peptides showed an explicit activity: AMV5 and AMV10. The first one against *C. ihumii* and the other against the three *Clostridium* tested. Curiously, the fractions 1 and 2 of AMV10 were active against *C. ihumii* unlike in *S. salivarius*. A really weak activity was also observed for the fraction 2 of AMV1 and the fraction 4 of AMV6 against *C. botulinum* and *C. difficile*, respectively.

Based on these results, the peptides AMV5 and AMV10 were used for the antimicrobial test in liquid medium. The

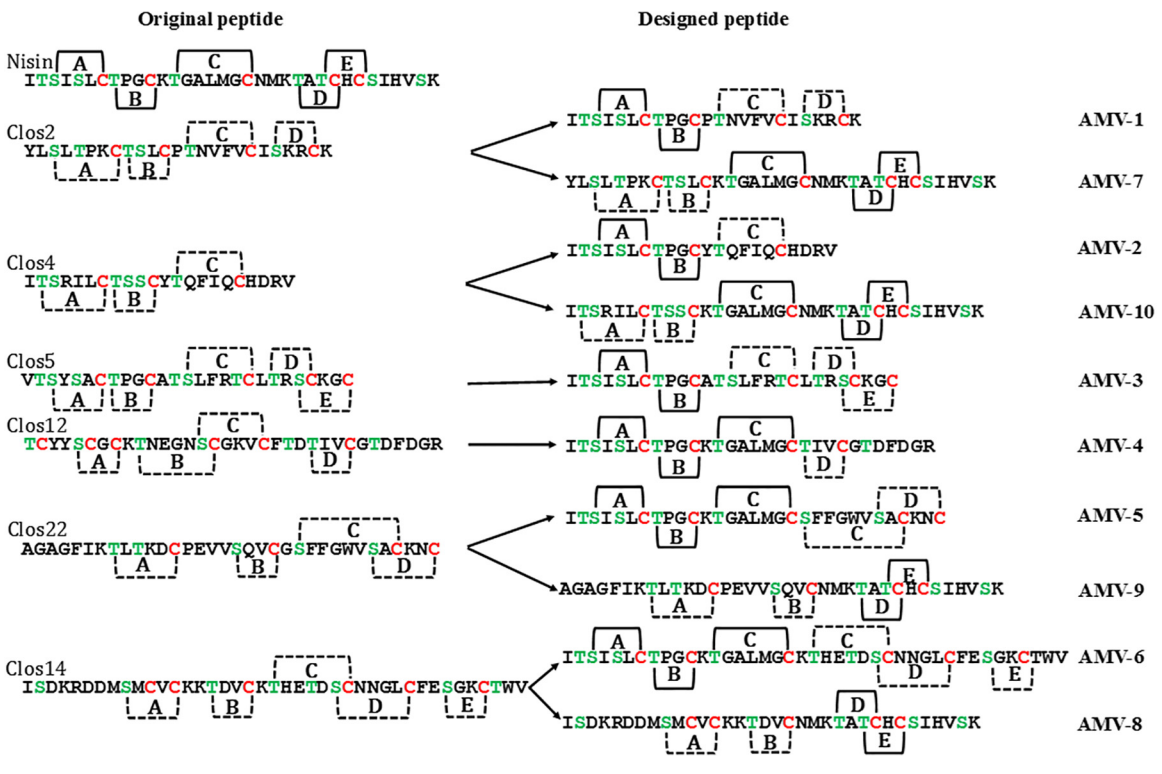

FIGURE 6 | Putative structure of the designed AMV_x peptides. Solid line, well-known rings formation and dot line, putative ring formation.

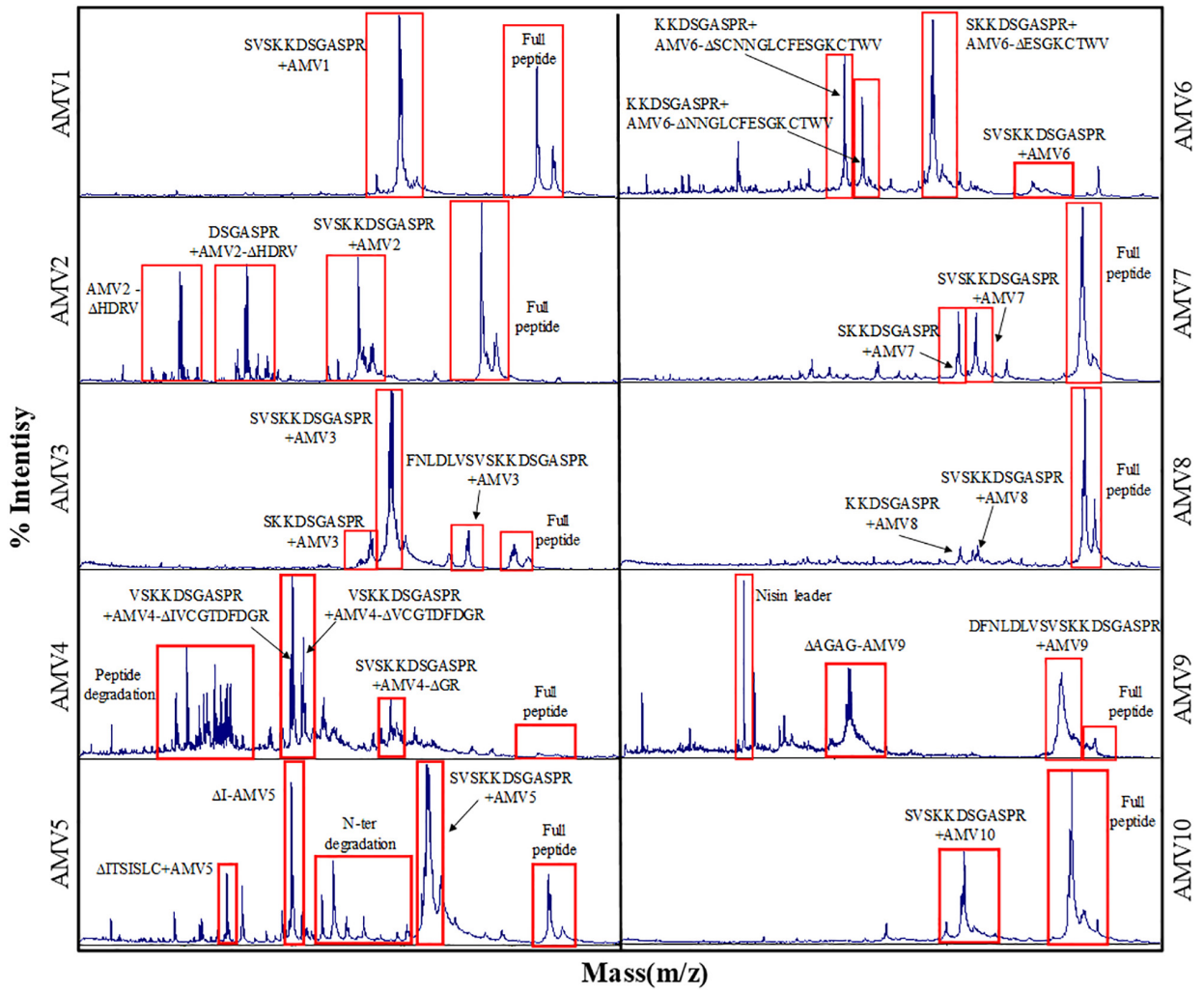

FIGURE 7 | MALDI-ToF chromatogram for AMV_x peptides indicating different degradation levels.

peptides were quantified using Qubit™ Protein Assay Kit and a fluorimeter, and then, they were assayed by triplicate at concentration ranged from 32 to 0.007 μg/mL against six different strains of *Clostridium*. NisP was added to the culture medium to ensure the release of the leader.

TABLE 6 | MIC values determined by broth microdilution method against several clostridial strains.

Strains	MIC (μg/mL)		
	AMV5	AMV10	Nisin
Clostridium beijerinckii NIZO B504	32	>32	8
C. botulinum CECT551	32	2	1
C. difficile CECT531	>32	2	0.03
C. ihumii AP5	32	1	0.5
C. sporogenes C22/10	>32	32	>32
C. tyrobutyricum NIZO B574	>32	>32	4

According to **Table 6**, AMV10 displayed a broad and high antimicrobial activity against some pathogenic *Clostridia*, such as *C. difficile* or *C. botulinum* with MIC values between 0.25 and 2 μg/mL. The same activity was observed for *C. ihumii*. *C. beijerinckii* was resistant to the higher concentration used, and *C. sporogenes* was sensitive to 32 μg/mL. AMV5 was less active than AMV10 being the only sensitive bacteria *C. ihumii* and *C. botulinum* (16 μg/mL). Prenisin was used in the same conditions as a positive control. As expected, a strong activity was observed against *C. difficile*, *C. botulinum*, and *C. ihumii*. *C. sporogenes* was resistant.

Finally the ring formation was analyzed for AMV5 and AMV10 (**Figure 8**). In general, the ring was installed. In the case of AMV10, in some cases one of the five rings was not installed for peptides with −8, −7, or −6, but interestingly, for the $-9H_2O$ peptide all the ring were installed. In the case of AMV5 one ring or two rings were not installed in some cases, even in the more dehydrated peptide ($-6H_2O$).

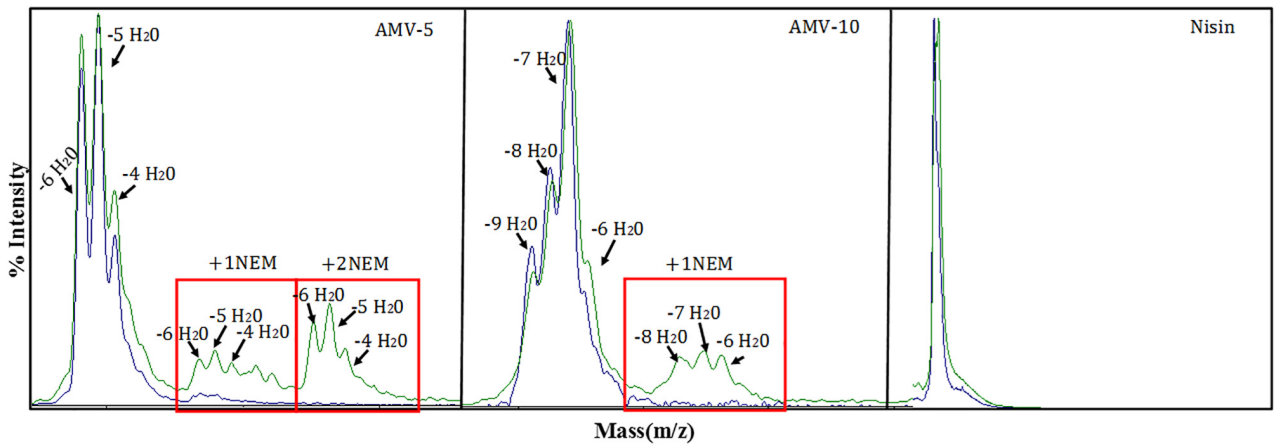

FIGURE 8 | Ring formation analysis. In blue, the peptide before NEM reaction; in green, after the reaction.

DISCUSSION

The treatment of infections caused by pathogenic *Clostridium* spp. poses a significant challenge in medicine, in particular by the ability of these bacteria to form spores that escape from the biocidal action of traditional antibiotics. Usually, the treatment requires the administration of antibiotics for a long time, and the broad activity of these antibiotics is related to the alteration of the gut microbiota. The most common pathogen of antibiotic-associated diarrhea is *C. difficile*. It is a Gram-positive, endospore-forming bacterium that has been recognized as one of the most frequent pathogens in nosocomial diseases, being related with a high index of morbidity and mortality (Miller et al., 2016). *C. difficile* is responsible for diarrhea and/or pseudomembranous colitis, and it is the first cause of antibiotic-associated diarrhea which is the most common adverse event related to antibiotic use (Dicks et al., 2018; Mullish and Williams, 2018). After long antibiotic treatments, the normal microbiota is damaged, and the spores of *C. difficile*, that are in virtually all healthy human, can germinate fast, releasing toxins and producing the infection. The ability of *C. difficile* spores to escape the biocidal action of the antibiotics used for its treatment produces relapses in the disease and recurrence (Mathias et al., 2019; Song and Kim, 2019).

The aim of this work was the design of new antimicrobials with potent and specific antimicrobial activity against *Clostridium* strains and especially against *C. difficile*. Starting from the premise that bacteriocins are usually active against bacteria closely related to the producing strain (Zacharof and Lovitt, 2012; Yang et al., 2014; Ventura et al., 2015), and using gene mining approaches (Weber et al., 2015; van Heel et al., 2016, 2018, 4; Montalbán-López et al., 2017), we have identified 54 putative lantibiotic sequences after the analysis of more than 560 *Clostridium* spp. genomes deposited in NCBI. From these putative lantibiotics, 10 were selected for its heterologous expression in *L. lactis* using the nisin biosynthetic machinery (Montalbán-López et al., 2017).

Among the genomes analyzed, the one from *C. ihumii* (Merhej et al., 2015) stands out since it encodes a class I lantibiotic cluster in where until 11 putative lantibiotics with a high range of diversity could be processed by a unique *lan*BTC system (**Figure 1**). This kind of lantibiotic island has been not described to date in other bacteria. However, it has been described that some bacteria have the ability to produce many different lanthipeptides (with the codifying gene dispersed in the genome) using only one biosynthetic enzyme as the ubiquitous marine cyanobacteria *Prochlorococcus* or *Synechococcus* (Cubillos-Ruiz et al., 2017). None of the *C. ihumii* putative peptides selected for heterologous expression was produced by *L. lactis*. In fact, only the peptides named Clos2, Clos4, and Clos5 from *C. beijerinckii* HUN142 were produced. Five different putative lantibiotics were identified in the genome of this bacteria divided into two complete clusters (one close to the other). Together with Clos2, Clos4, and Clos5, a variant of streptin was also present in the genome.

All these $Clos_x$ peptides showed a broad range of hetero-dehydration and some peaks observed in MALDI-ToF were matching with N-terminal leader peptide degradation (**Figure 3**). The purification of the pure form of a lantibiotic when it is hetero-dehydrated is laborious because of the impossibility to completely separate one fraction from the other. However, due to the differential hydrophobic properties of the lantibiotics depending on the dehydration level, in an RP-HPLC the more dehydrated forms elute later than, the less dehydrated (van Heel et al., 2016). Based on this and because the antimicrobial activity of the lantibiotics toward specific sensitive bacteria could be dehydration-level dependent, four HPLC fractions were assayed. In general, none displayed antimicrobial activity against the Gram-positive bacteria assayed and/or against *Clostridium* strains except a weak activity of fraction 4 of each peptide against *B. cereus*.

Nisin is well known to display potent antimicrobial activity against clostridial strains. However, as other antimicrobials, nisin is not active against spores (Mazzotta et al., 1997; Le Lay et al., 2016; El Jaam et al., 2017), and although there are still studies, nisin also seems to modify the gut microbiota (Gough et al., 2018; Jia et al., 2018). Based on this and following a

synthetic biology approach, 10 differences peptides (AMV_x) were designed by a combination of parts of nisin with parts of these putative lantibiotics. The idea was to obtain peptides as active as nisin and with specificity against *Clostridium*. Similar approaches to improve the activity of lantibiotics have recently published by Schmitt et al. (2019) but unlike that work, in this case, the lantibiotic used in the hybrid peptides are putative, the rings AB(C) part of nisin were changed in some of them and the design is focused toward a specific bacterial group, i.e., Clostridia.

Two groups of peptides were designed based on the use of the rings AB/ABC of CDE/DE of the nisin in combination with the putative rings of the peptides. Unlike $Clos_x$ peptides, all the new designed were heterologously expressed in *L. lactis*, but only AMV5, AMV7, and AMV10 were produced in concentrations similar to nisin production (**Figure 2**). After MALDI-ToF analysis, a putative N-terminal leader degradation was observed in all the peptides as well as a putative C-terminal degradation in the case of the peptides AMV2, AMV4, and AMV6 (**Figure 7**). Interestingly, in these peptides and according to their sequence no C-terminal ring could be formed (unlike AMV1, AMV3, AMV5) indicating a protective effect. No C-terminal degradation was observed for the peptides in which the last part of nisin was cloned (AMV7, AMV8, AMV9, and AMV10) (**Figures 6**, **7**). Finally, the N-terminal degradation of the leader was stronger for the peptides in which the C-terminal part of nisin was not present, suggesting that this part of nisin could be implicated in the resistance to proteases of prenisin. The presence and flexibility of the hinge region could be related to a major resistance to N-terminal degradation (Yuan et al., 2004; Zhou et al., 2015). In the case of AMV9, masses corresponding to the size of the peptide without the first four aa (AGAG) as well as a mass corresponding to the nisin leader were observed after the purification. We suggest that this peptide could be cleaved by another protease from the cell, e.g., by the intermembrane CAAX (CPBP family) proteases (Pei and Grishin, 2001; Pei et al., 2011). These proteases are related (at least) with the cleavage of class IIb bacteriocins (GG, GA, AG motifs) (Oliveira et al., 2017) and after a genome screening, at least five of these enzymes (llmg_0149, llmg_0198, llmg_0736, llmg_2326, and llmg_0852) are annotated in the chromosome of *L. lactis* MG1363 (mother strain of NZ9000).

With regard to the activity, none of the designed peptides displayed antimicrobial activity against the Gram-positive bacteria tested, with some exceptions. The HPLC fraction 4 of the truncated peptide AMV6 against *B. cereus* and the fractions 2, 3, and 4 of AMV10 against *S. salivarius*. A weak activity of the fraction of AMV1 and AMV8 was also observed against *B. cereus*. Interestingly, two peptides showed an evident activity against *Clostridium* strains, the fraction 4 of AMV5 and especially the fraction 2 of AMV10. In the case of AMV10 and unlike in *S. salivarius*, the active HPLC fractions were the numbers 1 and 2. This suggests that the dehydration level could be related to the specificity against certain bacteria.

Finally, the peptides AMV5 and AMV10 were selected for an extensive test against six different *Clostridium* strains. Concentrations ranging from 32 to 0.007 μg/mL were tested. We found that AMV10 is a potent peptide against pathogenic clostridia such as *C. difficile* or *C. botulinum*. Notably, AMV10 was not active against *C. beijerinckii*. AMV10 was obtained by the combination of the first two putative rings of Clos4 with the rings CDE of nisin, and Clos4 is a putative lantibiotic identified in the genome of other *C. beijerinckii* (**Figure 6**). This suggests that these strains could present specific resistance to these peptides and that the specificity toward clostridia is more related to the first rings (i.e., lipid II binding domain) than with the last one. However, *C. beijerinckii* was sensitive to AMV5 at the higher tested concentration as well as *C. ihumii* and *C. botulinum*. In this case, the first rings of the designed peptides are from *C. perfringens*. The rest of the species tested were resistant (**Table 6**). Respect the ring installation, only the peptide AMV10 with $-9H_2O$ is able to form all the rings. That means that probably only around the 10% of this peptide (**Table 4**) is the most active.

CONCLUSION

The primary objective of this work was the development of new antimicrobials with high specificity and activity against specific clostridial strains, especially pathogenic *Clostridia* as *C. difficile*. Using the combination of two different methodologies, genome mining of clostridial genomes and synthetic biology, 20 different peptides were heterologously expressed in *L. lactis* obtaining at the end two peptides (AMV5 and specially AMV10) that fulfilled the requirements set in this work: good heterologous expression levels and high specificity and activity toward *Clostridium*. The high specificity and activity observed for peptide AMV10 makes it a good candidate as an alternative to traditional antibiotics in the treatment of *C. difficile* infections, avoiding the side effects and the damage on the gut microbiota.

Finally, the methodology applied in this work has shown its robustness in the identification and design of new peptides with specificity and high activity against specific bacteria and could be applied for other fastidious bacteria which are hard to treat, such as *Mycobacterium* or Gram-negative/positive ESKAPE bacteria.

DATA AVAILABILITY

The datasets generated for this study are available on request to the corresponding author.

AUTHOR CONTRIBUTIONS

OK supervised the work. RC and OK conceived and designed the experiments. RC, AM-V, and AJ collected and analyzed the data.

RC and OK wrote and reviewed the manuscript. All authors read and approved the final manuscript.

FUNDING

RC was financially supported by the Spanish Ramon Areces Foundation and by the NWO-NACTAR (Project number 16433) program to enable this work. AJ was sponsored by the LPDP scholarship, from the Ministry of Finance of Republic of Indonesia, during his master degree in the University of Groningen.

SUPPLEMENTARY MATERIAL

The Supplementary Material for this article can be found online at: https://www.frontiersin.org/articles/10.3389/fmicb.2019.02154/full#supplementary-material

FIGURE S1 | MALDI-ToF data of the NisP leader cleavage efficiency for Clos2, Clos4, Clos5, and nisin during 3 h.

FIGURE S2 | MALDI-ToF data of the NisP leader cleavage efficiency for AMV_x peptides before (in blue) and after 3 h (in green).

TABLE S1 | Putative lantibiotics identified in *Clostridium* ssp. genomes after the genome mining, and NCBI genome reference number.

REFERENCES

Abts, A., Montalban-Lopez, M., Kuipers, O. P., Smits, S. H., and Schmitt, L. (2013). NisC binds the FxLx motif of the nisin leader peptide. *Biochemistry* 52, 5387–5395. doi: 10.1021/bi4008116

Aktypis, A., Kalantzopoulos, G., Huis in't Veld, J. H., and ten Brink, B. (1998). Purification and characterization of thermophilin T, a novel bacteriocin produced by *Streptococcus thermophilus* ACA-DC 0040. *J. Appl. Microbiol.* 84, 568–576. doi: 10.1046/j.1365-2672.1998.00383.x

Alvarez-Sieiro, P., Montalbán-López, M., Mu, D., and Kuipers, O. P. (2016). Bacteriocins of lactic acid bacteria: extending the family. *Appl. Microbiol. Biotechnol.* 100, 2939–2951. doi: 10.1007/s00253-016-7343-9

Bauer, M. P., Notermans, D. W., van Benthem, B. H. B., Brazier, J. S., Wilcox, M. H., Rupnik, M., et al. (2011). *Clostridium difficile* infection in Europe: a hospital-based survey. *Lancet* 377, 63–73. doi: 10.1016/S0140-6736(10)61266-4

Breukink, E., and de Kruijff, B. (2006). Lipid II as a target for antibiotics. *Nat. Rev. Drug. Discov.* 5, 321–332. doi: 10.1038/nrd2004

Candel-Pérez, C., Ros-Berruezo, G., and Martínez-Graciá, C. (2019). A review of *Clostridioides* [*Clostridium*] *difficile* occurrence through the food chain. *Food Microbiol.* 77, 118–129. doi: 10.1016/j.fm.2018.08.012

Cassir, N., Benamar, S., and La Scola, B. (2016). *Clostridium butyricum*: from beneficial to a new emerging pathogen. *Clin. Microbiol. Infect.* 22, 37–45. doi: 10.1016/j.cmi.2015.10.014

Cebrián, R., Baños, A., Valdivia, E., Pérez-Pulido, R., Martínez-Bueno, M., and Maqueda, M. (2012). Characterization of functional, safety, and probiotic properties of *Enterococcus faecalis* UGRA10, a new AS-48-producer strain. *Food Microbiol.* 30, 59–67. doi: 10.1016/j.fm.2011.12.002

Cheng, Y.-W., Phelps, E., Ganapini, V., Khan, N., Ouyang, F., Xu, H., et al. (2019). Fecal microbiota transplantation for the treatment of recurrent and severe *Clostridium difficile* infection in solid organ transplant recipients: a multicenter experience. *Am. J. Transplant.* 19, 501–511. doi: 10.1111/ajt.15058

Collins, J., and Auchtung, J. M. (2017). Control of *Clostridium difficile* infection by defined microbial communities. *Microbiol. Spectr.* 5:BAD-0009-2016. doi: 10.1128/microbiolspec.BAD-0009-2016

Cubillos-Ruiz, A., Berta-Thompson, J. W., Becker, J. W., van der Donk, W. A., and Chisholm, S. W. (2017). Evolutionary radiation of lanthipeptides in marine cyanobacteria. *Proc. Natl. Acad. Sci. U.S.A.* 114, E5424–E5433. doi: 10.1073/pnas.1700990114

Czepiel, J., Dróżdż, M., Pituch, H., Kuijper, E. J., Perucki, W., Mielimonka, A., et al. (2019). *Clostridium difficile* infection: review. *Eur. J. Clin. Microbiol. Infect. Dis.* 38, 1211–1221. doi: 10.1007/s10096-019-03539-6

de Ruyter, P. G., Kuipers, O. P., and de Vos, W. M. (1996). Controlled gene expression systems for *Lactococcus lactis* with the food-grade inducer nisin. *Appl. Environ. Microbiol.* 62, 3662–3667.

de Vos, W. M., Kuipers, O. P., van der Meer, J. R., and Siezen, R. J. (1995). Maturation pathway of nisin and other lantibiotics: post-translationally modified antimicrobial peptides exported by gram-positive bacteria. *Mol. Microbiol.* 17, 427–437. doi: 10.1111/j.1365-2958.1995.mmi_17030427.x

Dicks, L. M. T., Mikkelsen, L. S., Brandsborg, E., and Marcotte, H. (2018). *Clostridium difficile*, the difficult "kloster" fuelled by antibiotics. *Curr. Microbiol.* 76, 774–782. doi: 10.1007/s00284-018-1543-8

El Jaam, O., Fliss, I., and Aïder, M. (2017). Effect of electro-activated aqueous solutions, nisin and moderate heat treatment on the inactivation of *Clostridium sporogenes* PA 3679 spores in green beans puree and whole green beans. *Anaerobe* 47, 173–182. doi: 10.1016/j.anaerobe.2017.05.017

Fatima, R., and Aziz, M. (2019). The hypervirulent strain of *Clostridium difficile*: NAP1/B1/027 - A brief overview. *Cureus* 11:e3977. doi: 10.7759/cureus.3977

Geu-Flores, F., Nour-Eldin, H. H., Nielsen, M. T., and Halkier, B. A. (2007). USER fusion: a rapid and efficient method for simultaneous fusion and cloning of multiple PCR products. *Nucleic Acids Res.* 35:e55. doi: 10.1093/nar/gkm106

Gough, R., Cabrera Rubio, R., O'Connor, P. M., Crispie, F., Brodkorb, A., Miao, S., et al. (2018). Oral delivery of nisin in resistant starch based matrices alters the gut microbiota in mice. *Front. Microbiol.* 9:1186. doi: 10.3389/fmicb.2018.01186

Green, R., and Rogers, E. J. (2013). Chemical transformation of *E. coli*. *Methods Enzymol.* 529, 329–336. doi: 10.1016/B978-0-12-418687-3.00028-8

Grote, A., Hiller, K., Scheer, M., Münch, R., Nörtemann, B., Hempel, D. C., et al. (2005). JCat: a novel tool to adapt codon usage of a target gene to its potential expression host. *Nucleic Acids Res.* 33, W526–W531. doi: 10.1093/nar/gki376

Hasper, H. E., Kramer, N. E., Smith, J. L., Hillman, J. D., Zachariah, C., Kuipers, O. P., et al. (2006). An alternative bactericidal mechanism of action for lantibiotic peptides that target lipid II. *Science* 313, 1636–1637. doi: 10.1126/science.1129818

Hockett, K. L., and Baltrus, D. A. (2017). Use of the soft-agar overlay technique to screen for bacterially produced inhibitory compounds. *J. Vis. Exp.* 119:55064. doi: 10.3791/55064

Holo, H., and Nes, I. F. (1995). Transformation of *Lactococcus* by electroporation. *Methods Mol. Biol.* 47, 195–199. doi: 10.1385/0-89603-310-4.195

Hudson, G. A., and Mitchell, D. A. (2018). RiPP antibiotics: biosynthesis and engineering potential. *Curr. Opin. Microbiol.* 45, 61–69. doi: 10.1016/j.mib.2018.02.010

Jia, Z., Chen, A., Bao, F., He, M., Gao, S., Xu, J., et al. (2018). Effect of nisin on microbiome-brain-gut axis neurochemicals by *Escherichia coli*-induced diarrhea in mice. *Microb. Pathog.* 119, 65–71. doi: 10.1016/j.micpath.2018.04.005

Kiu, R., and Hall, L. J. (2018). An update on the human and animal enteric pathogen *Clostridium perfringens*. *Emerg. Microbes Infect.* 7:141. doi: 10.1038/s41426-018-0144-8

Kleerebezem, M., Boekhorst, J., van Kranenburg, R., Molenaar, D., Kuipers, O. P., Leer, R., et al. (2003). Complete genome sequence of *Lactobacillus plantarum* WCFS1. *Proc. Natl. Acad. Sci. U.S.A.* 100, 1990–1995. doi: 10.1073/pnas.0337704100

Le Lay, C., Dridi, L., Bergeron, M. G., Ouellette, M., and Fliss, I. L. (2016). Nisin is an effective inhibitor of *Clostridium difficile* vegetative cells and spore germination. *J. Med. Microbiol.* 65, 169–175. doi: 10.1099/jmm.0.000202

Lewies, A., Du Plessis, L. H., and Wentzel, J. F. (2018). Antimicrobial peptides: the Achilles' heel of antibiotic resistance? *Probiotics Antimicrob. Proteins* 11, 370–381. doi: 10.1007/s12602-018-9465-0

Mastrantonio, P., and Rupnik, M. (2018). "Erratum to: updates on *Clostridium difficile* in Europe," in *Updates on Clostridium difficile in Europe. Advances in Experimental Medicine and Biology*, eds P. Mastrantonio, and M. Rupnik, (Cham: Springer).

Mathias, F., Curti, C., Montana, M., Bornet, C., and Vanelle, P. (2019). Management of adult *Clostridium difficile* digestive contaminations: a literature review. *Eur. J. Clin. Microbiol. Infect. Dis.* 38, 209–231. doi: 10.1007/s10096-018-3419-z

Mazzotta, A. S., Crandall, A. D., and Montville, T. J. (1997). Nisin resistance in *Clostridium botulinum* spores and vegetative cells. *Appl. Environ. Microbiol.* 63, 2654–2659.

Merhej, V., Pfleiderer, A., Ramasamy, D., Lagier, J.-C., Michelle, C., Raoult, D., et al. (2015). Non-contiguous finished genome sequence and description of *Clostridium ihumii* sp. nov. *Stand Genomic Sci.* 10:63. doi: 10.1186/s40793-015-0025-x

Miller, A. C., Polgreen, L. A., Cavanaugh, J. E., Philip, M., Vernon, M., City, I., et al. (2016). Hospital *Clostridium difficile* infection (CDI) incidence as a risk factor for hospital-associated CDI. *Am. J. Infect Control* 44, 825–829. doi: 10.1016/j.ajic.2016.01.006.Hospital

Montalbán-López, M., Deng, J., van Heel, A. J., and Kuipers, O. P. (2018). Specificity and application of the lantibiotic protease NisP. *Front. Microbiol.* 9:160. doi: 10.3389/fmicb.2018.00160

Montalbán-López, M., van Heel, A. J., and Kuipers, O. P. (2017). Employing the promiscuity of lantibiotic biosynthetic machineries to produce novel antimicrobials. *FEMS Microbiol. Rev.* 41, 5–18. doi: 10.1093/femsre/fuw034

Mullish, B. H., and Williams, H. R. (2018). *Clostridium difficile* infection and antibiotic-associated diarrhoea. *Clin. Med.* 18, 237–241. doi: 10.7861/clinmedicine.18-3-237

Nelson, R. (2007). Antibiotic treatment for *Clostridium difficile*-associated diarrhea in adults. *Cochrane Database Syst. Rev.* 3:CD004610. doi: 10.1002/14651858.CD004610.pub3

Oliveira, L., Silveira, A. M. M., Monteiro, A. S., dos Santos, V. L., Nicoli, J. R., Azevedo, V. A. C., et al. (2017). *In silico* prediction, *in vitro* antibacterial spectrum, and physicochemical properties of a putative bacteriocin produced by *Lactobacillus rhamnosus* Strain L156.4. *Front. Microbiol.* 8:876. doi: 10.3389/fmicb.2017.00876

Pei, J., and Grishin, N. V. (2001). Type II CAAX prenyl endopeptidases belong to a novel superfamily of putative membrane-bound metalloproteases. *Trends Biochem. Sci.* 26, 275–277. doi: 10.1016/s0968-0004(01)01813-8

Pei, J., Mitchell, D. A., Dixon, J. E., and Grishin, N. V. (2011). Expansion of type II CAAX proteases reveals evolutionary origin of γ-secretase subunit APH-1. *J. Mol. Biol.* 410, 18–26. doi: 10.1016/j.jmb.2011.04.066

Peng, Z., Jin, D., Kim, H. B., Stratton, C. W., Wu, B., Tang, Y.-W., et al. (2017). Update on Antimicrobial resistance in *Clostridium difficile*: resistance mechanisms and antimicrobial susceptibility Testing. *J. Clin. Microbiol.* 55, 1998–2008. doi: 10.1128/JCM.02250-16

Plat, A., Kuipers, A., Rink, R., and Moll, G. N. (2013). Mechanistic aspects of lanthipeptide leaders. *Curr. Protein Pept. Sci.* 14, 85–96. doi: 10.1016/S0968-0004(01)01813-8

Ramai, D., Zakhia, K., Ofosu, A., Ofori, E., and Reddy, M. (2019). Fecal microbiota transplantation: donor relation, fresh or frozen, delivery methods, cost-effectiveness. *Ann. Gastroenterol.* 32, 30–38. doi: 10.20524/aog.2018.0328

Repka, L. M., Chekan, J. R., Nair, S. K., and van der Donk, W. A. (2017). Mechanistic understanding of lanthipeptide biosynthetic enzymes. *Chem. Rev.* 117, 5457–5520. doi: 10.1021/acs.chemrev.6b00591

Rink, R., Kuipers, A., de Boef, E., Leenhouts, K. J., Driessen, A. J. M., Moll, G. N., et al. (2005). Lantibiotic structures as guidelines for the design of peptides that can be modified by lantibiotic enzymes. *Biochemistry* 44, 8873–8882. doi: 10.1021/bi050081h

Sahl, H. G., Jack, R. W., and Bierbaum, G. (1995). Biosynthesis and biological activities of lantibiotics with unique post-translational modifications. *Eur. J. Biochem.* 230, 827–853. doi: 10.1111/j.1432-1033.1995.0827g.x

Sambrook, J., Fritsch, E. F., and Maniatis, T. (1990). *Molecular Cloning: A Laboratory Manual*. New York, NY: Cold Spring Harbor Laboratory Press.

Sasi Jyothsna, T. S., Tushar, L., Sasikala, C., and Ramana, C. V. (2016). Erratum to *Paraclostridium benzoelyticum* gen. nov. sp. nov., isolated from marine sediment and reclassification of *Clostridium bifermentans* as *Paraclostridium bifermentans comb*. nov. Proposal of a new genus *Paeniclostridium gen*. nov. to accommodate *Clostridium sordellii* and *Clostridium ghonii*. *Int. J. Syst. Evol. Microbiol.* 66:2459. doi: 10.1099/ijsem.0.001144

Schmitt, S., Montalbán-López, M., Peterhoff, D., Deng, J., Wagner, R., Held, M., et al. (2019). Analysis of modular bioengineered antimicrobial lanthipeptides at nanoliter scale. *Nat. Chem. Biol.* 15, 437–443. doi: 10.1038/s41589-019-0250-5

Seo, B., Yoo, J. E., Lee, Y. M., and Ko, G. (2017). Merdimonas faecis gen. nov., sp. nov., isolated from human faeces. *Int. J. Syst. Evol. Microbiol.* 67, 2430–2435. doi: 10.1099/ijsem.0.001977

Song, H. J., Shim, K.-N., Jung, S.-A., Choi, H. J., Lee, M. A., Ryu, K. H., et al. (2008). Antibiotic-associated diarrhea: candidate organisms other than *Clostridium difficile*. *Korean J. Intern. Med.* 23, 9–15. doi: 10.3904/kjim.2008.23.1.9

Song, J. H., and Kim, Y. S. (2019). Recurrent *Clostridium difficile* infection: risk factors, treatment, and prevention. *Gut Liver* 13, 16–24. doi: 10.5009/gnl18071

Todorov, S. D., de Melo Franco, B. D. G., and Tagg, J. R. (2019). Bacteriocins of Gram-positive bacteria having activity spectra extending beyond closely-related species. *Benef. Microbes* 10, 315–328. doi: 10.3920/BM2018.0126

Udaondo, Z., Duque, E., and Ramos, J.-L. (2017). The pangenome of the genus *Clostridium*. *Environ. Microbiol.* 19, 2588–2603. doi: 10.1111/1462-2920.13732

Van den Bogert, B., Boekhorst, J., Herrmann, R., Smid, E. J., Zoetendal, E. G., and Kleerebezem, M. (2013). Comparative genomics analysis of *Streptococcus* isolates from the human small intestine reveals their adaptation to a highly dynamic ecosystem. *PLoS One* 8:e083418. doi: 10.1371/journal.pone.0083418

van der Meer, J. R., Rollema, H. S., Siezen, R. J., Beerthuyzen, M. M., Kuipers, O. P., and de Vos, W. M. (1994). Influence of amino acid substitutions in the nisin leader peptide on biosynthesis and secretion of nisin by *Lactococcus lactis*. *J. Biol. Chem.* 269, 3555–3562.

van Heel, A. J., de Jong, A., Song, C., Viel, J. H., Kok, J., and Kuipers, O. P. (2018). BAGEL4: a user-friendly web server to thoroughly mine RiPPs and bacteriocins. *Nucleic Acids Res.* 46, W278–W281. doi: 10.1093/nar/gky383

van Heel, A. J., Kloosterman, T. G., Montalban-Lopez, M., Deng, J., Plat, A., Baudu, B., et al. (2016). Discovery, production and modification of five novel lantibiotics using the promiscuous nisin modification machinery. *ACS Synth. Biol.* 5, 1146–1154. doi: 10.1021/acssynbio.6b00033

van Heel, A. J., Montalban-Lopez, M., and Kuipers, O. P. (2011). Evaluating the feasibility of lantibiotics as an alternative therapy against bacterial infections in humans. *Expert Opin. Drug Metab. Toxicol.* 7, 675–680. doi: 10.1517/17425255.2011.573478

van Heel, A. J., Mu, D., Montalbán-López, M., Hendriks, D., and Kuipers, O. P. (2013). Designing and producing modified, new-to-nature peptides with antimicrobial activity by use of a combination of various lantibiotic modification enzymes. *ACS Synth. Biol.* 2, 397–404. doi: 10.1021/sb3001084

van Kraaij, C., de Vos, W. M., Siezen, R. J., and Kuipers, O. P. (1999). Lantibiotics: biosynthesis, mode of action and applications. *Nat. Prod. Rep.* 16, 575–587. doi: 10.1039/a804531c

Ventura, M., Turroni, F., and van Sinderen, D. (2015). "Chapter 4-bifidobacteria of the human gut: our special friends," in *Diet-Microbe Interactions in the Gut*, eds K. Tuohy, and D. Del Rio, (San Diego, CA: Academic Press), 41–51. doi: 10.1016/B978-0-12-407825-3.00004-6

Wang, S., Xu, M., Wang, W., Cao, X., and Piao, M. (2016). Systematic review : adverse events of fecal microbiota transplantation. *PLoS One* 11:e0161174. doi: 10.1371/journal.pone.0161174

Weber, T., Blin, K., Duddela, S., Krug, D., Kim, H. U., Bruccoleri, R., et al. (2015). antiSMASH 3.0—a comprehensive resource for the genome mining of biosynthetic gene clusters. *Nucleic Acids Res.* 43, W237–W243. doi: 10.1093/nar/gkv437

Wegmann, U., O'Connell-Motherway, M., Zomer, A., Buist, G., Shearman, C., Canchaya, C., et al. (2007). Complete genome sequence of the prototype lactic acid bacterium *Lactococcus lactis* subsp. cremoris MG1363. *J. Bacteriol.* 189, 3256–3270. doi: 10.1128/JB.01768-06

Wilkins, M. R., Gasteiger, E., Bairoch, A., Sanchez, J. C., Williams, K. L., Appel, R. D., et al. (1999). Protein identification and analysis tools in the ExPASy server. *Methods Mol. Biol.* 112, 531–552. doi: 10.1385/1-59259-584-7:531

Yakob, L., Riley, T. V., Paterson, D. L., Marquess, J., Magalhaes, R. J. S., Furuya-Kanamori, L., et al. (2015). Mechanisms of hypervirulent *Clostridium difficile* ribotype 027 displacement of endemic strains: an epidemiological model. *Sci. Rep.* 5:12666. doi: 10.1038/srep12666

Yang, S.-C., Lin, C.-H., Sung, C. T., and Fang, J.-Y. (2014). Antibacterial activities of bacteriocins: application in foods and pharmaceuticals. *Front. Microbiol.* 5:241. doi: 10.3389/fmicb.2014.00241

Yang, X., and van der Donk, W. A. (2015). The Michael-type cyclizations in lantibiotic biosynthesis are reversible. *ACS Chem. Biol.* 10, 1234–1238. doi: 10.1021/acschembio.5b00007

Yuan, J., Zhang, Z.-Z., Chen, X.-Z., Yang, W., and Huan, L.-D. (2004). Site-directed mutagenesis of the hinge region of nisin Z and properties of nisin Z mutants. *Appl. Microbiol. Biotechnol.* 64, 806–815. doi: 10.1007/s00253-004-1599-1

Zacharof, M. P., and Lovitt, R. W. (2012). Bacteriocins produced by lactic acid bacteria a review article. *APCBEE Procedia* 2, 50–56. doi: 10.1016/j.apcbee.2012.06.010

Zhou, L., van Heel, A. J., and Kuipers, O. P. (2015). The length of a lantibiotic hinge region has profound influence on antimicrobial activity and host specificity. *Front. Microbiol.* 6:11. doi: 10.3389/fmicb.2015.00011

Conflict of Interest Statement: The authors declare that the research was conducted in the absence of any commercial or financial relationships that could be construed as a potential conflict of interest.

frontiers in Microbiology

REVIEW
published: 06 August 2019
doi: 10.3389/fmicb.2019.01690

Bacterial Proteinaceous Compounds With Multiple Activities Toward Cancers and Microbial Infection

*Gisele Rodrigues[1], Gislaine Greice Oliveira Silva[2], Danieli Fernanda Buccini[2], Harry Morales Duque[1], Simoni Campos Dias[1,3] and Octávio Luiz Franco[1,2]**

[1] Centro de Análises Proteômicas e Bioquímicas, Programa de Pós-Graduação em Ciências Genômicas e Biotecnologia, Universidade Católica de Brasília, Brasília, Brazil, [2] S-Inova Biotech, Programa de Pós-Graduação em Biotecnologia, Universidade Católica Dom Bosco, Campo Grande, Brazil, [3] Pós-Graduação em Biologia Animal, Universidade de Brasilia, Brasília, Brazil

In recent decades, cancer and multidrug resistance have become a worldwide problem, resulting in high morbidity and mortality. Some infectious agents like *Streptococcus pneumoniae*, *Stomatococcus mucilaginous, Staphylococcus* spp., *E. coli. Klebsiella* spp., *Pseudomonas aeruginosa, Candida* spp., *Helicobacter pylori,* hepatitis B and C, and human papillomaviruses (HPV) have been associated with the development of cancer. Chemotherapy, radiotherapy and antibiotics are the conventional treatment for cancer and infectious disease. This treatment causes damage in healthy cells and tissues, and usually triggers systemic side-effects, as well as drug resistance. Therefore, the search for new treatments is urgent, in order to improve efficacy and also reduce side-effects. Proteins and peptides originating from bacteria can thus be a promising alternative to conventional treatments used nowadays against cancer and infectious disease. These molecules have demonstrated specific activity against cancer cells and bacterial infection; indeed, proteins and peptides can be considered as future antimicrobial and anticancer drugs. In this context, this review will focus on the desirable characteristics of proteins and peptides from bacterial sources that demonstrated activity against microbial infections and cancer, as well as their efficacy *in vitro* and *in vivo*.

Keywords: antimicrobial, anticancer, bacteriocin, protein, peptides

OPEN ACCESS

Edited by:
Bingyun Li,
West Virginia University, United States

Reviewed by:
Ramya Viswanathan,
National Institutes of Health (NIH), United States
Hai Liang,
National Institutes of Health (NIH), United States

****Correspondence:***
Octávio Luiz Franco
ocfranco@gmail.com

Specialty section:
This article was submitted to Antimicrobials, Resistance and Chemotherapy, a section of the journal Frontiers in Microbiology

Received: *14 April 2019*
Accepted: *09 July 2019*
Published: *06 August 2019*

Citation:
Rodrigues G, Silva GGO, Buccini DF, Duque HM, Dias SC and Franco OL (2019) Bacterial Proteinaceous Compounds With Multiple Activities Toward Cancers and Microbial Infection. Front. Microbiol. 10:1690. doi: 10.3389/fmicb.2019.01690

INTRODUCTION

In recent years, global health authorities have had to deal with two significant problems: the alarming number of people suffering from cancer and the rise of antimicrobial resistance (AMR). Cancer is the second most prevalent cause of death worldwide (O'Brien-Simpson et al., 2018; Shoombuatong et al., 2018). According to the World Health Organization (WHO) and the International Agency of Research on Cancer [IARC] (2018) in there were about 18.1 million new cases of cancer and 9.6 million deaths. The estimate for AMR is that 700,000 die annually worldwide, and the annual number of deaths is likely to increase to 10 million by 2050 (Arias and Murray, 2009; World-Health-Organisation [WHO], 2018; Ghosh et al., 2019).

Additionally, 16.1% of newly diagnosed cancers may be attributable to infections [National Cancer Institute – Epidemiology and Genomic Research Program[1] (accessed March 12, 2019)].

[1]https://epi.grants.cancer.gov/infectious-agents/#web

Oncologic patients are more susceptible to infectious complications caused by *Streptococcus pneumoniae*, *Stomatococcus mucilaginous, Staphylococcus* spp., *E. coli Klebsiella* spp., *Pseudomonas aeruginosa, Helicobacter pylori,* and *Candida* spp. (Zorina and Styche, 2015; Rolston, 2017). Another concern related to cancer patients are infections caused by viruses such as hepatitis B and C, and human papillomaviruses (HPV) (Vedham et al., 2014; Rolston, 2017).

In fact, patients with a chronic infection induced by *Staphylococcus aureus*, *Klebsiella pneumoniae, Acinetobacter baumanii, Pseudomonas aeruginosa*, and *Enterobacter* species have been shown to have greater susceptibility to cancer development, as a result of their precarious immune system (Felício et al., 2017; Rolston, 2017). At the same time, antibiotics are used to prevent microbial infection in post-cancer surgery, and after chemotherapy or radiotherapy (Thundimadathil, 2012; Gaspar et al., 2013; Felício et al., 2017; Leite et al., 2018; O'Brien-Simpson et al., 2018; Shoombuatong et al., 2018). Conventional cancer treatments do not act on specific targets, such as malignant cells, resulting in severe side effects for patients, and these may contribute to the selection of cells that are resistant to antibiotics and anticancer drugs (Vedham et al., 2014; Zorina and Styche, 2015).

As a result, the development of a new class of molecules with selectivity and specificity against microbial infection and cancer is essential (Gaspar et al., 2013; Felício et al., 2017; Shoombuatong et al., 2018). Bacteria have an arsenal of proteins and peptides with both antibacterial and antitumoral activity, which can be explored in the search for these new compounds (Karpinski and Adamczak, 2018).

Among these promising molecules are toxins, immunotoxins (Jain, 2001; Gorgal et al., 2012), enzymes (Chakrabarty et al., 2014), bacteriocins (which are part of the same group as peptides) and a vast range of proteins (Karpinski and Adamczak, 2018). Antimicrobial peptides (AMPs) with anticancer activity can be classified according to the spectrum of their activity on tumor cells, and they are divided into two main categories: (i) peptides that show potent activity against bacteria and tumor cells, without causing damage to mammalian cells; (ii) peptides that are toxic to cancer cells, bacteria and healthy cells (Hoskin and Ramamoorthy, 2008; Bandala et al., 2013).

Therefore, this review will focus on the desirable characteristics of proteins and peptides originating from bacteria that demonstrated activity against microbial infections and cancer, as well as their efficacy in clinical trials, and will discuss future prospects.

DUAL ACTIVITY FROM BACTERIAL PROTEINS AND PEPTIDES

Some proteins and peptides exhibit antimicrobial and anticancer activities. Therefore, bacteria use indirect and direct strategies to compete and survive. Host bacteria can show antimicrobial activity indirectly, by host immune system modulation (Belmadi et al., 2018). Alternatively, host bacteria can act directly by expressing proteins and peptides that are secreted to the extracellular environment and that target other bacteria (Cascales et al., 2007). Likewise, these proteins and peptides present variable structures linked to their activity, and these characteristics make their classification difficult (Daw and Falkiner, 1996; Vasilchenko and Valyshev, 2019). These structural diversities are represented in **Figure 1**, by toxins like colicin and pycin, and peptides represented by nisin, pediocin and plantaricin (Jain, 2001; Karpinski and Adamczak, 2018). Colicins are formed by three domains, the N-terminal, central and C- terminal, which act in membrane translocation, binding receptor and activity domain, respectively (Cascales et al., 2007). Pyocins are composed of four domains: domain I represents the receptor binding at the N-terminal, domain II has no defined function yet, domain III is responsible for translocation across the outer membrane and domain IV is responsible for DNase activity at the C-terminal end (Michel-Briand and Baysse, 2002). Nisin has two variants, A and Z, and the only difference between them is the change of His^{27} by Asn. They interact with the membrane surface in the C-terminal moiety (Lins et al., 1999). Pediocins interact with the target-cell surface in the N-terminal domain, and the C-terminal domain penetrates the membrane. Indeed, for pedicins, the domain is the major specificity determinant (Fimland et al., 2005). Plantaricin can present three variable forms, with 26-residue peptide and two N-terminal forms containing 23 and 22 residues; these forms result from a 48-residue precursor encoded by the plnA gene. Besides that, the amphiphilic nature of plnA can induced pore formation in cell membrane (Kaur and Kaur, 2015) (**Figure 1**).

In addition, several strategies could be designed to try to combat antimicrobial infection and carry out cancer therapy using proteins and peptides (Shilova et al., 2018). For example, proteins and peptides can be combined with conventional drugs (Liberio et al., 2013; Felício et al., 2017; Leite et al., 2018). They can be used as a heterologous compound infusion with other proteins or peptides that help in site-directed activity (Kawakami et al., 2006; Leshem and Pastan, 2019). It is possible to coat or conjugate proteins and peptides with polymers, such as polyethylene glycol (PEG) (Kelly et al., 2016). Another strategy is rational design for these molecules, because it then becomes possible to substitute naturally occurring amino acids with unnatural ones (Gordon et al., 2005; Uggerhøj et al., 2015).

In the various ways described above, these molecules have shown different applications and modes of action against antimicrobial infections and cancer. Nevertheless, in this study we focus on bacteriocins that have been previously characterized and/or synthesized with dual activity (**Figure 2**).

Bacteriocins

Bacteriocins make up a class of molecules (proteins and peptides) synthesized by ribosomes in several Gram-positive and negative bacteria. In 1925, the first bacteriocin isolated from *E. coli* discovered by Gratia (1925), was identified and later named colicin. Since then, several bacteriocins have been discovered in a variety of bacteria (Kaur and Kaur, 2015). Cationic peptides belonging to the bacteriocin class may be associated with biological functions in bacteria and may assist in the inhibition

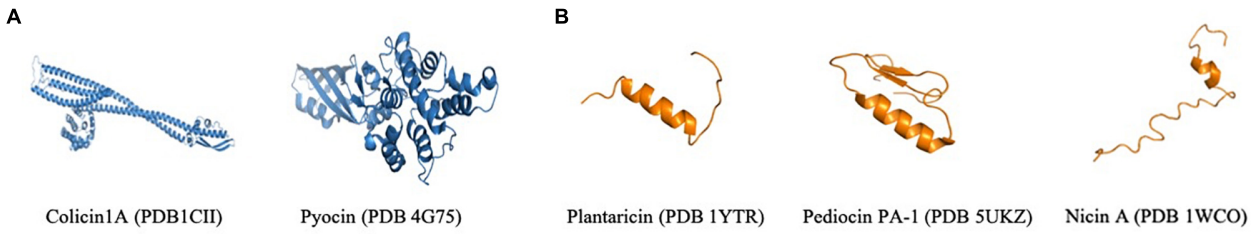

FIGURE 1 | An overview of different structures of bacteriocins, proteins **(A)** and peptides **(B)** with dual anticancer and antimicrobial activity. All of these structures are available on the PDB.

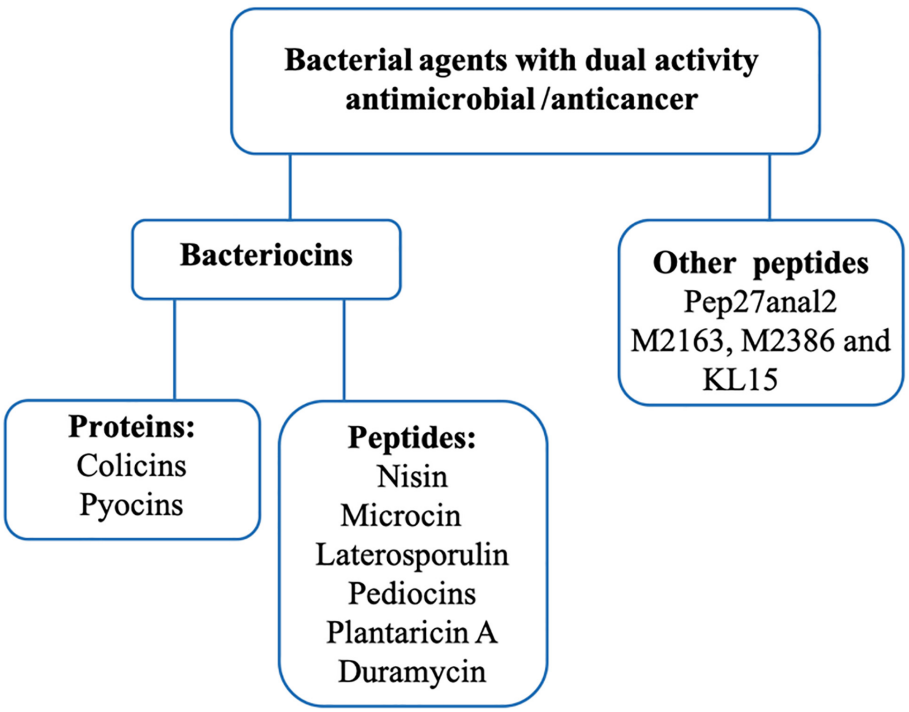

FIGURE 2 | Distribution of described anticancer and antimicrobial proteins and peptides.

and elimination of possible competing microorganisms in their natural environment (Nes and Holo, 2000).

As demonstrated above, proteins and peptides have variable structures (Vasilchenko and Valyshev, 2019). Regarding classification, which is a challenge, it is known that 80% of the bacteriocins are of cationic and amphipathic nature, due mainly to the excess of residues of lysine or arginine amino acids (Nes and Holo, 2000; Hammami et al., 2010). These characteristics of bacteriocins may be linked to their efficacy in combating cancer cells, possibly by the interaction of these cationic molecules with the negative surface charge of the cancerous cell membrane (Saito et al., 1979; Baindara et al., 2015). A visible example of such characteristics can be observed in lantipeptides, a class I bacteriocin, which can form pores, resembling cationic antimicrobial peptides (cAMPs) (Smith and Hillman, 2008). In addition, some bacteriocins produced by Gram-positive bacteria can resemble the defensins, AMPs produced by eukaryotic cells, which have membrane-permeabilizing characteristics (Singh et al., 2015).

Another relevant feature of bacteriocins is their low toxicity when in contact with mammalian cells. Due to these characteristics, bacterial strains producing bacteriocins have been implemented in foods as probiotics (Cutter and Siragusa, 1998). Their low toxicity has already been demonstrated in studies, for example, a bacteriocin named laterosporulin did not show hemolysis in the presence of erythrocytes, even at concentrations exceeding the minimum inhibitory concentration (MIC) values (Singh et al., 2015). The same can be observed in studies with penisin, a class IA lantibiotic, which in addition to not being hemolytic showed no cytotoxic activity against mouse macrophages (RAW) (Baindara et al., 2015). These characteristics are important from the point of view of the development of

new therapies, since their affinity with tumor cells and low toxicity show that the bacteriocins are excellent candidates for the treatment of cancer, besides presenting antibacterial activities (Chakrabarty et al., 2014; Yang et al., 2014; Kaur and Kaur, 2015; Karpinski and Adamczak, 2018).

In this section, we will address the issue of protein and peptide bacteriocins isolated from bacteria. Only those molecules with a molecular mass of 10 kDa or less will be classified as peptides. Among the bacteriocins studied to date, some have been submitted to tests with tumor cells. **Table 1** lists the bacteriocins that have been evaluated so far and have demonstrated activity against bacterial and cancer cells (**Figure 3**). These activities are divided into membrane adsorption (**Figure 3A**) and conformational change (**Figure 3B**). Membrane adsorption is represented by carpet model (in which the formation of membrane micellar structures occurs in an area with high peptide densities); barrel-stave model (protein and peptides form a pore in a perpendicular orientation to the membrane surface and interact with the phospholipid acyl chains); toroidal pore model (the contact of protein and peptides with the phospholipid head groups during the pore formations causes expanding membrane curvature); disordered toroidal pore (which promotes the internal curvature of lipid molecules for pore formation with few peptides; this process occurs in randomic form); non-bilayer intermediate (the peptide aggregation on the membrane surface activates the formation of the intermediate bilayer, causing membrane disruption, allowing the peptide to be translocated into the internal leaflet); membrane thinning/thickening (originates with peptides aligned parallel to the surface of the membrane, provoking thinning or thickening due to hydrophilic characteristics associated with the lipid bilayer) (Lohner, 2009; Haney et al., 2010; Nguyen et al., 2011; Gaspar et al., 2013; Gabernet et al., 2016). The conformational charge is represented by anion carrier (this model acts directly on the membrane through lipid isolation or addresses oxidized phospholipids, or even acts as a small anion carrier through the membrane); charge lipid cluster (cationic peptides interact with clustering of anionic lipids in the membrane region, and this interaction allows pore formation); electroporation (occurs subtly, when proteins or peptides bind small anions across the bilayer, inducing the efflux and changes in the membrane potential); non-lytic membrane depolarization (proteins and peptides induce charge modification, cause membrane instability, and allow the proteins and peptides to translocate across the cytoplasmic membrane); and oxidized lipid targeting [stimulating the formation of cellular reactive oxygen species (ROS) causing oxidative cellular damage, developing metabolites that can be mutagenic, cytotoxic and also promote cellular aging and apoptosis] (Gifford et al., 2005; Epand and Epand, 2011; Nguyen et al., 2011; Hasegawa et al., 2012; Gaspar et al., 2013; Gabernet et al., 2016; Alexander et al., 2019).

Colicins and Pyocins

There are a small number of proteins classified as bacteriocins, including colicin, pyocin, pesticin, butyricin, and megacin (Konisky, 1982). These proteins are used by bacterial species for intraspecies competition (Di Masi et al., 1973; Chai et al., 1982; Michel-Briand and Baysse, 2002; Spector et al., 2010; Yang et al., 2014). However, only colicin and pyocin have been reported in the literature as presenting dual activity.

Colicins are proteins produced by *E. coli,* and they present a diversity of molecules (E1-3, K, A, L, B, Ia, Ib, V, D, and M) with varied masses between 27 and 80 kDa (Konisky, 1982). The structure of colicin proteins presents three domains; these are the receptor-binding domain responsible for target interaction, the N-terminal domain that mediates interaction with transporters, and the cytotoxic domain that allows antibacterial activity (Vasilchenko and Valyshev, 2019). Colicins act by binding to the outer membrane of integral membrane protein receptors, transporting the colicin to the inner membrane through Tol complex, inducing membrane depolarization, and degradation of DNA, ribosomal RNA, or tRNA (Duché and Houot, 2019) (**Figure 3B**). Colicins show activity on a wide bacterial range (Duché and Houot, 2019), and they also showed cytotoxic activity on breast carcinoma, fibrosarcoma, leiomyosarcoma, osteosarcoma, and colon carcinoma (Bandala et al., 2013; Karpinski and Adamczak, 2018). In this sense, a study using the different isolates of colicins, E1, E6, E7, K, and M, was evaluated against *E. coli* strains from patients with bacteraemia of urinary tract origin. The colicin isolates were tested in concentrations of 1, 10, and 100 μg/ml. The results showed that colicin E7 was able to kill 87% of the strains tested. The results showed that colicin E7 at 10 μg. ml^{-1} was able to kill 87% of strains tested. The inhibitory activity of combinations of colicins E7, K, M and E1, E6, E7, K effectively inhibited the growth of pathogenic *E. coli* strains (Budič et al., 2011). Furthermore, colicin presents anticancer activity. This activity was elucidated by Chumchalova and Šmarda (2003), in a study that used four colicins (A, E1, U, E3) against 11 cancer cell lines. They detected anticancer activity in most of cell lines tested. Although fibrosarcoma HS913T has demonstrated 50% inhibition with colicin E1, it was also shown to be sensitive to colicin A and U. Only colicin E3 did not exhibit significant inhibition activity against tested cancer cells. Another study demonstrated the efficiency of colicin E3 against murine leukemia P388cells. It tested colicin E3 in final concentrations of 0.4 mg. ml^{-1}, 0.8 mg. ml^{-1}, 1.6 mg. ml^{-1}, and 3.2 mg. ml^{-1} for 0, 24, 48 and 72-h cultivations at 37°C. The results demonstrated the colicin E3 was able to inhibit the proliferation of murine leukemia cells in a time- and dose-dependent manner (Fuska et al., 1979).

Pyocins originate from *P. aeruginosa* (Ghequire and De Mot, 2018); their size varies between 77 and 157 amino acid residues (Ghequire and De Mot, 2014). Three different types of pyocins are described, namely the R, F, and S type. The R-type pyocins connect to the outer membrane receptor and induce the depolarization of the cytoplasmic membrane in relation to pore formation (**Figure 3A**). S-type or colicin-like pyocins show endonuclease activity when placed at the C-terminal end, and this activity induces cell death by interrupting DNA, RNA and protein syntheses (Michel-Briand and Baysse, 2002) (**Figure 3B**). These proteins act on Gram-negative bacteria (McCaughey et al., 2016), and demonstrated activity against embryonal ovary carcinoma, human hepatocellular carcinoma, and cervical adenocarcinoma (Karpinski and Adamczak, 2018).

TABLE 1 | Anticancer and antimicrobial activity of proteins and peptides from bacterial origins.

Protein	Bacterial origin	Size (kDa)	Net charge	Hydrophobicity < H >	Antibacterial activity	Cancer cell lines	References
Colicins	*E. coli*	27–80			Gram−	MCF-7, ZR75, BT549, BT474, MDA-MB-231, SKBR3, T47D, HOS, SKUT-1, HS913T, HT29, MRC5.	Karpinski and Adamczak, 2018; Duché and Houot, 2019
Pyocins	*P. aeruginosa*	77–157			Gram+	HFFF, HeLa, AS-II, HepG2, mKS-ATU-7, HCG-27.	Karpinski and Adamczak, 2018
Peptide	**Bacterial origin**	**Size (kDa)**	**Net charge**	**Hydrophobicity < H >**	**Antibacterial activity**	**Cancer cell lines**	**References**
Nisin A	*Lactococcus lactis*	3.49	3	0.569	Gram+/Gram−	MCF-7, HepG2, HNSCC, HT29, CaCo-2, SW480.	Kuwano et al., 2005; Maher and McClean, 2006; Joo et al., 2012; Shin et al., 2016; Ahmadi et al., 2017
Nisin Z	*Lactococcus lactis* SIK-83	3.47	3	0.548	Gram+/Gram−	HNSCC, HUVEC.	Kamarajan et al., 2015; Preet et al., 2015
Microcin E492	*Klebsiella pneumoniae*	7.8	−4	0.171	Gram−	Jurkat, RJ2.25 HeLa, CRC cells.	de Lorenzo, 1984; Hetz et al., 2002
Bovicin HC5	*Streptococcus bovis* HC5	2.4	–	–	Gram+/*Prevotella bryantii*	MCF-7, HepG2	Mantovani et al., 2002; Paiva et al., 2012
Laterosporulin- LS10	*Brevibacillus laterosporus* SKDU10	6.0	2	0.409	*Mycobacterium tuberculosis* and *S. aureus*	HeLa, H1299, HEK293T, HT1080, MCF-7	Baindara et al., 2015; Singh et al., 2015
Pediocin PA-1	*Pediococcus acidilactici* PAC1	4.6	3	0.343	Gram+	Lung carcinoma (A-549) and CRC (DDL1)	Henderson et al., 1992; Beaulieu, 2005
Pediocin K2a2-3	*Pediococcus acidilactici* K2a2-3	4.1	2	0.360	Gram+	HT29, Hela	Villarante et al., 2011
Pediocin CP2	*P. acidilactici* CP2 MTCC501	4.6	3	0.343	Gram+	Hela, HepG2, MCF-7, Sp2/0-Ag14	Kumar et al., 2011
Plantaricin A	*Lactobacillus plantarum* C11	2.4	6	0.369	Gram+/Gram−	Jurkat, GH_4, Reh, PC12, N2A.	Nissen-Meyer et al., 1993; Diep et al., 1996; Zhao et al., 2006
m2163	*Lactobacillus casei* ATCC334	2.7	3	0.508	Gram+	SW480	Tsai et al., 2015
m2386	*Lactobacillus casei* ATCC334	2.7	2	0.324	Gram+	SW480	Tsai et al., 2015
KL15	*Lactobacillus casei* ATCC334	1.9	5	0.491	Gram+/Gram−	SW480, CaCo-2	Chen et al., 2015
Duramycin	*Streptoverticillium cinnamoneus*	2.0	1	0.457	Gram+	AsPC-1, Caco-2, Colo320, CT116, JJN3, Lovo, MCF7, MDA-B-231, MIA PaCa-2, MM.1S, U266B1	Iwamoto et al., 2007; Broughton et al., 2016
Pep27	*Streptococcus pneumoniae*	2.8	4	0.040	Gram+/Gram−	Jurkat	Lee et al., 2005; Sung et al., 2007
Pep27anal2	*Streptococcus pneumoniae*	3.3	4	0.527	Gram+/Gram−	Jurkat, HL-60, AML-2, MCF-7, SNU-601	Lee et al., 2005; Sung et al., 2007
p28	*Pseudomonas aeruginosa* PAO1	2.8	−4	0.222	–	MCF-7, HCT-116, UISO-MEL-23, MNE-MB-231, p53wt (Mel-29), U87, LN229	Yamada et al., 2009; Mehta et al., 2011; Bernardes et al., 2013

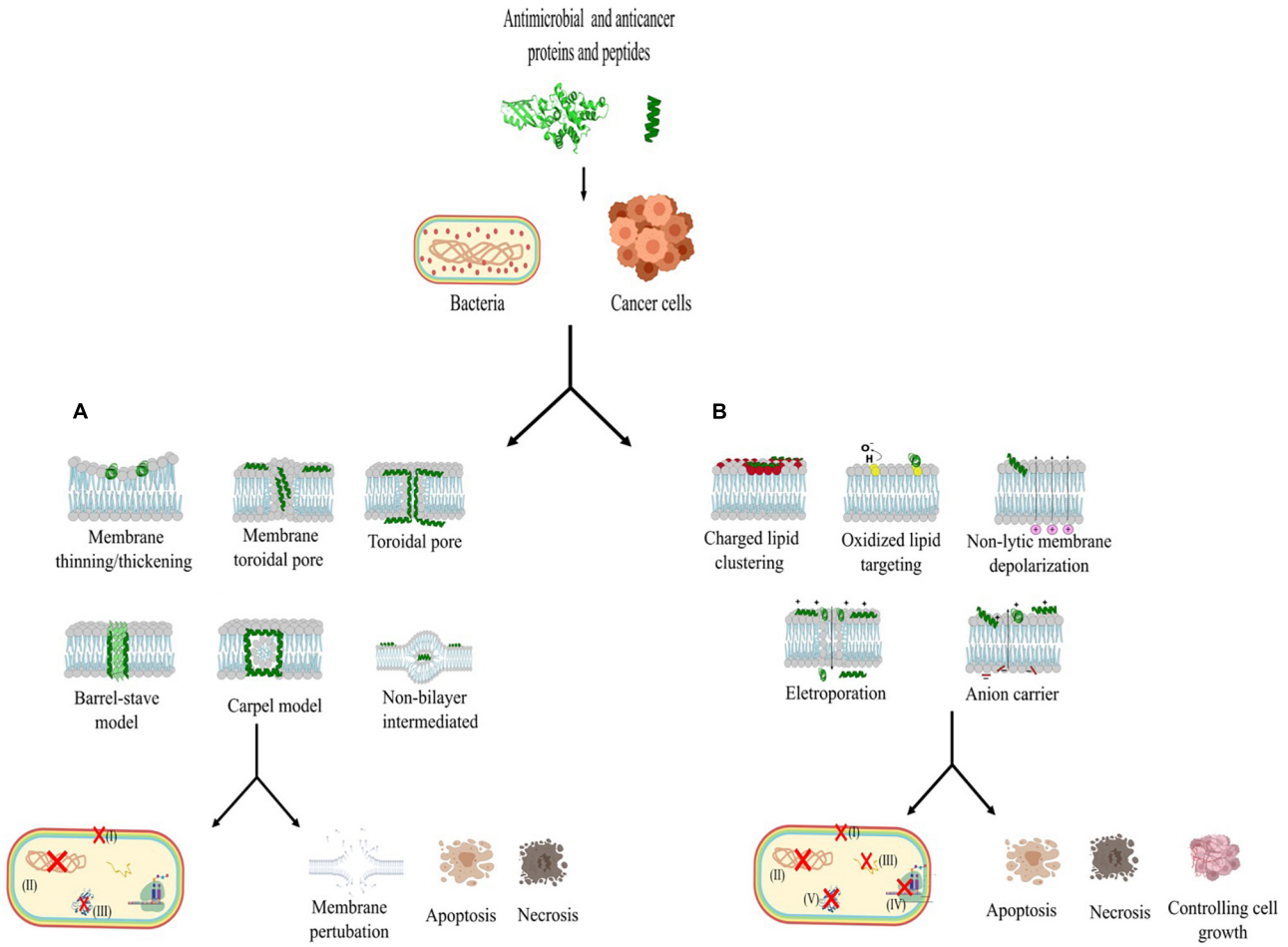

FIGURE 3 | Different mechanisms of action of proteins and peptides with anticancer and antibacterial activity. **(A)** This section represents the protein and peptide interaction with the carpet model, barrel-stave model, toroidal pore, disorder toroidal pore, non-bilayer intermediate and membrane thinning/thickening, which are mechanisms that act in the conformation of the external membrane (I), target the inhibition of phospholipase, lipid II and LPS permeabilization. In the inner membrane, these mechanisms act in DNA synthesis (II) and inhibition of fold protein (III). **(B)** This section represents the action of proteins and peptides interaction the other mechanisms described above, such as anion carrier, charged lipid clustering, electroporation, non-lytic membrane depolarization, and oxidized lipid targeting, act in the destabilization of membrane components (I): in addition, they act in the inner membrane by interrupting DNA (II), RNA(III), and protein syntheses (IV) and (V). All these mechanisms can cause bacterial death and, in cancer cells, can cause disruption of membrane, apoptosis, necrosis, and control of angiogenesis. The model described in **(A)** and **(B)** acting in bacteria and cancer cells.

Thus, Ling et al. (2010) studied the pyocin S5 in different concentrations (3.5, 14, 56, and 225 μg. ml^{-1}) against seven clinical *P. aeruginosa* isolates (DWW3, InA, InB, In3, In4, In7, and In8). Their results indicated that isolate DWW3 is most sensitive in an inhibitory concentration of 12.6l μg.ml^{-1}, and the other isolates were killed in a concentration of 225 μg. ml^{-1} isolates (Ling et al., 2010). Additionally, R-type pyocins were tested in a lethal mouse peritonitis model. The researchers infected female mice (Charles River Laboratories) with 0.5. ml^{-1} of inoculum of *P. aeruginosa* strain 13s per mouse, in concentrations of 10^6 to 10^7 CFU. ml^{-1}. The treatment with 0.1. ml^{-1} of pyocins was administered intraperitoneally (i.p.) and intravenously (i.v.). At 24 and 48 h after treatment inoculation, blood and spleen samples were evaluated. The result showed that i.p. and i.v. dose responses were similar, and pyocin killed approximately 99.99% of the bacteria in the blood and spleen samples. This study suggested that R-type pyocins could be an effective therapy (Scholl and Martin, 2008).

A different test using purified pyocin S2 and partially purified pyocin from *P. aeruginosa* 42A was evaluated against human tumor cell lines, HepG2 and Im9, and the normal human cell line HFFF (Human Fetal Foreskin Fibroblast). Pyocin S2 and partially purified pyocin were tested at concentrations of 6.25, 12.25, 25, and 50 U. ml^{-1}, for 5 days. The results showed cell line Im9 was more sensitive than HepG2, and maximum growth inhibition of 80% was observed at the maximum pyocin concentration of 50 U. ml^{-1} after 5 days (Abdi-Ali et al., 2004). According to the examples cited above, the colicins and pyocins demonstrated efficacious antimicrobial and anticancer activity.

Nisin

Nisin can be secreted by *Lactococcus lactis* subspecies lactis and has a low molecular mass of 3.49 kDa with 34 amino acid residues. This polycyclic peptide belongs to a class of lantibiotics, which have unusual amino acids such as lanthionines (Moll et al., 1997; de Arauz et al., 2009; Shin et al., 2016). Nisin exhibits stability at different temperatures and has potent activity against different bacteria, including pathogenic strains, acting primarily on Gram-positive bacteria (Jack et al., 1995; Severina et al., 1998). In view of this, nisins are classified as broad-spectrum peptides, presenting activity in different classes of bacteria (Shin et al., 2016). In addition, nisins share some similarities with pore-forming AMPs, such as positive net charge and amphipathicity. These peptides may exhibit different mechanisms of activity that may involve interaction with membranes facilitated by lipid II binding (Christ et al., 2007). This can lead to the formation of pores in the membrane (Moll et al., 1997) (**Figure 3**). Due to its low toxicity, this molecule has been used for a long time in food preservation (Gharsallaoui et al., 2016). In addition to its antibacterial activity, nisin and its natural variants have been shown to be effective in combating cancerous cells (Joo et al., 2012; Kamarajan et al., 2015).

In this sense, several studies have been carried out to demonstrate the efficiency of nisin against microorganisms. One of these studies purified nisin Z, which exhibits antimicrobial activity against *S. aureus* and *E. coli*. However, the test using nisin Z and 100 mM NaCl demonstrated activity just for *S. aureus* (Kuwano et al., 2005). Another study described the nisin activity against cariogenic microorganisms (*Streptococcus* spp., *Lactobacillus* spp., *Actinomyces* spp.). According to the researchers, electron microscopy showed that nisin exerted bactericidal activity by forming small pores on the surface of cells (Tong et al., 2010) (**Figure 3A**).

In addition, we described studies using nisin with anticancer activity. Joo et al. (2012) demonstrated that nisin decreases head and neck squamous cell carcinoma (HNSCC) tumorigenesis *in vitro* and *in vivo* by inducing increased cell apoptosis and decreased cell proliferation. For the *in vitro* test, the researchers used a concentration of 5, 10, 20, 40, and 80 $\mu g.ml^{-1}$ nisin against three different HNSCC cell lines, and after 24 h of treatment they observed increased levels of DNA fragmentation or apoptosis. *In vivo* tests were evaluated with a 150 mg/kg dose of nisin administered over the course of 3 weeks. They observed that mice that had received nisin treatment exhibited statistically significant reduced tumor volumes compared with control. These effects are associated with the activation of CHAC1, broadening calcium influxes and inducing cell cycle arrest (Joo et al., 2012).

Another group also tested the efficiency of nisin Z for the treatment of HNSCC *in vitro* and *in vivo*. They used nisin Z at different concentrations (0, 100, 400, and 800 $\mu g.ml^{-1}$) against normal-human umbilical vein endothelial cells (HUVECs) in an *in vitro* test. In *in vivo* tests, they used an oral cancer floor-of-mouth mouse model. The treatment started after confirmation that tumors were established, using a control group that was given water (equal volume/control), and the treatment groups were treated with nisin, at two different concentrations (400 and 800 mg/kg per day) by oral gavage for 3 weeks. The researchers observed that the *in vitro* test demonstrated notably increasing levels of apoptosis when compared to cells treated with control medium. Furthermore, the concentrations of nisin tested *in vivo* significantly decreased the tumor volumes (13.5 and 88.5 mm^3 for nisin ZP 800 mg/kg, nisin ZP 400 mg/kg, respectively) compared to controls (232.8 mm^3). The authors concluded that nisin is an alternative therapy for HNSCC, exhibiting HNSCC cell apoptosis, suppressing HNSCC cell proliferation, inhibiting angiogenesis, HNSCC and tumorigenesis *in vivo* (Kamarajan et al., 2015). Different studies demonstrated the capacity of nisin to reduce, control and increase the apoptosis of distinct types of tumor cells (Preet et al., 2015; Ahmadi et al., 2017).

In addition, bovicin HC5 is a peptide with a strong similarity to the structure and function of nisin. This peptide can cause cell membrane disruption through pore formation and by modifying cellular potassium efflux (**Figure 3A**). It is a lantibiotic secreted by *Streptococcus bovis* HC5 and presents about 2.4 kDa of molecular mass. It can be considered as an AMP with a broad spectrum of activity on Gram-positive and negative bacteria. It is considered a stable molecule at high temperatures and low pH, but it may undergo loss of activity in the presence of pronase E and trypsins (Mantovani et al., 2002). Bovicin HC5 has already demonstrated anticancer activity against human adenocarcinoma cells (MCF-7) and hepatocellular carcinoma (HepG2) (Paiva et al., 2012).

Microcin

Bacteria belonging to the Enterobacteriaceae family are responsible for the production of microcin. These peptides can have a molecular mass up to 10 kDa, and they present activity on different strains of pathogenic bacteria, such as *Salmonella, Enterobacter, Klebsiella, Escherichia,* and *Citrobacter* (de Lorenzo, 1984). The microcins are classified in two classes: class I is represented by peptides with molecular masses <5 kDa, being codified by cluster genes located either on plasmids or on the chromosome, like microcins B17, C (or C7, C51 or C7/C51), and J25.6. Class II is represented by higher molecular mass peptides ranging from 5- to 10-kDa. Additionally, they are subdivided into two subclasses, IIa and IIb. Class IIa presents three plasmid-encoded peptides, microcins L, V, 6 and N. They do not have post-translational modifications and can present two, one, and no disulfide bond(s), respectively. Class IIb is described as linear microcins with post-translational modification represented by microcins E492, M, H47, and presumably I47 and G492 (Rebuffat, 2013). The microcin act taking advantage of iron-siderophore receptors (FepA, Cir, Fiu). After receptor interaction, microcin was translocated though the TonB-ExbB-ExbD inner-membrane protein complex (Morin et al., 2011; Rebuffat, 2013). Thus, microcin induces depolarization of the cytoplasmic membrane, reaching a specific molecular target (de Lorenzo, 1984; de Lorenzo and Pugsley, 1985; Lagos et al., 1993; Hetz et al., 2002; Morin et al., 2011; Rebuffat, 2013) (**Figure 3A**).

The efficiency of microcin was studied by Yu et al. (2018). They tested microcin (MccJ25) against the ETEC K88 (serotype

O149:K91, K88ac) strain, which is a pathogen related with human infants and neonatal diarrhea. They used MccJ25 in 0.125 to 256 μg/mL concentrations. The results demonstrated the efficacy of MccJ25 at a concentration of 0.25 μg. ml^{-1} against ETEC K88. They observed that MccJ25 was not cytotoxic, and that is was also able to protect the intestine against ETEC K88-induced damage and inflammatory response. According to the authors, MccJ25 can be used as a novel prophylactic agent to reduce pathogenic infection in animals, food or humans.

Furthermore, the efficacy of microcin with *in vitro* tumor cells was described by Hetz et al. (2002). They studied microcin E492 produced by *Klebsiella pneumoniae* strain RYC492 with 7,887 Da. This peptide was tested against some human tumor cells such as Jurkat, RJ2.25, colorectal carcinoma (CRC) and HeLa to observe the capacity to induce apoptosis. The authors tested microcin E492 at different concentrations of 5, 10, and 20 μg/ml. The result demonstrated that at a concentration of 5 μg. ml^{-1} microcin induced tumor cells to apoptosis, and at concentrations of 10 and 20 μg. ml^{-1} necrosis was observed (Hetz et al., 2002).

Laterosporulins

Laterosporulins (LS) are peptides with low molecular masses (approximately 5.6 kDa) that present a strong similarity to defensins (Singh et al., 2015). This class of peptides exhibits amphiphilic helical structure, which permits laterosporulin to insert itself into the membrane of the target cell, inducing depolarization and death (Kaur and Kaur, 2015) (**Figure 3A**). These peptides were isolated from different strains, namely GI-9 and SKDU10, from *Brevibacillus* sp. and have showed potent antibacterial activity against several pathogens (Singh et al., 2015). One example is laterosporulin 10 (LS10) isolated from *Brevibacillus* SKDU10, with 6 kDa, which was tested at different concentrations of 4, 8, and 20 μM against *Staphylococcus aureus* and *Mycobacterium tuberculosis* (MtbH37Rv). The result showed that LS10 inhibited the growth of *S. aureus* with LD50 of 4.0 μM and *M. tuberculosis* (Mtb H37Rv) with LD50 of 0.5 μM. In addition, microscopic studies demonstrated that LS10 acts on *S. aureus* cell membrane and the Mtb H37Rv strain by disrupting cellular metabolic homeostasis. LS10 was able to alter the membrane of the Mtb H37Rv strain, which has a thick lipid layer (Baindara et al., 2016). Moreover, regarding LS10 antitumor activity, this peptide was tested in the concentrations 1–20 μM against HeLa, H1299, HEK293T, HT1080, MCF-7, and RWPE-1 cells. The results demonstrated that LS10 showed activity against diverse cancer cells like MCF-7, HEK293T, HT1080, HeLa, and H1299 in low concentrations (10 μM), but failed against RWPE-1 cells. Moreover, the LS10 at a concentration of 2.5 μM induced apoptosis (Baindara et al., 2018).

Pediocins

Pediocins originate from bacteria that produce lactic acid, mainly species of *Pediococcus* (Kumar et al., 2011). A variety of pediocins have been identified so far, namely, pediocin CP-2, F, K1, AcH, AcM SJ-1, and L50, some of which are cited in an extensive review by Porto et al. (2017). They can be considered as small plasmid-encoded cationic AMPs (>5 kDa), with high stability at a variety of temperatures and pHs. However, they may undergo actions of different proteolytic enzymes such as trypsin, α-trypsin, pepsin, papain, and proteases (Kumar et al., 2011). Their N-terminal region contains the conserved Y-G-N-G-V/L "pediocin box" motif and two conserved cysteine residues that are joined by a disulfide bridge, which forms a three-stranded antiparallel beta-sheet (Papagianni and Anastasiadou, 2009). Pediocins contain a conserved N-terminal region folded by disulfide bonds, and this domain mediates binding of class IIa bacteriocins to the target cell membrane. In contrast, the C-terminal region forms a hairpin that is able to penetrate the target cell membrane hydrophobic region, thereby mediating leakage through the membrane (Fimland et al., 2005; Drider et al., 2006) (**Figure 3A**). Pediocins have showed antimicrobial activity. According to Bédard et al. (2018), they synthesized pediocin PA-1 and demonstrated that it is a potent inhibitor of *Listeria monocytogenes* (MIC = 6.8 nM), similar to that produced naturally by *Pediococcus acidilactici*. Pediocin PA-1 was also tested against different strains of *Carnobacterium divergens* ATCC 35677 (MIC = 1.9 nM), *Leuconostoc mesenteroides* ATCC 23386 (MIC = 1.9 nM), *Listeria seeligeri* ATCC 35967 MIC = 4.7 nM), *Clostridium perfringens* AAC 1–222 (MIC = 37.8 nM), *Clostridium perfringens* AAC 1–223 (MIC = 75.7 nM), *Listeria murrayi* ATCC 25401 (MIC = 151.4 nM), and *Lactobacillus plantarum* ATCC 8014 (MIC = 605.5 nM). Studies have shown the antitumor activity of some pediocins, as exemplified by PA-1, a pediocin produced by *P. acidilactici* PAC1. In the presence of human lung carcinoma cells and colorectal adenocarcinoma, PA-1 inhibited the growth of these cells. Pediocin PA-1 isolated from *P. acidilactici* K2a2-3 has also been shown to be cytotoxic to human colon adenocarcinoma HT29 and HeLa cells, but the mechanism of cytotoxicity has not been studied (Villarante et al., 2011). As also observed, pediocin CP2 produced by *P. acidilactici* CP2 MTCC501 has antitumor activity on HEPg2, HeLa and MCF-7 human cancer cells (Kumar et al., 2011).

Plantaricin

The peptide plantaracin (Pln) is produced by different strains of *Lactobacillus plantarum* (C11, WCFS1, V90), showing low molecular mass (∼2.4 kDa) (Diep et al., 1996). The amphiphilic nature of the Pln peptide (class IIb), could facilitate the formation of membrane channels (Nissen-Meyer et al., 1993) (**Figure 3A**). In fact, Pln has already been shown to permeate eukaryotic cells, but demonstrates affinity to negatively charged membranes and exhibits strong interaction with glycolate membrane proteins (Sand et al., 2013). Some works have demonstrated a broad-spectrum activity of these peptides on different bacterial strains (Nissen-Meyer et al., 1993; Diep et al., 1996). A recent study demonstrated the antimicrobial activity of plantaricins (Pln) A, E, F, J, and K against *Staphylococcus epidermidis*. The plantaricins alone were tested at a concentration of 0.097 to 50 μM, and the plantaricins in association with the antibiotics were tested at concentrations12.5 and 6.25 μM. The results showed that *S. epidermidis* was more susceptible to PlnEF than PlnJK, with MIC 12.5 and 25 μM, respectively. PlnE, F, J and K inhibited bacterial growth, and PlnEF and PlnJK, at 25 and 50 μM, caused rapid bacterial lysis (data not shown). In addition, PlnA (50 μM) alone repressed bacterial growth. Pln in combination

with low concentrations of antibiotics displayed antimicrobial activity against *S. epidermidis*. According to results, Pln in combination with antibiotics in low concentration was efficient against *S. epidermidis* and exhibited strong potential to treat infections (Selegård et al., 2019). Pln also demonstrated activity on cancer cells (Zhao et al., 2006; Sand et al., 2010, 2013). This activity was shown in a study by Sand et al. (2010), in which they studied the effect of synthesized PlnA against normal human B and T cells, Reh cells (from human B cell leukemia), and Jurkat cells (from human T cell leukemia). The cell types were tested at a concentration of 10–100 μM PlnA. The results showed that all cells were affected by PlnA, but at low concentrations (10 μM) this did not demonstrate a strong effect. The mechanism of action was seen to be membrane permeabilization, leading to apoptosis along with necrosis.

Duramycin

Duramycin is a type of lantibiotic produced by streptomycetes. This tetracyclic peptide is synthesized by ribosomes and exhibits post-translational changes, as well as possessing antimicrobial activity. It consists of 19 amino acid residues corresponding to a molecular mass of ∼2 kDa (Phoenix et al., 2015; Broughton et al., 2016). The post-translational changes undergone by duramycin, such as the enzymatic addition of three thioether bonds, besides increasing the proteolytic stability of this molecule, also provide selectivity and binding to phosphatidylethanolamine (PE) present on the membrane of various cell types, including Gram-positive and negative bacteria (Iwamoto et al., 2007). The interaction of duramycin with target cells can trigger plasmatic membrane imbalance, affecting membrane integrity and influencing the ion transportation mediated by pore formation on the surface of the cell membrane (Sheth et al., 1992; Oliynyk et al., 2010) (**Figure 3A**).

Other effects of duramycin on the plasma membrane have been shown, such as an inhibitory effect on plasma membrane ATPase activity (Nakamura and Racker, 1984), an increase in cell membrane permeability, and inhibition of Na^+-K^+-ATPase in the cellular plasma membranes of Ehrlich ascites tumor cells (Nakamura and Racker, 1984). Due to these characteristics, the antineoplastic capacity of duramycin has been studied. Since the membrane surface of some cancer cells is positive for PE, the effectiveness of duramycin on these cells was visible, decreasing the proliferation of tumor cells and inducing apoptosis. In accordance with a study conducted by Broughton et al. (2016), it was shown that about 11 cancer cell lines (AsPC-1, Caco-2, Colo320, HCT116, JJN3, Lovo, MCF-7, MDA-MB-231, MIA PaCa-2, MM. 1S, and U266B1) expressed PE on the surface. Furthermore, cell death from necrosis in these cancer cells and the release of Ca 2^+ calcium ions were identified, depending on the time of exposure as well as the concentration of duramycin. Other findings such as morphological changes and influx of iodide have also been reported (Broughton et al., 2016).

Other Peptides

Pep27anal2

Pep27anal2 contains 27 amino acid residues and has a molecular mass of 3.3 kDa. This peptide is an analog of pep27, produced by *Streptococcus pneumoniae* (Sung et al., 2007). Therefore, pep27 showed MIC 12.5 for Gram-positive and Gram-negative bacteria without a hemolytic effect on human erythrocytes (Sung et al., 2007). Pep27anal2 has a higher number of hydrophobic residues compared to the native peptide pep27. This hydrophobic characteristic of pep27anal2 may be related to the interaction with cell membranes and possibly the anticancer activity that this peptide has demonstrated (**Figure 3A**) (Lee et al., 2005). It demonstrated activity against leukemia cancer cells (Jurkat, HL-60, AML-2), breast cancer (MCF-7) and gastric cancer (SNU-601). Besides the ability to permeate cancer cells, data indicate that the mechanism responsible for cytotoxicity in neoplastic cells arises from the induction of apoptosis of caspase-free and cytochrome-C. In addition, electron microscopy revealed that pep27anal2 induced the morphological features of apoptosis in Jurkat cells, and showed cytoplasmic condensation, cell shrinkage, loss of plasma membrane microvilli, condensed or fragmented nuclei, and the formation of membrane vesicles (Lee et al., 2005). Considering its potent activity against cancer cells, pep27anal2 is a potential candidate for antineoplastic therapy (Lee et al., 2005).

M2163, M2386, and KL15

Based on genomic analyses of *Lactobacillus casei* ATCC334, some DNA sequences responsible for the expression of the antimicrobial peptides m2163 and m2386 were identified (Tsai et al., 2015). These peptides demonstrated activity on different lactobacillus strains as well as species of *Listeria* sp. Furthermore, m2163 and m2386 showed effective activity on SW480 cancer cells, acting on the cell membrane and then penetrating the cell cytoplasm to induce apoptosis (**Figure 3B**) (Tsai et al., 2015). These bacteriocins, m2163 and m2386, were the sources of inspiration for the development of the KL15 antimicrobial peptide through *in silico* modifications in their sequences. KL15, besides having potent antibacterial activity on pathogenic bacteria such as *Enterococcus, Staphylococcus, Bacillus, Escherichia,* and *Listeria,* presented anticancer activity against SW480 and CaCo-2 human adenocarcinoma cells (Chen et al., 2015). Moreover, KL15 (50 μg. mL^{-1}) has been shown to be able to permeate the membranes of SW480 cells, resulting in the formation of porous structures, resulting in necrotic cell death. However, the 150 μg. mL^{-1} dose of KL15 showed cytotoxicity on human normal mammary epithelial cells H184B5F5/M10 (Chen et al., 2015).

FINAL REMARKS

As mentioned above, cancer and chronic infections are the predominant causes of death worldwide. The conventional treatment for these problems generates resistance against multiple drugs. Moreover, conventional treatments are not efficient and effective, inducing serious side effects in patients (Liu et al., 2015; Felício et al., 2017; Leite et al., 2018).

Thus, a new class of molecules needs to be developed and used to provide a more targeted therapy, by exploiting more specific interactions between the drugs and their targets

(Gaspar et al., 2013; Felício et al., 2017; Wang et al., 2017; Leite et al., 2018; Shoombuatong et al., 2018). To this end, bacteria have an arsenal of proteins and peptides with both antibacterial and antitumoral activity, which can be explored in the search for these new compounds (Karpinski and Adamczak, 2018).

Various approaches have been discussed here, demonstrating the properties of proteins and peptides derived from bacteria as an alternative strategy for cancer treatment. Among the proteins and peptides that act against bacterial and cancer cells, several stand out. Colicins act on a wide range of bacteria (Duché and Houot, 2019), and have also demonstrated activity against breast carcinoma, fibrosarcoma, leiomyosarcoma, osteosarcoma, and colon carcinoma (Karpinski and Adamczak, 2018). Another promising group is the nisins, which act on Gram-positive bacteria (Jack et al., 1995; Severina et al., 1998), and some nisin variations have demonstrated activity against Gram-negative bacteria (Kuwano et al., 2005), besides potent activity on HNSCC, reducing tumorigenesis (Joo et al., 2012).

Proteins and peptides have been studied for some years, but recently the number of publications and *in vivo* tests have increased. This has led to the rising number of proteins and peptides approved for use in medical practice. In addition, it is to be expected that in upcoming years these molecules may replace conventional treatments. Thus, it is necessary to improve some properties of these molecules in order to decrease or eliminate cytotoxic effects and increase the specificity of the targeting. Besides that, to expand the use of proteins and peptides it will be important to combine these molecules with conventional drugs. This can reduce costs per treatment, besides decreasing the resistance problem. Therefore, proteins and peptides derived from bacteria with dual activity are an important alternative to current treatments against infections and cancer, reducing side effects and curbing the rise of resistant bacteria.

AUTHOR CONTRIBUTIONS

All authors listed have made a substantial, direct and intellectual contribution to the work, and approved it for publication.

FUNDING

This work was supported by grants from Fundação de Apoio à Pesquisa do Distrito Federal (FAPDF), Coordenação de Aperfeiçoamento de Pessoal de Nível Superior (CAPES), Conselho Nacional de Desenvolvimento Científico e Tecnológico (CNPq), and Fundação de Apoio ao Desenvolvimento do Ensino, Ciência e Tecnologia do Estado de Mato Grosso do Sul (FUNDECT), Brazil.

REFERENCES

Abdi-Ali, A., Worobec, E. A., Deezagi, A., and Malekzadeh, F. (2004). Cytotoxic effects of pyocin S2 produced by *Pseudomonas aeruginosa* on the growth of three human cell lines. *Can. J. Microbiol.* 50, 375–381. doi: 10.1139/w04-019

Ahmadi, S., Ghollasi, M., and Hosseini, H. M. (2017). The apoptotic impact of nisin as a potent bacteriocin on the colon cancer cells. *Microb. Pathog.* 111, 193–197. doi: 10.1016/j.micpath.2017.08.037

Alexander, J. L., Thompson, Z., Yu, Z., and Cowan, J. A. (2019). Cu-ATCUN derivatives of Sub5 exhibit enhanced antimicrobial activity via multiple modes of action. *ACS Chem. Biol.* 14, 449–458. doi: 10.1021/acschembio.8b01087

Arias, C. A., and Murray, B. E. (2009). Antibiotic-resistant bugs in the 21st century—a clinical super-challenge. *N. Engl. J. Med.* 360, 439–443. doi: 10.1056/nejmp0804651

Baindara, P., Chaudhry, V., Mittal, G., Liao, L. M., Matos, C. O., Khatri, N., et al. (2015). Characterization of the antimicrobial peptide penisin, a class ia novel lantibiotic from *Paenibacillus* sp. Strain A3. *Antimicrob. Agents Chemother.* 60, 580–591. doi: 10.1128/AAC.01813-15

Baindara, P., Korpole, S., and Grove, V. (2018). Bacteriocins: perspective for the development of novel anticancer drugs. *Appl. Microbiol. Biotechnol.* 102, 10393–10408. doi: 10.1007/s00253-018-9420-8

Baindara, P., Singh, N., Ranjan, M., Nallabelli, N., Chaudhry, V., Pathania, G. L., et al. (2016). Laterosporulin10: a novel defensin like class IId bacteriocin from *Brevibacillus* sp. strain SKDU10 with inhibitory activity against microbial pathogens. *Microbiology* 162, 1286–1299. doi: 10.1099/mic.0.000316

Bandala, C., Perez-Santos, J. L. M., Lara-Padilla, E., Delgado, L., and Anaya-Ruiz, M. (2013). Effect of botulinum toxin A on proliferation and apoptosis in the T47D breast cancer cell line. *Asian Pac. J. Cancer Prev.* 14, 891–894. doi: 10.7314/apjcp.2013.14.2.891

Beaulieu, L. (2005). *Production, Purification et Caracterisation de la Pediocine PA-1 Naturelle et de ses Formes Recombinantes: Contribution a la Mise en Evidence d'une Nouvelle Activite Biologique*. Quebec, QC: Universite Laval.

Bédard, F., Hammami, R., Zirah, S., Rebuffat, S., Fliss, I., and Biron, E. (2018). Synthesis, antimicrobial activity and conformational analysis of the class IIa bacteriocin pediocin PA-1 and analogs thereof. *Sci. Rep.* 8:9029. doi: 10.1038/s41598-018-27225-3

Belmadi, N., Wu, Y., and Touqui, L. (2018). Immuno-modulatory functions of the type-3 secretion system and impacts on the pulmonary host defense: a role for ExoS of *Pseudomonas aeruginosa* in cystic fibrosis. *Toxicon* 143, 68–73. doi: 10.1016/j.toxicon.2018.01.004

Bernardes, N., Chakrabarty, A. M., and Fialho, A. M. (2013). Engineering of bacterial strains and their products for cancer therapy. *Appl. Microbiol. Biotechnol.* 97, 5189–5199. doi: 10.1007/s00253-013-4926-6

Broughton, L. J., Crow, C., Maraveyas, A., and Madden, L. A. (2016). Duramycin-induced calcium release in cancer cells. *Anticancer Drugs* 27, 173–182. doi: 10.1097/CAD.0000000000000313

Budič, M., Rijavec, M., Petkovšek, Ž, and Žgur-Bertok, D. (2011). *Escherichia coli* bacteriocins: antimicrobial efficacy and prevalence among isolates from patients with bacteraemia. *PLoS One* 6:e28769. doi: 10.1371/journal.pone.0028769

Cascales, E., Buchanan, S. K., Duché, D., Kleanthous, C., Lloubes, R., Postle, K., et al. (2007). Colicin biology. *Microbiol. Mol. Biol. Rev.* 71, 158–229. doi: 10.1128/MMBR.00036-06

Chakrabarty, A. M., Bernardes, N., and Fialho, A. M. (2014). Bacterial proteins and peptides in cancer therapy: today and tomorrow. *Bioengineered* 5, 234–242. doi: 10.4161/bioe.29266

Chai, T., Wu, V., and Foulds, J. (1982). Colicin A receptor: role of two *Escherichia coli* outer membrane proteins (OmpF protein and btuB gene product) and lipopolysaccharide. *J. Bacteriol.* 151, 983–988.

Chen, Y.-C., Tsai, T.-L., Ye, X.-H., and Lin, T.-H. (2015). Anti-proliferative effect on a colon adenocarcinoma cell line exerted by a membrane disrupting antimicrobial peptide KL15. *Cancer Biol. Ther.* 16, 1172–1183. doi: 10.1080/15384047.2015.1056407

Chumchalova, J., and Šmarda, J. (2003). Human tumor cells are selectively inhibited by colicins. *Folia Microbiol.* 48, 111–115. doi: 10.1007/BF02931286

Cutter, C. N., and Siragusa, G. R. (1998). Incorporation of nisin into a meat binding system to inhibit bacteria on beef surfaces. *Lett. Appl. Microbiol.* 27, 19–23. doi: 10.1046/j.1472-765X.1998.00381.x

Daw, M. A., and Falkiner, F. R. (1996). Bacteriocins: nature, function and structure. *Micron* 27, 467–479. doi: 10.1016/s0968-4328(96)00028-5

de Arauz, L. J., Jozala, A. F., Mazzola, P. G., and Penna, T. C. V. (2009). Nisin biotechnological production and application: a review. *Trends Food Sci. Technol.* 20, 146–154. doi: 10.1016/j.tifs.2009.01.056

de Lorenzo, V. (1984). Isolation and characterization of microcin E 492 from *Klebsiella pneumoniae*. *Arch. Microbiol.* 139, 72–75. doi: 10.1007/BF00692715

de Lorenzo, V., and Pugsley, A. P. (1985). Microcin E492, a low-molecular-weight peptide antibiotic which causes depolarization of the *Escherichia coli* cytoplasmic membrane. *Antimicrob. Agents Chemother.* 27, 666–669. doi: 10.1128/aac.27.4.666

Di Masi, D. R., White, J. C., Schnaitman, C. A., and Bradbeer, C. (1973). Transport of vitamin B_{12} in *Escherichia coli*: common receptor sites for vitamin B_{12} and the E colicins on the outer membrane of the cell envelope. *J. Bacteriol.* 115, 506–513.

Diep, D. B., Håvarstein, L. S., and Nes, I. F. (1996). Characterization of the locus responsible for the bacteriocin production in *Lactobacillus plantarum* C11. *J. Bacteriol.* 178, 4472–4483. doi: 10.1128/jb.178.15.4472-4483.1996

Drider, D., Fimland, G., Hechard, Y., McMullen, L. M., and Prevost, H. (2006). The continuing story of class IIa bacteriocins. *Microbiol. Mol. Biol. Rev.* 70, 564–582. doi: 10.1128/MMBR.00016-05

Duché, D., and Houot, L. (2019). Similarities and differences between colicin and filamentous phage uptake by bacterial cells. *EcoSal Plus* 8, doi: 10.1128/ecosalplus.ESP-0030-2018

Epand, R. M., and Epand, R. F. (2011). Bacterial membrane lipids in the action of antimicrobial agents. *J. Pept. Sci.* 17, 298–305. doi: 10.1002/psc.1319

Felício, M. R., Silva, O. N., Goncçalves, S., Santos, N. C., and Franco, O. L. (2017). Peptides with dual antimicrobial and anticancer activities. *Front. Chem.* 5:5. doi: 10.3389/fchem.2017.00005

Fimland, G., Johnsen, L., Dalhus, B., and Nissen-Meyer, J. (2005). Pediocin-like antimicrobial peptides (class IIa bacteriocins) and their immunity proteins: biosynthesis, structure, and mode of action. *J. Pept. Sci.* 11, 688–696. doi: 10.1002/psc.699

Fuska, J., Fusková, A., Šmarda, J., and Mach, J. (1979). Effect of colicin E3 on leukemia cells P 388 in vitro. *Experientia* 35, 406–407. doi: 10.1007/bf01964380

Gabernet, G., Müller, A. T., Hiss, J. A., and Schneider, G. (2016). Membranolytic anticancer peptides. *MedChemComm* 7, 2232–2245. doi: 10.1039/c6md00376a

Gaspar, D., Veiga, A. S., and Castanho, M. A. (2013). From antimicrobial to anticancer peptides. A review. *Front. Microbiol.* 4:294. doi: 10.3389/fmicb.2013.00294

Gharsallaoui, A., Oulahal, N., Joly, C., and Degraeve, P. (2016). Nisin as a food preservative: part 1: physicochemical properties, antimicrobial activity, and main uses. *Critic. Rev. Food Sci. Nutr.* 56, 1262–1274. doi: 10.1080/10408398.2013.763765

Ghequire, M. G., and De Mot, R. (2014). Ribosomally encoded antibacterial proteins and peptides from *Pseudomonas*. *FEMS Microbiol. Rev.* 38, 523–568. doi: 10.1111/1574-6976.12079

Ghequire, M. G., and De Mot, R. (2018). Turning over a new leaf: bacteriocins going green. *Trends Microbiol.* 26, 1–2. doi: 10.1016/j.tim.2017.11.001

Ghosh, C., Sarkar, P., Issa, R., and Haldar, J. (2019). Alternatives to conventional antibiotics in the Era of antimicrobial resistance. *Trends Microbiol.* 27, 323–338. doi: 10.1016/j.tim.2018.12.010

Gifford, J. L., Hunter, H. N., and Vogel, H. J. (2005). Lactoferricin. *Cell. Mol. Life Sci.* 62:2588.

Gordon, Y. J., Romanowski, E. G., and McDermott, A. M. (2005). A review of antimicrobial peptides and their therapeutic potential as anti-infective drugs. *Curr. Eye Res.* 30, 505–515. doi: 10.1080/02713680590968637

Gorgal, T., Charrua, A., Silva, J. F., Avelino, A., Dinis, P., and Cruz, F. (2012). Expression of apoptosis-regulating genes in the rat prostate following botulinum toxin type a injection. *BMC Urol.* 12:1. doi: 10.1186/1471-2490-12-1

Gratia, A. (1925). Sur un remarquable example d'antagonisme entre deux souches de colibacille. *Compt. Rend. Soc. Biol.* 93, 1040–1042.

Hammami, R., Zouhir, A., Le Lay, C., Hamida, J. B., and Fliss, I. (2010). BACTIBASE second release: a database and tool platform for bacteriocin characterization. *BMC Microbiol.* 10:22. doi: 10.1186/1471-2180-10-22

Haney, E. F., Nathoo, S., Vogel, H. J., and Prenner, E. J. (2010). Induction of non-lamellar lipid phases by antimicrobial peptides: a potential link to mode of action. *Chem. Phys. Lipids* 163, 82–93. doi: 10.1016/j.chemphyslip.2009.09.002

Hasegawa, Y., Shimizu, T., Takahashi, N., and Okada, Y. (2012). The apoptotic volume decrease is an upstream event of MAP kinase activation during staurosporine-induced apoptosis in HeLa cells. *Int. J. Mol. Sci.* 13, 9363–9379. doi: 10.3390/ijms13079363

Henderson, J. T., Chopko, A. L., and van Wassenaar, P. D. (1992). Purification and primary structure of pediocin PA-1 produced by *Pediococcus acidilactici* PAC-1.0. *Arch. Biochem. Biophys.* 295, 5–12. doi: 10.1016/0003-9861(92)90480-K

Hetz, C., Bono, M. R., Barros, L. F., and Lagos, R. (2002). Microcin E492, a channel-forming bacteriocin from *Klebsiella pneumoniae*, induces apoptosis in some human cell lines. *Proc. Natl. Acad. Sci. U.S.A.* 99, 2696–2701. doi: 10.1073/pnas.052709699

Hoskin, D. W., and Ramamoorthy, A. (2008). Studies on anticancer activities of antimicrobial peptides. *Biochim. Biophys. Acta* 1778, 357–375. doi: 10.1016/j.bbamem.2007.11.008

International Agency of Research on Cancer [IARC] (2018). *World Cancer Report*. Geneva: World-Health-Organisation.

Iwamoto, K., Hayakawa, T., Murate, M., Makino, A., Ito, K., Fujisawa, T., et al. (2007). Curvature-dependent recognition of ethanolamine phospholipids by duramycin and cinnamycin. *Biophys. J.* 93, 1608–1619. doi: 10.1529/biophysj.106.101584

Jack, R. W., Tagg, J. R., and Ray, B. (1995). Bacteriocins of gram-positive bacteria. *Microbiol. Mol. Biol. Rev.* 59, 171–200.

Jain, K. K. (2001). Use of bacteria as anticancer agents. *Exp. Opin. Biol. Ther.* 1, 291–300. doi: 10.1517/14712598.1.2.291

Joo, N. E., Ritchie, K., Kamarajan, P., Miao, D., and Kapila, Y. L. (2012). Nisin, an apoptogenic bacteriocin and food preservative, attenuates HNSCC tumorigenesis via CHAC1. *Cancer Med.* 1, 295–305. doi: 10.1002/cam4.35

Kamarajan, P., Hayami, T., Matte, B., Liu, Y., Danciu, T., Ramamoorthy, A., et al. (2015). Nisin ZP, a bacteriocin and food preservative, inhibits head and neck cancer tumorigenesis and prolongs survival. *PLoS One* 10:e0131008. doi: 10.1371/journal.pone.0131008

Karpinski, T. M., and Adamczak, A. (2018). Anticancer activity of bacterial proteins and peptides. *Pharmaceutics* 10:E54. doi: 10.3390/pharmaceutics10020054

Kaur, S., and Kaur, S. (2015). Bacteriocins as potential anticancer agents. *Front. Pharmacol.* 6:272. doi: 10.3389/fphar.2015.00272

Kawakami, K., Nakajima, O., Morishita, R., and Nagai, R. (2006). Targeted anticancer immunotoxins and cytotoxic agents with direct killing moieties. *Sci. World J.* 6, 781–790. doi: 10.1100/tsw.2006.162

Kelly, G. J., Kia, A. F.-A., Hassan, F., O'Grady, S., Morgan, M. P., Creaven, B. S., et al. (2016). Polymeric prodrug combination to exploit the therapeutic potential of antimicrobial peptides against cancer cells. *Org. Biomol. Chem.* 14, 9278–9286. doi: 10.1039/C6OB01815G

Kominami, K., Nakabayashi, J., Nagai, T., Tsujimura, Y., Chiba, K., Kimura, H., et al. (2012). The molecular mechanism of apoptosis upon caspase-8 activation: quantitative experimental validation of a mathematical model. *Biochim. Biophys. Acta Mol. Cell Res.* 1823, 1825–1840. doi: 10.1016/j.bbamcr.2012.07.003

Konisky, J. (1982). Colicins and other bacteriocins with established modes of action. *Annu. Rev. Microbiol.* 36, 125–144. doi: 10.1146/annurev.mi.36.100182.001013

Kumar, B., Balgir, P. P., Kaur, B., and Garg, N. (2011). Cloning and expression of bacteriocins of *Pediococcus* spp.: a review. *Arch. Clin. Microbiol.* 2, 1–18. doi: 10:3823/231

Kuwano, K., Tanaka, N., Shimizu, T., Nagatoshi, K., Nou, S., and Sonomoto, K. (2005). Dual antibacterial mechanisms of nisin Z against Gram-positive and Gram-negative bacteria. *Int. J. Antimicrob. Agents* 26, 396–402. doi: 10.1016/j.ijantimicag.2005.08.010

Lagos, R., Wilkens, M., Vergara, C., Cecchi, X., and Monasterio, O. (1993). Microcin E492 forms ion channels in phospholipid bilayer membranes. *FEBS Lett.* 321, 145–148. doi: 10.1016/0014-5793(93)80096-d

Lee, D. G., Hahm, K.-S., Park, Y., Kim, H.-Y., Lee, W., Lim, S.-C., et al. (2005). Functional and structural characteristics of anticancer peptide Pep27 analogues. *Cancer Cell. Int.* 5:21. doi: 10.1186/1475-2867-5-21

Leite, M. L., da Cunha, N. B., and Cost, F. F. (2018). Antimicrobial peptides, nanotechnology, and natural metabolites as novel approaches for cancer treatment. *Pharmacol. Ther.* 183, 160–176. doi: 10.1016/j.pharmthera.2017.10.010

Leshem, Y., and Pastan, I. (2019). *Pseudomonas* exotoxin immunotoxins and anti-tumor immunity: from observations at the patient's bedside to evaluation in preclinical models.*Toxins* 11:20. doi: 10.3390/toxins11010020

Liberio, M. S., Joanitti, G. A., Fontes, W., and Castro, S. (2013). Anticancer peptides and proteins: a panoramic view. *Protein a Peptide Lett.* 20, 380–391. doi: 10.2174/092986613805290435

Ling, H., Saeidi, N., Rasouliha, B. H., and Chang, M. W. (2010). A predicted S-type pyocin shows a bactericidal activity against clinical *Pseudomonas aeruginosa* isolates through membrane damage. *FEBS Lett.* 584, 3354–3358. doi: 10.1016/j.febslet.2010.06.021

Lins, L., Ducarme, P., Breukink, E., and Brasseur, R. (1999). Computational study of nisin interaction with model membrane. *Biochim. Biophys. Acta Biomembr.* 1420, 111–120. doi: 10.1016/S0005-2736(99)00090-5

Liu, X., Li, Y., Li, Z., Lan, X., Leung, P. H. M., Li, J., et al. (2015). Mechanism of anticancer effects of antimicrobial peptides. *J. Fiber Bioeng. Inform.* 8, 25–36. doi: 10.3993/jfbi03201503

Lohner, K. (2009). New strategies for novel antibiotics: peptides targeting bacterial cell. *Gen. Physiol. Biophys.* 28, 105–116. doi: 10.4149/gpb_2009_02_105

Maher, S., and McClean, S. (2006). Investigation of the cytotoxicity of eukaryotic and prokaryotic antimicrobial peptides in intestinal epithelial cells in vitro. *Biochem. Pharmacol.* 71, 1289–1298. doi: 10.1016/j.bcp.2006.01.012

Mantovani, H. C., Hu, H., Worobo, R. W., and Russell, J. B. (2002). Bovicin HC5, a bacteriocin from *Streptococcus bovis* HC5. *Microbiology* 148, 3347–3352. doi: 10.1099/00221287-148-11-3347

Martarelli, D., Pompei, P., and Mazzoni, G. (2009). Inhibition of adrenocortical carcinoma by diphtheria toxin mutant CRM197. *Chemotherapy* 55, 425–432. doi: 10.1159/000264689

McCaughey, L. C., Ritchie, N. D., Douce, G. R., Evans, T. J., and Walker, D. (2016). Efficacy of species-specific protein antibiotics in a murine model of acute *Pseudomonas aeruginosa* lung infection. *Sci. Rep.* 6:30201. doi: 10.1038/srep30201

Mehta, R. R., Yamada, T., Taylor, B. N., Christov, K., King, M. L., Majumdar, D., et al. (2011). A cell penetrating peptide derived from azurin inhibits angiogenesis and tumor growth by inhibiting phosphorylation of VEGFR-2, FAK and Akt. *Angiogenesis* 14, 355–369. doi: 10.1007/s10456-011-9220-6

Michel-Briand, Y., and Baysse, C. (2002). The pyocins of *Pseudomonas aeruginosa*. *Biochimie* 84, 499–510. doi: 10.1093/oxfordjournals.jbchem.a129929

Moll, G. N., Clark, J., Chan, W. C., Bycroft, B. W., Roberts, G. C., Konings, W. N., et al. (1997). Role of transmembrane pH gradient and membrane binding in nisin pore formation. *J. Bacteriol.* 179, 135–140. doi: 10.1128/jb.179.1.135-140.1997

Morin, N., Lanneluc, I., Connil, N., Cottenceau, M., Pons, A. M., and Sablé, S. (2011). Mechanism of bactericidal activity of microcin L in *Escherichia coli* and *Salmonella enterica*. *Antimicrob. Agents Chemother.* 55, 997–1007. doi: 10.1128/AAC.01217-10

Nakamura, S., and Racker, E. (1984). Inhibitory effect of duramycin on partial reactions catalyzed by sodium-potassium adenosinetriphosphatase from dog kidney. *Biochemistry* 23, 385–389. doi: 10.1021/bi00297a031

Nes, I. F., and Holo, H. (2000). Class II antimicrobial peptides from lactic acid bacteria. *Pept. Sci.* 55, 50–61. doi: 10.1002/1097-0282(2000)55:1<50::aid-bip50>3.0.co;2-3

Nguyen, L. T., Haney, E. F., and Vogel, H. J. (2011). The expanding scope of antimicrobial peptide structures and their modes of action. *Trends Biotechnol.* 29, 464–472. doi: 10.1016/j.tibtech.2011.05.001

Nissen-Meyer, J., Larsen, A. G., Sletten, K., Daeschel, M., and Nes, I. F. (1993). Purification and characterization of plantaricin A, a *Lactobacillus plantarum* bacteriocin whose activity depends on the action of two peptides. *J. Gen. Microbiol.* 139, 1973–1978. doi: 10.1099/00221287-139-9-1973

O'Brien-Simpson, N. M., Hoffmann, R., Chia, C. S. B., and Wade, J. D. (2018). Editorial: antimicrobial and anticancer peptides. *Front. Chem.* 6:13. doi: 10.3389/fchem.2018.00013

Oliynyk, I., Varelogianni, G., Roomans, G. M., and Johannesson, M. (2010). Effect of duramycin on chloride transport and intracellular calcium concentration in cystic fibrosis and non-cystic fibrosis epithelia. *APMIS* 118, 982–990. doi: 10.1111/j.1600-0463.2010.02680.x

Paiva, A. D., de Oliveira, M. D., de Paula, S. O., Baracat-Pereira, M. C., Breukink, E., and Mantovani, H. C. (2012). Toxicity of bovicin HC5 against mammalian cell lines and the role of cholesterol in bacteriocin activity. *Microbiology* 158, 2851–2858. doi: 10.1099/mic.0.062190-0

Papagianni, M., and Anastasiadou, S. (2009). Pediocins: the bacteriocins of *Pediococci*. Sources, production, properties and applications. *Microb. Cell Fact.* 8:3. doi: 10.1186/1475-2859-8-3

Phoenix, D. A., Harris, F., Mura, M., and Dennison, S. R. (2015). The increasing role of phosphatidylethanolamine as a lipid receptor in the action of host defence peptides. *Prog. Lipid Res.* 59, 26–37. doi: 10.1016/j.plipres.2015.02.003

Porto, M. C. W., Kuniyoshi, T. M., Azevedo, P. O. S., Vitolo, M., and Oliveira, R. P. D. S. (2017). *Pediococcus* spp.: an important genus of lactic acid bacteria and pediocin producers. *Biotechnol. Adv.* 35, 361–374. doi: 10.1016/j.biotechadv.2017.03.004

Preet, S., Bharati, S., Panjeta, A., Tewari, R., and Rishi, P. (2015). Effect of nisin and doxorubicin on DMBA-induced skin carcinogenesis—a possible adjunct therapy. *Tumor Biol.* 36, 8301–8308. doi: 10.1007/s13277-015-3571-3

Racker, E., Riegler, C., and Abdel-Ghany, M. (1984). Stimulation of glycolysis by placental polypeptides and inhibition by duramycin. *Cancer Res.* 44, 1364–1367.

Rebuffat, S. (2013). "Microcins," in *Handbook of Biologically Active Peptides*, ed. A. Kastin (Cambridge, MA: Academic Press), 129–137. doi: 10.1016/b978-0-12-385095-9.00020-8

Rolston, K. V. I. (2017). Infections in cancer patients with solid tumors: a review. *Infect. Dis. Ther.* 6, 69–83. doi: 10.1007/s40121-017-0146-1

Saito, H., Watanabe, T., and Tomioka, H. (1979). Purification, properties, and cytotoxic effect of a bacteriocin from *Mycobacterium smegmatis*. *Antimicrob. Agents Chemother.* 15, 504–509. doi: 10.1128/aac.15.4.504

Sand, S. L., Nissen-Meyer, J., Sand, O., and Haug, T. M. (2013). Plantaricin A, a cationic peptide produced by *Lactobacillus plantarum*, permeabilizes eukaryotic cell membranes by a mechanism dependent on negative surface charge linked to glycosylated membrane proteins. *Biochim. Biophys. Acta Biomembr.* 1828, 249–259. doi: 10.1016/j.bbamem.2012.11.001

Sand, S. L., Oppegård, C., Ohara, S., Iijima, T., Naderi, S., Blomhoff, H. K., et al. (2010). Plantaricin A, a peptide pheromone produced by *Lactobacillus plantarum*, permeabilizes the cell membrane of both normal and cancerous lymphocytes and neuronal cells. *Peptides* 31, 1237–1244. doi: 10.1016/j.peptides.2010.04.010

Scholl, D., and Martin, D. W. (2008). Antibacterial efficacy of R-type pyocins towards *Pseudomonas aeruginosa* in a murine peritonitis model. *Antimicrob. Agents Chemother.* 52, 1647–1652. doi: 10.1128/AAC.01479-07

Selegård, R., Musa, A., Nyström, P., Aili, D., Bengtsson, T., and Khalaf, H. (2019). Plantaricins markedly enhance the effects of traditional antibiotics against *Staphylococcus epidermidis*. *Fut. Microbiol.* 14, 195–205. doi: 10.2217/fmb-2018-0285

Severina, E., Severin, A., and Tomasz, A. (1998). Antibacterial efficacy of nisin against multidrug-resistant Gram-positive pathogens. *J. Antimicrob. Chemother.* 41, 341–347. doi: 10.1093/jac/41.3.341

Sheth, T. R., Henderson, R. M., Hladky, S. B., and Cuthbert, A. W. (1992). Ion channel formation by duramycin. *Biochim. Biophys. Acta Biomemb.* 1107, 179–185. doi: 10.1016/0005-2736(92)90345-M

Shilova, O. N., Shilov, E. S., Lieber, A., and Deyev, S. M. (2018). Disassembling a cancer puzzle: cell junctions and plasma membrane as targets for anticancer therapy. *J. Control. Rel.* 286, 125–136. doi: 10.1016/j.jconrel.2018.07.030

Shin, J. M., Gwak, J. W., Kamarajan, P., Fenno, J. C., Rickard, A. H., and Kapila, Y. L. (2016). Biomedical applications of Nisin. *J. Appl. Microbiol.* 120, 1449–1465. doi: 10.1111/jam.13033

Shoombuatong, W., Schaduangrat, N., and Nantasenamat, C. (2018). Unraveling the bioactivity of anticancer peptides as deduced from machine learning. *EXCLI J.* 17, 734–752. doi: 10.17179/excli2018-1447

Smith, L., and Hillman, J. D. (2008). Therapeutic potential of type A (I) lantibiotics, a group of cationic peptide antibiotics. *Curr. Opin. Microbiol.* 11, 401–408. doi: 10.1016/j.mib.2008.09.008

Singh, P. K., Solanki, V., Sharma, S., Thakur, K. G., Krishnan, B., and Korpole, S. (2015). The intramolecular disulfide-stapled structure of laterosporulin, a class IId bacteriocin, conceals a human defensin-like structural module. *FEBS J.* 282, 203–214. doi: 10.1111/febs.13129

Spector, J., Zakharov, S., Lill, Y., Sharma, O., Cramer, W. A., and Ritchie, K. (2010). Mobility of BtuB and OmpF in the *Escherichia coli* outer membrane:

implications for dynamic formation of a translocon complex. *Biophys. J.* 99, 3880–3886. doi: 10.1016/j.bpj.2010.10.029

Sung, W. S., Park, Y., Choi, C.-H., Hahm, K.-S., and Lee, D. G. (2007). Mode of antibacterial action of a signal peptide, Pep27 from *Streptococcus pneumoniae*. *Biochem. Biophys. Res. Commun.* 363, 806–810. doi: 10.1016/j.bbrc.2007.09.041

Thundimadathil, J. (2012). Cancer treatment using peptides: current therapies and future prospects. *J. Amino Acids* 2012, 1–13. doi: 10.1155/2012/967347

Tong, Z., Dong, L., Zhou, L., Tao, R., and Ni, L. (2010). Nisin inhibits dental caries-associated microorganism *in vitro*. *Peptides* 31, 2003–2008. doi: 10.1016/j.peptides.2010.07.016

Tsai, T.-L., Li, A.-C., Chen, Y.-C., Liao, Y.-S., and Lin, T.-H. (2015). Antimicrobial peptide m2163 or m2386 identified from *Lactobacillus casei* ATCC 334 can trigger apoptosis in the human colorectal cancer cell line SW480. *Tumor Biol.* 36, 3775–3789. doi: 10.1007/s13277-014-3018-2

Uggerhøj, L. E., Poulsen, T. J., Munk, J. K., Fredborg, M., Sondergaard, T. E., Frimodt-Moller, N., et al. (2015). Rational design of alpha- helical antimicrobial peptides: do's and don'ts. *ChemBioChem* 16, 242–253. doi: 10.1002/cbic.201402581

Vasilchenko, A. S., and Valyshev, A. V. (2019). Pore-forming bacteriocins: structural–functional relationships. *Arch. Microbiol.* 201, 147–154. doi: 10.1007/s00203-018-1610-3

Vedham, V., Divi, R. L., Starks, V. L., and Verma, M. (2014). Multiple infections and cancer: implications in epidemiology. *Technol. Cancer Res. Treat.* 13, 177–194. doi: 10.7785/tcrt.2012.500366

Villarante, K. I., Elegado, F. B., Iwatani, S., Zendo, T., Sonomoto, K., and de Guzman, E. E. (2011). Purification, characterization and in vitro cytotoxicity of the bacteriocin from *Pediococcus acidilactici* K2a2-3 against human colon adenocarcinoma (HT29) and human cervical carcinoma (HeLa) cells. *World J. Microbiol. Biotechnol.* 27, 975–980. doi: 10.1007/s11274-010-0541-1

Wang, L., Dong, C., Li, X., Han, W., and Su, X. (2017). Anticancer potential of bioactive peptides from animal sources. *Oncol. Rep.* 38, 637–651. doi: 10.3892/or.2017.5778

World-Health-Organisation [WHO] (2018). *Cancer: World Cancer Report*. Geneva: World-Health-Organisation.

Yamada, T., Mehta, R. R., Lekmine, F., Christov, K., King, M. L., Majumdar, D., et al. (2009). A peptide fragment of azurin induces a p53-mediated cell cycle arrest in human breast cancer cells. *Mol. Cancer Ther.* 8, 2947–2958. doi: 10.1158/1535-7163.MCT-09-0444

Yang, S. C., Lin, C. H., Sung, C. T., and Fang, J. Y. (2014). Antibacterial activities of bacteriocins: application in foods and pharmaceuticals. *Front. Microbiol.* 5:241. doi: 10.3389/fmicb.2014.00241

Yu, H., Ding, X., Shang, L., Zeng, X., Liu, H., Li, N., et al. (2018). Protective ability of biogenic antimicrobial peptide microcin J25 against Enterotoxigenic *Escherichia Coli*-induced intestinal epithelial dysfunction and inflammatory responses IPEC-J2 cells. *Front. Cell. Infect. Microbiol.* 8:242. doi: 10.3389/fcimb.2018.00242

Zhao, H., Sood, R., Jutila, A., Bose, S., Fimland, G., Nissen-Meyer, J., et al. (2006). Interaction of the antimicrobial peptide pheromone Plantaricin A with model membranes: implications for a novel mechanism of action. *Biochim. Biophys. Acta Biomembr.* 1758, 1461–1474. doi: 10.1016/j.bbamem.2006.03.037

Zorina, T., and Styche, A. (2015). "Infectious diseases in cancer patients: an overview," in *Infection and Cancer: Bi-Directorial*, eds M. Shurin, Y. Thanavala, and N. Ismail (Cham: Springer), 295–311. doi: 10.1007/978-3-319-20669-1_14

Conflict of Interest Statement: The authors declare that the research was conducted in the absence of any commercial or financial relationships that could be construed as a potential conflict of interest.

frontiers in Microbiology

REVIEW
published: 18 October 2019
doi: 10.3389/fmicb.2019.02340

Targeted Diphtheria Toxin-Based Therapy: A Review Article

Fatemeh Shafiee[1], Marc G. Aucoin[2] and Ali Jahanian-Najafabadi[1]†*

[1] Department of Pharmaceutical Biotechnology, School of Pharmacy and Pharmaceutical Sciences, Isfahan University of Medical Sciences, Isfahan, Iran, [2] Department of Chemical Engineering, Faculty of Engineering, University of Waterloo, Waterloo, ON, Canada

Cancer remains one of the leading causes of death worldwide. Conventional therapeutic strategies usually offer limited specificity, resulting in severe side effects and toxicity to normal tissues. Targeted cancer therapy, on the other hand, can improve the therapeutic potential of anti-cancer agents and decrease unwanted side effects. Targeted applications of cytolethal bacterial toxins have been found to be especially useful for the specific eradication of cancer cells. Targeting is either mediated by peptides or by protein-targeting moieties, such as antibodies, antibody fragments, cell-penetrating peptides (CPPs), growth factors, or cytokines. Together with a toxin domain, these molecules are more commonly referred to as immunotoxins. Targeting can also be achieved through gene delivery and cell-specific expression of a toxin. Of the available cytolethal toxins, diphtheria toxin (DT) is one of the most frequently used for these strategies. Of the many DT-based therapeutic strategies investigated to date, two immunotoxins, Ontak™ and Tagraxofusp™, have gained FDA approval for clinical application. Despite some success with immunotoxins, suicide-gene therapy strategies, whereby controlled tumor-specific expression of DT is used for the eradication of malignant cells, are gaining prominence. The first part of this review focuses on DT-based immunotoxins, and it then discusses recent developments in tumor-specific expression of DT.

Keywords: diphtheria toxin, immunotoxin, cancer, transcriptional targeting, fusion protein, bacterial toxin

OPEN ACCESS

Edited by:
Tomasz M. Karpiński, Poznań University of Medical Sciences, Poland

Reviewed by:
Mark Sutherland, Charité Medical University of Berlin, Germany
Daniel A. Vallera, University of Minnesota Twin Cities, United States

***Correspondence:**
Ali Jahanian-Najafabadi
jahanian@pharm.mui.ac.ir

†Present address:
Ali Jahanian-Najafabadi, Department of Chemical Engineering, Faculty of Engineering, University of Waterloo, Waterloo, ON, Canada

Specialty section:
This article was submitted to Antimicrobials, Resistance and Chemotherapy, a section of the journal Frontiers in Microbiology

Received: *12 April 2019*
Accepted: *25 September 2019*
Published: *18 October 2019*

Citation:
Shafiee F, Aucoin MG and Jahanian-Najafabadi A (2019) Targeted Diphtheria Toxin-Based Therapy: A Review Article. Front. Microbiol. 10:2340. doi: 10.3389/fmicb.2019.02340

INTRODUCTION

Too many deaths around the world can be attributed to one form of cancer or another. According to GLOBCAN, it is expected that the yearly death toll due to cancer will reach 16 million by 2040 (Ferlay et al., 2018). Along with deaths, it is associated with an incredible amount of pain and suffering, largely due to the non-specific nature of most conventional treatments. Conventional chemo- and radio-therapy strategies focus on mass cell killing, not limited to cancer cells (Padma, 2015). This non-specific toxicity to normal proliferating cells has resulted in low therapeutic indices and narrow therapeutic windows for conventional anti-cancer drugs (Ducry and Stump, 2010) and

Abbreviations: ADPR, adensosine diphosphate ribosyl; AML, acute myeloid leukemia; BPDCN, blastic plasmacytoid dendritic cell neoplasm; CCP, cell-penetrating peptide; CR, complete remissions; CTCL, cutaneous T-cell lymphoma; DT, diphtheria toxin; EGF, epidermal growth factor; GM-CSF, Granulocyte macrophage-colony stimulating factor; HD, Hodgkin's disease; MTD, maximum tolerated dose; NAD, nicotinamine dinucleotide; NHL, non-Hodgkin's lymphoma; PR, partial remissions; PTCL, peripheral T-cell lymphoma.

has encouraged the development of target-specific agents that are more effective and specific to tumor cells, lowering the probability of their affecting healthy tissues (He and Shi, 2014). Rapid progress in cancer research, including the determination of cancer-specific cellular processes and surface antigens, have allowed the combination of rational drug design and consideration of cancer biology for the development of novel targeted therapeutic strategies (Reiter, 2001; Kreitman, 2006).

The use of cell-surface molecules as recognition targets to selectively find and eliminate cancer cells while sparing normal cells is one approach for targeted cancer therapy (Denkberg et al., 2003). In this regard, a fusion protein consisting of a targeting moiety and an effector cytolethal moiety is produced. The targeting molecule is typically an antibody or antibody fragment or a ligand of a specific cell surface receptor that is either absent on the surface of normal cells or is highly up-regulated on cancer cells. Such a molecule is called an immunotoxin, especially when the targeting moiety is a molecule belonging to the immune system such as an antibody, cytokine, or growth factor (Jahanian-Najafabadi et al., 2012b).

Another strategy for the targeted killing of cancer cells is by delivering a gene of a cytolethal agent to cells and limiting its expression to within cancer cells through transcriptional regulation. This strategy, which might be called expression-targeting, uses specific transcriptional control elements such as enhancers or tumor-specific promoters to drive transcription of a particular gene in targeted cells (Fang et al., 2010; Javan and Shahbazi, 2017). Tumor-specific promoters are derived from genes with ectopic up-regulated levels of mRNA, and consequently protein, in cancer cells (Saukkonen and Hemminki, 2004). When these promoters are used upstream of a gene encoding for a toxic agent, no significant expression is expected to occur in normal cells even after taking up the expression cassette (Chen C. et al., 2018).

This review aims to highlight the advances in diphtheria toxin (DT)-based anti-cancer strategies as well as the targeting systems that are used to reduce non-specific destruction of non-cancerous cells. Specifically, the present manuscript will focus on DT or its derivatives as part of immunotoxins or targeted fusion proteins. We then review recent applications of the DT coding sequence used in DNA cassettes to mediate DT expression under the control of tumor-specific promoters. **Tables 1**, **2** summarize DT-based immunotoxins and gene therapy studies, respectively. Although we try to be as comprehensive as possible, we have limited our review mostly to those therapeutics that have advanced at least to *in vivo* studies.

IMMUNOTOXINS

Immunotoxins are fusion proteins comprised of a toxic moiety and a targeting moiety, in which a known toxin molecule is usually truncated to remove its native binding domain, which is replaced by a targeting molecule that allows concentration of the fusion protein at the plasma membrane of specific cell types (Jahanian-Najafabadi et al., 2012b). The toxic moieties of immunotoxins have been derived from bacterial, fungal, plant, and even animal toxins (Cao et al., 2012; Weidle et al., 2014), while growth factors, monoclonal antibodies, cytokines (Aruna, 2006), and cancer-specific cell-penetrating peptides (CPPs) (Kersemans and Cornelissen, 2010; Soleimani et al., 2016, 2019) have been used as targeting moieties. Of the bacterial toxins, *Vibrio cholerae* toxin (Sarnovsky et al., 2010), Shiga toxin (Al-Jaufy et al., 1994; Jahanian-Najafabadi et al., 2012a), Pseudomonas exotoxin A (Yu et al., 2017; Dhillon, 2018), and DT (Vallera et al., 1999; Liu et al., 2000; Vaclavkova et al., 2006) have been used as either an immunotoxin or some other form of targeted toxin. Among these, DT is the most widely used due to its easy expression, high activity, and minimal side effects in humans (Brinkmann et al., 1995). Furthermore, there is detailed information on the three-dimensional structure of DT and its various fragments, which helps in the selection of appropriate peptide linkers to conjugate the toxin fragment to a targeting moiety as well as to maintain the activity of both parts (Choe et al., 1992; Louie et al., 1997).

DIPHTHERIA TOXIN

Diphtheria toxin is a single chain, 62 kDa protein consisting of 535 amino acid residues that is produced by *Corynebacterium diphtheria* containing lysogenic beta phage (Holmes, 2000). DT mediates its cytolethal effect through the inhibition of protein synthesis in susceptible cells (Bennett and Eisenberg, 1994). As it schematically represented in **Figure 1**, DT is a Y shaped molecule containing two functionally different regions: A and B. The A fragment (located at the N-terminus), includes a catalytic domain (C domain; 22 KDa, residues 1–193) that stops protein synthesis within eukaryotic cells. The B fragment (located at the C-terminus), on the other hand, consists of two domains, a transmembrane domain (T domain, 22 KDa, residues 201–384), and a receptor-binding domain (R domain, 18 KDa, residues 385–455).

The T domain helps in the translocation of the C domain from the endosome to the cytosol, while the R domain helps to bind the heparin-binding epidermal growth factor receptor (HBEGFR) on the surfaces of susceptible cells (Bennett and Eisenberg, 1994). In the cytoplasm of susceptible cells, the catalytic domain first binds to nicotinamide dinucleotide (NAD) and then transfers an adenosine diphosphate ribosyl (ADPR) moiety to elongation factor 2, which subsequently inhibits protein synthesis (Collier, 2001). The interaction of DT with its cell surface receptor and its mechanism of action are summarized in **Figures 2**, **3**, respectively.

DIPHTHERIA TOXIN-BASED IMMUNOTOXINS

Truncated forms of DT have been successfully used to generate recombinant immunotoxins against cancer (Shapira and Benhar, 2010). Genetic substitution of the native DT R domain with cytokines, growth factors, cancer-specific CPPs, and generally any ligands specific for cancer cell antigens have resulted in the

TABLE 1 | List of immunotoxins containing different truncated forms of DT attached to various targeting moieties for cancer therapy.

Immunotoxin	Toxin/Toxin fragment	Targeting moiety	Target disease	Extent of studies	References
DAB486IL-2	DT486	IL-2	NHL, HD, CTCL/Rheumatoid arthritis	Clinical trial	LeMaistre et al., 1993; Moreland et al., 1995
DAB389IL-2 (Denileukin Diftitox™)	DT389	IL-2	NHL, HD, CTCL,	Clinical trial, FDA approved	Duvic et al., 2002
DT388-GM-CSF	DT388	GM-CSF	AML	Clinical trial	Frankel et al., 2002b
DT388-IL3	DT389	IL-3	AML, BPDCN	Clinical trial, FDA approved	Syed, 2019
DT389-EGF	DT389	EGF	Bladder cancer, lung cancer, glioblastoma	Clinical trial	Theodoulou et al., 1995
A-dmDT390-bisFV	Mutant DT390	A bispecific antibody against CD3	CTCL, PTCL, GVHD	Clinical trial	Frankel et al., 2015
DT2219	DT390	Bispecific scFv toward CD19 and CD22	B cell leukemia or lymphoma	Clinical trial	Bachanova et al., 2015
Tf-CRM107 (TransMID)	A mutated form of intact DT	Transferrin	Breast cancer, glioblastoma, medulloblastoma	Clinical trial	Yoon et al., 2010
DTAT/DTAT13/ DTATEGF	DT390	AT fragment of uPA/AT-IL13/AT-EGF	Glioblastoma	Xenograft nude mice	Ramage et al., 2003; Hall and Vallera, 2006; Huang et al., 2012
DTEGF13	DT390	EGF and IL13	Glioblastoma, prostate, and pancreatic cancer	Xenograft nude mice	Oh et al., 2010
DT-antiCCR4	DT390	scFv against CCR4	T-cell malignancies	Xenograft nude mice, cynomolgus monkeys	Wang et al., 2016
DT386-BR2	DT386	BR2 (a cancer-specific CPP)	Breast cancer, leukemia, cervical cancer	*In vivo* safety assessment in albino mice	Shafiee et al., 2016
DT390-biTMTP1/ DT390-triTMTP1	DT390	Double/Triple repeats of TMTP1synthetic pentapeptide (NVVRQ)	Highly metastatic cancer cells	Xenograft nude mice	Ma et al., 2013
DT-CD19	DT390	scFV against CD19	$CD19^{+}$ lymphoma	Xenografted immunodeficient NSG mice	Zheng et al., 2017
DTIL13	DT389	IL-13	Gleioblastoma	Xenograft nude mice	Rustamzadeh et al., 2006
DT-SCF	DT387	stem cell factor	Ovarian, pancreatic, stomach, and liver cancers	*In vitro*	Potala and Verma, 2010
DT389-GRP	DT389	gastrin-releasing peptide	Brest cancer, prostate cancer, colon cancer	*In vitro*	Vanderspek et al., 1997
DAB389-IL7	DT389	IL-7	Hematopoietic malignancies	*In vitro*	Sweeney et al., 1998
DL_9F and DL_2F	DT389	Basic fibroblast growth factor	Ovarian teratocarcinoma	*In vitro*	Beitz et al., 1992; Zhang et al., 2006
DT389GCSF	DT389	Granulocyte-colony stimulating factor	G-CSF receptor-overexpressing cancer cells	Not evaluated	Babavalian et al., 2019

formation of fusion proteins that retained the functions and activities of their constituent parts (Beilhartz et al., 2017). **Table 3** represents most of the cell surface receptors or antigens targeted for construction of DT-based immunotoxins to date. *In vitro,* these immunotoxins have shown very small IC_{50}s on the order of 10^{-9}–10^{-14} M, which validates their possible use as a targeted therapy. For cells that are not targeted or that do not contain a targeted receptor, DT-based immunotoxins tend to have an IC_{50} on the order of 10^{-7} M.

DAB486IL-2 and DAB389IL-2

Interleukin-2 (IL-2) is a cytokine that is primarily produced by CD4+ T-cells following their activation by antigens. Three different IL-2 receptor chains exist that together generate low-, intermediate-, and high-affinity IL-2 receptors. The ligand-specific IL-2 receptor α chain (IL-2Rα, Tac antigen) binds IL-2 with low affinity, the combination of IL-2Rβ and IL-2Rγc together forms an IL-2Rβ/γc complex that binds IL-2 with intermediate affinity, and when all three receptor chains are co-expressed, IL-2 is bound with high affinity (Kim et al., 2006). Some T-cell malignancies overexpress the IL2R, making it an ideal target for immunotoxins (Urba et al., 1990; Zachariae et al., 1991).

DAB486IL-2, a 68 kDa-recombinant protein, showed selective binding affinity to cells expressing high-affinity IL-2R (Williams et al., 1987, 1990). C91/PL, C8215, and CTLL2, which are IL-2R-positive cells, have been shown to be highly sensitive to this recombinant protein, with IC_{50}s ranging 0.1–50 $\times$ 10^{-10} M,

TABLE 2 | Gene cassettes used to drive DTA expression within cancer cells.

Expression cassette	Promoter	Target malignancy	Extent of studies	References
pDTA-PBH19	814 bp flanking the 5′-region of the H19 gene	Bladder, choriocarcinoma, colorectal, and ovarian cancers	Clinical Trial	Lavie et al., 2017
pP3-DTA and pP4-DTA/ pP4-DTA-P3-DTA	Insulin-like growth factor 2, promoters 3 and 4	Human bladder and hepatocellular carcinoma	Xenograft murine model	Ayesh et al., 2003; Amit et al., 2011
pAF-DTA	Alpha-fetoprotein promoter	Hepatocellular carcinomas and teratomas	Xenograft murine model	Kunitomi et al., 2000
pRAD51-DTA, pRAD51C-DTA, pXRCC2-DTA	Rad51, Rad51C, and XRCC2 regulatory elements	Various malignancies including breast and cervical cancers	Xenograft murine model	Hine et al., 2012; Cao et al., 2014; Chen Y. et al., 2018
pPSAR-PCPSA-DTA	Prostate-specific antigen promoter	Prostate cancer	Xenograft murine model, TRAMP mice	Zheng et al., 2003
Surp1430-DTA	Survivin promoter	Ovarian, gastric, non-small- and small-cell lung, and breast cancer	Xenograft murine model	Lin et al., 2015
V3-DTA	Heat shock promoter and upstream control element	Pancreatic cancer	Xenograft murine model	Fogar et al., 2010
phTERT-DTA	Human telomerase reverse transcriptase	Hepatocellular carcinoma, bladder carcinoma, and osteosarcoma	*In vitro*	Abdul-Ghani et al., 2000
CPT4-DTA	A synthetic β-catenin-dependent promoter	Hepatocellular carcinoma	*In vitro*	Lipinski et al., 2004
pTHA-47 or pTHA-49	Human chorionic gonadotropin α and β promoters	Breast and ovarian cancer	*In vitro*	Lidor et al., 1997
pTHA71	Immunoglobulin (Ig) kappa light chain gene regulatory sequences	B-cell malignancies	*In vitro*	Maxwell et al., 1992

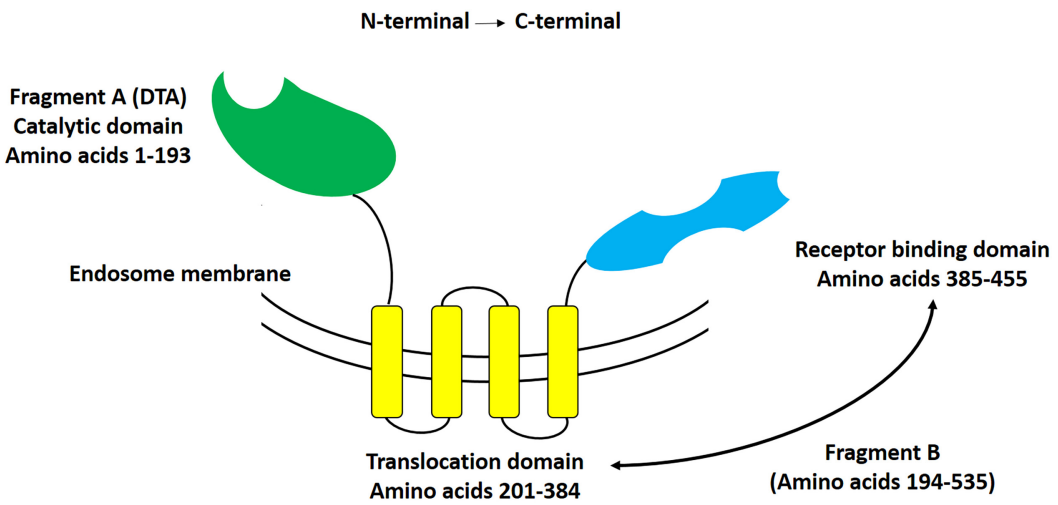

FIGURE 1 | Schematic representation of diphtheria toxin. This Y-shaped molecule consists of two different fragments, that at the N-terminal side being named fragment A, and that at the C-terminal side being named fragment B. Fragment A includes the catalytic domain of DT, whereas fragment B includes both the translocation (T), and receptor-binding (R) domains of DT.

whereas IL-2 negative cell lines had IC_{50}s greater than 10^{-7} M (Bacha et al., 1988; Waters et al., 1990, 1991).

DAB486IL-2 advanced to a phase I clinical trial for treatment of chemotherapy-resistant hematological malignancies. From 18 evaluable patients in the study, the maximum tolerated dose (MTD) was determined to be 100 μg/kg/day given as an intravenous (IV) bolus over 10 days. The main adverse effect was reversible elevations in hepatic transaminases. Other mild reversible side-effects included rash, nausea, elevated creatinine, chest tightness, and fever (LeMaistre et al., 1992). Furthermore, the MTD when infused for 90-min daily for five consecutive days was slightly higher, at 300 μg/kg/day, and higher doses resulted in renal insufficiency associated with hemolysis and thrombocytopenia (LeMaistre et al., 1993).

DAB486IL-2 has also advanced to clinical trials for treatment of rheumatoid arthritis (RA). In an open-label, phase I/II

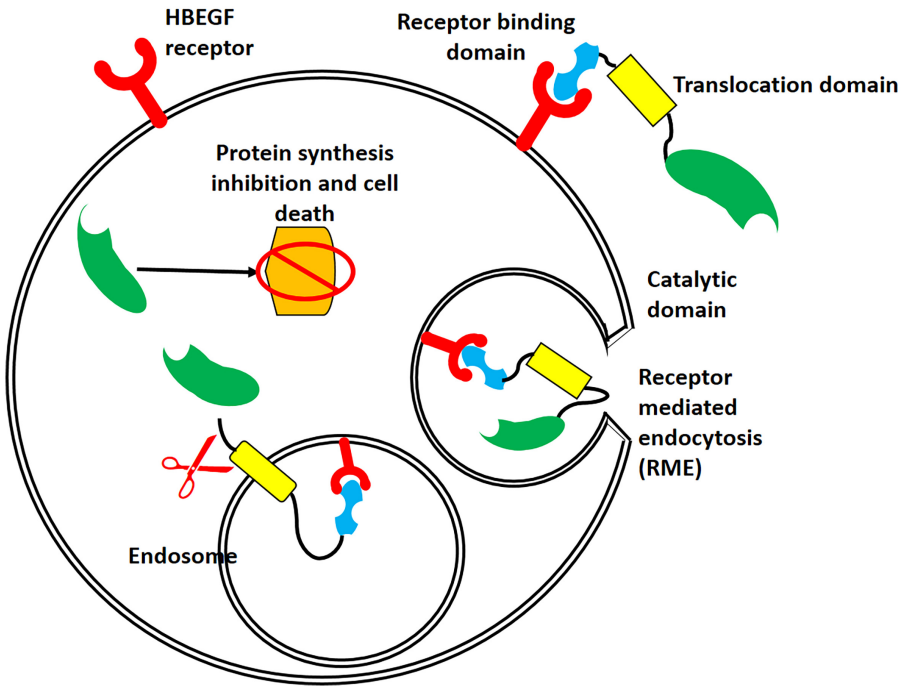

FIGURE 2 | Interaction of DT with its receptor, followed by its internalization. After binding of DT to the heparin-binding epidermal growth factor receptor (HBEGFR, red), receptor-mediated endocytosis relocates DT to the cytosol. The acidic pH of the endosome causes conformational changes in the T domain (yellow) and membrane, resulting in a large channel that allows translocation of the C domain (green) and its release into the cytoplasm.

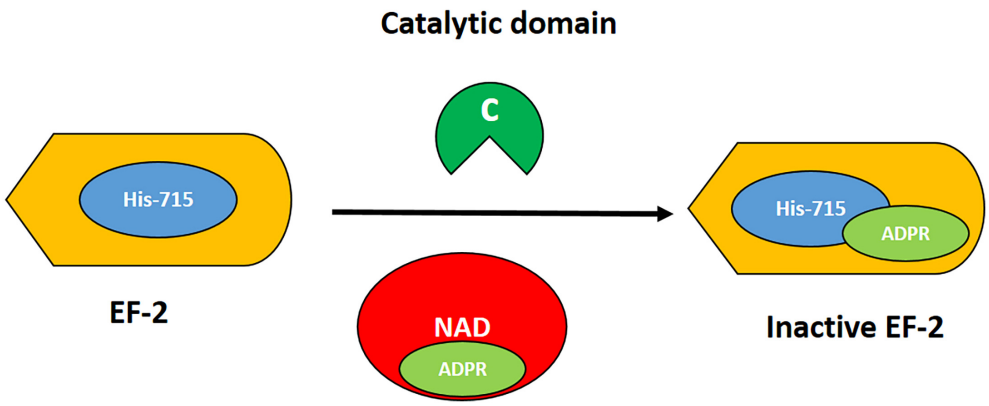

FIGURE 3 | Mechanism of action of DT. The catalytic domain (green) acts by transferring the ADPR moiety (light green) from NAD (red) to the post-transcriptionally modified histidine residue at 715 (diphthamide; blue) of elongation factor 2 (EF2, orange). Thus, the EF2 is irreversibly inactivated, resulting in inhibition of protein synthesis and cell death.

clinical trial on patients with RA refractory to methotrexate, nine patients showed a substantial or meaningful response. The MTD for patients receiving DT486IL-2 for 5 to 7 consecutive days was 0.1 mg/kg/day (Sewell et al., 1993), similar to the studies for the treatment of chemotherapy-resistant hematological malignancies. The anti-arthritic effect of this fusion protein was further evaluated in a subsequent pilot phase II, double-blind, placebo-controlled trial on 45 RA patients, and 18% of patients showed significant clinical improvement (Moreland et al., 1995).

To improve the short half-life of DT486IL-2, which is on the order of 5 min (Bacha et al., 1990), and to reduce the immunogenicity of the molecule, shorter DT fragments were investigated by removing the remaining hydrophobic sequences of its binding domain (Chaudhary et al., 1991; Kuzel et al., 1993). DAB389IL-2, which is a 58 kDa variant containing 97 fewer amino acids than its parent molecule, DAB486IL-2, showed a fivefold improvement in affinity for the IL-2R and an approximately 10-fold increase in cytotoxicity toward IL-2R-positive cancer cells (Bacha et al., 1991; Kiyokawa et al., 1991).

TABLE 3 | Cell surface receptors used as targets for DT-based immunotoxins and their presence in malignancies and normal tissue.

Targeted receptor or antigen	Targeted malignancies	Normal tissue	References
IL2 receptor	Some T-cell malignancies	T cells	Zachariae et al., 1991
GM-CSF receptor	Lymphoma	Multipotent myeloid progenitor cells, monocytes, DCs, macrophages, and neutrophils	Rozemuller et al., 1997; Westcott et al., 2004; Rosas et al., 2007
EGF receptor	Different malignancies including breast, lung, bladder, head-and-neck, and pancreatic cancers	Low expression in various normal tissues	Simon and Fitzgerald, 2016
IL3 receptor	Lymphoma	Multipotent and committed myeloid and lymphoid progenitors	Suda et al., 1985; Park et al., 1989
CD3	Malignant T-cells	T-cells	Frank et al., 1991
CD19	B cell leukemia or lymphoma	Late pre-B cells and B cells	Uckun et al., 1988
CD22	B cell leukemia or lymphoma	Pro-B cells and mature B cells	Sato et al., 1996
Transferin receptors (TfRs)	Various tumors	Low-level expression at most human tissues	Hagihara et al., 2000
uPA receptor	Many cancers including fibrosarcoma, melanoma, breast, prostate and colon carcinoma, leukemia	Many cell types including monocytes, granulocytes, endothelial cells, fibroblasts, keratocytes, and hepatocytes	Lanza et al., 1998
IL13 receptor	Renal cell carcinoma, malignant glioma, ovarian carcinoma, and squamous cell carcinoma of head and neck	Normal immune cells and tissues express very low levels	Joshi and Puri, 2009
CCR4	T-cell leukemia-lymphoma, adult peripheral T-cell lymphoma, T-cell acute lymphoblastic leukemia, and cutaneous T cell lymphoma	Effector Treg cells, and rare expression by CD8+ T cells, NK cells, CD14+ monocytes/macrophages, dendritic cells, and B cells	Sugiyama et al., 2013

Cell lines of hematopoietic malignancies expressing the high-affinity IL-2R displayed IC_{50}s of 10^{-12} to 10^{-11} M. Cells exhibiting an intermediate-affinity receptor had IC_{50}s on the order of 10^{-10} to 10^{-9} M, and cells with low-affinity IL-2R had IC_{50} values greater than 10^{-7} M (Bacha et al., 1991; Re et al., 1996). DAB389IL-2 has also shown an improved half-life of 72 min (LeMaistre et al., 1998).

In addition to IL-2R-positive malignancies, the effectiveness of DAB389IL-2 was also shown *in vitro* for the suppression of immunopathology in schistosomiasis (Ramadan et al., 1995) and HIV infection (Zhang et al., 1997) and also in clinical trials against psoriasis. For the latter, a phase I clinical study showed moderate to large improvement in 8 out of 10 psoriatic patients that received systemic injections of DAB389IL-2 (Gottlieb et al., 1995). However, despite promising antipsoriatic activity, a further phase II clinical study revealed high toxicity at the required doses and schedules for routine treatment of psoriasis (Bagel et al., 1998).

It is, however, with the IL-2R-positive malignancies that DAB389IL-2 has had the most encouraging results. Phase I/II clinical trials on relapsed cutaneous T-cell lymphoma (CTCL), non-Hodgkin's lymphoma (NHL), and Hodgkin's disease (HD) patients with confirmed expression of either p55 or p75 IL-2R subunits verified the activity and safety of DAB389IL-2. The MTD for patients that received up to eight courses of short IV infusions for 5 consecutive days, repeated every 2 days, was 27 μg/kg/day. At 31 μg/kg/day, patients became asthenic, which was considered the dose-limiting toxicity. Of the 73 patients included in the study (35 with CTCL, 17 with NHL, and 21 with HD), five complete and eight partial remissions (CR and PR, respectively) were obtained in CTCL patients; and one CR and two PRs were observed in NHL patients. No responses were observed in patients with HD (LeMaistre et al., 1998; Saleh et al., 1998). Further clinical studies of DAB389-IL2, including a phase III clinical study on 71 patients with biopsy-proven CTCL expressing the IL-2R (Olsen et al., 2001; Duvic et al., 2002) led to its approval by the FDA for the treatment of persistent or recurrent CTCL under the name denileukin diftitox (ONTAK^{TM}) in 2008.

Unfortunately, ONTAK^{TM} was discontinued in 2014 due to issues related to the production of the immunotoxin in Escherichia *coli* (Wang et al., 2017). DAB389IL-2 was revived as a better-formulated drug now referred to as E7777. E7777, which has improved purity and an increased percentage of active protein, is 1.5–2 times more bioactive than ONTAK^{TM} (Duvic et al., 2014), and a phase I clinical trial on Japanese patients with relapsed or refractory peripheral and cutaneous T-cell lymphoma revealed an MTD of 9 μg/kg/day (Maruyama et al., 2015; Ohmachi et al., 2018). Phase II and phase III clinical trials of E7777 are currently ongoing (ClinicalTrials.gov identifiers: NCT02676778 and NCT01871727, respectively).

Other attempts to improve the production or enhance the potency of DAB389IL-2 have also been reported. In a recent study, production and evaluation of a bivalent ONTAK^{TM}-like (DAB389-IL2IL2) protein in a DT resistant *Pichia pastoris* with 100-fold higher *in vitro* potency and comparable *in vivo* efficiency has been reported. However, this immunotoxin has not been evaluated clinically yet (Peraino et al., 2014; Wang et al., 2017). Another group also reported the expression and purification of a secreted biologically active Val6Ala mutant form of the DAB389IL2 [s-DAB-IL2(V6A)] in *C. diphtheria*. The mutation reduced vascular leaks, a usual side effect of DAB389IL2, and increased the MTD. The LD50 of the mutated molecule was 3.7-fold higher than DAB389IL-2 in mice. Expression in *C. diphtheria* also reduced the aggregation problems observed for ONTAK^{TM}

(Cheung et al., 2019). There is, therefore, still significant potential for an IL-2-targeting DT immunotoxin as a therapeutic approach.

DT388GMCSF

Granulocyte-macrophage colony-stimulating factor (GM-CSF) is a monomeric glycoprotein cytokine involved in the maturation and proliferation of white blood cells. Its receptor, GMCSFR, is overexpressed in leukemic cells, which could be targeted with GM-CSF (Rozemuller et al., 1997).

DT388GMCSF contains the C and T domains of DT fused to human GM-CSF. The IC_{50} of this immunotoxin against cell lines overexpressing GMCSFR such as HL60, U937, and TF1 was on the order of 10^{-12} M (Frankel et al., 1997). It has also been cytotoxic to chemotherapy-resistant cell lines, and on therapy-refractory progenitor cells separated from acute myeloid leukemia (AML) patients without being toxic to normal human myeloid progenitor cells (Hogge et al., 1998). In a preclinical *in vivo* study involving a xenograft model of human AML, anti-leukemic effects were shown through the treatment of abdominal masses formed from HL60 cells. The treatment consisted of 84 μg/kg/day of DT388GMCSF intraperitoneally injected on days 2 through 6, which showed to be the MTD in mice (Hall et al., 1999). In cynomolgus monkeys, however, an 11-fold lower MTD (7.5 μg/kg/day) was observed compared to mice. It was suggested that cross-reactivity of receptors in monkeys led to distinct dose-limiting toxicities (Hotchkiss et al., 1999).

Finally, in a phase I clinical trial involving AML patients, 15 min IV infusions for 5 consecutive days showed significant remission in patients. The MTD was determined to be 4 μg/kg/day. At doses around 4.5–5 μg/kg/day, liver injury was reported. Among nine patients treated at those doses, one patient developed liver failure, and one patient had transient hepatic encephalopathy. Although DT388GMCSF did not show any *in vivo* damaging effect on hepatic cell lines, the correlation of increased DT388GMCSF serum concentrations and increased serum aspartate aminotransferase levels, along with DT388GMCSF-induced cytokine release by macrophages, halted further clinical applications (Frankel et al., 2002b). A follow-up to determine the mechanism of the observed hepatotoxicity with a murine version of the fusion protein, DT390mGMCSF, showed that the observed hepatotoxicity was not a result of non-specific uptake but rather of the uptake of the fusion protein by GMCSF-receptor-positive hepatic macrophages (Kupffer cells), which causes their depletion (Westcott et al., 2004). This observation limited further studies on the production and application of GMCSFR-based immunotoxins.

DT388-IL3

Interleukin 3 (IL-3) is a growth factor that induces the proliferation and terminal differentiation of multipotent and committed myeloid and lymphoid progenitors without affecting hematopoietic stem cells (Suda et al., 1985). The IL-3 receptor (IL3R) consists of an α and a β subunit. While the α subunit is unique to the IL3R and is the site of ligand attachment and represents the specificity of the receptor, the β is a subunit shared with the GM-CSF and functions in signal transduction and internalization of the ligand–receptor complexes (Park et al., 1989).

Similar to DT388GMCSF, DT388-IL3 was developed to treat AML. A preliminary *in vitro* and *in vivo* (C57BL/6 mice) study using DT390mIL-3 (DT390 fused to mouse interleukin 3) confirmed the potential for application of IL-3 to target AML (Chan et al., 1996). DT388-IL3 was subsequently developed and showed cytolethal activity on different IL-3R-overexpressing human leukemia cell lines, with IC_{50} values ranging from 1 to 28 $\times$ 10^{-12} M. Receptor-negative cell lines were not impaired at concentrations exceeding 1.4 $\times$ 10^{-9} M (Frankel et al., 2000). Unlike DT388GMCSF, which showed a modest but significant toxicity against normal progenitor cell types (Feuring-Buske et al., 2000), a study on non-obese diabetic/severe combined immunodeficient (NOD/SCID) mice inoculated with human IL-3-receptor-positive AML blasts receiving DT388IL3 at daily doses of 0.045 μg/g for 5 consecutive days revealed no significant toxicity against equivalent normal cells, while it resulted in an up to 83% size reduction in AML engraftments. In addition, no evidence of leukemia was detected in two of the samples after 12 weeks (Feuring-Buske et al., 2002). Further toxicology and pharmacokinetic studies in cynomolgus monkeys revealed an MTD of 100 μg/kg/day when injected every other day over 12 days. At 150 μg/kg/day, subjects showed elevated liver enzyme concentrations, severe malaise and anorexia (Cohen et al., 2004, 2005).

A phase I clinical trial on 45 patients (40 AML and 5 myelodysplasia patients) established an MTD but had only moderate success. Patients were scheduled to receive one of five dose levels between 4 and 12.5 μg/kg/day as 15 min IV infusions every other day over 12 days. Due to the prolonged infusion schedule, many patients failed to receive the 6 doses. Still, the MTD was determined to be $>$ 12.5 μg/kg/day. Of the AML patients, one showed CR for 8 months and one showed PR for 3 months. Of the myelodysplasia patients, one showed PR for 4 months (Frankel et al., 2008).

A subsequent phase I/II clinical trial on 11 patients with blastic plasmacytoid dendritic cell neoplasm (BPDCN), however, established a role for DT388-IL3 in the management of BPDCN and other hematologic malignancies. BPDCN patients received 12.5 μg/kg/day DT388-IL3 (aka SL-401) IV over 15 min for up to 5 days. Three patients with an initial response to SL-401 received a second course in relapse. Seven of nine evaluable BPDCN patients had major responses, including five CR and two PR after a single course of SL-401 (Frankel et al., 2014). Further clinical and non-clinical evaluations of this immunotoxin (Pemmaraju et al., 2017; Sun et al., 2018) led to its approval by the FDA in 2018 for the treatment of adult and pediatric BPDCN under the name of Tagraxofusp^{TM} (Syed, 2019).

DAB389EGF and DAB486EGF

Another growth factor whose receptor is overexpressed in cancer cells is the EGF. It has been reported that the EGF receptor (EGFR) has a more than 320-fold overexpression in some human cancer cell lines (Pfeiffer et al., 1990). Preliminary *in vitro* studies on A431 (vulval carcinoma), KB (oral carcinoma), and A549 (lung adenocarcinoma) cell lines revealed a 10- to

100-fold higher potency for DAB389EGF over DAB486EGF, consistent with the findings for the DT-IL2 immunotoxins. IC_{50} values for DAB389EGF and DAB486EGF on A431 cells were 2×10^{-12} M and 1×10^{-10} M, respectively (Shaw et al., 1991). In addition, IC_{50} values ranging from 4×10^{-13} to 5×10^{-12} M were determined on 13 different human glioma cell lines overexpressing EGFR (Liu et al., 2003).

Preclinical animal studies on DAB389EGF in rats revealed an MTD of 30 μg/kg/day upon receiving daily bolus IV infusions for 10–14 days. Renal and hepatic injury was observed at higher doses (Cohen et al., 2003). Further preclinical animal studies on cynomolgus monkeys revealed a lower MTD of 20 μg/kg/day for 10 days, which is similar to that for the DT388GMSCF immunotoxin, potentially due to the cross-reactivity of receptors in monkeys. Again, hepatic and renal injuries were the dose-limiting toxicities in the studied monkeys. Afterward, the *in vivo* efficacy of the immunotoxin was evaluated in nude mice inoculated with human EGFR-positive A549 lung adenocarcinoma cells. Treatment of the xenografts with 25 μg/kg/day for 10 days resulted in 50% tumor growth inhibition and also complete tumor regression in 20% of the mice (Theodoulou et al., 1995). By considering the promising effect of DAB389EGF in the xenograft animal model, phase I/II clinical trials were carried out with bolus IV infusions of DAB389EGF over 1–3 weeks in 72 patients with EGFR-positive metastatic carcinomas. However, the results of the clinical trials showed only a 6-month partial remission in one patient with non-small cell lung carcinoma. The MTD was 6 μg/kg/day, with renal and liver injuries and chest pain as the most significant dose-limiting toxicities. Therefore, clinical study on this immunotoxin was discontinued (Theodoulou et al., 1995).

Recently, targeting the EGFR receptor with the conventional DAB389EGF immunotoxin or different DT fusion constructs has gained new research attention. In one study, Yang et al. (2013) evaluated the cytotoxicity of DAB389EGF on various bladder carcinoma cell lines. Their results revealed that the immunotoxin had a potent cytolethal effect on all cell lines including J82, RT4, CRL1749 (CRL), T24, TCCSUP (SUP), and HTB9, with IC_{50} values ranging from 3×10^{-11} to 1×10^{-10} M, while the IC_{50} was higher than 1×10^{-9} M for the EGFR-negative H520 control cell line. Next, they induced xenograft bladder tumors in C57BL/6 female nude mice by instilling 100 μL of 1.5×10^{6} HTB9-Luc cells (HTB9 cells stably transfected with a luciferase-expressing cassette for simpler *in vivo* imaging of tumor size changes) into the animal bladder. Once tumor implantation was confirmed at day 7, 70 μl of 1 μg/μl of the immunotoxin solution was injected into the animals' bladder. This intravesical treatment was repeated twice per week for 2 weeks. This study revealed a subjective decrease in luminescent activity after 1 week and a nearly uniform loss of luminescent activity after 2 weeks of treatment. In addition, no obvious behavioral or organ and tissue toxicity was observed in the treated animals, showing that, in contrast to the systemic administration of the DT386EGF, its intratumoral administration could be safe.

A variation on targeting EGFR is targeting EGFRvIII (de2-7 EGFR), a tumor-specific receptor produced by 801 bp in-frame deletion of the EGFR nucleotide sequence through alternative splicing. This receptor lacks 267 amino acids in the extracellular domain and also has a new glycine residue and unique peptide sequence at the splice site (Humphrey et al., 1990). EGFRvIII could not bind EGF but has constitutive kinase activity, resulting in hyperactivation of growth, promoting signaling and enhanced proliferation of the EGFRvIII-bearing cells (Nagane et al., 1996). EGFRvIII has been targeted using a novel immunotoxin, DT390-BiscFv806, composed of DT390 and a bivalent single-chain Fv antibody fragment derived from a mouse monoclonal anti-EGFRvIII antibody, Mab 806. *In vitro*, EGFRvIII-transfected U87 (U87-EGFRvIII) glioblastoma cells showed to be significantly more sensitive to DT390-BiscFv806, with an IC_{50} of 2.26×10^{-13} M, compared to U87 cells (IC_{50} 1.47×10^{-9} M). *In vivo*, DT390-BiscFv806 significantly reduced tumor size in both U87 and U87-EGFRvIII xenograft mouse models (Meng et al., 2015). To date, there no clinical information has been reported for DT390-BiscFv806.

A-dmDT390-bisFV

CD3 is a multimeric protein complex that functions as a T-cell co-receptor. Due to the lack of signaling capability in the cytoplasmic portion of the T-cell receptor (TCR), T-cell activation via TCR depends on the CD3 protein complex. CD3 is expressed on normal and malignant T-cells at their earliest developmental stages, so its targeting could be useful for the treatment of T-lineage neoplasms (Frank et al., 1991). CD3 was first targeted within the context of immunotoxins as an immunosuppressive agent to combat graft-versus-host disease. Primary attempts used either intact ricin A (RA) or DT bound to an intact anti-human CD3 murine monoclonal antibody (UCHT1). *In vitro* studies on human peripheral T-cells and T-leukemia cells (Jurkat cells) revealed that a 10–100 times lower concentration of UCHT1-DT was needed compared to UCHT1-RA to have an effect. UCHT1-DT also showed faster onset and greater selectivity between T-cells and stem cells than did UCHT1-RA (Youle et al., 1986). However, further *in vivo* mouse studies showed that intact anti-CD3 monoclonal antibodies activated T-cells via their Fc fragment and resulted in more non-specific toxicity than the immunotoxin made with an antibody fragment (Blazar et al., 1991; Vallera et al., 1995). In addition, another study showed that an immunotoxin made from a single-chain antibody and DT390 (DT390scFv) retained its cytotoxicity on T-cells, with an IC_{50} of about 4.8×10^{-11} M. Although this smaller immunotoxin showed 16 times less cytotoxicity than the intact UCHT1-derived immunotoxin (which had an IC_{50} of 2.9×10^{-12} M on T-cells), it was less affected by pre-existing neutralizing antibodies *in vivo* (Thompson et al., 1995). Meanwhile, an anti-monkey CD3 antibody (FN18) fused to intact (FN18-CRM9) or truncated (DT390-FN18sFv) DT yielded similar results, with the intact DT having better IC_{50} values (1×10^{-10} M) compared to the truncated version (1×10^{-8} M) (Knechtle et al., 1997; Ma et al., 1997).

A challenge with antibody- or antibody fragment-based immunotoxins is their production. In bacterial platforms such as recombinant *E. coli*, aggregation and subsequent solubilization and purification have been issues. These issues, however, are minimized by producing the protein in a higher eukaryotic

platform. CHO cells have been a *de facto* platform for therapeutic antibody production; however, CHO cells are sensitive to the DT. CHO K1 RE1.22c cells have been used to overcome this challenge and obtain correctly folded DT390-scFv (Liu et al., 2000). These cells were mutated to become ADP-ribosylation insensitive. Although the cells were able to produce and secrete the immunotoxin, the cytotoxicity of the immunotoxin toward target cells was reduced. Further investigation revealed N-glycosylation of the DT390 fragment at two sites (at N-glycosylation motifs 16-18 and 235-237). Mutations (Ser18Ala, and Asn235Ala) to remove these N-glycosylation sites increased the IC_{50} values from 4.8×10^{-10} M (N-glycosylated) to 4×10^{-12} M (Non-glycosylated, A-dmDT390-scFv) on Jurkat cells. A-dmDT390-scFv was 12 times more effective than the DT390-scFv immunotoxin expressed by *E. coli* cells (Liu et al., 2000). Subsequent *in vitro* studies showed 10-fold higher cytotoxicity by a bivalent single-chain fragment immunotoxin, A-dmDT390-bisFv. *In vivo* studies in transgenic heterozygote mice (tgE 600) expressing either human or mouse CD3 antigen on the surfaces of their T-cells showed that the bivalent immunotoxin had a 9- and 34-fold higher potency for depleting spleen and lymph node T-cells, respectively, compared to the monovalent immunotoxin (Thompson et al., 2001). In addition, a larger derivative of the immunotoxin is expected to have lower kidney clearance and accumulation, as reported before (Vallera et al., 2000, 2005b). This results in decreased renal toxicity and failure, a dose-limiting toxicity, which had been shown in a preclinical murine study on monovalent DT390anti-CD3sFv (Vallera et al., 1997).

Later, since the production yield of the A-dmDT390-bisFv in the mutated CHO cell line was very low (2–5 μg/ml), which was not sufficient to go through different phases of the clinical trials, *Pichia pastoris* was used as a production host, which finally gave a production yield of 37 μg/ml in an optimized expression condition (Woo et al., 2002, 2004). Further preclinical studies on the A-dmDT390-bisFv produced in *Pichia pastoris* revealed an IC_{50} of 1.7×10^{-14} M on CD3-positive Jurkat Cells. In addition, the LD_{10} (the dose resulting in 10% death) for 10-week-old Balb/C female mice was between 500 and 750 μg/kg (cumulative after eight injections administered twice daily for 4 days). Renal tubular necrosis was the dose-limiting toxicity (Woo et al., 2008b). Another animal study in rats and squirrel monkeys was performed to refine the pharmacokinetics and pharmacodynamics. In this study, an MTD of 200 μg/kg was reported. This amount was sufficient for antitumor activity *in vitro* as well as in the rat model. However, in order to maintain CD3 occupation of lower than 10% (to prevent any T-cell activation and cytokine release), doses of 2.5 μg/kg twice daily for 4 days (20 μg/kg total) was used as the starting dose of the first-in-human clinical trial of A-dmDT390-bisFv (Resimmune^{TM}) (Woo et al., 2008a). At those doses, in another primary phase I clinical trial, this one for CTCL patients, two PRs for 1 and 6 months were achieved. However, mild to moderate toxicities including fever, chills, nausea, transaminasemia, hypoalbuminemia, lymphopenia, and reactivation of the Epstein-Barr virus (EBV) and cytomegalovirus (CMV) were reported (Frankel et al., 2009). Recent updates on a Phase I/II clinical trial (http://clinicaltrials.gov identifier: NCT00611208) on 30 patients (including 25 with CTCL and three with peripheral T-cell lymphoma (PTCL)) showed responses for 36% of the CTCL patients, including four CR (ranging from 38 to 72 months) and five PR (ranging from 3 to 14 months). Results from Resimmune^{TM} are promising, and further studies in patients with low tumor burden stage IB-IIB CTCL is warranted (Frankel et al., 2015).

DT2219

CD19 is a surface glycoprotein that is mainly expressed on late pre-B cells and B cells. It is also widely expressed on B cell leukemia or lymphoma including B-lineage lymphoblastic leukemia, which is the most common form of childhood leukemia (Anderson et al., 1984; Uckun et al., 1988). CD22 is a key regulatory cytoplasmic protein that is primarily expressed on pro-B cells and is then expressed simultaneously with immunoglobulin D as a surface membrane receptor on most mature B cells. CD22 is also expressed on the surface of ∼70% of B-cell lymphomas and leukemias (Peaker and Neuberger, 1993; Sato et al., 1996).

DT2219 is a bispecific immunotoxin consisting of DT390 fused to single-chain antibody fragments targeted to the CD22 and CD19 antigens. DT2219 came about following studies on HD37-dgRTA and RFB4-dgRTA, which were conjugates of deglycosylated ricin A toxin and full murine monoclonal antibodies against CD19 or CD22, respectively. These immunotoxins proved to be effective in patients with B cell lymphoma in separate clinical trials (Conry et al., 1995; Stone et al., 1996). Combotox, an equimolar combination of the two immunotoxins, led to an even higher survival rate for xenograft SCID mice inoculated with the pre-B acute lymphoblastic leukemia cell line, NALM-6-UM1 (Herrera et al., 2000, 2003). Considering the disadvantages of simultaneous administration of two immunotoxins, especially with regards to the increased rate of side effects, and also to broaden the reactivity against B-cell leukemias and lymphomas, Vallera et al. (2005a) developed DT2219. On the $CD19^{+}CD22^{+}$ Daudi cell line, this immunotoxin had the lowest IC_{50} (2×10^{-9} M) of different combinations tested (DT-sFvCD19, DT-sFvCD19sFvCD19, DT-sFvCD22, and DT-sFvCD22sFvCD22). This was more than one order of magnitude smaller than the next most potent immunotoxin tested, DT-sFvCD19sFvCD19, which had an IC_{50} of 3.2×10^{-8} M (Vallera et al., 2005a). Mutations in three amino acids through site-directed mutagenesis of the anti-CD22 variable heavy region enhanced avidity toward the CD22 antigen and lowered the IC_{50} to 3×10^{-10} M. *In vivo* evaluation in xenograft mice with established flank Daudi tumors resulted in significant survival of mice that received four 20 μg doses on days 12, 13, 14, and 16 post tumor inoculation. In SCID mice made to have systemic leukemia tumors through the injection of Daudi cells, those that were treated with 20 μg of DT2219 on days 3, 6, 15, 19, 26, 31, 42, 45, and 49 post inoculation resulted in significant animal survival compared to the controls (Salvatore et al., 2002; Vallera et al., 2005a). DT2219 was further improved by reversing the orientation of the VH and VL chains and fusing each sFv to DT390 via an aggregation

reducing/stabilizing linker (ARL: GSTSGSGKPGSGEGSTKG). These changes improved the IC_{50} values to between 6×10^{-11} and 2×10^{-10} M. *In vivo,* xenograft mice inoculated with human Raji Burkitt's lymphoma cells treated with the improved DT2219 (now known as DT2219ARL) showed long-term tumor-free survivors. The MTD in rabbits receiving IV injections was 200 μg/kg of DT2219ARL when administered every other day over 7 days. At 500 μg/kg under the same regimen, hepatic failure was reported as the dose-limiting toxicity (Vallera et al., 2009). A phase I dose-escalation study to determine the safety, MTD, and efficacy of DT2219ARL included 25 patients with mature or precursor B-cell lymphoid malignancies expressing CD19 and/or CD22 antigens. The patients received DT2219ARL doses ranging from 0.5 μg/kg/day (about 1/500th of the MTD in rabbits) to 80 μg/kg/day intravenously (IV) every other day for 4 total doses (days 1, 3, 5, and 8). Clinical responses were observed at doses of 40 and 60 μg/kg/day, though the 4 doses were inadequate to induce deeper remission. However, one patient who achieved PR after 1 cycle was subjected to an additional cycle, and this led to complete tumor elimination. The safety and biological activity of DT2219ARL at doses of 40–80 μg/kg/day were subsequently approved (Bachanova et al., 2015), and the evaluation of the immunotoxin has proceeded to a phase I/II clinical trial (http://Clinicaltrials.gov identifier: NCT02370160). Although the completion of the study was slated for April 2018, there are still no reported data regarding the outcome of this study.

Tf-CRM107 (TransMID)

Transferrin is an iron-binding glycoprotein that controls the level of free iron found in blood plasma. Receptors for transferrin (TfRs) are overexpressed on various tumors, including carcinomas, glioblastomas, and medulloblastomas (Daniels et al., 2012).

Transferrin-CRM107 (Tf-CRM107) is unique among the immunotoxins discussed thus far. It is constructed by chemically coupling human transferrin to a mutant whole DT structure (S525F). The mutation reduced the native binding activity of the toxin 8,000-fold, but maintained intact translocation and catalytic functions. Conjugation of transferrin and the mutated DT was achieved by thioesterification of the two proteins (Greenfield et al., 1987). *In vitro* studies determined the IC_{50} values for Tf-CRM107 against T47D (breast carcinoma), SNB40 (human medulloblastoma), and U251 (Human glioblastoma astrocytoma) cells to be between 0.39 and 2.6×10^{-12} M. In nude mice with human gliomas (U251), significant tumor reduction was achieved when treated with Tf-CRM107 (Johnson et al., 1988; Laske et al., 1994; Hagihara et al., 2000). The findings of phase I/II clinical trial demonstrated its tumor-suppressive capacity in 35% of patients with malignant brain tumors refractory to conventional therapies, without severe neurologic or systemic toxicity (Weaver and Laske, 2003). However, despite promising results from phase I and II clinical trials that showed positive effects in glioblastoma patients, the results of a phase III clinical trial determined that Tf-CRM107 was unlikely to improve overall patient survival compared to the current standard of care (Yoon et al., 2010).

DTAT, DTAT13, and DTATEGF

Urokinase-type plasminogen activator (uPA) is a serine protease that catalyzes the conversion of plasminogen to plasmin. uPA interacts with the urokinase receptor (uPAR, aka CD87) to restrict plasminogen activation. In certain cancer cells such as glioblastoma cells uPAR is overexpressed (Mori et al., 2000). The IL-13 receptor has also been reported to be overexpressed on glioblastoma cells and minimally expressed on normal healthy cells. It has also been reported to be overexpressed in prostate and pancreatic cancer cells (Debinski et al., 1999; Li C. et al., 2002).

DTAT is an immunotoxin composed of the amino-terminal (AT) fragment of the uPA fused to the C-terminus of DT390. On U118MG, U373MG, and U87MG glioblastoma cells, DTAT had IC_{50}s $< 1 \times 10^{-9}$ M. Treatment of nude mice bearing U118MG human tumors with five 20 μg/day doses administered every other day resulted in a significant regression of tumor sizes. Similar doses in healthy C57BL/6 mice did not affect any tissues or organs (Vallera et al., 2002). On uPAR-positive AML blasts obtained from patients, the IC_{50} for DTAT was lower than 1×10^{-9} M (Frankel et al., 2002a). Moreover, for seven different AML cell lines, IC_{50} values of less than 3×10^{-11} M were obtained. The ML-1 cell line was the most sensitive, with an IC_{50} of 5×10^{-12} M (Ramage et al., 2003).

To enhance the specific cytolethal efficacy of DTAT, a bispecific immunotoxin consisting of both the uPA amino-terminal fragment and IL-13 fused to DT390 was constructed (DTAT13). While *in vitro* and *in vivo* xenograft cytotoxicity assessments revealed very similar efficacy for the three immunotoxins, safety studies on intratumorally and intracranially treated xenograft mice indicated that DTAT13 was at least 160-fold less toxic than DTAT and at least eightfold less toxic than DTIL13 (a fusion of DT390 with IL-13) (Todhunter et al., 2004; Hall and Vallera, 2006).

On the basis of reports on the presence of EGFR on non-small cell lung cancer, a new DTAT derived immunotoxin, DTATEGF was constructed. *In vitro* anti-proliferative assessment of PC9-BrM3 (human brain metastatic lung cancer cell line) cells treated with DTATEGF revealed an IC_{50} of 1×10^{-12} M, compared to 1×10^{-8} M for DTEGF and 1×10^{-9} M for DTAT, representing a more than 1000- to 10000-fold increase in activity compared to each monospecific fusion toxin. Moreover, xenograft nude mice inoculated with the human PC9-BrM3 and treated with DTATEGF, showed significantly longer survival lengths compared to control mice. DTATEGF was administered intracranially via a micro-osmotic pump, and the mice received 1 μg of DTATEGF over 7 days (Huang et al., 2012).

Overall, the efficacy and anti-tumor effects of the three uPAR directed immunotoxins (DTAT, DTAT13, and DTATEGF) have been shown by different in *in vitro* and *in vivo* studies. Even with the mostly positive outcomes, there are no registered clinical trials or clinical evaluations for any uPAR-based immunotoxins.

DTEGF13

DTEGF13 is a bispecific immunotoxin consisting of DT390 fused to EGF and IL-13, made to target a range of solid tumors including glioblastoma, prostate, and pancreatic cancers, which

overexpress receptors for both EGF and IL-13. Used against different human cancer cell lines, including PC-3, DU-145 (prostate cancer cell lines) (Stish et al., 2007), U87MG, U118 (glioblastoma cell lines), calu-3 (human lung cancer cell line) (Stish et al., 2008; Oh et al., 2009), Panc-1, MiaPaCa-2 (pancreatic cancer cells), and H2981-T3 (lung adenocarcinoma cells) (Vallera et al., 2008), DTEGF has shown some of the lowest IC_{50}s for immunotoxins studied to date, ranging from 4.2×10^{-14} M to 2×10^{-11} M. These values were around 905- to 2800-fold smaller, i.e., more toxic, than the corresponding monospecific DTEGF or DTIL13 immunotoxins.

In addition, separate *in vivo* studies in various established xenografts with flank PC-3, U87, or MiaPaCa-2 tumors revealed significant regression of the tumor masses and prolonged survival of the animals upon administration of four 2.5 μg intratumoral injections of DTEGF13. The fact that multiple injections of DTEGF13 were tolerated in the animals is important because human EGF and IL-13 are cross-reactive with mouse EGFR and IL-13R, thereby showing a higher specificity of DTEGF13 for tumor cells and lower safety concerns (Stish et al., 2008; Oh et al., 2009).

Further studies on DTEGF13 showed that a 200 μg bolus intraperitoneal (IP) dose of recombinant EGF13 a few minutes before administration of DTEGF13 in pancreatic cancer xenografted nude mice resulted in an over 15-fold increase in the MTD of the immunotoxin. With this "ToxBloc" strategy, the initial MTD was increased from 0.5 to 7.5 μg DTEGF13/injection (Oh et al., 2010). However, although this "ToxBloc" strategy showed to be efficient in widening the therapeutic window of the DTEGF13 immunotoxin, no further reports have been published regarding any preclinical or clinical study on this protein.

DT-AntiCCR4

CC chemokine receptor 4 (CCR4) is expressed on the surface of some T cell-derived tumors including adult T-cell leukemia-lymphoma, adult peripheral T-cell lymphoma, T-cell acute lymphoblastic leukemia, and CTCL (Chang et al., 2012). In addition, this receptor is especially expressed by effector Treg cells, while it is absent on the surface of naïve Treg cells and, Th1 cells and is rarely expressed by $CD8^+$ T cells, NK cells, $CD14^+$ monocytes/macrophages, dendritic cells, and B cells (Sugiyama et al., 2013).

Various forms of DT-antiCCR4 fusions have been investigated, including monovalent DT390-scFv, bivalent DT390-biscFv, and DT390-Fold-back diabody with the aims of directly depleting both human $CCR4^+$ tumor cells and $CCR4^+$ Tregs as a combined cancer treatment. On the human $CCR4^+$ acute lymphoblastic leukemia cell line, CCRF-CEM, the three variants (DT390-scFv, DT390-biscFv, DT390-Fold-back diabody) had IC_{50}s of 2×10^{-9}, 1×10^{-10}, and 1×10^{-11} M, respectively. *In vivo,* DT390-biscFv and DT390-Fold-back diabody outperformed DT390-scFv. IL2 receptor $\gamma^{-/-}$ NOD/SCID mice xenografted with CCRF-CEM cells were treated in two courses consisting of twice-daily administrations of 50 μg/kg of the three immunotoxins for 4 consecutive days. While significant survival was seen for DT390-biscFv and DT390-Fold-back diabody, DT390-scFv showed no improvement compared to the control (Wang et al., 2015). An *in vivo* study of two cynomolgus monkeys that received IV bolus of the fold-back diabody immunotoxin (25 μg/kg) twice a day for four consecutive days showed up to 89 and 96% depletion of their $CCR4^+$ cells in the peripheral blood and lymph nodes, respectively. Other cell populations, including $CD8^+$ T cells, other $CD4^+$ T cells, B cells, and NK cells, were unaffected. However, due to the presence of CCR4 on the surface of other cell populations, e.g., $CD4^+CCR4^+$ and $CD8^+CCR4^+$ T-cells, further preclinical studies are necessary to evaluate their potential depletion (Wang et al., 2016).

DT390-biTMTP1 and DT390-triTMTP1

Using bacterial display, a pentapeptide (NVVRQ) was isolated that specifically bound to highly metastatic cancer cells and yet had low affinity for poorly metastatic or non-metastatic tumor cells. Alone, this pentapeptide bound to prostate cancer PC-3M-1E8, breast cancer MDA-MB-435S, lung cancer PG-BE1, and gastric cancer MKN-45sci cell lines (Yang et al., 2008). As part of an immunotoxin, i.e., DT390-TMTP1, it showed little to no toxicity; however, DT immunotoxins with repeats of the pentapeptide, either as double or triple repeats (DT390-biTMTP1 or DT390-triTMTP1), were highly effective at killing PC-3M-1E8 and MKN-45 cells. In animal studies with established MKN-45 and PC-3M-1E8 tumor xenograft mouse models, injections of 10 μg DT390-biTMTP1 or DT390-triTMTP1 every 3 days for 21 days resulted in effective inhibition of subcutaneous tumor growth and prolonged mice survival (Ma et al., 2013). Despite the promising *in vitro* and *in vivo* results, no further preclinical studies on this immunotoxin have been reported.

DT-AntiCD19

Using a previously reported sequence for anti-human CD19 scFV (Nicholson et al., 1997), three different DT390-antiCD19 immunotoxins have been investigated. The three immunotoxins consisted of DT390 fused to either a monovalent (scFV), bivalent (biscFV), or fold-back diabody fragment. In this case, cells were more sensitive to the biscFV than the fold-back diabody-based immunotoxin. On $CD19^+$ JeKo (mantle cell lymphoma) cells, IC_{50}s of 2×10^{-10}, 1.7×10^{-11}, and 2×10^{-12} M were obtained for scFV, fold-back diabody, and biscFV forms, respectively. The potency and safety of the immunotoxins were evaluated in a JeKo-cell xenografted immunodeficient NSG mouse model. Similar to the *in vitro* results, the bivalent form showed higher activity *in vivo*. Four courses of 100 μg/kg of each immunotoxin that was IP-injected twice daily for 4 consecutive days extended the survival rate of the mice by about 9 days (40-day survival post tumor induction) compared to negative controls (31-day survival post tumor induction). Given that no significant toxicity was reported in the animals, the dose could be increased further (Zheng et al., 2017). To date, no further studies on these immunotoxins have been reported.

DT386-BR2

DT386-BR2 is a 47 KDa fusion protein containing the first 386 residues of DT fused via a rigid peptide linker, $(AP)_4$, to the antimicrobial peptide, BR2 (Shafiee et al., 2016, 2017c). BR2

is derived from bufoin IIb (RAGLQFPVG[RLLR]$_3$), a potent antimicrobial peptide with cell-penetrating and anti-cancer properties (Lee et al., 2008; Cho et al., 2009). BR2 has only two terminal RLLR repeats and is selective in its ability to penetrate and kill cancer cells without affecting normal cells (Lim et al., 2013; Shafiee et al., 2017b). *In vitro* studies showed that DT386-BR2 was cytotoxic against HeLa (cervical carcinoma) and MCF-7 (breast cancer) cells, with little toxicity to HEK 293 and HUVEC cells (Shafiee et al., 2016). Compared to other immunotoxins, however, the reported IC_{50}s between 10^{-8} and 4×10^{-8} M against HeLa and MCF-7 are relatively high. Still, intraperitoneal injection into healthy albino mice in a preclinical safety study revealed no significant non-specific toxicity. The LD_{50} was greater than 10 mg/kg (Shafiee et al., 2017a), and permission for further preclinical study on xenograft human tumors has been granted.

DT387-SCF

Stem cell factor (SCF) is a hematopoietic growth factor promoting the survival, proliferation, and differentiation of hematopoietic stem cells and progenitor cells by itself or in synergy with other cytokines (Brandt et al., 1992). Overexpression of its receptor, c-kit, has been reported in several cancers such as liver (Chung et al., 2005), ovarian (Raspollini et al., 2004), stomach (Hirota et al., 1998), pancreatic (Yasuda et al., 2006), and small cell lung carcinoma (Naeem et al., 2002). DT387-SCF targets c-kit-overexpressing malignancies. It has been shown to be cytotoxic against PANC-1 (pancreatic carcinoma), MOLT4 (acute lymphoblastic leukemia), HeLa, and K562 (chronic myelogenous leukemia) cells, with IC_{50}s ranging from 4×10^{-7} to 8.8×10^{-7} M. HuT78 (Human T-cell lymphoma) cells were unaffected by DT-SCF. Although DT387-SCF showed moderate cytotoxicity against certain cells, the high IC_{50} values may be one of the reasons that there have been no further reports on this fusion protein (Potala and Verma, 2010).

DT-Gastrin-Releasing Peptide

Based on various studies showing that the gastrin-releasing peptide (GRP, an autocrine growth factor) receptor is up-regulated on the surface of different malignant cell types including cell lines from small cell lung, breast, prostate, and colon cancers (Carney et al., 1987; Schutte and Seeber, 1993), an immunotoxin with GRP has been produced (DT389-GRP). The lowest IC_{50} of this fusion protein on small cell lung cancer cells tested was for NCI-H345, a cell line with the highest levels of GRP receptor expression. The IC_{50} was recorded as 1.1×10^{-9} M (Vanderspek et al., 1997). Despite a good correlation between levels of GRP and toxicity, no further studies have been published.

Immunogenicity of DT-Based Immunotoxins

Because the general population is usually vaccinated against diphtheria, most patients have pre-existing antibodies against the toxin. These antibodies can neutralize the immunotoxin and result in lower treatment efficiency. Even if a patient does not have a pre-existing immunity, treatment schedules that require multiple courses can suffer from the production of antibodies against the toxin moiety during the treatment (Frankel et al., 2003, 2009; Bachanova et al., 2015). Attempts have been made to deimmunize toxin moieties. The highly hydrophilic amino acids glutamine, arginine, lysine, aspartic acid, and glutamic acid have been shown to be highly immunogenic in different studies (Onda et al., 2006). Point mutations of these highly hydrophilic amino acids present on the molecular surface of truncated diphtheria (DT390) have led to lower levels of antibodies when the mutant form of the toxin has been used as the toxin moiety. In a series of steps, it has been shown that up to seven mutations (K125S, R173A, Q245S, K385G, E292S, Q184S, and K227S) could be made to the toxin moiety (dDT) of dDTEGF13 without losing more than a log of activity (Schmohl et al., 2015). In an animal study consisting of 12 injections (on days 0, 1, 14, 21, 28, 35, 42, 49, 56, 63, 70, 77) and evaluated on day 84, dDTEGF13 elicited only a minimal antibody response, while DTEGF13 had an average anti-DT390 response of greater than 1500 μg/mL (Schmohl et al., 2015).

Similarly, DT390 was replaced by dDT390 in DT2219 to form dDT2219. The newly engineered immunotoxin was tested for activity, efficacy, and specificity using functional assays, proliferation assays, and flow cytometry. In addition, the immunogenicity of the molecule was evaluated in BALB/c mice. dDT2219 induced significantly lower levels of neutralizing antibodies compared to DT2219 without compromising its specific cytholethal activity on two different $CD22^+CD19^+$ Burkitt-lymphoma cell lines (Schmohl et al., 2018).

EXPRESSION OF DT UNDER THE CONTROL OF SPECIFIC PROMOTERS

To bypass issues related to the production, purification, formulation, administration, and immunogenicity of DT-based immunotoxins, the genetic material that codes for the catalytic domain of DT (DTA) can be delivered instead. Expression of the gene *in vivo* can then be controlled using tumor-specific promoter sequences. **Figure 4** schematically illustrates the mechanism of tumor-specific expression of DTA.

H19 Regulatory Sequence

H19 is a non-protein-coding onco-fetal gene that acts as a riboregulator upon transcription. It is highly expressed in different tumor types including hepatocellular (Ariel et al., 1998), bladder (Ariel et al., 2000), and chorio- (Lustig-Yariv et al., 1997) carcinoma, in addition to colorectal (Cui et al., 2002) and ovarian (Tanos et al., 1999) cancers, but its expression in normal tissues is very low or undetectable (Kaplan et al., 2003). Using the 814 bp flanking the 5′-region of the H19 gene, expression of DTA was assessed based on the inhibition of luciferase activity when various quantities of pDTA-PBH19 were co-transfected with a set amount of pLuc4SV40 reporter plasmid (7 μg). A potent decrease in luciferase activity was observed in T24P bladder carcinoma cells. Using 0.05 to 1 μg/well of pDTA-PBH19 resulted in 30 to 90% inhibition, respectively. In IMR-90 cells, where the H19 regulatory element is inactive,

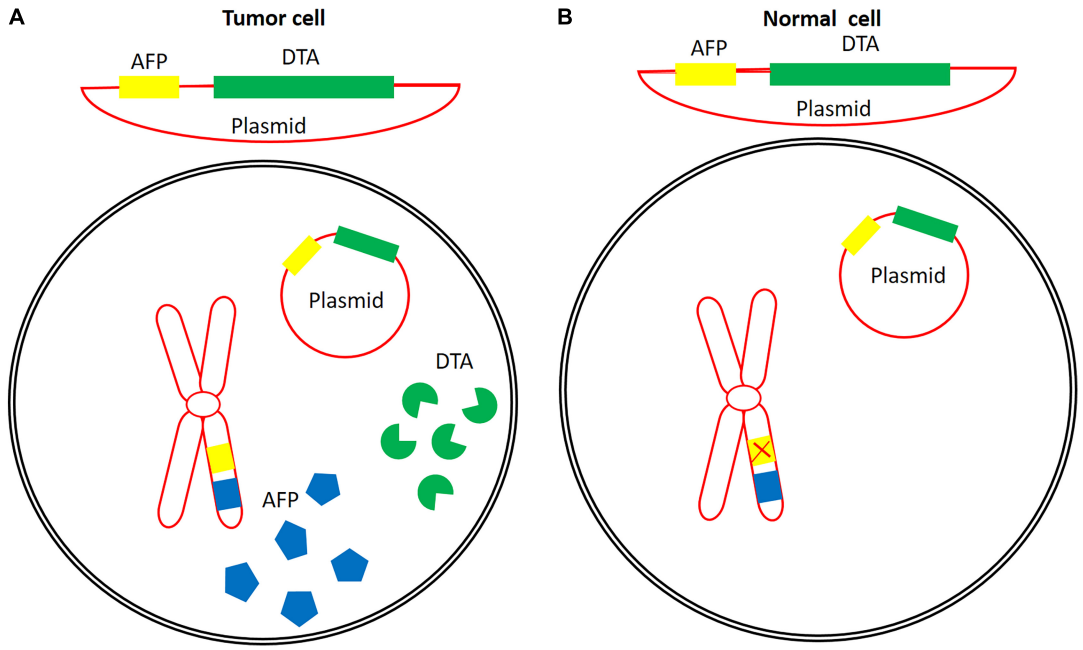

FIGURE 4 | An example of the concept of the application of a tumor-specific promoter for tumor-specific expression of DTA. Alpha feto-protein promoter is active in some cancers **(A)**, but is inactive in normal cells **(B)**. Construction of a plasmid containing the DTA coding sequence under the control of this promoter might lead to the expression of DTA in tumor cells with active AFP promoter without any expression in or cytotoxic effects on normal cells. Eukaryotic chromosome (red), AFP (blue), AFP promoter (yellow), and DTA (green).

no significant reduction in luciferase activity was observed. Substantial reductions in luciferase activity (about 85%) were also seen in Hep3B (human hepatocellular carcinoma) and MBT-2-t50 (mouse bladder carcinoma) cells, albeit with 0.5 μg/well of pDTA-PBH19 (Ohana et al., 2002). The anti-tumor potential of pDTA-PBH19 was assessed in a murine bladder carcinoma model established by subcutaneous injection of MBT-2-t50 cells. Intra-tumor administration of three 50 μg doses of pDTA-PBH19 as a calcium phosphate precipitate resulted in a 40% reduction in tumor size compared to the control groups, which received either the pLuc-PBH19 reporter plasmid or no treatment (Ohana et al., 2002). In a subsequent pilot clinical study, the safety and efficacy of the pDTA-PBH19 plasmid were evaluated in two human patients having recurrent superficial bladder carcinoma refractory to common treatments and whose cancer cells showed high levels of H19 RNA. A dose of 2 mg of the plasmid was delivered intravesically once a week for a total of 9 weeks. A reduction in tumor size of 75% without any significant adverse effects or traces of pDTA-PBH19 in their blood was seen for both patients (Ohana et al., 2004). pDTA-PBH19, now under the name BC-819, was subsequently evaluated in a phase I/II dose-escalation clinical trial on 18 patients with superficial bladder cancer refractory to intravesical therapy with the Bacillus Calmette–Guerin (BCG) vaccine. The patients received weekly intravesical doses of 2, 4, 6, 12, or 20 mg over 7 weeks. The doses were escalated if none of the first three patients in the preceding dose cohort experienced dose-limiting toxicity after the first three weekly intravesical treatments. Of the 18 patients, four went into CR and eight showed either complete ablation of marker tumors or at least a 50% reduction in marker lesions by week 12. No dose-limiting toxicity or death was observed during the study, confirming the safety of BC-819 (Sidi et al., 2008). The safety and efficacy results were also further confirmed by a phase IIb prospective, open-label, multicenter trial on patients with recurrent, multiple non-muscle-invasive bladder cancer with prior intravesical therapy failure. In that study, patients received intravesical instillations of six 20 mg plasmid DNA over 6 weeks. Following this period, patients were given 3-weekly maintenance treatment every 3 months for up to 1 year. Of the 39 evaluable patients, 64% were recurrence-free at 3 months. At 1 and 2 years, the recurrence-free rate was 45 and 40%, respectively. In addition, only one drug-related severe adverse effect was observed; one patient developed hematuria (Gofrit et al., 2014).

The anti-tumor potential of BC-819 was also evaluated in ovarian cancer cell lines. Co-transfection of 2 μg pLucSV40/well and 0.0125 μg pDTA-H19/well in OVCAR-3, TOV-112D, and ES-2 resulted in 30, 75, and 55% reductions in luciferase activity, respectively, compared to the controls. *In vivo* administration of four 25 μg injections of pDTA-H19 every other day to ES-2 cell line-xenografted nude mice inhibited tumor growth by 40% (Mizrahi et al., 2009). In a human case, an 80 mg intraperitoneal instillation of this construct to a woman with stage IIIc epithelial ovarian cancer showed no adverse effects. Gradually increasing the dose to 140 mg up to the 7th week led to complete resolution of the ascites and malignant cells with minimal adverse effects (Mizrahi et al., 2010a).

The synergistic activity of DTA and TNFα on ovarian tumor cell lines and nude mice ovarian cancer models has also

investigated. Expression of the two proteins under the control of the H19 promoter (pH19-TNF-IRES-DTA) occurred via an internal ribosomal entry site (IRES) element located at the 5′ end of the DTA fragment. Co-transfection of ES-2, TOV-122D, and SK-OV3 cell lines with 2 μg/well of a pLucSV40 and 0.025 μg/well of the pH19-TNF-IRES-DTA plasmid reduced the luciferase activity by 96%. The IC_{50} values for pH19-TNF-IRES-DTA on ES-2 and TOV-122D cells were lower than those for pH19-DTA on the same cell lines (0.0025 and 0.003 μg pH19-TNF—IRES-DTA/well for ES-2 and TOV-122D versus 0.004 μg pH19-DTA/well for both cell lines). Even the DTA- and TNF-resistant SK-OV3 cells were efficiently killed (IC_{50} value of 0.004 μg plasmid/well) using the pH19-TNF-IRES-DTA plasmid. In addition, 25 μg intra-tumoral injections of pH19-DTA or pH19-TNF-IRES-DTA into ectopically grown human ovarian tumors in athymic female nude mice inhibited tumor growth by 40% (Mizrahi et al., 2010b).

Further *in vitro* and *in vivo* preclinical studies also revealed potential for application of the pDTA-PH19 plasmid in the treatment of colorectal adenocarcinoma, lung cancer, and pancreatic cancer, alone or in combination with the chemotherapeutic agent gemcitabine (Hasenpusch et al., 2011; Sorin et al., 2011, 2012). Furthermore, an open-label, dose-escalation phase I/II clinical trial on nine patients with unresectable pancreatic adenocarcinoma showed promising results. The MTD for patients receiving a 4–8 mg intratumoral injection of the plasmid twice weekly for 2 weeks was greater than 8 mg/injection. Moreover, in addition to decreased tumor size in all of the patients, four patients who received the highest amount of the plasmid survived for more than 6 months, and 2 others survived for more than 12 months (Hanna et al., 2012). Recently, a phase I/IIa study on 14 patients with recurrent, platinum-resistant advanced-stage ovarian cancer or primary peritoneal carcinoma showed mixed results. The first cohort received a dose of 60 mg of BC-819 intraperitoneally, while subsequent cohorts received escalating doses of 120 and 240 mg. Results revealed only five drug-related adverse effects in four patients in the 60 and 120 mg cohorts, and no adverse effect was reported for the 240 mg cohort. Unfortunately, the overall survival seen in that study was between 6.3 and 15 months, which is similar to the median overall survival rate in heavily pretreated patients with recurrent platinum-resistant ovarian cancers. It has been suggested that a larger cohort study, with higher doses and longer periods of treatment in combination with other systemically administered drugs, is needed (Lavie et al., 2017).

Insulin-Like Growth Factor 2, Promoters 3 and 4

The human insulin-like growth factor 2 (IGF2) gene is transcribed under the control of four different promoters, P1–P4, which results in four different transcripts (Holthuizen et al., 1990). The P3 and P4 promoters are only active during embryogenesis and in some tumor tissues (Engstrom et al., 1998). Ayesh et al. (2003) verified the activity of these promoters in T24P (human bladder carcinoma), HepG2, and Skhep1 (hepatocellular carcinoma) cell lines using a reporter plasmid harboring the luciferase gene downstream of the P3 or P4 promoters. Their results confirmed the activity of both promoters in HepG2 and T24P cell lines; however, in Skhep1 cells, the promoters had limited functionality. When the same cells were co-transfected with plasmids bearing DTA under the control of either P3 (pP3-DTA) or P4 (pP4-DTA) promoters and pLucSV40 (a plasmid that allows constitutive expression of luciferase), a dose-dependent response was seen in all three cell types. A 50% reduction in luciferase activity was obtained following transfection of 0.01 and 0.015 μg/well pP3-DTA in HepG2 or T24P cells, respectively. In the same cells, transfecting with pP4-DTA only required 0.005 μg/well of the plasmid to achieve the same level of luciferase inhibition. However, for both P3-DT-A and P4-DT-A, higher concentrations were needed to achieve a 50% reduction in Skhep1.

Human P3 and P4 promoters are also active in the murine MBT-2-t50 bladder carcinoma cell line. To further test pP3-DTA, an animal model of the carcinoma was established by subcutaneous injection of the cells and treated by three 50 μg intratumoral injections of pP3-DTA over 5 days. Tumor growth was significantly inhibited (70%) compared to non-treated mice or mice injected with a LucP3 plasmid ($P < 0.0002$). In addition, a group of healthy animals receiving the same doses of pP3-DTA plasmid did not show any signs of toxicity after 24 days and continued to gain weight, similar to the healthy animals injected with LucP3. Furthermore, the histopathological examination of the two groups did not reveal any evidence for toxicity in any of their internal organs (liver, kidney, heart, spleen, pancreas, and adrenals) (Ayesh et al., 2003). To further improve the efficiency of these plasmids, Amit et al. (2011) developed a double-promoter plasmid by joining the two DTA-expressing cassettes. *In vitro* evaluation of the dual-cassette plasmid (pP4-DTA-P3-DTA) in various cancer cell lines showed that up to 70% inhibition of luciferase activity could be achieved with as little as 0.005 μg of plasmid preparation per well (Amit et al., 2013). *In vivo*, 3 doses of 25 mg intratumoral injections of the plasmids into a murine model of human bladder carcinoma over 5 days reduced tumor size by 70, 45, and 50% using pP4-DTA-P3-DTA, pP3-DTA, and p4-DTA, respectively (Amit et al., 2011). Despite the promising results *in vitro* and *in vivo*, there is no indication that these plasmids have progressed to preclinical or clinical studies.

Rad51, Rad51C, and XRCC2 Regulatory Elements

The Rad51 protein is involved in homologous recombination and has an essential role in repairing DNA double-strand breaks. The expression of Rad51 in normal cells is tightly controlled, but in a variety of tumors, it can be overexpressed (Raderschall et al., 2002). Hine et al. (2008) constructed a plasmid (pRAD51-DTA) expressing DTA under the control of the 6,532-bp Rad51 regulatory region and tested it on a panel of 13 normal and malignant cells. Cells were co-transfected with 0.01–0.1 μg of pRAD51-DTA together with a plasmid-bearing luciferase under the control of a constitutive promoter. All the tumor cell lines except MDA-MB-468 experienced a 10–100,000-fold decrease in protein synthesis. In normal cells, decreases in protein synthesis

were less than 10-fold. In addition, transfection with pRAD51-DTA resulted in a 20–80% reduction in viability in all of the cancer cell lines (HeLa, MCF-7, T47-D, HCC1954, GP2-293, HT1080, and MDA-MB-468) and had little to no effect on normal cell lines (HMEC-1, HMEC2, HMEC4, IMR90, WI-38, and HCA2).

In vivo effects of this construct were investigated in nude mice xenografted with human cervical cancer cells. The xenograft tumors were made by IP or SC injection of HeLa cells to the nude mice. The effect of the Rad51 controlled expression of DTA was evaluated following IP injections of Rad51-DTA plasmid in the case of IP tumors (receiving 6 doses of 100 μg plasmid over 15 days) or intratumoral injections to SC tumors (receiving 6 doses of 20 μg plasmid over 28 days). In the case of SC tumors, 50 percent of the mice were cancer-free after 6 doses of the plasmid injection. In addition, for intra-peritoneal tumors, IP administration of the plasmid resulted in a 90% increase of mean survival time compared to the controls (Hine et al., 2012).

Despite the promising cancer cell-selective activity of the pRAD51-DTA, its application was hindered due to the large size of the Rad51 regulatory element (6532 bp). Therefore, attempts were made to examine the tumor specificity of Rad51 paralogs having shorter regulatory nucleotide sequences. Cao et al. (2014) evaluated the expression level and specificity of four Rad51 paralogs, including Rad51B, Rad51C, Rad51D, and Rad52, with a panel of 14 different malignant and normal cell lines. Among these paralogs, Rad51C, with a ∼2000 bp length regulatory sequence, showed ninefold higher protein expression in cancer cells. In addition, transfection of normal and malignant cells by a plasmid driving DTA expression by the Rad51C promoter (pRAD51C-DTA) resulted in 7- to 10- fold greater inhibition of luciferase production and activity in cancer cells compared to normal cells (Cao et al., 2014). The use of XRCC2, another Rad51 paralog with a shorter regulatory sequence (∼2100 bp), resulted in an up to 90% reduction in luciferase activity in cancer cells, while only causing an up to 19% reduction in normal cells. The cytolethal effects after transfection of pXRCC2-DTA and pRAD51-DTA into HeLa cells were very similar (76.7 vs. 82.1%, respectively). Moreover, *in vivo* evaluation in nude mice, subcutaneously xenografted with HeLa cells, which consisted of 4 intratumoral injections of lentiviral vector containing the XRC22-DTA cassette in 11 days, resulted in a significant reduction in tumor size (Chen Y. et al., 2018).

Prostate-Specific Antigen Promoter

The promoter and upstream sequences (PSAR-PCPSA promoter) of human prostate-specific antigen (PSA) have been used to drive DTA expression in PSA-positive prostate cancer cells using the pPSAR-PCPSA-DTA plasmid. However, although liposome-based transfection of LNCaP (PSA positive prostate), DU145 (non-PSA-producing prostate), and R11 (renal) cell lines reduced the viability of LNCaP cells without significant effect on R11 and DU145 cells, the transfection efficiency was low (Pang, 2000). To overcome the low transfection efficiency, a lentiviral vector carrying the PSAR-PCPSA-DTA expression cassette was prepared and used to infect LNCaP and different PSA-negative control cell lines. Infection of the cells with MOIs of 0.5 or higher resulted in a 50–95% reduction in LNCaP cell viability but did not affect the control cell lines (Yu et al., 2001). In addition, intratumoral injection of the prepared lentiviral vectors in nude mice subcutaneously xenografted with LNCaP cells resulted in significant tumor regression 4–7 days post-injection, without any pathogenic effects even up to 90 days (Zheng et al., 2003).

Peng et al. (2005) also developed a viral vector-mediated approach using the PSA promoter. Using an adenoviral vector, they were able to show significant inhibition of protein synthesis by measuring luciferase enzyme activity in the LNCaP cell line. Furthermore, subcutaneous LNCaP tumors in nude mice were reduced in size by 50% upon intratumor injection of the adenoviral particles. This was also observed by intratumoral injection of the adenoviral particles into tumors of TRAMP mice, transgenic mouse models of prostate tumors. Taken together, the promoter sequence of PSA showed to be effective in tumor-specific expression of DTA fragments for the treatment of cancer.

Survivin Promoter

Survivin is type of inhibitor of the apoptosis protein family (Ambrosini et al., 1997), which is expressed in multiple types of cancers including ovarian (Chen et al., 2013), gastric (Meng et al., 2013), non-small- (Xu et al., 2012) and small-cell (Chen et al., 2014) lung, and breast cancer (Tanaka et al., 2000) but is undetectable in normal tissues (Chen et al., 2004). Evaluation of two different survivin promoter fragments, Surp269 and Surp1430 (269 or 1430 bp, respectively), to drive luciferase expression showed much higher activity for the longer fragment, Surp1430, in three different cancer cell lines (HeLa, Eca109, and ZR-7530). A lentiviral vector harboring a Surp1430-DTA expression cassette was used to transduce various normal and malignant cell lines. With 0.1 and 0.3 μg of the recombinant virus, a 42 to 92% reduction in cell viability was observed for the malignant cells, while the viability of normal cells was not affected. Furthermore, when nude mice xenografted with a ZR7530 breast cancer cell line were subjected to the Surp1430-DTA lentiviral vector 30, 40, and 50 days after implantation of the cells, significant regression of tumor masses was observed. However, the tumors were not completely eradicated, and a very small mass of tumors survived (Lin et al., 2015). This incomplete tumor mass regression, in addition to findings on survivin protein overexpression in megakaryocyte and erythrocytes and its up-regulation by β-catenin, has impeded further application of this promoter for tumor-targeted gene expression (Mccrann et al., 2008).

Alpha-Fetoprotein Promoter

Alpha-fetoprotein (AFP) is expressed during fetal development; however, after birth, its expression is negligible except in the case of certain malignancies including hepatocellular carcinomas and teratomas, where AFP is expressed at high levels (Chen et al., 2007). In one study, a plasmid containing DTA linked to the human AFP promoter and enhancer (pAF-DTA) was investigated for its selective cytolethal effects on AFP-producing cells HuH-7 and HepG2. Cells were co-transfected with both pAF-DTA and a plasmid bearing the chloramphenicol acetyltransferase (CAT) gene (pAF-CAT). CAT activity decreased with increasing

amounts of pAF-DTA from 0.5 to 3 μg/10^6 cells. Transfection of pAF-DTA in HuH-7 and HepG2 cells inhibited their growth, whereas following transfection of the AFP-negative cell line, MKN45, no growth inhibition was observed (Murayama et al., 1999). Furthermore, intra-tumor injection of the pAF-DTA plasmid in a hepatocellular carcinoma nude mouse model xenografted with HuH-7 tumors resulted in significant tumor weight reduction (0.62 ± 0.21 g) compared to PBS treated controls (2.07 ± 0.67 g) (Kunitomi et al., 2000). These results are promising for the treatment of cancerous cells expressing AFP without affecting other types of cells.

hTERT Promoter

Telomerase activity can be detected in about 85% of different malignant tumors but is absent in most normal cells (Ito et al., 1998). Therefore, human telomerase transcriptional regulatory sequences, hTER (responsible for the transcription of the RNA subunit of the human telomerase) and hTERT (responsible for transcription of the human telomerase reverse transcriptase subunit) have been targeted to drive the expression of DTA. These two regulatory sequences were tested by co-transfecting plasmids (phTER-DTA or phTERT-DTA) with a luciferase reporter plasmid in various cell lines with high-level telomerase activity (RT112 (bladder carcinoma) and HepG2 (hepatocellular carcinoma) cells), low-level telomerase activity (U2OS and Saos-2 osteosarcoma cells), or no telomerase activity (IMR-90 cells, a primary fibroblast cell line). A reduction in luciferase activity was observed in all of the malignant and normal cell lines, showing non-cancer cell specificity of hTER. However, highly tumor-specific reduction rates (82 to 55%) were observed for the phTERT-DTA, even in the low telomerase activity osteosarcoma cell lines, compared to the IMR-90 control cells (which had an up to 20% reduction). These results confirmed hTERT as a promising promoter for gene therapy applications (Abdul-Ghani et al., 2000).

Human Chorionic Gonadotropin α and β Promoters

Human chorionic gonadotropin (hCG) hormone is a glycoprotein composed of two non-covalently bound α and β subunits. Normally, this hormone is a sign of pregnancy and can be detected in the blood and urine of pregnant women; however, in cases of breast and ovarian cancer, free hCG α or β subunits can also be detected. In certain cancers, there is activation of the regulatory sequences controlling transcription of the hCG subunits (Cole et al., 1988). Therefore, to test if DTA could be preferentially expressed in cancer cells, plasmids were constructed that had DTA downstream of α or β hCG promoters (creating pTHA-47 or pTHA-49 plasmids, respectively). Co-transfecting these plasmids (individually) with a second plasmid harboring luciferase downstream of a constitutive promoter, the expression of DTA could be assessed through the inhibition of luciferase activity. Transfection into EBLY II, OVCAR-V, and OVCAR III cells resulted in up to 95% inhibition of luciferase compared to the control. Of the two promoters, the α subunit promoter yielded greater inhibition than the β subunit promoter. Unfortunately, luciferase inhibition, albeit small, was also seen when the plasmids were transfected into a normal ovarian cell line, thereby restricting further applications of these promoters (Lidor et al., 1997).

β-Catenin-Dependent Promoter

β-catenin is a component of cadherin-based adherens junctions. Deregulation in its structure and signaling properties often results in deregulated growth connected to cancer and metastases (De La Coste et al., 1998; Valenta et al., 2012). Lipinski et al. (2001) developed artificial β-catenin-dependent promoters that are highly active in cancer cells *in vitro* and *in vivo*. An adenovirus vector carrying DTA under the control of CTP4, an optimized β-catenin-dependent artificial promoter, was used to show a dose-dependent (adenoviral MOI) decreased cell survival in the β-catenin-deregulated tumor cell lines SW480 and HepG2 compared to control cells with regulated β-catenin activity, such as HeLa, HNX14C, and HUVEC (Lipinski et al., 2004).

Delivery of the DTA-Expressing Cassettes

In order to deliver DTA-expressing cassettes to cancer cells, different strategies, including the application of naked plasmids or viral vectors, have been considered. Usually, to improve cellular uptake of the intratumorally injected naked plasmids, they are prepared in a mixture of *in vivo* safe transfection reagents such as calcium phosphate (Ohana et al., 2002) or *in vivo*-jetPEI^{TM} (Hine et al., 2012). In some cases, delivery is enhanced using adeno- (Li Y. et al., 2002) or lenti- (Lin et al., 2015) viral vectors. One problem with preparation of DTA-encoding viral vectors is the leaky expression of DTA in packaging cell lines, which disturbs the host cell protein synthesis machinery and lowers viral particle titers or even prevents viral particle formation. To alleviate this problem, DT-resistant packaging cell lines such as HEK293T[mEF-2(G717R) (Mccrann et al., 2008) or 293DTRP#2 (Li Y. et al., 2002) were developed. Another strategy proposed to lessen the problem of leaky expression, especially in normal tissues, is using a two-plasmid (binary) system, in which one plasmid carries a silenced DTA gene separated from its promoter by a transcription terminator, and the second plasmid carries the encoding sequence for site-specific Cre recombinase under a cancer-specific promoter. Once inside the cancer cells, the recombinase removes the transcription terminator sequence flanked by attR and attL recombination sites and activates the expression of DTA. This could result in less DTA expression in normal cells and lower non-specific toxicity (Elias et al., 2018).

CONCLUSION

Diphtheria toxin is lethal and, without a targeted approach, significant toxicity can be experienced by the patient. In fact, certain clinical trials had to be cut short or failed once completed because of these effects. It is for this reason that strategies that can harness the power of the toxin while minimizing off-target effects are consistently being sought. It is clear that there is great potential for the catalytic domain of DT. However, this

potential is not new, and this review highlights work that dates back as early as the 1980s. Two broad approaches have been used for taming this toxin into serving as a therapeutic agent: direct toxin delivery or delivery of the gene for the production of the toxin *in vivo*. Amongst all of the examples described above, the only approved agents that reached the market are Ontak^{TM} and Tagraxofusp^{TM}. Some immunotoxins and gene-based constructs are still in pre-clinical and clinical trial stages, without any final decision on their overall clinical applicability. The development of more specific targeting strategies for the protein could result in fewer adverse and non-expected effects on normal cells and tissues. Moreover, the development of methods for enhanced delivery of the vectors for gene-based therapy with DTA should result in higher efficiency in eradicating tumor cells. However, in addition to the targeting and delivery issues with the DTA-based therapies, which are also common to other bacterial or plant toxins, is a preexisting immunity of the general population due to existing immunization schemes. This preexisting immunity could result in lower therapeutic responses or even clearance of the DT-fusion proteins by the patient immune system. This may give an advantage to gene-based DT therapeutics going forward.

AUTHOR CONTRIBUTIONS

FS, MA, and AJ-N took part in drafting, revising, and preparation of the manuscript. The manuscript was finalized and prepared for submission by AJ-N. Further revisions according to the reviewer comments were made by MA and AJ-N and finalized by AJ-N.

REFERENCES

Abdul-Ghani, R., Ohana, P., Matouk, I., Ayesh, S., Ayesh, B., Laster, M., et al. (2000). Use of transcriptional regulatory sequences of telomerase (hTER and hTERT) for selective killing of cancer cells. *Mol. Ther.* 2, 539–544. doi: 10.1006/mthe.2000.0196

Al-Jaufy, A. Y., Haddad, J. E., King, S. R., Mcphee, R. A., and Jackson, M. P. (1994). Cytotoxicity of a shiga toxin A subunit-CD4 fusion protein to human immunodeficiency virus-infected cells. *Infect. Immun.* 62, 956–960.

Ambrosini, G., Adida, C., and Altieri, D. C. (1997). A novel anti-apoptosis gene, survivin, expressed in cancer and lymphoma. *Nat. Med.* 3, 917–921. doi: 10.1038/nm0897-917

Amit, D., Tamir, S., Birman, T., Gofrit, O. N., and Hochberg, A. (2011). Development of targeted therapy for bladder cancer mediated by a double promoter plasmid expressing diphtheria toxin under the control of IGF2-P3 and IGF2-P4 regulatory sequences. *Int. J. Clin. Exp. Med.* 4, 91–102.

Amit, D., Tamir, S., and Hochberg, A. (2013). Development of targeted therapy for a broad spectrum of solid tumors mediated by a double promoter plasmid expressing diphtheria toxin under the control of IGF2-P4 and IGF2-P3 regulatory sequences. *Int. J. Clin. Exp. Med.* 6, 110–118.

Anderson, K. C., Bates, M. P., Slaughenhoupt, B. L., Pinkus, G. S., Schlossman, S. F., and Nadler, L. M. (1984). Expression of human B cell-associated antigens on leukemias and lymphomas: a model of human B cell differentiation. *Blood* 63, 1424–1433.

Ariel, I., Miao, H. Q., Ji, X. R., Schneider, T., Roll, D., De Groot, N., et al. (1998). Imprinted H19 oncofetal RNA is a candidate tumour marker for hepatocellular carcinoma. *Mol. Pathol.* 51, 21–25. doi: 10.1136/mp.51.1.21

Ariel, I., Sughayer, M., Fellig, Y., Pizov, G., Ayesh, S., Podeh, D., et al. (2000). The imprinted H19 gene is a marker of early recurrence in human bladder carcinoma. *Mol. Pathol.* 53, 320–323. doi: 10.1136/mp.53.6.320

Aruna, G. (2006). Immunotoxins: a review of their use in cancer treatment. *J. Stem Cells Regen. Med.* 1, 31–36.

Ayesh, B., Matouk, I., Ohana, P., Sughayer, M. A., Birman, T., Ayesh, S., et al. (2003). Inhibition of tumor growth by DT-A expressed under the control of IGF2 P3 and P4 promoter sequences. *Mol. Ther.* 7, 535–541. doi: 10.1016/s1525-0016(03)00056-x

Babavalian, E., Zeinoddini, M., Saeedinia, A. R., Mohammadi, R., and Xodadadi, N. (2019). Design of a recombinant immunotoxin against the human granulocyte-colony stimulating factor receptor. *Mol. Biol. Rep.* 46, 1093–1097. doi: 10.1007/s11033-018-4567-z

Bacha, P., Forte, S., Kassam, N., Thomas, J., Akiyoshi, D., Waters, C., et al. (1990). Pharmacokinetics of the recombinant fusion protein DAB486IL-2 in animal models. *Cancer Chemother. Pharmacol.* 26, 409–414. doi: 10.1007/bf02994090

Bacha, P., Williams, D. P., Waters, C., Williams, J. M., Murphy, J. R., and Strom, T. B. (1988). Interleukin 2 receptor-targeted cytotoxicity. *Interleukin* 2 receptor-mediated action of a diphtheria toxin-related interleukin 2 fusion protein. *J. Exp. Med.* 167, 612–622. doi: 10.1084/jem.167.2.612

Bacha, P. A., Forte, S. E., Mccarthy, D. M., Estis, L., Yamada, G., and Nichols, J. C. (1991). Impact of interleukin-2-receptor-targeted cytotoxins on a unique model of murine interleukin-2-receptor-expressing malignancy. *Int. J. Cancer* 49, 96–101. doi: 10.1002/ijc.2910490118

Bachanova, V., Frankel, A. E., Cao, Q., Lewis, D., Grzywacz, B., Verneris, M. R., et al. (2015). Phase I study of a bispecific ligand-directed toxin targeting CD22 and CD19 (DT2219) for refractory B-cell malignancies. *Clin. Cancer Res.* 21, 1267–1272. doi: 10.1158/1078-0432.CCR-14-2877

Bagel, J., Garland, W. T., Breneman, D., Holick, M., Littlejohn, T. W., Crosby, D., et al. (1998). Administration of DAB389IL-2 to patients with recalcitrant psoriasis: a double-blind, phase II multicenter trial. *J. Am. Acad. Dermatol.* 38, 938–944. doi: 10.1016/s0190-9622(98)70590-0

Beilhartz, G. L., Sugiman-Marangos, S. N., and Melnyk, R. A. (2017). Repurposing bacterial toxins for intracellular delivery of therapeutic proteins. *Biochem. Pharmacol.* 142, 13–20. doi: 10.1016/j.bcp.2017.04.009

Beitz, J. G., Davol, P., Clark, J. W., Kato, J., Medina, M., Frackelton, A. R., et al. (1992). Antitumor activity of basic fibroblast growth factor-saporin mitotoxin *in vitro* and *in vivo*. *Cancer Res.* 52, 227–230.

Bennett, M. J., and Eisenberg, D. (1994). Refined structure of monomeric diphtheria toxin at 2.3 A resolution. *Protein Sci.* 3, 1464–1475. doi: 10.1002/pro.5560030912

Blazar, B. R., Hirsch, R., Gress, R. E., Carroll, S. F., and Vallera, D. A. (1991). *In vivo* administration of anti-CD3 monoclonal antibodies or immunotoxins in murine recipients of allogeneic T cell-depleted marrow for the promotion of engraftment. *J. Immunol.* 147, 1492–1503.

Brandt, J., Briddell, R. A., Srour, E. F., Leemhuis, T. B., and Hoffman, R. (1992). Role of c-kit ligand in the expansion of human hematopoietic progenitor cells. *Blood* 79, 634–641.

Brinkmann, U., Brinkmann, E., and Pastan, I. (1995). Expression cloning of cDNAs that render cancer cells resistant to *Pseudomonas* and diphtheria toxin and immunotoxins. *Mol. Med.* 1, 206–216. doi: 10.1007/bf03401568

Cao, Y., Marks, J. D., Huang, Q., Rudnick, S. I., Xiong, C., Hittelman, W. N., et al. (2012). Single-chain antibody-based immunotoxins targeting Her2/neu: design optimization and impact of affinity on antitumor efficacy and off-target toxicity. *Mol. Cancer Ther.* 11, 143–153. doi: 10.1158/1535-7163.MCT-11-0519

Cao, Y., Xu, Y., Zhang, L., Li, Z., Jiang, Y., Tian, X., et al. (2014). Utilization of Rad51C promoter for transcriptional targeting of cancer cells. *Oncotarget* 5, 1805–1811.

Carney, D. N., Cuttitta, F., Moody, T. W., and Minna, J. D. (1987). Selective stimulation of small cell lung cancer clonal growth by bombesin and gastrin-releasing peptide. *Cancer Res.* 47, 821–825.

Chan, C. H., Blazar, B. R., Greenfield, L., Kreitman, R. J., and Vallera, D. A. (1996). Reactivity of murine cytokine fusion toxin, diphtheria toxin390-murine interleukin-3 (DT390-mIL-3), with bone marrow progenitor cells. *Blood* 88, 1445–1456.

Chang, D. K., Sui, J., Geng, S., Muvaffak, A., Bai, M., Fuhlbrigge, R. C., et al. (2012). Humanization of an anti-CCR4 antibody that kills cutaneous T-cell lymphoma

cells and abrogates suppression by T-regulatory cells. *Mol. Cancer Ther.* 11, 2451–2461. doi: 10.1158/1535-7163.MCT-12-0278

Chaudhary, V. K., Fitzgerald, D. J., and Pastan, I. (1991). A proper amino terminus of diphtheria toxin is important for cytotoxicity. *Biochem. Biophys. Res. Commun.* 180, 545–551. doi: 10.1016/s0006-291x(05)81099-x

Chen, C., Yue, D., Lei, L., Wang, H., Lu, J., Zhou, Y., et al. (2018). Promoter-operating targeted expression of gene therapy in cancer: current stage and prospect. *Mol. Ther. Nucleic Acids* 11, 508–514. doi: 10.1016/j.omtn.2018.04.003

Chen, Y., Li, Z., Xu, Z., Tang, H., Guo, W., Sun, X., et al. (2018). Use of the XRCC2 promoter for *in vivo* cancer diagnosis and therapy. *Cell Death Dis.* 9:420. doi: 10.1038/s41419-018-0453-9

Chen, G. G., Ho, R. L., Wong, J., Lee, K. F., and Lai, P. B. (2007). Single nucleotide polymorphism in the promoter region of human alpha-fetoprotein (AFP) gene and its significance in hepatocellular carcinoma (HCC). *Eur. J. Surg. Oncol.* 33, 882–886. doi: 10.1016/j.ejso.2007.02.036

Chen, J. S., Liu, J. C., Shen, L., Rau, K. M., Kuo, H. P., Li, Y. M., et al. (2004). Cancer-specific activation of the survivin promoter and its potential use in gene therapy. *Cancer Gene Ther.* 11, 740–747. doi: 10.1038/sj.cgt.7700752

Chen, L., Liang, L., Yan, X., Liu, N., Gong, L., Pan, S., et al. (2013). Survivin status affects prognosis and chemosensitivity in epithelial ovarian cancer. *Int. J. Gynecol. Cancer* 23, 256–263. doi: 10.1097/IGC.0b013e31827ad2b8

Chen, P., Zhu, J., Liu, D. Y., Li, H. Y., Xu, N., and Hou, M. (2014). Over-expression of survivin and VEGF in small-cell lung cancer may predict the poorer prognosis. *Med. Oncol.* 31:775. doi: 10.1007/s12032-013-0775-5

Cheung, L. S., Fu, J., Kumar, P., Kumar, A., Urbanowski, M. E., Ihms, E. A., et al. (2019). Second-generation IL-2 receptor-targeted diphtheria fusion toxin exhibits antitumor activity and synergy with anti-PD-1 in melanoma. *Proc. Natl. Acad. Sci. U.S.A.* 116, 3100–3105. doi: 10.1073/pnas.1815087116

Cho, J. H., Sung, B. H., and Kim, S. C. (2009). Buforins: histone H2A-derived antimicrobial peptides from toad stomach. *Biochim. Biophys. Acta* 1788, 1564–1569. doi: 10.1016/j.bbamem.2008.10.025

Choe, S., Bennett, M. J., Fujii, G., Curmi, P. M., Kantardjieff, K. A., Collier, R. J., et al. (1992). The crystal structure of diphtheria toxin. *Nature* 357, 216–222.

Chung, C. Y., Yeh, K. T., Hsu, N. C., Chang, J. H., Lin, J. T., Horng, H. C., et al. (2005). Expression of c-kit protooncogene in human hepatocellular carcinoma. *Cancer Lett.* 217, 231–236. doi: 10.1016/j.canlet.2004.06.045

Cohen, K. A., Liu, T., Bissonette, R., Puri, R. K., and Frankel, A. E. (2003). DAB389EGF fusion protein therapy of refractory Glioblastoma multiforme. *Curr. Pharm. Biotechnol.* 4, 39–49. doi: 10.2174/1389201033378039

Cohen, K. A., Liu, T. F., Cline, J. M., Wagner, J. D., Hall, P. D., and Frankel, A. E. (2004). Toxicology and pharmacokinetics of DT388IL3, a fusion toxin consisting of a truncated diphtheria toxin (DT388) linked to human interleukin 3 (IL3), in cynomolgus monkeys. *Leuk. Lymphoma* 45, 1647–1656. doi: 10.1080/10428190410001663572

Cohen, K. A., Liu, T. F., Cline, J. M., Wagner, J. D., Hall, P. D., and Frankel, A. E. (2005). Safety evaluation of DT388IL3, a diphtheria toxin/interleukin 3 fusion protein, in the cynomolgus monkey. *Cancer Immunol. Immunother.* 54, 799–806. doi: 10.1007/s00262-004-0643-4

Cole, L. A., Wang, Y. X., Elliott, M., Latif, M., Chambers, J. T., Chambers, S. K., et al. (1988). Urinary human chorionic gonadotropin free beta-subunit and beta-core fragment: a new marker of gynecological cancers. *Cancer Res.* 48, 1356–1360.

Collier, R. J. (2001). Understanding the mode of action of diphtheria toxin: a perspective on progress during the 20th century. *Toxicon* 39, 1793–1803. doi: 10.1016/s0041-0101(01)00165-9

Conry, R. M., Khazaeli, M. B., Saleh, M. N., Ghetie, V., Vitetta, E. S., Liu, T., et al. (1995). Phase I trial of an anti-CD19 deglycosylated ricin A chain immunotoxin in non-Hodgkin's lymphoma: effect of an intensive schedule of administration. *J. Immunother. Emphasis Tumor Immunol.* 18, 231–241. doi: 10.1097/00002371-199511000-00004

Cui, H., Onyango, P., Brandenburg, S., Wu, Y., Hsieh, C. L., and Feinberg, A. P. (2002). Loss of imprinting in colorectal cancer linked to hypomethylation of H19 and IGF2. *Cancer Res.* 62, 6442–6446.

Daniels, T. R., Bernabeu, E., Rodriguez, J. A., Patel, S., Kozman, M., Chiappetta, D. A., et al. (2012). The transferrin receptor and the targeted delivery of therapeutic agents against cancer. *Biochim. Biophys. Acta* 1820, 291–317. doi: 10.1016/j.bbagen.2011.07.016

De La Coste, A., Romagnolo, B., Billuart, P., Renard, C. A., Buendia, M. A., Soubrane, O., et al. (1998). Somatic mutations of the beta-catenin gene are frequent in mouse and human hepatocellular carcinomas. *Proc. Natl. Acad. Sci. U.S.A.* 95, 8847–8851. doi: 10.1073/pnas.95.15.8847

Debinski, W., Gibo, D. M., Hulet, S. W., Connor, J. R., and Gillespie, G. Y. (1999). Receptor for interleukin 13 is a marker and therapeutic target for human high-grade gliomas. *Clin. Cancer Res.* 5, 985–990.

Denkberg, G., Lev, A., Eisenbach, L., Benhar, I., and Reiter, Y. (2003). Selective targeting of melanoma and APCs using a recombinant antibody with TCR-like specificity directed toward a melanoma differentiation antigen. *J. Immunol.* 171, 2197–2207. doi: 10.4049/jimmunol.171.5.2197

Dhillon, S. (2018). Moxetumomab pasudotox: first global approval. *Drugs* 78, 1763–1767. doi: 10.1007/s40265-018-1000-9

Ducry, L., and Stump, B. (2010). Antibody-drug conjugates: linking cytotoxic payloads to monoclonal antibodies. *Bioconjug. Chem.* 21, 5–13. doi: 10.1021/bc9002019

Duvic, M., Kuzel, T. M., Dang, N. H., Prince, M., Feldman, T., Foss, F. M., et al. (2014). A dose finding lead-in study of E7777 (Diphtheria toxin fragment-Interleukin-2 Fusion Protein) in persistent or recurrent cutaneous T-cell lymphoma (CTCL). *Blood* 124, 3097–3097.

Duvic, M., Kuzel, T. M., Olsen, E. A., Martin, A. G., Foss, F. M., Kim, Y. H., et al. (2002). Quality-of-life improvements in cutaneous T-cell lymphoma patients treated with denileukin diftitox (ONTAK). *Clin. Lymphoma* 2, 222–228. doi: 10.3816/clm.2002.n.003

Elias, A., Gritsenko, N., Gorovits, R., Spector, I., Prag, G., Yagil, E., et al. (2018). Anti-cancer binary system activated by bacteriophage HK022 integrase. *Oncotarget* 9, 27487–27501. doi: 10.18632/oncotarget.25512

Engstrom, W., Shokrai, A., Otte, K., Granerus, M., Gessbo, A., Bierke, P., et al. (1998). Transcriptional regulation and biological significance of the insulin like growth factor II gene. *Cell Prolif.* 31, 173–189. doi: 10.1111/j.1365-2184.1998.tb01196.x

Fang, Y. X., Zhang, X. B., Wei, W., Liu, Y. W., Chen, J. Z., Xue, J. L., et al. (2010). Development of chimeric gene regulators for cancer-specific gene therapy with both transcriptional and translational targeting. *Mol. Biotechnol.* 45, 71–81. doi: 10.1007/s12033-010-9244-y

Ferlay, J., Ervik, M., Lam, F., Colombet, M., Mery, L., Piñeros, M., et al. (2018). *Global Cancer Observatory: Cancer Tomorrow*. Lyon: International Agency for Research on Cancer.

Feuring-Buske, M., Frankel, A., Gerhard, B., and Hogge, D. (2000). Variable cytotoxicity of diphtheria toxin 388-granulocyte-macrophage colony-stimulating factor fusion protein for acute myelogenous leukemia stem cells. *Exp. Hematol.* 28, 1390–1400. doi: 10.1016/s0301-472x(00)00542-7

Feuring-Buske, M., Frankel, A. E., Alexander, R. L., Gerhard, B., and Hogge, D. E. (2002). A diphtheria toxin-interleukin 3 fusion protein is cytotoxic to primitive acute myeloid leukemia progenitors but spares normal progenitors. *Cancer Res.* 62, 1730–1736.

Fogar, P., Navaglia, F., Basso, D., Zambon, C. F., Moserle, L., Indraccolo, S., et al. (2010). Heat-induced transcription of diphtheria toxin A or its variants, CRM176 and CRM197: implications for pancreatic cancer gene therapy. *Cancer Gene Ther.* 17, 58–68. doi: 10.1038/cgt.2009.48

Frank, S. J., Engel, I., Rutledge, T. M., and Letourneur, F. (1991). Structure/function analysis of the invariant subunits of the T cell antigen receptor. *Semin. Immunol.* 3, 299–311.

Frankel, A., Liu, J. S., Rizzieri, D., and Hogge, D. (2008). Phase I clinical study of diphtheria toxin-interleukin 3 fusion protein in patients with acute myeloid leukemia and myelodysplasia. *Leuk. Lymphoma* 49, 543–553. doi: 10.1080/10428190701799035

Frankel, A. E., Beran, M., Hogge, D. E., Powell, B. L., Thorburn, A., Chen, Y. Q., et al. (2002a). Malignant progenitors from patients with CD87+ acute myelogenous leukemia are sensitive to a diphtheria toxin-urokinase fusion protein. *Exp. Hematol.* 30, 1316–1323. doi: 10.1016/s0301-472x(02)00925-6

Frankel, A. E., Powell, B. L., Hall, P. D., Case, L. D., and Kreitman, R. J. (2002b). Phase I trial of a novel diphtheria toxin/granulocyte macrophage colony-stimulating factor fusion protein (DT388GMCSF) for refractory or relapsed acute myeloid leukemia. *Clin. Cancer Res.* 8, 1004–1013.

Frankel, A. E., Fleming, D. R., Powell, B. L., and Gartenhaus, R. (2003). DAB389IL2 (ONTAK) fusion protein therapy of chronic lymphocytic leukaemia. *Expert. Opin. Biol. Ther.* 3, 179–186. doi: 10.1517/14712598.3.1.179

Frankel, A. E., Hall, P. D., Burbage, C., Vesely, J., Willingham, M., Bhalla, K., et al. (1997). Modulation of the apoptotic response of human myeloid leukemia cells to a diphtheria toxin granulocyte-macrophage colony-stimulating factor fusion protein. *Blood* 90, 3654–3661.

Frankel, A. E., Mccubrey, J. A., Miller, M. S., Delatte, S., Ramage, J., Kiser, M., et al. (2000). Diphtheria toxin fused to human interleukin-3 is toxic to blasts from patients with myeloid leukemias. *Leukemia* 14, 576–585. doi: 10.1038/sj.leu.2401743

Frankel, A. E., Woo, J. H., Ahn, C., Foss, F. M., Duvic, M., Neville, P. H., et al. (2015). Resimmune, an anti-CD3epsilon recombinant immunotoxin, induces durable remissions in patients with cutaneous T-cell lymphoma. *Haematologica* 100, 794–800. doi: 10.3324/haematol.2015.123711

Frankel, A. E., Woo, J. H., Ahn, C., Pemmaraju, N., Medeiros, B. C., Carraway, H. E., et al. (2014). Activity of SL-401, a targeted therapy directed to interleukin-3 receptor, in blastic plasmacytoid dendritic cell neoplasm patients. *Blood* 124, 385–392. doi: 10.1182/blood-2014-04-566737

Frankel, A. E., Zuckero, S. L., Mankin, A. A., Grable, M., Mitchell, K., Lee, Y. J., et al. (2009). Anti-CD3 recombinant diphtheria immunotoxin therapy of cutaneous T cell lymphoma. *Curr. Drug Targets* 10, 104–109. doi: 10.2174/138945009787354539

Gofrit, O. N., Benjamin, S., Halachmi, S., Leibovitch, I., Dotan, Z., Lamm, D. L., et al. (2014). DNA based therapy with diphtheria toxin-A BC-819: a phase 2b marker lesion trial in patients with intermediate risk nonmuscle invasive bladder cancer. *J. Urol.* 191, 1697–1702. doi: 10.1016/j.juro.2013.12.011

Gottlieb, S. L., Gilleaudeau, P., Johnson, R., Estes, L., Woodworth, T. G., Gottlieb, A. B., et al. (1995). Response of psoriasis to a lymphocyte-selective toxin (DAB389IL-2) suggests a primary immune, but not keratinocyte, pathogenic basis. *Nat. Med.* 1, 442–447. doi: 10.1038/nm0595-442

Greenfield, L., Johnson, V. G., and Youle, R. J. (1987). Mutations in diphtheria toxin separate binding from entry and amplify immunotoxin selectivity. *Science* 238, 536–539. doi: 10.1126/science.3498987

Hagihara, N., Walbridge, S., Olson, A. W., Oldfield, E. H., and Youle, R. J. (2000). Vascular protection by chloroquine during brain tumor therapy with Tf-CRM107. *Cancer Res.* 60, 230–234.

Hall, P. D., Willingham, M. C., Kreitman, R. J., and Frankel, A. E. (1999). DT388-GM-CSF, a novel fusion toxin consisting of a truncated diphtheria toxin fused to human granulocyte-macrophage colony-stimulating factor, prolongs host survival in a SCID mouse model of acute myeloid leukemia. *Leukemia* 13, 629–633. doi: 10.1038/sj.leu.2401357

Hall, W. A., and Vallera, D. A. (2006). Efficacy of antiangiogenic targeted toxins against glioblastoma multiforme. *Neurosurg. Focus* 20:E23.

Hanna, N., Ohana, P., Konikoff, F. M., Leichtmann, G., Hubert, A., Appelbaum, L., et al. (2012). Phase 1/2a, dose-escalation, safety, pharmacokinetic and preliminary efficacy study of intratumoral administration of BC-819 in patients with unresectable pancreatic cancer. *Cancer Gene Ther.* 19, 374–381. doi: 10.1038/cgt.2012.10

Hasenpusch, G., Pfeifer, C., Aneja, M. K., Wagner, K., Reinhardt, D., Gilon, M., et al. (2011). Aerosolized BC-819 inhibits primary but not secondary lung cancer growth. *PLoS One* 6:e20760. doi: 10.1371/journal.pone.0020760

He, Q., and Shi, J. (2014). MSN anti-cancer nanomedicines: chemotherapy enhancement, overcoming of drug resistance, and metastasis inhibition. *Adv. Mater.* 26, 391–411. doi: 10.1002/adma.201303123

Herrera, L., Farah, R. A., Pellegrini, V. A., Aquino, D. B., Sandler, E. S., Buchanan, G. R., et al. (2000). Immunotoxins against CD19 and CD22 are effective in killing precursor-B acute lymphoblastic leukemia cells *in vitro*. *Leukemia* 14, 853–858. doi: 10.1038/sj.leu.2401779

Herrera, L., Yarbrough, S., Ghetie, V., Aquino, D. B., and Vitetta, E. S. (2003). Treatment of SCID/human B cell precursor ALL with anti-CD19 and anti-CD22 immunotoxins. *Leukemia* 17, 334–338. doi: 10.1038/sj.leu.2402790

Hine, C. M., Seluanov, A., and Gorbunova, V. (2008). Use of the Rad51 promoter for targeted anti-cancer therapy. *Proc. Natl. Acad. Sci. U.S.A.* 105, 20810–20815. doi: 10.1073/pnas.0807990106

Hine, C. M., Seluanov, A., and Gorbunova, V. (2012). Rad51 promoter-targeted gene therapy is effective for *in vivo* visualization and treatment of cancer. *Mol. Ther.* 20, 347–355. doi: 10.1038/mt.2011.215

Hirota, S., Isozaki, K., Moriyama, Y., Hashimoto, K., Nishida, T., Ishiguro, S., et al. (1998). Gain-of-function mutations of c-kit in human gastrointestinal stromal tumors. *Science* 279, 577–580. doi: 10.1126/science.279.5350.577

Hogge, D. E., Willman, C. L., Kreitman, R. J., Berger, M., Hall, P. D., Kopecky, K. J., et al. (1998). Malignant progenitors from patients with acute myelogenous leukemia are sensitive to a diphtheria toxin-granulocyte-macrophage colony-stimulating factor fusion protein. *Blood* 92, 589–595.

Holmes, R. K. (2000). Biology and molecular epidemiology of diphtheria toxin and the tox gene. *J. Infect. Dis.* 181(Suppl. 1), S156–S167.

Holthuizen, P., Van Der Lee, F. M., Ikejiri, K., Yamamoto, M., and Sussenbach, J. S. (1990). Identification and initial characterization of a fourth leader exon and promoter of the human IGF-II gene. *Biochim. Biophys. Acta* 1087, 341–343. doi: 10.1016/0167-4781(90)90010-y

Hotchkiss, C. E., Hall, P. D., Cline, J. M., Willingham, M. C., Kreitman, R. J., Gardin, J., et al. (1999). Toxicology and pharmacokinetics of DTGM, a fusion toxin consisting of a truncated diphtheria toxin (DT388) linked to human granulocyte-macrophage colony-stimulating factor, in cynomolgus monkeys. *Toxicol. Appl. Pharmacol.* 158, 152–160. doi: 10.1006/taap.1999.8691

Huang, J., Li, Y. M., Massague, J., Sicheneder, A., Vallera, D. A., and Hall, W. A. (2012). Intracerebral infusion of the bispecific targeted toxin DTATEGF in a mouse xenograft model of a human metastatic non-small cell lung cancer. *J. Neurooncol.* 109, 229–238. doi: 10.1007/s11060-012-0904-6

Humphrey, P. A., Wong, A. J., Vogelstein, B., Zalutsky, M. R., Fuller, G. N., Archer, G. E., et al. (1990). Anti-synthetic peptide antibody reacting at the fusion junction of deletion-mutant epidermal growth factor receptors in human glioblastoma. *Proc. Natl. Acad. Sci. U.S.A.* 87, 4207–4211. doi: 10.1073/pnas.87.11.4207

Ito, H., Kyo, S., Kanaya, T., Takakura, M., Inoue, M., and Namiki, M. (1998). Expression of human telomerase subunits and correlation with telomerase activity in urothelial cancer. *Clin. Cancer Res.* 4, 1603–1608.

Jahanian-Najafabadi, A., Bouzari, S., Oloomi, M., Roudkenar, M. H., and Mayr, L. M. (2012a). Attempts to express the A1-GMCSF immunotoxin in the baculovirus expression vector system. *Biosci. Biotechnol. Biochem.* 76, 749–754. doi: 10.1271/bbb.110862

Jahanian-Najafabadi, A., Bouzari, S., Oloomi, M., Roudkenar, M. H., and Shokrgozar, M. A. (2012b). Assessment of selective toxicity of insect cell expressed recombinant A1-GMCSF protein toward GMCSF receptor bearing tumor cells. *Res. Pharm. Sci.* 7, 133–140.

Javan, B., and Shahbazi, M. (2017). Hypoxia-inducible tumour-specific promoters as a dual-targeting transcriptional regulation system for cancer gene therapy. *Ecancermedicalscience* 11:751. doi: 10.3332/ecancer.2017.751

Johnson, V. G., Wilson, D., Greenfield, L., and Youle, R. J. (1988). The role of the diphtheria toxin receptor in cytosol translocation. *J. Biol. Chem.* 263, 1295–1300.

Joshi, B. H., and Puri, R. K. (2009). IL-13 receptor-α2: a novel target for cancer therapy. *Immunotherapy* 1, 321–327. doi: 10.2217/imt.09.8

Kaplan, R., Luettich, K., Heguy, A., Hackett, N. R., Harvey, B. G., and Crystal, R. G. (2003). Monoallelic up-regulation of the imprinted H19 gene in airway epithelium of phenotypically normal cigarette smokers. *Cancer Res.* 63, 1475–1482.

Kersemans, V., and Cornelissen, B. (2010). Targeting the Tumour: cell Penetrating Peptides for Molecular Imaging and Radiotherapy. *Pharmaceuticals* 3, 600–620. doi: 10.3390/ph3030600

Kim, H. P., Imbert, J., and Leonard, W. J. (2006). Both integrated and differential regulation of components of the IL-2/IL-2 receptor system. *Cytokine Growth Factor Rev.* 17, 349–366. doi: 10.1016/j.cytogfr.2006.07.003

Kiyokawa, T., Williams, D. P., Snider, C. E., Strom, T. B., and Murphy, J. R. (1991). Protein engineering of diphtheria-toxin-related interleukin-2 fusion toxins to increase cytotoxic potency for high-affinity IL-2-receptor-bearing target cells. *Protein Eng.* 4, 463–468. doi: 10.1093/protein/4.4.463

Knechtle, S. J., Vargo, D., Fechner, J., Zhai, Y., Wang, J., Hanaway, M. J., et al. (1997). FN18-CRM9 immunotoxin promotes tolerance in primate renal allografts. *Transplantation* 63, 1–6. doi: 10.1097/00007890-199701150-00002

Kreitman, R. J. (2006). Immunotoxins for targeted cancer therapy. *AAPS J* 8, E532–E551.

Kunitomi, M., Takayama, E., Suzuki, S., Yasuda, T., Tsutsui, K., Nagaike, K., et al. (2000). Selective inhibition of hepatoma cells using diphtheria toxin A under the control of the promoter/enhancer region of the human alpha-fetoprotein gene. *Jpn. J. Cancer Res.* 91, 343–350. doi: 10.1111/j.1349-7006.2000.tb00951.x

Kuzel, T. M., Rosen, S. T., Gordon, L. I., Winter, J., Samuelson, E., Kaul, K., et al. (1993). Phase I trial of the diphtheria toxin/interleukin-2 fusion

protein DAB486IL-2: efficacy in mycosis fungoides and other non-Hodgkin's lymphomas. *Leuk. Lymphoma* 11, 369–377. doi: 10.3109/10428199309067928

Lanza, F., Castoldi, G. L., Castagnari, B., Todd III, R. F., Moretti, S., Spisani, S., et al. (1998). Expression and functional role of urokinase-type plasminogen activator receptor in normal and acute leukaemic cells. *Br. J. Haematol.* 103, 110–123.

Laske, D. W., Ilercil, O., Akbasak, A., Youle, R. J., and Oldfield, E. H. (1994). Efficacy of direct intratumoral therapy with targeted protein toxins for solid human gliomas in nude mice. *J. Neurosurg.* 80, 520–526. doi: 10.3171/jns.1994.80.3.0520

Lavie, O., Edelman, D., Levy, T., Fishman, A., Hubert, A., Segev, Y., et al. (2017). A phase 1/2a, dose-escalation, safety, pharmacokinetic, and preliminary efficacy study of intraperitoneal administration of BC-819 (H19-DTA) in subjects with recurrent ovarian/peritoneal cancer. *Arch. Gynecol. Obstet.* 295, 751–761. doi: 10.1007/s00404-017-4293-0

Lee, H. S., Park, C. B., Kim, J. M., Jang, S. A., Park, I. Y., Kim, M. S., et al. (2008). Mechanism of anticancer activity of buforin IIb, a histone H2A-derived peptide. *Cancer Lett.* 271, 47–55. doi: 10.1016/j.canlet.2008.05.041

LeMaistre, C. F., Craig, F. E., Meneghetti, C., Mcmullin, B., Parker, K., Reuben, J., et al. (1993). Phase I trial of a 90-minute infusion of the fusion toxin DAB486IL-2 in hematological cancers. *Cancer Res.* 53, 3930–3934.

LeMaistre, C. F., Meneghetti, C., Rosenblum, M., Reuben, J., Parker, K., Shaw, J., et al. (1992). Phase I trial of an interleukin-2 (IL-2) fusion toxin (DAB486IL-2) in hematologic malignancies expressing the IL-2 receptor. *Blood* 79, 2547–2554.

LeMaistre, C. F., Saleh, M. N., Kuzel, T. M., Foss, F., Platanias, L. C., Schwartz, G., et al. (1998). Phase I trial of a ligand fusion-protein (DAB389IL-2) in lymphomas expressing the receptor for interleukin-2. *Blood* 91, 399–405.

Li, C., Hall, W. A., Jin, N., Todhunter, D. A., Panoskaltsis-Mortari, A., and Vallera, D. A. (2002). Targeting glioblastoma multiforme with an IL-13/diphtheria toxin fusion protein *in vitro* and *in vivo* in nude mice. *Protein Eng.* 15, 419–427. doi: 10.1093/protein/15.5.419

Li, Y., Mccadden, J., Ferrer, F., Kruszewski, M., Carducci, M., Simons, J., et al. (2002). Prostate-specific expression of the diphtheria toxin A chain (DT-A): studies of inducibility and specificity of expression of prostate-specific antigen promoter-driven DT-A adenoviral-mediated gene transfer. *Cancer Res.* 62, 2576–2582.

Lidor, Y. J., Lee, W. E., Nilson, J. H., Maxwell, I. H., Su, L. J., Brand, E., et al. (1997). *In vitro* expression of the diphtheria toxin A-chain gene under the control of human chorionic gonadotropin gene promoters as a means of directing toxicity to ovarian cancer cell lines. *Am. J. Obstet. Gynecol.* 177, 579–585. doi: 10.1016/s0002-9378(97)70149-2

Lim, K. J., Sung, B. H., Shin, J. R., Lee, Y. W., Kim, D. J., Yang, K. S., et al. (2013). A cancer specific cell-penetrating peptide, BR2, for the efficient delivery of an scFv into cancer cells. *PLoS One* 8:e66084. doi: 10.1371/journal.pone.0066084

Lin, B., Gao, A., Zhang, R., Ma, H., Shen, H., Hu, Q., et al. (2015). Use of a novel integrase-deficient lentivirus for targeted anti-cancer therapy with survivin promoter-driven diphtheria toxin A. *Medicine* 94:e1301. doi: 10.1097/MD.0000000000001301

Lipinski, K. S., Djeha, A. H., Ismail, T., Mountain, A., Young, L. S., and Wrighton, C. J. (2001). High-level, beta-catenin/TCF-dependent transgene expression in secondary colorectal cancer tissue. *Mol. Ther.* 4, 365–371. doi: 10.1006/mthe.2001.0468

Lipinski, K. S., Djeha, H. A., Gawn, J., Cliffe, S., Maitland, N. J., Palmer, D. H., et al. (2004). Optimization of a synthetic beta-catenin-dependent promoter for tumor-specific cancer gene therapy. *Mol. Ther.* 10, 150–161. doi: 10.1016/j.ymthe.2004.03.021

Liu, T. F., Cohen, K. A., Ramage, J. G., Willingham, M. C., Thorburn, A. M., and Frankel, A. E. (2003). A diphtheria toxin-epidermal growth factor fusion protein is cytotoxic to human glioblastoma multiforme cells. *Cancer Res.* 63, 1834–1837.

Liu, Y. Y., Gordienko, I., Mathias, A., Ma, S., Thompson, J., Woo, J. H., et al. (2000). Expression of an anti-CD3 single-chain immunotoxin with a truncated diphtheria toxin in a mutant CHO cell line. *Protein Expr. Purif.* 19, 304–311. doi: 10.1006/prep.2000.1255

Louie, G. V., Yang, W., Bowman, M. E., and Choe, S. (1997). Crystal structure of the complex of diphtheria toxin with an extracellular fragment of its receptor. *Mol. Cell* 1, 67–78. doi: 10.1016/s1097-2765(00)80008-8

Lustig-Yariv, O., Schulze, E., Komitowski, D., Erdmann, V., Schneider, T., De Groot, N., et al. (1997). The expression of the imprinted genes H19 and IGF-2 in choriocarcinoma cell lines. *Is H*19 a tumor suppressor gene? *Oncogene* 15, 169–177. doi: 10.1038/sj.onc.1201175

Ma, S., Hu, H., Thompson, J., Stavrou, S., Scharff, J., and Neville, D. M. Jr. (1997). Genetic construction and characterization of an anti-monkey CD3 single-chain immunotoxin with a truncated diphtheria toxin. *Bioconjug. Chem.* 8, 695–701. doi: 10.1021/bc9701398

Ma, X., Lv, P., Ye, S., Zhang, Y., Li, S., Kan, C., et al. (2013). DT390-triTMTP1, a novel fusion protein of diphtheria toxin with tandem repeat TMTP1 peptide, preferentially targets metastatic tumors. *Mol. Pharm.* 10, 115–126. doi: 10.1021/mp300125k

Maruyama, D., Tobinai, K., Ando, K., Ohmachi, K., Ogura, M., Uchida, T., et al. (2015). Phase I study of E7777, a diphtheria toxin fragment-interleukin-2 fusion protein, in japanese patients with relapsed or refractory peripheral and Cutaneous T-Cell lymphoma. *Blood* 126, 2724–2724.

Maxwell, I. H., Glode, L. M., and Maxwell, F. (1992). Expression of diphtheria toxin A-chain in mature B-cells: a potential approach to therapy of B-lymphoid malignancy. *Leuk. Lymphoma* 7, 457–462.

Mccrann, D. J., Yezefski, T., Nguyen, H. G., Papadantonakis, N., Liu, H., Wen, Q., et al. (2008). Survivin overexpression alone does not alter megakaryocyte ploidy nor interfere with erythroid/megakaryocytic lineage development in transgenic mice. *Blood* 111, 4092–4095. doi: 10.1182/blood-2007-11-122150

Meng, J., Liu, Y., Gao, S., Lin, S., Gu, X., Pomper, M. G., et al. (2015). A bivalent recombinant immunotoxin with high potency against tumors with EGFR and EGFRvIII expression. *Cancer Biol. Ther.* 16, 1764–1774. doi: 10.1080/15384047.2015.1095403

Meng, J. R., Tang, H. Z., Zhou, K. Z., Shen, W. H., and Guo, H. Y. (2013). TFF3 and survivin expressions associate with a lower survival rate in gastric cancer. *Clin. Exp. Med.* 13, 297–303. doi: 10.1007/s10238-012-0210-9

Mizrahi, A., Czerniak, A., Levy, T., Amiur, S., Gallula, J., Matouk, I., et al. (2009). Development of targeted therapy for ovarian cancer mediated by a plasmid expressing diphtheria toxin under the control of H19 regulatory sequences. *J. Transl. Med.* 7:69. doi: 10.1186/1479-5876-7-69

Mizrahi, A., Czerniak, A., Ohana, P., Amiur, S., Gallula, J., Matouk, I., et al. (2010a). Treatment of ovarian cancer ascites by intra-peritoneal injection of diphtheria toxin A chain-H19 vector: a case report. *J. Med. Case Rep.* 4:228. doi: 10.1186/1752-1947-4-228

Mizrahi, A., Hochberg, A., Amiur, S., Gallula, J., Matouk, I., Birman, T., et al. (2010b). Targeting diphtheria toxin and TNF alpha expression in ovarian tumors using the H19 regulatory sequences. *Int. J. Clin. Exp. Med.* 3, 270–282.

Moreland, L. W., Sewell, K. L., Trentham, D. E., Bucy, R. P., Sullivan, W. F., Schrohenloher, R. E., et al. (1995). Interleukin-2 diphtheria fusion protein (DAB486IL-2) in refractory rheumatoid arthritis. A double-blind, placebo-controlled trial with open-label extension. *Arthritis Rheum* 38, 1177–1186. doi: 10.1002/art.1780380902

Mori, T., Abe, T., Wakabayashi, Y., Hikawa, T., Matsuo, K., Yamada, Y., et al. (2000). Up-regulation of urokinase-type plasminogen activator and its receptor correlates with enhanced invasion activity of human glioma cells mediated by transforming growth factor-alpha or basic fibroblast growth factor. *J. Neurooncol.* 46, 115–123.

Murayama, Y., Tadakuma, T., Kunitomi, M., Kumai, K., Tsutsui, K., Yasuda, T., et al. (1999). Cell-specific expression of the diphtheria toxin A-chain coding sequence under the control of the upstream region of the human alpha-fetoprotein gene. *J. Surg. Oncol.* 70, 145–149. doi: 10.1002/(sici)1096-9098(199903)70:3<145::aid-jso1>3.0.co;2-o

Naeem, M., Dahiya, M., Clark, J. I., Creech, S. D., and Alkan, S. (2002). Analysis of c-kit protein expression in small-cell lung carcinoma and its implication for prognosis. *Hum. Pathol.* 33, 1182–1187. doi: 10.1053/hupa.2002.129199

Nagane, M., Coufal, F., Lin, H., Bogler, O., Cavenee, W. K., and Huang, H. J. (1996). A common mutant epidermal growth factor receptor confers enhanced tumorigenicity on human glioblastoma cells by increasing proliferation and reducing apoptosis. *Cancer Res.* 56, 5079–5086.

Nicholson, I. C., Lenton, K. A., Little, D. J., Decorso, T., Lee, F. T., Scott, A. M., et al. (1997). Construction and characterisation of a functional CD19 specific single chain Fv fragment for immunotherapy of B lineage leukaemia and lymphoma. *Mol. Immunol.* 34, 1157–1165. doi: 10.1016/s0161-5890(97)00144-2

Oh, S., Ohlfest, J. R., Todhunter, D. A., Vallera, V. D., Hall, W. A., Chen, H., et al. (2009). Intracranial elimination of human glioblastoma brain tumors in nude rats using the bispecific ligand-directed toxin, DTEGF13 and convection enhanced delivery. *J. Neurooncol.* 95, 331–342. doi: 10.1007/s11060-009-9932-2

Oh, S., Stish, B. J., Vickers, S. M., Buchsbaum, D. J., Saluja, A. K., and Vallera, D. A. (2010). A new drug delivery method of bispecific ligand-directed toxins, which reduces toxicity and promotes efficacy in a model of orthotopic pancreatic cancer. *Pancreas* 39, 913–922. doi: 10.1097/MPA.0b013e3181cbd908

Ohana, P., Bibi, O., Matouk, I., Levy, C., Birman, T., Ariel, I., et al. (2002). Use of H19 regulatory sequences for targeted gene therapy in cancer. *Int. J. Cancer* 98, 645–650. doi: 10.1002/ijc.10243

Ohana, P., Gofrit, O., Ayesh, S., Al-Sharef, W., Mizrahi, A., Birman, T., et al. (2004). Regulatory sequences of the H19 gene in DNA based therapy of bladder cancer. *Gene Ther. Mol. Biol.* 8, 181–192.

Ohmachi, K., Ando, K., Ogura, M., Uchida, T., Tobinai, K., Maruyama, D., et al. (2018). E7777 in Japanese patients with relapsed/refractory peripheral and cutaneous T-cell lymphoma: a phase I study. *Cancer Sci.* 109, 794–802. doi: 10.1111/cas.13513

Olsen, E., Duvic, M., Frankel, A., Kim, Y., Martin, A., Vonderheid, E., et al. (2001). Pivotal phase III trial of two dose levels of denileukin diftitox for the treatment of cutaneous T-cell lymphoma. *J. Clin. Oncol.* 19, 376–388.

Onda, M., Nagata, S., Fitzgerald, D. J., Beers, R., Fisher, R. J., Vincent, J. J., et al. (2006). Characterization of the B cell epitopes associated with a truncated form of *Pseudomonas* exotoxin (PE38) used to make immunotoxins for the treatment of cancer patients. *J. Immunol.* 177, 8822–8834. doi: 10.4049/jimmunol.177.12.8822

Padma, V. V. (2015). An overview of targeted cancer therapy. *Biomedicine* 5:19. doi: 10.7603/s40681-015-0019-4

Pang, S. (2000). Targeting and eradicating cancer cells by a prostate-specific vector carrying the diphtheria toxin A gene. *Cancer Gene Ther.* 7, 991–996. doi: 10.1038/sj.cgt.7700197

Park, L. S., Waldron, P. E., Friend, D., Sassenfeld, H. M., Price, V., Anderson, D., et al. (1989). Interleukin-3, GM-CSF, and G-CSF receptor expression on cell lines and primary leukemia cells: receptor heterogeneity and relationship to growth factor responsiveness. *Blood* 74, 56–65.

Peaker, C. J., and Neuberger, M. S. (1993). Association of CD22 with the B cell antigen receptor. *Eur. J. Immunol.* 23, 1358–1363. doi: 10.1002/eji.1830230626

Pemmaraju, N., Sweet, K. L., Lane, A. A., Stein, A. S., Vasu, S., Blum, W., et al. (2017). Results of pivotal phase 2 trial of SL-401 in patients with blastic plasmacytoid dendritic cell neoplasm (BPDCN). *Blood* 130, 1298–1298.

Peng, W., Chen, J., Huang, Y. H., and Sawicki, J. A. (2005). Tightly-regulated suicide gene expression kills PSA-expressing prostate tumor cells. *Gene Ther.* 12, 1573–1580. doi: 10.1038/sj.gt.3302580

Peraino, J. S., Zhang, H., Rajasekera, P. V., Wei, M., Madsen, J. C., Sachs, D. H., et al. (2014). Diphtheria toxin-based bivalent human IL-2 fusion toxin with improved efficacy for targeting human CD25(+) cells. *J. Immunol. Methods* 405, 57–66. doi: 10.1016/j.jim.2014.01.008

Pfeiffer, A., Rothbauer, E., Wiebecke, B., Pratschke, E., Kramling, H. J., and Mann, K. (1990). Increased epidermal growth factor receptors in gastric carcinomas. *Gastroenterology* 98, 961–967. doi: 10.1016/0016-5085(90)90020-2

Potala, S., and Verma, R. S. (2010). A novel fusion protein diphtheria toxin-stem cell factor (DT-SCF)-purification and characterization. *Appl. Biochem. Biotechnol.* 162, 1258–1269. doi: 10.1007/s12010-009-8896-1

Raderschall, E., Stout, K., Freier, S., Suckow, V., Schweiger, S., and Haaf, T. (2002). Elevated levels of Rad51 recombination protein in tumor cells. *Cancer Res.* 62, 219–225.

Ramadan, M. A., Gabr, N. S., Bacha, P., Gunzler, V., and Phillips, S. M. (1995). Suppression of immunopathology in schistosomiasis by interleukin-2-targeted fusion toxin, DAB389IL-2. I. Studies of in vitro and in vivo efficacy. *Cell Immunol.* 166, 217–226. doi: 10.1006/cimm.1995.9976

Ramage, J. G., Vallera, D. A., Black, J. H., Aplan, P. D., Kees, U. R., and Frankel, A. E. (2003). The diphtheria toxin/urokinase fusion protein (DTAT) is selectively toxic to CD87 expressing leukemic cells. *Leuk. Res.* 27, 79–84. doi: 10.1016/s0145-2126(02)00077-2

Raspollini, M. R., Amunni, G., Villanucci, A., Baroni, G., Taddei, A., and Taddei, G. L. (2004). c-KIT expression and correlation with chemotherapy resistance in ovarian carcinoma: an immunocytochemical study. *Ann. Oncol.* 15, 594–597. doi: 10.1093/annonc/mdh139

Re, G. G., Waters, C., Poisson, L., Willingham, M. C., Sugamura, K., and Frankel, A. E. (1996). Interleukin 2 (IL-2) receptor expression and sensitivity to diphteria fusion toxin DAB389IL-2 in cultured hematopoietic cells. *Cancer Res.* 56, 2590–2595.

Reiter, Y. (2001). Recombinant immunotoxins in targeted cancer cell therapy. *Adv. Cancer Res.* 81, 93–124. doi: 10.1016/s0065-230x(01)81003-4

Rosas, M., Gordon, S., and Taylor, P. R. (2007). Characterisation of the expression and function of the GM-CSF receptor α-chain in mice. *Eur. J. Immunol.* 37, 2518–2528. doi: 10.1002/eji.200636892

Rozemuller, H., Rombouts, E. J., Touw, I. P., Fitzgerald, D. J., Kreitman, R. J., Pastan, I., et al. (1997). Sensitivity of human acute myeloid leukaemia to diphtheria toxin-GM-CSF fusion protein. *Br. J. Haematol.* 98, 952–959. doi: 10.1046/j.1365-2141.1997.2893106.x

Rustamzadeh, E., Hall, W. A., Todhunter, D. A., Low, W. C., Liu, H., Panoskaltsis-Mortari, A., et al. (2006). Intracranial therapy of glioblastoma with the fusion protein DTIL13 in immunodeficient mice. *Int. J. Cancer* 118, 2594–2601. doi: 10.1002/ijc.21647

Saleh, M. N., Lemaistre, C. F., Kuzel, T. M., Foss, F., Platanias, L. C., Schwartz, G., et al. (1998). Antitumor activity of DAB389IL-2 fusion toxin in mycosis fungoides. *J. Am. Acad. Dermatol.* 39, 63–73. doi: 10.1016/s0190-9622(98)70403-7

Salvatore, G., Beers, R., Margulies, I., Kreitman, R. J., and Pastan, I. (2002). Improved cytotoxic activity toward cell lines and fresh leukemia cells of a mutant anti-CD22 immunotoxin obtained by antibody phage display. *Clin. Cancer Res.* 8, 995–1002.

Sarnovsky, R., Tendler, T., Makowski, M., Kiley, M., Antignani, A., Traini, R., et al. (2010). Initial characterization of an immunotoxin constructed from domains II and III of cholera exotoxin. *Cancer Immunol. Immunother.* 59, 737–746. doi: 10.1007/s00262-009-0794-4

Sato, S., Miller, A. S., Inaoki, M., Bock, C. B., Jansen, P. J., Tang, M. L., et al. (1996). CD22 is both a positive and negative regulator of B lymphocyte antigen receptor signal transduction: altered signaling in CD22-deficient mice. *Immunity* 5, 551–562. doi: 10.1016/s1074-7613(00)80270-8

Saukkonen, K., and Hemminki, A. (2004). Tissue-specific promoters for cancer gene therapy. *Expert Opin. Biol. Ther.* 4, 683–696. doi: 10.1517/eobt.4.5.683.31060

Schmohl, J. U., Todhunter, D., Oh, S., and Vallera, D. A. (2015). Mutagenic deimmunization of diphtheria toxin for use in biologic drug development. *Toxins* 7, 4067–4082. doi: 10.3390/toxins7104067

Schmohl, J. U., Todhunter, D., Taras, E., Bachanova, V., and Vallera, D. A. (2018). Development of a deimmunized bispecific immunotoxin dDT2219 against B-Cell malignancies. *Toxins* 10:E32. doi: 10.3390/toxins10010032

Schutte, J., and Seeber, S. (1993). Bombesin antagonists: experimental and clinical results. *Recent Results Cancer Res.* 129, 115–129. doi: 10.1007/978-3-642-84956-5_9

Sewell, K. L., Parker, K. C., Woodworth, T. G., Reuben, J., Swartz, W., and Trentham, D. E. (1993). DAB486IL-2 fusion toxin in refractory rheumatoid arthritis. *Arthritis Rheum* 36, 1223–1233. doi: 10.1002/art.1780360907

Shafiee, F., Enteshari, R., Rabbani, M., and Jahanian-Najafabadi, A. (2017a). In-vivo evaluation of DT386-BR2, a promising anticancer fusion protein in mice model. *J. Isfahan Med. Sch.* 35, 655–661. doi: 10.1016/j.mimet.2016.09.004

Shafiee, F., Minaiyan, G., Moazen, F., and Jahanian-Najafabadi, A. (2017b). Recombinant production and intein-mediated purification of an antimicrobial peptide, BR2. *Int. J. Peptide Res. Ther.* 23, 501–507. doi: 10.1007/s10989-017-9583-7

Shafiee, F., Rabbani, M., and Jahanian-Najafabadi, A. (2017c). Optimization of the expression of DT386-BR2 fusion protein in *Escherichia coli* using response surface methodology. *Adv. Biomed. Res.* 6:22. doi: 10.4103/2277-9175.201334

Shafiee, F., Rabbani, M., and Jahanian-Najafabadi, A. (2016). Production and evaluation of cytotoxic effects of DT386-BR2 fusion protein as a novel anti-cancer agent. *J. Microbiol. Methods* 130, 100–105. doi: 10.1016/j.mimet.2016.09.004

Shapira, A., and Benhar, I. (2010). Toxin-based therapeutic approaches. *Toxins* 2, 2519–2583. doi: 10.3390/toxins2112519

Shaw, J. P., Akiyoshi, D. E., Arrigo, D. A., Rhoad, A. E., Sullivan, B., Thomas, J., et al. (1991). Cytotoxic properties of DAB486EGF and DAB389EGF, epidermal

growth factor (EGF) receptor-targeted fusion toxins. *J. Biol. Chem.* 266, 21118–21124.

Sidi, A. A., Ohana, P., Benjamin, S., Shalev, M., Ransom, J. H., Lamm, D., et al. (2008). Phase I/II marker lesion study of intravesical BC-819 DNA plasmid in H19 over expressing superficial bladder cancer refractory to bacillus Calmette-Guerin. *J. Urol.* 180, 2379–2383. doi: 10.1016/j.juro.2008.08.006

Simon, N., and Fitzgerald, D. (2016). Immunotoxin therapies for the treatment of epidermal growth factor receptor-dependent cancers. *Toxins (Basel)* 8:137. doi: 10.3390/toxins8050137

Soleimani, M., Mahnam, K., Mirmohammad-Sadeghi, H., Sadeghi-Aliabadi, H., and Jahanian-Najafabadi, A. (2016). Theoretical design of a new chimeric protein for the treatment of breast cancer. *Res. Pharm. Sci.* 11, 187–199.

Soleimani, M., Sadeghi, H. M., and Jahanian-Najafabadi, A. (2019). A Bi-functional targeted P28-NRC chimeric protein with enhanced cytotoxic effects on breast cancer cell lines. *Iran J. Pharm. Res.* 18, 735–744. doi: 10.22037/ijpr.2019.2392

Sorin, V., Ohana, P., Gallula, J., Birman, T., Matouk, I., Hubert, A., et al. (2012). H19-promoter-targeted therapy combined with gemcitabine in the treatment of pancreatic cancer. *ISRN Oncol.* 2012:351750. doi: 10.5402/2012/351750

Sorin, V., Ohana, P., Mizrahi, A., Matouk, I., Birman, T., Hochberg, A., et al. (2011). Regional therapy with DTA-H19 vector suppresses growth of colon adenocarcinoma metastases in the rat liver. *Int. J. Oncol.* 39, 1407–1412. doi: 10.3892/ijo.2011.1171

Stish, B. J., Chen, H., Shu, Y., Panoskaltsis-Mortari, A., and Vallera, D. A. (2007). A bispecific recombinant cytotoxin (DTEGF13) targeting human interleukin-13 and epidermal growth factor receptors in a mouse xenograft model of prostate cancer. *Clin. Cancer Res.* 13, 6486–6493. doi: 10.1158/1078-0432.ccr-07-0938

Stish, B. J., Oh, S., and Vallera, D. A. (2008). Anti-glioblastoma effect of a recombinant bispecific cytotoxin cotargeting human IL-13 and EGF receptors in a mouse xenograft model. *J. Neurooncol.* 87, 51–61. doi: 10.1007/s11060-007-9499-8

Stone, M. J., Sausville, E. A., Fay, J. W., Headlee, D., Collins, R. H., Figg, W. D., et al. (1996). A phase I study of bolus versus continuous infusion of the anti-CD19 immunotoxin, IgG-HD37-dgA, in patients with B-cell lymphoma. *Blood* 88, 1188–1197.

Suda, T., Suda, J., Ogawa, M., and Ihle, J. N. (1985). Permissive role of interleukin 3 (IL-3) in proliferation and differentiation of multipotential hemopoietic progenitors in culture. *J. Cell Physiol.* 124, 182–190. doi: 10.1002/jcp.1041240203

Sugiyama, D., Nishikawa, H., Maeda, Y., Nishioka, M., Tanemura, A., Katayama, I., et al. (2013). Anti-CCR4 mAb selectively depletes effector-type FoxP3+CD4+ regulatory T cells, evoking antitumor immune responses in humans. *Proc. Natl. Acad. Sci. U.S.A.* 110, 17945–17950. doi: 10.1073/pnas.1316796110

Sun, W., Liu, H., Kim, Y., Karras, N., Pawlowska, A., Toomey, D., et al. (2018). First pediatric experience of SL-401, a CD123-targeted therapy, in patients with blastic plasmacytoid dendritic cell neoplasm: report of three cases. *J. Hematol. Oncol.* 11:61. doi: 10.1186/s13045-018-0604-6

Sweeney, E. B., Foss, F. M., Murphy, J. R., and Vanderspek, J. C. (1998). Interleukin 7 (IL-7) receptor-specific cell killing by DAB389 IL-7: a novel agent for the elimination of IL-7 receptor positive cells. *Bioconjug. Chem.* 9, 201–207. doi: 10.1021/bc9701757

Syed, Y. Y. (2019). Tagraxofusp: first global approval. *Drugs* 79, 579–583. doi: 10.1007/s40265-019-01087-z

Tanaka, K., Iwamoto, S., Gon, G., Nohara, T., Iwamoto, M., and Tanigawa, N. (2000). Expression of survivin and its relationship to loss of apoptosis in breast carcinomas. *Clin. Cancer Res.* 6, 127–134.

Tanos, V., Prus, D., Ayesh, S., Weinstein, D., Tykocinski, M. L., De-Groot, N., et al. (1999). Expression of the imprinted H19 oncofetal RNA in epithelial ovarian cancer. *Eur. J. Obstet. Gynecol. Reprod. Biol.* 85, 7–11. doi: 10.1016/s0301-2115(98)00275-9

Theodoulou, M., Baselga, J., Scher, H., Dantis, L., Trainor, K., Mendelsohn, J., et al. (1995). Phase I dose-escalation study of the safety, tolerability, pharmacokinetics and biologic effects of DAB389EGF in patients with solid malignancies that express EGF receptors (EGFR). *Proc. Am. Soc. Clin. Oncol.* 14:480.

Thompson, J., Hu, H., Scharff, J., and Neville, D. M. Jr. (1995). An anti-CD3 single-chain immunotoxin with a truncated diphtheria toxin avoids inhibition by pre-existing antibodies in human blood. *J. Biol. Chem.* 270, 28037–28041. doi: 10.1074/jbc.270.47.28037

Thompson, J., Stavrou, S., Weetall, M., Hexham, J. M., Digan, M. E., Wang, Z., et al. (2001). Improved binding of a bivalent single-chain immunotoxin results in increased efficacy for *in vivo* T-cell depletion. *Protein Eng.* 14, 1035–1041. doi: 10.1093/protein/14.12.1035

Todhunter, D. A., Hall, W. A., Rustamzadeh, E., Shu, Y., Doumbia, S. O., and Vallera, D. A. (2004). A bispecific immunotoxin (DTAT13) targeting human IL-13 receptor (IL-13R) and urokinase-type plasminogen activator receptor (uPAR) in a mouse xenograft model. *Protein Eng. Des. Sel.* 17, 157–164. doi: 10.1093/protein/gzh023

Uckun, F. M., Jaszcz, W., Ambrus, J. L., Fauci, A. S., Gajl-Peczalska, K., Song, C. W., et al. (1988). Detailed studies on expression and function of CD19 surface determinant by using B43 monoclonal antibody and the clinical potential of anti-CD19 immunotoxins. *Blood* 71, 13–29.

Urba, W. J., Steis, R. G., Longo, D. L., Kopp, W. C., Maluish, A. E., Marcon, L., et al. (1990). Immunomodulatory properties and toxicity of interleukin 2 in patients with cancer. *Cancer Res.* 50, 185–192.

Vaclavkova, P., Cao, Y., Wu, L. K., Michalek, J., and Vitetta, E. S. (2006). A comparison of an anti-CD25 immunotoxin, Ontak and anti-CD25 microbeads for their ability to deplete alloreactive T cells *in vitro*. *Bone Marrow Transplant* 37, 559–567. doi: 10.1038/sj.bmt.1705286

Valenta, T., Hausmann, G., and Basler, K. (2012). The many faces and functions of beta-catenin. *EMBO J.* 31, 2714–2736. doi: 10.1038/emboj.2012.150

Vallera, D. A., Chen, H., Sicheneder, A. R., Panoskaltsis-Mortari, A., and Taras, E. P. (2009). Genetic alteration of a bispecific ligand-directed toxin targeting human CD19 and CD22 receptors resulting in improved efficacy against systemic B cell malignancy. *Leuk. Res.* 33, 1233–1242. doi: 10.1016/j.leukres.2009.02.006

Vallera, D. A., Kuroki, D. W., Panoskaltsis-Mortari, A., Buchsbaum, D. J., Rogers, B. E., and Blazar, B. R. (2000). Molecular modification of a recombinant anti-CD3epsilon-directed immunotoxin by inducing terminal cysteine bridging enhances anti-GVHD efficacy and reduces organ toxicity in a lethal murine model. *Blood* 96, 1157–1165.

Vallera, D. A., Li, C., Jin, N., Panoskaltsis-Mortari, A., and Hall, W. A. (2002). Targeting urokinase-type plasminogen activator receptor on human glioblastoma tumors with diphtheria toxin fusion protein DTAT. *J. Natl. Cancer Inst.* 94, 597–606. doi: 10.1093/jnci/94.8.597

Vallera, D. A., Panoskaltsis-Mortari, A., and Blazar, B. R. (1997). Renal dysfunction accounts for the dose limiting toxicity of DT390anti-CD3sFv, a potential new recombinant anti-GVHD immunotoxin. *Protein Eng.* 10, 1071–1076. doi: 10.1093/protein/10.9.1071

Vallera, D. A., Seo, S. Y., Panoskaltsis-Mortari, A., Griffin, J. D., and Blazar, B. R. (1999). Targeting myeloid leukemia with a DT(390)-mIL-3 fusion immunotoxin: ex vivo and *in vivo* studies in mice. *Protein Eng.* 12, 779–785. doi: 10.1093/protein/12.9.779

Vallera, D. A., Stish, B. J., Shu, Y., Chen, H., Saluja, A., Buchsbaum, D. J., et al. (2008). Genetically designing a more potent antipancreatic cancer agent by simultaneously co-targeting human IL13 and EGF receptors in a mouse xenograft model. *Gut* 57, 634–641. doi: 10.1136/gut.2007.137802

Vallera, D. A., Taylor, P. A., Panoskaltsis-Mortari, A., and Blazar, B. R. (1995). Therapy for ongoing graft-versus-host disease induced across the major or minor histocompatibility barrier in mice with anti-CD3F(ab')2-ricin toxin A chain immunotoxin. *Blood* 86, 4367–4375.

Vallera, D. A., Todhunter, D. A., Kuroki, D. W., Shu, Y., Sicheneder, A., and Chen, H. (2005a). A bispecific recombinant immunotoxin, DT2219, targeting human CD19 and CD22 receptors in a mouse xenograft model of B-cell leukemia/lymphoma. *Clin. Cancer Res.* 11, 3879–3888. doi: 10.1158/1078-0432.ccr-04-2290

Vallera, D. A., Todhunter, D., Kuroki, D. W., Shu, Y., Sicheneder, A., Panoskaltsis-Mortari, A., et al. (2005b). Molecular modification of a recombinant, bivalent anti-human CD3 immunotoxin (Bic3) results in reduced *in vivo* toxicity in mice. *Leuk. Res.* 29, 331–341. doi: 10.1016/j.leukres.2004.08.006

Vanderspek, J. C., Sutherland, J. A., Zeng, H., Battey, J. F., Jensen, R. T., and Murphy, J. R. (1997). Inhibition of protein synthesis in small cell lung cancer cells induced by the diphtheria toxin-related fusion protein DAB389 GRP. *Cancer Res.* 57, 290–294.

Wang, Z., Pratts, S. G., Zhang, H., Spencer, P. J., Yu, R., Tonsho, M., et al. (2016). Treg depletion in non-human primates using a novel diphtheria toxin-based anti-human CCR4 immunotoxin. *Mol. Oncol.* 10, 553–565. doi: 10.1016/j.molonc.2015.11.008

Wang, Z., Wei, M., Zhang, H., Chen, H., Germana, S., Huang, C. A., et al. (2015). Diphtheria-toxin based anti-human CCR4 immunotoxin for targeting human CCR4(+) cells *in vivo*. *Mol. Oncol.* 9, 1458–1470. doi: 10.1016/j.molonc.2015.04.004

Wang, Z., Zheng, Q., Zhang, H., Bronson, R. T., Madsen, J. C., Sachs, D. H., et al. (2017). Ontak-like human IL-2 fusion toxin. *J. Immunol. Methods* 448, 51–58. doi: 10.1016/j.jim.2017.05.008

Waters, C. A., Schimke, P. A., Snider, C. E., Itoh, K., Smith, K. A., Nichols, J. C., et al. (1990). Interleukin 2 receptor-targeted cytotoxicity. Receptor binding requirements for entry of a diphtheria toxin-related interleukin 2 fusion protein into cells. *Eur. J. Immunol.* 20, 785–791. doi: 10.1002/eji.1830200412

Waters, C. A., Snider, C. E., Itoh, K., Poisson, L., Strom, T. B., Murphy, J. R., et al. (1991). DAB486IL-2 (IL-2 toxin) selectively inactivates high-affinity IL-2 receptor-bearing human peripheral blood mononuclear cells. *Ann. N. Y. Acad. Sci.* 636, 403–405. doi: 10.1111/j.1749-6632.1991.tb33479.x

Weaver, M., and Laske, D. W. (2003). Transferrin receptor ligand-targeted toxin conjugate (Tf-CRM107) for therapy of malignant gliomas. *J. Neurooncol.* 65, 3–13.

Weidle, U. H., Tiefenthaler, G., Schiller, C., Weiss, E. H., Georges, G., and Brinkmann, U. (2014). Prospects of bacterial and plant protein-based immunotoxins for treatment of cancer. *Cancer Genomics Proteomics* 11, 25–38.

Westcott, M. M., Abi-Habib, R. J., Cohen, K. A., Willingham, M. C., Liu, S., Bugge, T. H., et al. (2004). Diphtheria toxin-murine granulocyte-macrophage colony-stimulating factor-induced hepatotoxicity is mediated by Kupffer cells. *Mol. Cancer Ther.* 3, 1681–1689.

Williams, D. P., Parker, K., Bacha, P., Bishai, W., Borowski, M., Genbauffe, F., et al. (1987). Diphtheria toxin receptor binding domain substitution with interleukin-2: genetic construction and properties of a diphtheria toxin-related interleukin-2 fusion protein. *Protein Eng.* 1, 493–498. doi: 10.1093/protein/1.6.493

Williams, D. P., Snider, C. E., Strom, T. B., and Murphy, J. R. (1990). Structure/function analysis of interleukin-2-toxin (DAB486-IL-2). Fragment B sequences required for the delivery of fragment A to the cytosol of target cells. *J. Biol. Chem.* 265, 11885–11889.

Woo, J. H., Bour, S. H., Dang, T., Lee, Y. J., Park, S. K., Andreas, E., et al. (2008a). Preclinical studies in rats and squirrel monkeys for safety evaluation of the bivalent anti-human T cell immunotoxin, A-dmDT390-bisFv(UCHT1). *Cancer Immunol. Immunother.* 57, 1225–1239. doi: 10.1007/s00262-008-0457-x

Woo, J. H., Liu, J. S., Kang, S. H., Singh, R., Park, S. K., Su, Y., et al. (2008b). GMP production and characterization of the bivalent anti-human T cell immunotoxin, A-dmDT390-bisFv(UCHT1) for phase I/II clinical trials. *Protein Expr. Purif.* 58, 1–11. doi: 10.1016/j.pep.2007.11.006

Woo, J. H., Liu, Y. Y., Mathias, A., Stavrou, S., Wang, Z., Thompson, J., et al. (2002). Gene optimization is necessary to express a bivalent anti-human anti-T cell immunotoxin in Pichia pastoris. *Protein Expr. Purif.* 25, 270–282. doi: 10.1016/s1046-5928(02)00009-8

Woo, J. H., Liu, Y. Y., Stavrou, S., and Neville, D. M. Jr. (2004). Increasing secretion of a bivalent anti-T-cell immunotoxin by Pichia pastoris. *Appl. Environ. Microbiol.* 70, 3370–3376. doi: 10.1128/aem.70.6.3370-3376.2004

Xu, P., Xu, X. L., Huang, Q., Zhang, Z. H., and Zhang, Y. B. (2012). CIP2A with survivin protein expressions in human non-small-cell lung cancer correlates with prognosis. *Med. Oncol.* 29, 1643–1647. doi: 10.1007/s12032-011-0053-3

Yang, W., Luo, D., Wang, S., Wang, R., Chen, R., Liu, Y., et al. (2008). TMTP1, a novel tumor-homing peptide specifically targeting metastasis. *Clin. Cancer Res.* 14, 5494–5502. doi: 10.1158/1078-0432.CCR-08-0233

Yang, X., Kessler, E., Su, L. J., Thorburn, A., Frankel, A. E., Li, Y., et al. (2013). Diphtheria toxin-epidermal growth factor fusion protein DAB389EGF for the treatment of bladder cancer. *Clin. Cancer Res.* 19, 148–157. doi: 10.1158/1078-0432.CCR-12-1258

Yasuda, A., Sawai, H., Takahashi, H., Ochi, N., Matsuo, Y., Funahashi, H., et al. (2006). The stem cell factor/c-kit receptor pathway enhances proliferation and invasion of pancreatic cancer cells. *Mol. Cancer* 5:46.

Yoon, D. J., Kwan, B. H., Chao, F. C., Nicolaides, T. P., Phillips, J. J., Lam, G. Y., et al. (2010). Intratumoral therapy of glioblastoma multiforme using genetically engineered transferrin for drug delivery. *Cancer Res.* 70, 4520–4527. doi: 10.1158/0008-5472.CAN-09-4311

Youle, R. J., Uckun, F. M., Vallera, D. A., and Colombatti, M. (1986). Immunotoxins show rapid entry of diphtheria toxin but not ricin via the T3 antigen. *J. Immunol.* 136, 93–98.

Yu, D., Chen, D., Chiu, C., Razmazma, B., Chow, Y. H., and Pang, S. (2001). Prostate-specific targeting using PSA promoter-based lentiviral vectors. *Cancer Gene Ther.* 8, 628–635. doi: 10.1038/sj.cgt.7700344

Yu, Y., Li, J., Zhu, X., Tang, X., Bao, Y., Sun, X., et al. (2017). Humanized CD7 nanobody-based immunotoxins exhibit promising anti-T-cell acute lymphoblastic leukemia potential. *Int. J. Nanomedicine* 12, 1969–1983. doi: 10.2147/IJN.S127575

Zachariae, C., Larsen, C. S., Kaltoft, K., Deleuran, B., Larsen, C. G., and Thestrup-Pedersen, K. (1991). Soluble IL2 receptor serum levels and epidermal cytokines in mycosis fungoides and related disorders. *Acta Derm. Venereol.* 71, 465–470.

Zhang, H., Zhang, S., Zhuang, H., and Lu, F. (2006). Cytotoxicity of a novel fibroblast growth factor receptor targeted immunotoxin on a human ovarian teratocarcinoma cell line. *Cancer Biother. Radiopharm.* 21, 321–332. doi: 10.1089/cbr.2006.21.321

Zhang, L. J., Waters, C. A., Poisson, L. R., Estis, L. F., and Crumpacker, C. S. (1997). The interleukin-2 fusion protein, DAB389IL-2, inhibits the development of infectious virus in human immunodeficiency virus type 1-infected human peripheral blood mononuclear cells. *J. Infect. Dis.* 175, 790–794. doi: 10.1086/513972

Zheng, J. Y., Chen, D., Chan, J., Yu, D., Ko, E., and Pang, S. (2003). Regression of prostate cancer xenografts by a lentiviral vector specifically expressing diphtheria toxin A. *Cancer Gene Ther.* 10, 764–770. doi: 10.1038/sj.cgt.7700629

Zheng, Q., Wang, Z., Zhang, H., Huang, Q., Madsen, J. C., Sachs, D. H., et al. (2017). Diphtheria toxin-based anti-human CD19 immunotoxin for targeting human CD19(+) tumors. *Mol. Oncol.* 11, 584–594. doi: 10.1002/1878-0261.12056

Conflict of Interest: The authors declare that the research was conducted in the absence of any commercial or financial relationships that could be construed as a potential conflict of interest.

frontiers in Microbiology

ORIGINAL RESEARCH
published: 09 August 2019
doi: 10.3389/fmicb.2019.01836

Culture-Dependent Bioprospecting of Bacterial Isolates From the Canadian High Arctic Displaying Antibacterial Activity

Evangelos Marcolefas[1], Tiffany Leung[2], Mira Okshevsky[1], Geoffrey McKay[2], Emma Hignett[2], Jérémie Hamel[3], Gabriela Aguirre[1], Olivia Blenner-Hassett[1], Brian Boyle[3], Roger C. Lévesque[3], Dao Nguyen[2], Samantha Gruenheid[2] and Lyle Whyte[1]**

[1] Department of Natural Resource Sciences, McGill University, Sainte-Anne-de-Bellevue, QC, Canada, [2] Department of Microbiology and Immunology, McGill University, Montreal, QC, Canada, [3] Institute for Integrative Systems Biology, Université Laval, Quebec City, QC, Canada

OPEN ACCESS

Edited by:
Ana R. Freitas, University of Porto, Portugal

Reviewed by:
Teppo Rämä, UiT The Arctic University of Norway, Norway
Virginia Katrina Walker, Queen's University, Canada

***Correspondence:**
Samantha Gruenheid
samantha.gruenheid@mcgill.ca
Lyle Whyte
lyle.whyte@mcgill.ca

Specialty section:
This article was submitted to Antimicrobials, Resistance and Chemotherapy, a section of the journal Frontiers in Microbiology

Received: *20 March 2019*
Accepted: *25 July 2019*
Published: *09 August 2019*

Citation:
Marcolefas E, Leung T, Okshevsky M, McKay G, Hignett E, Hamel J, Aguirre G, Blenner-Hassett O, Boyle B, Lévesque RC, Nguyen D, Gruenheid S and Whyte L (2019) Culture-Dependent Bioprospecting of Bacterial Isolates From the Canadian High Arctic Displaying Antibacterial Activity. Front. Microbiol. 10:1836. doi: 10.3389/fmicb.2019.01836

The goal of this study was to isolate, screen, and characterize Arctic microbial isolates from Expedition Fjord, Axel Heiberg Island, Nunavut, Canada capable of inhibiting the growth of foodborne and clinically relevant pathogens. Arctic bacteria were isolated from twelve different high Arctic habitats pertaining to active layer permafrost soil, saline spring sediments, lake sediments, and endoliths. This was achieved using (1) the cryo-iPlate, an innovative *in situ* cultivation device within active layer permafrost soil and (2) bulk plating of Arctic samples by undergraduate students that applied standard culturing methods. To mitigate the possibility of identifying isolates with already-known antibacterial activities, a cell-based dereplication platform was used. Ten out of the twelve Arctic habitats tested were found to yield cold-adapted isolates with antibacterial activity. Eight cold-adapted Arctic isolates were identified with the ability to inhibit the entire dereplication platform, suggesting the possibility of new mechanisms of action. Two promising isolates, initially cultured from perennial saline spring sediments and from active layer permafrost soil (*Paenibacillus* sp. GHS.8.NWYW.5 and *Pseudomonas* sp. AALPS.10.MNAAK.13, respectively), displayed antibacterial activity against foodborne and clinically relevant pathogens. *Paenibacillus* sp. GHS.8.NWYW.5 was capable of inhibiting methicillin resistant and susceptible *Staphylococcus aureus* (MRSA and MSSA), *Listeria monocytogenes*, *Salmonella enterica* and *Escherichia coli* O157:H7. *Pseudomonas* sp. AALPS.10.MNAAK.13 was observed to have antagonistic activity against MRSA, MSSA, *Acinetobacter baumanii*, *Enterococcus faecium*, and *Enterococcus faecalis*. After whole genome sequencing and mining, the genome of *Paenibacillus* sp. GHS.8.NWYW.5 was found to contain seven putative secondary metabolite biosynthetic gene clusters that displayed low homology (<50% coverage, <30% identity, and e-values > 0) to clusters identified within the genome of the type strain pertaining to the same species. These findings suggest that cold-adapted Arctic microbes may be a promising source of novel secondary metabolites for potential use in both industrial and medical settings.

Keywords: Arctic, bioprospecting, antibiotics, secondary metabolites, microbial cultivation

INTRODUCTION

The rise of antibiotic resistance is one of the most urgent challenges the world currently faces. Antimicrobial resistance has steadily increased in clinical settings (Bitnun and Yeh, 2018). We are on the cusp of returning to a pre-antibiotic world in which common infections and minor injuries will once again become deadly (Laxminarayan et al., 2013; Ferri et al., 2017; Pawar et al., 2017). Simultaneously, natural product discovery efforts on the part of the pharmaceutical industry have largely dwindled since the end of the 20th century (Baker et al., 2007). Given that the current arsenal of effective antibiotics is decreasing, innovative discovery workflows for the identification of novel antibiotics are needed.

Enterococcus faecium, *Staphylococcus aureus*, *Klebsiella pneumoniae*, *Acinetobacter baumannii*, *Pseudomonas aeruginosa*, and *Enterococcus* species (ESKAPE) are recognized by the Infectious Disease Society of America as the bacteria posing the most significant risk to public health in the United States (Boucher et al., 2009). The ESKAPE pathogens are responsible for the majority of nosocomial infections in the United States, with an estimated 722,000 infections acquired in 2011 (Magill et al., 2014). Of particular concern are the increasing levels of antibiotic resistance occurring in these organisms, especially methicillin-resistant *S. aureus* (MRSA), vancomycin-resistant *E. faecium*, and fluoroquinolone-resistant *P. aeruginosa* (National Nosocomial Infections Surveillance System, 2004). MRSA infections are now responsible for more deaths in U.S. hospitals than HIV/AIDS and tuberculosis combined (Klevens et al., 2006; Boucher and Corey, 2008).

Many of the antibiotics currently in use are secondary metabolite natural products from soil bacteria, particularly from the *Streptomyces* genus. Since the pioneering experiments of Selman Waksman in the 1940's, this resource has been extensively studied (Waksman and Woodruff, 1940; Schatz et al., 1944). New approaches or modification to existing methods may be necessary to increase the probability of finding novel compounds. Once an isolate with antibiotic activity is identified, a "dereplication" procedure is required to avoid the re-discovery of already-known antibiotics. Compound extraction, purification and biochemical analyses are costly and technically challenging. Instead, we have employed a cell-based dereplication platform (Cox et al., 2017), in which isolates are tested for inhibitory activity against a panel of *Escherichia coli* strains expressing specific antibiotic resistance genes. The presence of inhibitory activity against all dereplication strains that comprise the Antibiotic Resistance Platform (ARP) suggests that the isolate produces antimicrobial secondary metabolite(s) with a potentially novel mechanism of action. As an additional dereplication measure, genomic sequencing and *in silico* genome mining could be used to prioritize isolates for downstream testing. Microbial genomic sequences could be mined *in silico* to detect secondary metabolite biosynthetic gene clusters (BGCs) using open source web-based pipelines such as the antibiotics and secondary metabolite analysis shell (antiSMASH) (Blin et al., 2019). Once microbial genomes have been mined, isolates can be prioritized on the basis of low BGC sequence homology to known clusters (Medema et al., 2015).

In the search for new antibiotics, interest has been growing in underexplored environments such as marine systems (Jang et al., 2013; Machado et al., 2015) and the deep biosphere (Orsi et al., 2013). The Canadian high Arctic is characterized by extreme environmental conditions such as high salt and prolonged subzero temperatures. The unique ecological niches (i.e., hypersaline springs, permafrost and endoliths) of the high Arctic harbor diverse microbial communities which remain largely unexplored (Perreault et al., 2007, 2008; Steven et al., 2007; Lay et al., 2013). Recent macro- and microdiversity studies have revealed that Arctic microbiomes do not always follow the latitudinal diversity paradigm, which states that diversity decreases towards the poles (Gregory et al., 2019). Arctic environments have been observed to be a cradle for microbial diversity (Gregory et al., 2019). Due to the rich microbial diversity and unique selective pressures experienced by the Arctic microbiome, we hypothesize that this extreme environment has potential for harboring novel antibacterial secondary metabolites. Previous bioprospecting studies conducted in polar cryohabitats have successfully identified microbial isolates expressing new natural products and encoding unknown secondary metabolite BGCs (Mitova et al., 2005; Tedesco et al., 2016; Dhaneesha et al., 2017). One such example includes the discovery of *Streptomyces artemisiae* MCCB 248 isolated from sediments in the Arctic fjord Kongsfjorden. This isolate was shown to produce secondary metabolites with anticancer properties and was found to encode unique polyketide synthetase (PKS) and non-ribosomal peptide (NRP) genes (Dhaneesha et al., 2017). Isolating secondary-metabolite-producing microbes from Arctic environments has the additional benefit of yielding strains with inhibitory activity at cold temperatures. Cold-active antimicrobial enzymes, such as cold-active alkaline phosphatases with antibiofilm activity, represent appealing biopreservatives for food processing industries since they can extend the shelf life of refrigerated consumables (Balabanova et al., 2017).

Identifying and isolating new antibacterial secondary metabolites often depends on cell-based screening of cultivable strains. Co-culture assays are known to activate silent BGCs in antibiotic-producing strains that would not be expressed in pure culture (Zarins-Tutt et al., 2016). Unfortunately, only a small percentage of all microbial species can be isolated using classic cultivation techniques (Winterberg, 1898; Ward et al., 1990). Innovative cultivation techniques are expanding the portion of cultivable isolates that could be phenotypically screened using cell-based assays (Vartoukian et al., 2010). The efficacy of such *in situ* cultivation techniques for drug discovery is illustrated by the recent discovery of the antibiotic Teixobactin, derived from an ichip isolate (Ling et al., 2015). Based on the initial design of the ichip, the cryo-iPlate prototype designed and implemented by Goordial et al. (2017) was the first *in situ* cultivation device deployed in the Arctic. Here, a re-designed and updated version of the cryo-iPlate is described for the first time and is used to isolate Arctic microorganisms for antibacterial screening. In addition to sampling unique ecological habitats and implementing the new cryo-iPlate cultivation device, the bioprospecting workflow described here uses a crowd-sourced screening approach first developed by Jo Handelsman at

Yale University in 2012, which harnesses the manpower of undergraduate microbiology teaching labs to screen bacterial isolates for antibiotic activity (Davis et al., 2017).

Here, we employed two cultivation methods to isolate and then screen bacteria derived from Canadian high Arctic habitats for antibacterial activities (**Figure 1**). Arctic isolates were screened for antibiotic activity against a collection of both foodborne and clinical pathogens. Cold-adapted antibiotic-producing bacteria were derived from Arctic permafrost, saline spring sediments, and cryptoendoliths suggesting that high Arctic environments could be a potentially untapped source of novel antibacterial secondary metabolites.

MATERIALS AND METHODS

Sampling Arctic Microbiomes

The various soil and rock samples used in this study were collected within the vicinity of the McGill Arctic Research Station (MARS) on Axel Heiberg Island, Nunavut, in the Canadian high Arctic. The sediment, soil and rock samples were collected for crowdsourced bulk plating whereas the *in situ* cryo-iPlate cultivation approach was only applied to active layer permafrost soil (described below). Sediments from spring outflow channels and soil in this study were collected with an ethanol-sterilized spatula used to exhume the first 15 cm of soil/sediment horizons. Rocks with visible lithic microbial biomass were sampled by breaking large rocks into smaller pieces using an ethanol-sterilized hammer and chisel. All rock and soil samples were collected in sterile WhirlPak bags and stored in coolers kept at 5°C until returned to McGill University. Upon return to the laboratory, all samples were stored at 5°C.

Cryo-iPlate Procedures

The cryo-iPlate design was based on the Nichols et al. (2010) ichip and the Goordial et al. (2017) cryo-iPlate prototype (Nichols et al., 2010; Goordial et al., 2017). It was designed using the Rhino 6 software and 3D-printed at Fablab Inc., Montreal, using durable PC-ISO polycarbonate plastic. Previous prototypes of the cryo-iPlate such as the one described in Goordial et al. (2017), consisted of empty pipette boxes that were not as durable in the field. The dimensions of the improved version of the cryo-iPlate described herein are 15 cm by 12 cm. It features 160 wells (as opposed to 96 in previous prototypes) that are 0.5 cm wide and deep. The wells of the central plate were filled with 2% w/v gellan gum (Alfa Aesar) prior to being deployed in the field. Based on previous studies of total microbial counts in active layer permafrost at the MARS study site, dilutions of the soil were made in the field using sterile water (Wilhelm et al., 2011). This device was only applied to active layer permafrost. Each individual well of the central plate was inoculated in the field with 10 μl of diluted soil containing ∼1–10 microbial cells. The top and bottom layers were overlaid with sterile semi-permeable 0.03 μm-pore-size polycarbonate membranes (Whatman^{TM}, GE Healthcare Life Sciences) and were glued using a silicon adhesive (DuPont). The assembly of three plates was then screwed together using eight stainless steel 10–24 screws and left to incubate *in situ*. After incubating in the field for 10 days, the cryo-iPlate was collected in a large sterile Whirl-Pak sampling bag along with the soil in which it was incubating. The assembly was stored in a cooler at 5°C during transport back to McGill University where it was subsequently incubated *ex situ* at 5°C for 3 months before being disassembled for subculturing. After disassembling the cryo-iPlates, well contents from the central plate were pushed into individual Eppendorf tubes containing 0.1% w/v pyrophosphate using sterile 1000 μl

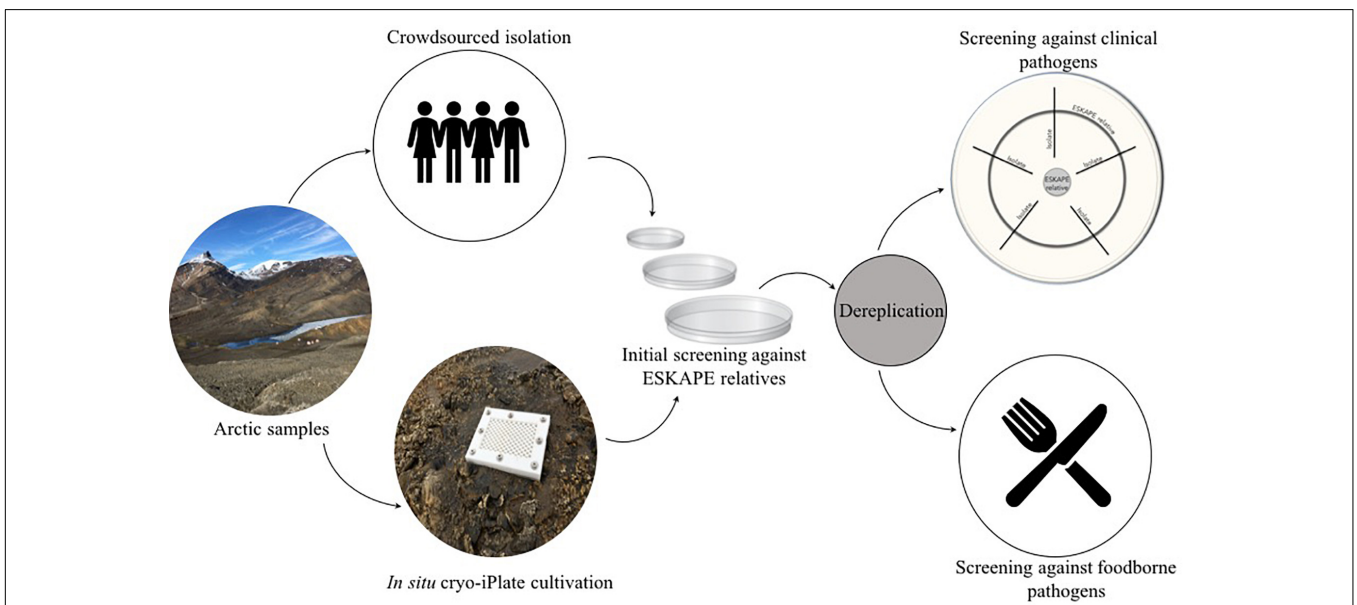

FIGURE 1 | Overview of the Arctic bioprospecting workflow.

pipette tips (Diamed Canada). Eppendorf tubes containing well contents from the cryo-iPlate in buffer solution were vortexed for 30 s and 100 μl of the solution was used to inoculate plates of 1/2 Reasoner's 2A (R2A) broth media solidified with 2% gellan gum (Alfa Aesar). The plates were incubated at room temperature for 2 weeks. Morphologically distinct colonies (selected based on distinct colony form, elevation, margin, size, texture and color) that grew on the 1/2 R2A plates were subcultured three times to attain clonal populations before being screened against the ESKAPE relative strains.

Crowdsourced Screening of Isolates Against ESKAPE Pathogen Relatives

The twelve sample types described in **Table 1** were processed by students in the Introduction to Microbiology Laboratory Course at McGill University in the following manner. One gram of sample was serially diluted in sterile water to 10^{-5}, and 100 μL of each dilution were spread onto lysogeny broth (LB) plates solidified with gellan, tryptic soy agar (TSA) (10% or 0.1%), potato dextrose agar or sheep blood agar. Each student pair participating in the course was provided with one of the Arctic samples and was allowed to select one of the aforementioned culturing media to increase the diversity of isolates obtained. Plates were incubated for 1 week at room temperature and morphologically distinct colonies were picked (selected based on colony form, elevation, margin, size, texture and color) and re-streaked to produce libraries of clonal populations. Isolates were screened against ESKAPE pathogen relatives (**Supplementary Table S1**) using the spread-patch technique (**Figure 2A**). Since antibiotic activity screening is performed in teaching labs, isolates were tested against non-pathogenic relatives of high priority threat pathogens. A diluted suspension of tester bacteria was evenly spread across on agar plate, and the Arctic isolates spotted on top. Plates were incubated for 1 week at room temperature and observed for a zone of pathogen inhibition surrounding isolates. All isolates that produced a zone of inhibition were given a name and stored as glycerol freezer stocks and selected for dereplication (**Figure 1**). If isolates were surrounded by a visually discernible zone of clearance devoid of any tester strain growth, then they were deemed to have positive antibacterial activity (**Figure 2A**).

Taxonomic Identification of Isolates

Isolates from the cryo-iPlate and from the crowdsourced bulk soil plating that displayed zones of inhibition against at least one of the ESKAPE relatives were selected for 16S rRNA gene sequencing. Colony PCR was first conducted to amplify the 16S rRNA gene using the 27F (forward) bacterial primer: 5′-AGAGTTACCTTGTTACGACTT-3′ and the 1492R (reverse) bacterial primer: 5′-GGTTACCTTGTTACGACTT-3′. The 16S rDNA amplification PCR reaction cycling program consisted of: (1) 95°C for 7 min, (2) 94°C for 45 s, (3) 55°C for 45 s, (4) 72°C for 1 min, (where steps 2 to 4 were repeated 30 times), (5) 72°C for 10 min. PCR products from the cryo-iPlate and from the bulk soil plating were sent for Sanger sequencing at the Plateforme d'Analyses Genomiques sequencing center at Laval University and the McGill University and at the Génome Québec Innovation Centre (respectively). All generated sequences were manually curated using 4Peaks software[1] where sequence segments with an average Q > 40 were used as queries against the EzBioCloud database for taxonomical identification (Yoon et al., 2017).

Dereplication Platform

Isolates that demonstrated antibacterial activity against at least one ESKAPE relative were tested against a dereplication platform described in **Supplementary Table S2**, and provided by the Wright lab at McMaster University (Cox et al., 2017). This dereplication platform consists of two parental strains: Wild type *E. coli* BW25113, and *E. coli* Δ*bamB* Δ*tolC* BW25113 harboring mutations to increase outer membrane permeability and decrease efflux pump activity, thereby increasing its susceptibility to antibiotics. In all cases except the *fluB* mutant, the Wright lab transformed these parent strains with plasmids harboring antibiotic resistance genes. Isolates were screened against the dereplication strains using the wagon-wheel assay, in which dereplication strains were streaked in a circle to form the "wheel" on LB plates, and Arctic isolates were streaked across the wheel to form "spokes" (**Figure 2B**). Plates were incubated for 1 week at room temperature and it was subsequently observed in which cases the isolates were able to inhibit the growth of the dereplication strain. Isolates able to inhibit the growth of all dereplication strains were considered to have "passed."

Screening Arctic Isolates That Passed the ARP Against ESKAPE Pathogens

Arctic isolates that passed the ARP were screened for inhibitory activities against a panel of ESKAPE pathogens, namely *Enterobacter cloacae* (strain CO794 provided by the G. Wright laboratory), methicillin-resistant *S. aureus* (MRSA) (ATCC 43300), methicillin-susceptible *S. aureus* (MSSA) (ATCC 29213), *K. pneumoniae* (clinical strain HO132323 provided by the G. Wright laboratory), *Acinetobacter baumanii* AB5075, *P. aeruginosa* WT PAO1, *E. faecium* (ATCC 700221) and *Enterococcus faecalis* (ATCC 29212), using the wagon-wheel co-culture technique as described above (**Figure 2B**). Frozen glycerol stock cultures of the Arctic isolates and of the tester pathogens were streaked on LB plates. The pathogen tester strains were incubated at 37°C for 18 h whereas Arctic isolates were incubated at room temperature for 48 h. Once sufficient growth appeared on plates, liquid cultures of the Arctic isolates and the pathogenic tester strains were made using LB media. Liquid cultures of the Arctic isolates were incubated with agitation at 250 rpm for 48 h at room temperature whereas pathogenic tester strains were incubated with agitation at 250 rpm for 24 h at 37°C. Loopfuls of the pathogenic strains in liquid culture were streaked in a circular line on a LB plate, while the Arctic isolates were streaked outward starting from the middle of the plate (**Figure 2B**). Triplicates of these co-culture plates were incubated at room temperature, and observed after 24, 48, and 72 h of incubation. Regions of contact between the Arctic isolate and pathogenic tester strain in which the tester strain did not produce visible growth were recorded as inhibition.

[1] https://nucleobytes.com/

TABLE 1 | Arctic samples collected from Expedition Fiord, Axel Heiberg Island, Nunavut, used as source material for bioprospecting of antibiotic-producing strains.

Sample type	Source location	Geographic coordinates	Habitat
Active Layer Permafrost	MARS station Expedition Fiord	(79.412872, – 90.740343)	Trough soil from polygonal tundra terrain
			Surface soil from polygonal tundra terrain
			Arid soil
			Active layer tundra permafrost
	Gypsum Hill, Expedition Fiord	(79.403906, – 90.732321)	Hummock soil
Sediments	Junction Diapir (Lost Hammer)	(79.076755, –90.195299)	Perennial hypersaline (22–23% salt) spring outflow channel sediment (Pollard et al., 2009)
	Color Lake, Expedition Fiord	(79.416300, – 90.764081)	Acidic (pH ˜3.6) freshwater lake sediment (Johannesson and Lyons, 1995)
			Acidic (pH ˜3.6) freshwater lake sediment covered with microbial mat (Johannesson and Lyons, 1995)
	Gypsum Hill, Expedition Fiord	(79.403906, – 90.732321)	Perennial saline (7.5–15.8% salt) spring sediment (Perreault et al., 2007)
	White Glacier, Expedition Fiord	(79.431663, – 90.647073)	Sediment from glacial terminus moraines
Lithic Communities	Gypsum Hill, Expedition Fiord	(79.412151, – 90.740644)	Gypsum cryptoendolith
	Junction Diapir (Lost Hammer)	(79.076755, – 90.195299)	Unknown rock cryptoendolith

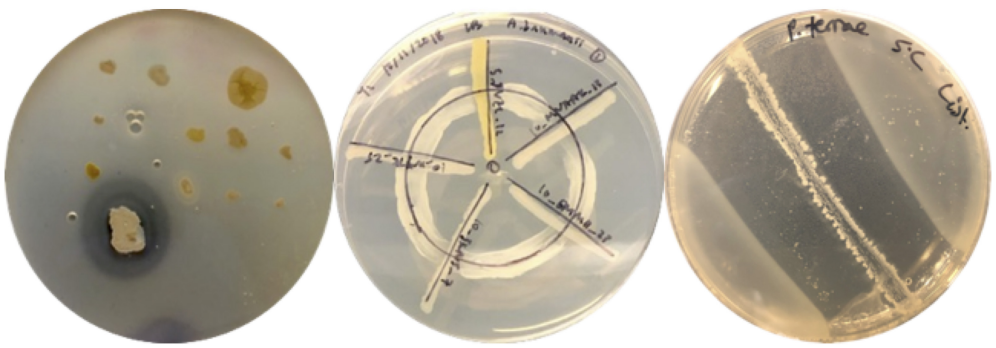

FIGURE 2 | Three different co-culture techniques used to screen Arctic isolates for antibacterial activity. **(A)** Spread-patch assay applied by the undergraduate crowdsourcing initiative to screen Arctic isolates against ESKAPE relatives. The image above features an Arctic bacterial isolate from the undergraduate crowdsourcing initiative exhibiting a zone of clearance against a lawn of an ESKAPE relative tester strain. **(B)** Wagon wheel assay used to dereplicate and screen Arctic isolates against clinically relevant pathogens. The image above displays five Arctic isolates: GHCE.5.JVZL.12, AALPS.10.MNAAK.13, AALPS.10.EMMH.23, AALPS.10.JKNJ.7, MAL.10.WYTK.25 (in clockwise order) tested against the tester pathogen *A. baumanii*. **(C)** Overlay assay used to screen Arctic isolates against foodborne pathogens. The image above displays the positive control strain *Paenibacillus terrae* NRRL B-30644 inhibiting the growth of *L. monocytogenes* at 5°C.

Assessing Growth of Arctic Isolates That Passed the ARP at Various Temperatures

Liquid TSB cultures of Arctic isolates were incubated with agitation at 250 rpm for 48 h at room temperature and then streaked on TSA plates. Inoculated plates were then incubated at 37, 25, 10, 5, 0, –5, and –10°C. TSA media intended for sub-zero incubation was amended with 3% v/v glycerol to avoid complete freezing of the media. Growth was visually assessed after 48 h of incubation at 37 and 25°C. The remaining incubations were assessed for growth after 20 days.

Screening Arctic Isolates That Passed the ARP Against Foodborne Pathogens

In addition to screening against clinical pathogens, all Arctic isolates that passed the dereplication assay were screened against foodborne pathogens using an overlay co-culture assay (**Figure 2C**). Liquid TSB cultures of Arctic isolates were incubated with agitation at 250 rpm for 2 days at room temperature and then streaked in a line in the center of the TSA plates. The TSA plates were then left to incubate at room temperature for 7 days. Following incubation, each Arctic isolate was overlaid with 7 ml of molten agar media inoculated with 100 μl of overnight liquid cultures of *S. aureus* WT, *Listeria monocytogenes* HPB# 1870 serotype 1/2c, *Salmonella enterica* serovar Heidelberg, and *E. coli* 0157:H7. To assess whether any of the secreted secondary metabolites produced by the Arctic isolates retained inhibitory activity at human body and standard refrigeration temperatures, the overlay plates were incubated at 37 and 5°C, respectively. Zones of inhibition were observed after 24 h of incubation for plates incubated at 37°C and after 20 days for those incubated at 5°C. This assay inherently relies on the diffusion of secreted molecules within the cultivation media's semisolid agar matrix. Specifically, in order to observe zones of clearance, diffusible biomolecules are required to reach the top agar layer to inhibit the tester strains. This co-culture assay was conducted in triplicate and an established antibiotic-producing strain, *Paenibacillus terrae* NRRL B-30644, was used a positive

control. This environmental strain has been previously reported to produce zones of inhibition in co-culture assays against foodborne pathogens (van Belkum et al., 2015). The zones of inhibition produced by *P. terrae* NRRL B-30644 served as a visual reference for positive inhibitory activity for all the co-culture assays conducted in this study (**Figure 2C**).

DNA Sequencing, Genome Assembly, and Analyses of Isolates Passing the ARP

Bacterial isolates were inoculated from single isolated colonies into R2A broth and grown at room temperature for periods ranging from 12 to 72 h. The genomic DNA was extracted using the E-Z 96 Tissue DNA Kit (Omega Bio-Tek, Norcross GA, United States). Between 250 and 700 ng of DNA were fragmented via sonication using a Covaris M220 (Covaris, Woburn, MA, United States) for 40 s at 18–22°C. The peak power was set at 50.0, duty factor at 20.0 and the number of bursts at 200. The libraries were prepared using the NEBNext Ultra II DNA library prep kit for Illumina (New England Biolabs, Ipswich MA, United States) following the manufacturer's instructions. The libraries were barcoded with TruSeq HT adapters (Illumina, San Diego, CA, United States) and sequenced using an Illumina MiSeq 300 bp paired-end run at the Plateforme d'Analyses Génomiques at the Institut de Biologie Intégrative et des Systèmes (Université Laval, Québec, Canada). The raw reads were assembled using the A5 pipeline (Tritt et al., 2012). Assemblies were validated using the metagenomic identification software Centrifuge and contig uniformity was verified to confirm that each assembly originated from the same source DNA and from not contaminants (Kim et al., 2016). To taxonomically identify the isolates that inhibited the ARP, their assembled genomes were first annotated using the Rapid Annotation using Subsystem Technology (RAST) version 2.0 using standard parameters (Aziz et al., 2008; Overbeek et al., 2013; Brettin et al., 2015). Following annotation, full 16S rRNA gene(s) were identified within each genome and subsequently used as a query sequences in the EzBioCloud database for corroborating taxonomical identification (Yoon et al., 2017). To predict the secondary metabolite BGCs within the genomes of the eight isolates of interest, all genomes were mined using the antiSMASH database v.4 using default search parameter settings (Medema et al., 2011; Blin et al., 2017). The BGCs of the isolates showing the broadest activity spectra were used as query sequence in a blastn alignment against genomes of type strains of the same species: *Pseudomonas prosekii* LMG 26867 (genome accession GCA_900105155.1), and *P. terrae* NRRL B-30644 (accession GCA_000943545.1). The assembled genomes of these two promising isolates were deposited at GenBank under the BioSample accessions (SAMN12211638 and SAMN12211639).

Organic Extraction Using Liquid Culture Supernatants From Two Promising Isolates

To confirm whether the antagonistic activities of promising isolates were caused by secreted secondary metabolites of bacterial origin, organic extracts using liquid culture supernatants were prepared. Isolates were incubated overnight in TSB media at room temperature with agitation at 250 rpm. Following overnight incubation, 14 mL of the cultures were mixed with 7.5 mL of ethyl acetate in a 50 mL Falcon tube (giving a final volume ratio of 2:1 culture supernatant to ethyl acetate). Solutions were vortexed on the highest setting until solutions were homogenized and then centrifuged at 7830 rpm for 15 min at room temperature. Following centrifugation, the organic layers were removed from both solutions and were collected in separate pre-weighed 7.5 mL borosilicate glass culture tubes using a Pasteur pipette. The ethyl acetate was then left to evaporate for 20 min by direct air filtered with a 0.3 μm HEPA filter (Whatman #0974479). After the solvent fully evaporated, both extracts were resuspended in 200 μL of methanol. To assess whether the crude organic extracts retained antibacterial activity, 30 μL of the extracts were spotted on agar plates. Once the methanol fully evaporated from the agar, 7 ml of molten agar containing the tester strains (*E. coli* ATCC 11775 and *E. coli* Δ*bam*Δ*tolC* BW25113) were poured over the dried extract spots. Control spots consisting only of methanol were plated to confirm that the observed zones of clearance did not arise from the solvent used to resuspend the extract. The plates were then incubated at room temperature for 24 h before being observed for zones of clearance.

RESULTS

Antibiotic Activity of Arctic Isolates Against ESKAPE Pathogen Relatives

Twelve environmental samples were collected in the regions of Expedition Fiord, Gypsum Hill, Lost Hammer, Color Lake and White Glacier on Axel Heiberg Island in the Canadian high Arctic. The sampled habitats included active layer permafrost, sediments, and lithic communities. Active layer permafrost samples included trough soil from polygonal tundra terrain, surface soil from polygonal tundra terrain, arid soil, and hummock soil. Sediment samples included perennial hypersaline spring outflow channel sediment, acidic freshwater lake sediment, acidic freshwater lake sediment covered with microbial mats, perennial saline spring sediment, and sediment from glacial terminus moraines. Lithic communities included gypsum cryptoendoliths and unknown rock cryptoendoliths (**Table 1**). All of these samples were distributed to the undergraduate students for traditional plate cultivation, and 3120 distinct colonies were subcultured and further tested. After co-culture screening, 54 isolates (1.7%) were identified as having antibacterial activity against at least one ESKAPE pathogen relative. Of these, three isolates originated from acidic freshwater lake sediment covered with microbial mat, four from a gypsum cryptoendolith, seven from Gypsum Hill hummock active layer permafrost, three from Gypsum Hill perennial saline spring sediment, one from a cryptoendolith collected at Lost Hammer, 25 from active layer tundra permafrost, seven from arid active layer permafrost, two from polygonal terrain surface soil, one from polygonal terrain trough soil, and one from glacial terminus moraine sediment (**Table 2**). The genera represented

TABLE 2 | Antibiotic activity of bulk soil isolates against ESKAPE pathogen relatives.

Source location	Habitat	Isolate name	Closest matching taxon	% identity	% coverage of 16S gene	*S. epidermidis*	*E. raffinosus*	*E. coli*	*P. putida*	*A. baylyi*	*E. aerogenes*
Color Lake, Expedition Fiord	Acidic freshwater lake sediment covered with microbial mat	CLMS.5.EMGM.4	*Janthinobacterium lividum*	99.87	54.6						
		CLMS.5.EMGM.9	*Pseudomonas yamanorum*	100	54.9						
		CLMS.6.VMCS.4	*Janthinobacterium lividum*	99.87	29.6						
Gypsum Hill, Expedition Fiord	Gypsum cryptoendolith	GHCE.C1.AWCA.27	*Streptomyces avidinii*	100	48.2						
		GHCE.C1.AWCA.31	*Mycetocola miduiensis*	99.75	56.3						
		GHCE.5.JVZL.12	*Pseudomonas fulva*	100	100						
		GHCE.5.JVZL.15	*Streptomyces avidinii*	100	46.4						
	Hummock soil	GHHS.3.LBZX.4	*Flavobacterium panaciterrae*	99	100						
		GHHS.3.LBZX.18	*Janthinobacterium svalbardensis*	100	59.5						
		GHHS.LB.ZXLB.24	*Pseudomonas helmanticensis*	99.75	54.8						
		GHHS.LB.ZXLB.15	*Pseudomonas helmanticensis*	100	54						
		GHHS.LB.ZXLB.15	*Pseudomonas arsenicoxydans*	100	54.8						
		GHHS.LB.ZXLB.9	*Pseudomonas arsenicoxydans*	100	46.2						
		GHHS.13.PTLY.2	*Pseudomonas arsenicoxydans*	100	53.9						
	Perennial saline spring sediment	GHS.C1.RZCG.3	*Bacillus nakamurai*	100	45.9						
		GHS.C1.RZCG.16	*Micrococcus aloeverae*	99.85	46.8						
		GHS.8.NWYW.5	*Paenibacillus terrae*	99.23	100						
Junction Diapir (Lost Hammer)	Unknown rock cryptoendolith	LCE.5.TZJR.21	*Pseudomonas lurida*	99.87	54.7						
MARS station Expedition Fiord	Active layer tundra permafrost	MAL.2.HSSH.5	*Pseudomonas kilonensis*	99.86	48.5						
		MAL.4.ABES.12	*Pseudomonas arsenicoxydans*	99.86	49.6						
		MAL.4.ABES.21	*Pseudomonas frederiksbergensis*	100	100						
		MAL.11.AHCHQX.12	*Pseudomonas arsenicoxydans*	100	100						
		MAL.10.WYTK.25	*Pseudomonas extremaustralis*	99.73	100						
		C2C25	*Curtobacterium pusillum*	99.54	100						
		C5C25	*Pseudomonas migulae*	99.6	100						
		HTAG2	*Pseudomonas jessenii*	99.34	100						
		C6A2	*Nocardia coeliaca*	99.62	100						
		C6A4	*Streptomyces netropsis*	100	100						
		C7A1	*Nocardia coeliaca*	99.61	100						
		C4F16	*Arthrobacter oryzae*	99.46	100						

(Continued)

TABLE 2 | Continued

Source location	Habitat	Isolate name	Closest matching taxon	% identity	% coverage of 16S gene	*S. epidermidis*	*E. raffinosus*	*E. coli*	*P. putida*	*A. baylyi*	*E. aerogenes*
		C6D6	*Nocardia globerula*	99.34	100						
		C6D9	*Pseudoarthrobacter phenanthrenivorans*	99.09	100						
		C7B19	*Nocardia coeliaca*	99.61	100						
		C7B21	*Bacillus mycoide*	99.69	100						
		C7D7	*Paenibacillus xylanexedens*	100	100						
		C8B11	*Rahnella inusitata*	98.59	100						
		C8C11.16	*Bacillus subtilis*	99.74	100						
		C10F22	*Nocardia coeliaca*	99.59	100						
		C10F26	*Pseudomonas fluorescens*	99.28	100						
		C10G6	*Nocardia globerula*	99.34	100						
		C11E10	*Bacillus subtilis*	100	100						
		C11E23	*Bacillus tequilensis*	99.87	100						
		MAL.11.SPBF.1	*Pseudomonas arsenicoxydans*	99.75	55.9						
	Arid soil	AALPS.3.MFAL.10	*Pseudomonas lutea*	100	36						
		AALPS.2.EKRD.20	*Pseudomonas mandelii*	99.73	100						
		AALPS.4.MSMB.5	*Pseudomonas mandelii*	99.66	100						
		AALPS.10.JKNJ.7	*Pseudomonas prosekii*	100	100						
		AALPS.10.EMMH.23	*Pseudomonas yamanorum*	98.68	100						
		AALPS.10.MNAAK.13	*Pseudomonas prosekii*	99.93	100						
		AALPS.13.YAYA.22	*Pseudomonas prosekii*	100	21						
	Surface soil from	PSALP.2.BBCP.18	*Pseudomonas lurida*	99.84	42.6						
	polygonal tundra	PSALP.2.JQGR.13	*Pseudomonas kilonensis*	99.87	53.8						
	terrain										
	Trough soil from polygonal tundra terrain	PWALP.2.KADK.9	*Pseudomonas fluorescens*	100	46.9						
White Glacier, Expedition Fiord	Sediment from glacial terminus moraines	GS.C1.SPSB.3	*Siccibacter turicensis*	100	53.9						

Red boxes: inhibitory activity. Black boxes: no inhibitory activity.

by these 54 isolates were *Pseudomonas* (27 isolates), *Bacillus* (5), *Nocardia* (6), *Janthinobacterium* (3), *Streptomyces* (3), *Paenibacillus* (2), *Mycetocola* (1), *Flavobacterium* (1), *Micrococcus* (1), *Curtobacterium* (1), *Arthrobacter* (1), *Pseudoarthrobacter* (1), *Rahnella* (1), and *Siccibacter* (1).

Microbial cultivation using the cryo-iPlate incubated in active layer permafrost soil within the vicinity of the MARS lead to the isolation of ∼300 morphologically distinct colonies. A total of 16 isolates (∼5%) exhibited antibacterial activity against at least one ESKAPE pathogen relative. All cryo-iPlate strains with antibacterial activity only displayed zones of inhibition against *P. putida* except for *Pedobacter* isolate B7.1 that inhibited *S. epidermidis,* and *Flavobacterium* strain C9.2 that inhibited the growth of *E. coli* and *P. putida* (**Table 3**). Genera represented by these 16 isolates were *Pseudomonas* (4 isolates), *Pedobacter* (3), *Flavobacterium* (3), *Janthinobacterium* (2), *Agreia* (1), *Pararhizobium* (1), *Sphingomonas* (1), and *Stenotrophomonas* (1) (**Table 3**). The genera isolated by both the classical soil plating approach and the cryo-iPlate were *Pseudomonas, Flavobacterium* and *Janthinobacterium*. Among both bulk plated and cryo-iPlate isolates, *Pseudomonas* represented the genus with the highest proportion of total isolated strains (50% of total bulk plated isolates and 25% of total cryo-iPlate isolates).

Antibacterial Activity of Arctic Isolates That Passed the ARP Against Clinical Pathogens

Eight (8) out of the total seventy (70) antibiotic-producing isolates (11%) were found to inhibit the growth of all strains comprising the ARP. These strains were prioritized for further investigation. To assess whether these isolates were capable of inhibiting the growth of clinically significant pathogens, the isolates were screened against ESKAPE organisms *P. aeruginosa*, MRSA, *A. baumanii,* MSSA, *E. cloacae*, *K. pneumoniae*, *E. faecium*, and *E. faecalis*. *Pseudomonas* sp. AALPS.10.MNAAK.13 was observed to have the broadest antibacterial activity spectrum. It inhibited the growth of MRSA, *A. baumanii*, MSSA, *E faecium*, and *E. faecalis* (**Table 5**). *Flavobacterium* sp. GHHS.3.LBZX.4 and *Pseudomonas* sp. MAL.4.ABES.21 were not observed to inhibited any of the pathogenic tester strains. *Pseudomonas* sp. MAL.10.WYTK.25, *Pseudomonas* sp. AALPS.4.MSMB.5 and *Bacillus* sp. C11E23 inhibited the growth of MRSA, MSSA, and *E. faecium*. *Paenibacillus* sp. GHS.8.NWYW.5 was capable of inhibiting MRSA and MSSA. Pseudomonas sp. GHCE.5JVZL.12 inhibited the growth of MRSA, *A. baumanii*, MSSA, and *K. pneumoniae*.

Growth of Arctic Isolates That Passed the ARP at Various Temperatures

After screening against clinically significant pathogens, we assessed whether the eight prioritized isolates were capable of growing at various temperatures (37, 25, 10, 5, 0, and −5°C). All eight isolates were capable of growth at 5°C. Only two isolates (*Paenibacillus* sp. GHS.8.NWYW.5 and *Pseudomonas* sp. GHCE.5.JVZL.12) were capable of growing at 37°C after 48 h of incubation. All isolates except *Pseudomonas* sp. GHCE.5.JVZL.12 grew at 0°C after 20 days of incubation. With the exception of *Flavobacterium* sp. GHHS.3.LBZX.4 and *Pseudomonas* sp. GHCE.5.JVZL.12, all other Arctic isolates that passed the ARP were capable of growing at −5°C after 20 days of incubation (**Supplementary Table S3**).

Antibacterial Activity of Prioritized Isolates Against Foodborne Pathogens

The eight prioritized isolates were tested for antibacterial activity against four foodborne pathogens (*S. aureus*, *L. monocytogenes*, *S. enterica* and *E. coli* O157:H7 at two different incubation temperatures (37 and 5°C). *Paenibacillus* sp. GHS.8.NWYW.5 was observed to inhibit the growth of *S. aureus*, *L. monocytogenes*, *S. enterica*, and *E. coli* O157:H7 at 37 and 5°C. *Pseudomonas* sp. AALPS.10.MNAAK.13 was observed to inhibit *S. aureus* at 37°C after 24 h of incubation. *Pseudomonas* sp. MAL.10.WYTK.25 was observed to inhibit the growth of *S. enterica at* 37°C after 24 h. *Bacillus* sp. C11E23 inhibited *L. monocytogenes* at 37 and 5°C (**Table 6**). The zones of inhibition produced by these Arctic isolates were consistent with the known antibiotic-producing strain *P. terrae* NRRL B-30644 which displayed inhibitory activity against all foodborne pathogens used in this assay.

Genomic Analysis of Bacterial Isolates Capable of Inhibiting the Entire ARP

After the Illumina MiSeq 300 bp paired-end run, the range of number of raw reads was 665502–2929247 and the fragment size range was 400–2000 bp (**Supplementary Table S4** and **Supplementary Figure S1**). The genomes of the eight prioritized isolates were then mined using the antiSMASH database to identify secondary metabolite gene clusters that they encode (**Table 4**). These genomes contained ≥ 6 putative BGCs that were homologous to NRP, PK, bacteriocin/ribosomally synthesized and post-translationally modified peptide (RiPP), and trans-polyketide synthetase (trans-PKS). All clusters labeled as "other" corresponded to either arylpolyene, terpene, betalactone, siderophore, N-acetylglutaminylglutamine (NAGGN) amide or phosphonate clusters (not shown in table). The genome of *Paenibacillus* sp. GHS.8.NWYW.5 featured the greatest number of BGCs compared to all other isolates with 23 secondary metabolite clusters. These clusters included 17 NRP clusters, three bacteriocin/RiPP clusters, one trans-PKS cluster, and two other clusters (one siderophore and one phosphonate cluster). The isolate featuring the least number of BGCs within its genome was *Flavobacterium* sp. GHHS.3.LBZX.4 with a total of six secondary metabolite clusters. These included one type-3 PK, one NRP and four other clusters (one arylpolyene cluster, two terpene clusters, and one betalactone cluster). *Pseudomonas* sp. AALPS.10.MNAAK.13 and *Paenibacillus* sp. GHS.8.NWYW.5 represent the two isolates that displayed the broadest spectra of antibacterial activities against foodborne and clinical pathogens. Eight BGCs were identified within the genome of *Pseudomonas* sp. AALPS.10.MNAAK.13 using antiSMASH (**Table 7**). After conducting a blastn alignment between the isolate's clusters with the *Pseudomonas prosekii* LMG 26867 type strain genome, none of the detected clusters displayed low homology within

TABLE 3 | Antibiotic activity of cryo-iPlate isolates against ESKAPE pathogen relatives.

Isolate name	Closest match	% identity	S. *epidermidis*	E. *raffinosus*	E. *coli*	P. *putida*	A. *baylyi*	E. *aerogenes*
A4.3Y	*Janthinobacterium lividum*	99.31						
B1.1W	*Pseudomonas trivialis*	100						
B4.6	*Pseudomonas migulae*	100						
B7.1	*Pedobacter humicola*	99.01						
C3.3	*Pedobacter alluvionis*	99.09						
C6.2	*Pseudomonas koreensis*	100						
C7.3	*Agreia pratensis*	100						
D4.1	*Pseudomonas arsenicoxydans*	100						
G2.2	*Flavobacterium oncorhynchi*	100						
F9.3	*Pedobacter terrae*	95.59						
D1.3	*Janthinobacterium lividum*	99.25						
C12.2A	*Stenotrophomonas rhizophila*	99.49						
C12.1B	*Flavobacterium frigidimaris*	99.2						
C11.2	*Pararhizobium herbae*	100						
C11.3	*Sphingomonas aerolata*	99.68						
C9.2	*Flavobacterium hydatis*	100						

Red boxes: positive inhibitory activity. Black boxes: negative inhibitory activity.

TABLE 4 | Identification of secondary metabolite biosynthetic gene clusters within genomes of isolates inhibiting the ARP.

Isolate	Genome size (Mb)	Isolate Identification	%16S gene ID	AntiSMASH (total clusters)	NRP[1]	PK[2]	Bacterion/ RiPP[3]	Trans PKS[4]	Other
GHHS.3.LBZX.4	6.1	*Flavobacterium panaciterrae*	87.54	6	1	1	0	0	4
GHS.8.NWYW.5	5.7	*Paenibacillus terrae*	99.23	23	17	0	3	1	2
MAL.10.WYTK.25	6.8	*Pseudomonas extremaustralis*	99.73	9	4	0	2	0	3
GHCE.5.JVZL.12	5	*Pseudomonas fulva*	100	11	9	0	0	0	2
AALPS.4.MSMB.5	6.3	*Pseudomonas mandelii*	99.66	10	3	0	3	1	3
AALPS.10.MNAAK.13	6.1	*Pseudomonas prosekii*	99.93	8	2	0	1	0	5
MAL.4.ABES.21	7.1	*Pseudomonas frederiksbergensis*	99.86	7	3	0	1	0	3
C11E23	4.3	*Bacillus tequilensis*	100	12	4	1	3	1	3

[1]Number of non-ribosomal peptide gene clusters identified using AntiSMASH. [2]Number of polyketide gene clusters identified using AntiSMASH. [3]Number of bacteriocin and ribosomally synthesized and post-translationally modified peptides (RiPP) identified using AntiSMASH. [4]Number of trans-polyketide gene clusters identified using AntiSMASH.

the type strain genome. The genome of the *Paenibacillus* sp. GHS.8.NWYW.5 featured 23 BGCs (**Table 7**). The clusters with low homology (<50% coverage, <30% identity, and e-values > 0) to the type strain genome of *P. terrae* NRRL B-30644 included: one NRP cluster displayed 11% coverage and 98% identity, one NRP cluster matching to pelgipeptin displayed 45% coverage and 97% identity, one NRP cluster displayed 41% coverage and 75% identity, and two unknown NRP clusters that did not have any significant homology with the type strain genome.

Organic Extraction Using Liquid Culture Supernatants

Organic extracts using liquid culture supernatants from isolates *Paenibacillus* sp. GHS.8.NWYW.5, *Pseudomonas* sp. AALPS.10.MNAAK.13, *Pseudomonas* sp. AALPS.10.EMMH.23, *Pseudomonas* sp. AALPS.10.JKNJ.7, *Pseudomonas* sp. AALPS.4.MSMB.5, *Pseudomonas* sp. GHCE.5.JVZL.12, *Pseudomonas* sp. MAL.10.WYTK.25 (same isolate as 7.EKIG.16 in **Figure 3**) were prepared using ethyl acetate. The crude organic extracts were then tested for retained antibacterial activity using a plate-based spot assay against the parental strains of the ARP (*E. coli* Δ*bam*Δ*tolC* BW25113 and *E. coli* BW25113). After 24 h of incubation at room temperature, the extracts of *Pseudomonas* sp. AALPS.10.MNAAK.13, *Pseudomonas* sp. AALPS.10.EMMH.23 and *Paenibacillus* sp. GHS.8.NWYW.5 exhibited zones of inhibition against *E. coli* Δ*bam*Δ*tolC* BW25113 (**Figures 3A,D**). The extract of *Pseudomonas* sp. AALPS.10.EMMH.23, yielded a zone of inhibition against *E. coli* BW25113 (**Figure 3B**).

DISCUSSION

Arctic Bacteria Demonstrate Antibiotic Activity Against ESKAPE Pathogen Relatives

Bacteria capable of inhibiting ESKAPE pathogen relatives were isolated from all sampled Arctic environments, with the

TABLE 5 | Screening Arctic isolates that inhibited the ARP against clinical pathogens.

Isolate name	Closest matching species	Closest matching strain	*P. aeruginosa*	*MRSA*	*A. baumanii*	*MSSA*	*E. cloacae*	*K. pneumoniae*	*E. faecium*	*E. faecalis*
GHHS.3.LBZX.4	*Flavobacterium panaciterrae*	DCY69(T)								
GHS.8.NWYW.5	*Paenibacillus terrae*	AM141(T)		+		+				
AALPS.10.MNAAK.13	*Pseudomonas prosekii*	LMG 26867		+	+	+			+	+
MAL.10.WYTK.25	*Pseudomonas extremaustralis*	14-3(T)		+		+			+	
GHCE.5.JVZL.12	*Pseudomonas fluorescens*	DSM 50090(T)		+	+	+		+		
AALPS.4.MSMB.5	*Pseudomonas mandelii*	NBRC 103147(T)		+		+			+	
MAL.4.ABES.21	*Pseudomonas frederiksbergensis*	JAJ28(T)								
C11E23	*Bacillus tequilensis*	KCTC 13622(T)		+		+			+	

(+) Positive inhibitory activity.

exception of perennial hypersaline spring sediment sample from Lost Hammer. A total of 70 antibiotic producing isolates were identified, with 54 coming from a classical bulk soil plating approach, and 16 from cryo-iPlate cultivation. More isolates were obtained from the bulk plating approach aided by the greater throughput of approximately 130 undergraduate students processing samples in parallel, while the cryo-iPlate samples were processed by only two graduate students. Additionally, the volume of Arctic samples used for classical plating to isolate microorganisms was ∼60 times greater than that used to inoculate the cryo-iPlate. None of the isolates with antibacterial activity were obtained from perennial hypersaline spring sediment from Lost Hammer, which may be because the salt content of the cultivation media was not adjusted to select for halophilic strains. It is known that the perennial hypersaline spring sediment at Lost Hammer hosts an active microbial community including members of the *Loktanella*, *Gillisia*, *Halomonas* and *Marinobacter* genera (Niederberger et al., 2010), and lack of isolates therefore cannot be attributed to lack of viable bacteria in the source material.

The sample type that yielded the greatest number of isolates with antibiotic activity was active layer soils overlaying permafrost, which consists of a low carbon mineral cryosol. It is ∼60 cm deep during the Arctic summer and completely freezes during winter and spring (Doran, 1993; Lau et al., 2015; Goordial et al., 2017). Previously cultured phylotypes from this habitat predominantly included Actinobacteria (Niederberger et al., 2010), and indeed 26% of isolates identified by the bulk soil plating approach belonged to the Actinobacteria. This phylum includes the genus *Streptomyces* which are known to be prolific producers of antibiotics (Kiesser et al., 2000; Manivasagan et al., 2014). A previous study using functional metagenomics showed that antibiotic resistance genes are present in similar permafrost soils at nearby Eureka, Ellesmere Island (Perron et al., 2015). The presence of antibiotics will create selective pressure for the development of antibiotic resistance. The presence of both antibiotic activity and antibiotic resistance therefore suggests interactions between these functions in the microbial permafrost community.

All cryo-iPlate strains were derived from active layer permafrost soil, because this was the only sample type in which the cryo-iPlate was incubated. The cryo-iPlate yielded genera (*Pararhizobium*, *Sphingomonas*, *Stenotrophomonas*, *Agreia*, *Pedobacter*) that were not observed in the strains isolated by the classical method from the same environment. In the initial implementation of the cryo-iPlate prototype, many of the same genera were isolated, including a putatively novel *Pedobacter* strain (Goordial et al., 2017). Similarly, *Pedobacter* strain F9.3 derived from the cryo-iPlate in this study was found to have 95.6% 16S rRNA gene sequence identity to its closest match *Pedobacter terrae* (**Table 3**). While none of the cryo-iPlate derived strains inhibited the entire ARP, they were able to inhibit the growth of both Gram-positive and Gram-negative relatives of the ESKAPE pathogens. Given that these strains were isolated from cryohabitats, their antibacterial activity has potential

TABLE 6 | Screening Arctic isolates that inhibited the ARP against foodborne pathogens.

			Staphylococcus aureus		*Listeria monocytogenes*		*Salmonella enterica*		*Escherichia coli O157:H7*	
Isolate name	**Closest matching species**	**Closest matching strain**	**37°C**	**5°C**	**37°C**	**5°C**	**37°C**	**5°C**	**37°C**	**5°C**
GHHS.3.LBZX.4	*Flavobacterium panaciterrae*	DCY69(T)								
GHS.8.NWYW.5	*Paenibacillus terrae*	AM141(T)	+	+	+	+	+	+	+	+
AALPS.10.MNAAK.13	*Pseudomonas prosekii*	LMG 26867	+							
MAL.10.WYTK.25	*Pseudomonas extremaustralis*	14-3(T)					+			
GHCE.5.JVZL.12	*Pseudomonas fluorescens*	DSM 50090(T)								
AALPS.4.MSMB.5	*Pseudomonas mandelii*	NBRC 103147(T)								
MAL.4.ABES.21	*Pseudomonas frederikbergensis*	JAJ28(T)								
C11E23	*Bacillus tequilensis*	KCTC 13622(T)			+	+				

(+) Positive inhibitory activity.

TABLE 7 | Comparing secondary metabolite gene clusters identified within genomes of promising isolates with type strains of the same species.

Isolate[a]	**Type strain genome**[b]	**BGC category**[c]	**Closest matching known BGC**[d]	**Coverage (%)**[e]	**ID (%)**[f]	**e-value**[g]
AALPS.10.MNAAK.13 (*Pseudomonas prosekii*)	*Pseudomonas prosekii* LMG 26867	NRP	pyoverdine	95	97.99	0
		betalactone	fengycin	100	98.3	0
		terpene	–	66	99.03	0
		arylpolyene	APE vf	95	98.63	0
		hserlactone	–	99	98.87	0
		bacteriocin	bacillomycin	100	98.22	0
		NAGGN	–	100	98.63	0
		NRP	pyoverdine	99	98.40	0
GHS.8.NWYW.5 (*Paenibacillus terrae*)	*Paenibacillus terrae* NRRL B-30644	NRP	tridecaptin	87	91	0
		siderophore	staphylobactin	88	95	0
		lanthipeptide	paenicidin B	100	96	0
		phosphonate	–	58	95	0
		lassopeptide	–	100	95	0
		NRP	–	54	93	0
				40	93	0
		NRP	calicheamicin	89	95	0
		NRP trans-ATPKS	paenilarvin	71	93	0
		NRP-betalactone	–	60	91	0
		NRP	–	58	94	0
		NRP		11	98	0
		bacteriocin	–	93	92	0
		NRP	fusaricidin	99	93	0
				37	65	0
		NRP	pelgipeptin	45	97	0
		NRP	–	*NA*	NA	NA
		NRP	–	41	75	0
		NRP	–	*NA*	NA	NA
		NRP	polymyxin	62	69	0
				44	69	7e-141
		NRP	tridecaptin	55	69	0
		NRP	–	46	73	8e-36
		NRP	–	95	73	0
				65	70	5e-38
				46	67	1e-33
		NRP	paenibacterin	38	74	1e-35
		NRP	–	61	69	3e-38

[a] *Prioritized isolates displaying widest spectra of antagonistic activity against foodborne and ESKAPE pathogens.* [b] *Corresponding type strain genome of isolates' species.* [c] *Category of secondary metabolite BGCs within genomes of isolates identified using the antiSMASH database.* [d] *Closest match to known secondary metabolite clusters within isolates' genomes.* [e] *Percent coverage of Arctic isolates' BGCs within reference genomes.* [f] *Percent identity of Arctic isolates' BGCs within reference genomes.* [g] *e-value of Arctic isolates' BGCs within reference genomes.*

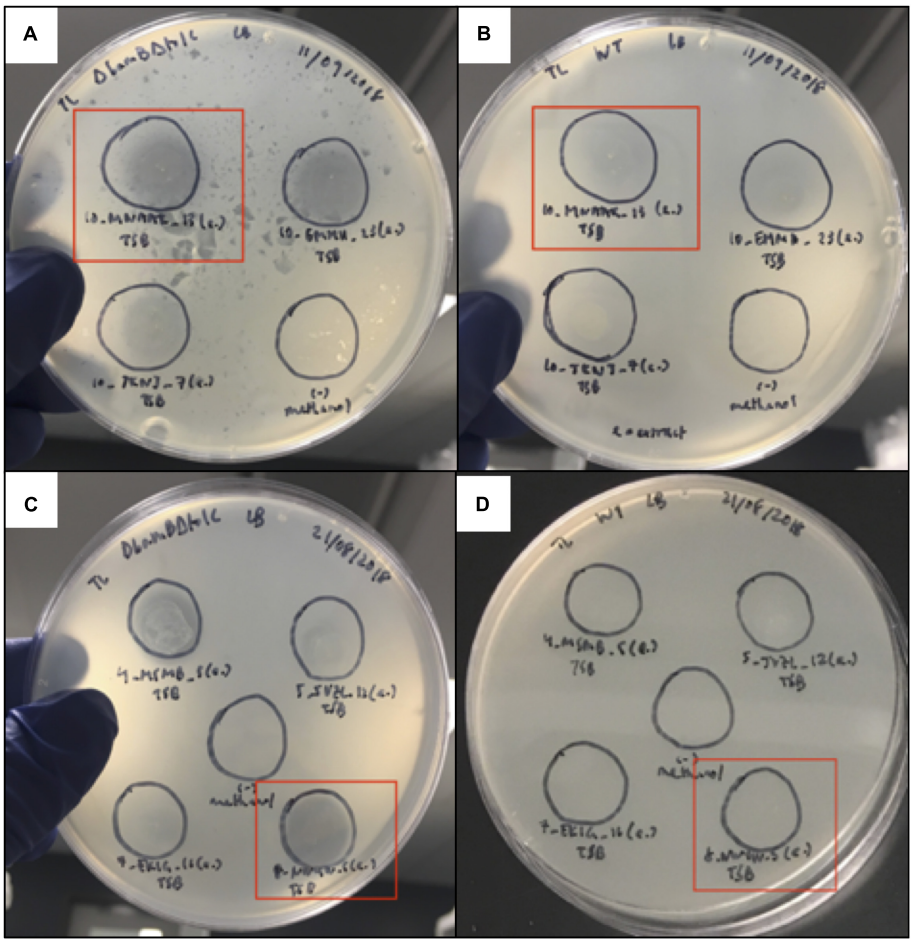

FIGURE 3 | Spot assay used to assess antibacterial activity of organic extracts derived from Arctic isolate supernatants. **(A,B)** Organic extracts of isolates *Pseudomonas* sp. AALPS.10.MNAAK.13, *Pseudomonas* sp. AALPS.10.EMMH.23 and *Pseudomonas* sp. AALPS.10.JKNJ.7 tested against both parental strains of the dereplication platform (*E. coli* Δ*bam*Δ*tolC* BW25113 and *E. coli* BW25113, respectively). Promising isolate *Pseudomonas* sp. AALPS.10.MNAAK.13 that displayed the broadest antibacterial activity in co-culture assays is boxed in red. Negative control spots solely consisting of the methanol are displayed at the bottom right in panels **(A,B)**. **(C,D)** Organic extracts of isolates *Paenibacillus* sp. GHS.8.NWYW.5, *Pseudomonas* sp. AALPS.4.MSMB.5, *Pseudomonas* sp. GHCE.5.JVZL.12, *Pseudomonas* sp. MAL.10.WYTK.25 (same isolate as 7.EKIG.16 in figure) tested against both parental strains of the dereplication platform (*E. coli* Δ*bam*Δ*tolC* BW25113 and *E. coli* BW25113, respectively). Promising isolate *Paenibacillus* sp. GHS.8.NWYW.5 that displayed the broadest antibacterial activity in co-culture assays is boxed in red. Negative control spots solely consisting of methanol are displayed in the center of panels **(C,D)**.

applications in food safety, where inhibitory activity is required at refrigeration temperatures.

Eight Arctic Bacterial Isolates Inhibited All ARP Strains

Here we have identified eight isolates able to inhibit the ARP which corresponded to either Firmicutes, Bacteroidetes or γ-Proteobacteria. It is worth noting that the dereplication method employed in this study is not a comprehensive approach in identifying isolates expressing novel antibiotic compounds. For example, if a given antibiotic-producing isolate expresses more than one antimicrobial secondary metabolite, it would be capable of inhibiting the growth of all strains comprising the ARP regardless of whether the mechanisms of action of its secondary metabolites are novel. Given this inherent limitation of the ARP, the benefit of using this platform is an initial quick and cost-effective method of screening isolates with inhibitory activities for potentially novel activities. Further identification and characterization of the causative agents responsible for the inhibitory activities are required to confirm the novelty of a natural product.

The phyla of the prioritized isolates are known to make up a significant proportion of the active layer permafrost microbial community and are established secondary metabolite producers (Pathma et al., 2011; Wilhelm et al., 2011). Five out of the eight isolates that passed dereplication were *Pseudomonas* spp. This observation is not unexpected, as these Gram-negative heterotrophic γ-Proteobacteria are routinely isolated from soil samples using classical cultivation techniques such as the ones employed here (Sbrana et al., 2002). Additionally, the microbial community living in active layer permafrost within the vicinity

of the MARS has been found to contain 19.4% γ-Proteobacteria (Wilhelm et al., 2011).

The only isolate that passed dereplication pertaining to the phylum Bacteroidetes was *Flavobacterium* sp. GHHS.3.LBZX.4. Two Firmicutes (one *Bacilllus* sp. and one *Paenibacillus* sp.) were also observed to inhibit all strains comprising the ARP. These two genera are well-documented secondary metabolite producers known to produce a plethora of antimicrobial compounds (Pathma et al., 2011; Caulier et al., 2019).

Interestingly, *Paenibacillus* sp. GHS.8.NWYW.5 and *Pseudomonas* sp. GHCE.5.JVZL.12 were the only isolates passing dereplication that were not derived from active layer permafrost. *Paenibacillus* sp. GHS.8.NWYW.5 was isolated from sediments of the Gypsum Hill saline spring (∼8% salts) and *Pseudomonas* sp. GHCE.5.JVZL.12 was isolated from a gypsum cryptoendolith. Our current knowledge of high Arctic saline spring sediments and cryptoendoliths as potential reservoirs of secondary metabolites is very limited and thus this finding serves as an interesting starting point for future studies.

Two Promising Isolates Inhibit the Growth of Foodborne and Clinically Relevant Pathogens

After the antibiotic activity of all eight isolates that passed the dereplication assay was tested against foodborne and clinically relevant pathogens, *Pseudomonas* sp. AALPS.10.MNAAK.13 and *Paenibacillus* sp. GHS.8.NWYW.5 were identified to have a broad spectrum of antibacterial activity. *Pseudomonas* sp. AALPS.10.MNAAK.13 was found to have the broadest activity against clinically relevant pathogens; inhibiting the growth of both Gram-positive and Gram-negative pathogens including MRSA, *A. baumanii*, MSSA, *E. faecium*, and *E. faecalis*. *Paenibacillus* sp. GHS.8.NWYW.5 was capable of inhibiting all four foodborne pathogens tested in this study. It displayed inhibitory effects at 37°C and at 5°C against *S. aureus*, *S. enterica*, *L. monocytogenes*, and *E. coli* O157:H7 (**Tables 5**, **6**). The zones of inhibition produced by these Arctic isolates were visually similar to ones produced by the environmental reference strain *P. terrae* NRRL B-30644 which was initially isolated from a Russian poultry production environment and documented to have inhibitory activity against the foodborne pathogen *Campylobacter jejuni* (Lohans et al., 2014). To confirm that the antagonistic activities observed during the initial co-culture assays were due to secreted bacterial biomolecules, promising isolates were selected for organic extraction and tested against the parental strains of the ARP. The organic extract of isolates *Pseudomonas* sp. AALPS.10.MNAAK.13, and *Paenibacillus* sp. GHS.8.NWYW.5 exhibited zones of clearance against *E. coli* Δ*bam*Δ*tolC* BW25113. These observations coupled with our detection of secondary metabolite gene clusters within Arctic isolates' genomes (**Table 7**), suggest that the inhibitory activities observed in this study arose from secreted antibacterial secondary metabolites. Ongoing testing is taking place to identify the causative agent(s) within the crude extracts and to determine their potency and spectrum of activity.

Interestingly, both of these Arctic isolates displayed antibacterial activity against MRSA and MSSA. MRSA's prevalence and the number of deaths it causes yearly qualify this pathogen as a major global public health concern (Martin et al., 2019), and antibacterial activity against MRSA is therefore of particular interest. The recent discovery of malacidin (effective against MRSA and other Gram-positive pathogens) illustrates how natural products from soil-dwelling bacteria continue to represent promising drug leads for endemic antibiotic resistant pathogens of the 21st century (Hover et al., 2018). The secondary metabolites expressed by the Arctic isolates surveyed herein will be further characterized in future studies to determine if they have any chemotherapeutic potential.

The genome of *Paenibacillus* sp. GHS.8.NWYW.5 was found to 7 BGCs displaying low homology with clusters of its respective type strains of the same species. Conversely, all clusters detected within the genome of *Pseudomonas* sp. AALPS.10.MNAAK.13 displayed high homology when aligned with the type strain genome sequence. The genome of *Paenibacillus* sp. GHS.8.NWYW.5 featured the greatest number of total BGCs with five NRP clusters displaying low homology to its corresponding type strain genome. The type strain of this isolate, *P. terrae* NRRL B-30644 has been shown to express paenicidins and tridecaptin A_1 (Lohans et al., 2014). Clusters encoding both paenicidin and tridecaptin were identified within the genome of *Paenibacillus* sp. GHS.8.NWYW.5, however, it was also found to encode five NRP clusters with low homology to the type strain genome. Follow-up experiments such as genome-wide transposon mutagenesis or targeted cloning and exogenous expression of specific clusters are required to determine which cluster(s) are responsible for the observed antibiotic activity exhibited by these isolates.

Arctic Isolates That Passed the ARP Are Capable of Growth at Refrigeration Temperatures

All isolates that passed the dereplication assay (except for *Pseudomonas* sp. GHCE.5.JVZL.12) were capable of growing at temperatures ≤ 0°C within 20 days of incubation and grew more quickly at room temperature. Only two isolates (*Paenibacillus* sp. GHS.8.NWYW.5 and *Pseudomonas* sp. GHCE.5.JVZL.12) were capable of growing at 37°C. This observation suggests that these isolates are eurypsychrophiles which are typically characterized by their tolerance to subzero temperatures and display optimal growth at ∼20°C (Raymond-Bouchard et al., 2018). Previous studies conducted with similar soil samples from the MARS site have led to the isolation of eurypsychrophillic strains including *Planococcus halocryophilus* Or1 that is capable of growth at –15°C (Mykytczuk et al., 2016). The initial incubation of the bulk soil plates was performed at room temperature precluded the isolation of stenopsychrophiles that would have required lower cultivation temperatures (Raymond-Bouchard et al., 2018).

The antibacterial activity of *Paenibacillus* sp. GHS.8.NWYW.5 against foodborne pathogens at common household refrigeration temperatures makes it a promising candidate for biotechnological applications in food-safety. The use of cold-adapted

environmental strains as biopreservatives intended to inhibit the growth of foodborne pathogens within refrigerated commodities have been previously developed (Rovira and Melero, 2018). For example, certain strains of bacteriocin-producing *Carnobacteria* spp. isolated from natural environments have been used to limit the growth of pathogens within preserved seafood products (Wiernasz et al., 2017). The isolates identified in this study that were capable of subzero growth and displayed antibacterial activity at refrigeration temperatures could serve as interesting starting points for future food-safety applications.

CONCLUSION

The results of our bioprospecting demonstrate how crowdsourced classical microbial cultivation and cryo-iPlate cultivation contribute to a culture-dependent workflow that can lead to the identification of Arctic bacteria capable of antibacterial activity. First results suggest that the habitats within the vicinity MARS on Axel Heiberg Island harbor promising cold-adapted bacteria with antibacterial activities against both foodborne and clinically significant pathogens. Further investigation will be required to identify the causative agents responsible for the observed antibacterial activities and to explore potential clinical and food-safety applications.

DATA AVAILABILITY

The raw data supporting the conclusions of this manuscript will be made available by the authors, without undue reservation, to any qualified researcher.

AUTHOR CONTRIBUTIONS

EM carried out field work, lab work, analysis, and writing. MO carried out analysis, participated in experimental design, and contributed significantly to writing. TL and GM conducted the dereplication assay and screening against clinical pathogens. EH conducted the dereplication assay and participated in isolating and screening cryo-iPlate strains. JH and BB conducted whole genome sequencing and assembly. GA and OB-H assisted in isolating and screening cryo-iPlate strains. RL and DN advised in experimental design and writing. SG coordinated the MIMM212 undergraduate crowdsourcing laboratory course, and advised and contributed significantly to writing and analysis. LW supervised the project and significantly contributed to project design, writing and analysis.

FUNDING

This work was supported by the Fonds de recherche du Québec – Nature et technologies (FRQNT), Northern Scientific Training Program (NSTP), and Polar Continental Shelf Project (PCSP).

ACKNOWLEDGMENTS

We acknowledge the hard work of the students and teaching assistants that participated in the MIMM212 Laboratory in Microbiology in 2016 and 2017. We thank Dr. Gerry Wright for generously providing the ARP strains, and Adam Classen, Maria Lee Ai Lan, Dr. Sudhakar G. Bhandare from the laboratories of Dr. Jennifer Ronholm and Dr. Lawrence Goodridge for providing the foodborne pathogens. We also thank the laboratory of Dr. J. C. Vederas for supplying our team with *P. terrae* NRRL B-30644, and Samy Coulombe for assisting in designing the cryo-iPlate and for subculturing Arctic isolates.

SUPPLEMENTARY MATERIAL

The Supplementary Material for this article can be found online at: https://www.frontiersin.org/articles/10.3389/fmicb.2019.01836/full#supplementary-material

REFERENCES

Aziz, R. K., Bartels, D., Best, A. A., DeJongh, M., Disz, T., Edwards, R. A., et al. (2008). The RAST server: rapid annotations using subsystems technology. *BMC Genomics* 9:75. doi: 10.1186/1471-2164-9-75

Baker, D. D., Chu, M., Oza, U., and Rajgarhia, V. (2007). The value of natural products to future pharmaceutical discovery. *Nat. Prod. Rep.* 24, 1225–1244.

Balabanova, L., Podvolotskaya, A., Slepchenko, L., Eliseikina, M., Noskova, Y., Nedashkovskaya, O., et al. (2017). Nucleolytic enzymes from the marine bacterium *Cobetia amphilecti* KMM 296 with antibiofilm activity and biopreservative effect on meat products. *Food Control* 78, 270–278. doi: 10.1016/j.foodcont.2017.02.029

Bitnun, A., and Yeh, E. A. (2018). Purpose of review the rise in antimicrobial resistance is an urgent public health threat which, in the absence of intervention, may result in a post-antibiotic era limiting the effectiveness of antibiotics to treat both common and serious infections. Globalization and human migration have profoundly contributed to the spread of drug-resistant bacteria. In this review, we summarize the recent literature. *Curr. Infect. Dis. Rep.* 20, 1–10. doi: 10.1007/s11908-018-0634-9

Blin, K., Shaw, S., Steinke, K., Villebro, R., Ziemert, N., Lee, S. Y., et al. (2019). antiSMASH 5.0: updates to the secondary metabolite genome mining pipeline. *Nucleic Acids Res.* 47, W81–W87. doi: 10.1093/nar/gkz310

Blin, K., Wolf, T., Chevrette, M. G., Lu, X., Schwalen, C. J., Kautsar, S. A., et al. (2017). antiSMASH 4.0—improvements in chemistry prediction and gene cluster boundary identification. *Nucleic Acids Res.* 45, W36–W41.

Boucher, H. W., and Corey, G. R. (2008). Epidemiology of methicillin-resistant *Staphylococcus aureus*. *Clin. Infect. Dis.* 46(Suppl. 5), S344–S349.

Boucher, H. W., Talbot, G. H., Bradley, J. S., Edwards, J. E., Gilbert, D., Rice, L. B., et al. (2009). Bad bugs, no drugs: no ESKAPE! an update from the infectious diseases society of America. *Clin. Infect. Dis.* 48, 1–12. doi: 10.1086/595011

Brettin, T., Davis, J. J., Disz, T., Edwards, R. A., Gerdes, S., Olsen, G. J., et al. (2015). RASTtk: a modular and extensible implementation of the RAST algorithm for building custom annotation pipelines and annotating batches of genomes. *Sci. Rep.* 5:8365. doi: 10.1038/srep08365

Caulier, S., Nannan, C., Gillis, A., Licciardi, F., Bragard, C., and Mahillon, J. (2019). Overview of the antimicrobial compounds produced by members of the *Bacillus subtilis* group. *Front. Microbiol.* 10:302. doi: 10.3389/fmicb.2019.00302

Cox, G., Sieron, A., King, A. M., De Pascale, G., Pawlowski, A. C., Koteva, K., et al. (2017). A common platform for antibiotic dereplication and adjuvant discovery. *Cell Chem. Biol.* 24, 98–109. doi: 10.1016/j.chembiol.2016.11.011

Davis, E., Sloan, T., Aurelius, K., Barbour, A., Bodey, E., Clark, B., et al. (2017). Antibiotic discovery throughout the small world initiative: a molecular strategy to identify biosynthetic gene clusters involved in antagonistic activity. *MicrobiologyOpen* 6:e00435. doi: 10.1002/mbo3.435

Dhaneesha, M., Naman, C. B., Krishnan, K., Sinha, R. K., Jayesh, P., Joseph, V., et al. (2017). Streptomyces artemisiae MCCB 248 isolated from Arctic fjord sediments has unique PKS and NRPS biosynthetic genes and produces potential new anticancer natural products. *3 Biotech* 7:32.

Doran, P. T. (1993). Sedimentology of Colour Lake, a nonglacial high Arctic lake, Axel Heiberg Island, NWT, Canada. *Arct. Alp. Res.* 25, 353–367.

Ferri, M., Ranucci, E., Romagnoli, P., and Giaccone, V. (2017). Antimicrobial resistance: a global emerging threat to public health systems. *Crit. Rev. Food Sci. Nutr.* 57, 2857–2876. doi: 10.1080/10408398.2015.1077192

Goordial, J., Altshuler, I., Hindson, K., Chan-Yam, K., Marcolefas, E., and Whyte, L. G. (2017). In situ field sequencing and life detection in remote (79° 26′ N) Canadian high arctic permafrost ice wedge microbial communities. *Front. Microbiol.* 8:2594. doi: 10.3389/fmicb.2017.02594

Gregory, A., Zayed, A., Conceição-Neto, N., Temperton, B., Bolduc, B., Alberti, A., et al. (2019). Marine DNA viral macro-and micro-diversity from pole to pole. *Cell* 177, 1109.e14–1123.e14. doi: 10.1016/j.cell.2019.03.040

Hover, B. M., Kim, S.-H., Katz, M., Charlop-Powers, Z., Owen, J. G., Ternei, M. A., et al. (2018). Culture-independent discovery of the malacidins as calcium-dependent antibiotics with activity against multidrug-resistant Gram-positive pathogens. *Nat. Microbiol.* 3:415. doi: 10.1038/s41564-018-0110-1

Jang, K. H., Nam, S. J., Locke, J. B., Kauffman, C. A., Beatty, D. S., Paul, L. A., et al. (2013). Anthracimycin, a potent anthrax antibiotic from a marine-derived actinomycete. *Angew. Chem. Int. Ed.* 52, 7822–7824. doi: 10.1002/anie.201302749

Johannesson, K. H., and Lyons, W. B. (1995). Rare-earth element geochemistry of Colour Lake, an acidic freshwater lake on Axel Heiberg Island, Northwest Territories, Canada. *Chem. Geol.* 119, 209–223. doi: 10.1016/0009-2541(94)00099-t

Kiesser, T., Bibb, M., Buttner, M., Chater, K., and Hopwood, D. (2000). *Practical Streptomyces Genetics*. Norwich: The John Innes Foundation.

Kim, D., Song, L., Breitwieser, F. P., and Salzberg, S. L. (2016). Centrifuge: rapid and sensitive classification of metagenomic sequences. *Genome Res.* 26, 1721–1729. doi: 10.1101/gr.210641.116

Klevens, R. M., Edwards, J. R., Tenover, F. C., McDonald, L. C., Horan, T., Gaynes, R., et al. (2006). Changes in the epidemiology of methicillin-resistant Staphylococcus aureus in intensive care units in US hospitals, 1992–2003. *Clin. Infect. Dis.* 42, 389–391. doi: 10.1086/499367

Lau, M. C., Stackhouse, B., Layton, A. C., Chauhan, A., Vishnivetskaya, T., Chourey, K., et al. (2015). An active atmospheric methane sink in high Arctic mineral cryosols. *ISME J.* 9, 1880–1891. doi: 10.1038/ismej.2015.13

Laxminarayan, R., Duse, A., Wattal, C., Zaidi, A. K., Wertheim, H. F., Sumpradit, N., et al. (2013). Antibiotic resistance—the need for global solutions. *Lancet Infect. Dis.* 13, 1057–1098. doi: 10.1177/1073110518782916

Lay, C.-Y., Mykytczuk, N. C., Yergeau, É, Lamarche-Gagnon, G., Greer, C. W., and Whyte, L. G. (2013). Defining the functional potential and active community members of a sediment microbial community in a high Arctic hypersaline subzero spring. *Appl. Environ. Microbiol.* 76, 3637–3648. doi: 10.1128/AEM.00153-13

Ling, L. L., Schneider, T., Peoples, A. J., Spoering, A. L., Engels, I., Conlon, B. P., et al. (2015). A new antibiotic kills pathogens without detectable resistance. *Nature* 517:455. doi: 10.1038/nature14098

Lohans, C. T., van Belkum, M. J., Cochrane, S. A., Huang, Z., Sit, C. S., McMullen, L. M., et al. (2014). Biochemical, structural, and genetic characterization of tridecaptin A1, an antagonist of *Campylobacter jejuni*. *Chembiochem* 15, 243–249. doi: 10.1002/cbic.201300595

Machado, H., Sonnenschein, E. C., Melchiorsen, J., and Gram, L. (2015). Genome mining reveals unlocked bioactive potential of marine Gram-negative bacteria. *BMC Genomics* 16:158. doi: 10.1186/s12864-015-1365-z

Magill, S. S., Edwards, J. R., Bamberg, W., Beldavs, Z. G., Dumyati, G., Kainer, M. A., et al. (2014). Multistate point-prevalence survey of health care–associated infections. *N. Engl. J. Med.* 370, 1198–1208. doi: 10.1056/nejmoa1306801

Manivasagan, P., Venkatesan, J., Sivakumar, K., and Kim, S.-K. (2014). Pharmaceutically active secondary metabolites of marine actinobacteria. *Microbiol. Res.* 169, 262–278. doi: 10.1016/j.micres.2013.07.014

Martin, P., Chakra, C. N. A., Williams, V., Bush, K., Dyck, M., Hirji, Z., et al. (2019). Prevalence of antibiotic-resistant organisms in Canadian Hospitals. Comparison of point-prevalence survey results from 2010, 2012, and 2016. *Infect. Control Hosp. Epidemiol.* 40, 53–59. doi: 10.1017/ice.2018.279

Medema, M. H., Blin, K., Cimermancic, P., de Jager, V., Zakrzewski, P., Fischbach, M. A., et al. (2011). antiSMASH: rapid identification, annotation and analysis of secondary metabolite biosynthesis gene clusters in bacterial and fungal genome sequences. *Nucleic Acids Res.* 39(Suppl. 2), W339–W346. doi: 10.1093/nar/gkr466

Medema, M. H., Kottmann, R., Yilmaz, P., Cummings, M., Biggins, J. B., Blin, K., et al. (2015). Minimum information about a biosynthetic gene cluster. *Nat. Chem. Biol.* 11:625.

Mitova, M., Tutino, M. L., Infusini, G., Marino, G., and De Rosa, S. (2005). Exocellular peptides from Antarctic psychrophilepseudoalteromonas haloplanktis. *Mar. Biotechnol.* 7, 523–531. doi: 10.1007/s10126-004-5098-2

Mykytczuk, N., Lawrence, J., Omelon, C., Southam, G., and Whyte, L. G. (2016). Microscopic characterization of the bacterial cell envelope of *Planococcus halocryophilus* Or1 during subzero growth at- 15 C. *Polar Biol.* 39, 701–712. doi: 10.1007/s00300-015-1826-5

National Nosocomial Infections Surveillance System (2004). National nosocomial infections surveillance (NNIS) system report, data summary from January 1992 through June 2004, issued October 2004. *Am. J. Infect. Control* 32, 470–485. doi: 10.1016/j.ajic.2004.10.001

Nichols, D., Cahoon, N., Trakhtenberg, E., Pham, L., Mehta, A., Belanger, A., et al. (2010). Use of ichip for high-throughput in situ cultivation of "uncultivable" microbial species. *Appl. Environ. Microbiol.* 76, 2445–2450. doi: 10.1128/AEM.01754-09

Niederberger, T. D., Perreault, N. N., Tille, S., Lollar, B. S., Lacrampe-Couloume, G., Andersen, D., et al. (2010). Microbial characterization of a subzero, hypersaline methane seep in the Canadian High Arctic. *ISME J.* 4, 1326–1329. doi: 10.1038/ismej.2010.57

Orsi, W. D., Edgcomb, V. P., Christman, G. D., and Biddle, J. F. (2013). Gene expression in the deep biosphere. *Nature* 499:205. doi: 10.1038/nature12230

Overbeek, R., Olson, R., Pusch, G. D., Olsen, G. J., Davis, J. J., Disz, T., et al. (2013). The SEED and the rapid annotation of microbial genomes using subsystems technology (RAST). *Nucleic Acids Res.* 42, D206–D214.

Pathma, J., Rahul, G., Kamaraj, K., Subashri, R., and Sakthivel, N. (2011). Secondary metabolite production by bacterial antagonists. *J. Biol. Control.* 25, 165–181.

Pawar, S. V., Ho, J. C., Yadav, G. D., and Yadav, V. G. (2017). The impending renaissance in discovery & development of natural products. *Curr. Top. Med. Chem.* 17, 251–267. doi: 10.2174/1568026616666160530154649

Perreault, N. N., Andersen, D. T., Pollard, W. H., Greer, C. W., and Whyte, L. G. (2007). Characterization of the prokaryotic diversity in cold saline perennial springs of the Canadian high Arctic. *Appl. Environ. Microbiol.* 73, 1532–1543. doi: 10.1128/aem.01729-06

Perreault, N. N., Greer, C. W., Andersen, D. T., Tille, S., Lacrampe-Couloume, G., Lollar, B. S., et al. (2008). Heterotrophic and autotrophic microbial populations in cold perennial springs of the high arctic. *Appl. Environ. Microbiol.* 74, 6898–6907. doi: 10.1128/AEM.00359-08

Perron, G. G., Whyte, L., Turnbaugh, P. J., Goordial, J., Hanage, W. P., Dantas, G., et al. (2015). Functional characterization of bacteria isolated from ancient arctic soil exposes diverse resistance mechanisms to modern antibiotics. *PLoS One* 10:e0069533. doi: 10.1371/journal.pone.0069533

Pollard, W., Haltigin, T., Whyte, L., Niederberger, T., Andersen, D., Omelon, C., et al. (2009). Overview of analogue science activities at the McGill Arctic research station, axel heiberg island, canadian high arctic. *Planet. Space Sci.* 57, 646–659. doi: 10.1016/j.pss.2009.01.008

Raymond-Bouchard, I., Tremblay, J., Altshuler, I., Greer, C. W., and Whyte, L. G. (2018). Comparative transcriptomics of cold growth and adaptive features of a eury-and steno-psychrophile. *Front. Microbiol.* 9:1565. doi: 10.3389/fmicb.2018.01565

Rovira, J., and Melero, B. (2018). "Protective cultures for the safety of animal-derived foods," in *Probiotics and Prebiotics in Animal Health and Food Safety*, eds D. Di Gioia and B. Biavati (Cham: Springer), 63–107. doi: 10.1007/978-3-319-71950-4_3

Sbrana, C., Agnolucci, M., Bedini, S., Lepera, A., Toffanin, A., Giovannetti, M., et al. (2002). Diversity of culturable bacterial populations associated to *Tuber borchii* ectomycorrhizas and their activity on *T. borchii mycelial* growth. *FEMS Microbiol. Lett.* 211, 195–201. doi: 10.1016/s0378-1097(02)00712-7

Schatz, A., Bugle, E., and Waksman, S. A. (1944). Streptomycin, a substance exhibiting antibiotic activity against gram-positive and gram-negative bacteria.*. *Proc. Soc. Exp. Biol. Med.* 55, 66–69. doi: 10.3181/00379727-55-14461

Steven, B., Briggs, G., McKay, C. P., Pollard, W. H., Greer, C. W., and Whyte, L. G. (2007). Characterization of the microbial diversity in a permafrost sample from the Canadian high Arctic using culture-dependent and culture-independent methods. *FEMS Microbiol. Ecol.* 59, 513–523. doi: 10.1111/j.1574-6941.2006.00247.x

Tedesco, P., Maida, I., Palma Esposito, F., Tortorella, E., Subko, K., Ezeofor, C., et al. (2016). Antimicrobial activity of monoramnholipids produced by bacterial strains isolated from the Ross Sea (Antarctica). *Mar. Drugs* 14:E83. doi: 10.3390/md14050083

Tritt, A., Eisen, J. A., Facciotti, M. T., and Darling, A. E. (2012). An integrated pipeline for de novo assembly of microbial genomes. *PLoS One* 7:e42304. doi: 10.1371/journal.pone.0042304

van Belkum, M. J., Lohans, C. T., and Vederas, J. C. (2015). Draft Genome sequences of *Paenibacillus polymyxa* NRRL B-30509 and *Paenibacillus terrae* NRRL B-30644, strains from a poultry environment that produce tridecaptin A and paenicidins. *Genome Announc.* 3:e00372-15. doi: 10.1128/genomeA.00372-15

Vartoukian, S. R., Palmer, R. M., and Wade, W. G. (2010). Strategies for culture of 'unculturable'bacteria. *FEMS Microbiol. Lett.* 309, 1–7.

Waksman, S. A., and Woodruff, H. B. (1940). Bacteriostatic and bactericidal substances produced by a soil Actinomyces. *Proc. Soc. Exp. Biol. Med.* 45, 609–614. doi: 10.3181/00379727-45-11768

Ward, D. M., Weller, R., and Bateson, M. M. (1990). 16S rRNA sequences reveal numerous uncultured microorganisms in a natural community. *Nature* 345:63. doi: 10.1038/345063a0

Wiernasz, N., Cornet, J., Cardinal, M., Pilet, M.-F., Passerini, D., and Leroi, F. (2017). Lactic acid bacteria selection for biopreservation as a part of hurdle technology approach applied on seafood. *Front. Mar. Sci.* 4:119. doi: 10.3389/fmars.2017.00119

Wilhelm, R. C., Niederberger, T. D., Greer, C., and Whyte, L. G. (2011). Microbial diversity of active layer and permafrost in an acidic wetland from the Canadian High Arctic. *Can. J. Microbiol.* 57, 303–315. doi: 10.1139/w11-004

Winterberg, H. (1898). Zur methodik der bakterienzählung. *Z. Hyg. Infektionskr.* 29, 75–93.

Yoon, S.-H., Ha, S.-M., Kwon, S., Lim, J., Kim, Y., Seo, H., et al. (2017). Introducing EzBioCloud: a taxonomically united database of 16S rRNA gene sequences and whole-genome assemblies. *Int. J. Syst. Evol. Microbiol.* 67, 1613–1617. doi: 10.1099/ijsem.0.001755

Zarins-Tutt, J. S., Barberi, T. T., Gao, H., Mearns-Spragg, A., Zhang, L., Newman, D. J., et al. (2016). Prospecting for new bacterial metabolites: a glossary of approaches for inducing, activating and upregulating the biosynthesis of bacterial cryptic or silent natural products. *Nat. Prod. Rep.* 33, 54–72. doi: 10.1039/c5np00111k

Conflict of Interest Statement: The authors declare that the research was conducted in the absence of any commercial or financial relationships that could be construed as a potential conflict of interest.

frontiers in Microbiology

ORIGINAL RESEARCH
published: 10 July 2019
doi: 10.3389/fmicb.2019.01556

Repurposed Antimicrobial Combination Therapy: Tobramycin-Ciprofloxacin Hybrid Augments Activity of the Anticancer Drug Mitomycin C Against Multidrug-Resistant Gram-Negative Bacteria

*Ronald Domalaon[1], Derek Ammeter[1], Marc Brizuela[1], Bala Kishan Gorityala[1], George G. Zhanel[2] and Frank Schweizer[1,2]**

[1] Department of Chemistry, University of Manitoba, Winnipeg, MB, Canada, [2] Department of Medical Microbiology and Infectious Diseases, University of Manitoba, Winnipeg, MB, Canada

OPEN ACCESS

Edited by:
Ana R. Freitas, University of Porto, Portugal

Reviewed by:
Rodolfo García-Contreras, National Autonomous University of Mexico, Mexico
Sidharth Chopra, Central Drug Research Institute (CSIR), India
Maria Bagattini, University of Naples Federico II, Italy
Tim Maisch, University of Regensburg, Germany

***Correspondence:**
Frank Schweizer
schweize@cc.umanitoba.ca

Specialty section:
This article was submitted to Antimicrobials, Resistance and Chemotherapy, a section of the journal Frontiers in Microbiology

Received: *12 March 2019*
Accepted: *21 June 2019*
Published: *10 July 2019*

Citation:
Domalaon R, Ammeter D, Brizuela M, Gorityala BK, Zhanel GG and Schweizer F (2019) Repurposed Antimicrobial Combination Therapy: Tobramycin-Ciprofloxacin Hybrid Augments Activity of the Anticancer Drug Mitomycin C Against Multidrug-Resistant Gram-Negative Bacteria. Front. Microbiol. 10:1556. doi: 10.3389/fmicb.2019.01556

The lack of therapeutic options to treat infections caused by multidrug-resistant (MDR) pathogens, especially Gram-negative bacteria, is apparent. Therefore, it is imperative to develop new strategies to address the problem of antimicrobial resistance. Repurposing non-antibiotic commercial drugs for antimicrobial therapy presents a viable option. We screened six anticancer drugs for their potential use in antimicrobial therapy. Here, we provide *in vitro* evidence that suggests feasibility to repurpose the anticancer drug mitomycin C against MDR Gram-negative bacteria. We also demonstrated that mitomycin C, etoposide and doxorubicin were affected by drug efflux in *Pseudomonas aeruginosa*. In combination with a tobramycin-ciprofloxacin antibiotic hybrid (TOB-CIP), the antibacterial activity of mitomycin C was enhanced against MDR clinical isolates of *P. aeruginosa*, *Acinetobacter baumannii*, *Escherichia coli*, *Klebsiella pneumoniae,* and *Enterobacter cloacae*. In fact, 4 μg/mL (3 μM) TOB-CIP reduced the minimum inhibitory concentration of mitomycin C to ≤1 μg/mL against MDR Gram-negative bacteria, except *A. baumannii*. We showed that synergy was inherent to TOB-CIP and that neither tobramycin nor ciprofloxacin individually synergized with mitomycin C. Our finding supports identifying adjuvant partners for mitomycin C, such as TOB-CIP, to enhance suitability for antimicrobial therapy.

Keywords: adjuvant, antibiotic hybrid, anticancer, antimicrobial, gram-negative bacteria, mitomycin C, repurposing, synergy

INTRODUCTION

There is a dire need to develop new strategies that can supplement our dwindling antibiotic armamentarium to address the growing threat of antimicrobial resistance (Luepke et al., 2017; Domalaon et al., 2018a; Koulenti et al., 2018). The shortage of available options is especially dire for the treatment of MDR Gram-negative bacterial infections. In fact, the

World Health Organization classified problematic Gram-negative bacteria, including carbapenem-resistant *P. aeruginosa*, carbapenem-resistant *A. baumannii* and carbapenem-resistant extended-spectrum β-lactamase-producing *Enterobacteriaceae*, to be of critical priority that urgently requires the development of antibiotics (Tacconelli et al., 2018). Promising strategies have emerged including anti-virulence therapy (Dickey et al., 2017), phage therapy (Kortright et al., 2019) and multicomponent combination therapy (Tyers and Wright, 2019). Repurposing non-antibiotic drugs for antimicrobial therapy offers a cost- and time-efficient method of discovery (Rangel-Vega et al., 2015; Soo et al., 2017; Polamreddy and Gattu, 2018; Cavalla, 2019). This is advantageous since the agents under study have well-characterized pharmacokinetic parameters and have undergone the rigorous process of safety evaluation from health agencies such as the United States' Food and Drug Administration (FDA) (Gns et al., 2019). Several non-antibiotic drugs have been described in the literature to display potential use for the treatment of MDR Gram-negative bacterial infections (Hennessy et al., 2016; Cheng et al., 2018; Lee and O'Neill, 2018; Domalaon et al., 2019).

Herein, we evaluate six anticancer agents (**Figure 1A**) for their ability to eradicate MDR Gram-negative bacteria, as stand-alone agents and in combination with our previously reported adjuvant TOB-CIP (**Figure 1B**; Gorityala et al., 2016a). TOB-CIP is an antibiotic hybrid composed of the aminoglycoside tobramycin covalently attached to the fluoroquinolone ciprofloxacin via a twelve carbon-long aliphatic linker (**Figure 1B**). Our previous study revealed that TOB-CIP possessed weak antibacterial activity on its own but augmented the activity and efficacy of other antibiotics in combination against MDR Gram-negative bacteria, through outer membrane permeabilization, inner membrane disruption and proton motive force dissipation (Gorityala et al., 2016a). We found that the anticancer agent mitomycin C possessed potent antibacterial activity against *Pseudomonas aeruginosa*, *Escherichia coli*, *Klebsiella pneumoniae,* and *Enterobacter cloacae*, while limited activity was observed against *Acinetobacter baumannii*. Moreover, our data revealed that mitomycin C was greatly affected by efflux in *P. aeruginosa* and was a good substrate for the MexAB-OprM efflux system. More importantly, we found that TOB-CIP further enhanced the already potent antibacterial activity of mitomycin C against antibiotic susceptible and MDR clinical isolates of Gram-negative bacteria. Our findings provide evidence to consider mitomycin C for antimicrobial therapy especially against MDR Gram-negative bacteria.

MATERIALS AND METHODS

Preparation of TOB-CIP Hybrid

The aminoglycoside tobramycin was covalently linked to the fluoroquinolone ciprofloxacin through an aliphatic hydrocarbon linker of twelve carbons-long, following our previous report (Gorityala et al., 2016a). The TOB-CIP (MW: 1131.44 g/mol for × 5 HCl salt) was characterized using one- and two-dimensional nuclear magnetic resonance and high-resolution matrix-assisted laser desorption ionization mass spectrometry experiments. Purity was then assessed for TOB-CIP using high-performance liquid chromatography and was found to be >95%.

Bacterial Strains and Growth Conditions

Anticancer agents (mitomycin C, etoposide, camptothecin, 5-fluorouracil, cisplatin and doxorubicin) in this study were obtained from commercial sources. Bacterial strains in this study were obtained from either the American type culture collection (ATCC) or the Canadian ward surveillance (CANWARD) study (Hoban and Zhanel, 2013). Bacterial isolates belonging to the CANWARD study were isolated from clinical specimens collected from patients suffering a presumed infectious disease that were admitted in participating medical centers across Canada. Efflux-deficient *P. aeruginosa* PAO200 lacked the MexAB-OprM efflux pump while PAO750 lacked five clinically relevant pumps (MexAB-OprM, MexCD-OprJ, MexEF-OprN, MexJK, and MexXY) and the outer membrane protein OpmH. Prior to conducting microbiological experiments, bacterial isolates were grown overnight in lysogeny/luria broth (LB) on an incubator shaker at 37°C.

Antimicrobial Susceptibility Assay

Antibacterial activity of the tested anticancer agents *in vitro* were assessed by microdilution broth susceptibility testing according to the Clinical and Laboratory Standards Institute (CLSI) guidelines (The Clinical and Laboratory Standards Institute, 2016). Bacterial cultures grown overnight were diluted in saline (0.85% NaCl) to achieve a 0.5 McFarland turbidity. Subsequently, the diluted bacterial culture was further diluted 1:50 in Mueller-Hinton broth (MHB) for inoculation to a final concentration of approximately 5×10^5 colony forming units/mL. Experiments were performed on 96-well plates, in which the tested agents were 2-fold serially diluted in MHB and incubated with equal volumes of bacterial inoculum at 37°C for 18 h. Minimum inhibitory concentration (MIC) values for the tested agents were determined as the lowest concentration to inhibit visible bacterial growth in the form of turbidity, which was confirmed via EMax Plus microplate reader (Molecular Devices, United States) at 590 nm wavelength. Wells with or without bacterial cells were used as positive or negative controls, respectively.

Checkerboard Assay

Experiments were performed on 96-well plates following previously described protocols (Domalaon et al., 2017, 2018b). The anticancer agents of interest were 2-fold serially diluted along the *x*-axis, while the TOB-CIP or other comparators were 2-fold serially diluted along the *y*-axis to create a matrix where each well consisted of a combination of both agents at different concentrations. Bacterial cultures grown overnight were then diluted in saline (0.85% NaCl) to 0.5 McFarland turbidity, subsequently followed by 1:50 further dilution in MHB and inoculation on each well to achieve a final concentration of approximately 5×10^5 colony forming units/mL. Wells consisting of MHB with or without bacterial cells were used as positive or negative controls, respectively. The 96-well plates

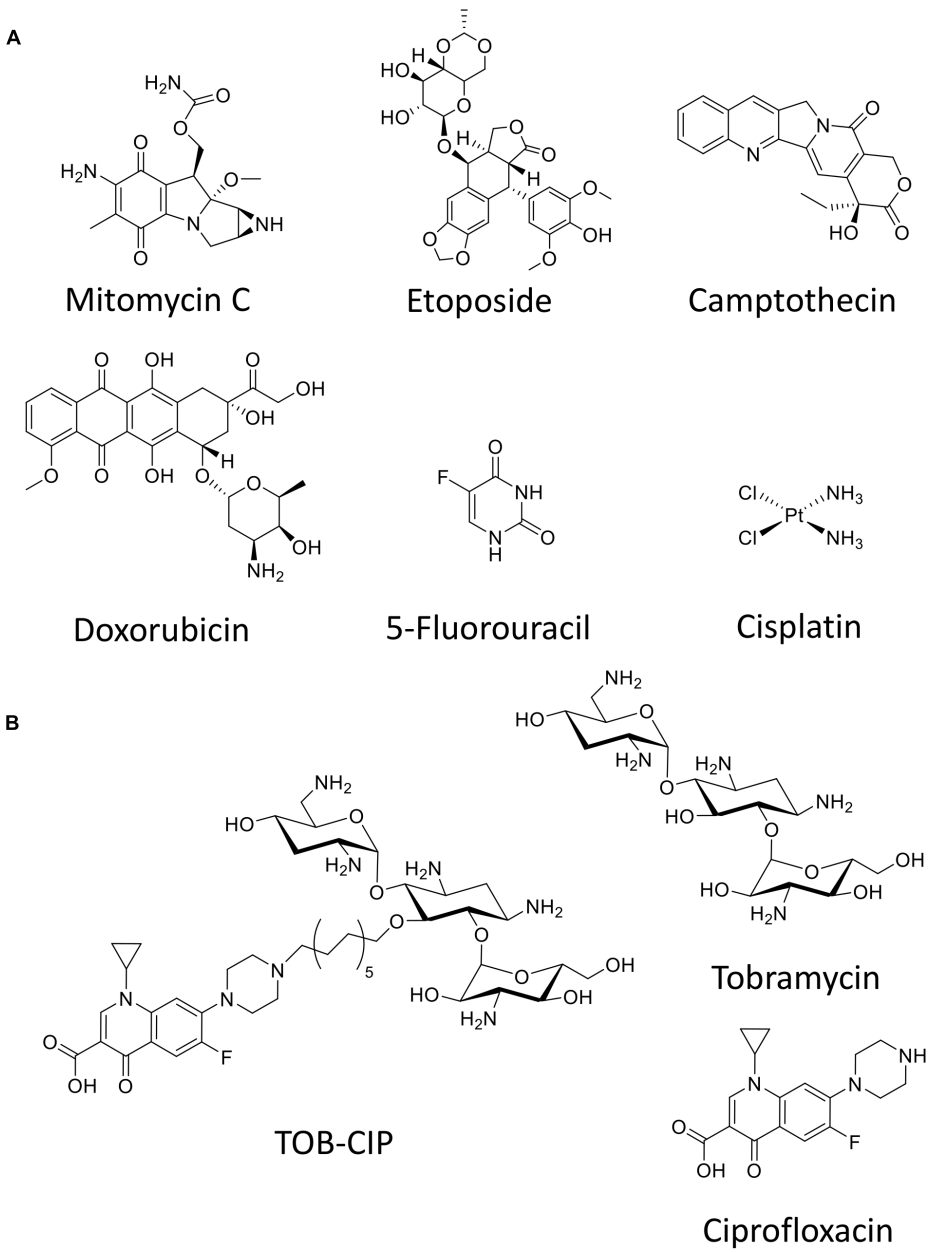

FIGURE 1 | Chemical structure of **(A)** six anticancer agents evaluated in this study and **(B)** tobramycin-ciprofloxacin (TOB-CIP) hybrid along with its individual antibiotic components.

were then incubated at 37°C for 18 h and were subsequently examined for visible turbidity, which was confirmed using an EMax Plus microplate reader (Molecular Devices, United States) at 590 nm wavelength. Fractional inhibitory concentration (FIC) of the anticancer agents were calculated by dividing the MIC of anticancer agents in the presence of TOB-CIP/comparators by the MIC of anticancer agents alone. Similarly, FIC of TOB-CIP/comparators were calculated by dividing the MIC of TOB-CIP/comparators in the presence of anticancer agents by the MIC of TOB-CIP/comparators alone. The FIC index was the summation of both FIC values. An FIC index of ≤ 0.5, $0.5 < \times < 4$, or ≥ 4 was interpreted as synergistic, additive, or antagonistic, respectively (Odds, 2003; Kalan and Wright, 2011).

RESULTS

Mitomycin C Possessed Potent Antibacterial Activity Against Gram-Negative Bacteria

The antibacterial activity of six anticancer agents were assessed against antibiotic susceptible strains (ASS) of *P. aeruginosa*,

A. baumannii, and *E. coli* using microdilution broth assay and activities were reported as their MIC or the minimum concentration of the agents to prevent visible bacterial growth. Anticancer agents (**Figure 1A**) included mitomycin C, etoposide, camptothecin, 5-fluorouracil, cisplatin and doxorubicin. Antibacterial activity of the individual anticancer agents were poor overall against the three Gram-negative bacteria with the exception of mitomycin C (**Table 1**). The MIC of mitomycin C against *P. aeruginosa* PAO1 (2 μg/mL) and *E. coli* ATCC 25922 (0.5 μg/mL) were significantly lower than against *A. baumannii* ATCC 17978 (16 μg/mL). Nonetheless, mitomycin C displayed better activity than the other five anticancer agents.

Efflux in *P. aeruginosa* Affected the Antibacterial Activity of Mitomycin C, Etoposide and Doxorubicin

Two efflux-deficient *P. aeruginosa* strains (PAO200 and PAO750) isogenic to the ASS PAO1 were used to explore the effects of efflux on the antibacterial activity of the six anticancer agents. Strain PAO200 lacked the MexAB-OprM efflux pump while strain PAO750 lacked five clinically relevant pumps (MexAB-OprM, MexCD-OprJ, MexEF-OprN, MexJK, and MexXY) and outer membrane protein OpmH. Mitomycin C appeared to be significantly affected by efflux since a 32- and 64-fold decrease in MIC were found against PAO200 and PAO750, respectively, relative to antibiotic susceptible PAO1 (**Table 2**). The MICs of etoposide (**Table 2**) were reduced by 4- and 32-fold against PAO200 and PAO750, respectively. Conversely, an 8- and 128-fold reduction on MIC (**Table 2**) were observed for doxorubicin against PAO200 and PAO750, respectively. No changes in the MICs were observed for camptothecin, 5-fluorouracil and cisplatin against the efflux-deficient *P. aeruginosa* strains.

TOB-CIP Enhanced Antibacterial Activity of Mitomycin C Against ASS of Gram-Negative Bacteria

The six anticancer agents were then screened in combinations with our previously reported TOB-CIP hybrid (**Figure 1B**) for potential synergy against ASS of *P. aeruginosa*, *A. baumannii,* and *E. coli* using checkerboard assay. We wondered whether the antibacterial activity of tested anticancer agents could be further augmented, as we have previously described with combinations of clinically used antibiotics and TOB-CIP (Gorityala et al., 2016a). FIC indices for each combination were calculated; and interpreted as synergistic, additive or antagonistic for FIC indices of ≤ 0.5, $0.5 < \times \leq 4$ and >4, respectively (Odds, 2003; Kalan and Wright, 2011). Out of the six anticancer agents, mitomycin C was consistently potentiated across the three tested ASS (**Figure 2**). However, it appeared that potentiation of other anticancer agents was only limited to certain organisms. Camptothecin did not synergize with TOB-CIP against antibiotic susceptible Gram-negative bacteria.

Mitomycin C Was Not Synergized by Either Components of TOB-CIP or Other Cationic Amphiphiles

Checkerboard assay was performed on combinations of mitomycin C and either tobramycin or ciprofloxacin against ASS of *P. aeruginosa*, *A. baumannii,* and *E. coli* to elucidate whether the observed potentiation stemmed from one or both of the TOB-CIP components (**Figure 1B**). Neither tobramycin nor ciprofloxacin synergized with mitomycin C against tested Gram-negative bacteria, having FIC indices ranging from 0.625 to 1.125 values (**Table 3**). Since our previous studies (Gorityala et al., 2016a) provided evidence that TOB-CIP potentiated antibiotics against Gram-negative bacteria by enhancing their intracellular accumulation through outer membrane permeabilization and proton-motive force disruption, we wondered whether synergy with mitomycin C could also be observed with other membrane-disputing agents. Combinations of mitomycin C and commercially used cationic amphiphiles/surfactants were then evaluated against same antibiotic susceptible Gram-negative bacteria. Cationic surfactant comparators included benzalkonium chloride, benzethonium chloride, and cetrimonium bromide. None of the comparators potentiated mitomycin C against tested ASS of *P. aeruginosa*, *A. baumannii,* and *E. coli* (**Figure 3**).

TABLE 1 | Minimum inhibitory concentration (MIC) of six anticancer drugs against ASS of *P. aeruginosa*, *A. baumannii,* and *E. coli*.

Anticancer drug	MIC, μg/mL		
	***P. aeruginosa* PAO1**	***A. baumannii* ATCC 17978**	***E. coli* ATCC 25922**
Mitomycin C	2	16	0.25
Etoposide	512	512	512
Camptothecin	256	256	256
5-Fluorouracil	64	256	32
Cisplatin	128	512	256
Doxorubicin	256	256	256

TABLE 2 | Effect of efflux on the antibacterial activity of tested anticancer drugs against isogenic *Pseudomonas aeruginosa* strains.

Anticancer drug	MIC, μg/mL		
	PAO1[a]	**PAO200[b]**	**PAO750[c]**
Mitomycin C	2	0.062	0.031
Etoposide	512	128	16
Camptothecin	256	512	256
5-Fluorouracil	64	64	64
Cisplatin	128	128	128
Doxorubicin	256	32	2
TOB-CIP	32	4	2

[a]P. aeruginosa antibiotic susceptible strain. [b]P. aeruginosa efflux-deficient strain lacking the MexAB-OprM pump. [c]P. aeruginosa efflux-deficient strain lacking five clinically relevant pumps (MexAB-OprM, MexCD-OprJ, MexEF-OprN, MexJK, and MexXY) and outer membrane protein OpmH.

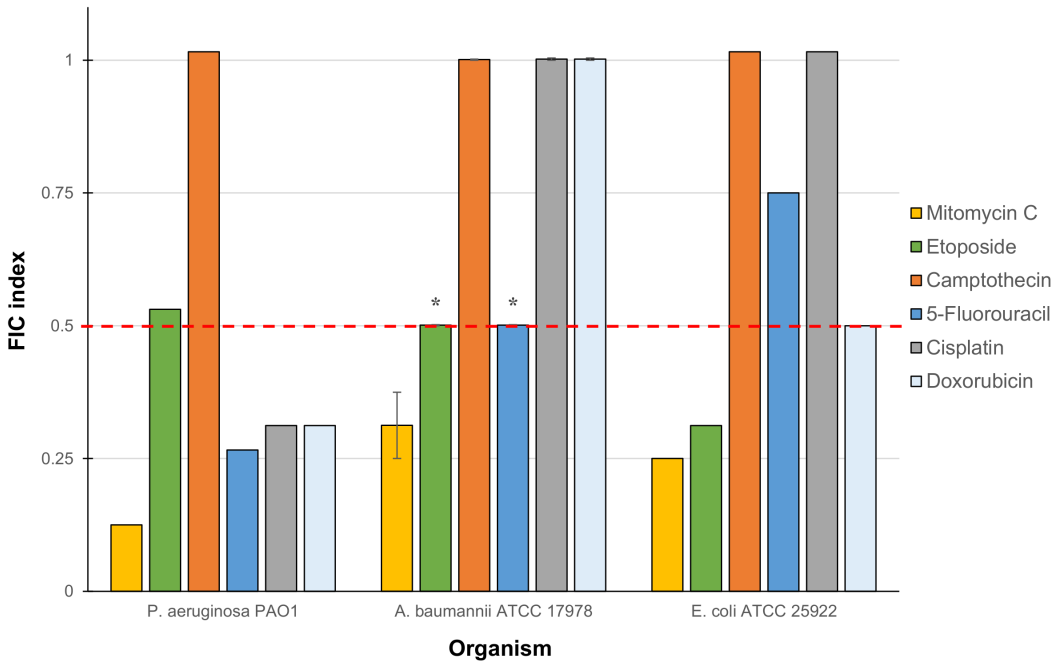

FIGURE 2 | Fractional inhibitory concentration (FIC) indices of combinations consisting of TOB-CIP and either of six anticancer agents against ASS of *P. aeruginosa*, *A. baumannii,* and *E. coli*. Red dashed line denotes the cutoff FIC index of ≤0.5 for synergistic interaction. Asterisk (*) indicates FIC indices of 0.501 which denotes for additive interaction. See **Supplementary Material** for MIC and FIC values.

TABLE 3 | Evaluation for synergy of combinations consisting of either tobramycin or ciprofloxacin and mitomycin C against ASS of *P. aeruginosa*, *A. baumannii,* and *E. coli*.

Organism	$MIC_{Mitomycin\ C}$ [MIC_{combo}], μg/mL	Adjuvant	$MIC_{Adjuvant}$ [MIC_{combo}], μg/mL	FIC index	Interpretation
P. aeruginosa PAO1	2 [1]	Tobramycin	1 [0.25]	0.750	Additive
A. baumannii ATCC 17978	16 [8]		1 [0.25]	0.750	Additive
E. coli ATCC 25922	0.25 [0.125]		2 [0.25]	0.625	Additive
P. aeruginosa PAO1	2 [1]	Ciprofloxacin	0.125 [0.031]	0.750	Additive
A. baumannii ATCC 17978	16 [8]		0.5 [0.125]	0.750	Additive
E. coli ATCC 25922	0.25 [0.25]		0.016 [0.002]	1.125	Additive

TOB-CIP Potentiated Mitomycin C Against MDR Clinical Isolates of Gram-Negative Bacteria

We then assessed the combination of mitomycin C and TOB-CIP against MDR clinical isolates of Gram-negative bacteria to provide *in vitro* evidence of therapeutic utility. The panel of MDR clinical isolates included *P. aeruginosa* (5), *A. baumannii* (4), *E. coli* (3), *K. pneumoniae* (3), and *E. cloacae* (3). Similar to what we have observed against ASS, mitomycin C displayed low MICs (**Tables 4**, **5**) against MDR clinical isolates of *P. aeruginosa* (2–4 μg/mL) and *Enterobacteriaceae* (0.062–8 μg/mL). Conversely, the antibacterial activity of mitomycin C alone (**Table 4**) appeared to be limited against MDR clinical isolates of *A. baumannii* (MIC range of 8–32 μg/mL). The combination of mitomycin C and TOB-CIP was synergistic against all (5/5) *P. aeruginosa* isolates while it was synergistic against (3/4) *A. baumannii* isolates (**Table 4**). At a working adjuvant concentration of 4 μg/mL (3 μM) TOB-CIP, mitomycin C was potentiated up to 128-fold against *P. aeruginosa* (**Table 4**). It should be noted that 4 μg/mL (3 μM) was the optimal adjuvant concentration for TOB-CIP, and other tobramycin-fluoroquinolone hybrids as determined in our previous studies (Gorityala et al., 2016a,b). Against *Enterobacteriaceae*, TOB-CIP was found to synergize with mitomycin C against all (3/3) *E. coli* isolates, all (3/3) *K. pneumoniae* isolates and (2/3) *E. cloacae* isolates (**Table 5**). Mitomycin C potentiation at a fixed concentration of 4 μg/mL (3 μM) TOB-CIP against *Enterobacteriaceae* was found to be up to 32-fold (**Table 5**). Indeed, the combination of the anticancer agent mitomycin C and TOB-CIP hybrid appeared to be synergistic against antibiotic susceptible but more importantly MDR Gram-negative bacteria.

DISCUSSION

The dearth of available therapeutics to treat MDR Gram-negative bacterial infections has energized the scientific community to

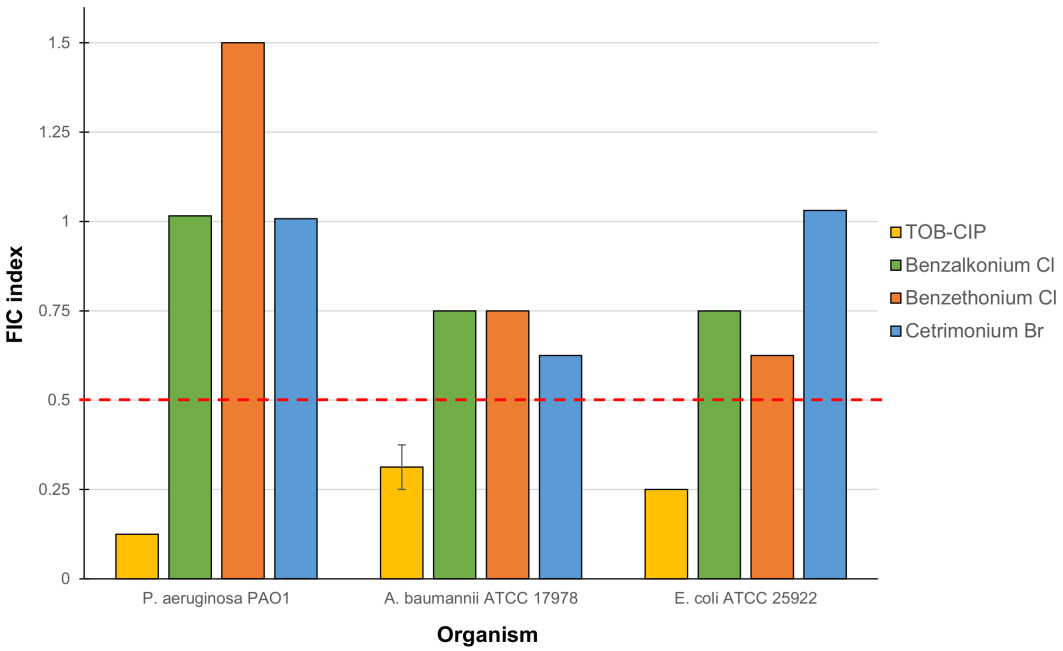

FIGURE 3 | Fractional inhibitory concentration (FIC) indices of combinations consisting of mitomycin C and either TOB-CIP or commercially used amphiphiles/surfactants against ASS of *P. aeruginosa*, *A. baumannii,* and *E. coli*. Red dashed line denotes the cutoff FIC index of ≤0.5 for synergistic interaction. See **Supplementary Material** for MIC and FIC values.

TABLE 4 | Evaluation for synergy of combinations consisting of TOB-CIP and mitomycin C against MDR clinical isolates of *P. aeruginosa* and *A. baumannii*.

Organism	$MIC_{Mitomycin\ C}$ [MIC_{combo}], μg/mL	$MIC_{TOB-CIP}$ [MIC_{combo}], μg/mL	FIC index	Interpretation	Absolute $MIC_{Mitomycin\ C}$,[a] μg/mL	Fold potentiation[b]
P. aeruginosa PA259-96918	2 [0.25]	128 [8]	0.187	Synergy	0.5	4-fold
P. aeruginosa PA260-97103	2 [0.031]	16 [2]	0.141	Synergy	0.016	128-fold
P. aeruginosa PA262-101856	2 [0.25]	256 [16]	0.187	Synergy	0.5	4-fold
P. aeruginosa PA264-104354	2 [0.125]	64 [8]	0.187	Synergy	0.25	8-fold
P. aeruginosa 100036	4 [0.25]	64 [4]	0.125	Synergy	0.25	16-fold
A. baumannii AB027	32 [8]	>128 [2]	0.250 < × < 0.266	Synergy	8	4-fold
A. baumannii AB031	32 [8]	128 [16]	0.375	Synergy	16	2-fold
A. baumannii 92247	8 [2]	64 [32]	0.750	Additive	8	1-fold
A. baumannii LAC-4	8 [1]	>128 [16]	0.125 < × < 0.250	Synergy	2	4-fold

[a]*MIC of mitomycin C in the presence of 4 μg/mL TOB-CIP.* [b]*Fold potentiation of mitomycin C in the presence of 4 μg/mL TOB-CIP.*

TABLE 5 | Evaluation for synergy of combinations consisting of TOB-CIP and mitomycin C against MDR clinical isolates of *Enterobacteriaceae*.

Organism	$MIC_{Mitomycin\ C}$ [MIC_{combo}], μg/mL	$MIC_{TOB-CIP}$ [MIC_{combo}], μg/mL	FIC index	Interpretation	Absolute $MIC_{Mitomycin\ C}$,[a] μg/mL	Fold potentiation[b]
E. coli 94393	1 [0.125]	>128 [1]	0.125 < × < 0.133	Synergy	0.125	8-fold
E. coli 94474	2 [0.25]	>128 [4]	0.125 < × < 0.156	Synergy	0.25	8-fold
E. coli 107115	1 [0.031]	>128 [2]	0.031 < × < 0.047	Synergy	0.031	32-fold
K. pneumoniae 113250	1 [0.25]	>128 [16]	0.125 < × < 0.375	Synergy	0.5	2-fold
K. pneumoniae 113254	2 [0.25]	>128 [16]	0.125 < × < 0.250	Synergy	0.5	4-fold
K. pneumoniae 116381	8 [0.5]	>128 [1]	0.062 < × < 0.070	Synergy	0.25	32-fold
E. cloacae 117029	4 [0.5]	>128 [2]	0.125 < × < 0.156	Synergy	1	4-fold
E. cloacae 118564	8 [1]	>128 [1]	0.125 < × < 0.133	Synergy	1	8-fold
E. cloacae 121187	0.062 [0.031]	>128 [0.5]	0.500 < × < 0.504	Additive	0.031	2-fold

[a]*MIC of mitomycin C in the presence of 4 μg/mL TOB-CIP.* [b]*Fold potentiation of mitomycin C in the presence of 4 μg/mL TOB-CIP.*

seek newer approaches and ingenious strategies. Instead of *de novo* development that are typically capital- and time-intensive, repurposing FDA-approved non-antibiotic drugs for antimicrobial therapy has recently gained significant traction as a method of discovery (Polamreddy and Gattu, 2018; Cavalla, 2019; Gns et al., 2019). We wondered whether anticancer agents could be repurposed as antimicrobials to eradicate MDR Gram-negative bacteria. Six anticancer agents (**Figure 1A**) that included DNA crosslinkers (mitomycin C and cisplatin), DNA topoisomerase blockers (etoposide, camptothecin, and doxorubicin), and thymidylate synthase inhibitors (5-fluorouracil) were evaluated against Gram-negative bacteria. Our initial assessment revealed that mitomycin C was potent against ASS of *P. aeruginosa* and *E. coli*, while moderate activity was observed against antibiotic susceptible *A. baumannii* (**Table 1**). The other five agents displayed poor antibacterial activity against Gram-negative bacteria (**Table 1**). Since anticancer agents are prone to drug efflux in rapidly dividing tumor cells (Choi and Yu, 2014; Fletcher et al., 2016), we wondered whether poor activity of these agents could be attributed to bacterial efflux systems. We probed the antibacterial activity of the six anticancer agents against efflux-deficient *P. aeruginosa* strains isogenic to antibiotic susceptible PAO1. We utilized PAO200 that lacked the MexAB-OprM efflux pump and PAO750 that lacked five clinically relevant pumps (MexAB-OprM, MexCD-OprJ, MexEF-OprN, MexJK, and MexXY) and outer membrane protein OpmH. Interestingly, the potent antibacterial activity of mitomycin C was further enhanced against the efflux pump-deletion mutants. For instance, the MIC of mitomycin C was reduced from 2 μg/mL against PAO1 to 0.062 μg/mL (32-fold reduction) against PAO200 and to 0.031 μg/mL (64-fold reduction) against PAO750 (**Table 2**). This significant reduction of MIC against efflux-deficient strains relative to antibiotic susceptible strain suggested that mitomycin C was a good substrate for at least the MexAB-OprM efflux system in *P. aeruginosa*. Interestingly, we found that etoposide and doxorubicin were also affected by efflux. The MICs of etoposide and doxorubicin were reduced by 4- and 8-fold, respectively, against PAO200 relative to PAO1 (**Table 2**). However, the MICs of etoposide and doxorubicin were more significantly reduced by 32- and 128-fold, respectively, against PAO750 relative to PAO1 (**Table 2**). These trends (of MIC reduction from PAO1 to PAO200 and PAO750) suggestively implied that both etoposide and doxorubicin were substrates for the MexAB-OprM efflux pump but as well as other efflux systems that were knocked-out in PAO750. Camptothecin, 5-fluorouracil and cisplatin appeared to be unaffected by bacterial efflux in *P. aeruginosa*.

We have previously reported antibiotic hybrids that could serve as adjuvants adjunct to antimicrobial therapy against Gram-negative bacteria (Domalaon et al., 2017, 2018a; Lyu et al., 2017a,b; Yang et al., 2017). Irrespective of their limited intrinsic antibacterial activity, these antibiotic hybrids efficiently permeabilize the outer membrane and perturb the inner membrane thereby resulting in dissipation of proton motive force (and de-energizing efflux systems) (Gorityala et al., 2016a,b; Yang et al., 2017). Therefore, they may be used in synergistic combinations with other agents that otherwise suffer from impeded intracellular accumulation due to their limited permeation of outer membrane and/or expulsion through efflux systems. We then explored the possibility of our antibiotic hybrid TOB-CIP, composed of the aminoglycoside tobramycin covalently linked to the fluoroquinolone ciprofloxacin via twelve carbons-long aliphatic tether (**Figure 1B**), to enhance antibacterial activity of the six tested anticancer agents, in a drug cocktail, against Gram-negative bacteria. Checkerboard assays revealed that mitomycin C synergized with TOB-CIP against ASS of *P. aeruginosa*, *A. baumannii,* and *E. coli* (**Figure 2**) while synergism with the other tested agents was only limited to certain organisms. These findings are promising since mitomycin C already possessed potent antibacterial activity (low MICs) as a stand-alone agent and that the addition of TOB-CIP further lowered the needed concentration to kill Gram-negative bacteria. This prompted our study to focus on the synergistic combination of mitomycin C and TOB-CIP against MDR bacteria.

Since TOB-CIP was fundamentally composed of tobramycin and ciprofloxacin fragments (**Figure 1B**), we questioned whether its synergism with mitomycin C stemmed from either or both components. Our data revealed that neither tobramycin nor ciprofloxacin potentiated mitomycin C (**Table 3**), confirming that hybridization of the two fragments is necessary to achieve synergy. We then explored other combinations consisting of mitomycin C and other cationic amphiphiles/surfactants that were known to disrupt bacterial membranes, that included benzalkonium chloride, benzethonium chloride and cetrimonium bromide. We found that the cationic amphiphile comparators did not synergize with mitomycin C (**Figure 3**), suggesting that membrane disruption may not be the sole function required to yield synergy. Comparison of TOB-CIP with polymyxin B nonapeptide (PMBN), perceived to be the "gold standard" for adjuvants that act through membrane permeabilization, showed comparable results (see **Supplementary Material**). Both TOB-CIP and PMBN reduced the MIC of mitomycin C against *P. aeruginosa*, *A. baumannii,* and *E. coli* to similar degree at the same adjuvant concentrations. Based on our observations that mitomycin C was affected by bacterial efflux, we then questioned whether the observed synergy may be due to TOB-CIP's ability to dissipate the proton motive force that may result in de-energized efflux systems. Note that PMBN and other polymyxins are also known to affect inner membrane components, such as vital respiratory enzyme type II NADH-quinone oxidoreductase, thereby affecting the proton motive force (Deris et al., 2014a,b). In line with this hypothesis, synergy between mitomycin C and TOB-CIP should be annulled in efflux pump-knocked out strains. Indeed, we found that the combination only yielded additive effects against efflux-deficient *P. aeruginosa* PAO200 and PAO750 strains (see **Supplementary Material**). Therefore, it is very likely that synergy is heavily due to TOB-CIP's disruptive effects on efflux systems thereby enhancing intracellular accumulation of mitomycin C. However, we do not dispute that TOB-CIP's outer membrane perturbation may also play a role. We also do not dispute that TOB-CIP may compete as a substrate for

efflux (as it is also affected by efflux shown in **Table 2**) relative to mitomycin C, rendering the latter agent to accumulate more efficiently in the bacterial cell. In fact, we suggest that these potential mechanisms of synergy work in synchrony, with the efflux-blocking effects being a major contributor. The effect of TOB-CIP on efflux is supported by the reduction of flagellum-dependent swimming motility of *P. aeruginosa* PAO1 as flagellar function requires an intact proton motive force (**Supplementary Material**).

To provide preliminary evidence for therapeutic utility using *in vitro* studies, we evaluated the combination of mitomycin C and TOB-CIP against MDR clinical isolates of Gram-negative bacteria (**Tables 4**, **5** and **Supplementary Material**). The combination was found to be synergistic in all tested isolates of *P. aeruginosa* (5), *E. coli* (3), and *K. pneumoniae* (3). Mitomycin C synergized with TOB-CIP in almost all tested *A. baumannii* (4/5) and *E. cloacae* (2/3) clinical isolates. At a working adjuvant concentration of 4 μg/mL TOB-CIP, we found that the MICs of mitomycin C against *P. aeruginosa*, *E. coli*, *K. pneumoniae,* and *E. cloacae* were significantly reduced to ≤ 1 μg/mL (**Tables 4**, **5**). In fact, the MIC of mitomycin C was potentiated 128-fold (from 2 to 0.016 μg/mL) against *P. aeruginosa* PA260-97103 in the presence of only 4 μg/mL (3 μM) TOB-CIP (**Table 4**). These findings suggested that the combination of mitomycin C and TOB-CIP may be of use to eradicate MDR *P. aeruginosa* and *Enterobacteriaceae*. However, the antibacterial effect of the combination appeared limited against clinical isolates of *A. baumannii* since the working adjuvant concentration of 4 μg/mL (3 μM) TOB-CIP did not lower the MIC of mitomycin C to 1 μg/mL (**Table 4**). Increasing the TOB-CIP concentration above 4 μg/mL may further reduce the MIC of mitomycin C, however, undesired toxicity of the adjuvant may be pronounced, as observed in our previous studies (Gorityala et al., 2016a,b).

First isolated from *Streptomyces caespitosus* in 1958 (Crooke and Bradner, 1976), mitomycin C has been an indispensable agent for cancer treatment since its FDA approval in 1974 (Bradner, 2001). It had been hinted early on (1961) that the DNA alkylating properties of the naturally occurring mitomycin C may not only be limited to fast-growing tumor cells but also to bacterial cells (Reich et al., 1960). Yet perhaps the availability of safer antibiotic alternatives, such as of the β-lactams, had relegated the therapeutic potential of mitomycin C in the past. With the increasing prevalence of MDR pathogens and the decline in available options to treat them, a revitalized interest in the antibacterial activity of mitomycin C is apparent. Our findings herein, along with others, suggests the potential of mitomycin C to be repurposed for antimicrobial therapy as either monotherapy or in combination with the adjuvant TOB-CIP. Mitomycin C have been shown to eradicate bacterial persister cells of *P. aeruginosa*, *E. coli,* and *Staphylococcus aureus* (Kwan et al., 2015). Furthermore, mitomycin C monotherapy showed efficacy in a *Caenorhabditis elegans* model of *E. coli* O157:H7 infection (Kwan et al., 2015). Another report (Cruz-Muniz et al., 2017) described the killing of MDR *A. baumannii* strains as well as the anti-biofilm properties of mitomycin C against *A. baumannii*. Moreover, it was reported that mitomycin C rescues *G. mellonella* from *A. baumannii* infections (Cruz-Muniz et al., 2017). However, antimicrobial therapy with mitomycin C is not without limitation. Peak plasma mitomycin C concentrations in humans were reported to vary per individual with a range of 0.4–3.2 μg/mL following intravenous administration (den Hartigh et al., 1983). Therefore, the effective concentration for mitomycin C to be used for antimicrobial therapy, especially against MDR Gram-negative bacteria, should be within or below this range. Based on our results, potentiators like TOB-CIP that significantly reduce the effective concentration of mitomycin C should gain broad interest to pursue this approach against MDR Gram-negative bacteria. Since our data suggest that mitomycin C is susceptible to bacterial efflux, one may postulate other favorable drug combinations that include efflux pump inhibitors and proton motive force uncouplers. Indeed, our future work includes evaluation of other adjuvants that may potentially be used in a cocktail with mitomycin C to treat complicated bacterial infections. But also, the biochemical and molecular interplay that result in synergy between mitomycin C and TOB-CIP will be elucidated.

DATA AVAILABILITY

The raw data supporting the conclusions of this manuscript will be made available by the authors, without undue reservation, to any qualified researcher.

AUTHOR CONTRIBUTIONS

RD, GZ, and FS conceived the study. DA and BG prepared and characterized the TOB-CIP. RD and MB performed all the microbiological experiments. GZ and FS guided the progress of the study. RD wrote the manuscript with inputs from DA, MB, GZ, and FS.

FUNDING

This work was supported by the Natural Sciences and Engineering Research Council of Canada NSERC-DG (2018-06047) and the University of Manitoba.

ACKNOWLEDGMENTS

We thank Dr. Ayush Kumar (Department of Microbiology, University of Manitoba) for generously providing efflux-deficient *P. aeruginosa* PAO200 and PAO750 strains.

SUPPLEMENTARY MATERIAL

The Supplementary Material for this article can be found online at: https://www.frontiersin.org/articles/10.3389/fmicb.2019.01556/full#supplementary-material

REFERENCES

Bradner, W. T. (2001). Mitomycin c: a clinical update. *Cancer Treat. Rev.* 27, 35–50. doi: 10.1053/ctrv.2000.0202

Cavalla, D. (2019). Using human experience to identify drug repurposing opportunities: theory and practice. *Br. J. Clin. Pharmacol.* 85, 680–689. doi: 10.1111/bcp.13851

Cheng, Y. S., Sun, W., Xu, M., Shen, M., Khraiwesh, M., Sciotti, R. J., et al. (2018). Repurposing screen identifies unconventional drugs with activity against multidrug resistant *Acinetobacter baumannii*. *Front. Cell. Infect. Microbiol.* 8:438. doi: 10.3389/fcimb.2018.00438

Choi, Y. H., and Yu, A.-M. (2014). ABC transporters in multidrug resistance and pharmacokinetics, and strategies for drug development. *Curr. Pharm. Des.* 20, 793–807. doi: 10.2174/13816128200514021 4165212

Crooke, S. T., and Bradner, W. T. (1976). Mitomycin c: a review. *Cancer Treat. Rev.* 3, 121–139.

Cruz-Muniz, M. Y., Lopez-Jacome, L. E., Hernandez-Duran, M., Franco-Cendejas, R., Licona-Limon, P., Ramos-Balderas, J. L., et al. (2017). Repurposing the anticancer drug mitomycin c for the treatment of persistent *Acinetobacter baumannii* infections. *Int. J. Antimicrob. Agents* 49, 88–92. doi: 10.1016/j.ijantimicag.2016.08.022

den Hartigh, J., McVie, J. G., van Oort, W. J., and Pinedo, H. M. (1983). Pharmacokinetics of mitomycin c in humans. *Cancer Res.* 43, 5017–5021.

Deris, Z. Z., Akter, J., Sivanesan, S., Roberts, K. D., Thompson, P. E., Nation, R. L., et al. (2014a). A secondary mode of action of polymyxins against Gram-negative bacteria involves the inhibition of NADH-quinone oxidoreductase activity. *J. Antibiot.* 67, 147–151. doi: 10.1038/ja.2013.111

Deris, Z. Z., Swarbrick, J. D., Roberts, K. D., Azad, M. A. K., Akter, J., Horne, A. S., et al. (2014b). Probing the penetration of antimicrobial polymyxin lipopeptides into gram-negative bacteria. *Bioconjug. Chem.* 25, 750–760. doi: 10.1021/bc500094d

Dickey, S. W., Cheung, G. Y. C., and Otto, M. (2017). Different drugs for bad bugs: antivirulence strategies in the age of antibiotic resistance. *Nat. Rev. Drug Discov.* 16, 457–471. doi: 10.1038/nrd.2017.23

Domalaon, R., De Silva, P. M., Kumar, A., Zhanel, G. G., and Schweizer, F. (2019). The anthelmintic drug niclosamide synergizes with colistin and reverses colistin resistance in gram-negative bacilli. *Antimicrob. Agents Chemother.* 63:e02574-18

Domalaon, R., Idowu, T., Zhanel, G. G., and Schweizer, F. (2018a). Antibiotic hybrids: the next generation of agents and adjuvants against Gram-negative pathogens? *Clin. Microbiol. Rev.* e00077-17. doi: 10.1128/CMR.00077-17

Domalaon, R., Sanchak, Y., Koskei, L. C., Lyu, Y., Zhanel, G. G., Arthur, G., et al. (2018b). Short proline-rich lipopeptide potentiates minocycline and rifampin against multidrug- and extensively drug-resistant *Pseudomonas aeruginosa*. *Antimicrob. Agents Chemother.* 62:e02374-17. doi: 10.1128/AAC.02374-17

Domalaon, R., Yang, X., Lyu, Y., Zhanel, G. G., and Schweizer, F. (2017). Polymyxin B3-tobramycin hybrids with *Pseudomonas aeruginosa*-selective antibacterial activity and strong potentiation of rifampicin, minocycline, and vancomycin. *ACS Infect. Dis.* 3, 941–954. doi: 10.1021/acsinfecdis.7b00145

Fletcher, J. I., Williams, R. T., Henderson, M. J., Norris, M. D., and Haber, M. (2016). ABC transporters as mediators of drug resistance and contributors to cancer cell biology. *Drug Resist. Updat.* 26, 1–9. doi: 10.1016/j.drup.2016.03.001

Gns, H. S., Gr, S., Murahari, M., and Krishnamurthy, M. (2019). An update on drug repurposing: re-written saga of the drug's fate. *Biomed. Pharmacother.* 110, 700–716. doi: 10.1016/j.biopha.2018.11.127

Gorityala, B. K., Guchhait, G., Fernando, D. M., Deo, S., McKenna, S. A., Zhanel, G. G., et al. (2016a). Adjuvants based on hybrid antibiotics overcome resistance in *Pseudomonas aeruginosa* and enhance fluoroquinolone efficacy. *Angew. Chem. Int. Ed. Engl.* 55, 555–559. doi: 10.1002/anie.201508330

Gorityala, B. K., Guchhait, G., Goswami, S., Fernando, D. M., Kumar, A., Zhanel, G. G., et al. (2016b). Hybrid antibiotic overcomes resistance in *P. aeruginosa* by enhancing outer membrane penetration and reducing efflux. *J. Med. Chem.* 59, 8441–8455. doi: 10.1021/acs.jmedchem.6b00867

Hennessy, E., Adams, C., Reen, F. J., and O'Gara, F. (2016). Is there potential for repurposing statins as novel antimicrobials? *Antimicrob. Agents Chemother.* 60, 5111–5121. doi: 10.1128/AAC.00192-116

Hoban, D. J., and Zhanel, G. G. (2013). Introduction to the canward study (2007-11). *J. Antimicrob. Chemother.* 68(Suppl. 1), i3–i5. doi: 10.1093/jac/dkt021

Kalan, L., and Wright, G. D. (2011). Antibiotic adjuvants: multicomponent anti-infective strategies. *Expert. Rev. Mol. Med.* 13:e5. doi: 10.1017/S1462399410001766

Kortright, K. E., Chan, B. K., Koff, J. L., and Turner, P. E. (2019). Phage therapy: a renewed approach to combat antibiotic-resistant bacteria. *Cell Host Microbe* 25, 219–232. doi: 10.1016/j.chom.2019.01.014

Koulenti, D., Song, A., Ellingboe, A., Abdul-Aziz, M. H., Harris, P., Gavey, E., et al. (2018). Infections by multidrug-resistant gram-negative bacteria: what's new in our arsenal and what's in the pipeline? *Int. J. Antimicrob. Agents* 53, 211–224. doi: 10.1016/j.ijantimicag.2018.10.011

Kwan, B. W., Chowdhury, N., and Wood, T. K. (2015). Combatting bacterial infections by killing persister cells with mitomycin c. *Environ. Microbiol.* 17, 4406–4414. doi: 10.1111/1462-2920.12873

Lee, V. E., and O'Neill, A. J. (2018). Potential for repurposing the personal care product preservatives bronopol and bronidox as broad-spectrum antibiofilm agents for topical application. *J. Antimicrob. Chemother.* 74, 907–911. doi: 10.1093/jac/dky520

Luepke, K. H., Suda, K. J., Boucher, H., Russo, R. L., Bonney, M. W., Hunt, T. D., et al. (2017). Past, present, and future of antibacterial economics: increasing bacterial resistance, limited antibiotic pipeline, and societal implications. *Pharmacotherapy* 37, 71–84. doi: 10.1002/phar.1868

Lyu, Y., Domalaon, R., Yang, X., and Schweizer, F. (2017a). Amphiphilic lysine conjugated to tobramycin synergizes legacy antibiotics against wild-type and multidrug-resistant. *Pseudomonas aeruginosa*. *Biopolymers* doi: 10.1002/bip.23091 [Epub ahead of print].

Lyu, Y., Yang, X., Goswami, S., Gorityala, B. K., Idowu, T., Domalaon, R., et al. (2017b). Amphiphilic tobramycin-lysine conjugates sensitize multidrug resistant gram-negative bacteria to rifampicin and minocycline. *J. Med. Chem.* 60, 3684–3702. doi: 10.1021/acs.jmedchem.6b01742

Odds, F. C. (2003). Synergy, antagonism and what the checkerboard puts between them. *J. Antimicrob. Chemother.* 52:1. doi: 10.1093/jac/dkg301

Polamreddy, P., and Gattu, N. (2018). The drug repurposing landscape from 2012 to 2017: evolution, challenges, and possible solutions. *Drug Discov. Today* 24, 789–795. doi: 10.1016/j.drudis.2018.11.022

Rangel-Vega, A., Bernstein, L. R., Mandujano-Tinoco, E. A., García-Contreras, S. J., and García-Contreras, R. (2015). Drug repurposing as an alternative for the treatment of recalcitrant bacterial infections. *Front. Microbiol.* 6:282. doi: 10.3389/fmicb.2015.00282

Reich, E., Shatkin, A. J., and Tatum, E. L. (1960). Bacteriocidal action of mitomycin c. *Biochim. Biophys. Acta* 45, 608–610. doi: 10.1016/0006-3002(60)91504-3

Soo, V. W., Kwan, B. W., Quezada, H., Castillo-Juárez, I., Pérez-Eretza, B., García-Contreras, S. J., et al. (2017). Repurposing of anticancer drugs for the treatment of bacterial infections. *Curr. Top. Med. Chem.* 17, 1157–1176. doi: 10.2174/1568026616666160930131737

Tacconelli, E., Carrara, E., Savoldi, A., Harbarth, S., Mendelson, M., Monnet, D. L., et al. (2018). Discovery, research, and development of new antibiotics: the WHO priority list of antibiotic-resistant bacteria and tuberculosis. *Lancet Infect. Dis.* 18, 318–327. doi: 10.1016/S1473-3099(17)30753-30753

The Clinical and Laboratory Standards Institute (2016). *Performance Standards for Antimicrobial Susceptibility Testing CLSI supplement M100S*, 26th Edn. Wayne, PA: Clinical and Laboratory Standards Institute.

Tyers, M., and Wright, G. D. (2019). Drug combinations: a strategy to extend the life of antibiotics in the 21st century. *Nat. Rev. Microbiol.* 17, 141–155. doi: 10.1038/s41579-018-0141-x

Yang, X., Goswami, S., Gorityala, B. K., Domalaon, R., Lyu, Y., Kumar, A., et al. (2017). A tobramycin vector enhances synergy and efficacy of efflux pump inhibitors against multidrug-resistant gram-negative bacteria. *J. Med. Chem.* 60, 3913–3932. doi: 10.1021/acs.jmedchem.7b00156

Conflict of Interest Statement: The authors declare that the research was conducted in the absence of any commercial or financial relationships that could be construed as a potential conflict of interest.

frontiers in Microbiology

ORIGINAL RESEARCH
published: 25 October 2019
doi: 10.3389/fmicb.2019.02431

Fluopsin C for Treating Multidrug-Resistant Infections: *In vitro* Activity Against Clinically Important Strains and *in vivo* Efficacy Against Carbapenemase-Producing *Klebsiella pneumoniae*

*Miguel Octavio Pérez Navarro[1], Ane Stefano Simionato[1], Juan Carlos Bedoya Pérez[2], André Riedi Barazetti[1], Janaina Emiliano[1], Erika Tyemi Goya Niekawa[1], Matheus Felipe de Lima Andreata[1], Fluvio Modolon[1], Mickely Liuti Dealis[1], Eduardo José de Almeida Araújo[3], Thalita Massi Carlos[3], Odair José Scarpelim[3], Denise Brentan da Silva[4], Andreas Lazaros Chryssafidis[5], Per Bruheim[6] and Galdino Andrade[1]**

[1] Microbial Ecology Laboratory, Department of Microbiology, State University of Londrina, Londrina, Brazil, [2] Institución Universitaria Colegio Mayor de Antioquia, Medellín, Colombia, [3] Department of Histology, State University of Londrina, Londrina, Brazil, [4] Biological and Health Sciences Centre, Federal University of Mato Grosso do Sul, Campo Grande, Brazil, [5] Veterinary Toxicology Laboratory, Department of Preventive Veterinary Medicine, State University of Londrina, Londrina, Brazil, [6] Department of Biotechnology and Food Science, NTNU – Norwegian University of Science and Technology, Trondheim, Norway

The increasing emergence of multidrug-resistant (MDR) organisms in hospital infections is causing a global public health crisis. The development of drugs with effective antibiotic action against such agents is of the highest priority. In the present study, the action of Fluopsin C against MDR clinical isolates was evaluated under *in vitro* and *in vivo* conditions. Fluopsin C was produced in cell suspension culture of *Pseudomonas aeruginosa* LV strain, purified by liquid adsorption chromatography and identified by mass spectrometric analysis. Bioactivity, bacterial resistance development risk against clinically important pathogenic strains and toxicity in mammalian cell were initially determined by *in vitro* models. *In vivo* toxicity was evaluated in *Tenebrio molitor* larvae and mice. The therapeutic efficacy of intravenous Fluopsin C administration was evaluated in a murine model of *Klebsiella pneumoniae* (KPC) acute sepsis, using six different treatments. The *in vitro* results indicated MIC and MBC below 2 μg/mL and low bacterial resistance development frequency. Electron microscopy showed that Fluopsin C may have altered the exopolysaccharide matrix and caused disruption of the cell wall of MDR bacteria. Best therapeutic results were achieved in mice treated with a single dose of 2 mg/kg and in mice treated with two doses of 1 mg/kg, 8 h apart. Furthermore, acute and chronic histopathological studies demonstrated absent nephrotoxicity and moderate hepatotoxicity. The results demonstrated the efficacy of Fluopsin C against MDR organisms in *in vitro* and *in vivo* models, and hence it can be a novel therapeutic agent for the control of severe MDR infections.

Keywords: antibiotic, murine sepsis model, resistant mutant, electronic microscopy, histopathology, metalloantibiotic

OPEN ACCESS

Edited by:
Ana R. Freitas,
University of Porto, Portugal

Reviewed by:
Divakar Sharma,
Indian Institute of Technology Delhi, India
Maurizio Sanguinetti,
Catholic University of the Sacred Heart, Italy

****Correspondence:***
Galdino Andrade
andradeg@uel.br

Specialty section:
This article was submitted to Antimicrobials, Resistance and Chemotherapy, a section of the journal Frontiers in Microbiology

Received: *25 February 2019*
Accepted: *08 October 2019*
Published: *25 October 2019*

Citation:
Navarro MOP, Simionato AS, Pérez JCB, Barazetti AR, Emiliano J, Niekawa ETG, Andreata MFdL, Modolon F, Dealis ML, Araújo EJdA, Carlos TM, Scarpelim OJ, da Silva DB, Chryssafidis AL, Bruheim P and Andrade G (2019) Fluopsin C for Treating Multidrug-Resistant Infections: In vitro Activity Against Clinically Important Strains and in vivo Efficacy Against Carbapenemase-Producing Klebsiella pneumoniae. Front. Microbiol. 10:2431. doi: 10.3389/fmicb.2019.02431

INTRODUCTION

The worldwide, intense and frequent use of antimicrobials is a selective pressure for resistant bacteria. The fast emergence of resistant microorganisms inside hospitals is causing a global health crisis, impairing the efficacy of antibiotics and jeopardizing the success of medical treatments. Tackling antimicrobial resistance (AMR), which includes multidrug resistance (MDR), is the main goal in order to increase treatment success and lower the number of deaths of severe hospital-acquired infections. The discovery and development of novel antibiotic molecules and compounds, with high activity against untreatable MDR bacteria, is necessary (Ventola, 2015). Vancomycin-resistant *Enterococcus* (VRE), methicillin-resistant *Staphylococcus aureus* (MRSA), and Carbapenem-resistant Enterobacteria (CRE), including Carbapenemase-producing *Klebsiella pneumoniae* (KPC), are among the greatest risks for health services due to their increasing rates of antibiotic resistance (Boucher et al., 2009; Arias and Murray, 2012).

The development of molecules complexed with metals as potential medicinal agents has been rising the last decade (Cardozo et al., 2013; de Oliveira et al., 2016; Kerbauy et al., 2016; Munhoz et al., 2017; Stringer et al., 2017). Previous studies demonstrated that specific fractions obtained from the culture of *Pseudomonas aeruginosa* LV strain (F3, F3D, and F4A) present very strong antimicrobial activity against many different pathogens (de Oliveira et al., 2011, 2016; Cardozo et al., 2013; Murate et al., 2015; Kerbauy et al., 2016; Munhoz et al., 2017; Simionato et al., 2017). Indeed, our research group demonstrated the strong antibiotic activity of these semi-purified fractions against planktonic cells and biofilm formation of MDR isolates (Kerbauy et al., 2016). The gene expression analysis of *P. aeruginosa* LV strain showed that, when it is cultured in the presence of copper chloride, the bioremediation of intracellular excess copper forms a compound with high antimicrobial activity (Gionco et al., 2017). This bioactive compound was identified as a metalloantibiotic (organocopper compound), which is a great candidate for the development of new antibiotics to control infections caused by MRSA, CRE, VRE, and KPC-producing strains (Cardozo et al., 2013; Kerbauy et al., 2016).

In the present study, this metalloantibiotic was identified as Fluopsin C (YC 73), a compound produced and isolated from *Pseudomonas* spp. and *Streptomyces* sp., with high antibacterial, antifungal and antitumor activity (Itoh et al., 1970; Otsuka et al., 1972; Ma et al., 2013). However, there is a lack of studies on microbial resistance development, ultrastructural effect in the target pathogens and *in vivo* efficacy of Fluopsin C, which may confirm the possible application of this compound as an alternative for the treatment of severe human infections.

New studies on the evaluation the bioactivity, resistance-development risk, toxicity and therapeutic efficacy of Fluopsin C are required to determine the suitability of its therapeutic application. Therefore, the objective of the present study was to verify the toxicity and the effects against MDR bacteria of Fluopsin C using *in vitro* and *in vivo* experiments. Mammalian blood and cells were used to determine the hemolytic and cytotoxic effects of the compound. *Tenebrio molitor* larvae were used to evaluate Fluopsin C lethal concentration. The therapeutic efficacy against carbapenemase-producing *K. pneumonia* (KPC-KP), as well as the hepatotoxic and nephrotoxic effects, were analyzed in a murine sepsis model.

MATERIALS AND METHODS

Microorganisms

The Fluopsin C was produced by *P. aeruginosa* LV strain (GenBank: QBLE00000000.1). These microorganisms were isolated from a citrus canker lesion on an orange (*Citrus sinensis* cv.Valence) at Astorga, Paraná, Brazil (Gionco et al., 2017). The pathogens *K. pneumoniae* ATCC 10031 and *Enterococcus faecium* ATCC 6569 were used as susceptible strains. Detailed descriptions of the resistant bacterial strains used in the present work (in lab-maintained strains MRSA N315 and MRSA BEC9393; clinically isolated strains VRE 170 and CRE-*Kpn 19*) can be found in the **Supplementary Table S1**. All bacteria were stored at −20°C or in liquid nitrogen. These strains were deposited in the Microbial Culture Collection of the Microbial Ecology Laboratory, Londrina State University, Brazil.

Production, Isolation and Identification of Fluopsin C

Fluopsin C production used a patented method (Patent PI0803350-1 – INPI 09/12/20092008)[1], with some modifications (Bedoya et al., 2019). Briefly, *P. aeruginosa* LV strain was cultured in nutrient broth supplied with 5 mg/L of cooper chloride. After 10 days, the bacterial culture was centrifuged for 20 min at 9000 rpm and 4°C, followed by the extraction of the supernatant with dichloromethane. The extract was purified by flash chromatography with silica gel 60 (0.04–0.062 mm, Macherey-Nagel), coupled to a low-pressure pump and washed with petroleum ether: dichloromethane: Ethyl Ether (65:25:10). A semi-preparative Agilent 1260 Infinity high performance liquid chromatography (HPLC) system, with SB-C18, 4.6 × 250 mm, 5 μm particle size column (Agilent Zorbax Sb-C18), monitored at 264 nm (UV –VIS), was used to purify the Fluopsin C. A gradient of acetonitrile, and water was used as the mobile phase (from 20/80 to 100/0 in 10 min, returning to the original phase for 5 min), with a flow rate of 2 mL.min^{-1} and injection volume of 100 μL. The pure compound was dried and dissolved in deuterated chloroform (CDCI3) or deuterated methanol (CD3OD) at 1,000 μgmL-1. Mass spectra were obtained with an ESI-MS Quattro LCZ (Micromass, Manchester, United Kingdom). ^{1}H and ^{13}C nuclear magnetic resonance spectra were recorded in solution using a Bruker Avance III 400 MHz spectrometer. X-ray microanalysis (EDS) was carried out using a FEI-Quanta 200 Scanning Electron Microscope with an accelerating voltage of 25 kV. In the experiments, Fluopsin C was reconstituted in DMSO 3%.

[1]http://www.inpi.gov.br

Antibiotic Activity Fluopsin C

The disk-diffusion agar test and minimum inhibitory/bactericidal concentration assays (MIC/MBC) were carried out for evaluating the *in vitro* antibiotic activity of Fluopsin C against different bacteria, in Muller Hinton agar (MHA) and cation-adjusted Muller Hinton broth (MHB), respectively. The tests followed CLSI guidelines (Clinical and Laboratory Standards Institute (CLSI), 2012).

Resistance Induction and Reversion Experiments

The determination of spontaneous resistant frequency was based on a variation and combination of multi/single passages and mutant prevention concentration (MPC) methods (Nagai et al., 2000; Metzler et al., 2013; Firsov et al., 2015). Briefly, for selecting Fluopsin C-resistant mutants (FC-RMs), serial passages of bacterial strains were performed daily, with MHB containing increasing concentrations of the compound. Initial inocula containing 10^6 CFU.mL^{-1} were placed into 96-well plates, with 100 μL per well. Fluopsin C was added at concentrations of 0, 0.25×, 0.5×, 1×, 2 × 4×, 8×, and 16× MIC, and plates were incubated at 35°C. Every 24 h, an aliquot of 1 μL was collected from the well treated with the highest concentration of Fluopsin C that presented visible bacterial growth. This aliquot was used to inoculate a fresh micro-broth plate. After 21 days of these sequential passages, the microorganisms from the wells with visible growth, in the highest antibiotic concentration, were distributed in three plates with Fluopsin C-free agar. The MIC and MBC were determined as described before.

For testing the stability of developed resistance, one FC-RM colony was used for serial passages for 10 days, without Fluopsin C, and MIC/MBC were re-evaluated. The remaining colonies were used to inoculate 100 mL of broth, incubated at 35°C for 18 h, under continuous shaking. An aliquot of 100 μL from the bacterial suspension was spread on agar containing 0, 1×, 2×, 4×, 8×, 16× MIC of Fluopsin C. The plates were incubated at 35°C for 48 h. The MPC, the resistance selection frequency in the original strain and their FC-RM clones, as well as their reverted mutant, were determined based on protocols described in literature (Metzler et al., 2013; Firsov et al., 2015).

Electron Microscopy Analysis

Bacterial suspensions (10^{10} CFU) of the N315 and Kpn19 strains, incubated with and without Fluopsin C, were spotted on polylysine-coated glass slides and kept at 28°C for 1 h for drying. The slides were fixed in a solution of 2% paraformaldehyde and 2.5% glutaraldehyde in 0.1 M sodium cacodylate buffer (pH 7) for 12 h. After fixation, the slides were washed with 0.1 M sodium cacodylate buffer (pH 7) and post-fixed in a 1% OsO_4 solution for 2 h. The samples were dehydrated in ethanol at concentrations of 70, 80, 90, and 100% and critical-point-dried in CO_2 (BALTEC CPD 030 Critical Point Dryer). After drying, the slides were coated with gold (BALTEC SDC 050 Sputter Coater) and visualized under scanning electron microscopy (SEM, FEI Quanta 200).

For the transmission electronic microscopy (TEM) assay, microorganisms were incubated with and without Fluopsin C and centrifuged at 4000 rpm for 5 min. The pellets were resuspended and washed with PBS, centrifuged and fixed as described before. After dehydration in a series of ethanol rinses, the material was included in Araldite®. Ultrathin cuts of 60–70 nm were collected (Leica Ultracut UCT), contrasted with 2% uranyl acetate (15 min) and lead citrate (20 min), and observed under a transmission electron microscope (FEI Tecnai12).

In vitro Cytotoxicity Assays

The viability of LLC-MK2 cells was determined by the MTT method [dimethylthiazol diphenyl tetrazolium bromide (Sigma Chemical Co., United States)] according to the manufacturer's recommendation. The antibiotic concentration that inhibited up to 50% of the viable cells, determined by regression analysis, corresponded to the 50% cytotoxic concentration ($CC_{50/24h}$). Human erythrocytes were used for the hemolytic assays.

Lethal Concentration Assay in Invertebrate Model

Tenebrio molitor bugs (Coleoptera) were maintained in our lab as described previously (de Souza et al., 2015). All growth stages were kept together in single plastic containers, with a rearing medium composed of white flour and wheat bran. Bread and vegetable fragments were added periodically. The surface of the culture was covered with filter and water was sprayed daily to provide adequate moisture. The containers were kept in the dark, under controlled environmental conditions (humidity of 70% and temperature at 28°C). *T. molitor* larvae that appeared clear, with uniform color, weighing 150 ± 20 mg, were collected and used in the experiment. For evaluating the lethal concentration of Fluopsin C, groups of larvae ($n = 10$) received intrahemocoelic injections with different drug concentrations (0.06–2 μg per larva). A control group received only sterile diluent (placebo, RPMI with DMSO 3%). Larvae were injected at the ventral surface of the second or third sternite, right above their legs, using a Hamilton syringe. After treatment, all larvae were incubated at 28°C, in Petri dishes containing rearing medium. The treated larvae were observed for 8 days and the following parameters were recorded: melanization of the puncture site, response to a gentle touch stimulus and larvae survival. The experiments were performed with two biological replicates.

Experimental Murine Model

All mouse experiments were approved by the Animal Care and Use Committee of the State University of Londrina (CEUA – UEL, protocol n°6886.2015.28), and all procedures were in accordance with the standard approved protocols for animal research. The mice were obtained from the UEL Central Animal Facility and acclimatized at the laboratory for at least 48 h. They were kept in polypropylene boxes with wood shaving bedding and placed on ventilated shelves with controlled environmental conditions (24°C, 55% humidity and 12/12 h photoperiod). Sterilized water and commercial feed (Nutival®) were provided *ad libitum* throughout the experiment.

Groups of 6 immunocompetent female Swiss albino mice (7 ± 1 week old and 32 ± 3 g), were inoculated intravenously (IV) with 0.1 mL of Fluopsin C in different concentrations (0.5 to 16 mg/kg) or infected intraperitoneally (IP) with 0.5 mL of different concentrations of CRE-Kpn19 strain (10^5 to 10^9 UFC/mL), for determining the Lethal Dose (LD) and Lethal Inoculum (LI), respectively. A negative control group was injected with placebo (sterile diluent, RPMI with DMSO 3%) or physiological solution. Mice survival was observed for 48 h.

For the *in vivo* evaluation of the Fluopsin C antimicrobial efficacy against MDR bacteria, groups of 12 randomly assigned mice were inoculated IP with 0.5 ml of CRE-Kpn19 (LI = 4.1×10^7 UFC/mL), and treatments started 2 h post-infection (hpi). Mice received drug injections according to their respective group: (i) control treated with placebo; (ii) a single IV dose of Fluopsin C at 1 mg/kg; (iii) a single IV dose of Fluopsin C at 2 mg/kg; (iv) a single IV dose of Fluopsin C at 3 mg/kg; (v) two IV doses of Fluopsin C at 1 mg/kg, 8 h apart; or (vi) two IV doses of Fluopsin C at 2 mg/kg, 8 h apart. Mortality was recorded over 96 hpi.

Histopathological Pilot Study

For the evaluation of histopathological toxicity, cohorts of 2 non-infected mice were euthanized at 1, 10, 20, and 40 days after treatment with 2 mg/kg of Fluopsin C or placebo (RPMI medium), both delivered IV. Their whole kidney and liver were collected and fixed in 10% neutral buffered formalin. The organs were dehydrated in ascending series of ethyl alcohol, diaphanized in xylol and included in paraffin. From the paraffin-embedded tissues, 5 μm sections were stained (hematoxylin-eosin) and analyzed qualitatively and quantitatively.

For quantitative analysis, specific portions of the organs were collected and compared using the ImageProPlus software (version 2.5.3). In the liver, the number of hepatocytes with one or two nuclei, hepatocytes with condensed chromatin, and hepatocytes with vacuolization in the cytoplasm were counted. In addition, the area comprising 100 hepatocytes nuclei was measured. In the kidneys, the Bowmann area of ten glomerular corpuscles, the diameter of 50 proximal tubules and 50 distal tubules were measured.

The qualitative analysis was performed by sampling ten random images of liver (400× magnification) and five random images of kidney (100× magnification) of each animal. The presence of inflammatory infiltration, capillary congestion, hemorrhage, cytoplasmic vacuolation, and necrosis was evaluated in both organs. Additionally, the nuclear scaling and position of the cells lining the tubules were observed in the kidney cortex. The severity of such findings was evaluated based on the following scores: 0 - absent, 1 - discrete, 2 - moderate and 3 - severe.

Serum antimicrobial concentrations were determined in seven groups of three healthy Swiss mice, treated with a single IV dose of Fluopsin C (2 mg/Kg). Each group was euthanized at a specific time point after treatment (0, 15, 30, 60, 120, 240, and 480 min post drug injection) and total blood was collected from the mice via cardiac puncture. The blood was immediately placed in microtubes and centrifuged at 3,000 rpm for 5 min at room temperature. The serum was separated and stored at −20°C until analysis. Extraction of Fluopsin C from the serum samples was performed using acetonitrile at low temperature (∼4°C). An internal standard was used for control (500 μg of Phenazine carboxamide (PCN) dissolved in acetonitrile was added to 100 μL of every serum sample before extraction). The sample was vortexed and centrifuged at 3,000 rpm for 5 min at 4°C. The ACN: H_2O phase was filtered using 13 mm PTFE syringe filters with pore size of 0.22 μm. Fluopsin C was quantified using ultra-pressure liquid chromatography-tandem mass spectrometry (UPLC-MS/MS).

Statistical Analysis

Statistical analysis and graphics were performed with Rstudio software (2018 RStudio, Inc., - Safari/538.1 Qt/5.4.1). The Kaplan–Meier estimator was applied to generate a survival curve. Statistical analysis was performed using Tukey test, with a confidence level of 95% (significance considered when $p < 0.05$).

RESULTS

Identification of Fluopsin C

Fluopsin C was extracted from *P. aeruginosa* LV strain cultures by partitioning their supernatant with dichloromethane and purified by chromatographic adsorption techniques. The fourth fraction obtained by flash chromatography (CF4) was collected and analyzed by HPLC, with about 80% of such fraction corresponding to Fluopsin C. The peak with retention time of 3.611 min was collected and identified using mass spectrometry (265.92 *m/z*), NMR, infrared spectroscopy and X-ray microanalysis (**Supplementary Figure S1**).

Antibiotic Activity and Resistance Assays

Fluopsin C presented very strong bactericidal activity against Gram-positive and Gram-negative pathogens, including their MDR variants (**Table 1**). Moreover, intense bioactivity against *S. aureus, E. faecium*, and *K. pneumoniae* was detected in concentrations below 2 μg/mL.

The generation of Fluopsin C-resistant mutants was tested with bacteria cultured in sub-MIC concentrations for 21 days (FC-RM21), as shown in **Figure 1**. Serial passaging of *K. pneumoniae* (ATCC 10031 and *Kpn*-KPC 19) cultures containing Fluopsin C led to a moderate loss in susceptibility, with Fluopsin C-MIC gradually increasing to 4-fold and 8-fold after the 21st passage, for ATCC 10031 and *Kpn*-KPC 19, respectively. The MIC decreased again when the mutants were serially passaged for 10 days in Fluopsin C-free culture (FC-RM + 10), indicating a tendency for bacterial resistance reversal and consequent return to the original MIC. No resistant mutants of *S. aureus* and *E. faecium* were detected after 21 days of serial passages in different concentrations of Fluopsin C.

Results from the susceptibility tests (i.e., disk diffusion (10 μg/disk), MIC and MBC), using FC-RM21 and FC-RM + 10, are presented in **Table 1**. The MPC was determined as the antibiotic concentration necessary to prevent the growth of FC-RMs on Fluopsin C-containing agar plates after recovering

TABLE 1 | The Fluopsin C susceptibility tests: disk diffusion on agar (10 μg/disc), MIC, MBC, MPC and mutant frequencies for parent strain and RMs.

Strain	Fluopsin C†	Halo (mm)	MIC (μg/mL)	MBC (μg/mL)	MPC (μg/mL)	Mutant frequency	
						2xMIC	4xMIC
MRSA N315	PS	40	0.5	1.0	4.0	$\sim 4.2 * 10^{-6}$	$\sim 9.2 * 10^{-9}$
	RM21	32	1.0	1.0	4.0	$\sim 2.6 * 10^{-8}$	$< 1.8 * 10^{-10}$
	RM + 10	39	0.5	1.0	4.0	$\sim 5.0 * 10^{-7}$	$< 1 * 10^{-10}$
MRSA BEC9393	PS	40	1.0	1.0	4.0	$\sim 6.3 * 10^{-8}$	$< 1.5 * 10^{-10}$
	RM21	38	1.0	1.0	4.0	$\sim 6.5 * 10^{-7}$	$< 2.5 * 10^{-10}$
	RM + 10	40	1.0	1.0	4.0	$\sim 8.8 * 10^{-7}$	$< 4.4 * 10^{-10}$
ATCC 6569	PS	36	1.0	1.0	4.0	$\sim 4.4 * 10^{-8}$	$< 6.0 * 10^{-9}$
	RM21	35	1.0	1.0	4.0	$\sim 6.0 * 10^{-7}$	$< 1.3 * 10^{-10}$
	RM + 10	33	1.0	1.0	4.0	$\sim 9.8 * 10^{-7}$	$< 2.4 * 10^{-10}$
VRE-170	PS	39	1.0	1.0	4.0	$\sim 8.0 * 10^{-8}$	$< 8.8 * 10^{-9}$
	RM21	28	2.0	2.0	8.0	$\sim 4.3 * 10^{-6}$	$< 2.5 * 10^{-10}$
	RM + 10	32	1.0	1.0	4.0	$\sim 8.4 * 10^{-7}$	$< 5.7 * 10^{-10}$
ATCC 10031	PS	30	1.0	1.0	4.0	$\sim 3.3 * 10^{-8}$	$< 1.6 * 10^{-10}$
	RM21	21	4.0	4.0	8.0	$\sim 3.8 * 10^{-7}$	$< 1.9 * 10^{-10}$
	RM + 10	28	2.0	2.0	4.0	$\sim 6.6 * 10^{-7}$	$< 3.2 * 10^{-10}$
CRE *kpn*19	PS	22	2.0	2.0	8.0	$\sim 4.0 * 10^{-8}$	$< 3.5 * 10^{-10}$
	RM21	9	16.0	16.0	16.0	$< 3.5 * 10^{-10}$	$< 3.5 * 10^{-10}$
	RM + 10	12	4.0	4.0	8.0	$\sim 4.8 * 10^{-7}$	$< 2.4 * 10^{-10}$

†*PS, parent strain; RM21, FC-RM strain after 21 passages of the parent strain on antibiotic-containing media; RM + 10, strain after 21 passages of the parent strain on antibiotic-containing media plus 10 passages on Fluopsin C-free media.*

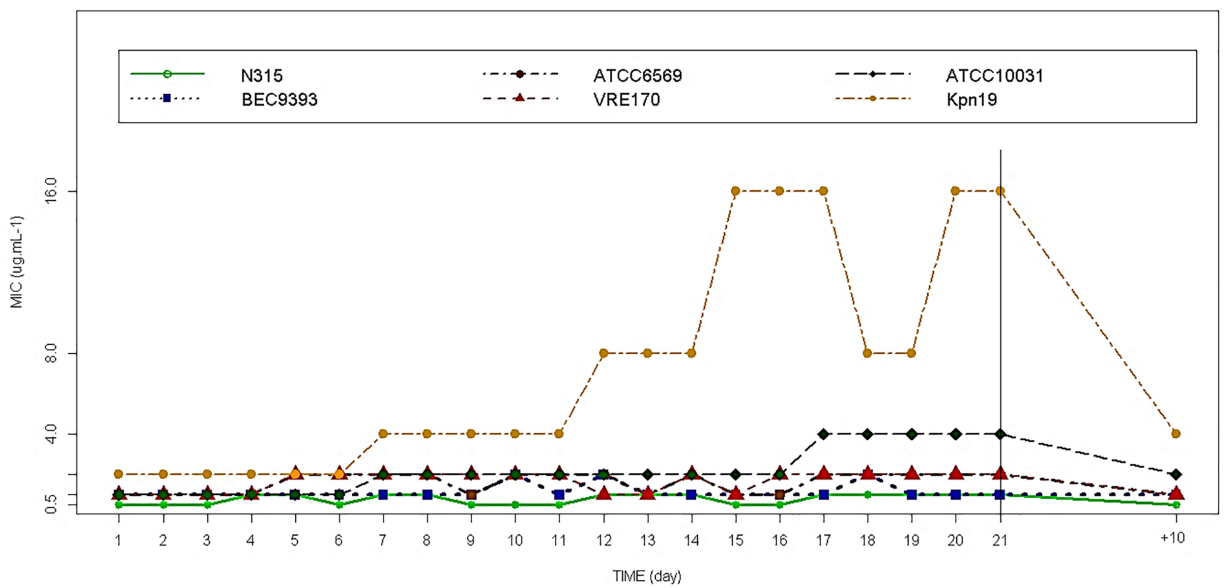

FIGURE 1 | Resistance development of *S. aureus, E. faecium* and *K. pneumoniae* during 21 serial passages in Fluopsin C-containing MHB (FC-RM21) and the final MIC, when the mutants were serially passaged for 10 days in Fluopsin C-free medium (FC-RM + 10).

$\sim 10^{10}$ CFU from the cell suspension culture. Following 48 h, no resistant colonies were observed, and all strains tested were unable to produce resistant mutants, when plating on media with Fluopsin C (4× MIC), giving the calculated frequency of resistance below 10^{-9}. The frequency of resistant clones cultured in 2× MIC of Fluopsin C was determined as well. The MPC and frequencies are shown in **Table 1** and **Figure 2**.

Ultrastructural Analysis

The ultrastructure of Fluopsin C-treated cells was evaluated by Scanning Electron Microscopy (SEM) and Transmission Electron Microscopy (TEM), after 1 h of incubation. Clinical isolates of *K. pneumoniae* (*Kpn*-KPC 19) and MRSA (N315) incubated with Fluopsin C presented reduced CFU and decreased extracellular matrix formation when compared to bacteria

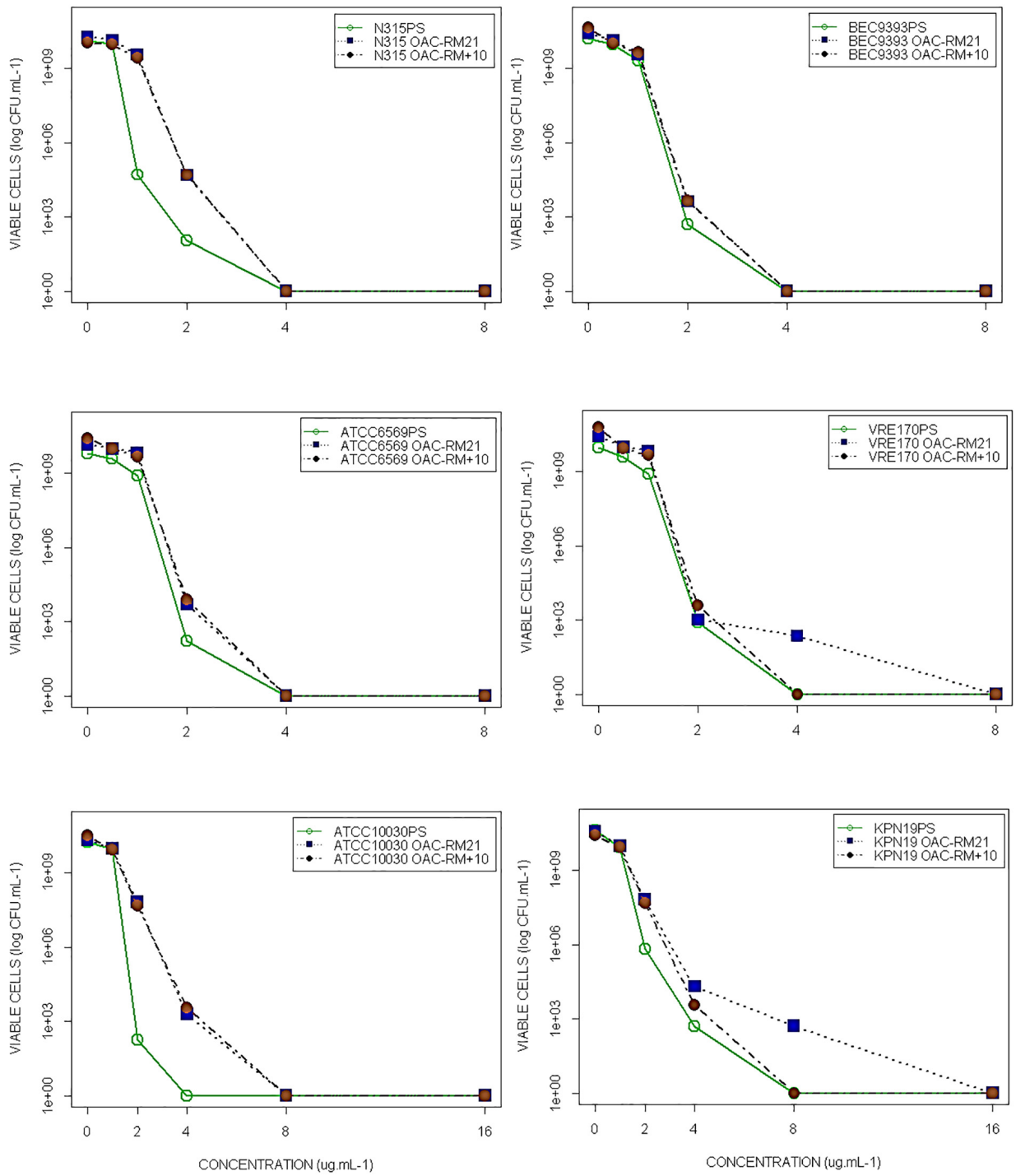

FIGURE 2 | Fluopsin C-MPC determination with *S. aureus* (MRSA N315 and MRSA BEC9393), *E. faecium* (ATCC6569 and VRE 170) and *K. pneumoniae* (ATCC 10031 and CRE-Kpn19) parent and FC-RMs strains.

incubated without the compound (**Figures 3**, **4**). Fluopsin C decreased the number of bacteria and generated morphological changes in bacterial cell shape, with marked depressions in the cell shape, lessened extracellular matrix and visible cell disruption (**Figures 3**, **4**). Cytoplasmic alteration and vacuolation were detected by TEM in cells treated with Fluopsin C when compared to non-treated cells (**Figures 5**, **6**). The plasma membrane was intact, but the cell showed low electron density,

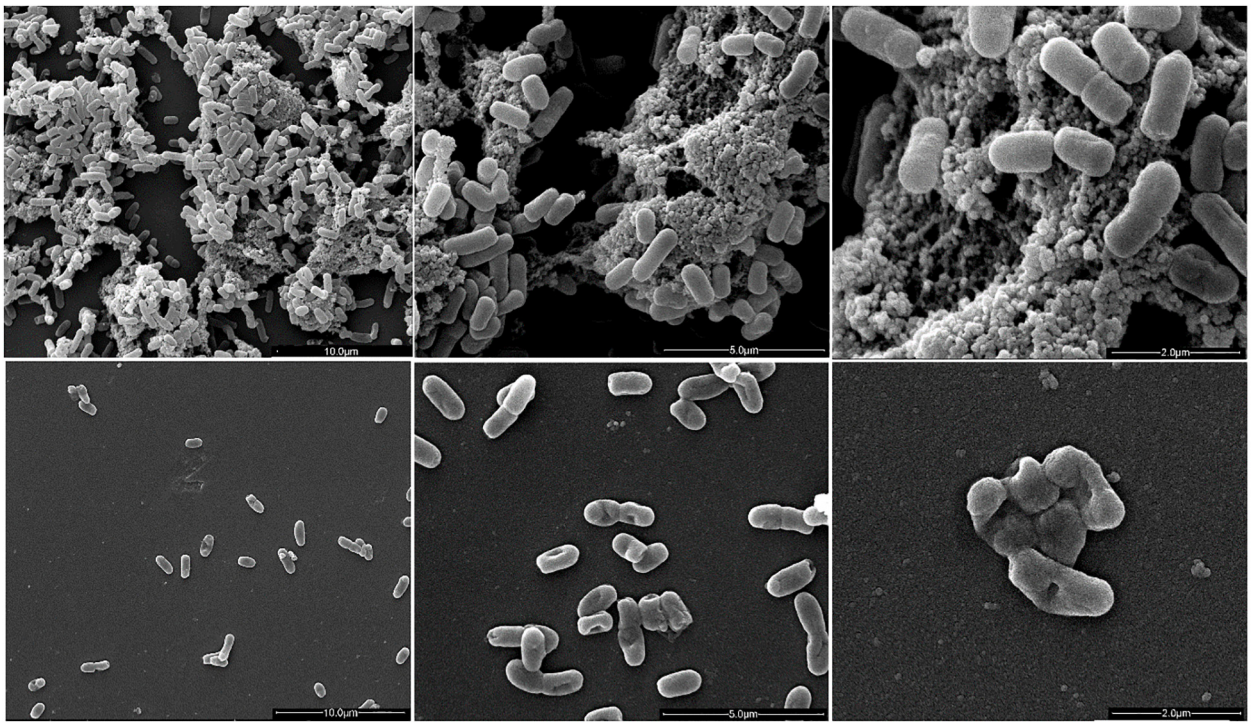

FIGURE 3 | Scanning electron micrographs (SEM). Above, control (not treated), large number of *K. pneumoniae* with intact appearance and high extracellular polysaccharide production. Below, *K. pneumoniae* treated with Fluopsin C (1 h), showing fewer microorganisms and bacteria presenting cell wall disruption, forming depressions in the configuration of the bacterial skeleton and lessened extracellular matrix.

probably caused by a failure in the ionic pumps of the plasma membrane.

In vitro and *in vivo* (Invertebrate Model) Toxicity Evaluation

The cytotoxic and hemolytic effects analyses were carried out using LLC-MK2 cells and human erythrocytes, respectively. Fluopsin C induced the highest toxic activities (>90%) with ≥20 μg/mL. The lowest toxic concentration ($CC_{50/24h}$) detected in both LLC-MK2 and red blood cells was near 2 μg/mL. When Fluopsin C concentration was below 2 μg/mL, no cytotoxic or hemolytic effect was observed (**Supplementary Figure S2**). Larvae of *T. molitor* treated with 0.06 and 0.12 μg of Fluopsin C, as well as control larvae, did not indicate any toxic effect. Larva groups treated with 0.25 and 0.5 μg presented mortality rates of 20 and 42%, respectively, whereas all larvae treated with 1 and 2 μg died after 96 hpi (**Supplementary Figure S3A**).

Antibiotic Activity Evaluation in Mice Model

Fluopsin C demonstrated strong antibiotic activity against *kpn*-KPC 19 strain in *in vitro* test (MIC = 2 μg/mL), as described above. Also, this concentration did not generate evident toxic effects. After these *in vitro* results were obtained, the effect of Fluopsin C for controlling *kpn*-KPC 19 experimental peritoneal infection of mice was evaluated. Initially, the lethal dose (LD) of Fluopsin C was determined, where concentrations below 4 mg/kg (LD_{50}) did not generate toxicity signs in treated mice after 96 h. However, higher doses produced lethality after 48 h (**Supplementary Figure S3B**). The presence of Fluopsin C in serum was assessed by UPLC-MS/MS, without detection in any time point.

The *in vivo* evaluation of Fluopsin C antibiotic activity was performed using a murine sepsis model. Swiss mice were infected by IP route with a lethal dose (LI_{90}) of *kpn*-KPC 19 cell suspension, being treated with Fluopsin C or placebo after infection. Mice treated with a single dose of 2 mg/kg and two doses of 1 mg/kg 8 h apart (experimental groups iii and v, respectively) presented survival rates of 50 and 42%, respectively, after 72 h of treatment. The group treated with one dose of 1 mg/kg (treatment ii) showed a survival rate of 25% after 48 h and 17% after 96 h. Groups iv and vi (3 mg/kg and two doses of 2 mg/kg/8 h, respectively) presented lower survival rates, reaching complete mortality even faster than control group (**Figure 7**).

Histopathological Examination

Liver and kidney of mice were collected at 1, 10, 20, and 40 days after treatment with Fluopsin C and placebo. The control group did not show overt alterations in the morphology of hepatic cells, but areas with discrete hepatocyte cytoplasm vacuolation and inflammatory infiltration were detected (**Figure 8**). Liver collected from mice treated with 2 mg/kg of Fluopsin C

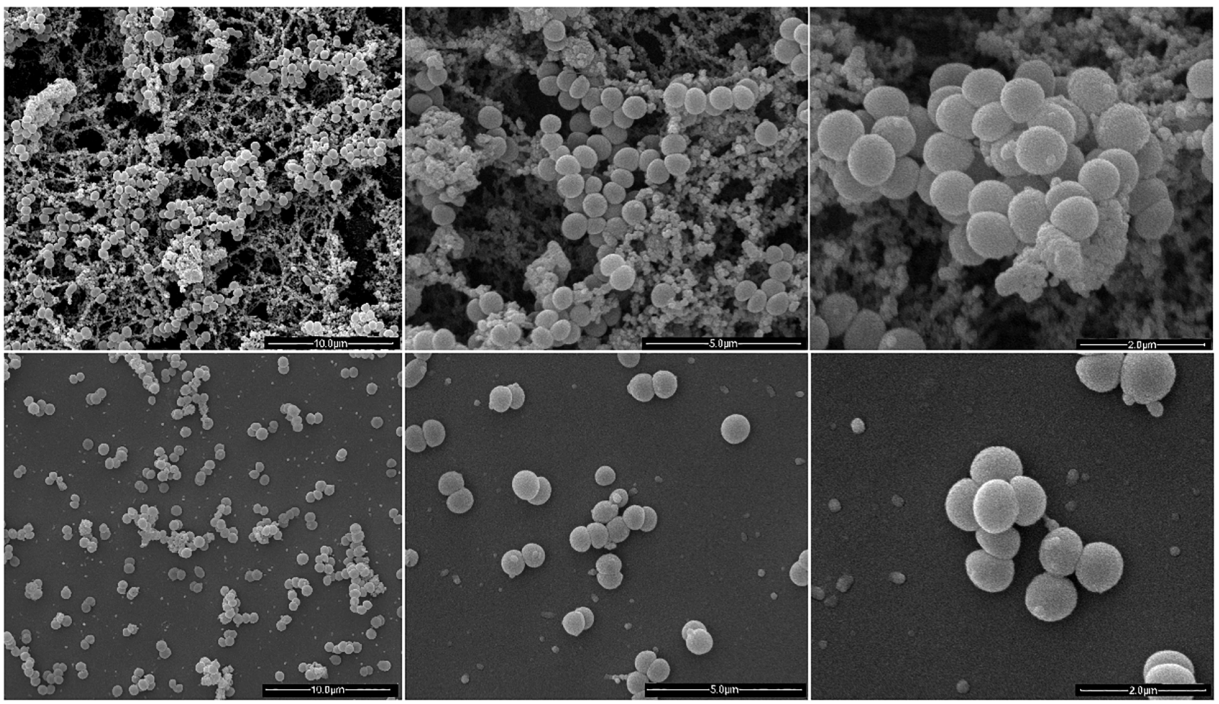

FIGURE 4 | Scanning electron micrographs (SEM). Above, MRSA-N315 control, great number of bacteria with intact appearance and high extracellular polysaccharide production. Below, MRSA-N315 strain treated with Fluopsin C (1 h), showing less bacteria and extracellular matrix.

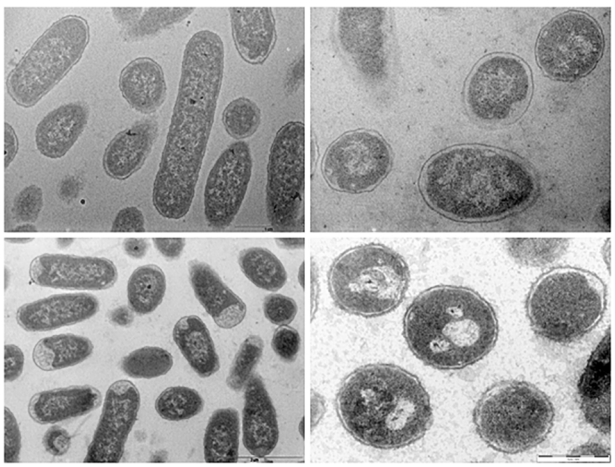

FIGURE 5 | Transmission electron micrographs. Control (above) and Fluopsin C-treated *K. pneumoniae* cells (below). TEM studies demonstrated that Fluopsin C induced internal cell damage.

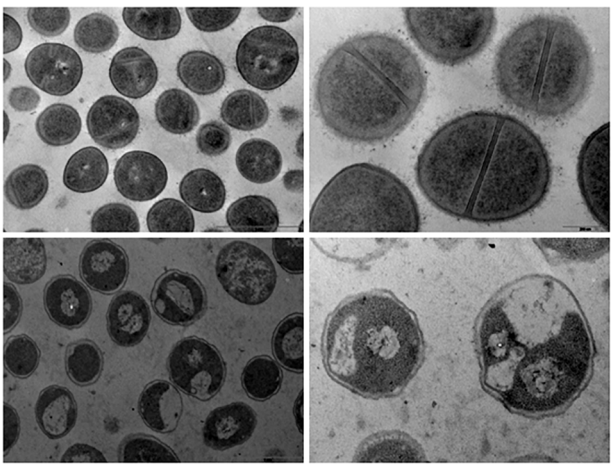

FIGURE 6 | Transmission electron micrographs. Control (above) and Fluopsin C-treated MRSA cells (below). TEM studies demonstrated that Fluopsin C induced internal cell damage.

presented moderate vessel congestion, inflammatory infiltration, hemorrhage and marked cytoplasmic vacuolation in all time points, but there was no sign of necrosis during the whole experiment (**Supplementary Table S2**). Fluopsin C did not cause significant changes in the number of hepatocytes, neither with one or two nuclei, nor with condensed chromatin. Mild differences of hepatocyte nuclear area were observed in both groups, in all time points. Hepatocytes with vacuolated cytoplasm and displaced nucleus were detected in treated mice (**Supplementary Table S3** and **Supplementary Figure S4**).

The qualitative analysis of kidney did not detect congestion, edema or necrosis in glomerular corpuscles (**Figure 9**). However, mild inflammatory infiltration and bleeding was present in treated mice. In the tubules, slight cytoplasmic vacuolation and

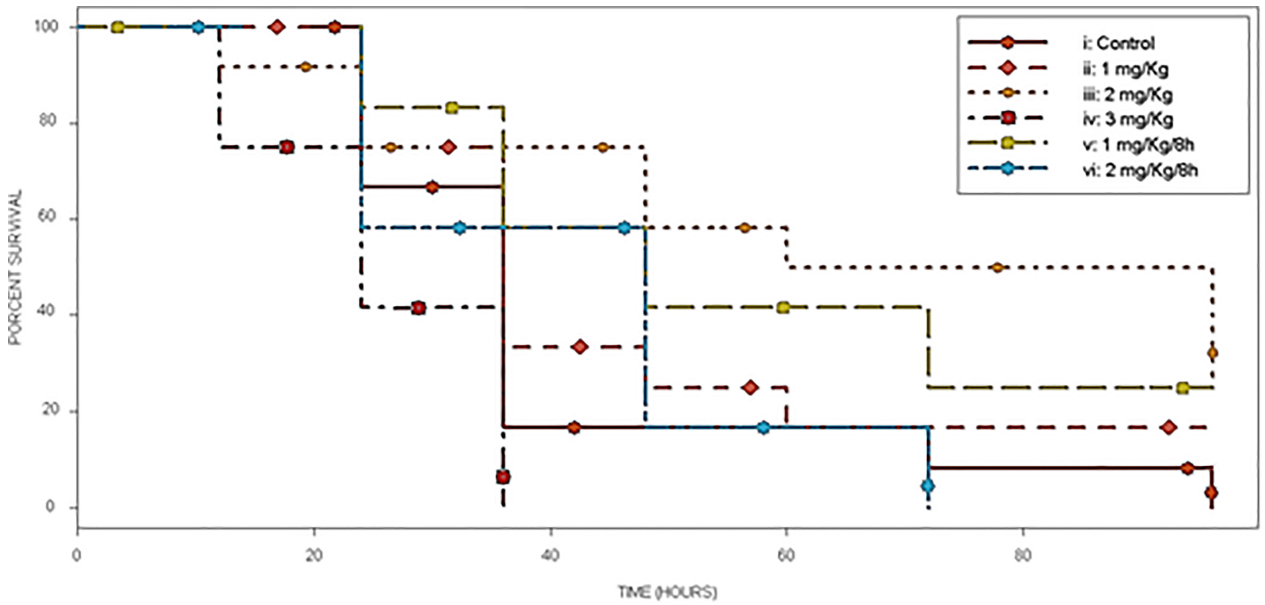

FIGURE 7 | Survival curve of the experimental murine model of MDR infection. Control (i) and 5 different treatments (ii–vi) with Fluopsin C, in septicemia protection model using CRE–Kpn19. Survival is depicted until 96 h after infection.

nuclei positioned at the cell center were observed. Differences in the number of glomerular corpuscles, changes in the Bowman's space and tubule diameters were observed (**Supplementary Table S4**). No significant differences were observed between the renal cortexes of mice treated with Fluopsin C and placebo (**Supplementary Figure S4**).

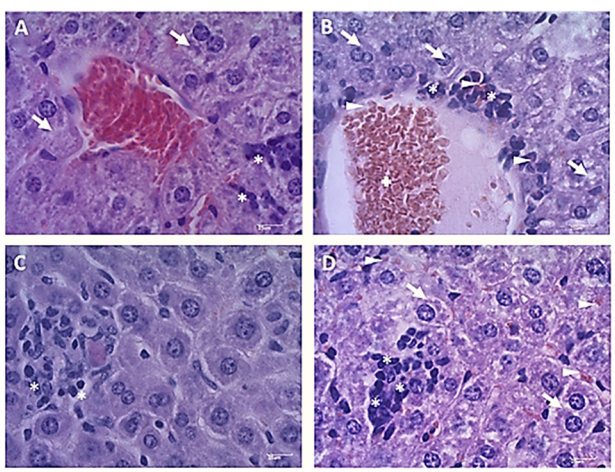

FIGURE 8 | Photomicrographs of mice liver 10 days after treatment with Fluopsin C or placebo. The control group **(A,C)** showed a slight cytoplasmic vacuolation of hepatocytes (arrow) and discrete inflammatory infiltrate (asterisk), while animals treated with Fluopsin C **(B,D)** presented moderate vessel congestion (cross), marked vacuolation of the cytoplasm (arrow), moderate inflammatory infiltrate (asterisk) and bleeding (arrowhead). Similar images were observed in other fields, in every time point. Color: HE. Scale bar: 25 μm.

DISCUSSION

Current treatments of MDR infections are often unsuccessful due to continuous selection of bacteria resistant to a large number of antibiotics. It seems that the biggest challenge now is to discover novel drug candidates that may overcome bacterial resistance mechanisms. Previous studies have reported the antibiotic effects of secondary metabolites of *Pseudomonas* sp. against many clinical pathogenic resistant microorganisms. The F3d fraction, produced by *P. aeruginosa* LV strain, demonstrated activity against N315, BEC9393, ATCC 10031, and *Kpn*-KPC 19 strains (Cardozo et al., 2013; Kerbauy et al., 2016), with the metalloantibiotic compound Fluopsin C being the major component with strong antibiotic activity (de Oliveira et al., 2016). Elementary analysis, mass spectrometry, chemical proprieties and biological activity evaluation proved that *P. aeruginosa* LV strain-metalloantibiotic is identical to Fluopsin C (YC 73), a compound described in earlier studies (Egawa et al., 1970, 1971; Itoh et al., 1970; Otsuka et al., 1972; Ma et al., 2013; de Oliveira et al., 2016).

Fluopsin C demonstrated a potential increase of 250-fold in biocidal activity when compared to the F3d fraction, and it required 50-fold less concentration to form equal or greater inhibition halos than the ones described in previous experiments with less purified fractions (Cardozo et al., 2013; Kerbauy et al., 2016). In addition, Fluopsin C decreased MIC 30- and 125-fold when tested against *K. pneumoniae* and *S. aureus,* respectively (Cardozo et al., 2013; Kerbauy et al., 2016). Fluopsin C was effective against Gram-positive and Gram-negative bacteria, with MICs comparable to commercial antibiotics commonly used in clinical practice, such as vancomycin, and new antibiotics, such as linezolid, teixobactin and daptomycin (Firsov et al., 2015;

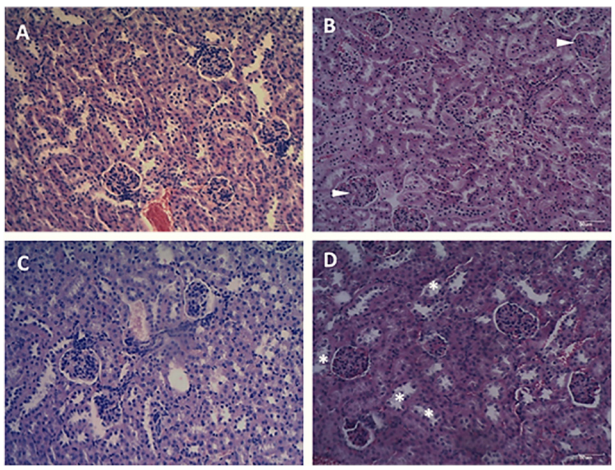

FIGURE 9 | Photomicrographs of the renal cortex of mice after 10 days of treatment with Fluopsin C or placebo. The control group **(A,C)** presented mild inflammatory infiltrate and bleeding in the glomerular corpuscles. In the tubules **(C)**, discrete cytoplasmic vacuolation could be observed and scaling was practically non-existent. The animals in the treated group **(B,D)** presented no glomerular changes (arrowheads), but a mild peeling of the tubular epithelium (asterisk) was detected. Similar images were observed in other fields and on other days. Color: HE. Scale bar: 25 μm.

Ling et al., 2015). The bactericidal activity of Fluopsin C was analyzed under electron microscopy, allowing the comparison between treated and non-treated bacterial cultures. In both SEM and TEM it was possible to observe that Fluopsin C caused cell lysis and degraded cellular matrix. Similar effects were observed when cells were treated with the semi-purified F3d fraction (Cardozo et al., 2013; Kerbauy et al., 2016). The present results raised the hypothesis that the primary target of Fluopsin C is the cell membrane, causing its disruption, but further studies need to be carried to better understand the action of Fluopsin C in the cell.

Previous studies using serial passages selected resistant mutants of *K. pneumoniae, S. aureus, Escherichia coli*, and *Streptococcus pneumoniae* for different antibiotics, such as Fluoroquinolones, Linezolid, Daptomycin and Vancomycin. Their respective MIC increased 100 times in a few days when compared to the original strain (Nagai et al., 2000; Firsov et al., 2006, 2015; Ling et al., 2015; Strukova et al., 2017). In the present study, FC-RMs did not generate spontaneous resistant mutants of Gram-positive bacteria during 21 serial passages with sub-inhibitory concentrations of Fluopsin C. On the other hand, *K. pneumoniae* ATCC 10031 strain produced FC-RM21, increasing the MIC 4-fold, but the resistance stability was affected at the 10th transfer to antibiotic-free media, when the original MIC was restored. The results indicated that Fluopsin C-tolerant clones of *K. pneumoniae* were obtained during the multi-passages, when the antibiotic was present, but the MIC increased below the level detected in previous studies with other antibiotics (Nagai et al., 2000; Firsov et al., 2006, 2015; Ling et al., 2015; Strukova et al., 2017). The *kpn*-KPC 19 produced after 21 passages (FC-RM21) increased MIC eight-fold (2 to 16 μg/mL) and the MPC only twofold (8 to 16 μg/mL), suggesting that it is hard for bacteria to generate resistance to Fluopsin C in concentrations above 16 μg/mL. Furthermore, the resistance frequency to Fluopsin C was low, with CFU below 10^{-9}. The MIC of *kpn*-KPC 19 possibly increased by intrinsic resistance mechanisms, such as efflux pumps, which could transport Fluopsin C to outside the cell, but further molecular studies should be made to determine which defense mechanisms are involved.

The methods applied in this study emphasized the importance of evaluating the emergence of microbial resistance to new antibiotic molecules, with little expenses. Molecular techniques (Martínez et al., 2011; Andersson, 2015) and dynamic models of "anti-mutant" ratios (Firsov et al., 2015; Strukova et al., 2017; Yu and Wang, 2017) are also important methods that can improve the prediction of mutational resistance rise to antimicrobial substances, even before their clinical use. Current antibiotic treatments for *K. pneumoniae* infections are often unsuccessful due to the increasing frequency of antibiotic resistance genes, which creates MDR strains, and the low number of drug candidates in clinical development. *P. aeruginosa* secondary metabolites, expressed in culture medium with copper, were used to identify a class of organic metal complexes with potent antibiotic activity. Fluopsin C demonstrated very strong biocidal activity in *in vitro* experiments against *K. pneumoniae*, including many resistant strains with different resistance genes (Kerbauy et al., 2016). Beyond that, this compound was active against Gram-positive bacteria, including clinical isolates of *S. aureus* MRSA and *E. faecium* VRE (Cardozo et al., 2013).

The chemotherapeutic potential of Fluopsin C has been highlighted since its first description, but the significant cytotoxicity against Ehrlich, Hela, and sarcoma 180 cells line, added to acute toxicity in animal models, suggested its unfeasibility to control infections in humans (Itoh et al., 1970; Otsuka et al., 1972). Fluopsin C also increased $CC_{50/24\ h}$ when compared to previous studies with semi-purified fractions, where the cytotoxicity was not detected with F3 and F3d fractions (Murate et al., 2015; Kerbauy et al., 2016). Probably, the activity of these fractions against LLCMK2 cell line was low because Fluopsin C was diluted in these fractions. The replacement of live animals by alternative models is desirable and studies for measuring bioactivity using invertebrate larvae increase each year (Desbois and Coote, 2011; Luther et al., 2014; de Souza et al., 2015). The *T. molitor* larva model indicated a LD_{50} of 0.5 μg per larvae (∼3 mg/kg), very close to the result found in the murine model (LD_{50} of 4 mg/kg), thus supporting the application of such a model and the reduction in the use of animals in the experiment.

The low pharmacokinetic properties can be an issue to most natural products (Das et al., 2016). From the best of our knowledge, there is no previous report of Fluopsin C detection in blood. In the present study, the compound could not be detected in the blood of treated mice, suggesting a low bioavailability. Despite that, the metalloantibiotic significantly increased the survival rate of Swiss mice infected with *kpn*-KPC 19, protecting a high percentage of the infected animals against sepsis. It is possible that Fluopsin C is quickly metabolized by the treated

organism and changed into a different molecule, or molecules, with distinct chemical properties, complicating its detection. Another possibility is that the compound may have such high affinity for the membrane cells, that it might be trapped on them. Still, further studies must be carried out to verify such hypotheses.

This is the first report of Fluopsin C efficacy in MDR-infected mice. In addition, Fluopsin C did not cause pathological alterations in kidney cells, such as glomerular corpuscles and the Bowman's space area, suggesting that Fluopsin C is not a nephrotoxic compound. On the other hand, the treatment increased the frequency of hepatocytes with vacuolated cytoplasm and displaced nucleus. These changes occur when triglyceride production increases during liver damage, suggesting that the antibiotic presents moderate hepatotoxicity (Ma et al., 2013). Likewise, many other antibiotics, such as isoniazid, rifampicin, and pyrazinamide, commonly used in clinical therapy, cause moderate liver damage during the treatment of tuberculosis patients, but they are still applied in the control of infection (Rossouw and Saunders, 1975). Vancomycin is indicated to treat Gram-positive bacteria, but it is not considered a first-choice drug because of the common adverse effects, like hepatotoxicity, nephrotoxicity and phlebotoxicity (Bruniera et al., 2014). In the same way, the intravenous formulation of colistin and polymyxin B were gradually abandoned in many countries in the early 1980s because of the high incidence of severe nephrotoxicity. However, due to the emergence of MDR in most of the antibiotic classes available and the lack of new antimicrobial against Gram-negative, the polymyxins were put back in use as a therapeutic option (Falagas and Kasiakou, 2005). The present study provides new information about the potent antibiotic activity of Fluopsin C against MDR isolates. Still, its toxicity and antibiotic selectivity should be better studied. Thus, despite the small gap between effective healing and toxic doses, Fluopsin C, or a possible derivative, may become a new member in the antibacterial arsenal against MDR infections.

CONCLUSION

The strong antibiotic activity of Fluopsin C under *in vitro* and *in vivo* conditions stressed the potential of this compound to control Gram-positive and Gram-negative MDR infections. However, the development of a less cytotoxic derivate or presentation is desirable. Additional studies aiming at the reduction of toxicity – by reducing the Fluopsin C effective concentration with possible synergic combinations with commercial antibiotics – as well as the elucidation of its pharmacokinetic properties and mechanisms of action will be carried out in the near future.

DATA AVAILABILITY STATEMENT

All datasets generated for this study are included in the manuscript/**Supplementary Files**.

ETHICS STATEMENT

All animal experimentation was carried out with the approval of the Animal Research Ethics Committee of the State University of Londrina (CEUA – UEL, protocol n°176;6886.2015.28) and all procedures were in accordance with the standard approved protocols for animal research and approved by the name of committee. The arrive checklist can be found in **Supplementary Material**.

AUTHOR CONTRIBUTIONS

GA and MN conceived the study and designed the experimental procedures. MN, AS, JP, AB, JE, EN, MA, FM, MD, TC, and OS carried out the experiments. MN, EA, DS, AC, and GA analyzed the data. EA, DS, and PB contributed the reagents and materials. MN and AC wrote the manuscript. GA supervised the project.

FUNDING

This work was supported by the Brazilian National Council for Scientific and Technological Development (CNPq) and Coordination for the Improvement of Higher Education Personnel (CAPES, Brazil).

ACKNOWLEDGMENTS

We would like to thank the Laboratory of Spectroscopy – ESPEC UEL/FINEP for the help with the NMR, X-ray, and infrared analysis. We would also like to thank the Laboratory for Electron Microscopy and Microanalysis – LMEM UEL/FINEP for the help with the electron microscopy experiments and the UEL Central Animal Facility for providing the mice.

SUPPLEMENTARY MATERIAL

The Supplementary Material for this article can be found online at: https://www.frontiersin.org/articles/10.3389/fmicb.2019.02431/full#supplementary-material

REFERENCES

Andersson, D. I. (2015). Improving predictions of the risk of resistance development against new and old antibiotics. *Clin. Microbiol. Infect.* 21, 894–898. doi: 10.1016/j.cmi.2015.05.012

Arias, C. A., and Murray, B. E. (2012). The rise of the *Enterococcus*: beyond vancomycin resistance. *Nat. Rev. Microbiol.* 10, 266–278. doi: 10.1038/nrmicro2761

Bedoya, J. C., Dealis, M. L., Silva, C. S., Niekawa, E. T. G., Navarro, M. O. P., Simionato, A. S., et al. (2019). Enhanced production of target bioactive metabolites produced by *Pseudomonas aeruginosa* LV strain. *Biocatal. Agric. Biotechnol.* 17, 653–664. doi: 10.1016/j.bcab.2019.01.025

Boucher, H. W., Talbot, G. H., Bradley, J. S., Edwards, J. E., Gilbert, D., Rice, L. B., et al. (2009). Bad bugs, no drugs: no ESKAPE! an update from the infectious diseases society of America. *Clin. Infect. Dis.* 48, 1–12. doi: 10.1086/595011

Bruniera, F. R., Ferreira, F. M., Savioli, L. R. M., Bacci, M. R., Feder, D., Pereira, E. C., et al. (2014). Endothelial, renal and hepatic variables in wistar rats treated with vancomycin. *An. Acad. Bras. Cienc.* 86, 1963–1971. doi: 10.1590/0001-3765201420140204

Cardozo, V. F., Oliveira, A. G., Nishio, E. K., Perugini, M. R. E., Andrade, C. G. T. J., Silveira, W. D., et al. (2013). Antibacterial activity of extracellular compounds produced by a *Pseudomonas* strain against methicillin-resistant *Staphylococcus aureus* (MRSA) strains. *Ann. Clin. Microbiol. Antimicrob.* 12:12. doi: 10.1186/1476-0711-12-12

Clinical and Laboratory Standards Institute (CLSI) (2012). *CLSI Document M07-A9. Methods for Dilution Antimicrobial S cally: Approved Standard*, 19th Edn. (Wayne, IL: CLSI).

Das, M., Sakha Ghosh, P., and Manna, K. (2016). A review on platensimycin: a selective FabF inhibitor. *Int. J. Med. Chem.* 2016, 1–16. doi: 10.1155/2016/9706753

de Oliveira, A. G., Murate, L. S., Spago, F. R., Lopes, L. D. P., Beranger, J. P. D. O., Martin, J. A. B. S., et al. (2011). Evaluation of the antibiotic activity of extracellular compounds produced by the *Pseudomonas* strain against the *Xanthomonas citri* pv. *citri* 306 strain. *Biol. Control* 56, 125–131. doi: 10.1016/j.biocontrol.2010.10.008

de Oliveira, A. G., Spago, F. R., Simionato, A. S., Navarro, M. O. P., da Silva, C. S., Barazetti, A. R., et al. (2016). Bioactive organocopper compound from *Pseudomonas aeruginosa* inhibits the growth of *Xanthomonas citri* subsp. *citri*. *Front. Microbiol.* 7:113. doi: 10.3389/fmicb.2016.00113

de Souza, P. C., Morey, A. T., Castanheira, G. M., Bocate, K. P., Panagio, L. A., Ito, F. A., et al. (2015). *Tenebrio molitor* (Coleoptera: Tenebrionidae) as an alternative host to study fungal infections. *J. Microbiol. Methods* 118, 182–186. doi: 10.1016/j.mimet.2015.10.004

Desbois, A. P., and Coote, P. J. (2011). Wax moth larva (*Galleria mellonella*): an in vivo model for assessing the efficacy of antistaphylococcal agents. *J. Antimicrob. Chemother.* 66, 1785–1790. doi: 10.1093/jac/dkr198

Egawa, Y., Umino, K., Awataguchi, S., Kawano, Y., and Okuda, T. (1970). Antibiotic YC 73 of *Pseudomonas* origin 1. Production, isolation and properties. *J. Antibiot.* 23, 267–270. doi: 10.7164/antibiotics.23.267

Egawa, Y., Umino, K., and Yukio, I. (1971). Antibiotic YC 73 of *Pseudomonas* origin. Ip structure and synthesis of thioformin and its cupric complex (YC 73). *J. Antibiot.* XXIV, 124–130. doi: 10.7164/antibiotics.24.124

Falagas, M. E., and Kasiakou, S. K. (2005). Colistin: the revival of polymyxins for the management of multidrug-resistant gram-negative bacterial infections. *Clin. Infect. Dis.* 40, 1333–1341. doi: 10.1086/429323

Firsov, A. A., Golikova, M. V., Strukova, E. N., Portnoy, Y. A., Romanov, A. V., Edelstein, M. V., et al. (2015). In vitro resistance studies with bacteria that exhibit low mutation frequencies: prediction of "Antimutant" linezolid concentrations using a mixed inoculum containing both susceptible and resistant *Staphylococcus aureus*. *Antimicrob. Agents Chemother.* 59, 1014–1019. doi: 10.1128/AAC.04214-14

Firsov, A. A., Smirnova, M. V., Lubenko, I. Y., Vostrov, S. N., Portnoy, Y. A., and Zinner, S. H. (2006). Testing the mutant selection window hypothesis with *Staphylococcus aureus* exposed to daptomycin and vancomycin in an in vitro dynamic model. *J. Antimicrob. Chemother.* 58, 1185–1192. doi: 10.1093/jac/dkl387

Gionco, B., Tavares, E. R., de Oliveira, A. G., Yamada-Ogatta, S. F., do Carmo, A. O., Pereira, U. D. P., et al. (2017). New insights about antibiotic production by *Pseudomonas aeruginosa*: a gene expression analysis. *Front. Chem.* 5:66. doi: 10.3389/fchem.2017.00066

Itoh, S., Inuzuka, K., and Suzuki, T. (1970). New antibiotics produced by bacteria grown on n-paraffin (mixture of C12, C 13 and C14 fractions). *J. Antibiot.* 23, 542–545. doi: 10.7164/antibiotics.23.542

Kerbauy, G., Vivan, A. C., Simões, G. C., Simionato, A. S., Pelisson, M., Vespero, E. C., et al. (2016). Effect of a metalloantibiotic produced by *Pseudomonas aeruginosa* on *Klebsiella pneumoniae* Carbapenemase (KPC)-producing *K. pneumoniae*. *Curr. Pharm. Biotechnol.* 17, 389–397. doi: 10.2174/1389201017041602151716 49

Ling, L. L., Schneider, T., Peoples, A. J., Spoering, A. L., Engels, I., Conlon, B. P., et al. (2015). A new antibiotic kills pathogens without detectable resistance. *Nature* 517, 455–459. doi: 10.1038/nature14098

Luther, M. K., Arvanitis, M., Mylonakis, E., and LaPlante, K. L. (2014). Activity of daptomycin or linezolid in combination with rifampin or gentamicin against biofilm-forming *Enterococcus faecalis* or *E. faecium* in an in vitro pharmacodynamic model using simulated endocardial vegetations and an in vivo survival assay using gal. *Antimicrob. Agents Chemother.* 58, 4612–4620. doi: 10.1128/AAC.02790-13

Ma, L.-S., Jiang, C.-Y., Cui, M., Lu, R., Liu, S.-S., Zheng, B.-B., et al. (2013). Fluopsin C induces oncosis of human breast adenocarcinoma cells. *Acta Pharmacol. Sin.* 34, 1093–1100. doi: 10.1038/aps.2013.44

Martínez, J. L., Baquero, F., and Andersson, D. I. (2011). Beyond serial passages: new methods for predicting the emergence of resistance to novel antibiotics. *Curr. Opin. Pharmacol.* 11, 439–445. doi: 10.1016/j.coph.2011.07.005

Metzler, K., Drlica, K., and Blondeau, J. M. (2013). Minimal inhibitory and mutant prevention concentrations of azithromycin, clarithromycin and erythromycin for clinical isolates of *Streptococcus pneumoniae*. *J. Antimicrob. Chemother.* 68, 631–635. doi: 10.1093/jac/dks461

Munhoz, L. D., Fonteque, J. P., Santos, I. M. O., Navarro, M. O. P., Simionato, A. S., Goya, E. T., et al. (2017). Control of bacterial stem rot on tomato by extracellular bioactive compounds produced by *Pseudomonas aeruginosa* LV strain. *Cogent Food Agric.* 3, 1–16. doi: 10.1080/23311932.2017.1282592

Murate, L. S., de Oliveira, A. G., Higashi, A. Y., Barazetti, A. R., Simionato, A. S., da Silva, C. S., et al. (2015). Activity of secondary bacterial metabolites in the control of citrus canker. *Agric. Sci.* 06, 295–303. doi: 10.4236/as.2015.63030

Nagai, K., Davies, T. A., Pankuch, G. A., Dewasse, B. E., Jacobs, M. R., and Appelbaum, P. C. (2000). In vitro selection of resistance to clinafloxacin, ciprofloxacin, and trovafloxacin in *Streptococcus pneumoniae*. *Antimicrob. Agents Chemother.* 44, 2740–2746. doi: 10.1128/AAC.44.10.2740-2746.2000

Otsuka, H., Niwayama, S., Tanaka, H., Take, T., and Uchiyama, T. (1972). An antitumor antibiotic, no. 4601 from *Streptomyces*, identical with YC 73 of *Pseudomonas origin*. *J. Antibiot.* 25, 369–370. doi: 10.7164/antibiotics.25.369

Rossouw, J. E., and Saunders, S. J. (1975). Hepatic complications of antituberculous therapy. *Q. J. Med.* 44, 1–16. doi: 10.1093/oxfordjournals.qjmed.a067410

Simionato, A. S., Navarro, M. O. P., de Jesus, M. L. A., Barazetti, A. R., da Silva, C. S., Simões, G. C., et al. (2017). The effect of phenazine-1-carboxylic acid on mycelial growth of *Botrytis cinerea* produced by *Pseudomonas aeruginosa* LV strain. *Front. Microbiol.* 8:1102. doi: 10.3389/fmicb.2017.01102

Stringer, T., Seldon, R., Liu, N., Warner, D. F., Tam, C., Cheng, L. W., et al. (2017). Antimicrobial activity of organometallic isonicotinyl and pyrazinyl ferrocenyl-derived complexes. *Dalt. Trans.* 46, 9875–9885. doi: 10.1039/C7DT01952A

Strukova, E. N., Portnoy, Y. A., Zinner, S. H., and Firsov, A. A. (2017). Species differences in ciprofloxacin resistance among Gram-negative bacteria: can "anti-mutant" ratios of the area under the concentration–time curve to the MIC be achieved clinically? *J. Chemother.* 29, 351–357. doi: 10.1080/1120009X.2017.1335980

Ventola, C. L. (2015). The antibiotic resistance crisis: part 1: causes and threats. *P T* 40, 277–283.

Yu, G., and Wang, G. (2017). Optimization of the biosynthesis conditions of daptomycin by the biostatistical methodology. *Interdiscip. Sci. Comput. Life Sci.* 9, 80–87. doi: 10.1007/s12539-015-0133-8

Conflict of Interest: The authors declare that the research was conducted in the absence of any commercial or financial relationships that could be construed as a potential conflict of interest.

frontiers in Microbiology

ORIGINAL RESEARCH
published: 19 March 2019
doi: 10.3389/fmicb.2019.00544

In silico and Genetic Analyses of Cyclic Lipopeptide Synthetic Gene Clusters in *Pseudomonas* sp. 11K1

*Hui Zhao[1], Yan-Ping Liu[1,2] and Li-Qun Zhang[1]**

[1] Department of Plant Pathology and MOA Key Laboratory of Pest Monitoring and Green Management, China Agricultural University, Beijing, China, [2] National Laboratory of Biomacromolecules, CAS Center for Excellence in Biomacromolecules, Institute of Biophysics, Chinese Academy of Sciences, Beijing, China

Pseudomonas sp. 11K1, originally isolated from rhizosphere, possesses inhibitory activity against plant pathogenic fungi and bacteria. Herein, the genome of strain 11K1 was sequenced and subjected to *in silico*, mutational, and functional analyses. The 11K1 genome is 6,704,877 bp in length, and genome mining identified three potential cyclic lipopeptide (CLP) biosynthetic clusters, subsequently named brasmycin, braspeptin, and brasamide. Insertional and deletion mutants displayed impaired brasmycin and braspeptin production, and lost antifungal activity, but retained antibacterial activity against *Xanthomonas oryzae*. The structures of these two active CLPs were predicted based on adenylation (A) domains. Brasmycin is composed of nine amino acids and belongs to the syringomycin class, while braspeptin is a 22 amino acid cyclic peptide belonging to the tolaasin group. Matrix-Assisted Laser Desorption/Ionization Time-of-Flight (MALDI-TOF) mass spectrometry analysis revealed that brasmycin and braspeptin have different molecular weights compared with known syringomycin and tolaasin members, respectively. Mutation of brasmycin and braspeptin gene clusters affected both biofilm formation and colony morphology. Collectively, these results indicate that *Pseudomonas* sp. 11K1 produces two novel CLPs that may help bacteria compete for nutrients and niches in the environment.

Keywords: *Pseudomonas*, genome mining, secondary metabolites, cyclic lipopeptides, NRPS, rhizosphere, antifungal activity, biofilm formation

OPEN ACCESS

Edited by:
Ana R. Freitas,
Universidade do Porto, Portugal

Reviewed by:
Maarten Ghequire,
KU Leuven, Belgium
Jon Y. Takemoto,
Utah State University, United States

****Correspondence:***
Li-Qun Zhang
zhanglq@cau.edu.cn

Specialty section:
This article was submitted to Antimicrobials, Resistance and Chemotherapy, a section of the journal Frontiers in Microbiology

Received: *06 December 2018*
Accepted: *01 March 2019*
Published: *19 March 2019*

Citation:
Zhao H, Liu Y-P and Zhang L-Q (2019) In silico and Genetic Analyses of Cyclic Lipopeptide Synthetic Gene Clusters in Pseudomonas sp. 11K1. Front. Microbiol. 10:544. doi: 10.3389/fmicb.2019.00544

INTRODUCTION

Pseudomonas spp. are ubiquitous in aquatic and terrestrial habitats, especially plant rhizospheres. Rhizosphere-derived pseudomonads have received much attention in recent decades because many are able to suppress plant diseases (Bender et al., 1999; Raaijmakers et al., 2002; Weller, 2007). Production of antimicrobial metabolites is one of the major mechanisms by which pseudomonads prevent microbial infection. *Pseudomonas* species exhibit extensive metabolic versatility and produce a remarkable spectrum of antimicrobial metabolites including cyclic lipopeptides (CLPs), 2,4-diacetylphloroglucinol (DAPG), phenazines (PHZs), pyrrolnitrin (PRN), pyoluteorin (PLT), 2,5-dialkylresorcinol, quinolones, gluconic acid, rhamnolipids, siderophores, and hydrogen cyanide (Gross and Loper, 2009; Masschelein et al., 2017).

Comparative genomics studies have revealed substantial diversity among different species of the *Pseudomonas* genus, and even among strains belonging to the same species (Loper et al., 2012). Many novel antimicrobial compounds have been discovered using genome analysis, including CLPs (de Bruijn et al., 2007; Gross and Loper, 2009; Nikolouli and Mossialos, 2012). CLPs are amphiphilic molecules composed of a cyclic oligopeptide lactone ring coupled to a fatty acid tail (Raaijmakers et al., 2010). CLPs are synthesized by non-ribosomal peptide synthases (NRPSs), large enzymes that are composed of a series of modules. Each module is a building block for the stepwise incorporation of an amino acid in the CLP peptide moiety and consists of an adenylation (A) domain, a thiolation (T) domain, and a condensation (C) domain. The A domain is responsible for amino acid selection and activation, the thiolation (T) domain catalyzes thioesterification of the activated amino acid, and C domain promotes peptide bond formation between two neighboring substrates to elongate the peptide chain. Based on their structural relationships, CLPs produced by *Pseudomonas* spp. are divided into at least six categories (Raaijmakers et al., 2006; Gross and Loper, 2009). Recently, Geudens and Martins (2018) further classified *Pseudomonas* spp. CLPs into 14 major groups, according to oligopeptide length and structure. Most CLPs produced by *Pseudomonas* species exhibit antifungal and antibacterial activity, and some possess antioomycete, antiviral, antiprotozoan, and antitumor activities (Masschelein et al., 2017).

Cyclic lipopeptides exert their antimicrobial activities by targeting either cell wall biosynthesis or cell membrane integrity. Friulimicin B from *Actinoplanes friuliensis* and the recently discovered CLP malacidin encoded in soil microbiomes inhibit cell wall biosynthesis (Schneider et al., 2009; Hover et al., 2018). Daptomycin produced by *Streptomyces roseosporus* and tridecaptin A1 produced by *Bacillus* and *Paenibacillus* species exert antimicrobial activity by disrupting membrane integrity (Straus and Hancock, 2006; Cochrane et al., 2016). Also *Pseudomonas* CLPs such as syringopeptins, cormycin, and massetolides exert their antibiosis activity by affecting membrane integrity. Overall, the molecular targets of most CLPs remain unknown (Masschelein et al., 2017).

In addition to antimicrobial activity, many CLPs produced by *Pseudomonas* spp. are involved in a wide range of other biological functions such as motility, biofilm formation, and virulence. Most CLPs produced by *Pseudomonas* spp. affect bacterial motility and biofilm formation as biosurfactants (Raaijmakers et al., 2010). Syringomycin and syringpeptin contribute to the virulence of *P. syringae* pv. *syringae* in cherry fruits (Scholz-Schroeder et al., 2001), and CLP sessilin hampers orfamide production in *Pseudomonas* sp. CMR12a (D'Aes et al., 2014).

We previously isolated *Pseudomonas* sp. 11K1 from *Vicia faba* rhizosphere in Yunnan province. This strain exhibits strong inhibitory activity against plant pathogens, including the fungal pathogen *Botryosphaeria dothidea* that causes canker of grapevines, and the bacterial pathogen *Xanthomonas oryzae* RS105 that causes bacterial blight of rice. In the present work, we sequenced the genome of strain 11K1, performed *in silico* and genetic analyses of putative secondary metabolite biosynthetic clusters, and identified two CLP clusters contributing to the antifungal activities displayed by this strain.

MATERIALS AND METHODS

Strains and Growth Conditions

Bacterial strains and plasmids used in this study are listed in **Supplementary Table S1**. *Pseudomonas* sp. 11K1 and its mutants were grown in lysogenic broth (LB), AB medium (ABM), or amended King's B medium (Proteose peptone No.3, 10 g; K_2HPO_4, 1.5 g; $MgSO_4 \cdot 7H_2O$, 1.5 g; glucose, 20 g; KBG) at 28°C. *Escherichia coli* cells were grown at 37°C in LB medium. *B. dothidea* was cultured in PDA medium, and *X. oryzae* RS105 cells were grown at 28°C in LB or PDA medium. Where indicated, media was supplemented with ampicillin (50 μg/mL) or kanamycin (50 μg/mL) and/or 5-bromo-4-chloro-3-indolyl-D-galactopyranoside (X-Gal; 40 μg/mL).

Genome Sequencing and Assembly

Genomic DNA from 11K1 was prepared from a culture grown from a single colony using a DNA purification kit (Promega, Beijing, China) and sequenced on a PacBio RS II platform (Pacific Biosciences, Menlo Park, CA, United States) following the manufacturer's instructions. *De novo* assembly of PacBio reads was performed using the Smartanalysis pipeline v2.3.0 in conjunction with the HGAP assembly protocol, and additional assembly was performed with minimus2. Open reading frames were identified and annotated using GeneMarkS, rRNAs were predicted by Barrnap and RNAmmer, and tmRNAs and tRNAs were predicted using ARAGORN and tRNAscan-SE, respectively. Other non-coding RNAs were predicted and classified by infernal conjunction with Rfam. The functions of genes were also annotated using the COG, KEGG, Pfam, TIGRFAMs, and SwissProt databases.

Genome Analysis of Putative Secondary Metabolite Clusters

The genome of the 11K1 strain was analyzed using the Antibiotics and Secondary Metabolite Analysis Shell (antiSMASH) pipeline (Blin et al., 2017). ClusterFinder and Use ClusterFinder algorithms were employed for biosynthetic gene cluster (BGC) border prediction and analysis. Complete genome sequences of 11K1, four strains of *P. brassicacearum*, and 15 well-studied biocontrol agents belonging to other species of the *Pseudomonas* genus were also analyzed using Extra Features (KnownClusterBlast, SubClusterBlast, and ActiveSiteFinder).

Mutation of Putative Secondary Metabolite Gene Clusters

Fragments of genes to be inactivated were PCR-amplified using primer pairs and PCR conditions listed in **Supplementary Table S2**. PCR products were cloned into the p2P24-Km suicide vector (Yan et al., 2017) to generate insertional mutant constructs, designated as p2P24-GC1, p2P24-GC4, p2P24-GC8, p2P24-GC26, p2P24-GC30, p2P24-GC28-1, and p2P24-28-2

(**Supplementary Table S1**). These were introduced individually into the *E. coli* DH5α donor strain then transferred into *Pseudomonas* sp. 11K1 by triparental mating (Thoma and Schobert, 2009). In brief, cells from 300 μL of overnight LB donor, helper DH5α (λπ) containing plasmid pRK600, and recipient cultures were washed twice with ddH_2O and resuspended in 300 μL of ddH_2O. The three suspensions were pooled (1:1:1) and cells were harvested by centrifugation. Bacterial pellets were resuspended in 100 μL of ddH_2O and spotted onto an LB plate (2 μL per droplet). After incubation for 6 h at 28°C, bacterial cells were removed from the medium, resuspended in 1 mL of ddH_2O, and 100 μL aliquots or serial dilutions were plated on ABM plates supplemented with kanamycin.

To further confirm the antimicrobial activities of lipopeptides, we constructed in-frame deletion mutants of gene clusters encoding brasmycin, braspeptin and brasamide, and combinations thereof (double and triple mutants). In-frame deletions were made using a two-step homologous recombination strategy. Briefly, ∼1 kb upstream and downstream fragments of brasmycin, braspeptin, and brasamide gene clusters were PCR-amplified from 11K1 genomic DNA using primers listed in **Supplementary Table S2**. PCR products were digested with restriction enzymes and cloned into the suicide vector p2P24-Km to generate plasmids p2P24-Δbam, p2P24-Δbap, and p2P24-Δbaa, which were individually introduced into strain 11K1 by triparental mating. Colonies appeared on LB plates containing kanamycin were picked up and inoculated in liquid LB medium without antibiotics. Overnight cultures were then plated on LB plates supplemented with 20% sucrose to generate the mutants Δbam, Δbap, and Δbaa, in which 38,432, 73,251, and 26,622 bp regions of the biosynthesis gene clusters were removed, respectively (Yan et al., 2017). All deletion mutants were screened and confirmed by PCR amplification (**Supplementary Figure S1**). The same method was used to generate double gene cluster deletion mutants ΔbamΔbap, ΔbamΔbaa, and ΔbapΔbaa, and the triple gene cluster deletion mutant ΔbamΔbapΔbaa (**Supplementary Table S1**).

Identification and Analysis of Domains in NRPS Genes

The antiSMASH 4.0 program was used for cluster analysis of the A, T, and C domains of predicted NRPS genes. Sequences from predicted A domains in 11K1 and known A domains from CLPs in other pseudomonads were aligned using ClustalW. Phylogenetic trees were inferred by the neighbor joining method using MEGA5 with 1,000 bootstrap replicates. The peptide moieties of putative CLP signature sequences identified in the A domains were predicted by NRPSpredictor2 as described previously (Röttig et al., 2011).

Extraction of Lipopeptides

Overnight liquid cultures of 11K1 in LB were spread onto PDA plates (100 μL). After incubation for 5 days at 28°C, agar was sliced into small pieces and extracted with water overnight at 28°C with shaking at 180 rpm in a 500 mL Erlenmeyer flask. The water extract was separated from agar by cheesecloth filtration and subsequently from cell debris by centrifugation (7000 *g*, 10 min) (Michelsen et al., 2015a,b). The supernatant pH was adjusted to pH 2 using 6 M HCl, and the sample was incubated overnight at 4°C before centrifugation (7000 *g*, 10 min). The pellet was collected and dried at 50°C, the crude peptide extract was resuspended in 1 mL of methanol (Biniarz et al., 2016), and analyzed by matrix-assisted laser desorption/ionization time-of-flight (MALDI-TOF) mass spectrometry (MS).

Matrix-Assisted Laser Desorption/Ionization Time-of-Flight (MALDI-TOF) MS Analysis

MALDI-TOF MS analysis was conducted on a Bruker UltrafleXtreme MALDI-TOF/TOF MS instrument (Ultraflextreme, Bruker, Germany) operated in reflection-positive ion mode with an acceleration voltage of 20 kV. The sample was mixed with matrix in a 1:1 (v/v) ratio. The matrix was α-cyano-4-hydroxycinnamic acid, which was dissolved in 50% acetonitrile containing 0.1% trifluoroacetic acid (TFA) (Monti et al., 2011). The nitrogen laser was set at a threshold adequate for signal generation that minimized fragmentation.

Swarming Motility and Biofilm Formation

Swarming motility was studied by spotting 5 μL of an overnight cell suspension on KBG medium solidified with 0.6% agar, and evaluating surface swarming motility after incubation at 28°C for 24 h (Olorunleke et al., 2017). Biofilm formation was quantified by incubating 11K1 and its mutants for 3 days at 28°C in glass tubes, and staining with 0.1% crystal violet. Stained biofilms on the inner-surface of glass tubes were subsequently extracted with 95% ethanol and quantified by measuring the absorbance of the solution at 570 nm (Spiers et al., 2003).

RESULTS

Genomic Features of *Pseudomonas* sp. 11K1

The 11K1 complete genome consists of a 6,682,832 bp chromosome and one 22,045 bp plasmid, p11K1. A total of 5,785 CDSs were predicted, of which 5,749 CDSs are chromosomal and 36 are encoded on the plasmid. 84 RNA genes including rRNA, tRNA and tmRNA genes were identified. In addition, 81 miscellaneous RNA genes were identified. The general features of the strain 11K1 genome are summarized in **Table 1**. Based on 16S rDNA sequence analysis, strain 11K1 was identified as a species in the *P. fluorescens* group (**Supplementary Figure S2**; Hesse et al., 2018).

Automated Searching for Secondary Metabolite Clusters Using the antiSMASH 4.0 Pipeline

The genome of 11K1 was subjected to an automated search using antiSMASH (version 4.0). When the "Extra Features" settings

TABLE 1 | Genome statistics for *Pseudomonas* sp. 11K1.

Feature	Chromosome	Plasmid	Total
Size (bp)	6,682,832	22,045	6,704,877
G+C content	60.3	53.2	60.3
Number of genes	5,913	37	5,950
Number of CDSs	5,749	36	5,785
Number of rRNAs	16	0	16
Number of tRNAs	67	0	67
Number of tmRNAs	1	0	1
Number of miscellaneous RNAs	80	1	81

TABLE 2 | Secondary metabolite and antibiotic gene clusters in *Pseudomonas* sp. 11K1 predicted by antiSMASH 4.0[a].

Cluster[b]	Type	Most similar known cluster[c]	MIBiG BGC-ID[d]
Cluster 1	Other	Mangotoxin biosynthetic gene cluster (71% of genes show similarity)	BGC0000387_c1
Cluster 4	Aryl polyene	APE Vf biosynthetic gene cluster (40% of genes show similarity)	BGC0000837_c1
Cluster 8	Bacteriocin	–	–
Cluster 14	NRPS	Pyoverdine biosynthetic gene cluster (11% of genes show similarity)	BGC0000413_c1
Cluster 26	NRPS	Syringopeptin biosynthetic gene cluster (100% of genes show similarity)	BGC0000438_c1
Cluster 28	NRPS	Syringomycin biosynthetic gene cluster (100% of genes show similarity)	BGC0000437_c1
Cluster 30	Hserlactone	–	–
Cluster 32	NRPS	Cupriachelin biosynthetic gene cluster (17% of genes show similarity)	BGC0000330_c1
Cluster 35	NRPS	Pyoverdine biosynthetic gene cluster (20% of genes show similarity)	BGC0000413_c1
Cluster 41	Lantipeptide		

[a]Clusters identified by antiSMASH 4.0 using the "Extra Features" settings and the gene clusters highlighted in gray were inactivated by site-directed insertional mutagenesis. [b]Cluster 28 contains two CLP gene clusters. [c]The percentage similarity between genes in predicted clusters and the most similar known cluster. A BLAST e-value <1E-05 was used as a significance threshold for genes showing similarity, along with 30% minimal sequence identity, and a shortest BLAST alignment coverage >25% of the sequence. [d]Hyperlinks to the MIBiG repository.

were applied, 10 gene clusters were identified (**Table 2**), five of which are NRPS-type gene clusters predicted to be involved in the biosynthesis of lipopeptides, pyoverdine, and cupriachelin, four were predicted to synthesize a bacteriocin, a homoserine lactone (Hserlactone), a aryl polyene, and a lantipeptide, and one designated "Other" accounts for biosynthesis of mangotoxin (**Table 2**). An "Extended" search found an additional 33 gene clusters (**Supplementary Table S3**), 24 of which had no predicted products or functions. Other clusters showed only low gene similarities (<40%) with known biosynthetic clusters except for gene cluster 39, which shares 80% gene similarities to the alginate BGC (**Supplementary Table S3**).

We compared the secondary compound profile as predicted for strain 11K1 with 19 other *Pseudomonas* strains, and siderophore production is the only common feature present in all strains (**Figure 1**). Other antimicrobial compounds (e.g., CLPs, DAPG, PLT, and PRN) are present in conserved genomic locations of some closely related strains (**Figure 1**). Group III *Pseudomonas* spp. including strain 11K1 all produce CLPs but not DAPG, PLT, or PRN (**Figure 1**). *Pseudomonas* strains from Group II only produce DAPG but not PLT, PRN, or CLPs (**Figure 1**). Group I, comprising five *P. protegens* strains, produces all four types of antimicrobial compounds (DAPG, PLT, PRN, and CLPs; **Figure 1**). These results indicate that different *Pseudomonas* strains, even those belonging to the same species, may produce different secondary compounds. Closely related strains share similar metabolite profiles, and strain 11K1 may produce multiple CLPs with similar chemical structures to the compounds produced by other members of Group III.

Identification of Gene Clusters Involved in Antibiosis Activity

Based on the results of the *in silico* analysis, we performed site-directed insertional mutagenesis of seven gene clusters (**Table 2**), to find out whether one or more of these clusters contribute to the antimicrobial activity of strain 11K1. Inactivated clusters included NRPS-type clusters 26 and 28. The latter cluster is predicted to produce two CLPs. The two CLPs synthetic gene clusters in cluster 28 are located next to each other, but their synthetic genes transcribe in opposite direction (**Figure 2**). The growth of *B. dothidea* was not affected by any of the site-directed insertional mutants except mutants 11K1-GC28-1::Km and 11K1-GC28-2::Km. These mutants were both hit in cluster 28. The former mutant displayed a reduced inhibition phenotype whereas the latter completely failed to inhibit *B. dothidea*. These results indicate that the two CLPs encoded by gene cluster 28 are potential antifungal compounds. The first of the CLP gene clusters in cluster 28 was predicted to encode a 22 amino acid lipopeptide, and the second was predicted to encode a 9 amino acid lipopeptide. Gene cluster 28 is similar to the syringomycin/syringopeptin BGC in *P. syringae* pv. *syringae* B301D, and the nunamycin/nunapeptin BGC in *P. fluorescens* In5 (**Supplementary Figure S3A**). The third CLP, encoded by gene cluster 26, was predicted to encode an 8 amino acid lipopeptide, and this cluster shares similarity with the syringopeptin gene cluster in *P. syringae* B301D and the cichopeptin gene cluster in *P. cichorii* SF1-54 (Scholz-Schroeder et al., 2001; Huang et al., 2015; **Supplementary Figure S3B**). We designated the predicted 22 amino acid CLP as braspeptin (bap), the 9 amino acid compound as brasmycin (bam), and the 8 amino acid peptide as brasamide (baa; **Figure 2**). All mutants retained their inhibitory activity against *X. oryzae* RS105, indicating that other compounds, but not CLPs, were responsible for inhibition of this bacterium.

To further evaluate the role of CLPs in antibiosis activity, we constructed deletion mutants of single gene clusters Δbam, Δbap, and Δbaa, double gene clusters ΔbamΔbap, ΔbamΔbaa, and ΔbapΔbaa, and the triple gene cluster ΔbamΔbapΔbaa. Mutants Δbam, ΔbamΔbap, ΔbamΔbaa, and ΔbamΔbapΔbaa failed to inhibit *B. dothidea* growth, whereas mutant Δbaa retained full antifungal activity comparable with that of the WT 11K1 strain. Mutants Δbap and ΔbapΔbaa displayed a reduced inhibition phenotype compared with the Δbaa and WT strains (**Figure 3A**). These results confirm the results of the insertional mutation analysis, and indicate that brasmycin is the major antifungal compound active against *B. dothidea*. In addition, all CLP deletion mutants retained antibacterial

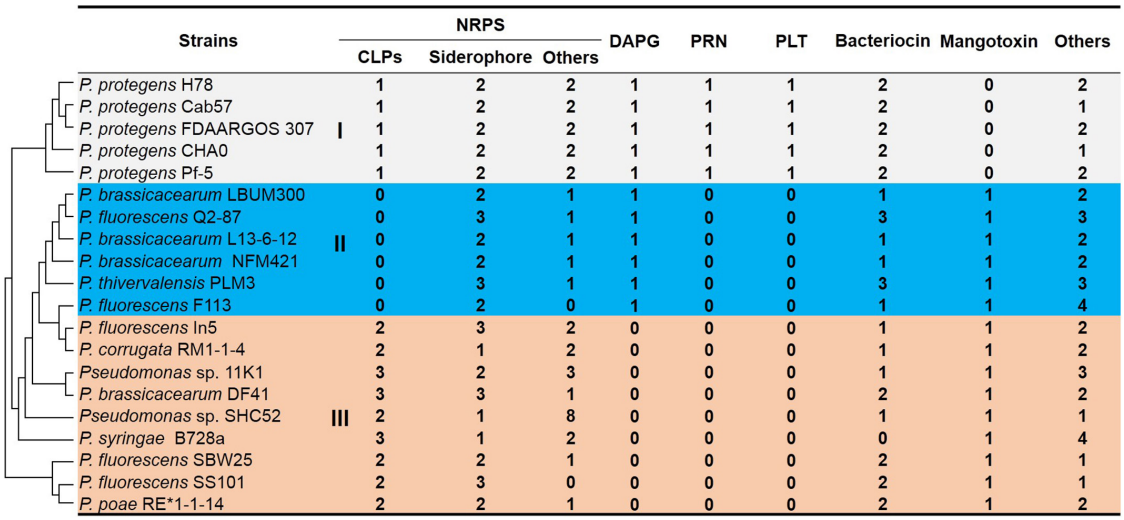

Strains		NRPS			DAPG	PRN	PLT	Bacteriocin	Mangotoxin	Others
		CLPs	Siderophore	Others						
P. protegens H78	I	1	2	2	1	1	1	2	0	2
P. protegens Cab57		1	2	2	1	1	1	2	0	1
P. protegens FDAARGOS 307		1	2	2	1	1	1	2	0	2
P. protegens CHA0		1	2	2	1	1	1	2	0	1
P. protegens Pf-5		1	2	2	1	1	1	2	0	2
P. brassicacearum LBUM300	II	0	2	1	1	0	0	1	1	2
P. fluorescens Q2-87		0	3	1	1	0	0	3	1	3
P. brassicacearum L13-6-12		0	2	1	1	0	0	1	1	2
P. brassicacearum NFM421		0	2	1	1	0	0	1	1	2
P. thivervalensis PLM3		0	3	1	1	0	0	3	1	3
P. fluorescens F113		0	2	0	1	0	0	1	1	4
P. fluorescens In5	III	2	3	2	0	0	0	1	1	2
P. corrugata RM1-1-4		2	1	2	0	0	0	1	1	2
Pseudomonas sp. 11K1		3	2	3	0	0	0	1	1	3
P. brassicacearum DF41		3	3	1	0	0	0	2	1	2
Pseudomonas sp. SHC52		2	1	8	0	0	0	1	1	1
P. syringae B728a		3	1	2	0	0	0	0	1	4
P. fluorescens SBW25		2	2	1	0	0	0	2	1	1
P. fluorescens SS101		2	3	0	0	0	0	2	1	1
P. poae RE*1-1-14		2	2	1	0	0	0	2	1	2

FIGURE 1 | *In silico* analysis and comparison of secondary metabolite production in *Pseudomonas* sp. 11K1 and strains of related species. Clusters accounting for biosynthesis of secondary metabolites were predicted by antiSMASH 4.0 using the "Extra Features" settings. Numbers represent the number of gene clusters within a genome. Abbreviations are as follows: CLPs, cyclic lipopeptides; DAPG, 2,4-diacetylphloroglucinol; PRN, pyrrolnitrin; PLT, pyoluteorin; NRPS, non-ribosomal peptide synthase. *Pseudomonas* strains were divided into groups I (gray), II (blue), and III (orange) based on profiles of secondary metabolites. Group I species produce all four antimicrobial compounds DAPG, PLT, PRN, and CLPs; *Pseudomonas* strains of Group II produce DAPG but not PLT, PRN, or CLPs; *Pseudomonas* strains of group III, including strain 11K1, produce CLPs but not DAPG, PLT, or PRN. The phylogenetic tree of 16S rDNA sequences (left) was constructed using the neighbor-joining method in MEGA version 5.0 after multiple sequence alignment by ClustalW.

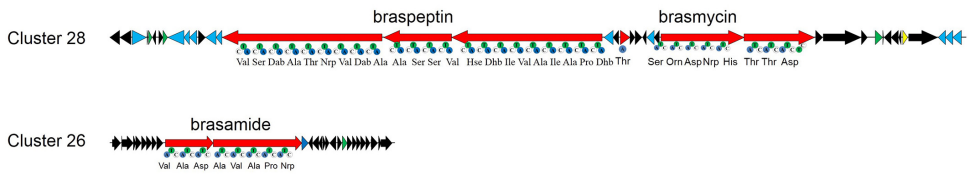

FIGURE 2 | The CLP gene clusters of *Pseudomonas* sp. 11K1. CLPs are synthesized by modular non-ribosomal peptide synthases (NRPSs), and each module contains an adenylation (A), condensation (C), and thiolation (T) domain. Red arrows indicate biosynthetic genes, blue arrows indicate transport-related genes, green arrows indicate regulatory genes, the yellow arrow indicates a predicted transposase, and other genes are indicated by black arrows.

activity against *X. oryzae* RS105 (**Figure 3B**), consistent with the above results obtained using insertional mutants, further confirming that CLPs were not the antibacterial compounds active against *X. oryzae* RS105.

Sequence-Based Structure Prediction of Brasmycin and Braspeptin

Bioinformatic analysis revealed that the predicted brasmycin BGC comprises nine modules, each of which consists of an adenylation (A), a thiolation (T), and a condensation (C) domain. Similar to nunamycin and syringomycin BGCs, the last module lacks the A domain, encoded by the first gene (**Figure 2**; Raaijmakers et al., 2006). The amino acid composition of CLPs could be predicated *in silico* based on A domain selectivity (Challis et al., 2000), and various A domain specificity features have been empirically determined (Röttig et al., 2011). We predicted the amino acid sequence of brasmycin based on a phylogenetic approach in which all A domains were compared with those of functionally characterized lipopeptides. The predicted brasmycin amino acid sequence was Ser-Orn-Asp-Nrp-His-Thr-Thr-Asp-Thr (**Figure 4A** and **Supplementary Figure S4**), which is most similar to thanamycin, although the fourth amino acid was uncertain. The predicted brasmycin sequence differs from nunamycin at amino acid 2 (Orn versus Dab), 3 (Asp versus Gly), and 5 (His versus Dab) and from syringomycin at amino acid 2 (Orn versus Ser), 3 (Asp versus Dab), 5 (His versus Arg), 6 (Thr versus Phe), and 7 (Thr versus Dhb) (**Figure 4A**), suggesting that brasmycin may represent a new member of the syringomycin group (Gross and Loper, 2009). These results are in agreement with a previous report showing that amino acids 2–7 of syringomycin group members are the most variable (Michelsen et al., 2015b).

The predicted amino acid sequence of braspeptin based on A domain phylogenetic analysis suggested that it belonged to the tolaasin group, but with differences from known members (**Figure 4B** and **Supplementary Figure S5**). Braspeptin shares conserved sites at amino acid 1 (Dhb), 2 (Pro), 5 (Ala), 13 (Ala),

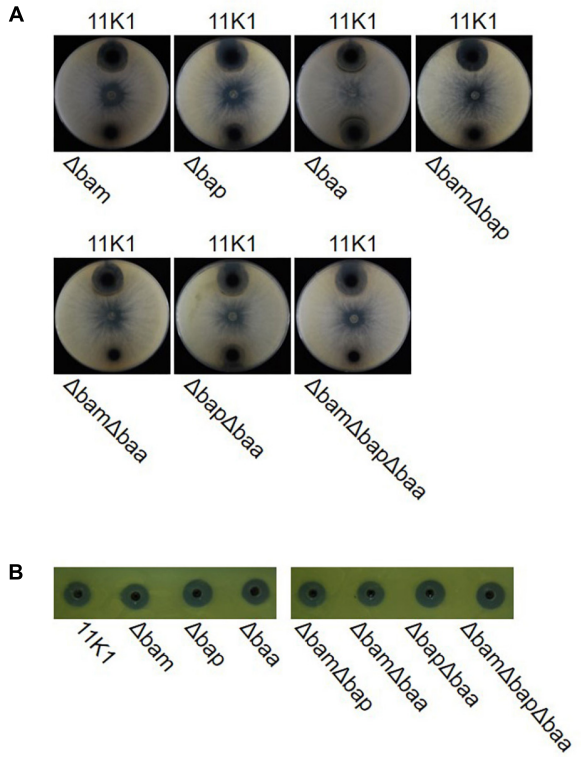

FIGURE 3 | (A) Antimicrobial activity of *Pseudomonas* sp. 11K1 and its mutants against *Botryosphaeria dothidea*, and **(B)** *Xanthomonas oryzae* RS105. *B. dothidea* disks (5 mm diameter) were placed in the center of each plate and 5 μL of an overnight culture of wild-type (WT) 11K1 or its mutants were inoculated near the edge of PDA medium plates. For antibacterial assays, 50 μL of sterile fermentation liquor was used to detect bacterial inhibition. Δbam, brasmycin gene cluster deletion mutant; Δbap, braspeptin gene cluster deletion mutant; Δbaa, brasamide gene cluster deletion mutant; ΔbamΔbap, brasmycin and braspeptin double gene cluster deletion mutant; ΔbamΔbaa, brasmycin and brasamide double gene cluster deletion mutant; ΔbapΔbaa, braspeptin and brasamide double gene cluster deletion mutant; ΔbamΔbapΔbaa, brasmycin, braspeptin, and brasamide triple gene cluster deletion mutant.

19 (Ala), and 20 (Dab) with corpeptin, nunapeptin, thanapeptin, and syringopeptin, but differs from corpeptin at amino acid 4 (Ile versus Ala), 7 (Ile versus Val), 11 (Ser versus Ile), 12 (Ser versus Dhp), 15 (Dab versus Ala), and 22 (Val versus Ile); it differs from nunapeptin at amino acid 4 (Ile versus Ala), 7 (Ile versus Ala), 9 (Hse versus Thr), 11 (Ser versus Ile), 12 (Ser versus Dhp), 15 (Dab versus Ala), and 22 (Val versus Ilx); it differs from thanapeptin at amino acid 4 (Ile versus Ala), 7 (Ile versus Val), 11 (Ser versus Ile), 12 (Ser versus Dhb), 15 (Dab versus Ala), and 22 (Val versus Ile); it differs from syringpeptin at amino acid 3 (Ala versus Val), 4 (Ile versus Val), 6 (Val versus Ala), 7 (Ile versus Val), 8 (Dhb versus Val), 9 (Hse versus Dhb), 10 (Val versus Ala), 11 (Ser versus Val), 12 (Ser versus Ala), 14 (Ala versus Dhb), 15 (Dab versus Thr), 16 (Val versus Ser), 18 (Thr versus Dhb), 21 (Ser versus Dab), and 22 (Val versus Tyr). Thus, although amino acid 17 remains uncertain (**Figure 4B**), braspeptin can be considered a new member of the tolaasin group.

Identification of CLPs in *Pseudomonas* sp. 11K1 Using MALDI-TOF MS

Lipopeptides from *Pseudomonas* sp. 11K1 contributing to its antibiosis activity were extracted, and analyzed using a Bruker UltrafleXtreme MALDI-TOF/TOF MS instrument to determine their molecular masses. In WT 11K1, two peaks were obtained at m/z 1,268.706 and 2,175.493 (**Figure 5A**), whereas only the m/z 2,175.493 peak was detected for the brasmycin gene cluster deletion mutant Δbam (**Figure 5B**), and only m/z 1,268.706 was detected in braspeptin gene cluster deletion mutant Δbap (**Figure 5C**). These results showed that the m/z 1,268.706 ion corresponds to the brasmycin lipopeptide, and the m/z 2,175.493 ion corresponds to the braspeptin lipopeptide. Molecular weights differ between brasmycin (m/z 1,268.706) and known syringomycin members nunamycin (m/z 1,138) (Michelsen et al., 2015a), thanamycin (m/z 1,291) (Van Der Voort et al., 2015), syringomycins (m/z 1,225, m/z 1,253) (Monti et al., 2011), and cormycin A (m/z 1274) (Scaloni et al., 2004). The molecular weight of braspeptin (m/z 2,175.493) is different from nunapeptins (m/z 2,023.22, m/z 2,037.24, and m/z 2,075.22) (Michelsen et al., 2015a), thanamycin (m/z 2,120.9) (Van Der Voort et al., 2015), syringopeptins (m/z 2,400, m/z 2,428) (Monti et al., 2011), corpeptins (m/z 2,095, m/z 2,121.2) (Licciardello et al., 2012; Strano et al., 2015), and sclerosis (m/z 2,095.3, m/z 2,123.3, m/z 2,145.3) (Berry et al., 2012). These results further confirm that brasmycin and braspeptin represent new members of the syringomycin and tolaasin lipopeptide groups, respectively.

Although it is currently impossible to accurately predict the fatty acid structures of brasmycin and braspeptin, we made a rough prediction based on molecular weights and predicted oligopeptide chains, in which uncertain amino acids were replaced with the most likely amino acids. The brasmycin might have a 12–15 carbon fatty acid tail (**Supplementary Figure S6**), and the fatty acid tail of braspeptin might contain 10–12 carbon atoms (**Supplementary Figure S7**).

Corroborating the results from dual-culture experiments (**Figure 3A**), crude peptides extracted from *Pseudomonas* sp. 11K1 containing both brasmycin and braspeptin, brasmycin extracted from mutant Δbap, and braspeptin extracted from mutant Δbam all inhibited mycelial growth of *B. dothidea* (**Figure 5D**).

Lipopeptides Affect Swarming Motility and Biofilm Formation in *Pseudomonas* sp. 11K1

Pseudomonas sp. 11K1 was able to swarm on soft KBG plates containing 0.6% agar. All three single lipopeptide gene cluster mutants Δbam, Δbap, and Δbaa exhibited reduced swarming motility to some degree, indicating that all three lipopeptides contribute to swarming motility (**Supplementary Figure S8**). However, double mutants ΔbamΔbap, ΔbamΔbaa, and ΔbapΔbaa, and triple mutant ΔbamΔbapΔbaa, did not further impair swarming motility (**Supplementary Figure S8**), indicating that lipopeptides were not the only surfactants contributing to swarming motility; other unknown surfactants were presumably produced under these conditions.

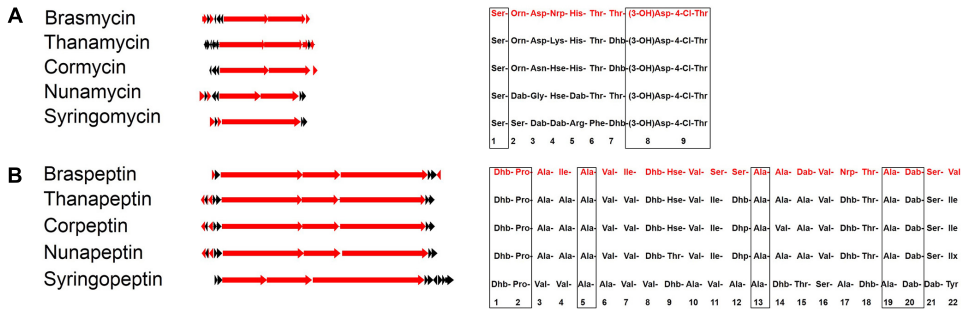

FIGURE 4 | Comparison of brasmycin **(A)** and braspeptin **(B)** gene clusters and the predicted amino acid sequences with those of similar CLPs. Red arrows indicate biosynthesis genes, while other genes are indicated by black arrows. Amino acid sequences of brasmycin and braspeptin (in red) were predicated based on A domain phylogenetic analysis. Cormycin and corpeptin from *P. corrugata* CFBP5454 (ATKI00000000), nunamycin and nunapeptin from *P. fluorescens* In5 (LIRD01000000), thanamycin and thanapeptin from *Pseudomonas* sp. SHC52 (CBLV000000000), syringomycin and syringopeptin from *P. syringae* pv. *syringae* B301D (CP005969). Consensus amino acids are denoted in boxes. Non-standard amino acids are abbreviated as follows: Dab, 2,4-diaminobutyric acid; Dhb, dehydrobutyrine; Dha, dehydroalanine; Orn, ornithine; Hse, homoserine, Nrp, uncertain amino acids.

Biofilm formation was tested in glass test tubes containing KGB liquid medium. Strain 11K1 formed a biofilm on the inner wall of tubes at the interface between air and liquid.

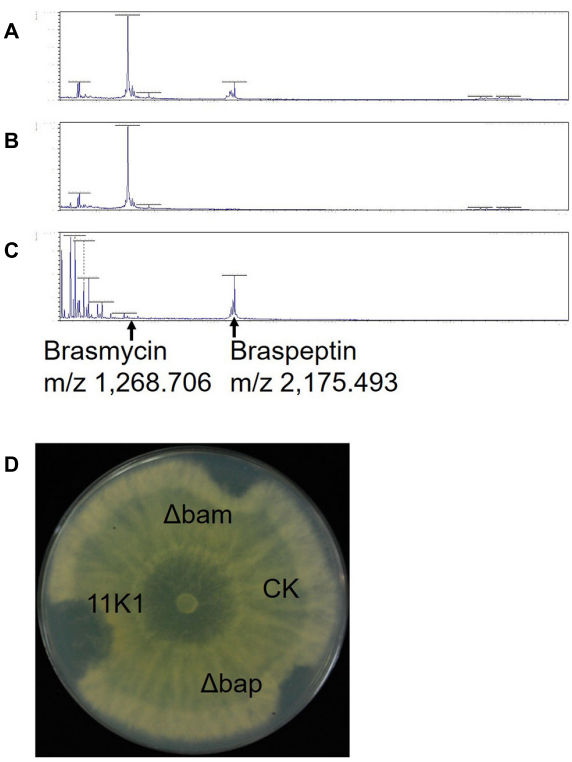

FIGURE 5 | MALDI-TOF MS analysis of CLPs extracted from **(A)** *Pseudomonas* sp. 11K1, **(B)** braspeptin gene cluster mutant Δbap, and **(C)** brasmycin gene cluster mutant Δbam. **(D)** Antifungal analysis of crude CLP extracts. Inhibition of *B. dothidea* mycelial growth by crude peptide extracts derived from *Pseudomonas* sp. 11K1 and its mutants was assessed. Extracts (20 μL) from 11K1, braspeptin gene cluster deletion mutant Δbap, and brasmycin gene cluster deletion mutant Δbam were spotted on agar plates. Methyl alcohol was applied as a control (CK).

The brasmycin gene cluster mutant Δbam formed markedly less biofilm, the braspeptin gene cluster mutant Δbap produced more biofilm than the WT 11K1 strain, and biofilm formation by mutant Δbaa was comparable to that of 11K1 (**Figure 6A**). Double and triple gene cluster mutants ΔbamΔbap, ΔbamΔbaa, and ΔbamΔbapΔbaa formed less biofilm, similar to brasmycin mutant Δbam, indicating that brasmycin was the most important lipopeptide involved in biofilm formation.

Mutation of lipopeptide biosynthesis gene clusters caused morphological changes of bacterial colonies on PDA plates. The WT 11K1 strain produced round colonies with a wrinkled surface, whereas all mutants containing brasmycin gene cluster mutations (Δbam, ΔbamΔbap, ΔbamΔbaa, and ΔbamΔbapΔbaa) formed smaller colonies with a smooth surface (**Figure 6B**). Mutant Δbaa formed typical WT colonies, whereas mutants Δbap and ΔbapΔbaa produced smaller colonies with a less wrinkled surface than WT colonies (**Figure 6B**).

DISCUSSION

Genome comparison of twenty *Pseudomonas* strains highlighted the tremendous diversity of gene sequences encoding secondary metabolites (**Figure 1**), suggesting strains from various environments encounter selective pressure, resulting in the acquisition or loss of gene clusters during evolution. The 20 *Pseudomonas* strains were clustered into three distinct groups according to secondary metabolite profiles. Compared to the vertical inheritance that is the process of genetic material from the parent to the offspring, horizontal genes transfer occurs between different species (Eisen, 2000). Group III is composed of different *Pseudomonas* species including *P. fluorescens*, *P. brassicacearum* and strain 11K1, all producing CLPs but not DAPG, PLT, or PRN. In contrast, *P. fluorescens* and *P. brassicacearum* in group II do not produce CLPs (**Figure 1**), indicating the horizontal transfer possibility of CLP biosynthesis gene clusters among *Pseudomonas* species. In addition, we found one transposase gene flanking the brasmycin and braspeptin

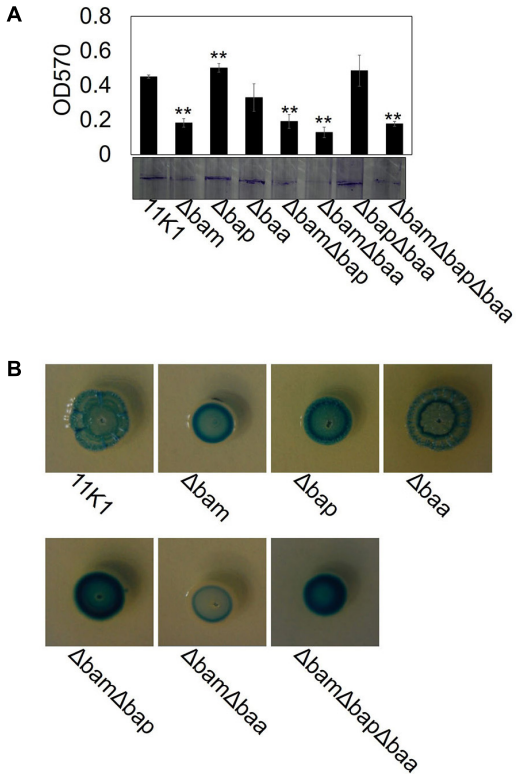

FIGURE 6 | Effects of CLP gene mutations on bacterial biofilm formation **(A)** and colony morphology **(B)**. **(A)** Spectrophotometric quantification of biofilms formed by *Pseudomonas* sp. 11K1 and CLP mutants. Mean values of three replicates are given, and error bars indicate standard error. Visual representation of biofilm formation by *Pseudomonas* sp. 11K1 and CLP mutants on tubes is shown. Biofilms were stained with Crystal Violet. **(B)** Colony morphology detected on PDA plates. A 5 μL sample of overnight culture of WT 11K1 or mutant strains was spot-inoculated in the center of a PDA plate and incubated for 48 h at 28°C. Δbam, brasmycin gene cluster deletion mutant; Δbap, braspeptin gene cluster deletion mutant; Δbaa, brasamide gene cluster deletion mutant; ΔbamΔbap, brasmycin and braspeptin double gene cluster deletion mutant; ΔbamΔbaa, brasmycin and brasamide double gene cluster deletion mutant; ΔbapΔbaa, braspeptin and brasamide double gene cluster deletion mutant; ΔbamΔbapΔbaa, brasmycin, braspeptin, and brasamide triple gene cluster deletion mutant.

synthetic gene cluster, which further indicates CLP gene clusters can be horizontally acquired (**Figure 2**).

The two active CLPs produced by strain 11K1 (brasmycin and braspeptin) belong to the syringomycin and tolaasin groups, respectively. CLPs in the syringomycin group consist of nine amino acids, including unusual amino acids (**Figure 4A**). All syringomycin group members possess antifungal ability (Sinden et al., 1971; Michelsen et al., 2015b; Trantas et al., 2015; Van Der Voort et al., 2015), and syringomycin is involved in the full virulence of *P. syringae* pv. *syringae* B301D, since syringomycin (*syrB1*) mutant was significantly reduced in virulence compared with its parental strain (Scholz-Schroeder et al., 2001). Compared with the syringomycin group, CLPs in the tolaasin group are much more diverse, both in the composition of the peptide chain, and in antimicrobial activities (**Figure 4B**). Syringopeptin and corpeptin display antifungal activity, but not antioomycete activity (Lavermicocca et al., 1997; Strano et al., 2015). By contrast, antifungal activity has not been observed for nunapeptin or thanapeptin, but these compounds inhibit oomycete growth (Michelsen et al., 2015b; Van Der Voort et al., 2015). Braspeptin, produced by 11K1, has antifungal activity, but no antioomycete activity (data not shown). Exactly why CLPs with similar composition exhibit different antimicrobial activities remains unclear. A possible explanation is that small structural changes in the peptide or lipid tail may affect their physicochemical properties and interactions with different types of cellular membranes (Kuiper et al., 2004; Raaijmakers et al., 2010).

Biosurfactants such as CLPs, rhamnolipids, and lipopolysaccharides are essential for bacterial swarming motility (Raaijmakers et al., 2006). Under suitable conditions, bacterial cells differentiate into hyperflagellated swarmers that are more motile on wet and viscous surfaces (Harshey, 2003). Biosurfactants produced by bacteria can change the viscosity of surfaces, thereby influencing cell differentiation and motility (McCarter and Silverman, 1990; Allison et al., 1993). Several studies showed that biosurfactants produced by pseudomonads and other bacteria can promote their surface motility. For example, orfamide and massetolide A are required as surfactants for the swarming ability of *Pseudomonas* strains CMR12a and SBW25, respectively, because swarming was completely abolished in CLP biosynthesis mutants (de Bruijn et al., 2007; D'Aes et al., 2014). Similarly, swarming of *P. aeruginosa* 57RP requires alkanoic acids that act as surfactants (Deziel et al., 2003). *Salmonella enterica* SJW1103 lipopolysaccharide biosynthesis gene mutants lose swarming motility (Toguchi et al., 2000). Our present study shows that the single lipopeptide gene cluster mutants Δbam, Δbap, and Δbaa in 11K1 display partly impaired swarming motility, indicating that all three lipopeptides contribute to swarming motility (**Supplementary Figure S8**). However, double mutants ΔbamΔbap, ΔbamΔbaa, and ΔbapΔbaa, and triple mutant ΔbamΔbapΔbaa, did not further impair swarming motility (**Supplementary Figure S8**), indicating that other biosurfactants contribute to the full swarming phenotype (**Supplementary Table S3**).

Cyclic lipopeptides play an important role in biofilm formation, although this can differ between CLP types. For example, a massetolide A-deficient mutant of *P. fluorescens* SBW25 forms less biofilm (de Bruijn et al., 2007), whereas a putisolvin-deficient mutant of *P. putida* PCL1445 displays enhanced biofilm formation (Kuiper et al., 2004). Orfamide has no effect on biofilm formation in *P. fluorescens* Pf-5 (Gross et al., 2007). In strain 11K1, the brasmycin gene cluster mutant Δbam formed markedly less biofilm, whereas the braspeptin gene cluster mutant Δbap produced more biofilm than the WT 11K1 strain (**Figure 6A**). The mechanisms by which CLPs affect biofilm formation remain unclear, but because CLPs play an important role in cell surface hydrophobicity, CLPs with different structures might differ in hydrophobicity, and their roles in biofilm formation could be entirely different (de Bruijn et al., 2008; Raaijmakers et al., 2010).

A tight correlation between wrinkled colony morphology and increased biofilm formation has been reported for various bacteria including *P. aeruginosa* PA14, *Burkholderia cenocepacia* H111, and *P. fluorescens* SBW25 (Spiers et al., 2003; Friedman and Kolter, 2004; Fazli et al., 2013), but there are exceptions. *B. subtilis* NCIB 3610 produces robust wrinkled colonies, but displays poor biofilm formation on glass surfaces, whereas *B. subtilis* JH642 readily forms biofilms on glass surfaces, but does not produce robust wrinkled colonies (Vlamakis et al., 2013). In the present work, both Δbam and Δbap mutants produce smooth surface colonies, but only Δbam forms less biofilm than the WT 11K1 strain, which produces wrinkled colonies (**Figure 6B**). Both biofilm formation and wrinkled colony morphology require exopolysaccharides, but the exopolysaccharides involved are not always the same (Fazli et al., 2014). Although acetylation of cellulose is essential for wrinkled colonies, it is not required for biofilm formation on tubes by *P. fluorescens* SBW25 (Spiers et al., 2003). Thus, the molecular relationship between biofilm formation and wrinkled colony morphology remains unclear.

The gene cluster of brasamide shares high similarity with some predicted CLP gene clusters in strains of the *P. fluorescens* group (**Supplementary Figure S9**), but the potential CLPs they encode have not yet been investigated. The predicted brasamide and its homologs contain eight amino acids with identical sequence, which are distinctly different from two known eight amino acid CLPs bananamide and pseudofactin (**Supplementary Figure S9B**; Janek et al., 2010; Nguyen et al., 2016). We cannot assign brasamide to any existing group because its chemical structure has not been experimentally resolved, but the distinctly different composition of predicted amino acids suggests that brasamide may belong to a new group of lipopeptides. Except for its contribution to bacterial swarming (**Supplementary Figure S6**), few information is available about its biological function. However, conserved distribution of brasamide-like CLPs in closely related pseudomonad strains strongly suggest that these CLPs fulfill an ecological function, which will be subject of future study.

DATA AVAILABILITY

This complete genome project has been deposited at GenBank under the accession numbers CP035088 (chromosome sequence) and CP035089 (plasmid sequence).

AUTHOR CONTRIBUTIONS

HZ and L-QZ designed the research. L-QZ supervised the study. Y-PL contributed to the MALDI-TOF MS. HZ performed the other experiments, analyzed the data, and wrote the manuscript together with L-QZ. All authors revised the manuscript and approved the final version for submission.

FUNDING

This work was supported by grants from Special Fund for Agro-scientific Research in the Public Interest (201503109), National Key Research and Development Program (2017YFD0201106), National Technology System for Grape Industry (CARS-29), and the National Natural Science Foundation of China (31572045 and 31872020).

SUPPLEMENTARY MATERIAL

The Supplementary Material for this article can be found online at: https://www.frontiersin.org/articles/10.3389/fmicb.2019.00544/full#supplementary-material

REFERENCES

Allison, C., Lai, H. C., Gygi, D., and Hughes, C. (1993). Cell differentiation of *Proteus mirabilis* is initiated by glutamine, a specific chemoattractant for swarming cells. *Mol. Microbiol.* 8, 53–60. doi: 10.1111/j.1365-2958.1993.tb01202.x

Bender, C. L., Rangaswamy, V., and Loper, J. (1999). Polyketide production by plant-associated Pseudomonads. *Annu. Rev. Phytopathol.* 37, 175–196. doi: 10.1146/annurev.phyto.37.1.175

Berry, C. L., Brassinga, A. K. C., Donald, L. J., Fernando, W. G. D., Loewen, P. C., and de Kievi, T. R. (2012). Chemical and biological characterization of sclerosin, an antifungal lipopeptide. *Can. J. Microbiol.* 58, 1027–1034. doi: 10.1139/w2012-079

Biniarz, P., Łukaszewicz, M., and Janek, T. (2016). Screening concepts, characterization and structural analysis of microbial-derived bioactive lipopeptides: a review. *Crit. Rev. Biotechnol.* 37, 393–410. doi: 10.3109/07388551.2016.1163324

Blin, K., Wolf, T., Chevrette, M. G., Lu, X., Schwalen, C. J., and Kautsar, S. A. (2017). AntiSMASH 4.0-improvements in chemistry prediction and gene cluster boundary identification. *Nucleic Acids Res.* 45, 36–41. doi: 10.1093/nar/gkx319

Challis, G. L., Ravel, J., and Townsend, C. A. (2000). Predictive, structure-based model of amino acid recognition by nonribosomal peptide synthetase adenylation domains. *Chem. Biol.* 7, 211–224. doi: 10.1016/S1074-5521(00)00091-0

Cochrane, S. A., Findlay, B., Bakhtiary, A., Acedo, J., Rodriguez-Lopez, E. M., Mercier, P., et al. (2016). Antimicrobial lipopeptide tridecaptin A1 selectively binds to Gram-negative lipid II. *Proc. Natl Acad. Sci.* 113, 11561–11566. doi: 10.1073/pnas.1608623113

D'Aes, J., Kieu, N. P., Léclère, V., Tokarski, C., Olorunleke, F. E., De Maeyer, K., et al. (2014). To settle or to move? The interplay between two classes of cyclic lipopeptides in the biocontrol strain *Pseudomonas* CMR12a. *Environ. Microbiol.* 16, 2282–2300. doi: 10.1111/1462-2920.12462

de Bruijn, I., de Kock, M., Yang, M., de Waard, P., van Beek, A., and Raaijmakers, J. M. (2007). Genome-based discovery, structure prediction and functional analysis of cyclic lipopeptide antibiotics in *Pseudomonas* species. *Mol. Microbiol.* 63, 417–428. doi: 10.1111/j.1365-2958.2006.05525.x

de Bruijn, I., de Kock, M. J., Waard, P., van Beek, T. A., and Raaijmakers, J. M. (2008). Massetolide A biosynthesis in *Pseudomonas fluorescens*. *J. Bacteriol.* 190, 2777–2789. doi: 10.1128/JB.01563-07

Deziel, E., Lepine, F., Milot, S., and Villemur, R. (2003). *rhlA* is required for the production of a novel biosurfactant promoting swarming motility in *Pseudomonas aeruginosa*: 3-(3-hydroxyalkanoyloxy) alkanoic acids (HAAs), the precursors of rhamnolipids. *Microbiology* 149, 2005–2013. doi: 10.1099/mic.0.26154-0

Eisen, J. A. (2000). Horizontal gene transfer among microbial genomes: new insights from complete genome analysis. *Curr. Opin. Gent. Dev.* 10, 606–611. doi: 10.1016/S0959-437X(00)00143-X

Fazli, M., Almblad, H., Rybtke, M. L., Givskov, M., Eberl, L., and Tolker-Nielsen, T. (2014). Regulation of biofilm formation in *Pseudomonas* and *Burkholderia* species. *Environ. Microbiol.* 16, 1961–1981. doi: 10.1111/1462-2920.12448

Fazli, M., McCarthy, Y., Givskov, M., Ryan, R., and Tolker-Nielsen, T. (2013). The exopolysaccharide gene cluster Bcam1330–Bcam1341 is involved in *Burkholderia cenocepacia* biofilm formation, and its expression is regulated by c-di-GMP and Bcam1349. *Microbiologyopen* 2, 105–122. doi: 10.1002/mbo3.61

Friedman, L., and Kolter, R. (2004). Genes involved in matrix formation in *Pseudomonas aeruginosa* PA14 biofilms. *Mol. Microbiol.* 51, 675–690. doi: 10.1046/j.1365-2958.2003.03877.x

Geudens, N., and Martins, J. C. (2018). Cyclic lipodepsipeptides from *Pseudomonas* spp. - biological swiss-army knives. *Front. Microbiol.* 9:1867. doi: 10.3389/fmicb.2018.01867

Gross, H., and Loper, J. E. (2009). Genomics of secondary metabolite production by *Pseudomonas* spp. *Nat. Prod. Rep.* 26, 1408–1446. doi: 10.1039/b817075b

Gross, H., Stockwell, V. O., Henkels, M. D., Nowak-Thompson, B., Loper, J. E., and Gerwick, W. H. (2007). The genomisotopic approach: a systematic method to isolate products of orphan biosynthetic gene clusters. *Chem. Biol.* 14, 53–63. doi: 10.1016/j.chembiol.2006.11.007

Harshey, R. M. (2003). Bacterial motility on a surface: many ways to a common goal. *Annu. Rev. Microbiol.* 57, 249–273. doi: 10.1146/annurev.micro.57.030502.091014

Hesse, C., Schulz, F., Bull, C. T., Elbourne, L. D. H., Yan, Q., Shapiro, N., et al. (2018). Genome-based evolutionary history of *Pseudomonas* spp. *Environ microbial.* 6, 2142–2159. doi: 10.1111/1462-2920.14130

Hover, B., Kim, S. H., Katz, M., Charlop-Powers, Z., Owen, J., Melinda, A., et al. (2018). Culture-independent discovery of the malacidins as calcium-dependent antibiotics with activity against multidrug-resistant Gram-positive pathogens. *Nat. Microbiol.* 3, 415–422. doi: 10.1038/s41564-018-0110-1

Huang, C., Pauwelyn, E., Ongena, M., Debois, D., Leclere, V., Jacques, P., et al. (2015). Characterization of Cichopeptins, new phytotoxic cyclic lipodepsipeptides produced by *Pseudomonas cichorii* SF1-54, and their role in bacterial midrib rot disease of lettuce. *Mol. Plant. Microbe Interact.* 28, 1109–1022. doi: 10.1094/MPMI-03-15-0061-R

Janek, T., Lukaszewicz, M., Rezanka, T., and Krasowska, A. (2010). Isolation and characterization of two new lipopeptide biosurfactants produced by *Pseudomonas* fluorescens BD5 isolated from water from the arctic archipelago of svalbard. *Bioresour. Technol.* 101, 6118–6123. doi: 10.1016/j.biortech.2010.02.109

Kuiper, I., Lagendijk, E. L., Pickford, R., Derrick, J., Lamers, G., Thomas-Oates, J., et al. (2004). Characterization of two *Pseudomonas putida* lipopeptide biosurfactants, putisolvin I and II, which inhibit biofilm formation and break down existing biofilms. *Mol. Microbiol.* 51, 97–113. doi: 10.1046/j.1365-2958.2003.03751.x

Lavermicocca, P., Iacobellis, N. S., and Simmaco, M. (1997). Biological properties and spectrum of activity of *Pseudomonas syringae* pv. *syringae toxins*. *Physiol. Mol. Plant* 50, 129–140. doi: 10.1006/pmpp.1996.0078

Licciardello, G., Strano, C. P., Bertani, I., Bella, P., Fiore, A., Fogliano, V., et al. (2012). N-acyl-homoserine-lactone quorum sensing in tomato phytopathogenic *Pseudomonas* spp. is involved in the regulation of lipodepsipeptide production. *J. Biotechnol.* 159, 274–282. doi: 10.1016/j.jbiotec.2011.07.036

Loper, J. E., Hassan, K. A., Mavrodi, D. V., Davis, E. W., Lim, C. K., Shaffer, B. T., et al. (2012). Comparative genomics of plant-associated *Pseudomonas* spp.: insights into diversity and inheritance of traits involved in multitrophic interactions. *PLoS Genet.* 8:e1002784. doi: 10.1371/journal.pgen.1002784

Masschelein, J., Jenner, M., and Challis, G. L. (2017). Antibiotics from Gram-negative bacteria: a comprehensive overview and selected biosynthetic highlights. *Nat. Pro. Rep.* 34, 712–783. doi: 10.1039/c7np00010c

McCarter, L., and Silverman, M. (1990). Surface-induced swarmer cell differentiation of *Vibrio parahaemolyticus*. *Mol. Microbiol.* 4, 1057–1062. doi: 10.1111/j.1365-2958.1990.tb00678.x

Michelsen, C. F., Jensen, H., Venditto, V. J., Hennessy, R. C., and Stougaard, P. (2015a). Bioactivities by a crude extract from the Greenlandic *Pseudomonas* sp. *In*5 involves the nonribosomal peptides, nunamycin and nunapeptin. *PeerJ* 3:e1476. doi: 10.7717/peerj.1476

Michelsen, C. F., Watrous, J., Glaring, M. A., Kersten, R., Koyamae, N., and Stougaarda, P. (2015b). Nonribosomal peptides, key biocontrol components for *Pseudomonas fluorescens* In5, isolated from a Greenlandic suppressive soil. *mBio* 6:e00079. doi: 10.1128/mBio.00079-15

Monti, S. M., Gallo, M., Ferracane, R., Borrelli, R. C., Ritieni, A., Greco, M. L., et al. (2011). Analysis of bacterial lipodepsipeptides by matrix-assisted laser desorption/ionisation time-of-flight and high-performance liquid chromatography with electrospray mass spectrometry. *Rapid Commun. Mass Spectrom.* 15, 623–628. doi: 10.1002/rcm.277

Nguyen, D. D., Melnik, A. V., Koyama, N., Lu, X. W., Schorn, M., Fang, J. S., et al. (2016). Indexing the *Pseudomonas* specialized metabolome enabled the discovery of poaeamide B and the bananamides. *Nat. Microbiol.* 2:16197. doi: 10.1038/NMICROBIOL.2016.197

Nikolouli, K., and Mossialos, D. (2012). Bioactive compounds synthesized by non-ribosomal peptide synthetases and type-I polyketide synthases discovered through genome-mining and metagenomics. *Biotechnol. lett.* 34, 1393–1403. doi: 10.1007/s10529-012-0919-2

Olorunleke, F. E., Kieu, N. P., De Waele, E., Timmerman, M., Ongena, M., and Höfte, M. (2017). Coregulation of the cyclic lipopeptides orfamide and sessilin in the biocontrol strain *Pseudomonas* sp. *CMR*12a. *Microbiologyopen* 6:e00499. doi: 10.1002/mbo3.499

Raaijmakers, J. M., de Bruijn, I., and de Kock, M. J. (2006). Cyclic lipopeptide production by plant-associated *Pseudomonas* spp.: diversity, activity, biosynthesis, and regulation. *Mol. Plant. Microbe. Interact.* 19, 699–710. doi: 10.1094/MPMI-19-0699

Raaijmakers, J. M., de Bruijn, I., Nybroe, O., and Ongena, M. (2010). Natural functions of lipopeptides from *Bacillus* and *Pseudomonas*: more than surfactants and antibiotics. *FEMS Microbiol. Rev.* 34, 1037–1062. doi: 10.1111/j.1574-6976.2010.00221.x

Raaijmakers, J. M., Vlami, M., and De Souza, J. T. (2002). Antibiotic production by bacterial biocontrol agents. *Antonie Van Leeuwenhoek* 81, 537–547. doi: 10.1023/A:1020501420831

Röttig, M., Medema, M. H., Blin, K., Weber, T., Rausch, C., and Kohlbacher, O. (2011). NRPSpredictor2-a web server for predicting NRPS adenylation domain specificity. *Nucleic Acids Res.* 39, 362–367. doi: 10.1093/nar/gkr323

Scaloni, A., Dalla Serra, M., Amodeo, P., Mannina, L., Vitale, R. M., Segre, A. L., et al. (2004). Structure, conformation and biological activity of a novel lipodepsipeptide from *Pseudomonas corrugata*: cormycin A1. *Biochem. J.* 384, 25–36. doi: 10.1042/BJ20040422

Schneider, T., Gries, K., Josten, M., Wiedemann, I., Pelzer, S., Labischinski, H., et al. (2009). The lipopeptide antibiotic friulimicin B inhibits cell wall biosynthesis through complex formation with bactoprenol phosphate. *Antimicrob. Agents Chemother.* 53, 1610–1618. doi: 10.1128/AAC.01040-08

Scholz-Schroeder, B. K., Hutchison, M. L., Grgurina, I., and Gross, D. (2001). The contribution of syringopeptin and syringomycin to virulence of *Pseudomonas syringae* pv. *syringae* strain B301D on the basis of sypA and syrB1 biosynthesis mutant analysis. *Mol. Plant Microbe. Interact.* 14, 336–348. doi: 10.1094/MPMI.2001.14.3.336

Sinden, S. L., De Vay, J. E., and Backman, P. A. (1971). Properties of syringomycin, a wide spectrum antibiotic and phytotoxin produced by *Pseudomonas syringae*, and its role in the bacterial canker disease of peach trees. *Physiol. Plant Pathol.* 1, 199–200. doi: 10.1016/0048-4059(71)90029-4

Spiers, A. J., Bohannon, J., Gehrig, S. M., and Rainey, P. (2003). Biofilm formation at the air-liquid interface by the *Pseudomonas fluorescens* SBW25 wrinkly spreader requires an acetylated form of cellulose. *Mol. Microbiol.* 50, 15–27. doi: 10.1046/j.1365-2958.2003.03670.x

Strano, C. P., Bella, P., Licciardello, G., Lo Piero, A. R., Fogliano, V., Venturi, V., et al. (2015). Pseudomonas corrugata *crpCDE* is part of the cyclic lipopeptide corpeptin biosynthetic gene cluster and is involved in bacterial virulence in tomato and in hypersensitive response in *Nicotiana benthamiana*. *Mol. Plant Pathol.* 16, 495–506. doi: 10.1111/mpp.12207

Straus, S. K., and Hancock, R. E. W. (2006). Mode of action of the new antibiotic for Gram-positive pathogens daptomycin: comparison with cationic antimicrobial peptides and lipopeptides. *Biochim. Biophys. Acta* 1758, 1215–1223. doi: 10.1016/j.bbamem.2006.02.009

Thoma, S., and Schobert, M. (2009). An improved *Escherichia coli* donor strain for diparental mating. *FEMS Microbiol. Lett.* 294, 127–132. doi: 10.1111/j.1574-6968.2009.01556.x

Toguchi, A., Siano, M., Burkkart, M., and Harshey, R. (2000). Genetics of swarming motility in *Salmonella enterica* serovar typhimurium: critical role for lipopolysaccharide. *J. Bacteriol.* 182, 6308–6321. doi: 10.1128/JB.182.22.6308-6321.2000

Trantas, E. A., Licciardello, G., Nalvo, F., Almeida, N., Witek, K., Strano, C., et al. (2015). Comparative genomic analysis of multiple strains of two unusual plant pathogens: *Pseudomonas corrugata* and *Pseudomonas mediterranea*. *Front. Microbiol.* 6:811. doi: 10.3389/fmicb.2015.00811

Van Der Voort, M., Meijer, H., Schmidt, Y., Watrous, G., Dekkers, E., Mendes, E., et al. (2015). Genome mining and metabolic profiling of the rhizosphere bacterium *Pseudomonas* sp. *SH-C*52 for antimicrobial compounds. *Front. Microbiol.* 6:693. doi: 10.3389/fmicb.2015.00693

Vlamakis, H., Chai, Y., Beauregard, P., Losick, R., and Kolter, R. (2013). Sticking together: building a biofilm the *Bacillus subtilis* way. *Nat. Rev. Microbiol.* 11, 157–168. doi: 10.1038/nrmicro2960

Weller, D. M. (2007). *Pseudomonas* biocontrol agents of soilborne pathogens: looking back over 30 years. *Phytopathology* 97, 250–256. doi: 10.1094/phyto-97-2-0250

Yan, X., Yang, R., Zhao, R. X., Han, J. T., Jia, W. J., Li, D. Y., et al. (2017). Transcriptional regulator PhlH modulates 2, 4-Diacetylphloroglucinol biosynthesis in response to the biosynthetic intermediate and end product. *Appl. Environ. Microbiol.* 83:e1419-17. doi: 10.1128/AEM.01419-17

Conflict of Interest Statement: The authors declare that the research was conducted in the absence of any commercial or financial relationships that could be construed as a potential conflict of interest.

frontiers in Microbiology

ORIGINAL RESEARCH
published: 15 March 2019
doi: 10.3389/fmicb.2019.00484

Characterization of Subtilin L-Q11, a Novel Class I Bacteriocin Synthesized by *Bacillus subtilis* L-Q11 Isolated From Orchard Soil

Yuxuan Qin[1,2], Yao Wang[1], Yinghao He[2], Ying Zhang[1], Qianxuan She[2], Yunrong Chai[2], Pinglan Li[1] and Qingmao Shang[3]**

[1] Beijing Advanced Innovation Center for Food Nutrition and Human Health, College of Food Science and Nutritional Engineering, Key Laboratory of Functional Dairy, China Agricultural University, Beijing, China, [2] Department of Biology, Northeastern University, Boston, MA, United States, [3] Key Laboratory of Biology and Genetic Improvement of Horticultural Crops, The Institute of Vegetables and Flowers, Chinese Academy of Agricultural Sciences, Beijing, China

OPEN ACCESS

Edited by:
Ana R. Freitas, Universidade do Porto, Portugal

Reviewed by:
Ana P. Tedim, Neiker Tecnalia, Spain
Dzung B. Diep, Norwegian University of Life Sciences, Norway

***Correspondence:**
Pinglan Li
lipinglan@cau.edu.cn
Qingmao Shang
shangqingmao@caas.cn

Specialty section:
This article was submitted to Antimicrobials, Resistance and Chemotherapy, a section of the journal Frontiers in Microbiology

Received: *03 December 2018*
Accepted: *25 February 2019*
Published: *15 March 2019*

Citation:
Qin Y, Wang Y, He Y, Zhang Y, She Q, Chai Y, Li P and Shang Q (2019) Characterization of Subtilin L-Q11, a Novel Class I Bacteriocin Synthesized by Bacillus subtilis L-Q11 Isolated From Orchard Soil. Front. Microbiol. 10:484. doi: 10.3389/fmicb.2019.00484

Bacteriocins are peptides or proteins synthesized by bacterial ribosomes that show killing or inhibitory activities against different groups of bacteria. Bacteriocins are considered potential alternatives to traditional antibiotics, preservatives in pharmaceutical and food industries. A strain L-Q11 isolated from orchard soil was phylogenetically characterized as *Bacillus subtilis* based on 16S rRNA gene sequencing analysis. A novel class I bacteriocin (Subtilin L-Q11), was identified and purified from L-Q11 cell-free supernatant in a four-step procedure, including salt precipitation, cation exchange, gel filtration, and reverse-phase high-performance liquid chromatography (RP-HPLC). The molecular mass (3,552.9 Da) of this novel bacteriocin was determined by Matrix-assisted laser desorption/ionization time-of-flight mass spectrometry (MALDI-TOF-MS). The purified Subtilin L-Q11 exhibited optimal features in pH tolerance, thermostability, and sensitivity to proteases. Further, Subtilin L-Q11 showed inhibitory activities against a number of bacteria including some human pathogens and food spoilage bacteria, in particular *Staphylococcus aureus.* All these important features make this novel bacteriocin a potential candidate for the development of a new antibacterial drug or food preservative in the future.

Keywords: Subtilin L-Q11, *Bacillus subtilis*, bacteriocin, antibacterial activity, antibacterial mechanism

INTRODUCTION

Bacillus subtilis is a Gram-positive, spore-forming soil bacterium, which is known to produce more than twenty different, structurally diverse antimicrobial compounds (Stein, 2005). The majority of these compounds are peptide-based antibiotics. There are two principal synthetic pathways for biosynthesis of peptide-based antibiotics in *B. subtilis*: (i) non-ribosomal synthesis of peptides by non-ribosomal peptide synthetases (NRPSs), and (ii) ribosomally synthesized antimicrobial peptides (Giessen and Marahiel, 2012).

Bacteriocins are ribosomally synthesized peptide antibiotics, which show antagonistic activities toward different bacteria, especially to those that are genetically close to the producing strains

(Klaenhammer, 1988). Bacteriocins are often employed as a weapon by the producing bacteria to compete and protect themselves in the natural environment. In the food industry, bacteriocins produced by lactic acid bacteria have long been applied in food preservation (Tagg et al., 1976). Bacteriocins also demonstrate great potentials as antimicrobial compounds in pharmaceutical, agricultural, and biochemical engineering industries (Dischinger et al., 2014). Bacteriocins have become more popular in recent years due to their therapeutic effects in treating bacterial infection, even against certain multidrug resistant bacteria (Garneau et al., 2002; Cotter et al., 2005). Furthermore, compared to chemically synthesized traditional antibiotics or food preservatives, bacteriocins present low toxicity toward human hosts because human cells do not possess a receptor recognized by bacteriocins (Kanmani et al., 2013; Yang et al., 2014). Bacteriocins were originally only found to be synthesized by *Lactobacillus*. It is now believed that more than 99% of bacteria can produce at least one type of bacteriocins, however, the majority of them are yet to be identified (Riley and Wertz, 2002).

An average of 4 and 5% of the *B. subtilis* genome is believed to be involved in the biosynthesis of various antimicrobial compounds (Stein, 2005). Thus, species from the *Bacillus* genus represent a great pool for screen and discovery of novel bacteriocins (Phelan et al., 2013). Based on distinct structural and functional characteristics, bacteriocins can be divided into different classes. Class I bacteriocins are also named lantibiotics. Most of the bacteriocins produced by *Bacillus* species belong to the class I bacteriocins (Singh et al., 2012).

In this study, we purified and characterized Subtilin L-Q11, a novel class I bacteriocin from *B. subtilis* L-Q11, a strain isolated from the orchard soil in Beijing, China. We demonstrated that this new bacteriocin has great potential to be used as a biologically synthesized antibiotic or food preservative in agricultural field and food industry. We also investigated the mode of action of this novel bacteriocin against the bacterial pathogen *S. aureus* ATCC 29213.

MATERIALS AND METHODS

Bacterial Strains and Growth Conditions

The spore-forming strain L-Q11 is a bacteriocin-producing bacterium isolated from the orchard soil in Beijing, China. Briefly, in order to isolate the spore-forming bacteria from natural environment. Soil samples from orchard was heated to kill non-spore-forming mesophiles, and then plated on rich media after dilution by sterilized water and incubated aerobically at 30°C. Thermophiles would not grow at this temperature, and anaerobic spore-formers (e.g., *Clostridium*) will not grow aerobically. Other mesophilic aerobic endospore-formers (e.g., *Heliospirillum*) are phototrophic, scarce, and require lots of light for growth.

Bacillus subtilis was grown in Luria-Bertani (LB) broth at 37°C under the shaking condition (200 rpm). *Staphylococcus aureus* 29213 was used as an indicator strain for antibacterial activities of the Subtilin L-Q11 and it was also cultured in LB broth at 37°C.

Phylogenetic Characterization of the Strain L-Q11

The bacteriocin-producing *B. subtilis* strain was phylogenetically identified by 16S rRNA gene sequencing analysis. Briefly, the genomic DNA of L-Q11 was prepared by using a bacterial genomic extraction kit (TianGen, Beijing, China) according to the manufacturer's instructions. A region in the 16s rRNA gene was amplified by PCR using two universal primers (27F: 5′-AGAGTTTGATCMTGGCTCAG-3′ and 1492R: 5′-TACGGYTACCTTGTTACGACTT-3′) (Lane, 1991). Thermal cycling consisted of initial denaturation at 95°C for 10 min, followed by 30 cycles of denaturation at 95°C for 30 s, annealing at 50°C for 1 min, and elongation at 72°C for 1 min, and finally, at 72°C for 10 min for completion. The PCR product was sent for sequencing after purification using GeneJET Gel Extraction Kit (QIAGEN, Germany). The sequencing result was blasted against the NCBI GenBank database[1]. If the similarity of the 16s rRNA gene sequence of this strain valued >97% when compared with a certain species, we considered that this strain belonged to this species.

Crude Bacteriocin Preparation and Antibacterial Activity Assay

Bacillus subtilis L-Q11 was inoculated in 50 mL of LB broth and grown overnight, 1% of the overnight culture was re-inoculated into 1 L of LB broth and incubated at 37°C under the shaking condition at 200 rpm. Samples were collected every 4 h to record the medium pH and cell optical density ($O.D._{600}$). Meanwhile, cell-free supernatant (CFS) from each time point was used to test the antibacterial activity against an indicator strain (*S. aureus* ATCC 29213). Briefly, we centrifuged the culture samples at 12,000 rpm for 15 min at 4°C to remove the cell pellets. The supernatant was filter-sterilized by passing through the Nalgene^{TM} Rapid-Flow^{TM} Sterile Disposable Filter (0.22 μm, Thermo Fisher Scientific, MA, United States) to obtain the CFS. The antibacterial activity of the crude bacteriocin in the CFS was determined by measuring the diameter of the inhibition zone with vernier caliper using *S. aureus* ATCC 29213 as an indicator strain. The antibacterial activity was presented as an arbitrary unit per milliliter of culture medium (AU/mL) and one AU was defined as the reciprocal of the highest 2-fold dilution exhibiting a clear zone of inhibition of the indicator strain (Deraz et al., 2005).

Purification of Subtilin L-Q11

CFS was first mixed with 70% (w/v) ammonium sulfate at 4°C overnight under the continuous stirring and then centrifuged at 9,000 *g* for 20 min at 4°C. After that, the precipitation was collected and dissolved in 10 mL of PBS buffer (pH 7.0). The crude extract obtained after ammonium sulfate precipitation was applied onto the CM Sepharose Fast Flow cation-exchange column (16 mm × 200 mm, GE, Sweden) equilibrated and washed with 50 mM PBS (pH 6.0) linked to AKTA purifier 100 system (GE, Sweden). The elution was

[1]http://www.ncbi.nlm.nih.gov/BLAST

carried out by a linear gradient (from 0 to 1 M of NaCl) in the same buffer as equilibration for 60 min at a flow rate of 1 mL/min and monitored by an UV detector at the wavelength of 280 nm.

The active fractions obtained from the last step of purification were loaded onto a Sephadex G-10 (12 mm × 200 mm, GE, Sweden) column equilibrated with PBS buffer (pH 6.0) and connected to an AKTA purifier 100 system (GE, Sweden). The elution was carried out at the flow rate of 0.5 mL/min and recorded by UV at the wavelength of 280 nm by the same buffer.

The active fractions from above were applied onto a reverse phase high-performance liquid chromatography (RP-HPLC) system (Agilent, CA, United States) equipped with C18 reverse-phase column (5 μm, 4.6 mm × 250 mm, Agilent, United States) for further purification. The elution was performed using 5–95% linear gradient of acetonitrile containing 0.1% trifloroacetic acid (TFA) with a flow rate of 1 mL/min for 30 min and monitored by UV at the wavelength of 280 nm.

The collected fractions were concentrated and tested for antibacterial activities as described by An et al. (2017), and then stored at −80°C. The BCA kit (Thermo Fisher Scientific, MA, United States) was used for the protein concentration analysis.

Molecular Weight and Amino Acid Sequence Determination

The molecular mass of the bacteriocin in the active fractions obtained after the HPLC purification were determined by matrix-assisted laser desorption ionization–time-of-flight (MALDI-TOF) mass spectrometry (MS) (Applied Biosystems, Foster city, CA, United States) in the positive mode. The active fraction was mixed together with the same volume of matrix solution contained 0.1% (v/v) of α-cyano-4-hydroxycinnamic acid (CHCA, Sigma, United States) dissolved in trifluoroacetic acid and 50% (v/v) of acetonitrile. For the MALDI analysis, 1 μl of the mixture was deposited directly onto the MALDI plate for drying. For identifying N-terminal amino sequence of Sublitin L-Q11, the purified Sublitin L-Q11 electrophoresed by SDS-PAGE was transferred to PVDF membrane (Millipore, United States). Residue amino sequence identified by Edman degradation was then compared with other published bacteriocin sequences by NCBI blast.

Antimicrobial Spectrum Assay

To investigate the antimicrobial spectrum of Subtilin L-Q11, partially purified Subtilin L-Q11 preparation from cation exchange chromatography was adjusted to pH 6.0 by using 1 M NaOH, and the spectrum of antibacterial activity was determined against a series of food-borne and food-spoilage pathogens (**Table 1**) by using the pour plate method described by An et al. (2017).

Determination of Physicochemical Characteristics of Subtilin L-Q11

To evaluate the physicochemical characteristics of Subtilin L-Q11, proteolytic, thermal, pH, and surfactant sensitivities of the bacteriocin were tested. To test the proteolytic sensitivity of Subtilin L-Q11, different types of proteases including Pepsin (pH 3.0), Papain (pH 6.5), Proteinase K (pH 7.5), Trypsin (pH 7.6), and Chymotrypsin (pH 7.8), were incubated with the bacteriocin at a final concentration of 1 mg/mL for 3 h. After incubation, the mixture was heated to 100°C for 5 min to terminate the enzymatic reaction. To test its thermal sensitivity, Subtilin L-Q11 was heated to 60, 80, and 100°C, respectively, for 15 and 30 min, and 121°C for 20 min. The pH tolerance of the bacteriocin was measured by adjusting the pH of the buffer to a range of 2–11 using 5 M NaOH or HCl for 2 h. Various chemical reagents, including 1% (v/v) of ethylene diamine tetraacetic acid (EDTA), Tween 20, Tween 80, and urea were incubated with the bacteriocin for 5 h at 37°C to determine its tolerance to the chemical reagents.

After each treatment from above, the antibacterial activity of the residual bacteriocin was measured and compared to the untreated bacteriocin to estimate the loss of the bacteriocin after each of the above treatments.

TABLE 1 | Antibacterial spectrum of Subtilin L-Q11.

Indictor strain	Source	Diameter of inhibition zone (mm)
Gram-positive bacteria		
Bacillus amyloliquefaciens ATCC 15841	ATCC	16.2 ± 0.2
B. amyloliquefaciens L-S60	Qin et al., 2015b	16.1 ± 0.3
B. amyloliquefaciens L-H15	Qin et al., 2015a	16.0 ± 0.3
B. cereus ATCC 14579	ATCC	16.4 ± 0.2
Lactococcus lactis NZ9000	Linares et al., 2010	9.4 ± 0.2
L. lactis MG1363	Linares et al., 2010	9.1 ± 0.3
Lactobacillus plantarum S-35	Wang et al., 2018	10.3 ± 0.2
L. plantarum γ-35	Wang et al., 2018	11.0 ± 0.3
Staphylococcus aureus ATCC 29213	ATCC	16.4 ± 0.4
S. aureus ATCC 43300	ATCC	16.3 ± 0.4
S. aureus ATCC 26112	ATCC	16.1 ± 0.4
Enterococcus faecalis ATCC 29212	ATCC	16.2 ± 0.4
E. faecalis ATCC 51299	ATCC	8.2 ± 0.2
E. faecalis M2	Wang et al., 2018	6.3 ± 0.5
Gram-negative bacteria		
Escherichia coli DH5α	Takara	0
E. coli BL21	Takara	0
E. coli BW25113	Grenier et al., 2014	0
E. coli JM109	Takara	0
Fungi		
Saccharomyce cerevisiae	Wang et al., 2018	0
Pichia pastoris GS115	Thermo Fisher Scientific	0

Antibacterial Activity of Subtilin L-Q11 Against *S. aureus*

In order to determine the action mode of Subtilin L-Q11, *S. aureus* ATCC 29213 was cultured overnight in TSB broth (BD Biosciences, United States) at 37°C with shaking (200 rpm). Cells were spun down and readjusted to a final density of

10^7 CFU/mL by using 0.9% sterile NaCl. The final concentration of the bacteriocin was adjusted to 64 μg/mL (MIC_{50} of Subtilin L-Q11 against *S. aureus* ATCC 29213) and the sample with the same amount of TSB broth was used as a control. All the samples for the test were incubated at 37°C under shaking (200 rpm) for 5 h. The cell optical density ($O.D._{600}$) and the number of viable cells were measured every hour (Deraz et al., 2007).

Scanning and Transmission Electron Microscopy

In order to observe the morphological changes of *S. aureus* ATCC 29213 cells after treated with Subtilin L-Q11, scanning electron microscopy (SEM) was used. *S. aureus* ATCC 29213 cells (1×10^7 CFU/ml) in LB broth were mixed with 256 μg/mL ($4 \times MIC_{50}$) of Subtilin L-Q11 and incubated at 37°C for 1, 2, and 3 h, respectively. Cells without bacteriocin treatment were set as a control. Cells in both the bacteriocin treatment and control groups were collected by centrifugation and washed with phosphate buffer (0.1 M, pH 7.0). Cells for SEM observation were fixed for 4 h in 2.5% glutaraldehyde at 4°C and then dehydrated with gradient ethanol solutions (30, 50, 80, 90, and 100%). After that, ethanol was replaced by 100% tertiary butyl ethanol. Cells were then freeze-dried (Wheeler et al., 1975), coated with gold, and imaged using a FEI Quanta 200 SEM.

For observation of intracellular differences between cells in the Subtilin L-Q11 treatment and control groups, transmission electron microscopy was performed as previously described (Yamanaka et al., 2005) with minor modifications. Briefly, cells were fixed as described above. After that, samples for imaging were osmicated in 2% osmium tetroxide at 4°C for 4 h, and then were dehydrated with gradient ethanol solutions as described above. Embedding was performed in epoxy resin at 60°C for 48 h. The sections were then coated with an amorphous carbon film and stained with 2% uranyl acetate and lead citrate. Ultrastructure observation and photomicrographs were then carried out using a JEM-1200EX TEM (Japan Electronics Co., Ltd., Japan).

Statistical Analysis

Data in this study were presented as means ± standard deviations (SD). One-way analysis of variance (ANOVA) and Duncan's multiple range test of the data were carried out by SPSS 23.0, and $p < 0.05$ was considered statistically significant. All the experiments were preformed in triplicate.

RESULTS

Phylogenetic Characterization of the Strain L-Q11

We performed BLAST search using the DNA sequence of the 16S rRNA gene of L-Q11 as a query against the NCBI GenBank database. Our result indicated that the 16S rRNA gene sequence of L-Q11 showed extremely high similarity (identity ≥ 99%, E value = 0) to *B. subtilis*. We finally classified the strain L-Q11 as *B. subtilis*.

Dynamic Production of the Antibiotic Against *S. aureus* by *B. subtilis* L-Q11

The dynamic profile of antibiotic production by *B. subtilis* L-Q11 during growth was investigated when cells were cultured in LB broth under the shaking condition (200 rpm) at 37°C. The inhibitory activity of the CFS against growth of the indicator strain *S. aureus* ATCC 29213 was used as a measurement of antibiotic production. The growth profile of L-Q11 showed that the culture transitioned to early exponential phase 2 h after inoculation, entered stationary phase at 8 h and remained in stationary phase until end of the experiment (**Figure 1**). The antibacterial activity in the CFS against *S. aureus* ATCC 29213 was evaluated by measuring the diameter of the inhibition zone. The bacteriocin begun to be produced after cells entered early stationary phase (8 h) and reached maximum at 20 h. Although the antibacterial capacity in the CFS produced by L-Q11 begun to decrease after 20 h, it showed inhibitory activity during the entire stationary phase (**Figure 1**). The pH of the broth was also measured once every 4 h during the entire experiment. We found that the pH of the medium dropped from 7.0 to 5.2 during the exponential phase and then went back to almost 7.0 (**Figure 1**). The observed pH changes in the medium indicate that the metabolic capacity of this strain meets the basic requirement of industrial fermentation.

Purified Bacteriocin From L-Q11 Showed Strong Bacterial Inhibitory Activity

The CFS collected after 20 h of incubation under the shaking condition was used for bacteriocin extraction and purification by a four-step procedure as described in the Methods. The yield and characteristics of the bacteriocin after each purification step were shown in **Table 2**. The crude bacteriocin in the CFS was first extracted by ammonium sulfate precipitation and approximately 2-fold enrichment of the bacteriocin was achieved at this stage as measured by the inhibitory activity against *S. aureus* ATCC 29213 (**Table 2**). For further purification the crude bacteriocin was subjected to a SP-Sepharose Fast Flow cation exchange column. Five main peaks were obtained and separated into five different fractions at this stage. We then tested all five fractions and found that only fraction 5 showed antibacterial activity (**Figures 2Aa,b**). In addition, we achieved 41-fold enrichment after this step; the antibacterial activity of bacteriocin increased from 1,500 to 37,000 AU/mg against the indicator strain. Next, the active fraction (fraction 5) was injected into a Sephadex G-10 gel-filtration chromatography for the subsequent purification step. During this step, two separate peaks were observed by measuring the absorbance at the wavelength of 220 nm. However, only fraction 1 retained the antibacterial activity (**Figures 2Ba,b**). Meanwhile, the bacteriocin activity increased 80-fold after this purification step. RP-HPLC was applied in the final purification step of the bacteriocin. The corresponding fraction to this peak showed a strong antibacterial activity against *S. aureus* ATCC 29213 (**Figures 2Ca,b**). In summary, after series of purification steps, the antibacterial activity of the bacteriocin

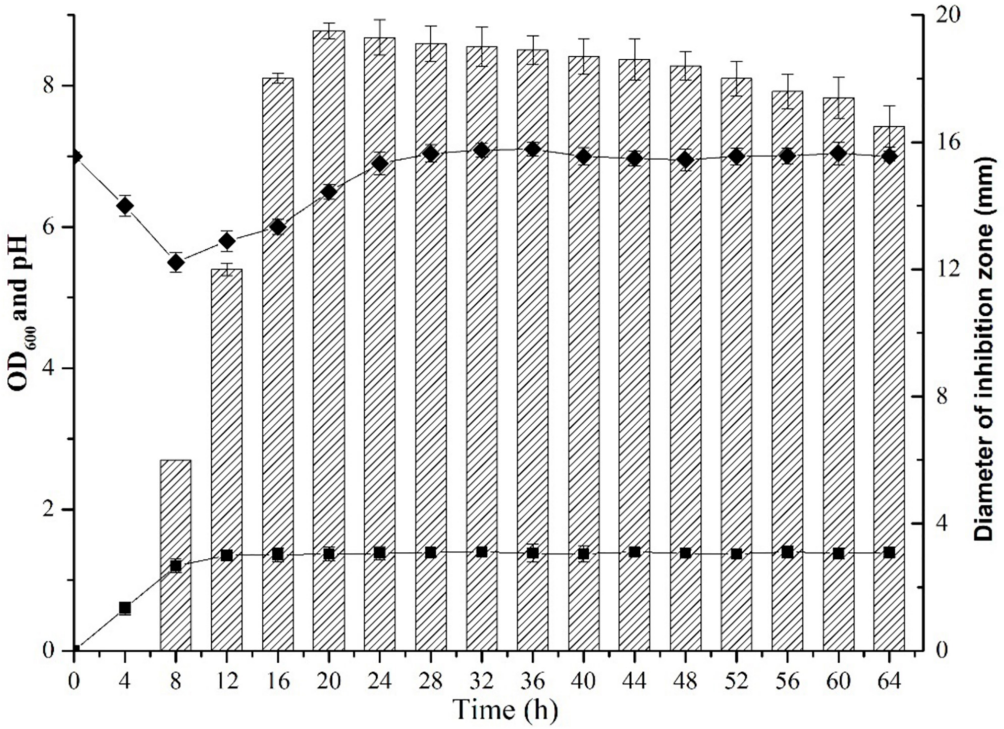

FIGURE 1 | Growth and dynamics of bacteriocin production by *B. subtilis* L-Q11. "♦" represents the growth curve of L-Q11; "■" represents values of pH in the culture medium; "▨" represents inhibitory activity against the indicator strain *S. aureus* ATCC 29213.

TABLE 2 | Purification of the bacteriocin produced by L-Q11.

Purification Stage	Volume (mL)	Total protein (mg)	Total activity (AU)	Specific activity (AU/mg)	Purification fold	Recovery (%)
Culture supernatant	200	1156	1,024,000	885	1	100
Ammonium sulfate precipitation	20	531	820,000	1,500	2	80
SP-sepharose fast flow	5	17	612,000	37,000	41	35
Sephadex G10	1	4	313,000	71,000	80	13
RP-HPLC	0.3	1	104,000	104,000	117	2

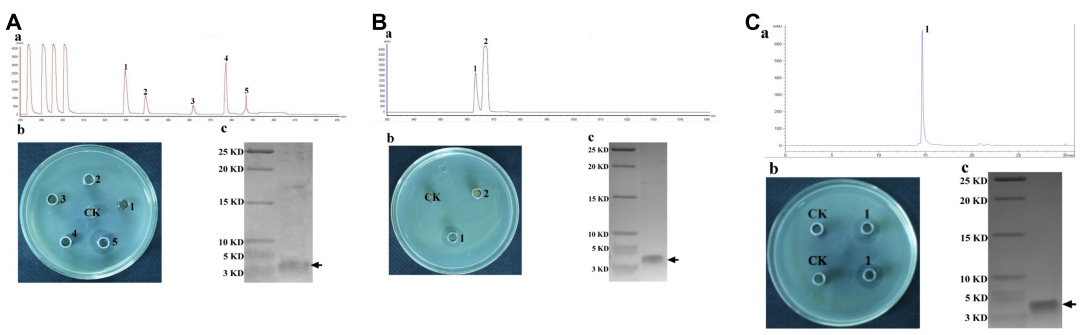

FIGURE 2 | Purification of Subtilin L-Q11 by chromatography. **(A)** cation exchange column; **(B)** gel filtration chromatography; **(C)** RP-HPLC. **(a)** process of purification; **(b)** the assay of antibacterial activity against the indicator strain from the absorbance peaks versus CK (control) by agar well diffusion assay; **(c)** Tricine-SDS-PAGE of the purified active fraction. The arrows indicate the active fraction after each step of purification on Tricine-SDS-PAGE gel.

increased 117-fold compared to that in the initial CFS, reaching 104,000 AU/mg.

Molecular Mass and Amino Acid Sequence Determination

The molecular mass of the purified bacteriocin produced by *B. subtilis* L-Q11 is 3,552.9 Da as determined by MALDI-TOF MS (**Figure 3A**). The molecular mass of the bacteriocin produced by *B. subtilis* L-Q11 is different from any of the published bacteriocins. According to the genome sequence analysis of *B. subtilis* L-Q11, the entire amino acid sequence of the bacteriocin was MSKFDDFDLDVV KVSKQDSKITPQWKSESVCTPGCVTGILQTCFLQSITCNCRL SK. Aligned with published bacteriocins from *Bacillus* spp. (Barbosa et al., 2015), bacteriocin produced by *B. subtilis* L-Q11 showed highly similarity to class I bacteriocin but was not identical (**Figure 3B**). We thus believe that it is a novel Class I bacteriocin and named it Subtilin L-Q11.

Subtilin L-Q11 Showed a Broad Range of Antibacterial Activities

Subtilin L-Q11 showed a wide range of an antibacterial spectrum (**Table 1**). It could inhibit the growth of various Gram-positive bacteria including *Bacillus amyloliquefaciens*, *Lactococcus lactis*, *Lactobacillus plantarum*, *Staphylococcus aureus*, and *Enterococcus faecalis*. Some of them are important spoilage bacteria in food industry and human pathogens, such as *S. aureus* ATCC 29213 and species from *Bacillus* genus. However, it showed no inhibitory activity on any of the tested Gram-negative bacteria and fungi (**Table 1**).

Subtilin L-Q11 Demonstrated Desirable Thermostability, pH Tolerance, Resistance to Chemical Reagents, and Sensitivity to Proteases

We next tested several physicochemical characteristics of Subtilin L-Q11, including thermostability, pH tolerance, resistance to chemical reagents, and sensitivity to proteases. In thermostability test, more than 97% of the bacterial inhibitory activity was retained after 15 or 30 min of heat treatment at 60 or 80°C, respectively. Further, the activity was decreased significantly ($p < 0.05$) when under the treatments of 100°C for 15 and 30 min, or at 121°C for 20 min, but there was still more than 54% of activity retained (**Figure 4A**). Subtilin L-Q11 retained more than 90% of the antimicrobial activity in buffers with the pH ranged from 2 to 7. Although in the buffer of pH 8–10, the antimicrobial activity of Subtilin L-11 decreased significantly ($p < 0.05$), it still showed some activity at pH 10 (27.83%) (**Figure 4B**). We also tested the impact of several detergents on the activity of the bacteriocin. We found that Subtilin L-Q11 showed great tolerant character after 3 h treatment by 1% (V/V) of Tween-20, Tween-80, Urea and EDTA. It still retained 97.9, 97.2, 95.9 and 98.3% of the activities after treated by above detergents, respectively, (**Figure 4C**). The activity of the bacteriocin from L-Q11 was

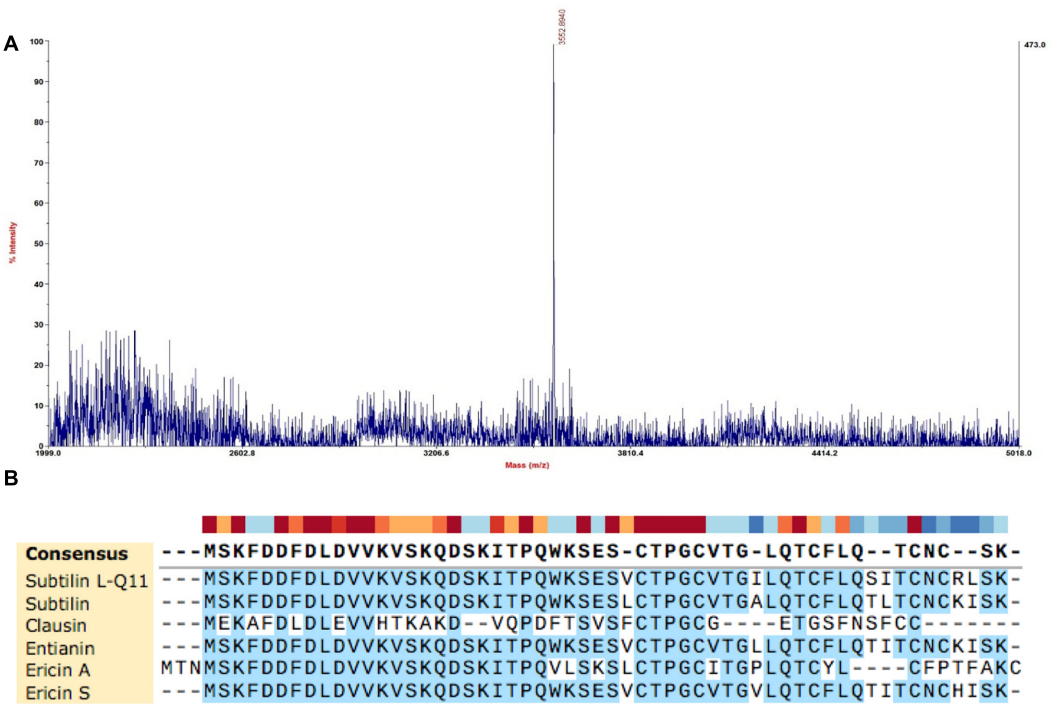

FIGURE 3 | Molecular mass determination and amino acid sequence alignment of Subtilin L-Q11. **(A)** The mass spectrum shown corresponded to the absorbance peak after purification using RP-HPLC in **Figure 2C**. **(B)** Alignment of published class I bacteriocins from *Bacillus* spp. and Subtilin L-Q11. Alignments were obtained by SnapGene V4.2.6 with default settings.

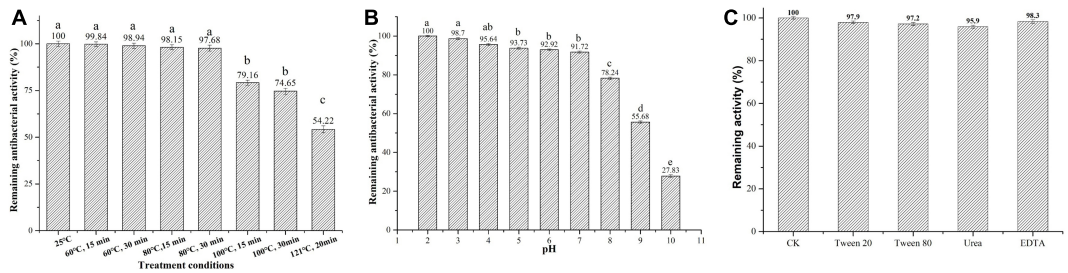

FIGURE 4 | Subtilin L-Q11 demonstrated optimal thermostability, pH tolerance, and resistance to chemical reagents. The effects of pH **(A)**, temperature **(B)** and surfactant **(C)** on the bacteriocin activity produced by L-Q11 were assayed. Relative ratios in percentages were applied to represent retained antibacterial activities of the bacteriocin samples after various treatments when compared to the untreated control group. "abcde" indicates the significant difference among different conditions, the same letter represents no significant differences among those groups and different letters represents significant differences ($p < 0.05$) among those groups.

totally lost after treatment by any of the three important human digestive proteases, trypsin, chymotrypsin, and pepsin. Also, the commonly used proteinase K could completely eliminate the activity of bacteriocin.

Subtilin L-Q11 Induced Serious Morphological and Intracellular Changes in *S. aureus* Cells

We were interested in better understanding the inhibitory mechanism of Subtilin L-Q11 against *S. aureus* ATCC 29213. Upon treatment of Subtilin L-Q11 for 3 h, the viable number of *S. aureus* ATCC 29213 cells dropped from 8 to 6 [log (cfu/mL)] and the optical density of the culture decreased from 1 to 0.25 ($O.D._{600}$) (**Figure 5**). This implies that Subtilin L-Q11 induced cell lysis in *S. aureus* ATCC 29213.

To demonstrate in detail, the potential morphological and intracellular changes in *S. aureus* ATCC 29213 cells upon cell lysis caused by Subtilin L-Q11, Scanning Electron Microscope (SEM) and Transmission Electron Microscope were used. Morphological changes in *S. aureus* ATCC 29213 cells were shown in **Figure 6**. Compared to the regular shape and smooth surface of cells in the control group (**Figure 6A**), *S. aureus* ATCC 29213 cells treated with 256 μg/mL ($4 \times MIC_{50}$)

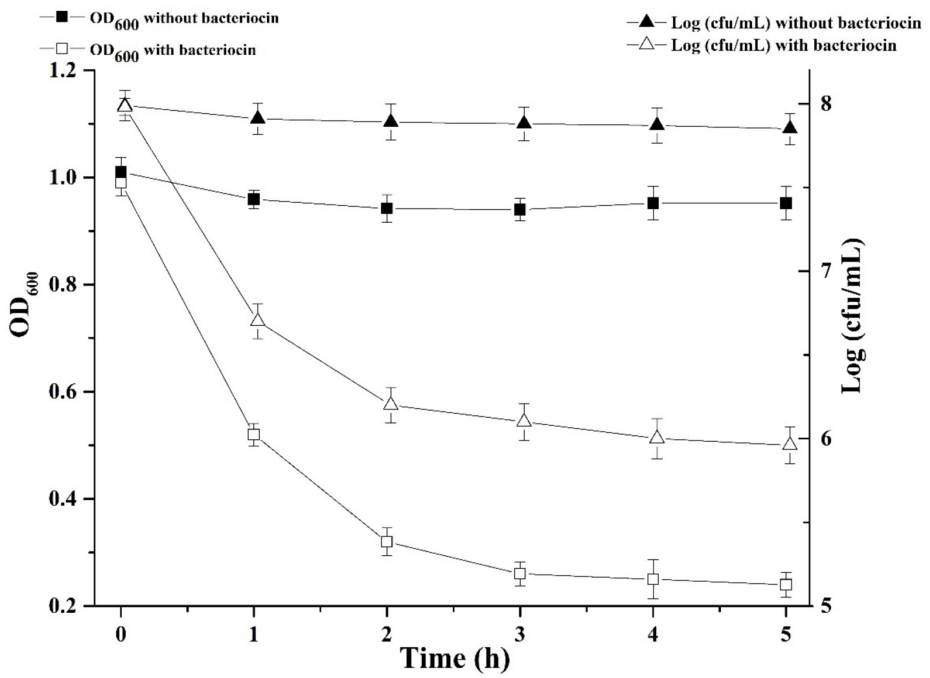

FIGURE 5 | Subtilin L-Q11 treatment triggered cell lysis in *S. aureus*. "▲" represents viable cell count of untreated *S. aureus* ATCC 29213; "△" represents viable cell count of *S. aureus* ATCC 29213 with the treatment of bacteriocin; "■" represents cell optical density at the wavelength of 600 nm ($O.D._{600}$) without bacteriocin treatment; "□" represents optical density at the wavelength of 600 nm with bacteriocin treatment.

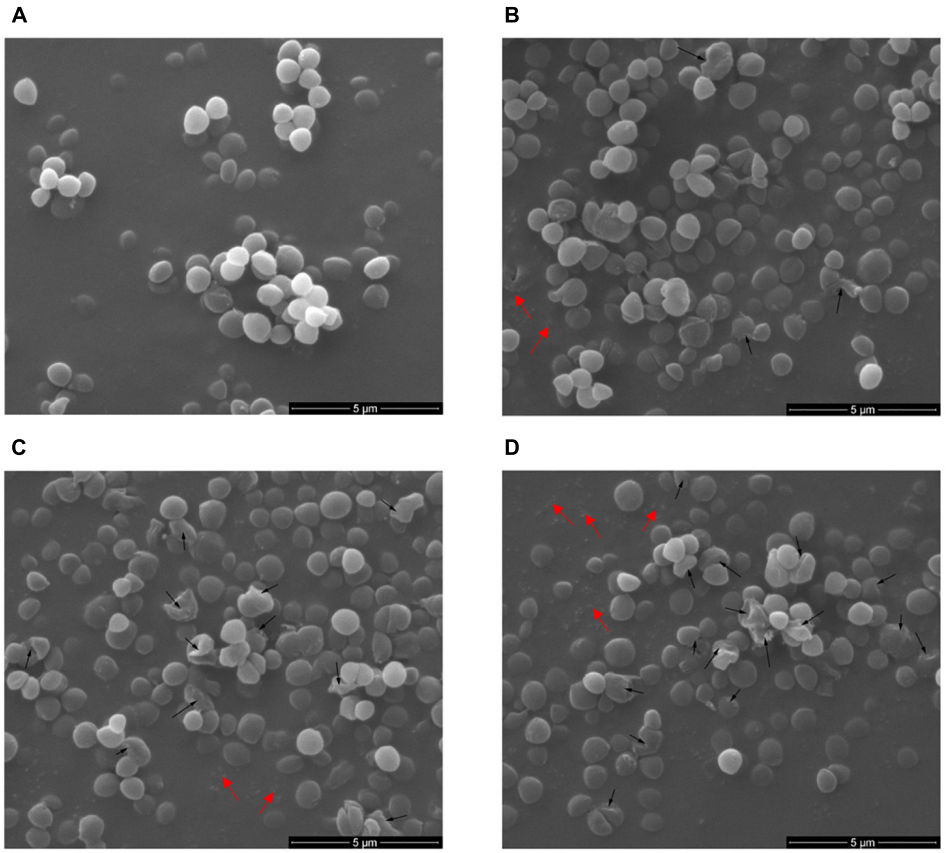

FIGURE 6 | Scanning electron microscopy of *S. aureus* cells treated by Subtilin L-Q11. **(A)** *S. aureus* ATCC 29213 cells from the untreated control group; **(B–D)** *S. aureus* ATCC 29213 cells treated with 256 μg/mL (4 × MIC_{50}) of Subtilin L-Q11 for 1, 2, and 3 h, respectively. Scale bars: 500 nm. Black arrows: the cell hollowness and membrane disruption; red arrows: cell fragments. For the sample preparation of TEM and SME, cell cultures were concentrated by centrifuging. During the sample preparation, large amount of the lysed cell (cell fragments) would lost.

Subtilin L-Q11 for 1 h showed slight hollowness on the surface (black arrows, **Figure 6B**). After exposed to the bacteriocin for 2 to 3 h (**Figures 6C,D**), the surface of cells showed more serious hollowness and clear membrane disruption (black arrows). Also fragments of lysed cell were seen in **Figures 6B–D** (red arrows). Moreover, the bacteriocin-induced deformation of *S. aureus* ATCC 29213 cells happened in a time-related manner.

The intracellular changes of *S. aureus* ATCC 29213 cells treated with Subtilin L-Q11 were observed by TEM. Under TEM, cells in the untreated control group showed features characterized as typical cell wall, and intact and smooth cell membrane (**Figure 7A**). Also, the biomass and the seemingly genomic DNA were evenly distributed in the cytoplasm. In contrast, after exposure to 256 μg/mL (4 × MIC_{50}) Subtilin L-Q11 for 1 h, the intracellular organization of cells was significantly disrupted, showing condensation of genomic DNA and vacuolization (**Figure 7B**). Moreover, the cytoplasm began to leak slightly (arrow 2 in **Figure 7B**). When the exposure time was prolonged to 2 h, although the entire cell structure was still largely retained, the seriously disrupted cell membrane was clearly visible as shown in **Figure 7C**. Also, loss of cytoplasm could be observed in the cells of the treatment group, and the leaked biomass from the cytoplasm could be observed around cell (arrow 1 in **Figure 7C**). After 3 h of treatment by the bacteriocin, the cytoplasm of the treated cells showed a lower density compared to that of the cells in control group, probably due to the loss of solutes (**Figure 7D**). Also, a discontinuity and ruptured cell membrane surface of treated cells was shown (arrow 3 in **Figure 7D**). This indicates that these cells were already lysed. All these observations showed that Subtilin L-Q11 induced serious disruption of the intracellular organization of *S. aureus* ATCC 29213 cells.

DISCUSSION

In this study, we reported a novel bacteriocin, Subtilin L-Q11, synthesized by *B. subtilis* L-Q11 isolated from orchard soil that demonstrated great biophysical characteristics, which makes it a potential candidate as both an antibacterial compound and a food preservative. A four-step procedure consisting of ammonium sulfate precipitation, SP-sepharose Fast Flow, Sephadex G10 and RP-HPLC, was used for the

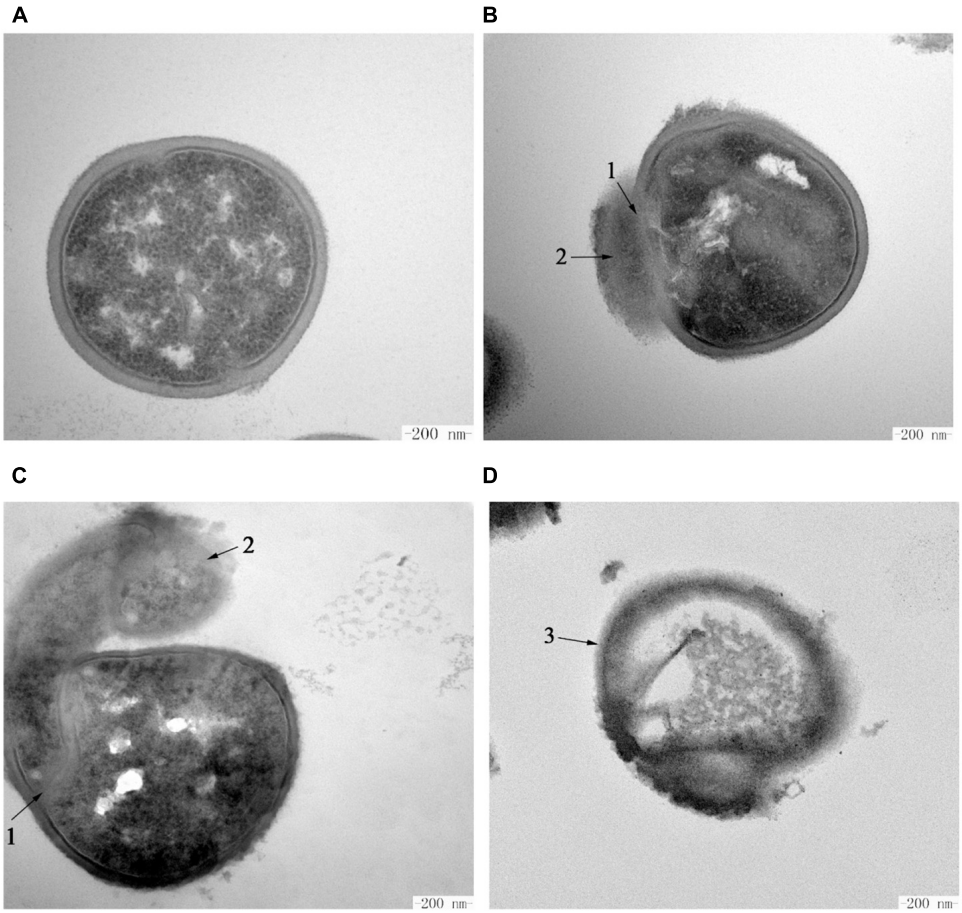

FIGURE 7 | Transmission electron microscopy of *S. aureus* cells treated by Subtilin L-Q11. **(A)** *S. aureus* ATCC 29213 cells from the untreated control group; **(B–D)** *S. aureus* ATCC 29213 cells treated with 256 μg/mL (4 × MIC_{50}) of Subtilin L-Q11 for 1, 2, and 3 h, respectively. Scale bars: 200 nm. Arrows numbered 1: the damaged cell membrane. Arrows numbered 2: the leaked intracellular substance. The arrow numbered 3: the ruptured cells.

purification of the bacteriocin. Subtilin L-Q11 retained strong antibacterial activity after purification. According to the genome sequence analysis, the entire amino acid sequence of the Subtilin L-Q11 was determined as MSKFDDFDLDVVKVSKQDSKITPQWKSESVCTPGCVTGILQ TCFLQSITCNCRLSK. The amino acid sequence is similar, but not identical, to the reported Class I bacteriocins (Barbosa et al., 2015). The molecular mass of the purified bacteriocin is 3,552.9 Da, determined by MS. This is different from other known bacteriocins, such as Sentianin (MW = 3446.6 Da) (Fuchs et al., 2011),Ericin S (MW = 3342.8 Da),Ericin A (MW = 2987.7 Da) (Stein et al., 2002), Clausin (MW = 2107.5 Da) (Bressollier et al., 2014), subtilomycin (MW = 3235 Da) (Phelan et al., 2013), Thuricin 4A-4 (MW = 2786.3 Da), and Thuricin 4A-4D (MW = 2886.3 Da) (Xin et al., 2015). We thus believe that the Subtilin L-Q11 produced by L-Q11 is a novel Class I bacteriocin.

For the food industry, pasteurization and high temperature sterilization are the two commonly used strategies for sterilization (Zhao et al., 2016). The thermostability of Subtilin L-Q11 was tested under the conditions of both pasteurization and high temperature sterilization. Our results showed that after treatment it could preserve more than 96 and 58% of the antibacterial activity, respectively, compared to the untreated. Therefore, our newly reported bacteriocin showed great utilization potential in the food industry, especially in the dairy industry. This bacteriocin also showed tolerance to a broad range of pH changes (pH 2.0–9.0), which makes it an excellent food preservative candidate in both acid and alkaline food processing procedures. We also found that the activity of the bacteriocin could be completely destroyed by human digestive enzymes, such as pepsin, trypsin, and chymotrypsin. In other words, the bacteriocin can be decomposed *in vivo* and is thus safe to human health (Hu et al., 2013). Nevertheless, more *in vivo* toxicity experiments should be carried out in the future to confirm the biosafety of the bacteriocin.

We showed that the amount of the important human opportunistic pathogen and food contaminating bacterium *S. aureus* ATCC 29213 decreased 100-fold from 10^8 to 10^6 cfu/mL after 3 h treatment by Subtilin L-Q11. The molecular mechanism of the killing of *S. aureus* ATCC 29213 by this new bacteriocin remains unknown. Some of the previously published results

showed that one of the major killing mechanisms by some Class I bacteriocins is the disruption of the membrane integrity. Those bacteriocins may cause tiny pores on the bacterial cell membrane (Ennahar et al., 2000; Perez et al., 2014). To further investigate the antibacterial mechanism of Subtilin L-Q11, SEM and TEM were used to show the impacts of Subtilin L-Q11 on the ultra cell structures of *S. aureus* ATCC 29213. The TEM results showed that the intracellular organization of *S. aureus* ATCC 29213 cells upon bacteriocin treatment was seriously damaged, which likely led to cell death (**Figure 7**). Under SEM, we observed relatively modest changes in *S. aureus* ATCC 29213 cell morphology (**Figure 6**). Cell membrane damage and leak of biomass from the cytoplasm were clearly observed in bacteriocin treated *S. aureus* ATCC 29213 cells; some cells were even partially lysed. Our observations were also consistent to those previously observed by other bacteriocins. For example, similar cytoplasm damages were reported in nisin and pediocin treated bacteria cells (Kalchayanand et al., 2004; Pattanayaiying et al., 2014). Since membrane damage caused by the pore-forming compounds would lead to severe membrane permeability and leak of the biomass, imbalance of inner and outer membrane (Liu et al., 2017), we believe that the antibacterial mode of action of Subtilin L-Q11 can be further investigated by measuring bacterial membrane potential, intracellular ATP levels, and electric conductivity before and after treatment. Meanwhile, the transcriptomic and proteomic data may also help us to reveal the antibacterial mechanism at the global transcriptional and translational levels. These are ongoing investigations currently in the lab.

CONCLUSION

In conclusion, Subtilin L-Q11 not only can inhibit the growth of different types of food-borne pathogens but also show great biophysical characteristics such as thermostability, pH-tolerance, resistance to chemical reagents, and sensitivity to various human proteases. Our results suggest that Subtilin L-Q11 has great potential in both the food industry and the agricultural field, as a new biological food preservative and an antibacterial drug.

DATA AVAILABILITY

The datasets generated for this study can be found in Genbank, MK156679.

AUTHOR CONTRIBUTIONS

YQ, QMS, and PL designed the experiments. YQ, YW, YH, YZ, and QXS performed the experiments. YQ and YW analyzed the results. YQ and YC wrote the manuscript.

FUNDING

This work was supported by the Special Fund for Agro-scientific Research in the Public Interest of China (201303014) and a scholarship to YQ from the China Scholarship Council (file No. 201606350112).

REFERENCES

An, Y., Wang, Y., Liang, X. Y., Yi, H. X., Zuo, Z. H., Xu, X. X., et al. (2017). Purification and partial characterization of M1-UVs300, a novel bacteriocin produced by *Lactobacillus plantarum* isolated from fermented sausage. *Food Control* 81, 211–217. doi: 10.1016/j.foodcont.2017.05.030

Barbosa, J., Caetano, T., and Mendo, S. (2015). Class I and Class II lanthipeptides produced by *Bacillus* spp. *J. Nat. Prod.* 78, 2850–2866. doi: 10.1021/np500424y

Bressollier, P., Brugo, M. A., Robineau, P., Schmitter, J. M., Sofeir, M., Urdaci, M. C., et al. (2014). "Peptide compound with biological activity, its preparation and its applications". Google Patents.

Cotter, P. D., Hill, C., and Ross, R. P. (2005). Bacterial lantibiotics: strategies to improve therapeutic potential. *Curr. Protein Pept. Sci.* 6, 61–75. doi: 10.2174/1389203053027584

Deraz, S. F., Karlsson, E. N., Hedstrom, M., Andersson, M. M., and Mattiasson, B. (2005). Purification and characterisation of acidocin D20079, a bacteriocin produced by *Lactobacillus acidophilus* DSM 20079. *J. Biotechnol.* 117, 343–354. doi: 10.1016/j.jbiotec.2005.02.005

Deraz, S. F., Karlsson, E. N., Khalil, A. A., and Mattiasson, B. (2007). Mode of action of acidocin D20079, a bacteriocin produced by the potential probiotic strain, *Lactobacillus acidophilus* DSM 20079. *J. Ind. Microbiol. Biotechnol.* 34, 373–379. doi: 10.1007/s10295-007-0206-8

Dischinger, J., Chipalu, S. B., and Bierbaum, G. (2014). Lantibiotics: promising candidates for future applications in health care. *Int. J. Med. Microbiol.* 304, 51–62. doi: 10.1016/j.ijmm.2013.09.003

Ennahar, S., Sashihara, T., Sonomoto, K., and Ishizaki, A. (2000). Class IIa bacteriocins: biosynthesis, structure and activity. *FEMS Microbiol. Rev.* 24, 85–106. doi: 10.1111/j.1574-6976.2000.tb00534.x

Fuchs, S. W., Jaskolla, T. W., Bochmann, S., Kotter, P., Wichelhaus, T., Karas, M., et al. (2011). Entianin, a novel subtilin-like lantibiotic from *Bacillus subtilis* subsp. *spizizenii* DSM 15029T with high antimicrobial activity. *Appl. Environ. Microbiol.* 77, 1698–1707. doi: 10.1128/AEM.01962-10

Garneau, S., Martin, N. I., and Vederas, J. C. (2002). Two-peptide bacteriocins produced by lactic acid bacteria. *Biochimie* 84, 577–592. doi: 10.1016/S0300-9084(02)01414-1

Giessen, T. W., and Marahiel, M. A. (2012). Ribosome-independent biosynthesis of biologically active peptides: application of synthetic biology to generate structural diversity. *FEBS Lett.* 586, 2065–2075. doi: 10.1016/j.febslet.2012.01.017

Grenier, F., Matteau, D., Baby, V., and Rodrigue, S. (2014). Complete genome sequence of *Escherichia coli* BW25113. *Genome Announc.* 2:e01038-14. doi: 10.1128/genomeA.01038-14

Hu, M., Zhao, H., Zhang, C., Yu, J., and Lu, Z. (2013). Purification and characterization of plantaricin 163, a novel bacteriocin produced by *Lactobacillus plantarum* 163 isolated from traditional chinese fermented vegetables. *J. Agric. Food Chem.* 61, 11676–11682. doi: 10.1021/jf403370y

Kalchayanand, N., Dunne, P., Sikes, A., and Ray, B. (2004). Viability loss and morphology change of foodborne pathogens following exposure to hydrostatic pressures in the presence and absence of bacteriocins. *Int. J. Food Microbiol.* 91, 91–98. doi: 10.1016/S0168-1605(03)00324-6

Kanmani, P., Satish, K. R., Yuvaraj, N., Paari, K. A., Pattukumar, V., and Arul, V. (2013). Probiotics and its functionally valuable products-a review. *Crit. Rev. Food Sci. Nutr.* 53, 641–658. doi: 10.1080/10408398.2011.553752

Klaenhammer, T. R. (1988). Bacteriocins of lactic-acid bacteria. *Biochimie* 70, 337–349. doi: 10.1016/0300-9084(88)90206-4

Lane, D. J. (1991). "16S/23S rRNA Sequencing," in *Nucleic Acid Techniques in Bacterial Systematics,* eds E. Stackebrandt and M. Goodfellow (New York, NY: John Wiley and Sons), 115–175.

Linares, D. M., Kok, J., and Poolman, B. (2010). Genome sequences of *Lactococcus lactis* MG1363 (Revised) and NZ9000 and comparative physiological studies. *J. Bacteriol.* 192, 5806–5812. doi: 10.1128/JB.00533-10

Liu, G., Ren, G., Zhao, L., Cheng, L., Wang, C., and Sun, B. (2017). Antibacterial activity and mechanism of bifidocin a against *Listeria monocytogenes*. *Food Control* 73, 854–861. doi: 10.1016/j.foodcont.2016.09.036

Pattanayaiying, R., H-Kittikun, A., and Cutter, C. N. (2014). Effect of lauric arginate, nisin Z, and a combination against several food-related bacteria. *Int. J. Food Microbiol.* 188, 135–146. doi: 10.1016/j.ijfoodmicro.2014.07.013

Perez, R. H., Zendo, T., and Sonomoto, K. (2014). Novel bacteriocins from lactic acid bacteria (LAB): various structures and applications. *Microb. Cell Fact.* 13(Suppl 1):S3. doi: 10.1186/1475-2859-13-S1-S3

Phelan, R., Barret, M., Cotter, P. D., Connor, P. D., Chen, R., Morrissey, J. P., et al. (2013). Subtilomycin: a new lantibiotic from *Bacillus subtilis* strain MMA7 isolated from the marine sponge *Haliclona simulans*. *Mar. Drugs* 11, 1878–1898. doi: 10.3390/md11061878

Qin, Y. X., Han, Y. Z., Shang, Q. M., and Li, P. L. (2015a). Complete genome sequence of *Bacillus amyloliquefaciens* L-H15, a plant growth promoting rhizobacteria isolated from cucumber seedling substrate. *J. Biotechnol.* 200, 59–60. doi: 10.1016/j.jbiotec.2015.02.020

Qin, Y. X., Han, Y. Z., Yu, Y. Q., Shang, Q. M., Zhang, B., and Li, P. L. (2015b). Complete genome sequence of *Bacillus amyloliquefaciens* L-S60, a plant growth-promoting and antifungal bacterium. *J. Biotechnol.* 212, 67–68. doi: 10.1016/j.jbiotec.2015.08.008

Riley, M. A., and Wertz, J. E. (2002). Bacteriocins: evolution, ecology, and application. *Ann. Rev. Microbiol.* 56, 117–137. doi: 10.1146/annurev.micro.56.012302.161024

Singh, P. K., Chittpurna, Ashish, Sharma, V., Patil, P. B., and Korpole, S. (2012). Identification, purification and characterization of Laterosporulin, a Novel bacteriocin produced by *Brevibacillus* sp. Strain GI-9. *PLoS One* 7:e31498. doi: 10.1371/journal.pone.0031498

Stein, T. (2005). *Bacillus subtilis* antibiotics: structures, syntheses and specific functions. *Mol. Microbiol.* 56, 845–857. doi: 10.1111/j.1365-2958.2005.04587.x

Stein, T., Borchert, S., Conrad, B., Feesche, J., Hofemeister, B., Hofemeister, J., et al. (2002). Two different lantibiotic-like peptides originate from the ericin gene cluster of *Bacillus subtilis* A1/3. *J. Bacteriol.* 184, 1703–1711. doi: 10.1128/JB.184.6.1703-1711.2002

Tagg, J. R., Dajani, A. S., and Wannamaker, L. W. (1976). Bacteriocins of gram-positive bacteria. *Bacteriol. Rev.* 40, 722–756.

Wang, Y., Qin, Y. X., Xie, Q., Zhang, Y., Hu, J. R., and Li, P. L. (2018). Purification and Characterization of plantaricin LPL-1, a novel class IIa bacteriocin produced by *Lactobacillus plantarum* LPL-1 isolated from fermented fish. *Front. Microbiol.* 9:2276. doi: 10.3389/fmicb.2018.02276

Wheeler, E. E., Gavin, J. B., and Seelye, R. N. (1975). Freeze-drying from tertiary butanol in the preparation of endocardium for scanning electron microscopy. *Stain Technol.* 50, 331–337. doi: 10.3109/10520297509117083

Xin, B., Zheng, J., Xu, Z., Song, X., Ruan, L., Peng, D., et al. (2015). The *Bacillus cereus* group is an excellent reservoir of novel lanthipeptides. *Appl. Environ. Microbiol.* 81, 1765–1774. doi: 10.1128/AEM.03758-14

Yamanaka, M., Hara, K., and Kudo, J. (2005). Bactericidal actions of a silver ion solution on *Escherichia coli*, studied by energy-filtering transmission electron microscopy and proteomic analysis. *Appl. Environ. Microbiol.* 71, 7589–7593. doi: 10.1128/AEM.71.11.7589-7593.2005

Yang, S. C., Lin, C. H., Sung, C. T., and Fang, J. Y. (2014). Antibacterial activities of bacteriocins: application in foods and pharmaceuticals. *Front. Microbiol.* 5:241. doi: 10.3389/fmicb.2014.00241

Zhao, S., Han, J., Bie, X., Lu, Z., Zhang, C., and Lv, F. (2016). Purification and characterization of plantaricin JLA-9: a novel bacteriocin against *Bacillus* spp. produced by *Lactobacillus plantarum* JLA-9 from Suan-Tsai, a traditional chinese fermented cabbage. *J. Agric. Food Chem.* 64, 2754–2764. doi: 10.1021/acs.jafc.5b05717

Conflict of Interest Statement: The authors declare that the research was conducted in the absence of any commercial or financial relationships that could be construed as a potential conflict of interest.

Advantages of publishing in Frontiers

OPEN ACCESS
Articles are free to read for greatest visibility and readership

FAST PUBLICATION
Around 90 days from submission to decision

HIGH QUALITY PEER-REVIEW
Rigorous, collaborative, and constructive peer-review

TRANSPARENT PEER-REVIEW
Editors and reviewers acknowledged by name on published articles

Frontiers
Avenue du Tribunal-Fédéral 34
1005 Lausanne | Switzerland

Visit us: www.frontiersin.org
Contact us: info@frontiersin.org | +41 21 510 17 00

REPRODUCIBILITY OF RESEARCH
Support open data and methods to enhance research reproducibility

DIGITAL PUBLISHING
Articles designed for optimal readership across devices

FOLLOW US
@frontiersin

IMPACT METRICS
Advanced article metrics track visibility across digital media

EXTENSIVE PROMOTION
Marketing and promotion of impactful research

LOOP RESEARCH NETWORK
Our network increases your article's readership